EM 4300: INORGANIC CHEMISTRY



Larry Mink
CSU San Bernardino

LibreTexts™

CSU San Bernardino

EM 4300: Inorganic Chemistry

Larry Mink

This text is disseminated via the Open Education Resource (OER) LibreTexts Project (https://LibreTexts.org) and like the thousands of other texts available within this powerful platform, it is freely available for reading, printing, and "consuming."

The LibreTexts mission is to bring together students, faculty, and scholars in a collaborative effort to provide an accessible, and comprehensive platform that empowers our community to develop, curate, adapt, and adopt openly licensed resources and technologies; through these efforts we can reduce the financial burden born from traditional educational resource costs, ensuring education is more accessible for students and communities worldwide.

Most, but not all, pages in the library have licenses that may allow individuals to make changes, save, and print this book. Carefully consult the applicable license(s) before pursuing such effects. Instructors can adopt existing LibreTexts texts or Remix them to quickly build course-specific resources to meet the needs of their students. Unlike traditional textbooks, LibreTexts' web based origins allow powerful integration of advanced features and new technologies to support learning.



LibreTexts is the adaptable, user-friendly non-profit open education resource platform that educators trust for creating, customizing, and sharing accessible, interactive textbooks, adaptive homework, and ancillary materials. We collaborate with individuals and organizations to champion open education initiatives, support institutional publishing programs, drive curriculum development projects, and more.

The LibreTexts libraries are Powered by NICE CXone Expert and was supported by the Department of Education Open Textbook Pilot Project, the California Education Learning Lab, the UC Davis Office of the Provost, the UC Davis Library, the California State University Affordable Learning Solutions Program, and Merlot. This material is based upon work supported by the National Science Foundation under Grant No. 1246120, 1525057, and 1413739.

Any opinions, findings, and conclusions or recommendations expressed in this material are those of the author(s) and do not necessarily reflect the views of the National Science Foundation nor the US Department of Education.

Have questions or comments? For information about adoptions or adaptions contact info@LibreTexts.org or visit our main website at https://LibreTexts.org.

This text was compiled on 03/11/2026

TABLE OF CONTENTS

Licensing

1: Atomic Structure

- 1.1: Historical Development of Atomic Theory
- 1.2: The quantum-mechanical model of the atom
- 1.3: Periodic Properties of Atoms
- 1.4: Concept Review Questions Chapter 1
- 1.5: Homework Problems Chapter 1

2: Symmetry and Group Theory

- 2.1: Symmetry Elements and Operations
- 2.2: Point Groups
- 2.3: Matrix Representations of Symmetry Operations and Character Tables
- 2.4: Concept Review Questions Chapter 2
- 2.5: Homework Problems Chapter 2

3: Review of Chemical Bonding

- 3.1: Prelude to Chemical Bonding
- 3.2: Valence Bond Theory- Lewis Dot Structures, the Octet Rule, Formal Charge, Resonance, and the Isoelectronic Principle
- 3.3: The Shapes of Molecules (VSEPR Theory) and Orbital Hybridization
- 3.4: Bond Polarity and Bond Strength
- 3.5: Discussion Questions
- 3.6: Problems
- 3.7: References

4: Molecular Orbital Theory

- 4.1: Prelude to Molecular Orbital Theory
- 4.2: Constructing Molecular Orbitals from Atomic Orbitals
- 4.3: Orbital Symmetry
- 4.4: σ, π, and δ orbitals
- 4.5: Diatomic Molecules
- 4.6: Orbital Filling
- 4.7: Periodic Trends in π Bonding
- 4.8: Three-center Bonding
- 4.9: Building up the MOs of More Complex Molecules- NH_3, P_4
- 4.10: Homology of σ and π orbitals in MO diagrams
- 4.11: Chains and Rings of π-Conjugated Systems
- 4.12: Discussion Questions
- 4.13: Problems
- 4.14: References

5: Coordination Chemistry I - Structures and Isomers

- 5.1: History
- 5.2: Nomenclature
- 5.3: Coordination Numbers and Structures
- 5.4: Isomerism
- 5.5: Concept Review Questions Chapter 5
- 5.6: Homework Problems Chapter 5

6: Coordination Chemistry III - Bonding

- 6.1: 7.1 Bonding in Coordination Compounds
- 6.2: Concept Review Questions Chapter 7
- 6.3: Homework Problems Chapter 7

7: Metals and Alloys- Structure, Bonding, Electronic and Magnetic Properties

- 7.1: Prelude to Metals and Alloys
- 7.2: Unit Cells and Crystal Structures
- 7.3: Bravais Lattices
- 7.4: Crystal Structures of Metals
- 7.5: Bonding in Metals
- 7.6: Conduction in Metals
- 7.7: Atomic Orbitals and Magnetism
- 7.8: Ferro-, Ferri- and Antiferromagnetism
- 7.9: Hard and Soft Magnets
- 7.10: Discussion Questions
- 7.11: Problems
- 7.12: References

8: Metals and Alloys - Mechanical Properties

- 8.1: Defects in Metallic Crystals
- 8.2: Work Hardening, Alloying, and Annealing
- 8.3: Malleability of Metals and Alloys
- 8.4: Iron and Steel
- 8.5: Amorphous Alloys
- 8.6: Discussion Questions
- 8.7: Problems
- 8.8: References

9: Ionic and Covalent Solids - Structures

- 9.1: Prelude to Ionic and Covalent Solids - Structures
- 9.2: Close-packing and Interstitial Sites
- 9.3: Structures Related to NaCl and NiAs
- 9.4: Tetrahedral Structures
- 9.5: Layered Structures and Intercalation Reactions
- 9.6: Bonding in TiS_2, MoS_2, and Pyrite Structures
- 9.7: Spinel, Perovskite, and Rutile Structures
- 9.8: Discussion Questions

- 9.9: Problems
- 9.10: References

10: Ionic and Covalent Solids - Energetics

- 10.1: Ionic Radii and Radius Ratios
- 10.2: Structure Maps
- 10.3: Energetics of Crystalline Solids- The Ionic Model
- 10.4: Born-Haber Cycles for NaCl and Silver Halides
- 10.5: Kapustinskii Equation
- 10.6: Discovery of Noble Gas Compounds
- 10.7: Stabilization of High and Low Oxidation States
- 10.8: Alkalides and Electrides
- 10.9: Resonance Energy of Metals
- 10.10: Prelude to Ionic and Covalent Solids - Energetics
- 10.11: The Strange Case of the Alkali Oxides
- 10.12: Lattice Energies and Solubility
- 10.13: Discussion Questions
- 10.14: Problems
- 10.15: References

11: Electronic Properties of Materials - Superconductors and Semiconductors

- 11.1: Prelude to Electronic Properties of Materials - Superconductors and Semiconductors
- 11.2: Metal-Insulator Transitions
- 11.3: Superconductors
- 11.4: Periodic Trends- Metals, Semiconductors, and Insulators
- 11.5: Semiconductors- Band Gaps, Colors, Conductivity and Doping
- 11.6: Semiconductor p-n Junctions
- 11.7: Diodes, LEDs and Solar Cells
- 11.8: Amorphous Semiconductors
- 11.9: Discussion Questions
- 11.10: Problems
- 11.11: References

12: Physical Techniques in Inorganic Chemistry

13: Coordination Chemistry IV - Electronic Spectra

- 13.1: Microstates and Terms
- 13.2: Term splitting in ligand fields, selection rules, Tanabe-Sugano diagrams. Metal to ligand, and ligand to metal transitions
- 13.3: Concept Review Questions Chapter 8
- 13.4: Homework Problems Chapter 8

14: Coordination Chemistry V - Reactions and Mechanisms

- 14.1: Substitution Reactions and their Mechanisms
- 14.2: Concept Review Questions Chapter 9
- 14.3: Homework Problems Chapter 9

15: Acid-Base Chemistry

- 15.1: Prelude to Acid-Base Chemistry
- 15.2: Brønsted and Lewis Acids and Bases
- 15.3: Hard and Soft Acids and Bases
- 15.4: The Electrostatic-Covalent (ECW) Model for Acid-Base Reactions
- 15.5: Frustrated Lewis Pairs
- 15.6: Discussion Questions
- 15.7: Problems
- 15.8: References

16: Redox Stability and Redox Reactions

- 16.1: Prelude to Redox Stability and Redox Reactions
- 16.2: Balancing Redox Reactions
- 16.3: Electrochemical Potentials
- 16.4: Latimer and Frost Diagrams
- 16.5: Redox Reactions with Coupled Equilibria
- 16.6: Pourbaix Diagrams
- 16.7: Discussion Questions
- 16.8: Problems
- 16.9: References

17: Transition-Metal Storage, Transport, and Biomineralization

- 17.1: Biological Significance of Iron, Zinc, Copper, Molybdenum, Cobalt, Chromium, Vanadium, and Nickel
- 17.2: Biological Systems of Metal Storage
- 17.3: Chemical Properties Relative to Storage and Transport
- 17.4: Iron Biomineralization
- 17.5: Transport of Iron
- 17.6: Transport of Zinc, Copper, Vanadium, Chromium, Molybdenum, and Cobalt

Index

Glossary

Detailed Licensing

Licensing

*A detailed breakdown of this resource's licensing can be found in **Back Matter/Detailed Licensing**.*

CHAPTER OVERVIEW

1: Atomic Structure

1.1: Historical Development of Atomic Theory

1.2: The quantum-mechanical model of the atom

1.3: Periodic Properties of Atoms

1.4: Concept Review Questions Chapter 1

1.5: Homework Problems Chapter 1

Dr. Kai Landskron (Lehigh University). If you like this textbook, please consider to make a donation to support the author's research at Lehigh University: Click Here to Donate.

This page titled 1: Atomic Structure is shared under a not declared license and was authored, remixed, and/or curated by Kai Landskron.

1.1: Historical Development of Atomic Theory

Development of Atomic Theory

Since the ancient times, humans thought of explaining the material world in all of its complexity. The basic idea behind all element theories is that the matter that surrounds us is composed of more simple matter. This matter may be composed of even simpler matter. The most simple matter would be called an element.

The first element theories were one element theories: The greek philosopher Thales thought water was the only element, and everything was a form of water. Anaximenes thought air was the only element, and Heraclitus believed fire was the only element (Figure 1.1.1).



Figure **1.1.1** Thales (640-545 BC) (Attribution: Ernst Wallis et al [Public domain] https://commons.wikimedia.org/wiki/File:Illustrerad_Verldshistoria_band_I_Ill_107.jpg), Anaximenes (585-525 BC) (Attribution: https://commons.wikimedia.org/wiki/File:Anaximenes_of_Miletus_Painting.jpg) and Heraclitus (544 – 483 BC) (Attribution: RoyFokker [CC BY-SA (https://creativecommons.org/licenses/by-sa/4.0)]), respectively.

However, with only one element assumed it was difficult to explain the material world in all its complexity satisfactorily. This could be done more satisfactorily by a multi-element theory. The first philosopher who introduced a multi-element theory was Empedocles. He suggested a four-element theory with fire, air, water, and soil as the elements (Figure 1.1.2).



Figure 1.1.2 Empedocles (495 – 435 BC) (Attribution: Thomas Stanley, The history of philosophy, 1655 [Public domain] https://commons.wikimedia.org/wiki/F...Philosophy.jpg)

First atomistic ideas



Figure 1.1.3 Democrites (460 – 370 BC) (Attribution: Strannik 92 [CC BY-SA (https://creativecommons.org/licenses/by-sa/3.0)] https://commons.wikimedia.org/wiki/File:Demokrit.jpg)

The element theories of Thales, Anaximenes, Heraklitus, and Empedocles were all non-atomistic. This means that they did not include the idea that elements were made of small particles that were indivisible. The first greek philosophers that introduced atomistic element theory were Leukippes, and Democrites (Figure 1.1.3). They assumed that particles cannot be divided into smaller particles infinitely often. Ultimately, after many divisions, one would arrive at particles that could not be further divided, and these particles would be called atoms. Atomistic element theory allows for many different elements which helps to explain the complexity of the material world satisfactorily. However, Leukippes and Democrites did not know how many different elements there were, and how different atoms of different elements were actually distinguished. This question would not be answered until about 2000 years later.

Modern Atomic Theories



Figure 1.1.4 Antoine Lavoisier, the father of modern chemistry, discovered the law of conservation of mass in 1774. (Attribution: Louis Jean Désiré Delaistre (1800–1871); drawing by Julien Léopold Boilly (1796–1874). [Public domain], https://commons.wikimedia.org/wiki/F...sier_color.jpg)

Although the atomistic idea was already known in the antique, it became forgotten for a long time and was only reintroduced about 2000 years later with Dalton's atom hypothesis. What lead to Dalton's atom hypothesis? The first discovery that was important to the development of modern atomic theory was the law of the conservation of mass by Antoine Lavoisier (Fig. 1.1.4). Historically, the conservation of mass and weight was kept obscure for millennia by the buoyant effect of the Earth's atmosphere on the weight of gases, an effect not understood until the vacuum pump first allowed the effective weighing of gases using scales. Until then, in many instances mass seemed to appear or disappear. For example, the mass of wood seems to disappear when it is burned. However, the mass of the wood actually does not disappear it is just converted into the mass of gases, mainly carbon dioxide. When scientists realized that mass never disappeared they could for the first time embark on quantitative studies of the transformations of substances. This in turn led to the idea of chemical elements, as well as the idea that all chemical processes and transformations are simple reactions between these elements. The **law of conservation of mass** states that the mass of a closed system of substances will remain constant, regardless of the processes acting inside the system. An equivalent statement is that matter cannot be created or destroyed, although it may change form. This implies that for any chemical process in a closed system, the mass of the reactants must equal the mass of the products.

Law of Constant Composition

The discovery of the law of the conservation of mass led to the discovery of the law of the constant composition (also called law of definitive proportions) by Joseph Proust (Fig. 1.1.5). This law was the result of chemical analysis that determined the mass ratio of

elements in pure substances. It was found that a pure substance always contains exactly the same proportion of elements by mass. For example the element analysis of pure substances containing the elements carbon and oxygen would be either 42.9% carbon and 57.1% oxygen or 27.3% carbon and 72.7% oxygen.



Figure 1.1.5 Joseph Proust (1754-1826) (Attribution: The original uploader was HappyApple at English Wikipedia. [Public domain] https://commons.wikimedia.org/wiki/F...ust_joseph.jpg)

The law was questioned by Proust's fellow Frenchman Claude Louis Berthollet, who argued that the elements could combine in any proportion. The very existence of this debate was because at the time the distinction between pure chemical compounds and mixtures had not yet been fully developed. When two pure compounds of two different elements are mixed, then the mixture can have a continuous mass ratio between the two elements because compounds can be mixed at any ratio. So, for the example in the two compounds between carbon and oxygen, in mixtures of the two there could be carbon to oxygen ratios varying continuously between 27.7 % to 42.9% carbon, and 42.9% to 72.7% oxygen. It was an accomplishment of Proust that he was able to correctly distinguish between pure compounds and mixtures.

The Law of Multiple Proportions



Figure 1.1.6 John Dalton 1766-1844 (Attribution: Charles Turner [Public domain] https://commons.wikimedia.org/wiki/F...les_Turner.jpg)

John Dalton (Fig. 1.1.6) discovered the law of multiple proportions by close analysis of Proust’s law of constant composition. He noticed that if two elements form more than one compound between them, then the ratios of the masses of the second element which combines with a fixed mass of the first element will be the ratios of small whole numbers, also called integer numbers. Let us see what is the meaning of the law of the multiple proportions by an example:

Example 1.1.1

The first compound contains 42.9% by mass carbon and 57.1% by mass oxygen.

The second compound contains 27.3% by mass carbon and 72.7% by mass oxygen.

Show that the data are consistent with the Law of Multiple Proportions!

Solution

In 100 g of the first compound (100 is chosen to make calculations easier) there are 57.1 g O and 42.9 g C.

The mass of O per gram C is:

57.1 g O / 42.9 g C = 1.33 g O per g C

In 100 g of the second compound, there are 72.7 g O and 27.3 g C.

The mass of oxygen per gram of carbon is:

72.7 g O / 27.3 g C = 2.66 g O per g C

Dividing the mass O per g C of the second (larger value) compound by the mass O per g C of the first compound gives:

2.66 : 1.33 = 2 : 1

2 and 1 are both integer numbers.

Dalton's Atom Hypothesis

Dalton argued that atoms could explain the law of the multiple proportions. If one assumed that elements were made of the same type of indivisible particles, that are identical in mass and all properties then, because these particles can only come in integer numbers, different atoms can be combined to form compounds also only in integer numbers. Thus, in a pure compound atoms of unlike elements would be combined in small whole number ratios. Consequently a given compound always has the same relative number and types of atoms. Chemical reactions would involve reorganization of atoms, but the atoms would retain their identity. Atoms could be rearranged in a chemical reaction but not created or destroyed.

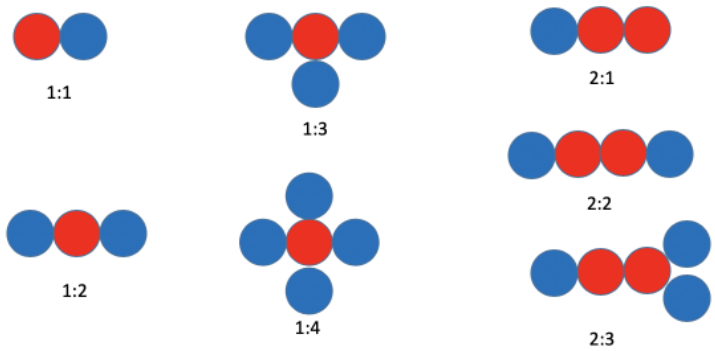


Figure 1.1.7 Illustration of the law of the multiple proportions for two generic, different atoms (red and blue balls).

Figure 1.1.7 is a simple illustration how atoms can explain the law of multiple proportions. The blue and red balls symbolize different atoms of different elements. It is possible to combine a red atom with one, two, three, or four blue atoms to make four different compounds. It is for example also possible to combine two red atoms with one, two or three blue atoms. In all of these compounds as well as in all other thinkable ones, the blue and red atoms can only be combined in integer numbers.

Dalton's Atom Symbols

Dalton also thought of symbols for the atoms of the different elements. The symbols are different from the element symbols that are used today, but the concept is the same. You can see some of them in Figure 1.1.8. For example oxygen is represented by a white ball, while carbon is symbolized by a black ball. You can also see that Dalton already combined atom symbols of different elements to illustrate compounds. For example he combined one white ball with one black ball to indicate carbon monoxide, while he combined two white balls with one black ball to indicate carbon dioxide. In this case he correctly identified the ratios of atoms in the two compounds. However, you can see that this is not always the case. For example, he combined one hydrogen atom (white ball with a dot in the middle) with one oxygen atom to indicate the composition of water. However, as we know today, a water molecule has two hydrogen atoms and one oxygen atom. Why has he been right with the carbon-oxygen compounds, but wrong about the water? The answer is that at the time he could determine the atom ratios only from the law of the multiple proportions. At the time there was only one compound known that was made of hydrogen and oxygen, water, so he assumed the simplest atom ratio of 1:1. If he had known hydrogen peroxide, which has the composition H_2O_2, and thus half as much hydrogen per oxygen, he would have probably correctly assigned the correct hydrogen to oxygen ratio to water. In the case of the carbon oxides, he assigned the compositions correctly because both carbon monoxide and carbon dioxide were known at the time.

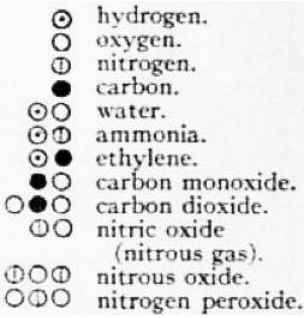


Figure 1.1.8 Dalton's atom symbols (Attribution: Encyclopædia Britannica, 1911 [Public domain] https://commons.wikimedia.org/wiki/F...an_symbols.png)

Subatomic Particles

Dalton's atomic theory stated that different elements were made of different atoms, but did not explain what made the atoms different. The answer is that atoms are composed of subatomic particles, protons, neutron, and electrons, and the number of the protons and electrons in an atom defines the element it represents. So after all, atoms are not so indivisible. However, an atom can still be seen as the smallest particle that represents the full properties of an element. If an atoms gets divided further into subatomic particles then these properties are being lost. To understand atoms further, we must therefore understand the subatomic particles they are made of. The first subatomic particle that was discovered was the electron. It was found through the investigation of so-called cathode rays which were a mysterious phenomenon at the time. Cathode rays occur when a high voltage of about 10-20 kV is applied to an evacuated tube (0.0001 mm Hg). You can see such a tube with a cathode ray going through in Figure 1.1.9. The big question was: What causes these rays?

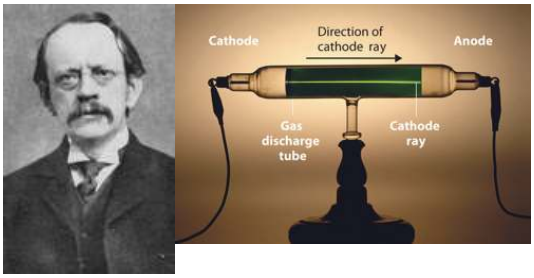


Figure 1.1.9 Joseph John Thomson (1856-1940) (Attribution: https://commons.wikimedia.org/wiki/F....J_Thomson.jpg, PD-US-expired)
and his experimental apparatus (Attribution: Chemlibetexts https://chem.libretexts.org/@api/dek...338&height=228, creativecommons.org/licenses/by-nc-sa/3.0/us/).

The answer was found by John Joseph Thomson. He applied electric and magnetic fields to these rays and found them deflected. When an electric field was applied the beam was deflected toward the positive pole. When an equally strong electric and magnetic field was applied, and the magnetic field was perpendicular to the electric field then these fields canceled out, and the rays were no longer deflected. Thomson concluded that these rays must consist of negatively charged particles emitted by the negatively charged electrode because they were attracted by the positive pole of the electric field: Electrons. Knowing the forces associated with the electrical and magnetic fields, he was able to calculate a mass to charge ratio of the electrons which is 5.6857 x 10E-9 g/C. After Thomson, Robert Millikan performed another experiment, the so-called oil drop experiment, that allowed to determine the charge and the mass of the electron. The charge of an electron is -1.6 x 10E-19 C, and its mass is 9.1 x 10E-28 g.

Thomson's plum pudding atomic model

The discovery of the electron led Thomson to the development of a first atomic model that would include a subatomic particle. It is named plum pudding model (Fig. 1.1.10). In the Thomson atom model electrons are embedded as little particles in a positively charged mass like raisins are embedded in a cake. This atom model is still far from the atom model that we accept today, but it represented an important step forward, because it introduced for the first time the idea that atoms are not indivisible, but contain subatomic particles.

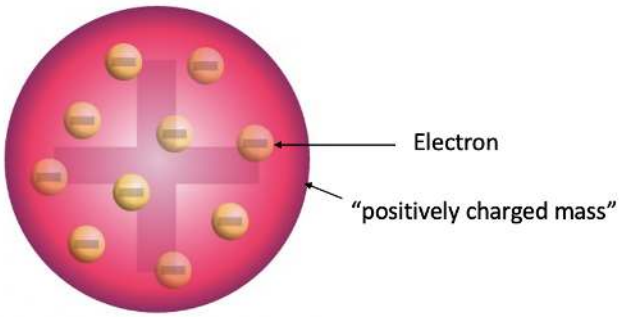


Figure 1.1.10 Thomson's plum pudding atomic model (Attribution: Fatfission (public domain) https://commons.wikimedia.org/wiki/File:Plum_pudding_atom.svg)

Rutherford's Atom Model

Ernest Rutherford (Fig. 1.1.11) wanted to test Thomson's plum pudding atom model by experiment. To do so, he placed a photographic film around a gold foil (Figure 1.1.12). In the following he bombarded the gold foil with alpha radiation. Alpha radiation is a form of radioactivity and consists of helium nuclei, also called alpha-particles. It was known at this time the alpha-particles were positively charged and had a large mass compared to an electron. Rutherford's hypothesis was that if Thomson's atom model was true, then the alpha particles should all go straight through the gold foil like a bullet going through a plum pudding. Therefore, a blackening of the photographic film, which served as the alpha radiation detector, should only occur directly behind the gold film.



Figure 1.1.11 Sir Ernest Rutherford (1871-1931) who earned the Nobel prize for chemistry 1908. (Attribution: George Grantham Bain Collection (Library of Congress) [Public domain], commons.wikimedia.org/wiki/F...erford_LOC.jpg)

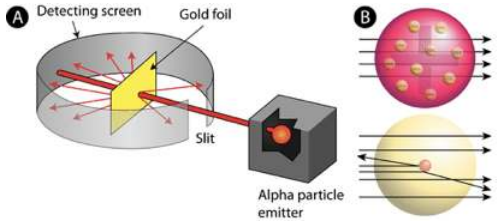


Figure 1.1.12 Rutherford's Gold Foil Experiment

However, what Rutherford observed was that while most of the alpha-particles went straight through the gold foil, some of them were deflected, and a few of them were even reflected. Rutherford concluded that Thomson's plum pudding model must be wrong. A bullet shot at a plum pudding would just never be reflected by the plum pudding and come back at you.

He suggested that the atom would be made of a positively charged nucleus where almost the entire mass of the atom would be concentrated. In the event of a collision between the alpha particle and that nucleus, the alpha particle would be reflected. In the event of an alpha particle passing by the nucleus close, the alpha particle would be deflected. In the event of an alpha particle passing the nucleus in larger distance, the alpha particle would pass the atom practically non-deflected. The observation that most of the alpha particles were not deflected led Rutherford to the conclusion that the overall atom must be much larger than the nucleus, in fact, the data allowed him to calculate that the radius of the atom would be about 10,000 times larger than the radius of the nucleus. This implies that the atoms would be mostly empty space. To explain the empty space, Rutherford assumed that the electrons would move in orbits around the nucleus like planets around the sun. This would be called the planetary model of the atom (Fig. 1.1.13).

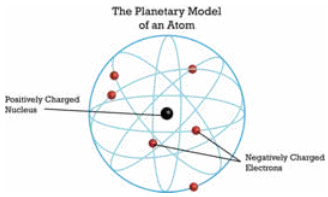


Figure 1.1.13 Rutherford's Atom Model

Bohr's Atom Model

Rutherford's atom model was another big step forward in the development of atomic theory, however there were inherent problems with it as it violated fundamental principles of physics. An electron in an orbit is a self-accelerating electrically charged particle, and according to the laws of physics such particles must emit electromagnetic radiation. However, under normal circumstances atoms do not emit electromagnetic radiation. Secondly, even if the electron emitted electromagnetic radiation, then this would mean that the electron would lose energy because electromagnetic radiation is a form of energy. However, an electron constantly losing energy would make it unstable in its orbit around the nucleus, and it should spiral downward closer to the nucleus until the atom was eventually collapsed. It is however, experimentally not observed that atoms collapse, they are quite stable species. These difficulties of the Rutherford atom model meant that it could not be the final answer to atomic structure. Niels Bohr (Fig. 1.1.14) was aware of the problems of the Rutherford model, and two new developments in physics, namely the concept of the quantization of energy and atomic spectra helped him to develop an improved atom model, known as Bohr model. To understand this model let us look first at the quantization of energy and atomic spectra.



Figure 1.1.14 Niels Bohr (1885 - 1962) (Attribution: Bain News Service, publisher Restored by: Bammesk [Public domain], commons.wikimedia.org/wiki/F...in_-_35303.jpg)

Blackbody Radiation

The quantization of energy was discovered in the context of the physical phenomenon called "blackbody radiation". Blackbody radiation is the electromagnetic radiation any object sends out due to its temperature (Fig. 1.1.15).



Figure 1.1.15 An example of blackbody radiation emitted by hot, volcanic lava. (Attribution: Hawaii Volcano Observatory (DAS) [Public domain], commons.wikimedia.org/wiki/F...hoehoe_toe.jpg)

It's distribution of wavelengths follows curves that depend on the temperature and are shown in Figure 1.1.16. You can see that for each temperature the intensity first increases with increasing wavelength, then goes through a maximum, and finally decreases again. You can also see that the overall intensity of the blackbody radiation increases with temperature and that the maximum of the curve shifts to smaller wavelengths with increasing temperature. Objects at room temperature do not emit much blackbody radiation and the wavelengths are far longer than visible for the human eye. However, when an object is heated high enough, intensity increases and wavelength decreases, and the object starts to glow. For instance, lava (Figure 1.1.15) has a temperature high enough so that its blackbody radiation is visible for the human eye. With increasing temperature objects first glow red, then orange, then yellow, and eventually white. This is because red is the color associated with the largest wavelength, and as

temperature increases other colors mix into red, until the object glows white. At extremely high temperatures the blackbody radiation also has a significant intensity in the UV region. Such temperatures occur in welding processes, for example, and for this reason welders need to wear glasses that block the UV radiation. The wavelength and intensity of blackbody radiation can be easily measured, but at the beginning of the 20th century there was no good explanation for its behavior. Classical theory predicted that intensity would continuously increase with decreasing wavelength at any temperature which was not in accordance with experimental observation.

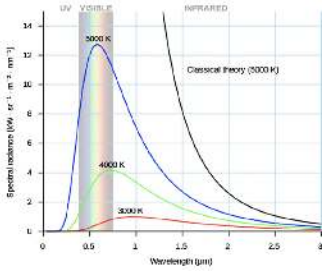


Figure 1.1.16 Experimentally measured intensity of blackbody radiation as a function of wavelength for 3000, 4000, and 5000 K vs. intensity predicted by classical theory (5000 K). (Attribution: Darth Kule commons.wikimedia.org/wiki/F...Black_body.svg)

To bring experiment and theory in accordance, Max Planck made the radical assumption that the energy associated with radiation of a given wavelength or a given frequency was quantized. It would be an integer multiple n of that frequency ν, multiplied with proportionality constant h, know today as the Planck constant.

$$E = n\,h\,\nu$$

Equation 1.1.1 The Planck-Einstein equation.

Using this assumption he was able to derive the Planck equation (Equation 1.1.2) which correctly describes the intensity and wavelength distribution of the blackbody radiation for any temperature. The correct description of blackbody radiation strongly supported Planck's assumption that energy was quantized, but it did not prove it or explain it. The proof and the explanation was found only later. Initially Planck assumed it merely to fit the data.

$$E(\lambda, T) = \frac{2hc^2}{\lambda^5} * \frac{1}{e^{\left(\frac{hc}{\lambda kT}\right)} - 1}$$

h = Planck's constant = $6.626 * 10^{-34}\ J * s$
c = speed of light = $2.997925 * 10^{8}\ m / sec$
λ = wavelength (m)
k = Boltzmann's constant = $1.381 * 10^{-23}\ J/K$
T = temperature (K)

Equation 1.1.2 Planck's equation

Bohr's Atom Model

The second development that contributed to Bohr's atom model was the absorption and emission spectra of atoms. It was experimentally observed that under certain circumstances atoms would send out or absorb electromagnetic radiation of discreet wavelengths that were characteristic for an atom. For example, H atoms would absorb or emit at four discreet wavelengths in the visible region of the electromagnetic spectrum (Fig. 1.1.17).



Figure 1.1.17 The hydrogen emission spectrum in the visible region (Balmer series). (Attribution: Merikanto, Adrignola [CC0], commons.wikimedia.org/wiki/F...spectrum-H.svg)

This is known as the Balmer series named after its discoverer Johann Balmer. Friedrich Paschen and Chester Lyman later found that H also absorbs and emits at discreet wavelengths in the IR and UV region respectively. These wavelengths are known as the

Paschen and Lyman series, respectively (Fig. 1.1.18).



Figure 1.1.18 Friedrich Paschen (1865 – 1947) (Attribution: www.maerkischeallgemeine.de [Public domain], commons.wikimedia.org/wiki/F...n_Physiker.jpg) and Chester Lyman (1814-1988) (Attribution: commons.wikimedia.org/wiki/F...mith_Lyman.jpg), respectively.

For the absorption and emission spectra of H a simple mathematical relationship between the energies associated with the wavelengths can be found. The energy is proportional to a constant, today known as the Rydberg constant, times one over an integer number square minus one over another integer number square, whereby the second integer number would be larger than the first one (Eq. 1.1.3). The observation of integer numbers showed that also the energy and the wavelengths of the atomic absorption and emission spectra are quantized. The question was what the quantization of the absorption spectra meant for atomic structure.

$$\Delta E = R_H \left(\frac{1}{n_{low}^2} - \frac{1}{n_{high}^2} \right)$$

Equation 1.1.3 Rydberg formula for the emission of light with particular energies.

Bohr answered the question the following way. He argued, that like in the Rutherford model the electrons would move in orbits around the nucleus. A balance of opposite centrifugal forces and Coulomb attractions would hold the electron stable in the orbit. However, because energy is quantized, also the angular momentum of the electron would be quantized, and thus, only discreet radii would be allowed. The most inner orbit would have the quantum number n=1, the next higher orbit the quantum number n=2, and so forth (Fig. 1.1.19).

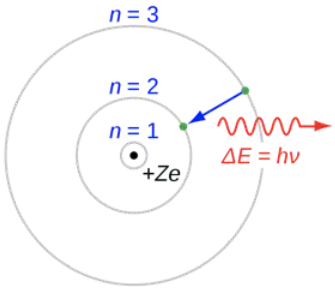


Figure 1.1.19 Bohr atom model (Attribution: JabberWok [CC BY-SA (http://creativecommons.org/licenses/by-sa/3.0/)], commons.wikimedia.org/wiki/F...atom_model.svg)

The quantization of the electron energies and the radii would be the explanation why electrons, despite self-accelerating, do not continuously emit electromagnetic radiation. Electromagnetic radiation is only emitted when an electron jumps from an outer orbit of higher energy to an inner orbit of lower energy. This radiation must have a discreet wavelength because the energy difference between two orbits is discreet. Vice versa, an atom can adsorb electromagnetic radiation of specific wavelength and energy that is suitable to make the electron jump from an inner to an outer orbit. In sum, the quantization of the energy and the radii would explain the quantization of the absorption and emission spectra. The question is: Can the radii be calculated, and what are the associated energies of the electrons in the orbits?

Definition: Bohr's Postulates (1913)

1. An electron in an atom moves in a circular orbit about the nucleus under the influence of the Coulomb attraction between the electron and the nucleus, obeying the laws of classical mechanics.

2. Instead of the infinity of orbits which would be possible in classical mechanics, it is only possible for an electron to move in an orbit for which its orbital angular momentum L is an integral multiple of h/2π.

3. Despite the fact that it is constantly accelerating, an electron moving in such an allowed orbit does not radiate electromagnetic energy. Thus, its total energy E remains constant.

4. Electromagnetic radiation is emitted if an electron, initially moving in an orbit of total energy, discontinuously changes its motion so that it moves in an other orbit of total energy. The frequency of the emitted radiation is equal to the quantity divided by h.

To calculate the radii and energies of the electron in the H atom Bohr made two assumptions: Firstly, the centrifugal force associated with the electron moving in the orbit would be assumed equal to the Coulomb force between the electron and the proton so that the electron would be stable in the orbit. Secondly, the angular momentum of the electron would be quantized and an integer multiple of the Planck constant h. The factor 2π is because E = h/2π x angular frequency. The angular frequency (also called angular speed) is the angular displacement (in degree or rad) per time unit. Angular frequency is frequency x 2π. We can rearrange this equation by solving it for *v* and then insert the equation into equation I giving the result as shown in Fig. 1.1.20.

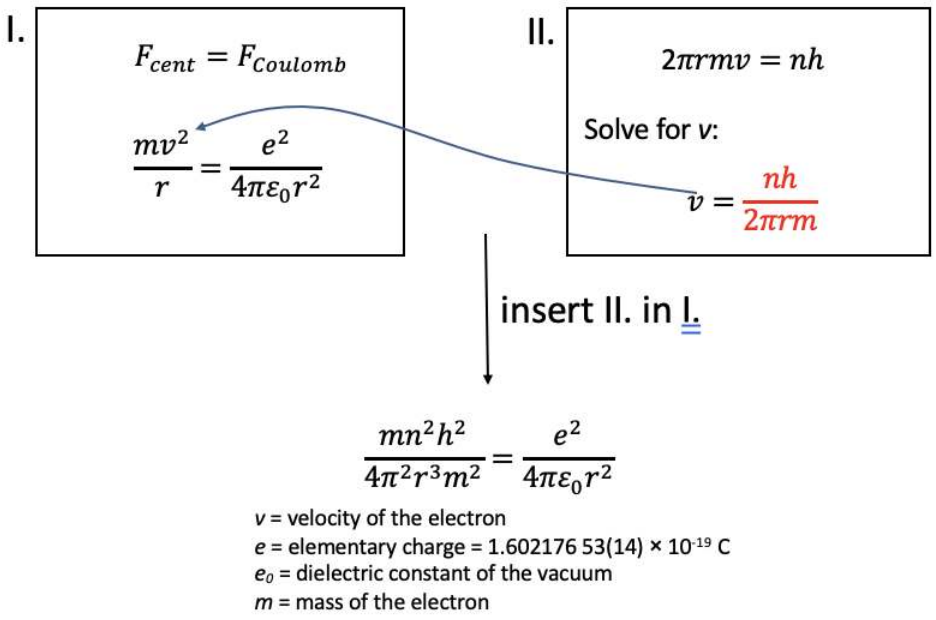


Figure 1.1.20 Derivation of the radii of the electron orbits (part 1).

We can then multiply this equation by $4\pi\varepsilon_0 r^2$, divide by e^2, and multiply it by r. This gives us the term $r=(n^2h^2\varepsilon_0)/(\pi me^2)$. Analyzing the term shows us that r is only a function of the quantum number n, specifically the radius is proportional to n^2 (Fig. 1.1.21). All other terms are constants, namely the Planck constant h, the dielectric constant of the vacuum, π, the mass of the electron, and the elementary charge. By inserting the quantum numbers into the equation we can calculate the actual values for the radii. For example, when we insert 1 for the quantum number n, we get the radius for the most inner orbit of the electron in the H atom. It is 5.29 x 10^{-11} m. If we inserted 2 for n, we would get the second radius, if we inserted 3, we would get the third radius and so on.

$$\frac{mn^2h^2}{4\pi^2r^3m^2} = \frac{e^2}{4\pi\varepsilon_0 r^2} \quad |\times 4\pi\varepsilon_0 r^2$$

$$\frac{n^2h^2\varepsilon_0}{\pi rm} = e^2 \quad |\div e^2 \quad |\times r$$

$$r = \frac{n^2h^2\varepsilon_0}{\pi me^2}$$

For the first radius (n=1): $r = \frac{1^2h^2\varepsilon_0}{\pi me^2} = 5.29\times10^{-11}m$

Figure 1.1.21 Continuation of the derivation of the radii of the electron orbits.

Now let us calculate the energies of the electron on these radii. Generally, the overall energy of the electron is the sum of the kinetic and potential energies. The kinetic energy of a moving object is given by $E_{kin}=1/2\ mv^2$. We know that m must be the mass of the electron, but what is the velocity of the electron? We can derive it from equation I we previously used by solving it for v^2 (Fig. 1.1.20). We can then insert the term for v^2 into the equation $E_{kin}=1/2\ mv^2$, which gives $E_{kin}=e^2/(8\pi\varepsilon_0 r)$, Fig. 1.1.23.

Now let us consider the potential energy. The potential energy is the Coulomb energy between the proton and the electron in the H atom. The formula for the Coulomb energy of two particles having two opposite elementary charges is $E_{pot}=-e^2/(4\pi\varepsilon_0 r)$. Note that this energy has a negative algebraic sign because the forces between the proton and the electron are attractive (Fig. 1.1.23).

$$E = E_{kin} + E_{pot}$$

$$E_{kin} = {}^1/_2\, mv^2 \qquad E_{pot} = -\frac{e^2}{4\pi\varepsilon_0 r}$$

Equation I: $\frac{mv^2}{r} = \frac{e^2}{4\pi\varepsilon_0 r^2}$

$$v^2 = \frac{e^2}{4\pi\varepsilon_0 rm}$$

$$E_{kin} = \frac{e^2}{8\pi\varepsilon_0 r}$$

Figure 1.1.23 Derivation of kinetic, potential, and overall energies of the H electron (part 1).

We can now add up the kinetic and the potential energy to give the overall energy which is $E = E_{kin}+E_{pot}= [e^2/(8\pi\varepsilon_0 r)] - [e^2/(4\pi\varepsilon_0 r)] = e^2/(\pi\varepsilon_0 r)\ (1/8-1/4) = -e^2/(8\pi\varepsilon_0 r)$. We can then use the term we previously calculated for r (Fig. 1.1.21) and insert it into the term for the overall energy. As a result the overall energy becomes $E=-(e^4m)/(8\varepsilon_0{}^2n^2h^2)$, Fig. 1.1.24. As we can see, the energies for the electrons in the different orbits are also only a function of the quantum number n, specifically, they are a function of $1/n^2$. Note also that the overall energy is negative. This is because the energy is a binding energy. Because of the negative algebraic sign, a higher quantum number n means a higher, because less negative energy. At very high quantum numbers n the value for E would approach zero, meaning that the binding energy for the electron would approach zero. The higher the orbit of the electron the more energy it has and the less strongly it is bound to the atom.

$$E = E_{kin} + E_{pot} = \frac{e^2}{8\pi\varepsilon_0 r} - \frac{e^2}{4\pi\varepsilon_0 r} = \frac{e^2}{\pi\varepsilon_0 r}\left(\frac{1}{8} - \frac{1}{4}\right) = -\frac{e^2}{8\pi\varepsilon_0 r}$$

B/c we had calculated before: $r = \frac{n^2h^2\varepsilon_0}{\pi me^2} \longrightarrow E = -\frac{e^4m}{8\varepsilon_0^2 n^2h^2}$

Figure 1.1.24 Continued derivation for the energies of the H electron.

Formula for energy of electron in a specific orbit:

$$E = -\frac{e^4 m}{8\varepsilon_0^2 n^2 h^2}$$

Formula for energy difference between two orbits:

$$\Delta E = -\frac{e^4 m}{8\varepsilon_0^2 n_{high}^2 h^2} - -\frac{e^4 m}{8\varepsilon_0^2 n_{low}^2 h^2} = \frac{e^4 m}{8\varepsilon_0^2 h^2}\left(\frac{1}{n_{low}^2} - \frac{1}{n_{high}^2}\right)$$

Empirically Rydberg found the H spectrum:

$$\Delta E = R_H\left(\frac{1}{n_{low}^2} - \frac{1}{n_{high}^2}\right)$$

Because ΔE (theory) = ΔE (empirical):

$$R_H = \frac{e^4 m}{8\varepsilon_0^2 h^2}$$

Figure 1.1.25 Comparing derived energies of the H electron with those experimentally found in the H spectrum.

Finally let us calculate energy differences between electrons in different orbits. Subtraction of the terms for the energies of two electrons in two different orbits gives $\Delta E=(e^4m)/(8\varepsilon_0^2h^2)\ (1/(n_{low}^2) - 1/(n_{high}^2))$, Fig. 1.1.25. The calculated and empirically found ΔE match excellently, the empirically found Rydberg constant matches the theoretically derived constant $(e^4m)/(8\varepsilon_0^2h^2)$. Thus experiment and theory are in accordance. Bohr's theory is able to explain the H spectra very well, and can predict both radii of electron orbits and energies. The Bohr model for the first time introduced the quantization of electron states in atoms, and in this regard in was a big step forward. However, there were still problems with Bohr's theory. It could only explain the H spectra well, but failed to explain the spectra of all other atoms. Secondly, Bohr's postulates seemed ad hoc and lacked an explanation. There was no good explanation why an electron in a quantized orbit would not emit electromagnetic radiation continuously. Thus, the Bohr model could still not be the final answer to atomic theory. In fact, it lacks to take an important property of the electron into account: The wave-particle dualism of the electron.

Definition: Problems with Bohr's Theory

1. It can explain only the H spectrum and fails to explain all the spectra of all other atoms.
2. Bohr's postulates are ad hoc. They lack an explanation.

Dr. Kai Landskron (Lehigh University). If you like this textbook, please consider to make a donation to support the author's research at Lehigh University: Click Here to Donate.

This page titled 1.1: Historical Development of Atomic Theory is shared under a not declared license and was authored, remixed, and/or curated by Kai Landskron.

- **1.1: Historical Development of Atomic Theory** by Kai Landskron is licensed CC BY 4.0.

1.2: The quantum-mechanical model of the atom

Wave Particle Dualism

The phenomenon of the wave-particle dualism was first discovered for electromagnetic radiation, and the extended to all other particles including the electron. It began with the investigation of the photoelectric effect by Albert Einstein (Fig. 1.2.1 and Fig. 1.2.2).

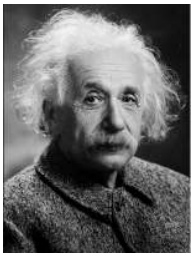


Figure 1.2.1 Albert Einstein, Nobel Prize 1921. (Attribution: Photograph by Orren Jack Turner, Princeton, N.J. Modified with Photoshop by PM_Poon and later by Dantadd. [Public domain], commons.wikimedia.org/wiki/F...lanck_1933.jpg)

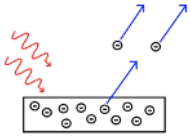


Figure 1.2.2 The photoelectric effect (Attribution: Wolfmankurd [CC BY-SA (http://creativecommons.org/licenses/by-sa/3.0/)]. commons.wikimedia.org/wiki/F...ric_effect.svg)

The photoelectric effect occur when a metal surface is irradiated by light. Above a certain frequency, or below a certain wavelength, light is able to eject electrons from the metal surface. The threshold frequency depends on the metal. Below the threshold frequency no electrons get ejected. Einstein investigated the maximum kinetic energy of the ejected electrons as a function of the frequency of the light. He found that there was a linear relationship. He analyzed the slope of this line and found that the slope was the Planck constant h. This would mean that electrons had an energy E=hν minus an energy E_B that would be needed to overcome the binding energy, also called the work function, of the electron in the metal (Figure 1.2.3, left).

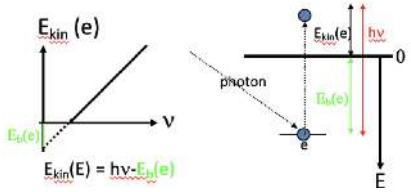


Figure 1.2.3 Maximum kinetic energy of the ejected electron as a function of the frequency of light (left), and mechanistic interpretation of the photoelectric effect (right).

The equation E=hν was previously derived by Planck (Fig. 1.2.4) based on the assumption that energy was quantized, and now Einstein had experimentally found it again in the quest to explain the photoelectric effect. This would mean that light was quantized. The quantization would be explained by the fact that light would not only have wave but also particle properties, and these particles would be called photons. Assuming photons the photoelectric effect could be easily explained (Figure 1.2.3, right). When light hits the metal surface the photon collides with the electron. Only when the photon had an energy larger than the work function of the metal, the electron would be ejected and would have a kinetic energy equal to the difference between the energy of the photon and the binding energy. The wave-particle dualism of light, and electromagnetic radiation in general can also be mathematically derived. Because mass can be converted into electromagnetic radiation according to the equation $E = mc^2$, and the energy of electromagnetic radiation is E=hν, mc^2=hν. We can solve the equation for ν, and then it is ν=mc^2/h. With ν=c/λ, and solved for λ, the equation becomes λ=h/mc. This equation shows the wave particle-dualism of electromagnetic radiation because it relates a wavelength to a mass. In fact, the mass of the particle associated with electromagnetic radiation, the photon, is inverse proportional to the wavelength of the electromagnetic radiation. The discovery of the wave-particle dualism of electromagnetic radiation was a radically new concept that is difficult to grasp intellectually up to this date because the human mind tends to see waves and particles to be mutually exclusive. However, it is one of the most fundamental principles of nature. As we will see later, not only electromagnetic radiation shows the wave particle dualism, but all particles including electrons.



Figure 1.2.4 Max Planck, Nobel Prize 1918 (Attribution: commons.wikimedia.org/wiki/F...lanck_1933.jpg)

Wave Particle Dualism of Massive Particles

The wave-particle dualism was originally thought to be valid for the photon only. A young French physics PhD student, Louis De Broglie had the radical idea that not only the photon, but all particles would exhibit the wave particle dualism, including the electron. Einstein's formula λ = h/mc would just need to be slightly rearranged into λ = h/mv, whereby m would be the mass of the particle, and v would be the velocity of the particle. This idea was much disputed at the time, and Louis De Broglie's PhD thesis was almost not accepted. However, eventually the wave-particle dualism of the electron was proven by electron diffraction experiments, and Louis De Broglie was awarded the Nobel prize in 1929. Today, we believe that all particles show the wave-particle dualism, and no experiment up to this date indicates an exception.



Figure 1.2.5 Louis de Broglie 1892-1987, Nobel Prize 1929 (Attribution: Unknown commons.wikimedia.org/wiki/F...roglie_Big.jpg, PD-US expired)

Standing Waves

With the discovery of the wave-particle dualism of the electron, and the observation of the quantization of electronic states in atoms led physicists focus on a field in physics in which waves are quantized. The field of standing waves (Fig. 1.2.6).

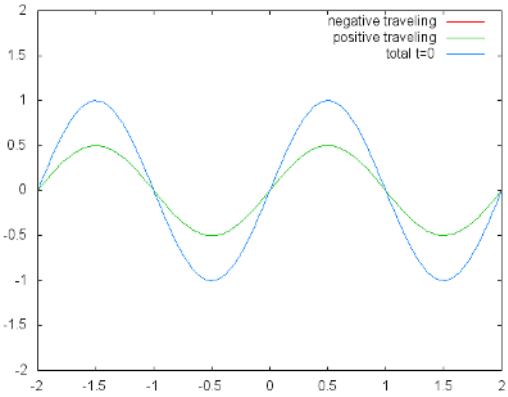


Figure 1.2.6 Two confined traveling waves (red and green) producing a standing wave (blue) due to their interference. (Attribution: Govindabalan [CC BY-SA (https://creativecommons.org/licenses/by-sa/3.0)], commons.wikimedia.org/wiki/F..._animation.gif)

Standing waves are a quite common phenomenon. You can for example trigger a standing waves by plucking a guitar string. This causes the guitar string to vibrate in standing waves with discreet, quantized wavelengths. The vibration with the longest wavelength is the so-called ground vibration. Its wavelength is two times the length of the guitar string. In addition, so-called higher harmonics are possible. The first harmonic has a wavelength equal to the length of the guitar string, the second one, has a wavelength equal to two-thirds of the length of the string, the third one has a wavelength equal to half of the length of the string, the fourth one has a wavelength equal to one third of the length of the guitar string, and so fourth (Fig. 1.2.7).



Figure 1.2.7 Standing waves (Attribution: Adjwilley [CC BY-SA (https://creativecommons.org/licenses/by-sa/3.0)], commons.wikimedia.org/wiki/F...n_a_string.gif)

It can be easily seen that the possible wavelengths at which the string can vibrate follow the equation $\lambda=2L/n$, whereby n is an integer, or a quantum number, and L is the length of the guitar string. Thus, we can say that the waves associated with the guitar string vibrations are quantized. Why are these waves called standing waves? This is because the positions of the crests and the troughs and the nodes do not move. They remain at the same position on the guitar string at any point in time. It should be said here that the standing nature of the waves is actually an illusion. There are actually two waves traveling in opposite direction on the guitar string, and these waves interfere with each other so that a standing wave is produced (this is illustrated in Fig. 1.2.6). When the guitar string is plucked two waves are sent into opposite direction on the guitar string toward the two opposite ends on the guitar string. Once they have reached these ends they get reflected and sent into the opposite direction until they again reach the ends of the guitar string where they get reflected again. During this process, which happens over and over again, the two waves interfere and produce the standing wave. In sum, the fact that the wave is confined within the guitar string, leads to the quantized standing waves.

Electron in a One-Dimensional Box

Let us know go from a vibrating guitar string to an electron in a one-dimensional box of length *a* having infinitely high walls. Inside the box the potential energy of the electron is zero, in the walls the potential energy is infinite (Figure 1.2.8).

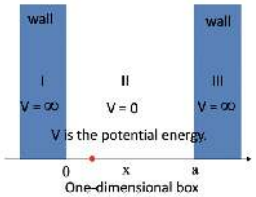


Figure 1.2.8 Electron (red dot) in a one-dimensional box with a potential energy V=0 within the box and infinite potential energy within the walls (the walls may be thought infinitely high).

Due to its kinetic energy the electron can travel on a line within the box until it hits the wall (Fig. 1.2.9, A). At the wall it is getting reflected and forced to travel into the opposite direction until it again hits the wall where it reverses direction again, and so forth. Consider now that the electron does not only have particle, but also wave properties. Because of that also a wave travels along the line, gets reflected at the wall, travels into opposite direction, gets reflected again and so on. These waves can interfere with it other just like the waves traveling on the guitar string to produce a standing wave. Thus, the electron in the one-dimensional box should behave like a standing wave, and this wave should be quantized (Fig. 1.2.9, B-F).

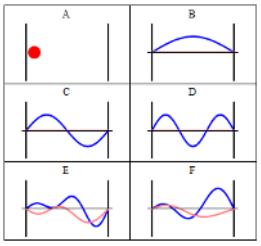


Figure 1.2.9 Electron traveling in a one-dimensional box acting as a standing wave (Attribution: Sbyrnes321 [CC0], commons.wikimedia.org/wiki/F...lAnimation.gif)

How can we mathematically describe the electron in the box as a standing wave? Generally, you can describe a standing wave by a wave function. A wave function tells the amplitude of the standing wave at a particular position in the one-dimensional box. How can we find the wave function? We can start out from a differential equation that is generally valid for standing waves (Eq. 1.2.1).

$$\frac{d^2\Psi(x)}{dx^2} = -\left(\frac{2\pi}{\lambda}\right)^2 \Psi(x)$$

Equation 1.2.1 Standing wave differential equation.

It says that the second derivative of the amplitude of the wave function at the position x is equal to $-(2\pi/\lambda)^2$ multiplied with the amplitude of the wave function at the position x. Let us now consider that the kinetic energy of the electron is $E = 1/2mv^2$ and expand the equation by m.

$$E = \tfrac{1}{2} mv^2$$

$$E = (mv)^2/2m \rightarrow (mv)^2 = 2mE \rightarrow mv = [2mE]^{1/2} \rightarrow \lambda = h/[2mE]^{1/2}$$

$$\lambda = h/mv \rightarrow mv = h/\lambda$$

Equation 1.2.2 Solving for λ from kinetic energy equation and De Broglie equation.

Let us then solve the equation for (mv) . Now let us solve the De Broglie equation for mv and insert mv by h/λ in the previous equation. Finally, let us solve the equation by λ and we will get $\lambda = h/[2mE]^{1/2}$, Eq. 1.2.2. We can now substitute λ by $h/[2mE]^{1/2}$ in the differential equation. Slightly rearranged this equation becomes the Schrödinger equation for the electron in the one-dimensional box (Equation 1.2.3).

$$\left[\frac{d^2}{dx^2}\frac{-h^2}{8\pi^2 m}\right]\Psi(x) = E_{kin}\Psi(x)$$

Equation 1.2.3 Schrödinger Equation for the electron in a 1-D box.

The Schrödinger equation is a differential equation. To get the wave function that describes the electron in the box we need to solve the differential equation. One possibility solve a differential equation is to guess its solution, and after that show that the solution is right. This is the approach we want to pursue here. A very general wave function is one that is a sum of a sinus term and a cosinus term of the coordinate x whereby we shall assume two general coefficients r and s in front of x, and two other general coefficients A and B in front of the sinus and the cosinus term, respectively.

$$\Psi = A \sin rx + B \cos sx$$

Equation 1.2.4 Generic solution to the differential equation.

We can now think of so-called boundary conditions for the wave function which will make the wave function more specific. A boundary condition is a property the wave function must have to be a sensible solution to the differential equation. We can assume a first boundary condition which assumes that at the position x=0 the amplitude of the wave function must be 0. This can be assumed because at these positions the "electron wave" gets reflected at the wall. That means that the wave function cannot have a cosinus term and thus B must be 0. If the wave function had a cosinus term it would not be 0 at x = 0 because the cosinus of 0 is not 0.

$$B = 0 \qquad \Psi = A \sin rx$$

Equation 1.2.5 Boundary condition 1 for the wave function

The second boundary condition is that the amplitude of the wave function is zero at x = a. Again, this is because the electron hits the wall at x = a and reverses its direction. The sinus function is only zero at x = a when ra is an integer number n times π: ra=nπ. This means that r must be nπ/a.

$$ra = n\pi \quad or \quad r = n\pi/a$$

Equation 1.2.6 Boundary condition 2 for the wave function

Thus, the wave function must be A=sin(nπx/a). We can see that the wave function that describes the electron as a standing wave in the one-dimensional box is quantized because the quantum number n appears.

$$\Psi = A \sin(n\pi x/a)$$

Equation 1.2.7 The wave function considering boundary conditions 1 and 2.

Inserting the quantum numbers n into the wave functions produces all the standing waves the electron can adopt (Fig. 1.2.10). You can see that the number of nodes and the wavelengths of the waves depend on the quantum number n. For n = 0 there is no node and the wavelength is twice the length of the box, for n = 2 there is one node and the wavelength is equal to the length of the box, for n =3 there are three nodes and the wavelength of the wave is 2/3 of the lengths of the box and so forth. We can illustrate that the wave function describes the waves depicted in Figure 1.2.10 by an example. The amplitude for the wave for n=2 is zero in the middle of the box where x = a/2. If we insert a/2 into the equation for Ψ then Ψ = A sin(nπ2a/a)= A sin(nπ) = 0 because it is the property of a sinus function to be 0 at an integer number multiple of π. We could also insert other values for x and n into the wave function, and would get the expected amplitude. This shows that the wave function correctly represents the standing waves the electron can adopt.

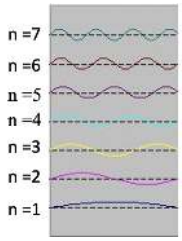


Figure 1.2.10 Standing waves corresponding to the wave function for different quantum numbers n.

We are still not quite finished with the wave function because we have not determined the parameter A in front of the sinus term. To obtain it we need to consider a third boundary condition (Eq. 1.2.8).

$$\int_0^a \Psi^2 dx = 1$$

Equation 1.2.8 Boundary condition 3.

It says that the integral of the square of the wave function over the length of the box must be equal to one. We can understand this boundary condition when we consider that the square of the wave function represents the probability to find the electron at a particular position in the box. The value the square of Ψ adopts at a position x within the box represents the probability to find the electron at this position when we consider the electron as a particle. This is called the Born interpretation of the wave function, named after the German physicist Max Born.

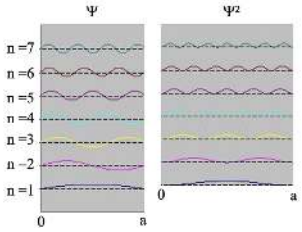


Figure 1.2.11 Standing waves corresponding to the wave function and its square.

Because the probability to find the electron anywhere in the box must be 100%, the integral of the square of the wave function over the entire box must be 100% or 1. One can show, and we omit the necessary mathematical steps for clarity here, that the boundary condition is only fulfilled when A is equal to the square root of 2/a. The final wave function is then psi is equal to 2/a sin(nπx/a). The factor square root of 2/a is called the normalization constant of the wave function because it adjusts the amplitude of the wave function so that the probability to find the electron anywhere in the box is 100%.

The Schrödinger Equation for the H Atom

Let us now go from an electron in a 1-dimensional box to the electron in the hydrogen atom. What is similar and what is different between these two cases. A similarity is that the electron is confined in an atom just like the electron is confined in the 1D box. Thus, like in the 1-dimensional box the electron should behave like a standing wave. While in the one-dimensional box there is only one coordinate to consider, there are three coordinates to consider for the electron in the atom. This is because an atom is spherical and thus three coordinates x, y, and z are necessary to describe a position within the atom. A second major difference is that the potential energy of the electron is zero at any position within the box, while it is not zero in the hydrogen atom. This is because in an atom there are attractive Coulomb forces between the nucleus and the electron. The further away the electron is from the nucleus the higher its potential energy. This is because it takes energy to pull the electron away from the nucleus.



Figure 1.2.12 Erwin Schrödinger (1887-1961), Nobel Prize 1933 (Attribution: Nobel foundation [Public domain] commons.wikimedia.org/wiki/F...ger_(1933).jpg)

We therefore need to modify the Schrödinger equation that we used previously for the one-dimensional box the following way. Firstly, we need to expand the operator for the kinetic energy from one to three dimensions and introduce the coordinates y and z in addition to x. Secondly, we have to add an operator for the potential energy to the equation. The potential energy is the Coulomb energy between the proton and the electron. It is similar to the term we previously used for the calculation of the potential energy of the electron in the Bohr model. Instead of the radius r we use now the square root of the sum of the square of the three coordinates x, y, and z, to indicate the Coulomb energy of the electron at any position within the atom. Our wave function will now be a function of three coordinates x, y, and z. This means our wave function will now be three-dimensional and represent three-dimensional standing waves. Three-dimensional waves are harder to imagine compared to 1-dimensional ones, but have the same properties, which are that the position of the crests, troughs, and nodes does not move.

$$\left[\left(\frac{d^2}{dx^2}+\frac{d^2}{dy^2}+\frac{d^2}{dz^2}\right)\frac{-h^2}{8\pi^2 m}+\frac{e^2}{4\pi\varepsilon_0\sqrt{x^2+y^2+z^2}}\right]\Psi(x,y,z)=E\,\Psi(x,y,z)$$

Operator for kinetic energy + Operator for potential energy (Coulomb energy)

Equation 1.2.9 Schrödinger equation for the H atom.

In order to get the wave functions for the electron we need to solve the Schrödinger equation for the hydrogen atom. To do so, we need to think about the boundary conditions for the wave function. One condition is that the square of the wave function approaches zero when we go very far from the nucleus, and r, the distance from the nucleus approaches infinite. Secondly, like in the one-dimensional box, the integral over the square of the wave function must be one. This is because the probability to find the electron somewhere in the atom must be 100%. Thirdly, it would be sensible to assume that the wave function must be continuously differentiable and single valued (Fig. 1.2.13).

Boundary conditions for ψ:
$\Psi^2 = 0$ for $r \rightarrow \infty$
$\int \Psi^2 dr = 1$
-continuously differentiable and single valued

Figure 1.2.13 Boundary conditions for the wave function of the electron in the hydrogen atom.

The Spherical Polar Coordinate System

The mathematical process to solve the Schrödinger equation is beyond the scope of this course and you are referred to Physical Chemistry classes and textbooks for the details. We shall only provide an brief outline of the process here. It is mathematically simpler to solve the Schrödinger equation in spherical polar coordinates instead of cartesian coordinates. Therefore, we obtain the solutions of the Schrödinger equation, the wavefunctions, in polar coordinates. The position of a point is specified by three numbers: the *radial distance* of that point from a fixed origin, its *polar angle* measured from a fixed zenith direction, and the *azimuthal angle* of its orthogonal projection on a reference plane that passes through the origin and is orthogonal to the zenith, measured from a fixed reference direction on that plane (Fig. 1.2.14).

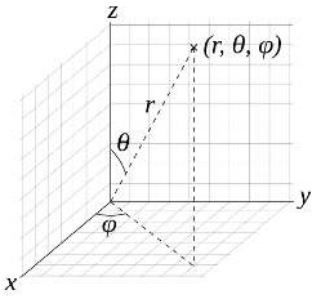


Figure 1.2.14 Illustration of the spherical polar coordinate system.

Solutions of the Schrödinger Equation

The wavefunction is then a function of r, θ and φ, in particular it is a product of a radial wave function which is function of r, a colatitude wave function, which is a function of θ, and an azimuthal wave function which is a function of φ (Eq. 1.2.10). You can see the explicit forms of the radial, colatitude, and azimuthal functions in Fig. 1.2.15.

$$\Psi(r,\theta,\phi) = R(r) \times \Theta(\theta) \times \Phi(\phi)$$

Equation 1.2.10 The wave function for the electron in the H atom as a function of r, θ and φ

Radial wave function ⟶ $R_{n,l} = r^l L_{n,l} e^{-r/na_0}$

Colatitude wave function ⟶ $\Theta(\theta) = (-1)^m \sqrt{\frac{2l+1}{2\pi}\frac{(l-m)!}{(l+m)!}} P_l^m(\cos\theta).$

Azimuthal equation ⟶ $\Phi(\phi) = \frac{1}{\sqrt{2\pi}} e^{im\phi}.$

Figure 1.2.15 Explicit forms of the radial, colatitude and azimuthal functions

We do not need to understand all details here, but need to realize that these wavefunctions are functions of quantum numbers. In contrast to the electron in the one-dimensional box not only one, but three quantum numbers need to be considered. Beyond the quantum number n, which is the called the principal quantum number, there is also a so-called orbital quantum number l, and a magnetic quantum number m. The quantum number n only occurs in the radial wave function, the quantum number l only occurs in the radial and colatitude function, and the quantum number m only occurs in the colatitude and the azimuthal part of the wave function. The values the orbital quantum number l can adopt depends on n, it can be between 0 and n-1 for a given quantum number n. The magnetic quantum number m depends on the quantum number l, and can run from –l to +l. So, for example when n is equal to 2, l can vary between 0 and 1, and for l equal to 2, m can adopt any value between -2 and 2, namely -2,-1, 0, +1, and +2 (Fig. 1.2.16).

Principal quantum number: n
Orbital quantum number: l (l = 0.....n-1)
Magnetic quantum number m (m = -l.....+l)

Figure 1.2.16 The quantum numbers of the wave function of the H atom.

These wave functions have a particular name in chemistry. They are called orbitals. One can understand an orbital as the three-dimensional wave function that describes the electron in an atom as a standing wave. Thus, an orbital is a state the electron can adopt, and when we say that an electron is in a particular orbital we mean that the electron is in a particular state.

The spin quantum number s

Within an orbital an electron can adopt two different spins described by the spin quantum number s. This quantum number is not a result of the Schrödinger equation, but was found experimentally. The spin quantum number s can adopt two values: +1/2 and -1/2. We say an electron is spin up when s = +1/2, and spin down when s = -1/2.

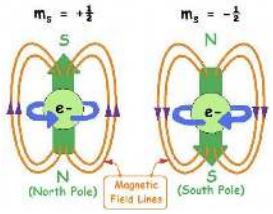


Figure 1.2.17 Electron spin (Attribution: Chemlibretexts.org chem.libretexts.org/@api/dek...jpg?revision=1, CC BY-NC-SA 3.0)

The spin quantum number is understood most easily when you view the electron as a particle rotating around its own axis. A counter-clockwise rotation would be associated with s=+1/2, a clockwise rotation would be associated with s=-1/2. The rotation produces a magnetic field with the direction of the field lines depending on the direction of rotation.

The 1s Orbital

Let us now insert the quantum numbers into the general form of the wave function for the electron in the hydrogen atom, and calculate their explicit mathematical forms. Let us start with the smallest possible numbers. When we insert n=1, l=0, and m=0 we get the wave function for the 1s orbital (Eq. 1.2.11).

$$\Psi_{1s} = \underset{\frac{1}{\sqrt{2\pi}}}{\Phi(\phi)} \times \underset{\frac{1}{\sqrt{2}}}{\Theta(\theta)} \times \underset{\frac{2}{a_0^{3/2}} e^{-r/a_0}}{R(r)}$$

Equation 1.2.11 Wave function for the 1s orbital

You can see that the colatitude and azimuthal parts of the wave functions, together also called the angular part of the wave function, are simple numbers, namely one over the square root of two pi, and one over the square root of two respectively. The angles theta and phi do not appear and that means that the wave function is angle-independent. This implies that the orbital has a spherical shape.

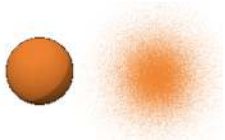


Figure 1.2.18 Common depictions of the 1s orbital

The radial part of the wave function has an exponential term e to the power of –r over a_0. The number ***e*** is the Euler number, that is the base of the natural logarithm. It is approximately equal to 2.71828. a_0 is the Bohr radius, which is the distance of the electron from the proton for the electron on its first orbit according to the Bohr atom model. We calculated it previously, and it was 5.29 x 10^{-11}m. r is the distance from the nucleus. This exponential term has a constant in front of it which is 1 over the Bohr radius to the power of three over two. Because the radial part of the wave function is e to the power of –r, the amplitude of the radial part of the wave function declines exponentially with increasing distance r from the nucleus. This is true for the entire wave function because the angular parts of the wave function are just simple numbers. You can see the exponential decline of the amplitude of the wave function as a function of the radius r in units of the Bohr radius a_0 in the graph below (Fig. 1.2.19).

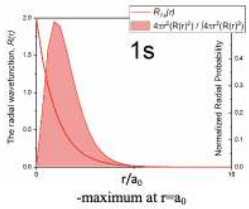


Figure 1.2.19 Amplitude of the radial wave function R of the 1s orbital as a function of the radius r in units of the Bohr radius a_0, and radial probability function (Attribution: Chemlibretexts chem.libretexts.org/@api/deki/files/205599/clipboard_e63775e352caeb1d434fe16aa3fa22d21.png?revision=1, http://creativecommons.org/licenses/by-nc-sa/3.0/us/)

This means that the 1s orbital must be a spherical orbital with its amplitude exponentially declining with increasing distance from the nucleus. This can be graphically depicted via a density of points around the nucleus (Fig. 1.2.18). A higher density of points means higher amplitude and a lower density of points means smaller amplitude. The fact that the amplitude is the highest closest to the nucleus means that the probability to find the electron in a particular point in space is the highest closest to the nucleus. This is because the square of the wave function for the 1s orbital represents the probability to find the electron at a particular point in space. However, the probability to find the electron at a certain distance from the nucleus is not the highest closest to the nucleus. This is because the probability to find the electron at a certain distance from the nucleus is the probability to find the electron at a particular point in space times the number of points in space that have that particular distance. The number of points in space that have a particular distance r from the nucleus is related to the surface of a sphere with the a radius r. The surface of a sphere A is given by the formula $A=4\pi r^2$. Thus, the probability to find the electron at a particular distance r from the nucleus is equal to the surface of a sphere with the radius r times the radial wave function square. This defines the radial probability function $R_P=4\pi r^2R^2$.

The graph for the radial probability function is depicted in Figure 1.2.19. You can see that it is zero when r=0 which is due to the r^2 term which becomes zero at r = 0. At small r values the $4\pi r^2$ term dominates the overall function and the probability to find the electron increases with r. However, because the exponential term of the radial function becomes more and more

significant at larger r values, the radial probability function goes through a maximum and then declines. At distances r approaching infinite the function approaches zero. The maximum of the curve represents the distance at which it is most likely to find the electron. Interestingly, it is equal to the Bohr radius r. That means that Bohr was not so wrong after all. However, he was wrong in the sense that he viewed the electron as a classical particle being only at that radius. Instead, the electron, due to its wave properties, it is not only at the Bohr radius r_0, but most likely we can find it there.

The result that the probability to find the electron at a specific point in space is the greatest at the nucleus does away with the question of why the H atom does not collapse. Because the amplitude of the wave function is the greatest closest to the nucleus we can actually say in a way that the atom is collapsed. Nonetheless, the atom is mostly empty space because of the delocalization of the wave function that describes the state of the electron. The delocalization of the electron due to its wave properties also makes the question of the size of an orbital non-trivial. The wave function approaches zero only for r approaching infinite, but never becomes zero. This means that to account for all electron density the orbital would be infinitely large. This however would not be a sensible definition. The commonly accepted definition is that the size of an orbital is defined by the space that contains 90% of its electron density. We can depict orbitals according to this definition. For the case of the 1s orbital the radius of the sphere that represents the 1s orbital is chosen so that the probability to find the electron within a sphere of that radius is 90%.

The 2s Orbital

Inserting n=2, l=0, and m=0 into the general wave function gives us the wave function for the 2s orbital (Eq. 1.2.12).

$$\Psi_{2s} = \underset{\frac{1}{\sqrt{2\pi}}}{\Phi(\phi)} \times \underset{\frac{1}{\sqrt{2}}}{\Theta(\theta)} \times \underset{\frac{1}{2\sqrt{2}\,a_0^{3/2}}\left[2-\frac{r}{a_0}\right]e^{-r/2a_0}}{R(r)}$$

Equation 1.2.12 Wave function for the 2s orbital

Like in the case of the 1s orbital, the angular parts of the wave function are only simple numbers. Thus, the 2s orbital is also a spherical orbital. Like in the 1s orbital, the radial part of the wave function has an exponential term of the type e^{-r} and a simple coefficient. However, there is an additional term $2\text{-}r/a_0$. Due to the exponential term, the amplitude of the wave function declines exponentially with r. However, because of the term $2\text{-}r/a_0$ the wave function becomes negative, and then approaches 0. The radius at which the wave function changes its algebraic sign is called a spherical node. The node is spherical because it describes the surface is a sphere. On the surface of this sphere the amplitude of the wave function is zero. The radius at which the wave function changes its algebraic sign is $2a_0$. This becomes clear when we consider that the term $2\text{-}r/a_0$ becomes zero when $r=2a_0$ because $2\text{-}2a_0/a_0=0$. When this term is zero then the entire wave function becomes zero. We can illustrate the change of the algebraic sign in the 2s orbital using colors as shown below (Fig. 1.2.20).

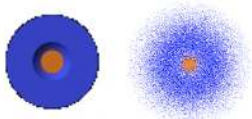


Figure 1.2.20 Common depictions of the 2s orbital.

The orange sphere indicates the space in which the amplitude of the 2s orbital is positive, and the blue area indicates where it is negative. The interface area where the color changes represents the node. By multiplying the square of the radial wave function R with $4\pi r^2$ we obtain the radial probability function for the 2s orbital (Fig. 1.2.21).

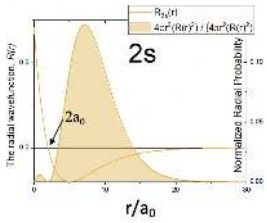


Figure 1.2.21 Amplitude of the wave function of the 2s orbital as a function of the radius r in units of the Bohr radius a_0 a well as the radial probability function (Attribution: Chemlibretexts https://chem.libretexts.org/@api/dek...png?revision=1, http://creativecommons.org/licenses/by-nc-sa/3.0/us/)

You can see that similar to the 1s orbital, the probability to find the electron on a radius closest to the nucleus is 0. However, unlike the 1s orbital there are now two maxima instead of only one. This second maximum is imposed by the spherical node of the 2s orbital. The second maximum is larger than the first one. Generally, the probability to find the electron further away from the nucleus is greater compared to the 1s orbital. That means that the 2s orbital is larger than the 1s orbital. This reflects the general trend that orbitals with a higher quantum number n tend to be larger and the probability to find the electron further away from the nucleus is greater.

The 3s Orbital

Let us look at one more s orbital, the 3s orbital (Eq. 1.2.13).

$$\Psi_{3s} = \underset{\frac{1}{\sqrt{2\pi}}}{\Phi(\phi)} \times \underset{\frac{1}{\sqrt{2}}}{\Theta(\theta)} \times \underset{\frac{2}{81\sqrt{3}\,a_0^{3/2}}\left[27-18\frac{r}{a_0}+2\frac{r^2}{a_0^2}\right]e^{-r/3a_0}}{R(r)}$$

Equation 1.2.13 Wave function for the 3s orbital.

The angular parts of the wave function for the 3s orbital are again simple numbers, which implies that the orbital is again spherical. Generally all s orbitals are spherical.

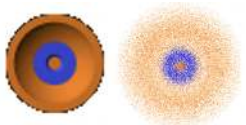


Figure 1.2.22 Common depictions of the 3s orbital

The radial part of the wave function can be divided into the parts. The first part is a simple number, then there is the term $27\text{-}18r/a_0+ 2r^2/a_0^{2,}$ and the exponential term $e^{-r/3a_0}$. Because of the exponential part the amplitude of the wave function declines exponentially with increasing r. However, then the wave function becomes negative, goes through a minimum, then becomes positive again, goes through a small maximum, and finally approaches zero. The fact that the wave function changes its algebraic sign two times means that the 3s orbital has two spherical nodes. These spherical nodes are due to the second term which is a square function of the type $ax^2 + bx + c$, whereby in this case $a = 2/a_0^2$, $b = -18/a_0$ and $c=27$. When this term becomes

zero the entire wave function becomes zero. Square functions have two solutions according the formula $x=(-b\pm\sqrt{(b^2-4ac)})/2a$. The solutions give the radii for the two spherical nodes of the 3s orbital. We omit the exact calculation of the radii for briefness and clarity reasons here. You may calculate them as a homework.

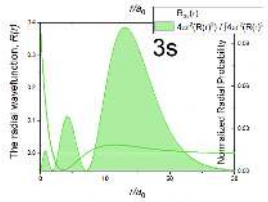


Figure 1.2.23 Amplitude of the wave function of the 3s orbital as a function of the radius r in units of the Bohr radius a_0 as well as radial probability function. (Attribution: Chemlibretexts https://chem.libretexts.org/@api/dek...png?revision=1, http://creativecommons.org/licenses/by-nc-sa/3.0/us/)

Because of the two spherical nodes, the radial probability function R_p has three maxima. A very small one close to the nucleus, are larger one further away from the nucleus, and the largest one at even greater distance from the nucleus. Overall, the 3s orbital is larger than the 2s orbital confirming the general trend that s orbitals increase in size with increasing quantum number n.

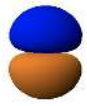
The $2p_z$ Orbital

Now let us look at orbitals in which the orbital quantum number l is larger than 0. When l is equal to 1, then n must be at least 2. An orbital with n=2 and l=1 is a 2p orbital. Overall, three 2p orbitals must exist because for l=1, the magnetic quantum number m can adopt three values: -1, 0, and +1. The orbital with m=0 is called the $2p_z$ orbital. Let us look at the mathematical form of this wave function (Eq. 1.2.14).

$$\Psi_{2p_z} = \underbrace{\frac{1}{\sqrt{2\pi}}}_{\Phi(\phi)} \times \underbrace{\frac{\sqrt{6}}{2}\cos\theta}_{\Theta(\theta)} \times \underbrace{\frac{1}{2\sqrt{6}\,a_0^{3/2}}\frac{r}{a_0}\,e^{-r/2a_0}}_{R(r)}$$

Equation 1.2.14 Wave function for the $2p_z$ orbital

Analyzing the angular parts of the wave function shows that while the azimuthal part is still a simple number, the colatitude part is not, it is a function of θ. This means that the amplitude of the wave function is now angle dependent, which implies that the orbital cannot be spherical. Instead the 2p orbital has the shape of a dumbbell which is oriented along the z-axis. One lobe is above the xy plane, and the other lobe is below the xy plane. These two different lobes have a different algebraic sign, indicated by different colors (Fig. 1.2.24).



$2p_z$ (l=1, m=0)
planar node (xy plane)

Figure 1.2.24 Common depiction for the $2p_z$ orbital

Within the xy plane the amplitude of the wave function is zero. The xy plane represents a so-called planar node. A planar node is a type of an angular node. The name angular node is because it is due to the fact that the angular part of the wave function is not a simple number, but a function of an angle, in this case θ. We can show that the angular part of the wave function produces the planar node in the xy plane when we convert it from spherical into Cartesian coordinates (Eq. 1.2.15).

$$\Theta\Phi(x,y,z) = \frac{1}{2}\sqrt{\frac{3z}{\pi r}} \quad \text{is 0 for } z = 0$$

Equation 1.2.15 Angular part of the wave function of $2p_z$ in cartesian coordinates. The function becomes zero when z=0.

We can see that the angular part of the wave function is only a function of z. We can also see, that the angular part of the wave function becomes zero when z=0. When the angular part of the wave function becomes zero, then the wave function of the entire orbital becomes zero. Z is zero only in the xy plane, and this explains why the xy plane is a planar node.

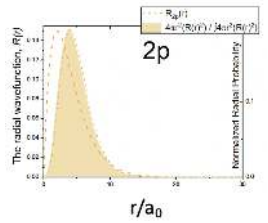


Figure 1.2.25 Amplitude of the wave function of the $2p_z$ orbital as a function of the radius r in units of the Bohr radius a_0 as well as radial probability function. (Attribution: Chemlibretexts https://chem.libretexts.org/@api/dek...png?revision=1, http://creativecommons.org/licenses/by-nc-sa/3.0/us/)

Now let us look at the radial part of the wave function. It is made of three terms: a simple constant, the term r/a_0, and the exponential term $e^{-r/2a_0}$. Because of the term r/a_0 the radial part of the wave function is zero at r=0. This means that it is very unlikely to find the electron at a point in space directly at the nucleus. This behavior is opposite to s orbitals. Because the r/a_0 term dominates the behavior of the wave function at small r value, the amplitude first increases. However, at larger r values the exponential term becomes more an more important which forces the amplitude of the radial function through a maximum, after which it declines and approaches zero. The radial wave function never changes algebraic sign. Therefore, the $2p_z$ orbital does not have a spherical node. The radial probability function has a similar shape compared to the radial function. It is zero at r=0 and goes through a maximum before it declines again and approaches zero (Figure 1.2.25).

The $2p_x$ and $2p_y$ Orbital

The $2p_x$ and the $2p_y$ orbitals are obtained when the quantum numbers m are 1, and -1, respectively.

$$\Psi_{2p_{x/y}} = \underbrace{\frac{1}{\sqrt{2\pi}}e^{\pm i\phi}}_{\Phi(\phi)} \times \underbrace{\frac{\sqrt{3}}{2}\sin\theta}_{\Theta(\theta)} \times \underbrace{\frac{1}{2\sqrt{6}\,a_0^{3/2}}\frac{r}{a_0}\,e^{-r/2a_0}}_{R(r)}$$

Equation 1.2.16 Wave function for the $2p_x$ and $2p_y$ orbital

They have the same shape as the $2p_z$ orbital, but their orientation is different. The dumbbell of the $2p_x$ orbital is oriented along the x-axis, and that of the $2p_y$ orbital is oriented along the y-axis.

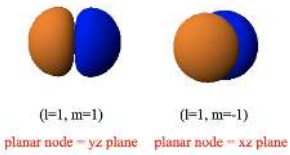


Figure 1.2.26 Common depictions for the $2p_x$ and $2p_y$ orbitals, respectively

This is because the $2p_x$ orbital has a planar node in the yz plane, and the $2p_y$ orbital has a planar node in the xz plane. The planar nodes are due to the angular part of the wave functions of these orbitals.

$$\Theta\Phi(x,y,z) = \frac{1}{2}\sqrt{\frac{3x}{\pi r}} \text{ is 0 for x = 0}$$
$$\Theta\Phi(x,y,z) = \frac{1}{2}\sqrt{\frac{3y}{\pi r}} \text{ is 0 for y = 0}$$

Equation 1.2.17 Angular part of the wave function of $2p_x$ and $2p_y$, respectively. The wave functions become 0 for x=0 and y=0, respectively.

As one can see, the angular parts of the wave function contain both the angles θ and Φ. When converted into Cartesian coordinates (Eq. 1.2.17) one can see that the angular function of the $2p_x$ orbital is only a function of x, and the angular function of the $2p_y$ orbital is only a function of y. The functions become zero for x=0 and y=0, respectively. X is zero only in the yz plane, and y is zero only in the xz plane, hence these nodes are planar nodes. The radial wave function is exactly the same as for the $2p_z$ orbital.

The 3p Orbitals

Now let us look at the 3p orbitals. In a 3p orbital the quantum number n=2 and l=1. Like for the case of the 2p orbitals there are three p orbitals because the magnetic quantum number m can adopt the values -1, 0, and +1. The wave function of the $3p_z$ orbital is shown below (Eq. 1.2.18).

$$\begin{array}{lccc} & \Phi(\phi) & \Theta(\theta) & R(r) \\ \Psi\, 3p_z = & \frac{1}{\sqrt{2\pi}} & \frac{\sqrt{6}}{2}\cos\theta & \frac{4}{81\sqrt{6}\,a_0^{3/2}}\left[6 - \frac{r}{a_0}\right]\frac{r}{a_0}e^{-r/3a_0} \end{array}$$

Equation 1.2.18 Wave function for the $3p_z$ orbital

One can see that the angular part of the wave function is exactly the same as for the $2p_z$ orbital. This means that like in the $2p_z$ orbital there must be a planar node in the xy plane. When you look at the radial part of the wave function you can see that it is composed of four terms, a simple constant, a term $6\text{-}r/a_0$, the term r/a_0, and the exponential term $e^{-r/3a_0}$. Because of the term r/a_0 the wave function becomes zero at r=0. Because of the term $6\text{-}r/a_0$ the wave function has a spherical node. This is because when $6\text{-}r/a_0=0$ the entire wave function becomes 0. We can determine the radius at which the wave function becomes zero by solving the equation $6\text{-}r/a_0=0$ for r, which gives $r=6a_0$. Overall, the radial function is zero at r=0, goes through a maximum, changes its algebraic sign at the spherical node at $r=6a_0$, has a minimum, and then approaches zero for very large distances r (Fig. 1.2.28).

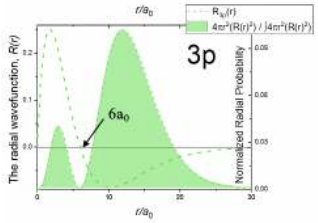


Figure 1.2.28 Amplitude of the wave function of the $3p_z$ orbital as a function of the radius r in units of the Bohr radius a_0 as well as radial probability function

The radial probability function has two maxima, a small one close to the nucleus, and a larger one further away from the nucleus. Overall the radial probability function is further away from the nucleus compared to the 2p orbitals, which implies that the 3p orbital is larger.

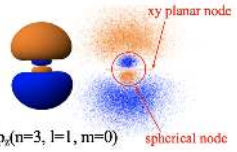


Figure 1.2.29 Common depiction for the $3p_z$ orbital

The overall shape of the $3p_z$ orbital is determined by the both the spherical and the planar node (Fig.1.2.29). Due to the planar node in the xy plane it has a dumbbell shape and is oriented in z direction. However, because of the spherical node the algebraic sign of the wave function changes within the two lobes of the dumbbell. Finally let us consider the $3p_x$ and the $3p_y$ orbitals. They would have the same shape as the $3p_z$ orbital, but they would be oriented in the x and the y direction respectively. We could also think about what would happen to the p orbitals if we increased the quantum number n further. In this case the dumbbell shape would remain, but additional spherical nodes would be introduced. A 4p orbital would have two spherical nodes, a 5p orbital three spherical nodes, and so on. The size of these p orbitals would also increase with the quantum number n.

The $3d_{z^2}$ Orbital

Now let us consider the orbitals with the orbital quantum number l=2. These orbitals are so-called d-orbitals. Because the principal quantum number n always has to be at least one integer number larger than the quantum l, the d orbitals with the smallest quantum number n are the 3d orbitals. For each quantum number n there must be five d orbitals because for l=2 the magnetic quantum number m can adopt the values -2, -1, 0, -1, +1, and +2. Let us first look at the 3d orbital with m=0. This orbital is called the $3d_{z^2}$ orbital. Its wave function is shown below (Eq. 1.2.19).

$$\Psi_{3d_{z^2}} = \underbrace{\frac{1}{4}\sqrt{\frac{5}{\pi}}(3\cos^2\theta - 1)}_{\Phi(\phi)\,\Theta(\theta)} \quad \underbrace{\frac{1}{81\sqrt{15}}\left[\frac{2}{a_0}\right]^{3/2}\frac{r^2}{a_0^2}e^{\frac{-r}{3a_0}}}_{R(r)}$$

Equation 1.2.19 Wave function for the $3d_{z^2}$ orbital

You can see that the radial function is a product of three terms: a constant, a term r^2/a_0^2, and the exponential term $e^{-r/3a_0}$. The exponential term is the same as for the 3p orbitals. Because of the term r^2/a_0^2 the amplitude of the wave function is 0 at r=0. The amplitude then increases with r, goes through a maximum, and then approaches zero. This means that the wave function never changes its algebraic sign, and therefore it does not have spherical nodes. The radial probability function has a similar shape compared to the radial function (Figure 1.2.30). The electron probability is somewhat further away from the nucleus compared to the 3p orbitals, meaning that the 3d orbital is somewhat larger than the 3p orbital.

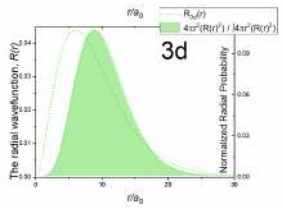


Figure 1.2.30 Amplitude of the wave function of the $3d_{z^2}$ orbital as a function of the radius r in units of the Bohr radius a_0 as well as radial probability function

You can see that the angular part of the wave function is a function of θ which means that the orbital will be non-spherical and there will be at least one angular node. In this case the angular nodes are two conical nodes. These nodes describe two cones that give the orbital its characteristic shape. It is a doughnut ring in the xy plane around a dumbbell pointing into z direction. The dumbbell and the doughnut have different algebraic signs indicated by different colors (Figure 1.2.31). Note that in contrast to the p orbitals the two lobes of the dumbbell have the same algebraic sign.

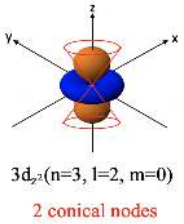


Figure 1.2.31 Common depiction for the $3d_{z^2}$ orbital with conical nodes (red).

We can understand that the $3d_{z^2}$ orbital has two conical nodes when we convert the angular part of the wave function into Cartesian coordinates (Eq. 1.2.20).

$$\Theta\Phi(x,y,z) = \frac{1}{4}\sqrt{\frac{5}{\pi}}\frac{(2z^2 - x^2 - y^2)}{r^2}$$

Equation 1.2.20 Angular part of the wave function of the $3d_{z^2}$ orbital in cartesian coordinates.

You can see that it is a function of $2z^2$-x^2-y^2. This is the mathematical form of cones. The angular part of the wave function becomes 0 when $2z^2=x^2$-y^2 which is true on the surface of two cones, one above the xy plane and one below the xy plane. The name of the $3d_{z^2}$ orbital is because it is a function of z^2.

The $3d_{x^2-y^2}$ Orbital

Let us next look at the $3d_{x^2-y^2}$ orbital (Eq. 1.2.21).

$$\Psi_{3d_{x^2-y^2}} = \underbrace{\frac{1}{4}\sqrt{\frac{15}{\pi}}\sin^2\theta\cos^2 2\phi}_{\Phi(\phi)\,\Theta(\theta)} \quad \underbrace{\frac{1}{81\sqrt{15}}\left[\frac{2}{a_0}\right]^{3/2}\frac{r^2}{a_0^2}e^{\frac{-r}{3a_0}}}_{R(r)}$$

Equation 1.2.21 Wave function for the $3d_{x^2-y^2}$ orbital

The radial part of the wave function is the same as the one for the $3d_{z^2}$ orbital. The angular part of the wave function is both a function of θ and Φ and thus there are angular nodes to expect. We can find them again when we convert the angular part of the wave function from spherical to Cartesian coordinates.

$$\Theta\Phi(x,y,z) = \frac{1}{4}\sqrt{\frac{15}{\pi}}\frac{(x^2 - y^2)}{r^2}$$

Equation 1.2.22 Angular part of the wave function of the $3d_{x^2-y^2}$ orbital in cartesian coordinates.

You can see that the angular function is a function of x^2-y^2. The function becomes zero when x^2-y^2=0. This is the case when x=y or x=-y. X is equal to y on two lines that bisect the 90 degree angle between the x and the y axis. The coordinate z is completely variable. Thus, overall, the wave function becomes zero on two planes that stand perpendicular to the xy plane and bisect the 90 degree angle between the x and the y axis. These two planes are therefore the two planar nodes of the orbital.

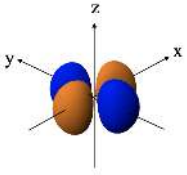


Figure 1.2.32 Common depiction of the $3d_{x^2-y^2}$ orbital

Because of the two planar nodes the orbital has four lobes lying on the x and the y axis, respectively. Lobes lying on the x-axis have the opposite algebraic sign compared to those lying on the y-axis. The name of the dx^2-y^2 orbital is because it is a function of x^2-y^2.

The $3d_{xy}$, $3d_{yz}$ and $3d_{xz}$ orbitals

The remaining d orbitals are the $3d_{yz}$, the $3d_{xz}$, and the $3d_{xy}$. The radial function of these orbitals is just like the ones we previously discussed. The angular part of the wave functions is shown here directly in Cartesian coordinates. The d_{yz} orbital is a function of yz. The function becomes zero when either y=0 or z=0. y is zero in the xz plane, and z is zero in the xy plane. Therefore these planes are planar nodes of the orbital. Because of these nodes, the orbital has four lobes which lie in the yz plane whereby the lobes are in between the y and the z axes. Note that adjacent lobes have opposite algebraic sign, and opposite lobes have the same algebraic sign.

$3d_{yz}$  $\Theta\Phi(x,y,z)=\frac{1}{2}\sqrt{\frac{15}{\pi}}\frac{yz}{r^2}$

Figure 1.2.33 Angular wave function for the $3d_{yz}$ orbital, and the common depiction for this orbital

The $3d_{xz}$ orbital is a function of xz, and thus the function becomes zero with x=0 or z=0. This defines that yz and the xy planes as the two planar nodes. The orbital has the same shape as the $3d_{yz}$, except that the four lobes lie within the xz plane instead the yz plane.

$3d_{xz}$  $\Theta\Phi(x,y,z)=\frac{1}{2}\sqrt{\frac{15}{\pi}}\frac{xz}{r^2}$

Figure 1.2.34 Angular Wave function for the $3d_{xz}$ orbital, and the common depiction for this orbital

The $3d_{xy}$-orbital is a function of xy, and thus its wave function becomes zero at x=0 or y=0. Therefore, the xz and the yz planes are the planar nodes and the orbital has four lobes in the xy plane in between the x and the y axis. Note that the $3d_{xy}$ and the $3d_{x^2-y^2}$ look very similar but are different. The difference is that the $3d_{x^2-y^2}$ orbital has its lobes on the x and the y axis, while the $3d_{xy}$ orbital has the lobes in between the x and the y axis. One can also say that the $3d_{x^2-y^2}$ orbital is rotated by 45 degree around z with respect to the $3d_{xy}$ orbital.

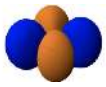
$3d_{xy}$  $\Theta\Phi(x,y,z)=\frac{1}{4}\sqrt{\frac{15}{\pi}}\frac{xy}{r^2}$

Figure 1.2.35 Angular wave function for the $3d_{xy}$ orbital, and the common depiction for this orbital

Rules for Angular and Spherical Nodes

Of course, we could now discuss the size and shape of many other orbitals such a the 4d orbitals or the 4f orbitals, but this will be beyond scope. Instead, let us think about if there are general rules that allow the prediction of the number of spherical and angular nodes in an orbital. The number of radial nodes is always equal to n-l-1, the number of angular nodes is equal to l, and the total number of nodes is always n-1. This means that the number of nodes increases with the quantum number n. If we increase the quantum number l for a given quantum number n, then we replace spherical nodes by angular nodes. This is summarized in Figure 1.2.36.

- $R(r) = 0 \rightarrow$ spherical node (spherical nodal surface)
- Number of radial nodes is n - l – 1.
- $\Phi(\phi)\ \Theta(\theta) = 0 \rightarrow$ angular node
  (This can be a planar or conical nodal surface)
- Number of spherical nodes is equal to the orbital quantum number l .
- Total number of nodes is always n-l

Figure 1.2.36 Rules for angular and spherical nodes

The Orbital Energies for the H Atom

The Schrödinger equation does not only allow to calculate the orbitals of the hydrogen atom, but also their energies. The energies of Bohr and Schrödinger model match: $E = \text{constant}/n^2$: This means that orbitals with the same quantum number n have the same energies. The energies are **not** a function of the quantum numbers l and m. The energies are negative because they are binding energies. In other words: Adding an electron to a proton is an exothermic process. The binding energy for the energy increases as the orbital energy decreases (Fig. 1.2.37).

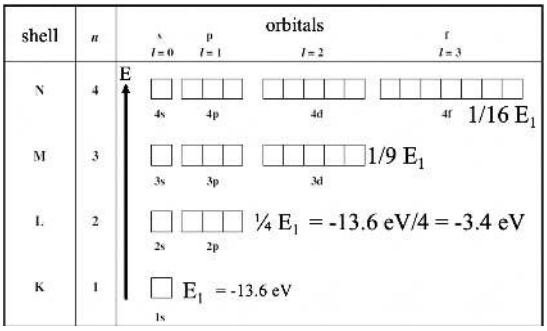


Figure 1.2.37 Orbital energies from the 1s orbital to 4f orbital. K, L, M, N indicate the shells associated with a quantum number n.

For the 1s orbital of H the energy is -13.6 eV, the energy of the 2s and the 2p orbitals are ¼ of that, the energy of the 3s, 3p, and 3d orbitals are 1/9 of the energy of the 1s orbital and so forth. Note at ¼ and 1/9th of -13.6 eV is more than -13.6 eV due to the negative algebraic sign. The electron volt is a unit of energy. It is the amount of kinetic energy gained by a single unbound electron when it passes through an electrostatic potential difference of one volt, in vacuum.

$$1\ \text{eV} = 1.602176\ 53(14)\times10^{-19}\ \text{J}.$$

Equation 1.2.23 The electron volt to joule unit conversion.

In other words, it is equal to one volt (1 volt = 1 joule per coulomb) times the charge of a single electron (in coulombs). It is a very small unit of energy which is practical for orbital energy calculations because the orbital energies are very small (Eq. 1.2.23).

Multi-electron Atoms

Thus far we have only considered the orbitals for the hydrogen atom which contains only one electron. Can we also solve the Schrödinger equation for atoms that have more than one electron and get the exact energies of the orbitals? The answer is no, this mathematically not possible. The process is just already too complex even for only two electrons. The Schrödinger equation can only be solved for one electron systems. Therefore, the description of the atomic structure of all other atoms must work with approximations. Let us first consider the He atom. It has only one more electron than hydrogen. It is a useful approach to approximate multi-electron atoms as one-electron systems first, and then approximate the electron-electron interactions. Electron energies in an atom with more than one proton should follow the equation $E_n=-Z^2$x13.6 eV/n^2, whereby Z is the number of protons.

$$E_n = -\frac{Z^2\ 13.6\ eV}{n^2}$$

Equation 1.2.24 The orbital energies for atoms with more than one proton

The binding energy of the electron increases proportionally to the square of the number of protons because the attractive Coulomb forces that act on the negatively charged electrons increases with the number of positively charged protons in the nucleus. One can experimentally measure the orbital energies via ionization energies. The energy required to remove an electron in a particular orbital from the atom is equal to the binding energy for the electron in that orbital. Therefore the ionization energy IE = $-E_n$ (E_n = orbital energy). According to the Schrödinger model the orbital energy for a helium electron in a 1s orbital should be $E_{1s}=-(2^2\times13.6\ eV)/1^1$ =-54.4 eV (Eq. 1.2.25).

$$E_{1s} = -\frac{2^2\times13.6\ eV}{1^1} = -54.4\ eV$$

Equation 1.2.25 Energy for a helium electron in a 1s orbital.

However, the experimentally measured ionization energy of the electron is +24.6 eV, which means that the real orbital energy is -24.6 eV, and not -54.4 eV. On the other hand, the ionization of a He^+ ion is +54.4 eV which is exactly what we would expect. We can explain this phenomenon by the fact that the Schrödinger model works for a single electron only and must neglect electron interactions. In a He^+ ion there is only one electron, therefore the Schrödinger model correctly predicts the energy of the electron. However, in a helium atom there are two electrons, and the Schrödinger model cannot account for the electron-electron interactions. Therefore, it does not give the correct energy for the electrons in a Helium atom. The electron-electron interactions can be viewed as shielding effects. This means that the first electron shields part of the nuclear charge from the second electron. Therefore, the second electron experiences a reduced Coulomb force from the nucleus. Because of the reduced Coulomb force, the binding energy is smaller. It is reduced from -54.4 eV to -24.6 eV. It should be pointed out that the two electrons in the 1s orbital of the He atom are indistinguishable, that means they both have the reduced binding energy. The binding energy only increases to -54.4 eV after one of the two electrons has been removed.

The net positive charge from the nucleus after accounting for shielding effects is called the effective nuclear charge. For the helium atom the effective nuclear charge is 1.34. We can calculate the effective nuclear charge from the experimentally measured first ionization energy. Solving the equation for Z_{eff} gives Z_{eff}=1.34 (Eq. 1.2.26).

$$E = -\frac{Z_{eff}^2}{n^2}\times13.6\ eV = -24.6\ eV \quad \text{b/c } IE(He) = 24.6\ eV$$

$$Z_{eff} = \sqrt{n^2\times\frac{24.6\ eV}{13.6\ eV}} = \sqrt{1^2\times\frac{24.6\ eV}{13.6\ eV}} = 1.34$$

Equation 1.2.26 Calculation of Z_{eff} in the Helium atom from first ionization energies.

The Lithium Atom

Now let us go to the atom with three electrons, the lithium atom. Following the so-called Aufbau principle we would fill the first two electrons into the 1s orbital, because the 1s orbital is the orbital with the the lowest energy. However, the third electron does not fit into the 1s orbital because of the Pauli principle.



Figure 1.2.38 Wolfgang Pauli (1900-1958), Nobel prize 1945 (Attribution: Nobel foundation [Public domain], commons.wikimedia.org/wiki/File:Pauli.jpg, PD-US-expired)

The Pauli principle states that no two electrons in an atom can have the same four quantum numbers. For that reason an orbital cannot accommodate more than two electrons. Within an orbital two electrons must have different spin quantum numbers s. We can indicate this by writing the electrons as arrows pointing up and down into a square box which represents the orbital. The third electron of the lithium would need to go to the orbital with the next higher energy.

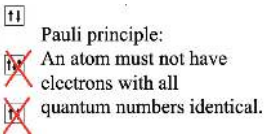
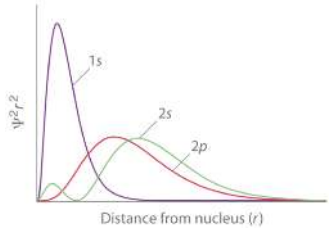


Figure 1.2.39 Illustration of the Pauli Principle

According to the Schrödinger model, the energy of an orbital is only a function of the quantum number n, and we would have two choices: The 2s and the 2p orbitals. Both of them would have the same energy. However, in the lithium atom the 2s orbital has a somewhat lower energy than the 2p orbital. This can again be explained by shielding effects. The 2s orbital penetrates the 1s orbital slightly better than the 2p orbitals. Because of that, the 1s orbital shields the nuclear charge from the nucleus less for the 2s orbital compared to the 2p orbitals. The ground state electron configuration, which is the atom electron configuration having the lowest energy, must therefore be $1s^2\ 2s^1$. We can see that the 2s orbital penetrates the 1s orbital slightly better than the 2p orbital from the graph for the radial probability functions of the orbitals shown in Figure 1.2.40.



Graph of radial probability functions of the 1s, 2s, and 2p orbitals (Attribut
es/Inorganic_Chemistry/Map%3A_Inorganic_Chemistry_(Miessler%2C_Fischer%2C_Tarr)/2%3A_Atomic_Structure/2.2%3A_The_Schr%C3%B6dinger_equation%2C_particle_in_a_box%2C_and_atomic_wave
censes/by-nc-sa/4.0/)

The second large maximum of the function of the 2s orbital is actually further away from the nucleus compared to the maximum associated with the 2p orbital. However, because the 2s orbital has a small second maximum very close to the nucleus, the 2s orbital overall penetrates the 1s orbital better, and therefore the shielding effect of the 1s orbital on the 2s orbital is smaller compared to the 2p orbitals.

Generally we can say, the smaller the quantum number l for a given quantum number n, the better the penetration ability of this orbital. Due to the better penetration ability, the shielding is less and thus the effective nuclear charge that acts on the electron in the orbital is higher. The higher effective nuclear charge leads to a lower energy of this orbital. For that reason the energy sequence of orbitals with the same quantum number n increases from s to p to d to f.

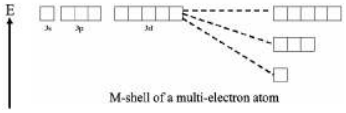


Figure 1.2.41 The energy sequence of orbitals with the quantum number n=3 in a multi-electron atom.

For example, a 3s orbital has a lower energy then a 3p orbital which has a lower energy than a 3d orbital (Fig. 1.2.41).

Slater's Rules

Because an orbital energy can be calculated from the effective nuclear charge, it would be useful if the effective nuclear charge could be somehow estimated by simple approximations.



Figure 1.2.42 John C. Slater (1900-1976) (Attribution: Biographical Memoirs, National Academy of Sciences, vol. 53. 1982., http://scarc.library.oregonstate.edu/coll/pauling/bond/pictures/portrait-slater.html)

The so-called Slater rules, named after their developer John C. Slater (Fig. 1.2.42), are a simple tool that give a good estimate for the effective nuclear charge of orbitals in multi-electron atoms. The Slater rules estimate a shielding constant σ that allows to calculate the effective nuclear charge Z_{eff} from the nuclear charge according to $Z_{eff}=Z-\sigma$.

The rules for the estimation of σ are the following. Firstly, we need to recognize that the rules for s and p electrons are slightly different than those for d and f electrons. This is because s and p electrons of the same quantum number n have somewhat higher penetration abilities compared to d and f electrons. For both groups the first step is the same. We write out the electron configuration of the atom according to their quantum numbers n and l as shown below (Fig. 1.2.43).

(1s) (2s, 2p) (3s, 3p) (3d) (4s, 4p) (4d) (4f) (5s, 5p)….

Figure 1.2.43 First step to calculate the shielding constant σ

Note that this order does not exactly reflect the order of energy. Electrons that have similar shielding effects are grouped together in parentheses. You can see that s and p orbitals of the same quantum number n build a group, all other orbitals are their own group.

To estimate the shielding constant for an s or a p orbital we can now apply the following rules:

a) Electrons to the right of the (ns, np) group contribute nothing to σ. This is because these electrons are further away from the nucleus than the electron of consideration.

b) Each of the other electrons in the same (ns, np) group contribute 0.35 to σ. These electrons are in the same shell as the electron of consideration, and thus have similar distance to the nucleus. For this reason their shielding is modest only and can be estimated to be about 35% of a full elementary charge, or 0.35.

c) Each electron in the n-1 shell contributes 0.85 to σ. Those electrons are significantly closer to the nucleus compared to the electron of consideration. For that reason they shield significantly better, approximately 85% of an elementary charge, or 0.85.

d) Each electron in the n-2 shell or below contributes 1.00 to σ. Those electrons are much closer to the nucleus than the electron of consideration and can fully shield an elementary charge. Its contribution to the shielding constant is therefore approximated to be 1.

Now let us look at the Slater rules for d and f electrons.

a) Electrons to the right of the (nd) or (nf) group contribute nothing to σ. This is again because the electron is further away from the nucleus than the electron of consideration, and thus cannot contribute to shielding.

b) Each of the other electrons in the same (nd) or (nf) group contribute 0.35 to σ. This is again because these electrons have similar distance compared to the electron for which we calculate the shielding constant, and thus the shielding is modest.

c) Each electron to the left of the (nd) or (nf) group contributes 1 to σ. Those electrons are considered much closer to the nucleus, and thus they shield a full elementary charge.

Note that the values 0.35, 0.85, and 1 have been chosen so that the results from the Slater rules are in the best possible accordance with experimental measurements of orbital energies. Remember, when we discussed the helium atom we said that the measurement of ionization energies can provide experimental orbital energies.

Slater's Rules Applied to Multi-Electron Atoms

Let us practice the Slater rules by a few examples. We can, for instance, calculate the effective nuclear charge that acts on a 2p electron in an oxygen atom. To answer this question we need to first write out the electron configuration according to the quantum numbers n and l and group the orbitals correctly (Fig. 1.2.44).

Electron configuration $(1s^2)(2s^2\ 2p^4)$

Figure 1.2.44 Slater electron configuration of oxygen

Next, we need to consider that the effective nuclear charge Z_{eff} is the nuclear charge Z minus the shielding constant σ. Then, because oxygen has eight protons, the nuclear charge is 8. From that we need to subtract the shielding constant. Firstly, we need to realize that there are 5 electrons in the same group as the 2p electron of consideration. These are the two 2s electrons and the three other 2p electrons. These five electrons shield with a factor of 0.35 because they are in the same group as the 2p electron for which we want to calculate the shielding constant. Note that this fourth 2p electron does not get a factor because it is the electron for which we calculate the shielding constant. In addition, we need to consider the two 1s electrons. They are in an n-1 shell, therefore they contribute with a factor of 0.85. Overall, the effective nuclear charge on the 2p electron is 8-(2 x 0.85)-(5 x 0.35)= 4.55 (Fig. 1.2.45).

$$Z^* = Z - \sigma$$
$$= 8 - \underset{(2s,\,2p)}{[5 \times (0.35)]} - \underset{(1s)}{[2 \times (0.85)]} = 4.55$$

Figure 1.2.45 Effective nuclear charge on the 2p electron of an oxygen atom

We can also ask what is the effective nuclear charge on a 1s electron in the oxygen atom. It is 8-0.35=7.65 (Fig. 1.2.46).

$$\underset{(1s)}{Z_{eff}} = 8 - 0.35 = 7.65$$

Figure 1.2.46 Effective nuclear charge on the 1s electron of an oxygen atom

This is because we only need to consider the second electron in the 1s orbital to calculate the shielding constant σ. It contributes with a factor of 0.35 because it is in the same group as the 1s electron of consideration. The 2s and the 2p electrons are in a group right to the 1s orbital, therefore they do not contribute to the shielding.

Slater's Rules and the Aufbau Principle

The Slater rules are of great help to understand the so-called Aufbau principle, which says that for an atom in the ground state the electrons are in the orbitals of the lowest energy. To some extent the orbitals energies follow the quantum number n, but this is not always the case. For example, the element potassium has the electron configuration $1s^2\ 2s^2\ 2p^6\ 3s^2\ 3p^6\ 3d^0\ 4s^1$ and not $1s^2 2s^2 2p^6\ 3s^2 3p^6\ 3d^1$. This means that the energy of the 3d orbital must be higher than the energy of the 4s orbital. Can the Slater rules predict that? Let us therefore calculate the energy of the 3d and 4s orbital using the Slater rules, and see if the energy of the 3d orbital comes out higher than the electron of the 4s orbital.

For the 3d orbital, the shielding constant is 18x1=18 because there are 18 electrons besides the 3d electron of consideration, and all the 18 electrons are in a lower shell. Therefore, they all contribute with a factor of 1. The nuclear charge Z of the potassium is 19. Therefore, the effective nuclear charge Z_{eff}= 19-18=1 (Fig. 1.2.47).

$$\sigma = 18 \times 1 \rightarrow Z_{eff} = 19 - 18 = 1$$

Figure 1.2.47 Calculation of effective nuclear charge for the 3d electron of potassium

Now let us do the analogous calculation for the 4s electron. For the 4s electron the Slater rules for s electrons apply. According to that, the two 3s and the six 3p electrons contribute 0.85 to the shielding constant because they are in an n-1 shell. The remaining two 1s, two 2s, and six 2p electrons are in an n-2 or lower shell and therefore contribute with the factor of 1. Therefore, the overall shielding constant is 8 x 0.85 + 10 x 1 = 16.8. The effective nuclear charge Z_{eff} is therefore 19-16.8=2.2 (Fig. 1.2.48).

$$\sigma = 8 \times 0.85 + 10 \times 1 = 16.8 \rightarrow Z_{eff} = 2.2$$

Figure 1.2.48 Calculation of the effective nuclear charge for the 4s electron of potassium

We can see that a higher effective nuclear charge acts on a 4s electron compared to a 3d electron, which indicates that the orbital energy for the 4s electron will be lower compared to the 3d electron. We can calculate the orbital energies by using the formula $E=(Z_{eff}^2)/n^2 \times 13.6$ eV (Eq. 1.2.27).

$$E = -\frac{Z_{eff}^2}{n^2} \times 13.6\ eV$$

Equation 1.2.27 Equation for orbital energies

For the 3d electron we insert Z_{eff}=1 and n=3 which gives -1.51 eV, Eq. 1.2.28.

$$E(3d) = \frac{-1^2\ 13.6\ \text{eV}}{3^2} = -1.51\ \text{eV}$$

Equation 1.2.28 Equation for orbital energy of the 3d electron of potassium

For the 4s electron insert Z_{eff}=2.2 and n=4 which gives -4.14 eV.

$$E(4s) = \frac{-2.2^2\ 13.6\ \text{eV}}{4^2} = -4.14\ \text{eV}$$

Equation 1.2.29 Equation for orbital energy of the 4s electron of potassium

As expected, the energy of the 4s electron is lower than the energy of the 3d electron. This explains why the electron configuration with the 4s electron as the valence electron is preferred over that with the 3d electron as the valence electron. Overall, we can see that the Slater rules can correctly predict electron configurations of atoms and the Aufbau principle.

Let us do another, more complex example: There are two conceivable electron configurations for Fe. One in which the 4s subshell is filled before the 3d subshell, and one in which the 3d subshell is filled before the 4s subshell. For the first case the electron configuration is $1s^2 2s^2 2p^6 3s^2\ 3p^6\ 4s^2\ 3d^6$. For the second case, the second electron configuration is $1s^2\ 2s^2\ 2p^6\ 3s^2\ 3p^6\ 3d^8\ 4s^0$. We can see that the two electron configurations are the same for the 1s, 2s, 2p, 3s, and 3p electrons. We therefore focus on the remaining eight electrons, denoted in red, and calculate their energies.

In this case, we need to compare the sum of the electron energies for both electron configurations to be able to decide which electron configuration is favored. We calculate the sum of the energies of the eight electrons for the first electron configuration the following way: In the first step we need to rewrite the electron configuration in Slater form: $(1s^2)(2s^2\ 2p^6)(3s^2\ 3p^6)(3d^6)(4s^2)$.

Next, we can calculate the shielding constant for a 3d electron. We can ignore the two 4s electrons because they are to the right of the d electron of consideration, and do not contribute to the shielding. However, we do need to consider the five other 3d electrons that are in the same group as the 3d electron of consideration. They contribute with the factor of 0.35. The other 18 electrons contribute 1.00 because they are in a lower shell. Because the effective nuclear charge of Fe is 26, the effective nuclear charge Z_{eff} is Z_{eff}=26-19.75=6.25 (Eq. 1.2.30).

$$\sigma_{3d}= 5(0.35)+18(1.00)=19.75 \quad Z_{eff}(3d)=26-19.75=6.25$$

Equation 1.2.30 Equation for the shielding constant and effective nuclear charge of the 3d electron of an iron atom

For a 4s electron, there is one other 4s electron in the same group which contributes with a factor of 0.35. In addition, there are 14 electrons in an n-1 shell, namely the 3s, the 3p, and the 3d electrons. They contribute 0.85 to the shielding constant. The remaining 10 electrons are in an n-2 shell or lower, therefore they contribute with the factor 1.00. This gives an overall shielding constant of 22.25. From that we can calculate the effective nuclear charge for a 4s electron which is 26-22.25=3.75.

$$\sigma_{4s}=1(0.35)+14(0.85)+10(1.00)=22.25 \quad Z_{eff}(4s)=26-22.25=3.75$$

Equation 1.2.31 Equation for shielding constant and effective nuclear charge of the 4s electron of an Fe atom

We can now calculate the electron energies. It is the sum of the energies for the 3d and 4s electrons. The electron energy for a single electron is $E=-(Z_{eff}^2)/n^2 \times 13.6$ eV= $-(6.25^2)/3^2 \times 13.6$ eV=-59.03 eV. Because we have six 3d electrons, the overall energy for the six electrons is 6 x -59.03 eV = -354.17 eV (Eq. 1.2.32).

$$E(3d) = -\frac{Z_{eff}^2}{n^2} \times 13.6\ eV = -\frac{6.25^2}{3^2} \times 13.6\ eV = -59.03\ eV.$$

$$\text{For six 3d electrons: } E(3d) = 6 \times -59.03 eV = -354.17 eV$$

Equation 1.2.32 Equation for the electron energies of the six 3d electrons in an iron atom

The energy of a single 4s electron is $E=-(3.75^2)/4^2 \times 13.6$ eV=-11.95 eV. For two 4s electrons the energy is 2 x -11.95 eV= -23.90 eV.

$$E(4s) = -\frac{3.75^2}{4^2} \times 13.6\ eV = -11.95\ eV$$

$$\text{For two 4s electrons: } E(4s) = 2 \times -11.95 eV = -23.90 eV$$

Equation 1.2.33 Equation for the electron energies of the 4s electron in iron

The sum of all electrons is then -354.17 eV + (-23.90 eV) = -378.1 eV (Eq. 1.2.34).

$$E(4s + 3d) = -354.17 eV - 23.90 eV = -378.1 eV$$

Equation 1.2.34 Equation for the sum of all electrons

Now let us calculate the energy for the second electron configuration. First we need this electron configuration in Slater configuration. Next, we can calculate the shielding constant for the d electrons. It is σ_{3d} = 7(0.35) + 18(1.00) = 20.45 because there are seven other 3d electrons in the same group and 18 electrons in lower shells. The effective nuclear charge is then Z_{eff} (3d) = 26- 20.45 = 5.55.

$$\sigma_{3d} = 7(0.35) + 18(1.00) = 20.45$$
$$Z_{eff}(3d) = 26 - 20.45 = 5.55$$

Equation 1.2.35 Equation for the shielding constant and effective nuclear charge of the 3d electrons of iron (second configuration)

The sum of the electron energies for the eight d electrons is then $E(\Sigma\ 3d)=-8(5.55^2/3^2)$ eV=-372.3 eV, Eq. 1.2.36.

$$E(\Sigma\ 3d) = -8\frac{5.55^2}{3^2} eV = -372.3\ eV$$

Equation 1.2.36 Equation for the sum of the electron energies for the eight d electrons of iron

We can can see the energy of the second electron configuration is somewhat higher, and thus less preferred. This is in accordance with the experimentally observed ground state electron configuration of the Fe atom. Again, we see that the Slater rules can correctly predict the ground state electron configuration of atoms.

The Aufbau Principle and the Spin Pairing Energy

The Slater rules are suitable to account for shielding effects in multi-electron atoms which are of electrostatic nature. However, not only electrostatic effects influence the orbital energies, there are also magnetic effects. This is because each electron has a spin with a magnetic field associated with it. The electrons behave like little magnets that can interact with each other. These interactions can be either attractive or repulsive, which influences the electron energies. The electron energies are usually minimized when the number of electrons with the same spin is maximized. This is known as Hund's (Fig. 1.2.49) rule of maximum spin multiplicity.



Figure 1.2.49 Friedrich Hund (1898-1997) (Attribution: GFHund [CC BY (https://creativecommons.org/licenses/by/3.0)], commons.wikimedia.org/wiki/F...%B6ttingen.jpg)

In the previously example we have seen that the electron configuration $4s^2\ 3d^6$ is favored in Fe because of electrostatic shielding effects. In addition, it also favored by magnetic effects. In this electron configuration there are four unpaired electrons, while in the electron configuration $3d^8$ there are only two unpaired electrons.

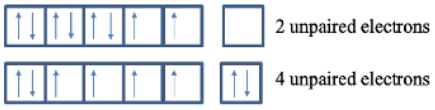


Figure 1.2.50 Electron configuration of Fe depicted regarding spin pairing

We can now understand the Aufbau principle for multi-electron atoms (Figure 1.2.51).

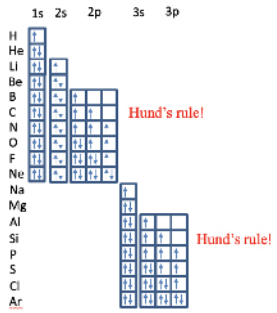


Figure 1.2.51 Electron configuration of atoms following the Aufbau principle

For H and He the 1s orbital gets filled. From lithium to beryllium the 2s subshell gets filled, and from boron to neon the 2p subshell gets filled under consideration of Hund's rule. You can see that for carbon the two 2p electrons are both spin up in different 2p orbitals. For nitrogen there are three unpaired electrons in the 2p orbitals. From the element oxygen on, we have to start pairing spins until all spins are paired in neon. From Na to Ar the 3s and the 3p orbitals get filled according to the same principles.

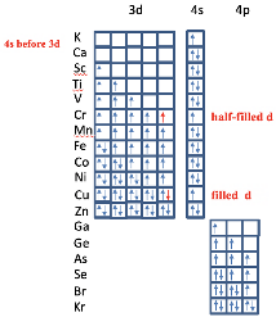


Figure 1.2.52 Continuation of electron configuration of atoms following the Aufbau principle

After that, the 4s orbitals of K and Ca get filled, and then the 3d orbitals of the elements from Sc to Zn (Fig. 1.2.52). We have seen previously that the Slater rules nicely show why. You can see that there are two anomalies though. For the chromium, the electron configuration is $4s^1\ 3d^5$ and not $4s^2\ 3d^4$. This is because there are more unpaired spins in this electron configuration, and a half-filled 3d subshell with unpaired spins only represents a particularly stable electron configuration. The second anomaly occurs for the element Cu which has an electron configuration $4s^1 3d^{10}$ and not $4s^2 3d^9$. This is because a d^{10} electron configuration is a particular stable electron configuration. After the 3d subshell is filled, the 4p subshell is filled for the elements from Ga to Kr. Again, the electrons are filled into the orbitals according to Hund's rule. We could extend our consideration to even heavier elements, but will be beyond scope.

Dr. Kai Landskron (Lehigh University). If you like this textbook, please consider to make a donation to support the author's research at Lehigh University: Click Here to Donate.

This page titled 1.2: The quantum-mechanical model of the atom is shared under a not declared license and was authored, remixed, and/or curated by Kai Landskron.

- **1.2: The quantum-mechanical model of the atom** by Kai Landskron is licensed CC BY 4.0.

1.3: Periodic Properties of Atoms

The Periodic Table of Elements

Having understood the Aufbau principle we can now understand the periodic table of the elements. The periodic table was actually invented a long time before the quantum-mechanical atom model was developed. It was first introduced by Mendeleev and Meyer who ordered the elements according to their masses in a row. Whenever an element had a property similar to an element that already was previously considered a new row was begun. This gave a table with rows and columns. Within a row the mass of the elements would increase, within a column one would find the elements that had similar properties. The rows would be called periods, and the columns would be called groups, hence the name periodic table of the elements. At the time Mendeleev and Meyer invented the periodic table, there were still many elements undiscovered visible as “holes” within the periodic table. However, over time the periodic table became complete (Fig. 1.3.1).

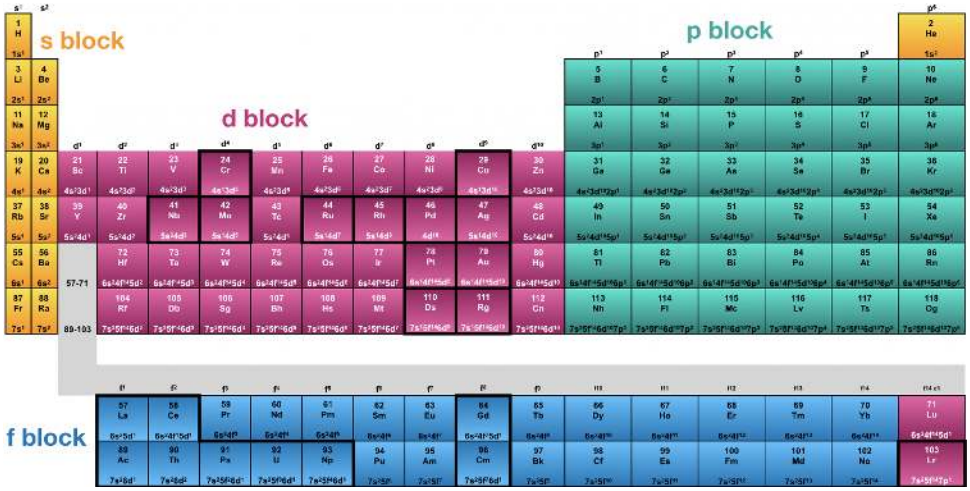


Figure 1.3.1 The periodic table of elements (Attribution: Kathryn Haas https://chem.libretexts.org/Bookshel...bau_Principle#)

Today we know 118 elements completing seven periods and 18 groups. Today, the elements are not ordered by mass, but by the atomic number (number of protons), however this did not change the original periodic table much because except for a very few elements the mass of the elements follows the atomic number. Before the quantum-mechanical model was developed, it was not understood why elements within the same group had similar properties. When you analyze the electron configuration of the atoms you can see that all atoms in the same group have the same type of outmost electrons, also called valence electrons. These electrons are the electrons that have the greatest distance from the nucleus and have the highest energies. Because they have the highest energies, they are also the electrons that are most reactive, and determine the chemical and physical properties of the element. For example, in the first group all elements have one s electron as the valence electron. Because these electrons have the highest energy and are most reactive, they determine the properties of the atom, and thus the elements in the first group have similar properties.

When you look into group 2, all the electrons have two s electrons as the valence electrons. An exception is the element helium which is placed into group 18 which is called the group of the noble gases. The other group 18 elements have two s and six p electrons of the same quantum number n as valence electrons. The behavior of He is much more similar to that of the other group 18 elements, namely it is a gas with extremely low reactivity. This property is due to the fact that like the other noble gases He has a full shell. Elements with a full shell are particularly unreactive because full shells represent particularly stable electron configurations, also called noble gas configurations.

Group 1, group 2 and He are called the s-block of the periodic table because they are the elements that only have s electrons as valence electrons. From group 3 to group 12 there are elements with s and d electrons as valence electrons. These elements are the d-block of the periodic table. The d-block begins with group 3 where there is only one d electron together with two s electrons, and ends with group 12 where there are ten d and two s electrons. In group 12 the d subshell is completely filled with electrons. From group 13 to group 18 we find electrons that have p electrons as valence electrons. There are six groups because p orbitals can accommodate up to six p electrons. In group 13 there is only one p valence electron, in group 14 there are two, in group 15 there are three, in group 16 four, in group 17 five, and in group 18 there a six except the Helium which we previously discussed already.

Group 13 to 18 is called the p block of the periodic table. The s-block and the p block elements together are also called the main group elements, the elements of the d-block are called the transition metals. The elements of the main groups have specific names. Group 1 elements except hydrogen are called the alkali metals, group 2 elements the earth alkaline metals, group 13 elements the triels, group 14 elements the tetrels, group 15 elements the pnictides, group 16 elements are the chalcogens, group 17 elements the halogens, and group 18 elements the noble gases.

Finally, there is the f block of the periodic table. The f-block contains the elements with f-valence electrons. Because there are seven f-orbitals for a given quantum number n, the f orbitals can accommodate up to 14 electrons, and thus there are 14 groups. The f block is actually located in between the s block and the d block of the periodic table, but is typically written underneath the rest of the periodic table. This is done because the periodic table would become too wide if it was placed between the s and the d block. Note that the f-block elements do not have a group number. Note also that the elements on the left end of the f-block, lanthanum and actinium, actually do not have f-valence electrons. They are actually group 3 elements located underneath the elements scandium and yttrium. The first row of the f-block is are called the lanthanides, which is the greek meaning the elements following the lanthanum. Only the elements following the lanthanum have f-valence electrons. Analogously, the actinium is not an actual f-block element, only the elements that follow the actinium. They are called the actinides.

The quantum mechanical model of the atoms also explains why the periodic table has periods. Each period is associated with a quantum number n, the first period with n=1, second period with n=2 and so forth. Within a period the available s and p valence orbitals of a specific quantum number n are getting filled. Subshells of a lower quantum number may also be filled within the period. For example, the 3d subshell gets filled within the fourth period, and the 4f subshell gets filled in the 6th period.

Elements with electron configurations that deviate from the expected electron configuration are highlighted in bold (Figure 1.3.1). There are only exceptions for the d-block and f-block elements. We discussed some of them already, for example the Cr and the Cu. In addition, for instance, Pd has the electron configuration $4d^{10}$ instead of $5s^24d^8$, and Pt has the electron configuration $6s^15d^9$ instead of $6s^25d^8$. We can explain these exceptions when considering the complex electrostatic and magnetic interactions of electrons in multi-electron atoms. Not everything can be explained by the simple concepts of Slater rules and Hund's rule.

As chemists we should always know our periodic table. Learning is easier with music, and there is a fabulous song by Tom Lehrer that can help you to learn the periodic table. The link to a respective YouTube video is provided below.

https://www.youtube.com/watch?v=DYW50F42ss8

Atomic Radii

Let us now look at what is called the periodic properties of atoms. These are properties which change due to the position of the element within the periodic table. Let us first consider how the atomic radii of the atoms depend on the position of the atom in the periodic table, Fig. 1.3.2.

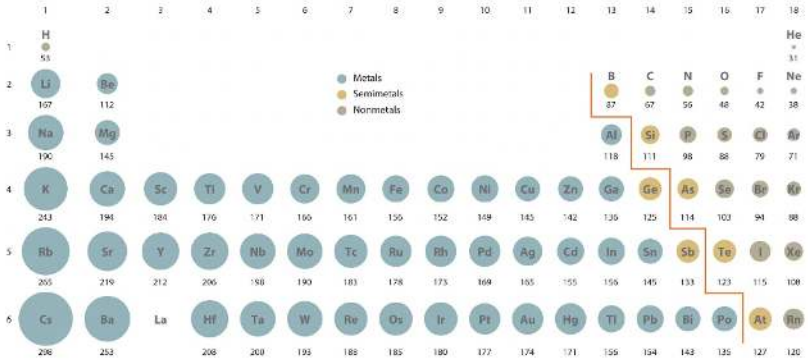


Figure 1.3.2 Calculated atomic radii of the elements in the periodic table (Attribution: Webelements.com, https://chem.libretexts.org/@api/deki/files/27875/bd05f43d0392ab934fc21044ccca1cfd.jpg?revision=1 http://creativecommons.org/licenses/by-nc-sa/3.0/us/)

When you look at how the atomic radii change within a period you can easily see that they decrease from the left to the right in the periodic table. The decrease is more significant for the s and p block elements compared to the d block elements. We can explain this effect using the concept of effective nuclear charge. As we go from the left to the right in the periodic table we add electrons to

the same shell. Because also a proton is added to the nucleus with each electron added, the electron experiences a greater attractive force from the nucleus. This effect tends to increase the effective nuclear charge. However, there is also an opposite effect. Because there is one more electron, there are more electron-electron repulsion and shielding effects, and this tends to decrease the effective nuclear charge. Because the new electron is added to the same shell, the shielding effects do not fully compensate for the additional Coulomb force coming from the additional proton in the nucleus, and thus the effective nuclear charge increases. This higher effective nuclear charge pulls the electrons closer to the nucleus, and thus the atom size decreases. For the d-block elements new d electrons get added to a more inner subshell, for example for the d-block elements of the 4th period the d electrons get added to the 3d subshell. Because of that, these 3d electrons can more effectively shield nuclear charge from the outmost two 4s electrons, and thus the decrease of the atomic radius is less pronounced. In summary:

Trend 1: Atomic radius decreases continuously within a period.

A second trend is that each time a new period is begun the atomic radius jumps dramatically. For example it jumps from 31 pm to 167 pm as we go from the helium to the lithium, and from 38 pm to 190 pm as you go from the neon to the sodium. This trend is because the electrons get filled into a new, more outer shell when a new period is begun. This outer shell is located much farther away from the nucleus, and thus the radius of the atom increases. In addition, the electrons in the inner shells can very effectively shield the nuclear charge from the electron added to the new shell which tends to increase atom radius. In summary:

Trend 2: Atomic radius jumps when a new period is begun.

As a third trend you can see that the atomic radii increase as you go down a group. This is because within a group there are the same number and type of valence electrons, but the valence electrons are in a more outer shell associated with a higher quantum number n. In a somewhat different view we can also argue that the first two trends add up to give the third trend. The effect of jump of atomic radius when a new period is begun is greater than the effect of decline of the radius within a period. As a result, the radius tends to increase as you go down a group. In summary:

Trend 3: Atomic radius increases continuously within a group.

The determination of an atomic radius is not as trivial at it may seem. You can obtain it either from quantum mechanical calculations, or determine it experimentally. If you calculate it, then the radius is defined as the radius that defines the volume in which the electron can be observed with 90% probability. The radii that you see in Figure 1.3.2 are actually calculated radii. If you determine the radius experimentally, then there are again different subtypes of radii. The so-called metallic, or crystal radii, the vanderWaals radii, and the covalent radii. The covalent radius is the half of the distance between two, same atoms in a molecule held together in a single covalent bond.

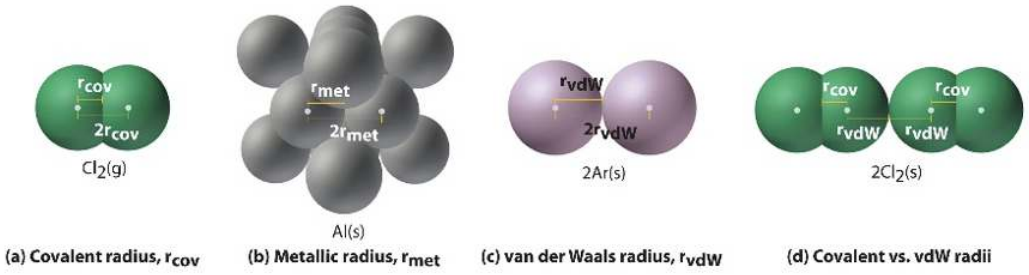


Figure 1.3.3 Atomic radii for a) covalent radius b) metallic radius c) van der Waals radius d) covalent vs vdW radii (Attribution: Chemlibretexts. https://chem.libretexts.org/@api/dek...jpg?revision=1 http://creativecommons.org/licenses/by-nc-sa/3.0/us/)

This is unambiguous for molecules such as Cl_2, the other halogens, and for other cases such as hydrogen, carbon (as diamond), sulfur, and a few other cases. However for oxygen, O_2, the situation is less clear as the order of the oxygen-oxygen bond is 2. In this case, it is necessary to infer the covalent radius from molecules containing O-O single bonds or from molecules containing an E-X single bond (E=element) in which the covalent radius of X is known. The van der Waals radius is half the distance between two same atoms in a crystal when there is no actual bonding between the atom except weak van der Waals forces. For example, in solid argon, there are only van der Waals forces between the atoms, and half the distance between the atoms in solid argon is the Van der Waals radius. For chlorine, for example, the van der Waals radius is half the distance between two chlorine atoms of two different Cl_2 molecules in solid Cl_2. Note that the van der Waals radius of chlorine is different than the covalent radius of chlorine. This again shows that there is a certain ambiguity when determining an atomic radius, and therefore it is always important to say

what definition of atomic radius you use. Lastly, there is also the metallic radius that applies to solid metals in which metal atoms are held together by metallic bonding. The metallic radius is the defined as half the distance between the centers of two metal atoms within a metal.

First Ionization Energy

The first ionization energy is another important periodic property of the elements. It is defined as the energy required to remove an electron from a neutral atom in the gas phase. It is important to understand that we refer to an atom in the gas phase here, because only in the gas phase atoms do not significantly interact with each other. Therefore, only when looking at an atom in the gas phase we can truly determine the properties of single, isolated atoms. Let us look at the two images (Figure 1.3.4) to determine periodic trends.

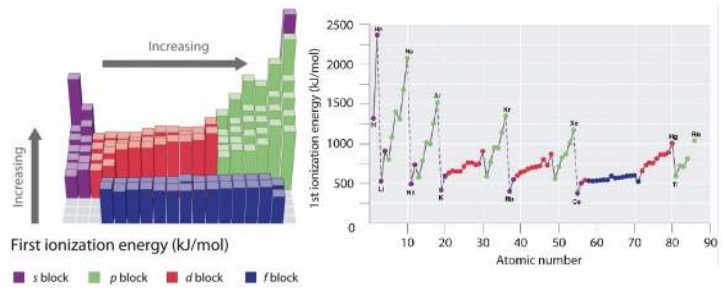


Figure 1.3.4 First ionization energies as a third dimension in the periodic table (left) and as function of atomic number (right) (Attribution: ChemlibreTexts https://chem.libretexts.org/@api/dek...png?revision=1 http://creativecommons.org/licenses/by-nc-sa/3.0/us/)

First of all we need to realize that all 1st ionization energies are positive. This means that it always requires energy to remove an electron from a neutral atom. You can understand this when you consider that all electrons in an atom are bound to the nucleus via a binding energy. If an ionization energy was negative then this would mean that the atom would spontaneously lose an electron, and spontaneously ionize. This would be unreasonable.

Now let us see how the first ionization energy changes within a period. We can see that it increases as we go from the left to the right within a period. This trend can be explained by the fact that the effective nuclear charge increases from the left to the right within a period. As the effective nuclear charge increases, the pull of the nucleus on the outmost electron increases, and thus the harder it is to remove this electron from the atom. You can see, however, that within the main group elements the trend is two times broken. The group 13 elements have a lower ionization energy than the group 2 elements, and the group 16 elements have a lower ionization energy than the group 15 elements. This phenomenon can be explained by the fact that the filled and half-filled subshells in group 2 and group 15 represent particularly stable electron configurations, and thus the electrons within these subshells have unusually low energy. For that reason these electrons are harder to remove from the atoms. The group 2 elements have filled s subshells, and the group 15 elements have half-filled p subshells. You can also notice that the increase in ionization energy is less pronounced within the d-block, and even less pronounced with in the f-block. This is because the effective nuclear charge on the outmost electrons does not increase as much because inner d and f orbitals are getting filled. You can also see that the group 13 elements have a lower ionization energy than the group 12 elements. This is because in group 13 a new p subshell is begun and the new electrons get added to the outmost shell where shielding effects are smaller.

As a second trend you can see that whenever a new period is begun, the ionization energy drastically drops. This is because the new electron is added to a new, more outer shell where the effective nuclear charge acting on the new electron is much smaller. The third trend is that the ionization energy becomes smaller as we go down a group. This is because the effective nuclear charge on the valence electrons decreases because the quantum number n of the valence electrons increases. There is one peculiarity that needs additional explanation. The drop of ionization energy from hydrogen to lithium in the first group is unusually large. This is because hydrogen is the only element for which there are no shielding effects, simply because the hydrogen has only one electron. For that reason the valence 1s electron of the hydrogen is far harder to remove than the valence s electrons of the other group 1 elements.

Electron Affinity

Now let us consider the first electron affinity (Figure 1.3.5). It is defined as the energy required or released when you add an electron to a neutral atom in the gas phase. Again, we look at an atom in the gas phase, because we want to consider an isolated atom that does not make significant interactions with other atoms.

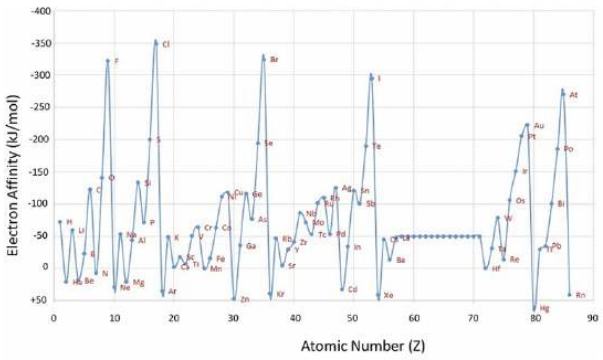


Figure 1.3.5 Electron affinity vs Atomic Number (Attribution: Chemlibretexts. https://chem.libretexts.org/@api/dek...780&height=456 http://creativecommons.org/licenses/by-nc-sa/3.0/us/)

We can see from the graph that most elements have negative electron affinities, meaning that the addition of a free electron to a neutral atom is exothermic, and releases energy, however, this is not always the case. Some elements have negative electron affinities, in particular the noble gases, but also Be, N, Mg, Zn, Cd, and Hg. Zn, Cd, and Hg, are group 12 elements with a full d subshell which is particularly stable. An additional electron would need to be added to a p orbital of a higher shell which is energetically quite unfavorable. Similarly, Be and Mg have filled s subshells which are also fairly stable. Adding an additional electron would need to start an new subshell, which is energetically not favorable. You can see that Ca and Sr have electron affinities of about 0, and that of Ba is only slightly negative showing that higher periods make the addition of an electron to a new p shell slightly more favorable. Nitrogen has a half-filled p subshell, which is also a quite stable electron configuration, and therefore adding an electron is not favorable. The addition of an electron is slightly more favorable for the other group 15 elements, however, these also tend to have rather low electron affinities.

Generally, for the main group elements the electron affinity tends to increase from the group 1 to group 17. However, the trend is broken for group 2 and group 15 elements because these elements have full and half-filled subshells, respectively. In addition, it is noteworthy that group 1 elements have higher electron affinities than group 3 elements. This is because adding an electron to a group 1 element produces a full s subshell which is fairly stable. For the d-block elements, the electron affinity tends to increase from group 3 to group 11, but the trend is broken multiple times showing that each element would need to be investigated individually which is beyond the scope here. There is a big drop in electron affinity from group 17 to group 18 which is easily explained by the fact that the addition of an electron to a group 17 element produces a filled shell, while a group 18 element already has a full shell, and the addition of an electron would start a new shell. Similarly, there is a sharp drop in electron affinity from group 11 to group 12, as an addition of an electron to a group 11 atom produces a full subshell, while the addition of an electron to a group 12 element would require the start of new, more outer subshell. For the p block elements the electron affinity tends to first increase from period 2 to 3, and then decrease. For the s-block there is a steady decrease down a group. For d block elements there is no clear trend for the electron affinity.

Electronegativity

Lastly, let us study the electronegativity as a periodic property. The electronegativity is the measure of the ability of an atom to attract electrons within a chemical bond. It is related to the electron affinity in the sense that both period properties measure the force by which an electron is attracted to a neutral atom. However, the electron affinity is associated with isolated atoms, that do not make bonds to neighbored atoms, while the electronegativity refers to atoms that are bonded to neighbored atoms. The importance of the electronegativity stems largely from its ability to predict and understand the nature of the bonding between atoms, in particular, covalent, ionic, and metallic bonding.

Electronegativity Scales

Electronegativity was a concept first developed by Linus Pauling to describe the relative polarity of bonds and molecules. He argued that the electronegativity of an atom could be derived from bond energy differences between homoleptic and heteroleptic bonds (Eq. 1.3.1).

$$\chi(A)-\chi(B) = c\,[(E(A\text{-}B) - \{E(A\text{-}A)\cdot E(B\text{-}B)\}^{1/2}),\ eV].$$

Here E(A-B), E(A-A) and E(B-B) are energies of A-B, A-A and B-B bonds respectively.
c is a constant.

Equation 1.3.1 Electronegativity according to Pauling, eV = electron volts.

For example, the energy required to break the bond in H_2 is 432 kJ mol^{-1}, and for F_2 it is 159 kJ mol^{-1}. However the energy required to break a bond in HF is 565 kJ mol^{-1}, which is much higher than expected just by averaging the energy of the two homonuclear bonds (296 kJ mol^{-1}). Pauling argued that the difference could be assigned to electrostatic attractions between the F and H "ends" of the molecule whereby the F end has more electron density and the H end has less electron density. The greater the difference between the average energy of the homoleptic bonds and the heteroleptic bonds, the greater the electronegativity difference between the atoms, and the greater the polarity of the heteroleptic bond.

First, Pauling used the arithmetic means of the heteroleptic bond energies, later he used the geometric means, because he found empirically that it worked better (Equation 1.3.1). The geometric mean of the homoleptic bond energies is the square root of the product of the homoleptic bond energies. This method only provided electronegativity differences. He therefore needed to define a reference atom with an arbitrarily defined electronegativity value, and then determine the electronegativity values of all other atoms relative to that value. He chose the most electronegative atom, the fluorine atom, as the standard and assigned a value of 4.0. The values of all other atoms vary between 0.7 (Fr) and 3.44 (O), and are shown in the periodic table on the below (Fig. 1.3.6).

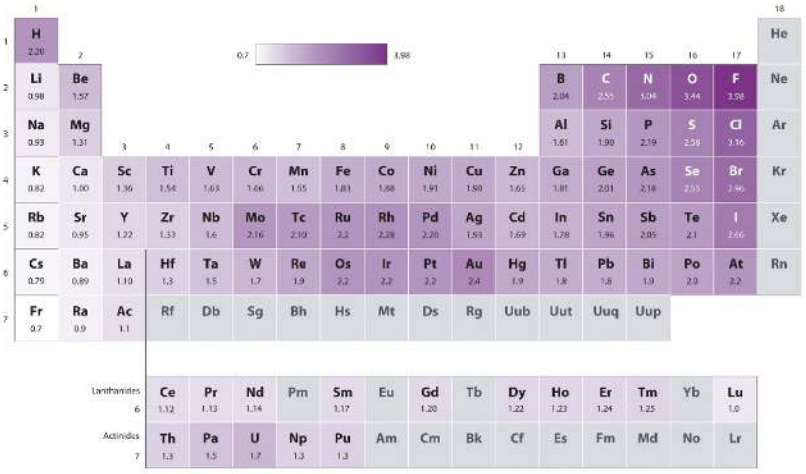


Figure 1.3.6 Periodic trends of electronegativity (Attribution: Chemlibretexts https://chem.libretexts.org/@api/dek...jpg?revision=1 http://creativecommons.org/licenses/by-nc-sa/3.0/us/)

What are the periodic trends? One can see that within a period the electronegativity values of the main group elements strictly increase with the group number. Note though that the noble gases do not have a Pauling electronegativity because, with few exceptions, noble gases do not make compounds and thus no bond energies are available for them. We can also see that for main group elements the electronegativity strictly decreases down a group. This makes the fluorine the most electronegative atom, and the cesium the least electronegative atom. Cesium has an electronegativity value of 0.7. We ignore the radioactive francium here. For the d-block, the trends are less strict, but there is a tendency of electronegativity increase from group 3 to group 11. All group 12 elements have smaller electronegativities compared to their neighbored group 11 elements. What about trends within a group? In group 3 to group 5 there is a small decrease in electronegativity down a group. For group 6 and 9, the period 5 elements have higher values than their neighbored elements in period 4 and 6. For group 10 to 12 the electronegativity increases down a group. The d-block element with the highest electronegativity is the gold, it has a value of 2.4. Note that this is similar to the electronegativity of non-metals such as I, S, and P. For these reasons, sometimes gold can behave like a non-metal in compounds with very low electronegativity. For example, there is the compound cesium auride (CsAu) which is a transparent, ionic crystalline

compound due to the high electronegativity difference between cesium and gold. The f-block elements generally have low electronegativity.

The Pauling electronegativity scale is derived from empirical data on bond energies. It works very well in practice and it is up to date the most used electronegativity scale. However, it does not to relate electronegativity to other periodic properties, and the quantum-mechanical model of the atoms. One electronegativity scale that addresses this short-coming the Allred-Rochow scale. It relates the electronegativity to the Coulomb force that acts on an electron on the surface of an atom. The Coulomb force is proportional to the effective nuclear charge Z* and inverse proportional to the atomic radius square. Z^*/r^2 is multiplied with a factor of 3590 and a value of 0.744 is added to this term. These numbers are empirically chosen so that the values of the Allred-Rochow scale become comparable to the Pauling scale.

$$\text{Allred-Rochow: } \chi = [0.744+3590 \cdot Z^*/r^2]$$

Here Z^* is effective nuclear charge and r is atomic radius.

Equation 1.3.2 Allred-Rochow definition of electronegativity

Another frequently used scale is the Mulliken electronegativity scale. The Mulliken scale relates the electronegativity to the sum of the first ionization energy IE and the first electron affinity EA. We would intuitively agree that the ability of an atom to attract electrons within a chemical bond is the higher, the harder it is to remove an electron from an isolated atom, and the easier it is to add an electron to an isolated atom. The numbers 0.118 and -0.207 are empirically chosen to make comparisons to the Pauling scale possible. The Mulliken scale is related to the Allred-Rochow scale in the sense that you can explain ionization energies and electron affinities of atoms with the concept of the effective nuclear charge.

$$\text{Mulliken: } \chi = [0.118 \cdot (IE+EA)-0.207]$$

Here IE is ionization energy and EA is electron affinity of an atom

Equation 1.3.3 Mulliken definition of electronegativity

Another electronegativity scale has been developed by Leland C. Allen. It designed for main group elements in particular. It argues that the electronegativity is proportional to the average energy of the s and p valence electrons in the atom. This electronegativity concept also has a relationship to that of Allred-Rochow, because orbital energies can be calculated from the effective nuclear charge.

$$\text{Allen: } \chi = [(me_p+ne_s)/(m+n)]$$

Here e_p is the energy of p-electrons and e_s is the energy of s-electrons; m and n are populations of p- and s-orbitals respectively.

Equation 1.3.4 Leland C. Allen definition of electronegativity

Overall, you can see that the electronegativity scales are inter-related, they say essentially the same, but present electronegativity from a somewhat different perspective.

Electronegativity of the Elements and Chemical Bonding

One of the most powerful attributes of electronegativity is that it can predict what type of chemical bond is to expect in elements and compounds. Let us first look at the bonding between elements.

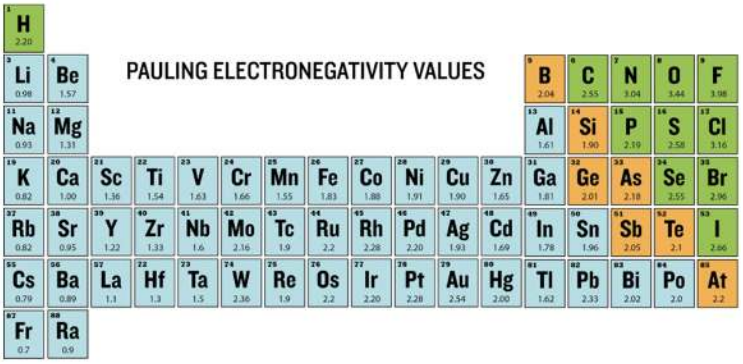


Figure 1.3.7 Pauling electronegativity values for the elements (Attribution: Ck12.org https://www.ck12.org/flx/show/default/image/user%3Ack12editor/20141124141684723269001l_ab8840393ea93a2a7c9fc01e395da3b2-20141124141684756943010 7.png https://creativecommons.org/licenses/by-nc/3.0/legalcode)

In the depicted periodic table (Figure 1.3.7) you can see the type of chemical bonding between atoms indicated by different colors. There is metallic bonding in metals, indicated by the color blue. In metallic bonds the electrons are shared between atoms but are delocalized over many atoms in the metal. The green color indicates covalent bonding seen in non-metals. In covalent bonding the electrons are shared, but localized in between typically two atoms. Metalloids have chemical bonding with a mix of covalent and metallic character shown in orange. There is electron-sharing with a moderate degree of delocalization. The Pauling electronegativity values of the elements are written underneath the element symbols.

Can we relate the electronegativity values to the chemical bonding in the elements? We can clearly see that elements with high electronegativity values significantly above 2.0, the non-metals, tend to make covalent bonds in between them. All metalloids with a hybrid covalent-metallic character, have intermediate electronegativity around 2.0. Most metals have low electronegativity values below 2.0 except noble metals like Pt and Au. Overall, we can say that there is a clear relationship between the bonding type in an element and its electronegativity. Now let us see if electronegativity can also predict chemical bonding in compounds.

Ketelaar's Triangle

The ability of electronegativity to predict the bonding type in compounds can be understood by Ketelaar's triangle, named after J.A.A. Ketelaar.

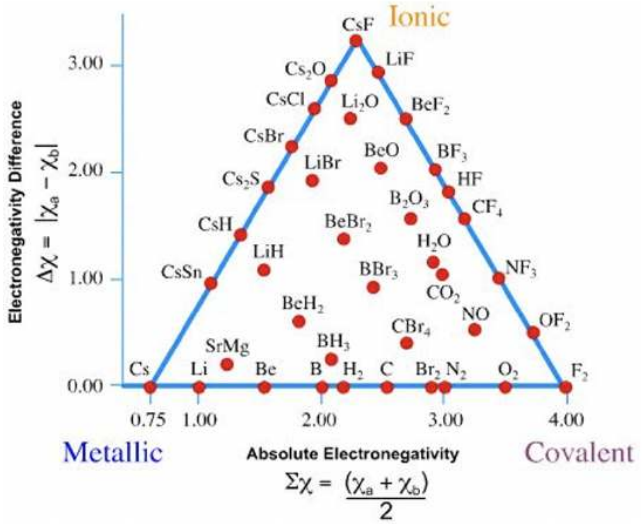


Figure 1.3.8 Ketelaar's Triangle (Attribution: Chemlibretexts https://chem.libretexts.org/@api/dek...jpg?revision=2 http://creativecommons.org/licenses/by-nc-sa/3.0/us/)

You can see that Ketelaar's triangle has three corners (Figure 1.3.8). Two of the corners are occupied by the elements F and Cs, and the third corner is occupied by CsF. All elements are located on the horizontal edge of the triangle, and there many compound indicated by dots either on the two other edges or within the triangle. There are no compounds or elements outside of the triangle. How can we understand this triangle and what does it say about the relationship between bonding character and electronegativity?

To understand this, look at the two axes. The horizontal x-axis represents the average electronegativity of the atoms in an element or a compound. The vertical y-axis represents the electronegativity difference between the atoms in the elements or the compound. For elements the electronegativity difference between the atoms is zero, because in an element all atoms are of the same type. Therefore, all the elements lie on the horizontally oriented edge of the triangle. Because Cs is the element with the lowest electronegativity, it lies furthest to the left on this edge. Fluorine is the element with the highest electronegativity, and thus lies the furthest on the right side. The other elements are in located in between the cesium and the fluorine on the edge. The higher the electronegativity of the elements, the further right their position on this edge of the triangle.

For compounds, the electronegativity difference between atoms is never exactly zero, therefore all compounds are located above the horizontal edge of the triangle. The compound with the highest electronegativity difference is the CsF. Its average electronegativity is the sum the electronegativity of Cs and F divided by 2: Therefore, CsF defines the third corner of the triangle. All other compounds must lie on the edges or within the triangle. All cesium compounds are located on the edge between the Cs and CsF, and all the fluorine compounds are located on the edge between CsF and F2. The compounds of all other elements are inside the triangle. The position of the compound on or in the triangle defines its bonding character. The closer the position of the compound toward the Cs corner, the more metallic, the closer the position is to the F2 corner, the more covalent, and the closer it is to the CsF corner, the more ionic. For example Li_2O is located close to CsF, and the bonding would be predominantly ionic, although there is also a small degree of covalent and metallic bonding. In contrast to that, SrMg has mostly metallic bonding, a little bit of covalent bonding, and even less ionic bonding. The bonding situation in LiH is in between metallic and ionic, with a little bit of covalent bonding character mixed in. Note that a 100% ionic bond is not possible because the electronegativity difference is finite, and thus there must always be a certain degree of electron sharing. In contrast to that, a 100% covalent bond is possible because electrons can be equally shared between two atoms when the electronegativity difference is zero.

The take home message is that in compounds and elements there is usually a mix of bonding types, and not a single bonding type, even through one bonding type may strongly dominate. The concept of electronegativity, and Ketelaar's triangle in particular, is extremely helpful to predict to which degree the three bonding types are present in a substance.

Dr. Kai Landskron (Lehigh University). If you like this textbook, please consider to make a donation to support the author's research at Lehigh University: Click Here to Donate.

This page titled 1.3: Periodic Properties of Atoms is shared under a not declared license and was authored, remixed, and/or curated by Kai Landskron.

- **1.3: Periodic Properties of Atoms** by Kai Landskron is licensed CC BY 4.0.

1.4: Concept Review Questions Chapter 1

Concept Review Questions

Section 1

1. Which were the elements in the antique non-atomistic element theories?
2. Explain the definition of the term “atom” as introduced by Leukippes and Demokrites.
3. What does the law of the conservation of mass state?
4. Who discovered the law of the conservation of mass?
5. What obscured the discovery of the law of the conservation of mass for a long time?
6. Explain why the discovery of the law of the conservation of mass was important for the development of atomic theory.
7. What does the law of the constant compositions state?
8. Who discovered the law of the constant compositions?
9. What does the law of the multiple proportions state?
10. Who discovered the law of the multiple proportions?
11. Explain why the law of the multiple proportions can be explained by Dalton’s hypothesis.
12. Explain what cathode rays are and how they are being produced.
13. Explain how Thomson identified electrons in cathode rays.
14. Explain why Rutherford’s gold foil experiment disproves Thomson’s atom model.
15. Describe Rutherford’s atom model and explain why it is in agreement with his gold foil experiment.
16. Which two opposing forces keep electrons stable in the orbit around the nucleus according to Rutherford’s atom model?
17. What are the two basic problems with Rutherford’s atom model?
18. What is blackbody radiation?
19. What assumption did Max Planck make to explain the spectra of blackbody radiation?
20. Objects first start to glow red, then, orange, and finally white with increasing temperature. Explain why.
21. What is meant by the “Balmer series”, the “Paschen series” and the “Lyman series”?
22. Explain why the atomic absorption and emission spectra inspired the Bohr atom model?
23. What is the meaning of an angular momentum in physics?
24. Name the four postulates of Niels Bohr that lead to his atom model.
25. Mathematically derive the terms for the allowed radii and the allowed energies for the electron in an H atom according to Bohr.
26. Explain why the results of the above calculations explain the atomic spectra of the H atom.
27. What are the two major problems of the Bohr atom model?

Section 2

1. What is the photoelectric effect?
2. Explain how Einstein verified Planck’s law by investigating the photoelectric effect.
3. Explain why the wave-particle dualism can explain the photoelectric effect.
4. What is the name of the particle associated with electromagnetic radiation?
5. Derive the formula for the wave-particle dualism of electromagnetic radiation.

6. Give a definition for standing matter waves.

7. Explain why standing matter waves are quantized.

8. Derive the Schroedinger equation for the electron in the one-dimensional box.

9. What are the boundary conditions for the wavefunctions describing the electron in a one-dimensional box.

10. Derive the wavefunction for the electron in the one-dimensional box.

11. Explain qualitatively what are the major similarities and differences for an electron in a one-dimensional box compared to an electron in a hydrogen atom.

12. What are the quantum numbers in the solution of the Schroedinger equation for the hydrogen atom?

13. The radial probability function is the product of the formula for the surface of a sphere multiplied with the square of the radial function. Explain why this product gives the probability to find the electron at a certain distance (radius) from the nucleus.

14. At which radius r has the radial probability function of the 1s orbital its maximum?

15. What is a spherical node in an orbital?

16. What is an angular node in an orbital?

17. What types of angular nodes do we know?

18. Can an s orbitals have angular nodes?

19. Can p and d orbitals have spherical nodes?

20. Name an orbital that has a conical node.

21. What are the formulas for the number of radial, angular, and total number of nodes in an atom?

22. On which quantum number do the orbital energies in the H atom depend on according to the wavemechanical model of the H atom?

23. The energy of an electron in the ground state of the hydrogen is -13.6 eV. Explain why this energy is negative.

24. What are the energies of the electron in the hydrogen atom when the electron is in a 2p and 4f orbital respectively?

25. Explain the concept of shielding in multi-electron atoms.

26. Explain why the energy of a 2s orbital in Li is smaller than that of a 2p orbital.

27. What are the Slater rules for s,p,d, and f electrons respectively?

28. What is special about the electron configurations of Cr and Cu?

29. Explain the concept of the spin-pairing energy.

30. What does Hund's rule state?

Section 3

1. Write down the periodic table of the elements for the elements with the atomic numbers 1 to 86. Include element symbols only.

2. Listen to Tom Lehrer's "The Elements" song. Relax.

3. Which are the three periodic trends for the atomic radii of the elements of the periodic table? Explain these trends.

4. What is the definition of the ionization energy, the electron affinity, and the electronegativity?

5. Which are the three periodic trends for the first ionization energies of the elements of the periodic table? Explain these trends INCLUDING their exceptions.

6. The electron affinities of the group 2, 12, and 18 elements as well as the electron affinity of N are negative. Explain.

7. Alkali metals have a relatively high electron affinity. Explain.

8. Explain how Pauling derived his electronegativity scale.

9. What the periodic trends for the electronegativity of the elements of the periodic table?

10. Explain why CsAu is an ionic crystal.

11. Explain why electronegativity differences are related to the dissociation energy differences of homonuclear and heteronuclear bonds.

12. Explain the concepts of the Allred-Rochow, Mulliken, and Allen electronegativity scale.

13. Which of the four electronegativity scales we talked about in class cannot make statements about the electronegativity of noble gases like Ne or He. Why?

14. We combine two elements of low electronegativity to form a compound. Which bonding type would you expect for this compound?

15. If two elements with high electronegativity are combined, which bonding results then?

16. If two elements of very different electronegativities are combined, what is the bonding in the compound?

17. Explain the concept of Ketalaar's triangle.

18. Can there be any compounds outside Ketelaar's triangle?

Dr. Kai Landskron (Lehigh University). If you like this textbook, please consider to make a donation to support the author's research at Lehigh University: Click Here to Donate.

1.4: Concept Review Questions Chapter 1 is shared under a not declared license and was authored, remixed, and/or curated by LibreTexts.

- **Concept Review Questions Chapter 1** by Kai Landskron is licensed CC BY 4.0.

1.5: Homework Problems Chapter 1

Homework Problems

Section 1

Exercise 1

Cobalt forms two sulfides, CoS and $Co_2 S_3$. Predict the ratio of the masses of sulfur that combine with a fixed mass of cobalt to form CoS and Co_2S_3

Answer

In Co_2S_3 there are 1.5 S atoms per Co atom

In CoS there is 1 S atom per Co atom

Mass ratio of S in the two compounds is 1:1.5 = **2:3**

Exercise 2

What is true about the Rutherford atom model?

a. It explains why atoms do not send out electromagnetic radiation permanently
b. It explains why alpha particles get scattered by atoms
c. It explains the atomic spectrum of the hydrogen atom
d. It explains the wave-particle dualism

Answer

b) It explains why alpha particles get scattered by atoms

Exercise 3

The Bohr radius (the radius of the electron orbit for the H atom in its ground state) is 5.29×10^{-11} m. Calculate the radius of an electron in the third shell of the H atom according to the Bohr atom model.

Answer

$r_3 = 3^2 \times 5.29 \times 10^{-11}$ m = 47.61×10^{-11} m.

Section 2

Exercise 1

The electron in an H atom undergoes an electronic transition from the 3rd to the 2nd shell. What frequency does the light that is emitted have? The energy of the electron in the first shell is -2.18×10^{-18} J.

Answer

Energy of electron in the 3rd shell: $E_3 = -2.18 \times 10^{-18}$ J / $3^2 = -0.24 \times 10^{-18}$ J

Energy of electron in the 2nd shell: $E_2 = -2.18 \times 10^{-18}$ J / $2^2 = -0.545 \times 10^{-18}$ J

Energy difference between the two electrons: E_3-$E_2 = 0.305 \times 10^{-18}$ J

Frequency of emitted light: $n=(E_3-E_2)/h = 0.305 \times 10^{-18}$ J/ 6.63×10^{-34} Js = 4.60×10^{14} s^-

Exercise 2

What is the mass of a photon with a wavelength of 400 nm that travels though space?

Answer

$\lambda = h/mc \rightarrow m = h/\lambda c = 6.63 \times 10^{-34} Js / (400 \times 10^{-9} m \times 3.00 \times 10^{8} m/s) = 5.525 \times 10^{-36} kg.$

Exercise 3

Two objects are moving at the same speed. Which (if any) of the following statements are true?

a. The DeBroglie wavelength of the heavier object is longer than that of the lighter one.
b. If one object has twice as much mass as the other, its wavelength is one-half of the other
c. Doubling the speed of one of the objects will have the same effect on its wavelength as doubling its mass.

Answer

a) If one object has twice as much mass as the other, its wavelength is one-half of the other

b) Doubling the speed of one of the objects will have the same effect on its wavelength as doubling its mass

Exercise 4

The power of a red laser with a wavelength of 630 nm) is 1.00 Watt (1.00 Js). How many photons per second does the laser emit?

Answer

$\nu = c/\lambda = 3.00 \times 10^{8} m/s / 630 \times 10^{-9} m = 4.76 \times 10^{14} s^{-1}$

$E = h\nu = 6.63 \times 10^{-34} Js \times 4.76 \times 10^{14} s^{-1} = 3.157 \times 10^{-19} J$

$\# photons = 1 J / 3.157 \times 10^{-19} J = 3.2 \times 10^{18}$

Exercise 5

Which of the following waves would you consider to be standing matter wave?

a. The vibration of a drum.
b. Sound traveling through open air.
c. A tsunami.
d. None of the above.

Answer

a) The vibration of a drum.

Exercise 6

Assume an electron travels in a one-dimensional box (as discussed in class) of the length of 1 m. Look up relevant constants in the internet or a suitable textbook.

a. What is the wavelength of the associated standing matter wave in the ground state?
b. What is the velocity of the electron in the ground state?
c. What is the energy of the electron in the ground state?

Answer

a) $\lambda = 2L = 2m$

b) $$v = \frac{h}{m\lambda} = \frac{6.63\times10^{-34}\,m^2kg}{9.1\times10^{-31}\,kgs\times 2m} = 3.6\times10^{-4}\,m/s$$

c) $$E = \frac{1}{2}mv^2 = \frac{1}{2}\times 9.1\times10^{-31}\,kg\times(3.6\times10^{-4})^2\,\frac{m^2}{s^2} = 5.9\times10^{-38}\,J$$

Alternatively the energy can also be calculated the following way giving the same result (within rounding errors):

$$E = \frac{n^2h^2}{8ma} = \frac{1^2\times(6.63\times10^{-34}\,m^2kg/s)^2}{8\times9.1\times10^{-34}\,kg\times1m} = 6.0\times10^{-38}\,J$$

Exercise 7

An electron in the first excited state travels with a velocity of 15 m/s within a one-dimensional box. What is the length of the box?

Answer

$$\lambda = \frac{h}{mv} = \frac{6.63\times10^{-34}\,m^2kg/s}{9.1\times10^{-31}\,kg\times15m/s} = 4.9\times10^{-5}\,m$$

In the first excited state n =2. For n = the length of the box is equal to the wavelength. Therefore the length of the box is 4.9 x 10^{-5} m.

Exercise 8

What are orbitals (more than one answer can be correct)?

a. Wave functions that describe the electrons as three-dimensional standing matter waves in an atom.
b. Spaces inside an atom in which the electron travels as a classical particle.
c. Solutions of the Schrödinger equation for the hydrogen atom.

Answer

a) Wave functions that describe the electrons as three-dimensional standing matter waves in an atom.

c) Solutions of the Schrödinger equation for the hydrogen atom.

Exercise 9

Which quantum numbers l are allowed when the quantum number n is 4?

Answer

l can be 3,2,1,0

Exercise 10

Which quantum numbers m are allowed when the quantum number l is 3?

Answer

-3,-2,-1,0,+1,+2,+3

Exercise 11

What is true about the following wave function?

$$\Psi = \frac{1}{\sqrt{2\pi}} \quad \frac{\sqrt{6}}{2}\cos\theta \quad \frac{4}{81\sqrt{6}a_0 3/2}\left[6 - \frac{r}{a_0}\right]\frac{r}{a_0}e^{-r/3a_0}$$

a. Its does not have angular nodes
b. Its does not have spherical nodes
c. Its amplitude is 0 at the nucleus
d. The wave function represents an s orbital

Answer

c) Its amplitude is 0 at the nucleus

Exercise 12

The angular part of the wavefunction of an orbital has the following form:

$$\Theta\Phi(x,y,z) = \frac{1}{4}\sqrt{\frac{15}{\pi}}\frac{(x^2-y^2)}{r^2}$$

Which planes are the planar nodes in this orbital?

Answer

The wavefunction is 0 for x=y and x=-y. So it is two planes that bisect the x and the y axis.

Exercise 13

Order the following orbitals with respect to their penetration abilities:

4s, 4p, 4d, 4f

Answer

4s > 4p > 4d > 4f

Exercise 14

What is the effective nuclear charge on an electron in an He^+ ion?

Answer

$$\sigma = 0 \rightarrow Z_{eff} = Z = 2$$

Exercise 15

Calculate the orbital energy of a 3p electron in a sulfur atom using the Slater rules.

Answer

$(1s^2)\ (2s^2\ 2p^6)\ (3s^2\ 3p^4)$

$$\sigma = 5\times 0.35 + 8\times 0.85 + 2\times 1 = 10.55$$
$$Z_{eff} = Z - \sigma = 16 - 10.55 = 5.45$$
$$E = -\frac{Z_{eff}^2 \times 13.6eV}{n^2} = -\frac{5.45^2 \times 13.6eV}{3^2} = -44.9eV$$

Exercise 16

Calculate the orbital energy of a 3d electron in a palladium atom using the Slater rules.

Answer

$(1s^2)\ (2s^2\ 2p^6)\ (3s^2\ 3p^6)(3d^{10})(4s^24p^6)(4d^8)(5s^2)$

$$\sigma = 9\times 0.35 + 18 = 21.15$$
$$Z_{eff} = Z - \sigma = 46 - 21.15 = 24.85$$
$$E = -\frac{Z_{eff}^2 \times 13.6eV}{n^2} = -\frac{24.85^2 \times 13.6eV}{3^2} = -933eV$$

Exercise 17

Calculate how much higher the first ionization energy of an oxygen atom is compared to a fluorine atom. Use the Slater rules to answer the question.

Answer

O: $(1s^2\ )\ (2s^2\ 2p^4)$

$$\sigma(2p_{oxygen}) = 5\times 0.35 + 2\times 0.85 = 3.45$$
$$Z_{eff}(2p_{oxygen}) = Z(2p_{oxygen}) - \sigma(2p_{oxygen}) = 8 - 3.45 = 4.55$$
$$E(2p_{oxygen}) = -\frac{Z_{eff}^2 \times 13.6eV}{n^2} = -\frac{4.55^2 \times 13.6eV}{2^2} = -70.4eV$$

$$\sigma(2p_{fluorine}) = 6\times 0.35 + 2\times 0.85 = 3.8$$
$$Z_{eff}(2p_{fluorine}) = Z(2p_{fluorine}) - \sigma(2p_{fluorine}) = 9 - 3.8 = 5.2$$
$$E(2p_{fluorine}) = -\frac{Z_{eff}^2 \times 13.6eV}{n^2} = -\frac{5.2^2 \times 13.6eV}{2^2} = -91.9eV$$

$$E(2p_{fluorine}) - E(2p_{oxygen}) = -91.9eV - (-70.4eV) = -21.5eV$$
$$\rightarrow \Delta IE = IE_{fluorine} - IE_{oxygen} = 21.5eV$$

Dr. Kai Landskron (Lehigh University). If you like this textbook, please consider to make a donation to support the author's research at Lehigh University: Click Here to Donate.

1.5: Homework Problems Chapter 1 is shared under a not declared license and was authored, remixed, and/or curated by LibreTexts.

- **Homework Problems Chapter 1** by Kai Landskron is licensed CC BY 4.0.

CHAPTER OVERVIEW

2: Symmetry and Group Theory

2.1: Symmetry Elements and Operations

2.2: Point Groups

2.3: Matrix Representations of Symmetry Operations and Character Tables

2.4: Concept Review Questions Chapter 2

2.5: Homework Problems Chapter 2

Dr. Kai Landskron (Lehigh University). If you like this textbook, please consider to make a donation to support the author's research at Lehigh University: Click Here to Donate.

This page titled 2: Symmetry and Group Theory is shared under a not declared license and was authored, remixed, and/or curated by Kai Landskron.

2.1: Symmetry Elements and Operations

Symmetry in Chemistry

Symmetry is actually a concept of mathematics and not of chemistry. However, symmetry, and the underlying mathematical theory for symmetry, group theory, are of tremendous importance in chemistry because they can be applied to many chemistry problems. For example it helps us to classify the structures of molecules and crystals, understand chemical bonding, predict vibrational spectra, and determine the optical activity of compounds. We will therefore first discuss the general foundations of symmetry and group theory, and then apply them to chemical problems, in particular chemical bonding.

Let us first find a definition for symmetry. Symmetry is very familiar to us as we associate symmetry with beauty, but very familiar things are not necessarily easy to define scientifically. One common definition is that symmetry is the self-similarity of an object. The more similar parts it has the more symmetric it appears. For example, we would argue that the two wings of the butterfly depicted look similar. If the left wing was very different from the right wing the butterfly would look less symmetric.



Figure 2.1.1 Symmetry depicted through an image of a butterfly (Attribution: Chemlibretexts https://chem.libretexts.org/@api/dek...jpg?revision=2 http://creativecommons.org/licenses/by-nc-sa/3.0/us/)

How can we measure the self-similarity, or symmetry of an object quantitatively? We can do this using the concept of the symmetry operation. It is defined as a movement of an object into an equivalent indistinguishable orientation. The number and kind of symmetry operations that can be carried out defines the symmetry of the object.

Definition: Symmetry Operation

Movement of an object into an equivalent indistinguishable orientation

Symmetry operations are carried out around so-called symmetry elements. A symmetry element is a point, line, or plane about which a symmetry operation is carried out. Let us understand know what symmetry elements and operations exist.

Definition: Symmetry Element

A point, line or plane about which a symmetry operation is carried out

The Identity Operation (*E*)

The most simple operation is the identity operation. It can be denoted by the Schoenflies symbol *E*. Schoenflies symbols are the most common symbols to denote a symmetry operation. The identity operation says that each object is self-similar to itself when you do not move it in any way. This is a trivial statement, but as we will see later, the identity operation is necessary to make the mathematical framework of symmetry, group theory, complete. The identity operation is present in any object. In the example of the depicted snail shell it is the only operation (Fig. 2.1.2).



Figure 2.1.2 Snail shell (Attribution: Petr Kratochvil http://res.publicdomainfiles.com/pdf...8045418010.jpg)

The Proper Rotation Operation

The proper rotation operation is a counter-clockwise rotation about a proper rotational axis by an angle of 360° over an integer number n. After that rotation the object must be indistinguishable from its original form. That means that the object after the rotation must superimpose the original object before the rotation. For example, when n=4, then we rotate around 90°, and after that the object must superimpose its original form. The proper rotational axis is the symmetry element associated with the proper rotation operation. It's Schoenflies symbol is C_n, whereby n is called the order of the rotational axis. A proper rotational operation has the symbol C_n^m, whereby m counts the number of times the operation is carried out. Overall we rotate by and angle of 360°× m/n when we carry out an operation C_n^m. This means that when m=n, then we have rotated around 360° (Fig. 2.1.3). Then all points in the object are at their original position. It is as though we had done nothing with the object. We can also say we have reached the identity *E*. In mathematical form we can say that C_n^n=E. If we rotated one more time, $C_n^{(n+1)}$, then this would be equal to rotating only one time, and thus $C_n^{(n+1)}=C_n^1$. For example if n=4, then rotating four times around 90° will produce the identity. We have rotated around 4 x 90°=360° which is the same a though we had not rotated at all, because all points in the object are in their original position after a 360° rotation. If we rotated 5 times around 90°, it would the same as rotating only one time.

$$C_n^m = 360° \times \frac{m}{n}$$

$$C_n^n = E$$

$$C_n^{n+1} = C_n^1$$

Figure 2.1.3 Properties of the proper rotation operation

If an object has several axes with different order n, then the one with the highest order is called the *principal axis.* If there is more than one axis of the same order, then they get distinguished by primes if they are not conjugate. We will learn about the exact definition of conjugation somewhat later, we can however often see by inspection if two axes are conjugate. This is usually the case when they pass through the object in a equivalent way, and rotate the object in an equivalent way. Axes that pass through less many bonds, get less many primes. This is just a convention, but you have to follow it. An additional rule is that an axis which is in the same position as the principal axis gets the least number of primes. For example, a square planar molecule such as $PtCl_4^{2-}$ has a C_4 principal axis standing perpendicular to the square plane of the molecule. There is an additional C_2 axis where the C_4 axis runs. It is present because one can also rotate around 180°, and not only around 90°. This C_2 axis does not get any prime. You an see that there are four additional C_2 axes, two of them are denoted C_2', and two others are denoted C_2''. You can see that the two axes which only have one prime pass through two Pt-Cl bonds, while the ones that have two primes, do not pass through any bonds. The two C_2' axes are conjugate, meaning that they transform the object in an equivalent way. The two C_2'' axes are also conjugate.

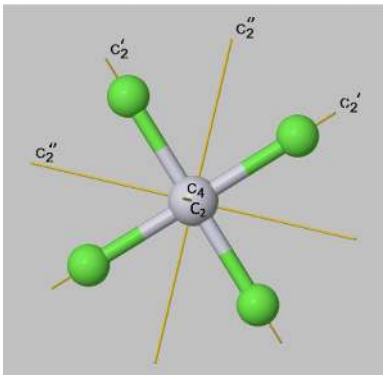


Figure 2.1.4 Proper rotational axes in the $PtCl_4^{2-}$ molecular anion. (Attribution: symotter.org/gallery)

We can now think about how we can write out the axes and their associated proper rotational operations in a systematic way. Let us first look at the symmetry elements, the proper axes: We conventionally write the principal axis first, and then all other axes from their highest to their lowest order. When there are axes of the same order, those with the least number of primes get denoted first, and those with the highest number of primes last. If there are conjugate axes then their number is placed in front of their Schoenflies symbol. For the proper axes of the $PtCl_4^{2-}$ the notation would therefore be: C_4, C_2, $2C_2'$, $2C_2''$. Now let us see how to denote the rotation operations that are associated with these symmetry elements. The notation follows the same rules as for the symmetry elements. In addition, we have to consider that we must not count identical operations twice, we also do not denote the operations that are the same as the identity. For the C_4 axis there are four operations until we reach the identity. C_4^1, C_4^2, C_4^3, and C_4^4. For each of the C_2, C_2', and C_2'' elements there are two operations until the identity is reached. C_2^1, C_2^2, $C_2^{1'}$, $C_2^{2'}$, $C_2^{1''}$, $C_2^{2''}$. The C_4^4, the C_2^2, the $C_2^{2'}$, and the $C_2^{2''}$are the same as the identity and therefore we do not consider them. In addition we can see that the C_4^2 is the same as the C_2^1. This is because the C_4 and the C_2 axes are in the same location, and rotating two times around 90° is the same as rotating one time around 180°. By convention we eliminate the operation associated with the higher order, thus the C_4^2. The overall notation would then be: C_4^1, C_4^3, C_2^1, 2 $C_2^{1'}$ 2 $C_2^{1''}$ (Fig. 2.1.5).

Rotation symmetry operations are: C_4^1, C_4^3, C_2^1, 2 $C_2^{1'}$ 2 $C_2^{1''}$

($C_4^4 = E$, $C_4^2 = C_2^1$, $C_2^2 = E$, $C_2^{2'} = E$, $C_2^{2''} = E$)

Figure 2.1.5 Proper rotation operations in $PtCl_4^{2-}$

The Reflection Operations (σ)

Let us look at reflection operations which are carried out around reflection planes, or mirror planes. Mirror planes have the Schoenflies symbol σ. When we carry out a reflection operation, then we move any point of the object to the other side of the mirror plane. There are two types of mirror planes, so-called horizontal mirror planes and vertical mirror planes. A horizontal mirror plane always stands perpendicular to the principal axis. For example in the depicted BH_3 molecule there is a horizontal mirror plane that stands perpendicular to a C_3 principal axis (Fig. 2.1.6). A horizontal mirror plane has the Schoenflies symbol σ_h.

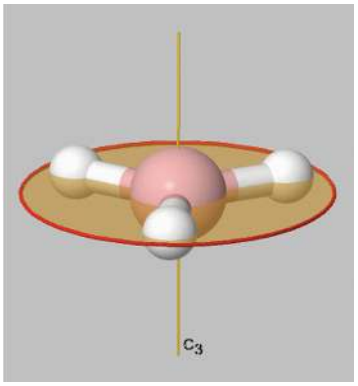


Figure 2.1.6 Visual depiction of the horizontal mirror plane of BH_3, σ_h (Attribution: symotter.org/gallery)

A vertical mirror plane has the property that it contains the principal axis, this means that it is part of the principal axis. It is denoted σ_v. The BH_3 molecule has three vertical axes that pass through the three B-H bonds. You can see that each of them contain

the principal C_3 axis (Fig. 2.1.7). The three vertical mirror planes are conjugate, and therefore they are not distinguished by primes. We can write a coefficient 3 in front of the symbol σ_v to indicate that there are three conjugate vertical mirror planes.

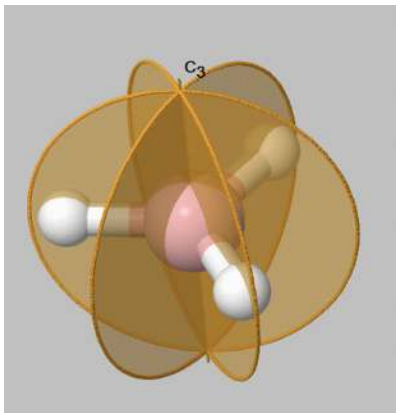


Figure 2.1.7 Visual depiction of the vertical mirror planes of BH_3, 3 σ_v (Attribution: symotter.org/gallery)

Now let us look at how many symmetry operations are associated with a particular mirror plane. Fortunately, things are simple here: There is only one reflection operation associated with one mirror plane. This because reflecting two times at a mirror plane produces the identity E: σ_v^2=E. More generally, when we reflect n times, and n is an even number then this is the same as the identity or, σ_v^n=E (n is even). When n is odd the reflecting n times is the same a reflecting only one time or, $\sigma_v^n=\sigma_v^1$ (n=odd).

The horizontal mirror plane of the BH_3 molecule deserves an additional comment. Carrying out the horizontal reflection does not change the position of any atom. It is important to understand why the operation does exist despite the fact it does not change the position of any atom. The criterion is not whether the position of an atom is changed, but whether the position of the points in the object changes. In the case of the BH_3 molecule the part of the molecule that is located above the mirror plane will be located below the mirror plane after the reflection operation has been carried out. Vice versa any part of the molecule that was formerly below the mirror plane will be located above the mirror plane after the reflection operation has been carried out. For example the lower half of the B atom with be above the mirror plane, and the half above the plane will be below the plane after the execution of the reflection operation.

Like non-conjugate proper rotations are distinguished by primes, also non-conjugate vertical mirror planes must be distinguished by primes. The smaller the number of bonds the vertical mirror plane contains, the larger the number of primes.

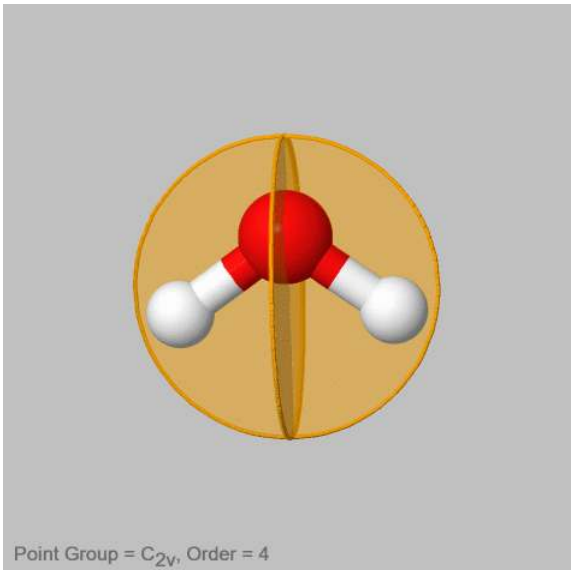


Figure 2.1.8 Non-conjugate vertical mirror planes of H_2O (Attribution: symotter.org/gallery)

For example in the water molecule (Fig. 2.1.8) there are two non-conjugate vertical mirror planes. One contains the two O-H bonds, the other stands perpendicular to the first mirror plane. It is easy to see that these two mirror planes will not move the points

in the atom in an equivalent way, and therefore they are not conjugate. The first mirror plane does not change the position of any atom, while the second one swaps the positions of the two hydrogen atoms. Therefore, the second mirror plane not containing any O-H bonds gets one prime the one that contains the O-H bonds doe not get a prime.

Dihedral Reflection Planes (σ_d)

A special case of a vertical mirror plane is a dihedral mirror plane, denoted σ_d. A dihedral mirror plane bisects the angle between two conjugate C_2 axes.

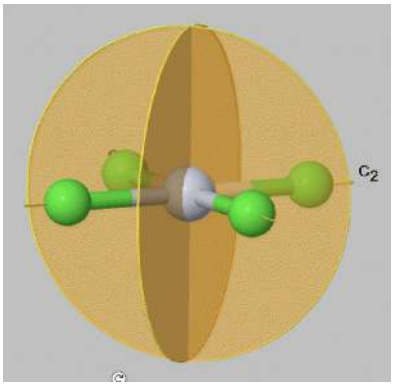


Figure 2.1.9 Dihedral mirror planes of $PtCl_4^{2-}$ (Attribution: symotter.org/gallery)

For example, in the $PtCl_4^{2-}$ anion (FIg. 2.1.9) there are two vertical mirror planes that bisect the angle between the two conjugate C_2 axes that pass through the Pt-Cl bonds. Therefore, these mirror planes are vertical mirror planes σ_d.

The Inversion Operation (*i*)

Let us look next at the inversion operation which is symbolized by a Schoenflies symbol *i*. The symmetry element associated with an inversion, is the inversion center, also called center of symmetry. It is a single point. When an inversion operation is performed, then each point of the object is moved through the inversion center to the other side. Each coordinate in the object (x,y,z) is inverted into the coordinates (-x,-y,-z).

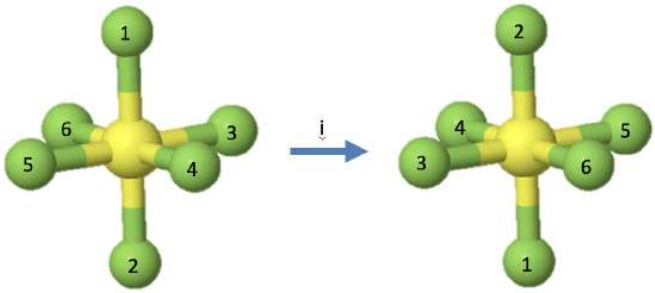


Figure 2.1.10 The inversion operation for SF_6 (Attribution: symotter.org/gallery)

For example, the octahedral molecule SF_6 has an inversion center in the center of the molecule (Fig. 2.1.10). When the inversion operation is carried out, then each fluorine atom is moved through the inversion center to the other side. This means that the fluorine atoms 1 and 2 swap up their positions, the fluorine atoms 3 and 5 swap up their positions, and so do the fluorine atoms 4 and 6. The sulfur atom does not change its position. There is only one inversion operation associated with each inversion center. Inverting two times, or more generally, an integer number of two times produces the identity. Inverting an odd number of times is the same as inverting one time.

The Rotation-Reflection Operation (S_n)

The rotation-reflection operation S_n is the most complex symmetry operation. It is carried out in two steps. First, a rotation around an improper axis is carried out. The angle is determined by the order n of the improper axis, and is 360°/n. This axis is called improper, because the object does not need to superimpose the original object after the rotation. Achieving superposition requires the second step which is the reflection at a mirror plane that stands perpendicular to the improper axis. Only after the second step

the operation is complete. The presence of the rotation-reflection does not require a proper rotational axis or a regular mirror plane σ to exist, however it also do not preclude their existence.

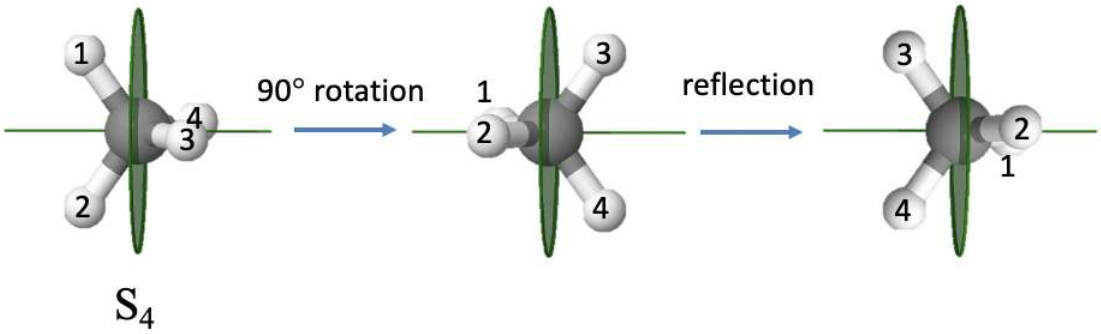


Figure 2.1.11 The improper S_4 rotation for CH_4 (Attribution: symotter.org/gallery)

An example of a molecule with an improper axis is the methane molecule (Fig. 2.1.11). It has an S_4 improper axis. The axis bisects the H-C-H tetrahedral bond angle. The order of the axis is four which requires that we rotate by 90° around this axis. You can see that after we carry out the rotation, the molecule does not superimpose the original molecule. Only after we reflect the rotated molecule at a mirror plane standing perpendicular to the improper axis the molecule superimposes the original molecule.

Properties of the Rotation-Reflection Operation (S_n)

The rotation-reflection has a number of interesting properties. One of the them is that an S_1 operation is the same as a reflection. This is because the order 1 implies a rotation around 360° which produces the identity, and all points within the object are in their original position. This is the same as though we had not rotated at all. This means actually we only did the second step, the reflection, and therefore the S_1 is identical to a "regular" reflection. The second property is that an S_2 operation is the same as an inversion. When you rotate around 180° and then reflect perpendicular to the improper axis of rotation, the positions of the points in the object change exactly the same way as they do when you invert through an inversion center.

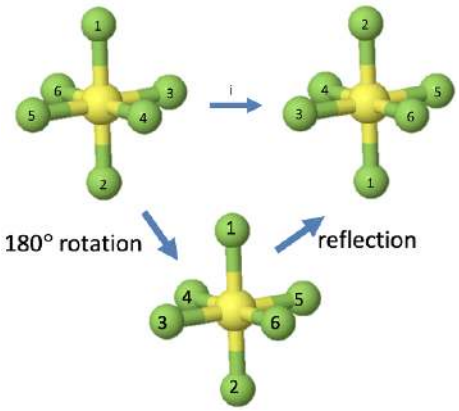


Figure 2.1.12 Rotation-Reflection operations for SF_6 (Attribution: symotter.org/gallery)

Look for example at the SF_6 molecule again (Fig. 2.1.12) which has an inversion center in the center of the atom. We previously saw that when we carry out the inversion, the atoms 1 and 2 swap their position, and so do the atoms 3 and 5, as well as the atoms 4 and 6. Let us carry out the rotation-reflection, and see if the atoms change the same way. Firstly we rotate 180° around an axis that goes through the atoms 1 and 2. This leaves the positions of the atoms 1 and 2 unchanged, but swaps up the positions of the atoms 3 and 5, as well as the atoms 4 and 6. Next we must do a reflection at a plane that stands perpendicular to the improper axis. It is the plane defined by the atoms 3, 4, 5, and 6. Reflection at this plane does not change the positions of the atoms 3, 4, 5, and 6, but it swaps up the positions of the atoms 1 and 2, which lie above and below the plane, respectively. We can see that the positions of the atoms are the same as after the inversion.

The fact that we can express a reflection by an S_1 rotation-reflection, and an inversion by a S_2 rotation-reflection means that the reflection and the inversion are not independent symmetry operations, and we would not need them. The symmetry of an object could be fully described by the identity, proper rotations, and rotation-reflections. However, by convention, we use reflections and

inversions instead of S_1 and S_2, simply because it is easier for the human mind to perform 1-step operations, rather than 2-step operations.

Improper rotations have different properties depending on whether the order of the axis is even or odd. For even orders, the presence of an S_n improper rotational axis implies that there must also be a proper rotational axis with an order n/2. For improper axes of even orders n the identity is produced after n rotation-reflections (Fig. 2.1.13).

$$S_n \text{ with n even} \rightarrow \text{molecule contains } C_{n/2}$$

$$S_n^n = E$$

Figure 2.1.13 Properties of improper rotations with even order *n*

For improper axes of odd order n, carrying out the rotation-reflection n times is the same as carrying out a reflection at a horizontal mirror plane. We need to do the rotation-reflection 2n times to reach the identity (Fig. 2.1.4).

$$S_n \text{ with n odd} \rightarrow \text{molecule contains } C_n \text{ and } \sigma_h$$

$$S_n^n = \sigma_h$$

$$S_n^{2n} = E$$

Figure 2.1.14 Properties of improper axes of odd order *n*

Rotation-Reflections of PF_5 (an example with odd order)

Let us show these properties using two examples. Let us first look at an example with an improper rotation of odd order. The PF_5 molecule has trigonal pyramidal shape with three F atoms in the equatorial plane, and two additional F atoms above and below the plane. The F atoms have been numbered from 1 to 5 as indicated by the subscripts that follow the element symbol (Fig. 2.1.15). The PF_5 has an improper rotational axis S_3 that stands perpendicular to the equatorial plane going through the P-F_1 and P-F_2 bonds. Let us carry out the S_3 symmetry operations step by step and see how the atoms move.

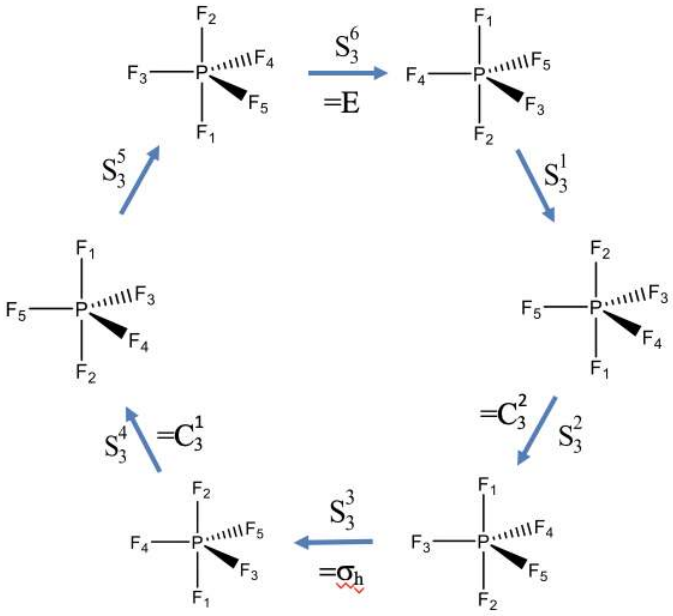


Figure 2.1.15 S_3 symmetry operations for PF_5

We would expect that after we carry out the operation six times the identity will be produced. After three rotation-reflections we would expect that the object has been moved the same way a horizontal mirror plane would do. After the first rotation-reflection the atoms F_1 and F_2 have swapped their positions, and the three F atoms in the equatorial plane have been rotated by 120 degrees counter-clockwise. The F_5 atom now occupies the position of the F_4, the F_4 has been rotated into the position of the F_3, and the F_3 has been moved into the position of the F_5. The second S_3 operation again swaps up the F_2 and F_1 atoms, and rotates the remaining F atoms by 120°. Now the F_5 atoms points toward us, the F_4 atom points away from us, and the F_3 atoms is in the paper plane. Carrying out the operation a third time again swaps the F_1 and F_2 and rotates F_3, F_4, and F_5 counter-clockwise by 120°. Now let us

compare the position of the atoms with the atom positions of the molecule we started with. We see that the position of the equatorial F atoms are same as in the beginning, but the position of the axial F_1 and F_2 atoms have been swapped up. This is equivalent to a reflection at a horizontal mirror plane located within the equatorial plane. This horizontal mirror plane would only swap up the axial F atoms, but would not move the equatorial ones. The S_3^4 operation again swaps up the position of the F_1 and the F_2 atoms, and rotates the equatorial F atoms by 120° counter-clockwise. Now, F_4 points toward us, F_3 points away, and F_5 is in the paper plane. After the fifth rotation-reflection F_1 and F_2 are again swapped so that F_1 is below and F_2 is above the equatorial plane. The atoms F_3, F_4 and F_5 are rotated so that F_3 is in the paper plane, F_5 points toward us, and F_4 points away from us. The sixth rotation-reflection again swaps up F_1 and F_2, and rotates the other F atoms around 120° counter-clockwise. We can now see that the produced molecule is the same as the one we started with, and the identity has been produced.

It is also noteworthy that the S_3^2 and the S_3^4 operation can be expressed by simpler operations, namely C_3^2 and C_3^1 proper rotation operations. We can understand this considering that an S_3^2 operation requires that we reflect two times, and reflecting two times is just like not reflecting at all. So effectively, we only have two rotations around 120° which is equivalent to C_3^2. Similarly, the S_3^4 operation requires to reflect four times, which is the same as not reflecting at all. Thus, effectively, we only rotate four times around 120°. This is the same as rotating only one time around this angle, which is equivalent to a C_3^1 operation.

Using similar considerations, we can also understand why the S_3^3 operation is equivalent to a σ_h. In this case, we rotate 3 x 120° = 360°, and rotating around 360° is the same as not rotating at all. In addition, we carry out a reflection three times. Reflecting an odd number of times is the same as reflecting only one time. Thus overall, we effectively carry out a single reflection only.

Overall, only the S_3^1 and the S_3^5 operations are unique, all others can be expressed by other, simpler operations.

Rotation-Reflections of CH_4 (an example with even order)

Let us illustrate the properties of an improper rotational axis with even order using the example methane (Fig. 2.1.16).

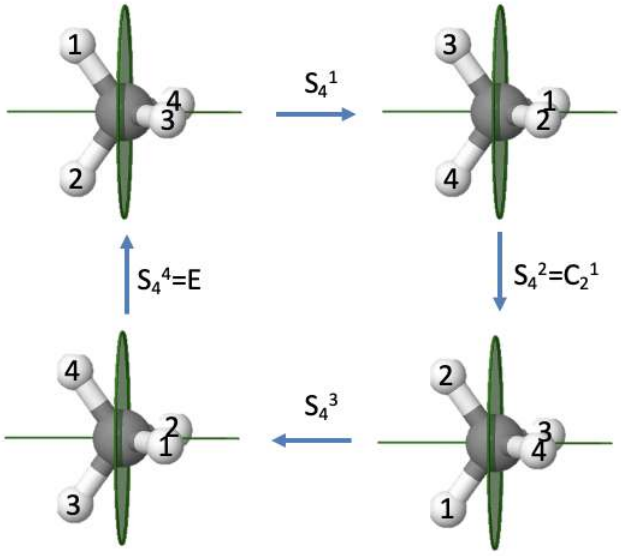


Figure 2.1.16 S_4 symmetry operations for CH_4 (Attribution: symotter.org/gallery)

We previously saw that the methane molecule has an S_4 improper axis. Executing the symmetry operation once moves the H atoms 1 and 2 to the right, whereby atom 1 points to the back and atom 2 points to the front. After the second rotation-reflection the atoms 1 and 2 are reflected back to the left side, but because we have rotated two times by 90° atom 2 points up, and atom 1 points down. Similarly, atoms 3 and 4 are reflected back to the right side, but atom four points toward us and atom 3 points to the back. After three rotation-reflections, the atoms 1 and 2 are again on the right side with atom 2 pointing to the back and atom 1 pointing to the front. Atoms 3 and 4 are on the left with atom 4 pointing up, and atom 3 pointing downward. After the operation is carried out four times, all atoms are back in their original position, meaning the identity has been produced. This is what we expected for an improper rotation of even order. We can see in addition that the S_4^2 operation is the same as an C_2 operation. Rotating two times about 90° is the same as rotating about 180°. Reflecting two times is the same as not reflecting at all. Therefore, effectively, we

only rotated by 180° which is the same as what a C_2^1 operation does. Because an S_4^2 can be expressed by a C_2^1, and an S_4^4 is the same as the identity, only the S_4^1 and the S_4^3 are unique symmetry operations.

The Symmetry of a Molecule

We have now discussed all types of symmetry elements and operations that can exist in an object. Next, let us think about how we can define the overall symmetry of an object. The **overall symmetry** of an object is defined as the sum of all the symmetry operations for this object. If two objects have exactly the same symmetry elements and operations then their symmetry is the same. Using the mathematical language of group theory, the mathematical theory for symmetry, we can say they belong to the same point group. The name point group comes from the fact, that it has at least one invariant point. The number of symmetry operations belonging to a point group is called the order of the point group. Let us see next what different point groups we know and how we can systematically classify them.

Dr. Kai Landskron (Lehigh University). If you like this textbook, please consider to make a donation to support the author's research at Lehigh University: Click Here to Donate.

This page titled 2.1: Symmetry Elements and Operations is shared under a not declared license and was authored, remixed, and/or curated by Kai Landskron.

- **2.1: Symmetry Elements and Operations** by Kai Landskron is licensed CC BY 4.0.

2.2: Point Groups

The Low Symmetry Point Groups

C_1 Point Group

Overall, we divide point groups into three major categories: High symmetry point groups, low symmetry point groups, dihedral point groups, and rotational point groups. Let us begin with the low symmetry point groups. As the name says, these point groups only have few symmetry elements and operations. The point group C_1 is the point group with the lowest symmetry. Molecules that belong to this point group only have the identity as symmetry element.

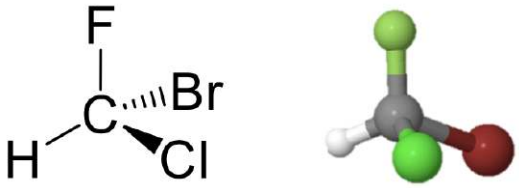


Figure 2.2.1 C_1 point group of bromochlorofluromethane (Attribution: symotter.org/gallery)

An example is the bromochlorofluromethane molecule (Fig. 2.2.1). It has no symmetry element, but the identity. The name C_1 comes from the symmetry element C_1. A C_1 operation is the same as the identity.

C_s Point Group

The point group C_s has a mirror plane in a addition to the identity. An example is the 1,2-bromochloroethene molecule (Fig. 2.2.2).

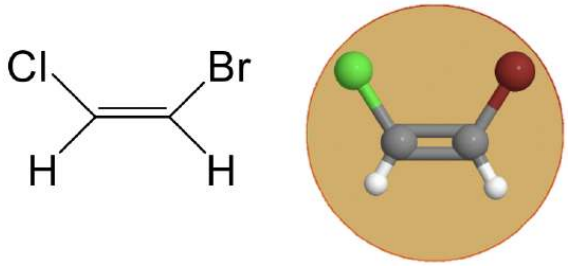


Figure 2.2.2 C_s point group of 1, 2-bromochloroethene (Attribution: symotter.org/gallery)

This is a planar molecule and the mirror plane is within the plane of the molecule. This mirror plane does not move any atoms when the reflection operation is carried out, nonetheless it exists because any point of the molecule above the mirror plane will be found below the mirror plane after the execution of the operation. Vice versa, any point below the mirror plane will be above the mirror plane. This mirror plane does not have a vertical or horizontal mirror plane designation because no proper rotational axes exist.

C_i Point Group

The point group C_i has the inversion as the only symmetry element besides the identity. The point group C_i is sometimes also called S_2 because an S_2 improper rotation-reflection is the same as an inversion. An example is the 1,2-dibromo 1,2-dichloro ethane (Fig. 2.2.3).

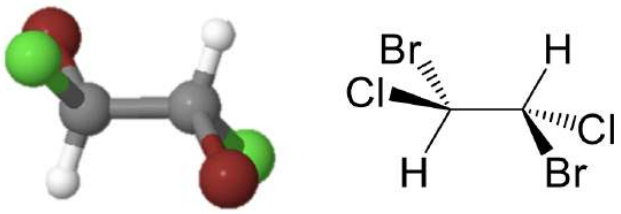


Figure 2.2.3 The C_i point group: 1,2-dibromo 1,2-dichloro ethane (Attribution: symotter.org/gallery)

This molecule looks quite symmetric, but it has inversion center in the middle of the carbon-carbon bond as the only symmetry element. Upon execution of the inversion operation, the two carbons swap up their positions, and so do the two bromine, the two chorine, and the two hydrogen atoms.

The High Symmetry Point Groups

The symmetry elements of the high symmetry point groups can be more easily understood when the properties of platonic solids are understood first. Platonic solids are polyhedra made of regular polygons. In a platonic solid all faces, edges, and vertices (corners) are symmetry-equivalent. We will see that this is a property that can be used to understand the symmetry elements in high symmetry point groups. There are only five possibilities to make platonic solids from regular polygons (Fig. 2.2.4).

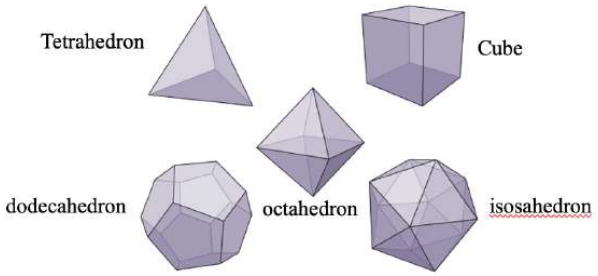


Figure 2.2.4 The platonic solids (Attribution: Drummyfish [CC0] https://commons.wikimedia.org/wiki/F...ransparent.svg)

The first possibility is to construct a tetrahedron from four regular triangles. The second platonic solid is the octahedron made of eight regular triangles. The third possibility is the icosahedron made of twenty triangles. In addition, six squares can be connected to form a cube, and twelve pentagons can be connected to form a dodecahedron. There are no possibilities to connect other regular polygons like hexagons to make a platonic solid.

The icosahedron is the most complex of all platonic solids. If you would like to see and study an icosahedron from the outside and inside, there is one for study on the playground of the Allentown Cedar Beach Park, in Allentown, Pennsylvania.



Figure 2.2.5 Icosahedron at Allentown Cedar Beach Park

The T_d Point Group

The tetrahedron, as well as tetrahedral molecules and anions such as CH_4 and BF_4- belong to the high symmetry point group T_d. Let us find the symmetry elements and symmetry operations that belong to the point group T_d. First, we should not forget the identity operation, E. Next, it is useful to look for the principal axes.

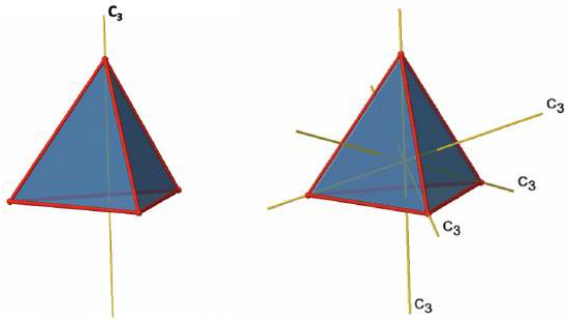


Figure 2.2.6 The C_3 axes in a tetrahedron (Attribution: symotter.org/gallery)

The tetrahedron has four principal C_3 axes (Fig. 2.2.6). It is a property of the high-symmetry point groups that they have more than one principal axis. The C_3 axes go through the vertices of the tetrahedron. Because each C_3 axis goes through one vertex, there are four vertices, and we know that in a platonic solid all vertices are symmetry-equivalent, we can understand that there are four C_3 axes. How many unique C_3 operations are associated with these axes? After three rotations around 120° we reach the identity. Therefore C_3^3=E, and we only need to consider the C_3^1 and the C_3^2 rotation about 120 and 240° respectively. Because there are four C_3 axes, there are four C_3^1 and four C_3^2 operations and eight C_3 operations overall. We can express this by writing the respective numbers as coefficients in front of the Schoenflies symbol for the operations (Fig. 2.2.7).

Symmetry operations: E, $8C_3$

Symmetry operations in detail: E, 4 C_3^1, 4 C_3^2 ($C_3^3 = E$)

Figure 2.2.7 Symmetry operations associated with the C_3 axes in the point group T_d

In addition to the C_3 axes there are C_2 axes (Fig. 2.2.8).

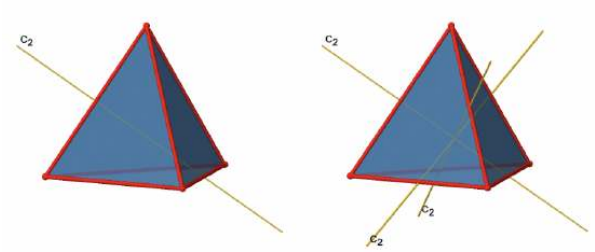


Figure 2.2.8 The C_2 axes in a tetrahedron belonging to the point group T_d (Attribution: symotter.org/gallery)

You can see that a C_2 axis goes through two opposite edges in the tetrahedron. Because a tetrahedron has six edges, and each C_2 axis go through two edges there are 6/2=3 C_2 axes. There is only one C_2 symmetry operation per C_2 axis because we produce the identity already after two rotations. Therefore there are three C_2^1 operations overall (Fig. 2.2.9).

Symmetry operations: $3C_2$

Symmetry operations in detail: 3 C_2^1

Figure 2.2.9 Symmetry operations associated with the C_2 axes in the point group T_d

In addition, the T_d point group has S_4 improper rotation reflections. Like the C_2 axes, they pass through the middle of two opposite edges. This also means that they are superimposing the C_2 axes. Because there are six edges, and two S_4 axes per edge there are 6/2=3 S_4 axes (Fig. 2.2.10).

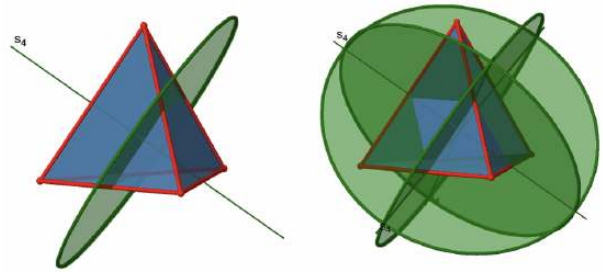


Figure 2.2.10 The S_4 axes in a tetrahedron (Attribution: symotter.org/gallery)

How many operations are associated with these S_4 axes? The order of the axes are even, and therefore we need four S_4 operations to produce the identity. The S_4^2 operation is the same as a C_2^1 operation because reflecting two times is equivalent to not reflecting at all, and rotating two times by 90° is the same as rotating about 180°. Therefore overall, only S_4^1 and S_4^3 operations are unique operations. S_4^2 and S_4^4 can be expressed by the simpler operations C_2^1 and E respectively. Because there are 3 S_4 axes, there are three S_4^1 and three S_4^3 operations. Overall there are six S_4 operations (Fig. 2.2.11).

Symmetry operations: $6S_4$

Symmetry operations in detail: 3 S_4^1, 3 S_4^3

($S_4^4 = E$, $S_4^2 = C_2^1$)

Figure 2.2.11 Symmetry operations associated with the S_4 axes in the point group T_d

There are also mirror planes (Fig. 2.2.11). The planes contain a single edge of the tetrahedron, thereby bisecting the tetrahedron. There a six edges in a tetrahedron, and therefore there are 6/1=6 mirror planes.

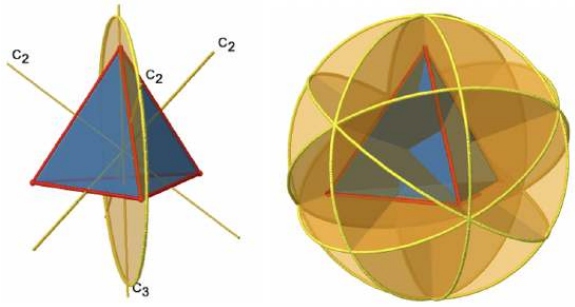


Figure 2.2.12 The mirror planes and C_2 axes in a tetrahedron belonging to the point group T_d (Attribution: symotter.org/gallery)

These planes are dihedral planes because each plane contains a C_3 principal axis and is bisects the angle between two C_2 axes. Overall, there are three C_2 axes and three C_2 operations. There is one reflection operation per mirror plane because reflecting two times produces the identity. Therefore, there are six σ_d reflection operations (Fig. 2.2.12, right and Fig. 2.2.13).

Symmetry operations: $6\sigma_d$

Symmetry operations in detail:6 σ_d

Figure 2.2.13 Reflection operations associated with the σ_d mirror planes in T_d

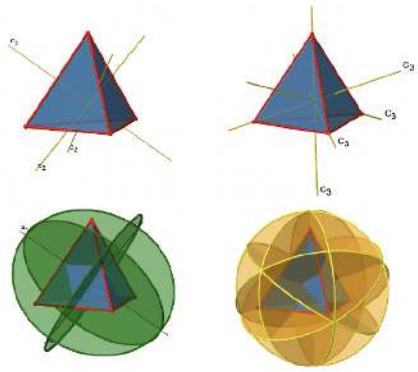


Figure 2.2.14 Summary of symmetry axes and planes in a tetrahedron with the point group T_d (Attribution: symotter.org/gallery)

In sum (Fig.2.2.14 and 2.2.15) we can denote the overall symmetry of the T_d point group the following way: E, $8C_3$, $3C_2$, $6S_4$, $6\sigma_d$. In detail the unique symmetry operations are E, $4C_3^1$, $4C_3^2$, $3C_2^1$, $3S_4^1$, $3S_4^3$, $6\sigma_d$.

Symmetry operations: E, $8C_3$, $3C_2$, $6S_4$, $6\sigma_d$

Symmetry operations in detail: E, 4 C_3^1, 4 C_3^2, 3 C_2^1, 3 S_4^1, 3 S_4^3, 6 σ_d

($C_3^3 = E$, $S_4^4 = E$, $S_4^2 = C_2^1$)

Figure 2.2.15 Summary of the symmetry operations for the point group T_d

The Rotational Subgroup T

The high symmetry point group T is the so-called rotational subgroup of the point group T_d. A rotational subgroup is a point group in which all symmetry operations but the identity and the proper rotations have been removed from a high-symmetry point group. For the point group T this leaves the $4C_3$, the four C_3^2 and the three C_2 operations (Fig. 2.2.17). The S_4 rotation-reflections and the mirror planes have been removed. The point group T is rare.

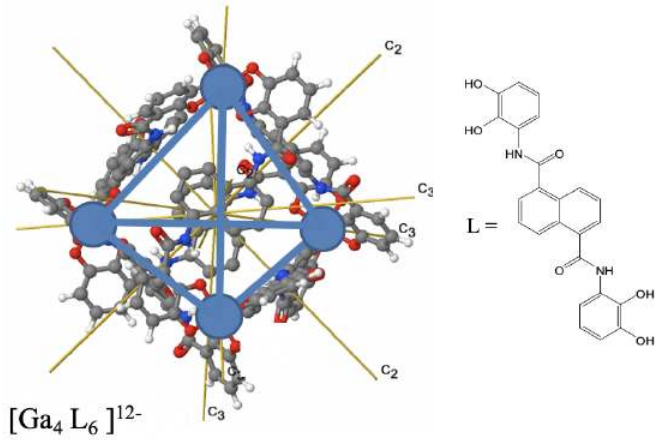


Figure 2.2.16 Symmetry elements in the Ga_4L_6 cage belonging to the point group T (Attribution: symotter.org/gallery)

An example is the depicted Ga_4L_6 cage (Fig. 2.2.16). The Ga atoms occupy the vertices of a tetrahedron, but the point group is not T_d but T because of the shape of the ligands that connect the four Ga atoms.

Symmetry operations: E, $4C_3$, $4C_3^2$, $3C_2$

Figure 2.2.17 Symmetry operations for the Ga_4L_6 cage

The Octahedral Point Group O_h

Another high symmetry point group is the point group O_h. Both the octahedron as well as the cube belong to this point group despite their very different shape (Fig. 2.2.18). Because they belong to the same point group they must have the same symmetry elements and operations. There are many octahedrally shaped molecules, such as the SF_6.

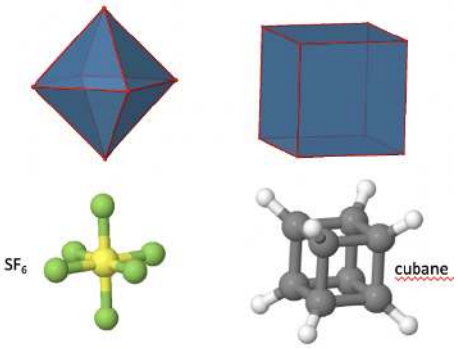


Figure 2.2.18 SF_6 and cubane with cubic and octahedral shape, respectively, belong to the point group O_h (Attribution: symotter.org/gallery)

Molecules with cubic shapes are far less common, because a cubic shape often leads to significant strain in the molecule. An example is cubane C_8H_8. Let us determine the symmetry elements and operations for the point group O_h using the example of the octahedron. If we used the cube, we would get exactly the same results.

There are three C_4 principal axes in the octahedron. They go through two opposite vertices of the octahedron (Fig. 2.2.19). There are three C_4 axes because an octahedron has six vertices which are all symmetry-equivalent because the octahedron is a platonic solid.

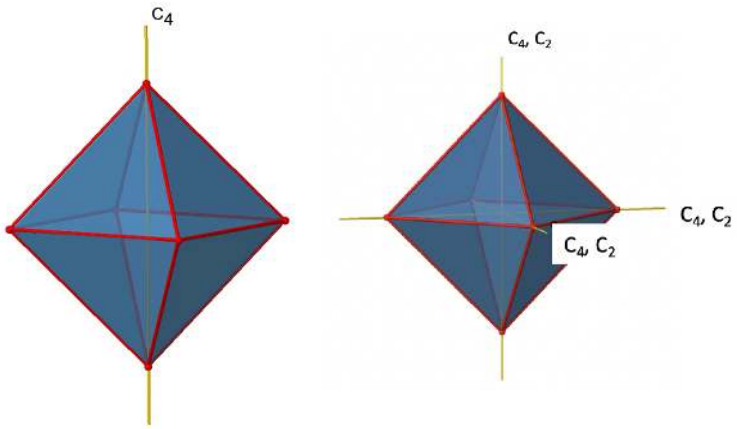


Figure 2.2.19 The C_4 and C_2 axes in the octahedral point group O_h (Attribution: symotter.org/gallery)

We can see that there are also C_2 axes where the C_4 axes run. This is because rotating two times around 90° is the same as rotating around 180°. What are the symmetry operations associated with these symmetry elements? Rotating four times around 90° using the C_4 axes produces the identity. So we have to consider the operations C_4^1, C_4^2, C_4^3 and C_4^4. How many of these are unique? C_4^4 is the same as the identity, so it is not unique, In addition a C_4^2 is identical to a C_2^1, and thus C_4^2 is also not unique, and can be expressed by the simpler operation C_2^1. That leaves the C_4^1 and the C_4^3 as the only unique symmetry operations. Because we have three C_4 axes, there are 2x3=6 C_4 operations, in detail there are $3C_4^1$ and three C_4^3 operations. In addition, there are the three C_2^1 operations belonging the the three C_2 axes (Fig. 2.2.20).

Symmetry elements: E, $3C_4$, 3 C_2

Symmetry operations: E, 6 C_4, 3 C_2
In detail: E, 3 C_4^1, 3 C_4^3
($C_4^2 = C_2^1$, C_4^4 = E)

Figure 2.2.20 C_4 and C_2 symmetry operations in the octahedral point group O_h

In addition, there are four C_3 axes (Fig. 2.2.21). They are going through the center of two opposite triangular faces of the octahedron.

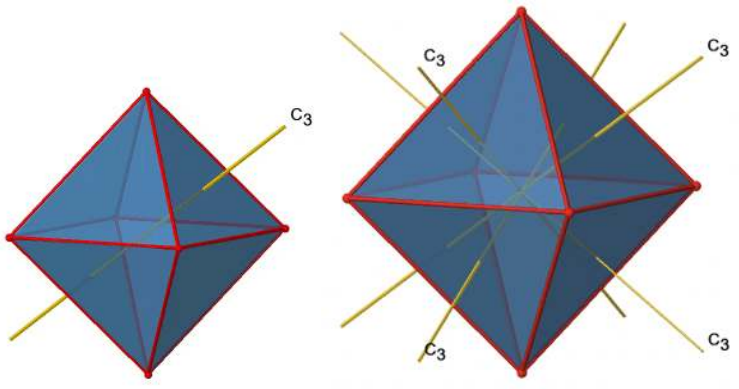


Figure 2.2.21 The C_3 axes in the octahedral point group O_h (Attribution: symotter.org/gallery)

You see above a single C_3 axis, and on the right hand side all four of these axes. How can we understand that there are four axes? An octahedron has overall eight triangular faces, and each C_3 axis goes through two opposite faces, so there are 8/2=4 C_3 axes. Each C_3 axis has the C_3^1 and the C_3^2 as unique symmetry operations. The C_3^3 is the same as the identity. So overall we have 4x2=8 operations, four of them are C_3^1, and four of them are C_3^2 (Fig. 2.2.22).

Symmetry elements: $4C_3$
Symmetry operations: $8\ C_3$
In detail: $4\ C_3^1$, $4\ C_3^2$
$(C_3^3 = E)$

Figure 2.2.22 Symmetry operations of C_3 in the octahedral point group O_h

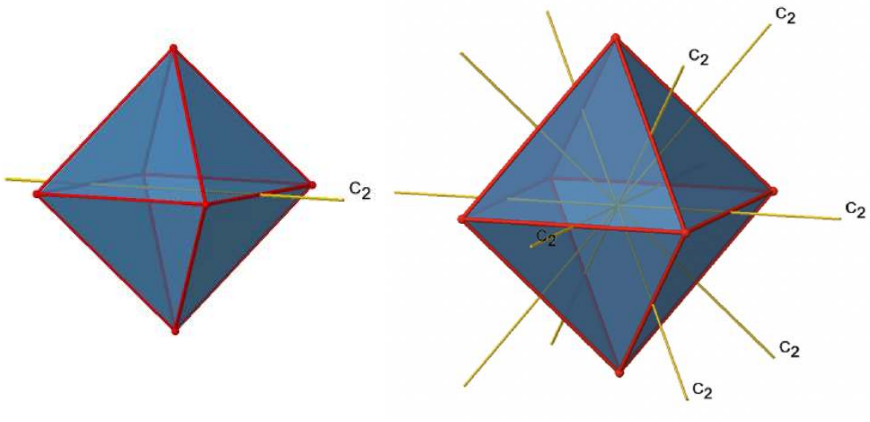


Figure 2.2.23 The C_2' axes in the octahedral point group O_h (Attribution: symotter.org/gallery)

In addition to the C_2 axes that superimpose the C_4 axes, there are C_2' axes which go though two opposite edges of the octahedron (Fig. 2.2.23). How many of them are there? An octahedron has twelve edges, and because each C_2' passes through two edges, there must be 12/2=6 C_2' axes. These axes have primes because they are not conjugate to the C_2 axes that superimpose the C_4 axes. For each C_2' axis there is only the C_2'^{1} as the unique symmetry operation, and therefore there are overall 6 C_2'^{1} symmetry operations (Fig. 2.2.24).

Symmetry elements: $6\ C_2$'
Symmetry operations: $6\ C_2$'^{1}

Figure 2.2.24 Symmetry operations of C_2' in the octahedral point group O_h

Let us look at the mirror planes next (Fig. 2.2.25). There are horizontal mirror planes that stand perpendicular to the C_4 principle axes. You can see a single one of them below on the left.

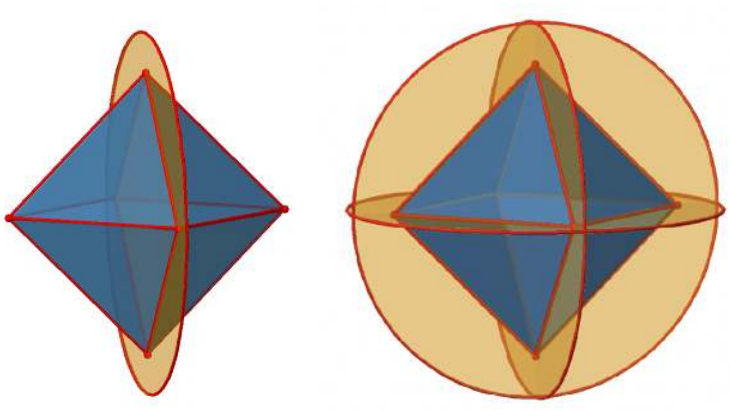


Figure 2.2.25 The horizontal mirror planes in the octahedral point group O_h (Attribution: symotter.org/gallery)

Note that this mirror plane also contains two axes, in addition to the one to which it stands perpendicular. Because it contains two principal C_4 axes, it has also properties of a vertical mirror plane. Nonetheless, we call it a horizontal mirror plane because it stands perpendicular to the third C_4. The horizontal properties trump the vertical ones, so to say. You can see that a single mirror plane contains four edges of the octahedron. Because there are twelve edges, there are 12/4=3 horizontal mirror planes. There is one

mirror plane per principal C_4 axis. There are three horizontal reflection operations because there is always only one reflection operation per mirror plane (Fig. 2.2.26).

Symmetry elements: $3\sigma_h$
Symmetry operations: $3\sigma_h$

Figure 2.2.26 Symmetry operations associated with horizontal mirror planes in the octahedral point group O_h

Next let us look for vertical mirror planes (Fig. 2.2.27). A vertical mirror plane is depicted below on the left.

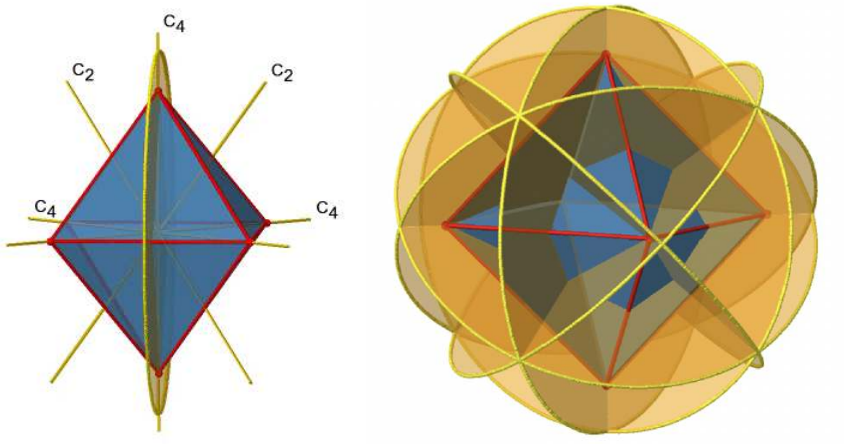


Figure 2.2.27 The vertical mirror planes in the octahedral point group O_h (Attribution: symotter.org/gallery)

You can see that - contrast to the horizontal mirror planes - it does not contain any edges. Rather, it cuts through two opposite edges. You can see that this plane contains a C_4 axis, but it does not stand perpendicular to the other two C_4 axes. Therefore it has only the properties of a vertical mirror plane. You can see however, that the mirror plane bisects the angle between two C_2' axes which also depicted. This makes the vertical mirror planes dihedral mirror planes, σ_d. How may of them do we have? As previously mentioned, each mirror plane cuts through two opposite edges. There are twelve edges in an octahedron, and thus there are 12/2=6 dihedral mirror planes. You can see all of them on the right side of Fig. 2.2.27. Each mirror plane is associated with one reflection operation, therefore there are six dihedral reflection operations (Fig. 2.2.28).

Symmetry elements: $6\ \sigma_d$
Symmetry operations: $6\ \sigma_d$

Figure 2.2.28 Symmetry operations associated with vertical mirror planes in the octahedral point group O_h

Next we can ask if the point group O_h has an inversion center? Yes, there is one in the center of the octahedron (Fig. 2.2.29)!

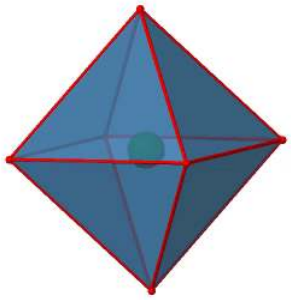


Figure 2.2.29 The inversion center of the octahedral point group O_h (Attribution: symotter.org/gallery)

Each point in the octahedreon can be moved through the inversion center to the other side, and the produced octahedron will superimpose the original one. There is always one inversion operation associated with an inversion center (Fig. 2.2.30).

Symmetry elements: i
Symmetry operations: i

Figure 2.2.30 Symmetry operations associated with the inversion center in the octahedral point group

Next, let us look for rotation-reflections. You can see an S_6 rotation-reflection operation below (Fig. 2.2.31, left).

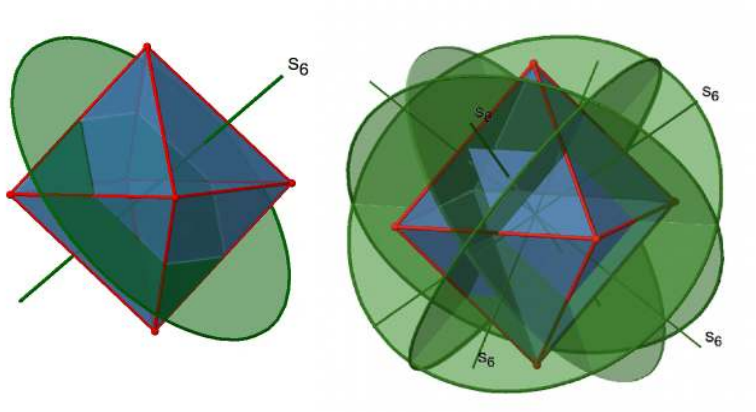


Figure 2.2.31 The S_6 rotation-reflection element of the octahedral point group O_h (Attribution: symotter.org/gallery)

The improper S_6 axis passes though the centers of two opposite triangular faces. One can see that rotation about 60° alone does not make the octahedron superimpose. The reflection at a plane perpendicular to the improper axis is required to achieve superposition. Overall, the rotation-reflection swaps up the position of the two opposite triangular faces. How many S_6 improper axes are there? Since each S_6 passes through two faces, and an octahedron has 8 faces there must be 8/2=4 S_4 axes. You can see all of them above (Fig. 2.2.31, right). Note that they are in the same position as the $4C_3$ axes we previously discussed. How many unique operations are associated with them? For an S_6 axis we need to consider operations from S_6^1 to S_6^6. S_6^6 is the same as the identity so it is not unique. The S_6^2 is the same as a C_3^1 because rotating two times round 60° is the same as rotating around 120°, and reflecting twice is the same as not reflecting at all. Similarly, an S_6^4 is the same as an C_3^2. Rotating four time by 60° is the same as rotating two times by 120° and reflecting four times is the same as not reflecting at all. Further, an S_6^3 is the same as an inversion. After three 60° rotations we have rotated by 180°. If we reflect after that, then this is the same as an S_2^1 operation which is the same as an inversion. Therefore, only the S_6^1 and the S_6^5 operations are unique, all other operations can be expressed by simpler operations (Fig. 2.2.32).

Symmetry elements: 4 S_6
Symmetry operations: 8 S_6
In detail $4S_6^1$, $4S_6^5$
($S_6^2=C_3^1$, $S_6^3=i$, $S_6^4=C_3^2$, $S_6^6=E$)

Figure 2.2.32 Symmetry operations of the rotation-reflection S_6 of the octahedral point group O_h

The octahedron also has S_4 improper axes, and you can see one of them below (Fig. 2.2.33, right).

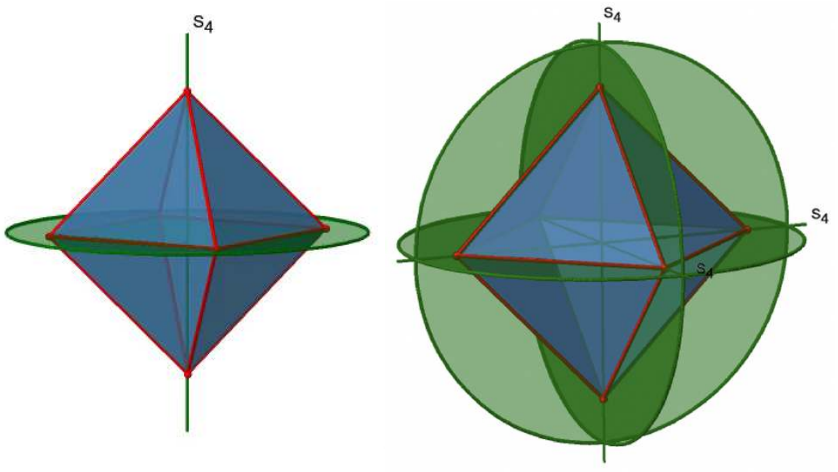


Figure 2.2.33 The S_4 improper axis of the octahedral point group O_h (Attribution: symotter.org/gallery)

It goes through two opposite corners of the octahedron. The S_4 improper axis seemingly does the same as the C_4 axis that goes through the same two opposite vertices, but actually does not. While rotating around 90° already makes the octahedron superimpose with its original form, executing the reflection operation after the rotation swaps up the position of the two vertices, and generally all points of the octahedron above and below the plane, respectively. Overall the S_4 moves the points within the object differently compared to the C_4 which makes it an additional, unique symmetry element. There are overall three S_4 improper axes because the octahedron has six vertices and one S_4 passes through two vertices (Fig. 2.2.34).

Symmetry elements: 3 S_4
Symmetry operations: 6 S_4
In detail: $3S_4^1$, $3S_4^3$
($S_4^2=C_2'$, $S_4^4=E$)

Figure 2.2.34 Symmetry operations associated with the S_4 improper axis of the octahedral point group O_h

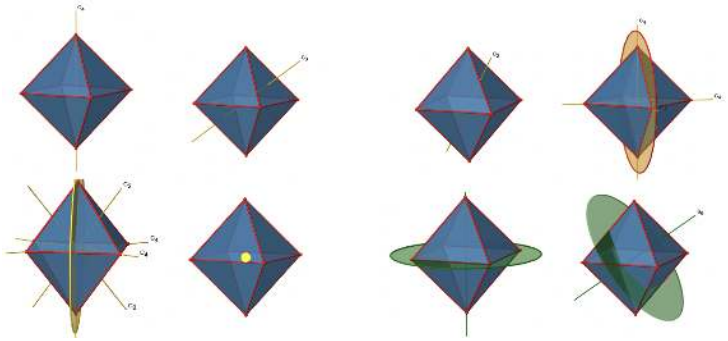


Figure 2.2.35 An overview over all symmetry elements in the octahedral point group O_h (Attribution: symotter.org/gallery)

Here is an overview over all the symmetry elements and operations (Fig. 2.2.35 and 2.2.36). Overall, there are 48 different unique operations that one can perform!

Symmetry elements: E, i, $4S_6$, $4C_3$, $3S_4$, $3C_4$, $6C_2$, $3\,C_2$, $3\sigma_h$, $6\sigma_d$
Symmetry operations: E, i, $8\,S_6$, $8\,C_3$, $6\,S_4$, $6\,C_4$, $6\,C_2$, $3\,C_2$, $3\,\sigma_h$, $6\,\sigma_d$
In detail: E, i, $4\,S_6^1$, $4\,S_6^5$, $4\,C_3^1$, $4\,C_3^2$, $3\,S_4^1$, $3\,S_4^3$, $3\,C_4^1$, $3\,C_4^3$, $6\,C_2$, $3\,C_2$, $3\,\sigma_h$, $6\,\sigma_d$
($S_6^2=C_3^1$, $S_6^3=i$, $S_6^4=C_3^2$, $S_6^6=E$; $C_3^3=E$. $S_4^2=C_2^1$, $S_4^4=E$, $C_4^2=C_2^1$, $C_4^4=E$)

Figure 2.2.36 Summary over all symmetry operations and elements of the octahedral point group O_h

Like the point group T_d , also the point group O_h has a rotational subgroup, named O. It has the identity and the same proper rotations as the point group O_h, but no other symmetry operations (Fig. 2.2.38). An example is the polyoxometalate cluster core shown below (Fig. 2.2.37). Polyoxometalates are cluster anions of the group 5 and 6 elements.

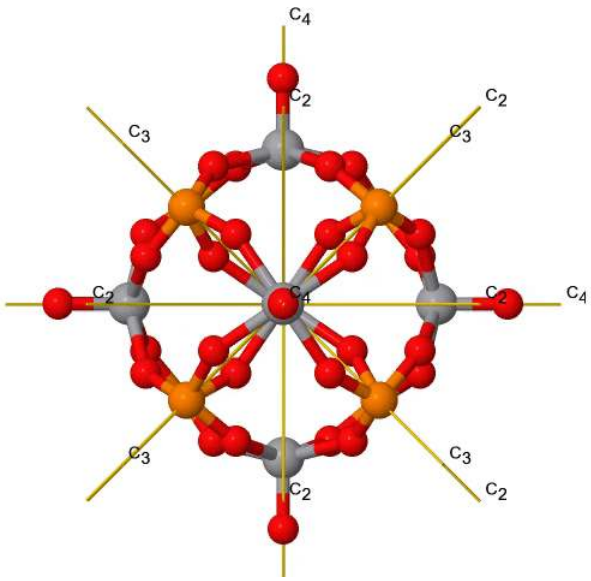


Figure 2.2.37 Proper rotations in a $V_6P_8O_{24}$ polyoxometalate cluster core. The C_3 rotation is animated. (Attribution: symotter.org/gallery)

The point group O is generally rare.

Symmetry elements: E, ~~i, $4S_6$~~, $4C_3$, ~~$3S_4$~~, $3C_4$, $6C_2$, $3\ C_2$, ~~$3\sigma_h$, $6\sigma_d$~~
Symmetry operations: E, ~~i, $8\ S_6$~~, $8\ C_3$, ~~$6\ S_4$~~, $6\ C_4$, $6\ C_2$, $3\ C_2$, ~~$3\ \sigma_h$, $6\ \sigma_d$~~
In detail: E, ~~i, $4\ S_6^1$, $4\ S_6^5$~~, $4\ C_3^1$, $4\ C_3^2$, ~~$3\ S_4^1$, $3\ S_4^3$~~, $3\ C_4^1$, $3\ C_4^3$, $6\ C_2$, $3\ C_2$, ~~$3\ \sigma_h$, $6\ \sigma_d$~~

Figure 2.2.38 Symmetry elements and operations in the point group O (relative to O_h)

Another high symmetry point group is the point group T_h. It can also be derived from the point group O_h. In this case the S_4, the C_4, the C_2', and the σ_d operations are removed from the octahedral symmetry. An example is the hexapyridyl iron (2+) cation (Fig. 2.2.39).

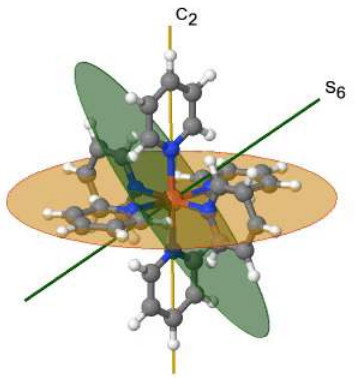


Figure 2.2.39 The hexapyridyl iron (2+) cation and its S_6 and C_2 symmetry elements. An S_6 operation is animated.

You can see that the N-atoms of the pyridyl-ligands surround the Fe atoms octahedrally, but the symmetry is reduced from O_h to T_h because of the planar shape of the pyridyl-ligands. In particular the C_4 symmetry is reduced to C_2. This reduction in symmetry leads to elimination of the S_4, the C_2', and the σ_d symmetry elements (Fig. 2.2.40).

T_h group (symmetry elements: E, i, $4S_6$, $4C_3$, $3C_2$, $3s_h$) can also be considered as a result of reducing **O_h** group symmetry (E, i, $4S_6$, $4C_3$, ~~$3S_4$, $3C_4$, $6C_2$~~, $3\ C_2$, $3\sigma_h$, ~~$6\sigma_d$~~)
by eliminating C_4, S_4 and some C_2 axes and s_d planes

Symmetry operations: i, $8\ S_6$, $8\ C_3$, $3\ C_2$, $3\ \sigma_h$,

Figure 2.2.40 Symmetry operations in $Fe(py)_6^{2+}$ in the point group T_h

The I_h Point Group

The two remaining platonic solids, the icosahedron and the dodecahedron, belong both to the icosahedral point group I_h. This is despite they are made of different polygons (Fig. 2.2.41).

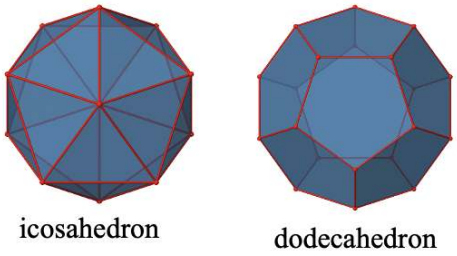


Figure 2.2.41 The icosahedron and dodecahedron of the I_h point group (Attribution: symotter.org/gallery)

Because they belong to the same point group, they have exactly the same symmetry operations. An example for a molecule with icosahedral shape is the molecular anion $B_{12}H_{12}^{2-}$. An example for a molecule with dodecahedral shape is the dodecahedrane $C_{20}H_{20}$.

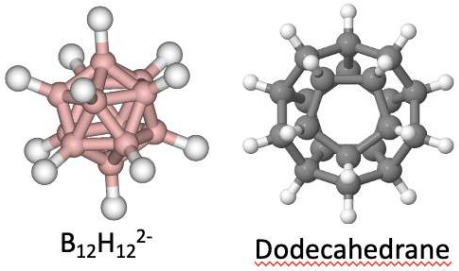


Figure 2.2.42 $B_{12}H_{12}^{2-}$ and the dodecahedrane (Attribution: wikiwand.com https://upload.wikimedia.org/Wikipedia/commons/thumb/9/97/Dodecaborane-3D-balls.png/640px-Dodecaborane-3D-balls.png)

Let us determine the symmetry elements and symmetry operations for the example of the icosahedron. We could also use the dodecahedron, and the results would be the same. The principal axes of the icosahedron are the C_5 axes. You can see one of them, going through the center of the pnetagon comprised of five triangular faces below (Fig. 2.2.43).

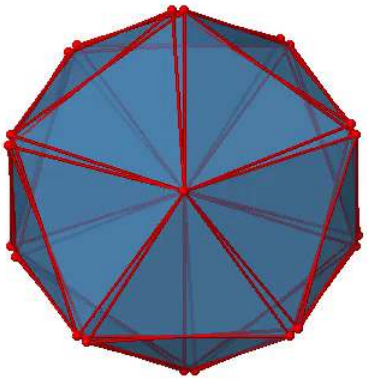


Figure 2.2.43 One of the C_5 axes of the icosahedron stands perpendicular to the paper plane going through the center of a pentagon of the icosahedron (Attribution: symotter.org/gallery)

You can understand that there is a C_5 when considering that there are five triangular faces making a pentagon. The C_5 axis sits in the center of the pentagon. We can see that when we rotate around this C_5 axis, then the produced icosahedron superimposes the original one. The C_5 axis goes through two opposite vertices of the icosahedron. Because an isosahedron has 12 vertices, there must be six C_5 axes overall. You can see all of them below (Fig. 2.2.44).

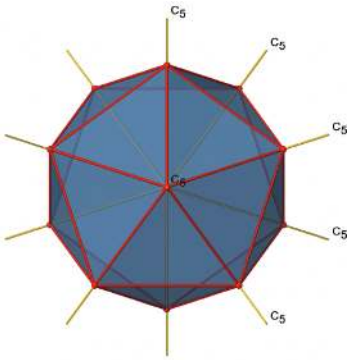


Figure 2.2.44 The C_5 axes of the icosahedron (Attribution: symotter.org/gallery)

There are four unique symmetry operations associated with a single C_5 axis, namely the C_5^1, the C_5^2, the C_5^3, and the C_5^4. The C_5^5 is the same as the identity. Because there are six C_5 axes, there are overall 6x4=24 C_5 symmetry operations (Fig. 2.2.45).

Symmetry elements: 6 C_5
Symmetry operations: 24 C_5
In detail: 6 C_5^1, 6 C_5^2, 6 C_5^3, 6 C_5^4 (C_5^5=E)

Figure 2.2.45 Symmetry operations associated with the C_5 axis of icosahedral point group

In addition, there are C_3 axes. One of them is shown below, and you can see that it passes through the centers of two opposite triangular faces (Fig. 2.2.46).



Figure 2.2.46 One of the C_3 axes of the icosahedral point group (Attribution: symotter.org/gallery)

As one rotates by 120° the atoms on the triangular faces change their position, and the resulting icosahedron superimposes the original one. As the name icosahedron says, there are twenty faces overall.

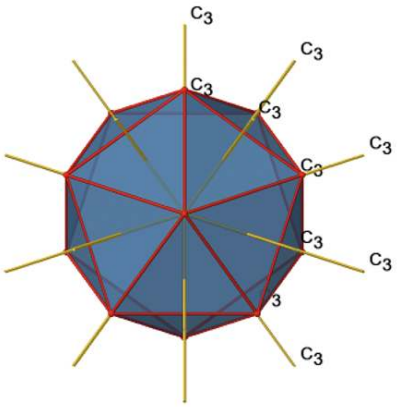


Figure 2.2.47 The C_3 axes of the icosahedral point group (Attribution: symotter.org/gallery)

Because one C_3 passes through two opposite axes, there are 20/2=10 C_3 axes overall (Fig. 2.2.47). Each C_3 axis is associated with two symmetry operations, namely C_3^1, and C_3^2. Thus, there are overall 10x2=20 C_3 symmetry operations.

Symmetry elements: 10 C_3
Symmetry operations: 20 C_3
In detail: 10 C_3^1, 10 C_3^2 (C_3^3=E)

Figure 2.2.48 Symmetry operations of the C_3 axes of the icosahedral point group

There are also C_2 axes (Fig. 2.2.49). They pass through the centers of two opposite edges of the icosahedron. Rotating around the C_2 axis shown makes the icosahedron superimpose.

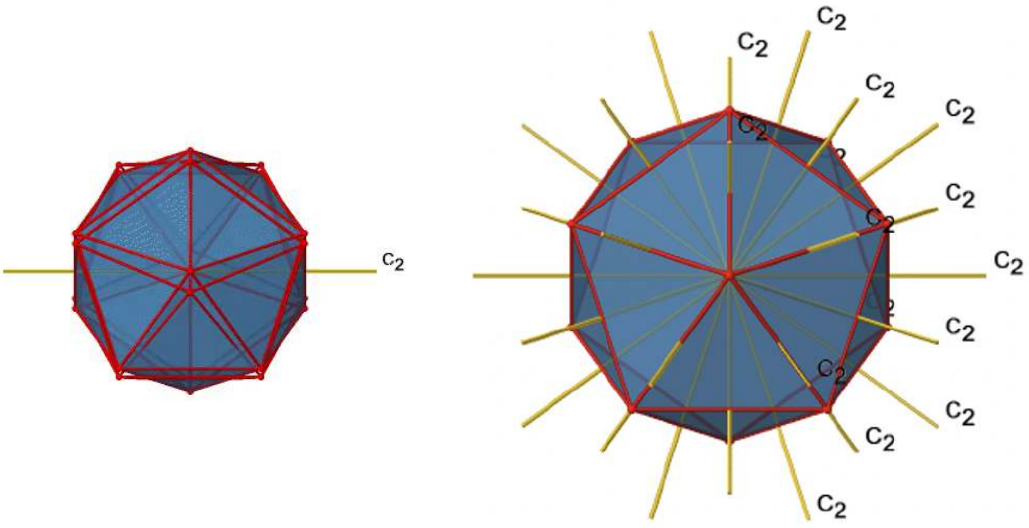


Figure 2.2.49 The C_2 axes of the icosahedral point group (Attribution: symotter.org/gallery)

An isosahedron has overall 30 edges. Because one C_2 axis passes through the centers of two opposite edges, we can understand that there are 30/2=15 C_2 axes. There is one unique C_2 operation per axis, and therefore there are 15 C_2 operations (Fig. 2.2.50).

Symmetry elements: 15 C_2
Symmetry operations: 15 C_2'
In detail: 15 C_2'^{1}

Figure 2.2.50 Symmetry operations associated with the C_2 axes of the icosahedral point group

We have now found all proper rotations. Let us look for mirror planes, next. You can see a mirror plane below (Fig. 2.2.51).

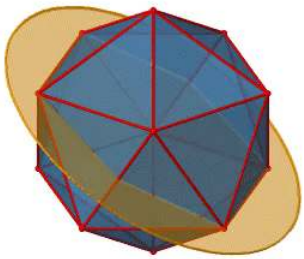


Figure 2.2.51 A mirror plane in the icosahedral point group (Attribution: symotter.org/gallery)

It contains two opposite edges. It also bisects two other edges. An icosahedron has overall 30 edges, therefore there are 30/2=15 mirror planes. You can see all of them below (Fig. 2.2.52 and Fig. 2.2.53)).

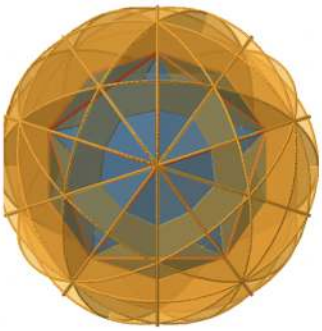


Figure 2.2.52 All the mirror planes in the icosahedral point group (Attribution: symotter.org/gallery)

Symmetry elements: 15 σ
Symmetry operations: 15 σ

Figure 2.2.53 Symmetry operations of the mirror planes in the icosahedral point group

The icosahedron also has an inversion center in the center of the icosahedron (Fig. 2.2.54 and Fig. 2.2.55)).



Figure 2.2.54 The inversion center in the icosahedron (Attribution: symotter.org/gallery)

As we carry out the associated, one symmetry operation, all points in the isosahedron move through the inversion center to the other side.

Symmetry elements: i
Symmetry operations: i

Figure 2.2.55 Symmetry operations of the inversion planes in the icosahedral point group

Let us now look for improper rotations. The improper rotational axes with the highest order are S_{10} axes. They are located in the same position as the C_5 axes, and go through two opposite corners (Fig. 2.2.56).

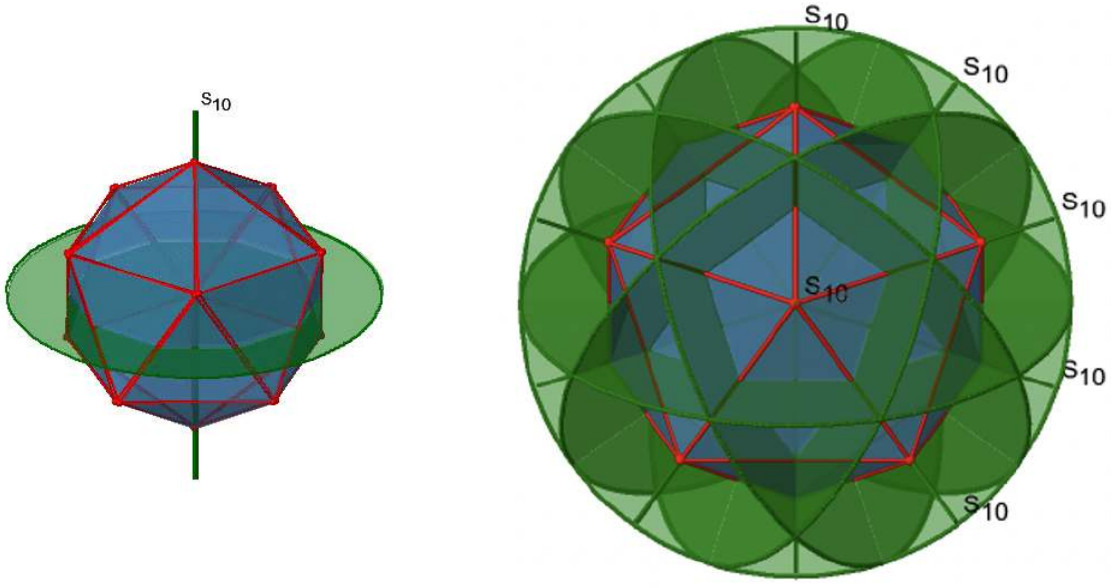


Figure 2.2.56 The S_{10} improper rotational axes in the icosahedral point group (Attribution: symotter.org/gallery)

The S_{10} exists because in an icosahedron there are pairs of co-planar pentagons that are oriented staggered relative to each other. The rotation around 36° brings one pentagon in eclipsed position relative to the other, but superposition is only achieved after the reflection at the mirror plane perpendicular to the rotational axis. Because one S_{10} passes through two opposite vertices, and there

are 12 vertices there are 6 S_{10} improper axes. For each axis there are four unique symmetry operations, the S_{10}^1, the S_{10}^3, the S_{10}^7, and the S_{10}^9. Therefore, there are overall 4x6=24 operations possible (Fig. 2.2.57).

Symmetry elements: 6 S_{10}
Symmetry operations: 24 S_{10}
In detail: 6 S_{10}^1, 6 S_{10}^3, 6 S_{10}^7, 6 S_{10}^9 ($S_{10}^2=C_5^1$, $S_{10}^4=C_5^2$, $S_{10}^5=i$, $S_{10}^6=C_5^3$, $S_{10}^8=C_5^4$)

Figure 2.2.57 Symmetry operations associated with the S_{10} improper rotational axes of the icosahedral point group

Are the lower order improper rotational axes? Yes, there are S_6 axes that pass through the centers of two opposite triangular faces (Fig. 2.2.58). This symmetry element exists because the two triangular faces are in staggered orientation to each other. Rotation alone brings one face in eclipsed orientation relative to the other, but reflection at a mirror plane perpendicular to the axis is required to achieve superposition. The S_6 axes are in the same location as the C_3 axes.

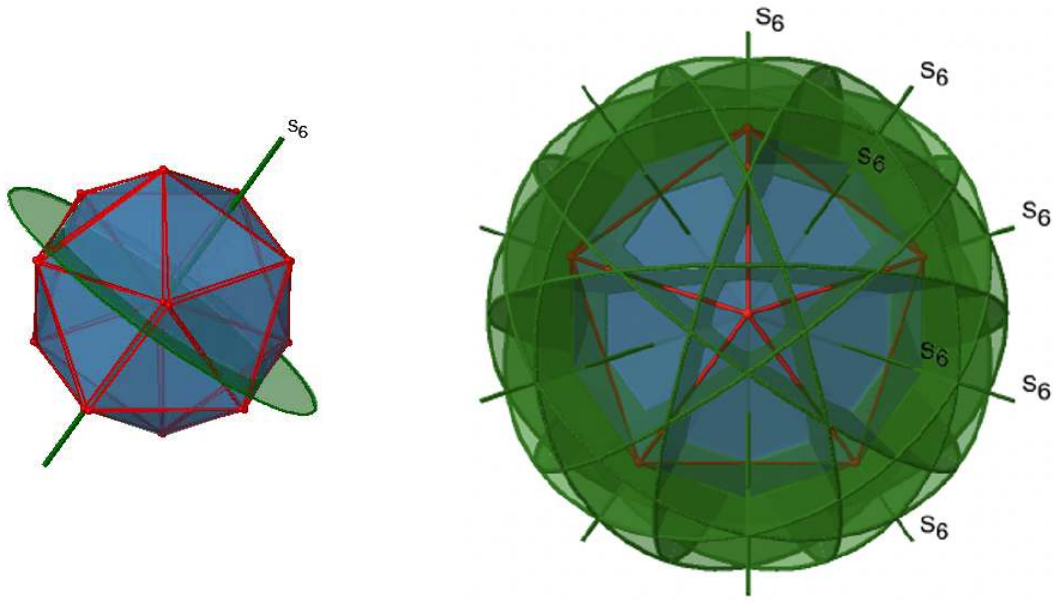


Figure 2.2.58 The S_6 rotation-reflections in the icosahedral point group (Attribution: symotter.org/gallery)

There are 10 S_6 axes because there are twenty faces and one axis passes through two opposite faces. Only the S_6^1 and the S_6^5 operations are unique S_6 operations, all others can be expressed by simpler operations. Therefore there are overall 10 S_6^1+10 S_6^5 = 20 S_6 operations (Fig. 2.2.59).

Symmetry elements: 10 S_6
Symmetry operations: 20 S_6
In detail: 10S_6^1, 10 S_6^5 ($S_6^2=C_3^1$, $S_6^3=i$, $S_6^4=C_3^2$)

Figure 2.2.59 Symmetry operations associated with the S_6 rotation-reflections in the icosahedral point group

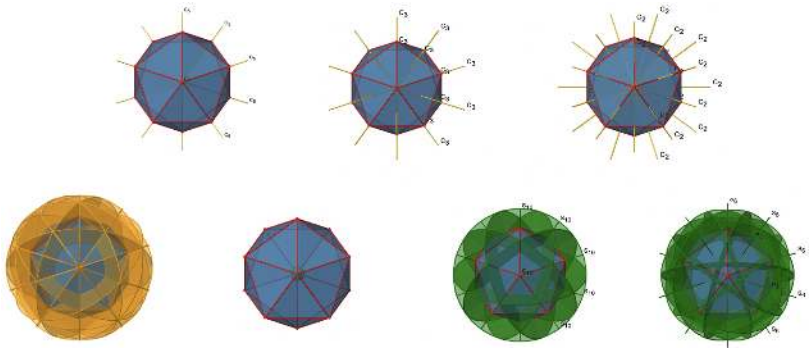


Figure 2.2.60 The symmetry elements of the icosahedral point group (Attribution: symotter.org/gallery)

We have now found all symmetry operations for the I_h symmetry. There are overall 120 operations making the point group I_h the point group with the highest symmetry (Fig. 2.2.60 and Fig. 2.2.61).

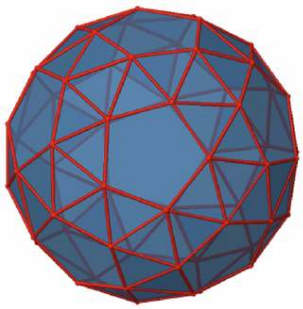
Symmetry elements: E, 6 C_5, 10 C_3, 15 C_2, 15 σ, i, 6 S_{10} , 10 S_6

Symmetry operations: E, 24 C_5, 20 C_3 , 30 C_2', 15 σ, i, 24 S_{10}, 20 S_6

In detail: E, 6 C_5^1, 6 C_5^2, 6 C_5^3, 6 C_5^4, 10 C_3^1, 10 C_3^2, 30 C_2'^{1}, 15 σ, i, 6 S_{10}^1, 6 S_{10}^3, 6 S_{10}^7, 6 S_{10}^9, 10S_6^1, 10 S_6^5

Figure 2.2.61 Summary of the symmetry operations of the icosahedral point group

Also the point group I_h has a rotational subgroup.



Snub-dodecahedron

Figure 2.2.62 The snub-dodecahedron belonging to the point group I (Attribution: symotter.org/gallery)

It is called I. An example of an object with this symmetry is the snub-dodecahedron (Fig. 2.2.62). It has the identity, and all the proper rotation operations of the point group O_h, but the inversion, the rotation-reflections, and the mirror planes are eliminated (Fig. 2.2.63).

Symmetry elements: E, 6 C_5, 10 C_3, 15 C_2, ~~15 σ, i, 6 S_{10} , 10 S_6~~

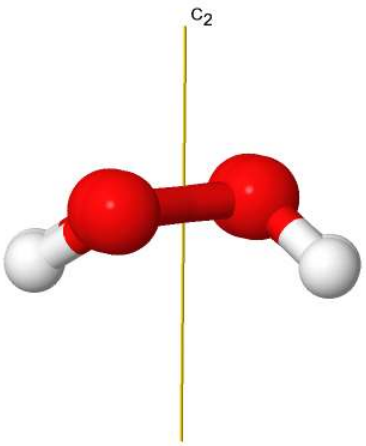
Symmetry operations: E, 24 C_5, 20 C_3 , 30 C_2', ~~15 σ, i, 24 S_{10}, 20 S_6~~

In detail: E, 6 C_5^1, 6 C_5^2, 6 C_5^3, 6 C_5^4, 10 C_3^1, 10 C_3^2, 30 C_2'^{1}, ~~15 σ, i, 6 S_{10}^1, 6 S_{10}^3, 6 S_{10}^7, 6 S_{10}^9, 10S_6^1, 10 S_6^5~~

Figure 2.2.63 Symmetry operations of the icosahedral rotational sub group I (relative to I_h)

Cyclic Point Groups

After having discussed high and low symmetry point groups, let us next look at cyclic point groups. They have the property that they have only a single proper n-fold rotational axis, but no other proper axes. In the most simple case they do not have any additional symmetry element such as mirror planes or rotation-reflections. These point groups are denoted C_n whereby n is the order of the proper axis. An example is the hydrogen peroxide molecule H_2O_2 (Fig. 2.2.64).



Point Group = C_2, Order = 2

Figure 2.2.64 The C_2 rotational axis of hydrogen peroxide

It has a so-called roof-structure due to its non-planarity. One hydrogen atom points toward us, and the other points away from us. This structure is due to the two electron-lone pairs at each sp^3-hybridized oxygen atom. These electron-lone pairs consume somewhat more space than the H atoms, and there is electrostatic repulsion between the electron lone pairs. Therefore, the electron lone pairs at the different oxygen atoms try to achieve the greatest distance from each other. This forces the H-atoms out of the plane, leading to the roof-structure of the hydrogen peroxide. Because the H_2O_2 molecule is not planar, it only has a single C_2 axis, but no other symmetry element besides the identity. The C_2 axis passes through the center of the O-O bond. Execution of the C_2 operation swaps up both the O and the H atoms.

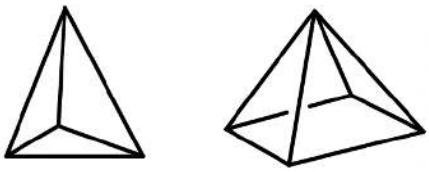
$$C_2 - H_2O_2 \text{ (elements: E, } C_2)$$

Figure 2.2.65 Symmetry elements in the hydrogen peroxide molecule

Definition: Cyclic Groups C_n

Cyclic groups have one rotational axiPyramidal Groups

Another class of groups are the pyramidal groups, denoted C_{nv}. They have n vertical mirror planes containing the principal axis C_n in addition to the principal axis C_n. Generally molecules belonging to pyramidal groups are derived from an n-gonal pyramid. An n-gonal pyramid has an n-gonal polygon as the basis which is capped (Fig. 2.2.66).



N-gonal pyramid

Figure 2.2.66 n-gonal pyramids (n=3,4)

For example a trigonal pyramid has a triangular basis which is capped, a tetragonal pyramid has a square which is capped, and so on. The proper axis associated with a specific pyramid has the order n and goes through the tip of the pyramid and the center of the polygon. An example of a molecule with a trigonal pyramidal shape is the NH_3 (Fig. 2.2.67).

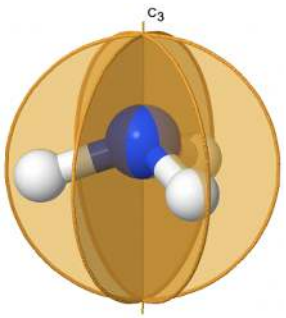


Figure 2.2.67 C_3 axis and vertical mirror planes in NH_3

The three H atoms form the triangular basis of the pyramid, which is capped by the N atom. The NH_3 molecule belongs to the point group C_{3v}. The C_3 axis goes though the N atom which is the tip of the pyramid, and the center of the triangle defined by the H atoms. There are three vertical mirror planes that contain the C_3 axis. Each of them goes through an N-H bond (Fig. 2.2.68).

$$C_{3v} - NH_3 \text{ (elements: E, } C_3, 3\sigma_v)$$

Figure 2.2.68 Symmetry elements in NH_3

Definition: Pyramidal Groups C_{nv}

Pyramidal groups have n vertical plane(s) in addition to the principal axis C_n.

The Linear Group $C_{\infty v}$

A special n-gonal polygon is the cone. A cone can be conceived as an n-gonal pyramid with an infinite number *n* of corners at the base (Fig. 2.2.69).

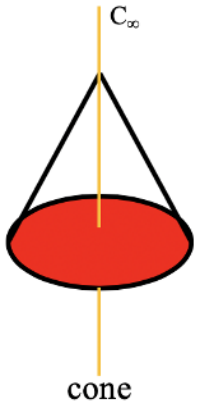


Figure 2.2.69 Cone having a proper rotational axis with infinite order.

In this case the order of the rotational axis that passes through the tip of the cone and the center of the circular basis is infinite. This also means that there is an infinite number of vertical mirror planes that contain the C_∞ axis (Fig. 2.2.71). The point group describing the symmetry of a cone is called the linear point group $C_{\infty v}$. Polar, linear molecules such as CO, HF, N_2O, and HCN belong to this point group. You can see the HCN molecule with its C_∞ axis and its infinite number of vertical mirror planes below (Fig. 2.2.70).

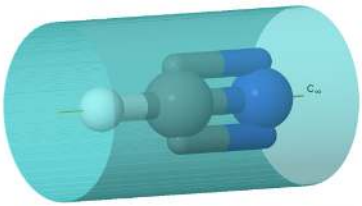


Figure 2.2.70 C_∞ axis of the HCN molecule

The infinite number of mirror planes, shown in blue are forming a cylinder that surround the molecule.

(**elements**: E, C_∞, $\infty\sigma_v$)

Figure 2.2.71 Symmetry elements of polar linear molecules

Definition: Linear group $C_{\infty v}$

The linear group $C_{\infty v}$ has an infinite number of vertical mirror planes containing a C_∞ axis

Reflection Groups

If we add a horizontal mirror plane instead of n vertical mirror planes to a proper rotational axis C_n we arrive at a the reflection point group type C_{nh}. The presence of the horizontal mirror planes also generates an improper axis of the order n. This is because when one can rotate and reflect perpendicular to the rotational axes independently, then it must also be possible to do it in combination. An example of a molecule belong to a reflection group is the trans-difluorodiazene N_2F_2 (Fig. 2.2.72).

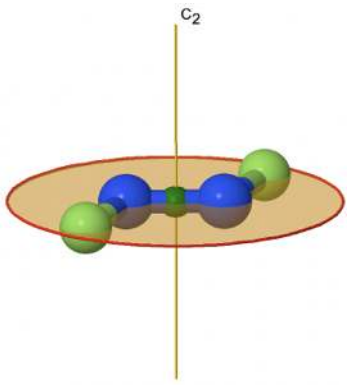


Figure 2.2.72 C_2 axis and horizontal mirror plane in trans-N_2F_2

It is a planar molecule with a C_2 axis going through the middle of the N-N double bond, and standing perpendicular to the plane of the molecule. The horizontal mirror plane stands perpendicular to the C_2 axis, and is within the plane of the molecule. There is an additional inversion center because an S_2 must exist which is the same as an inversion center. The inversion center is in the middle of the N-N bonds. Overall, the molecule has the symmetry C_{2h}.

C_{2h} – *trans*-F-N=N-F (**elements**: E, C_2, *i*, σ_h)

Figure 2.2.73 Symmetry elements in N_2F_2

Definition: Reflection Group C_{nh}

A reflection group has a horizontal plane perpendicular to the principal axis C_n

Dihedral Groups

Dihedral groups are point groups that have n additional C_2 axes that stand perpendicular to the principal axis of the order n. If there are no other symmetry elements, then the point group is of the type D_n.

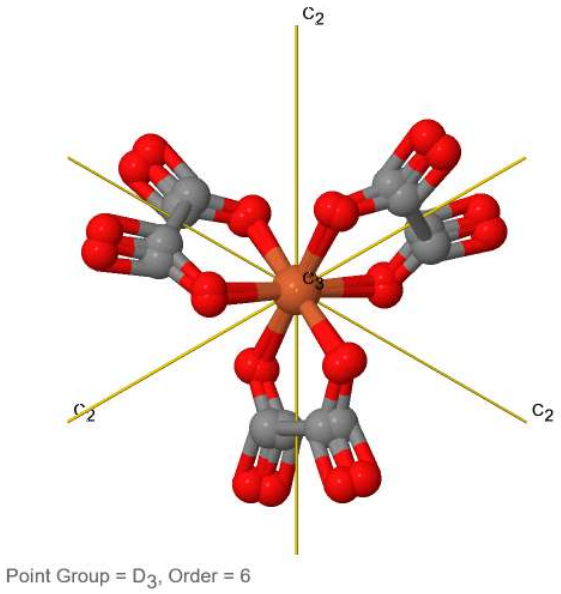


Figure 2.2.74 The tris-oxolato ferrate (3-) ion and its symmetry elements

For example in the point group D_3 there is a C_3 principal axis, and three additional C_2 axes, but no other symmetry element (Fig. 2.2.75). The tris-oxolato ferrate (3-) ion belongs to this point group (Fig. 2.2.75). You can see that the C_3 axis stands perpendicular to the paper plane, and there are three C_2 axes in the paper plane.

D_3 – (**elements**: E, C_3, $3C_2$)

Figure 2.2.75 Symmetry elements in the dihedral group D_3

Definition: Dihedral Groups D_n

In a point group of the type D_n there is a principal axis of order n, n C_2 axes, but no other symmetry elements.

If a horizontal mirror plane is added to the C_n axis and the n C_2 axes we arrive at the prismatic point groups D_{nh} (Fig. 2.2.76). The addition of the horizontal mirror plane generates further symmetry elements namely an S_n and n vertical mirror planes.

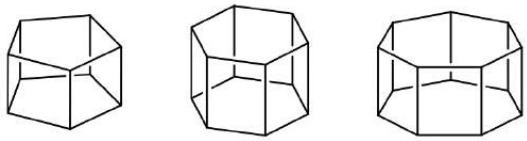


Figure 2.2.76 N-gonal prisms belong to the point group type D_{nh}

Generally, molecules belonging to this point group derive from n-gonal prisms. The order of the principal axis is the same as the number of corners of the polygons the prism are made of.

Definition: Prismatic Groups D_{nh}

In prismatic point groups there is a horizontal mirror plane perpendicular to the principal axis C_n. There are also n C_2 axes.

An example for a molecule belonging to a prismatic point group is PF_5 (Fig. 2.2.77).

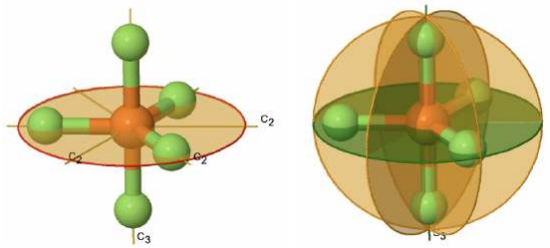


Figure 2.2.77 The PF_5 molecule belonging to the point group D_{3h} and its symmetry elements.

It has a trigonal bipyramidal shape. The C_3 axis goes through the axial F atoms of the molecule, and the three C_2 axes go through the three equatorial F atom. The horizontal mirror plane stands perpendicular to the principal C_3 axis and is located within the equatorial plane of the molecule. In addition, there are the vertical mirror planes that contain the C_3 axis, and go through the three equatorial P-F bonds. There is also an S_3 axis which superimposes the C_3 axis. In sum:

D_{3h} – PF_5 (**elements**: E, C_3, $3C_2$, σ_h, S_3, $3\sigma_v$)

Figure 2.2.78 Symmetry elements of PF_5

A special case of a D_{nh} group is the linear group $D_{\infty h}$. An object that has this symmetry is a cylinder. A cylinder can be conceived as a prism with an infinite number of vertices. Thus, the principal axis that passes through a cylinder has infinite order. Because of the infinite order of the principal axis, there is an infinite number of C_2 axes that stand perpendicular to the principal axis. You can see one such C_2 going though the cylinder (Fig. 2.2.79).

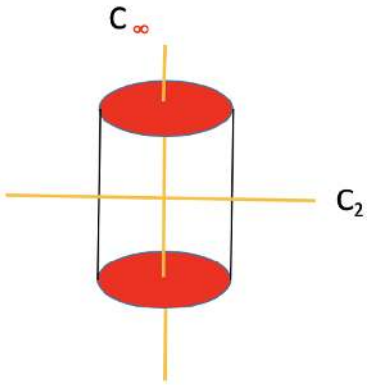


Figure 2.2.79 Cylinder as an example of linear group $D_{\infty h}$

There is now also an improper axis of infinite order, as well as an infinite number of vertical mirror planes. Non-polar linear molecules like H_2, CO_2, and acetylene C_2H_2 belong to the point group $D_{\infty h}$. You can see the C_∞ axis passing through a CO_2 molecule below (Fig. 2.2.80).

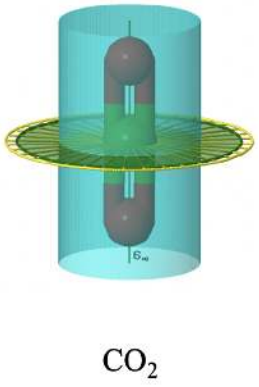


Figure 2.2.80 C_∞ in a CO_2 molecule

You can see the infinite number of vertical mirror planes as a blue cylinder. The infinite number of C_2 axes is shown a yellow lines going around the molecule. In sum:

$$E, C_\infty \infty C_2, \sigma_h, S_\infty, \infty \sigma_v, i$$

Figure 2.2.81 Symmetry elements of linear group $D_{\infty h}$

Definition: Linear Group D_{ooh}

In the point group $D_{\infty h}$ there is an infinite number of n C_2 axes in addition to the principal axis of infinite order, an infinite number of vertical mirror planes, and one horizontal mirror plane.

If we add n vertical mirror planes to the principal axis and the n C_2 axes, we arrive at the point group D_{nd}. The vertical mirror planes are dihedral mirror planes because they bisect the angle between the C_2 axes. An example is the ethane molecule in staggered conformation which has the symmetry D_{3d} (Fig. 2.2.82).

Figure 2.2.1: Paste Caption Here

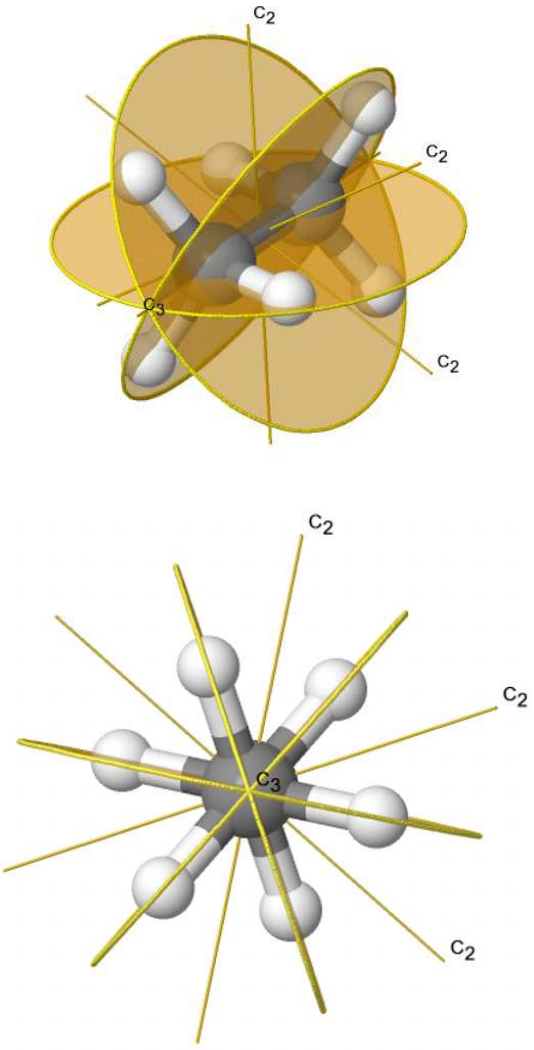


Figure 2.2.82 The ethane molecule in the staggered conformation belongs to the point group type D_{nd}

The C_3 axis goes along the C-C bond, and the $3C_2$ axes pass through the middle of the carbon-carbon bond, and bisect the angle between two hydrogens and one carbon atom. The three dihedral mirror planes pass through the C-H bonds. In addition, the ethane molecule has an S_6 axis, and an inversion center. In sum:

D_{3d} – ethane/staggered (elements: E, C_3, S_6, $3C_2$, 3 σ_d, i)

Figure 2.2.83 Symmetry elements in ethane

Definition: D_{nd}

In this point group type there are n dihedral mirror planes that contain the C_n and bisect the angle between adjacent C_2 axes

Improper Rotational Point Groups

The last class of point groups to be discussed are the improper rotation point groups. The only have one proper rotational axis, and an improper rotational axis that has twice the order of the proper rotational axis (Fig. 2.2.85). There may be an inversion center

present depending on the order of the proper and improper axes. An example the tetramethylcycloocta-tetraene molecule (Fig. 2.2.84).

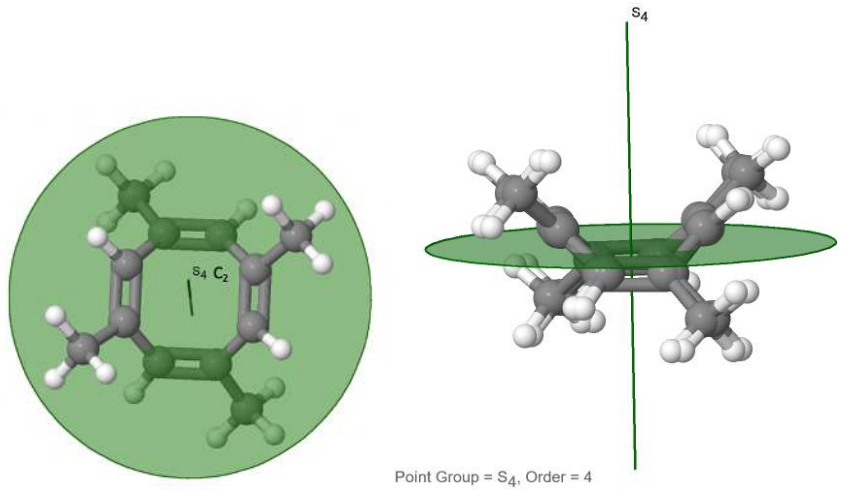


Figure 2.2.84 The S_4 and an C_2 axes of tetramethyl cycloocta-tetraene

It has an S_4 and an C_2 axis as the only symmetry elements besides the identity. Rotating by 90° alone does not superimpose the molecule because two C-C double bonds lie above the plane and two below the plane. In addition, two opposite methyl groups lie above and below the plane respectively. Therefore it needs the additional reflection to achieve superposition. There is also a C_2 axis which is in the same locations as the S_4 axis.

Symmetry elements: E, S_{2n}, C_n

May have inversion center *i*

Figure 2.2.85 Symmetry elements of improper rotational point groups

Guide for the Determination of Point Groups

With the knowledge you have, you can unambiguously identify the point group of a molecule. The key to success is that you are able to see the symmetry elements in the molecule. This takes practice. With enough practice you can identify the point group of a molecule immediately. Until, you can use guides, that you can follow to identify a point group. Such a guide asks systematic questions about the presence or absence of a symmetry element. Depending on whether you answer the question with yes or no you can follow the guide in a particular direction. Eventually, after having answered enough questions the guide will lead you to the respective point group. You can see such a chart below (Fig. 2.2.86).

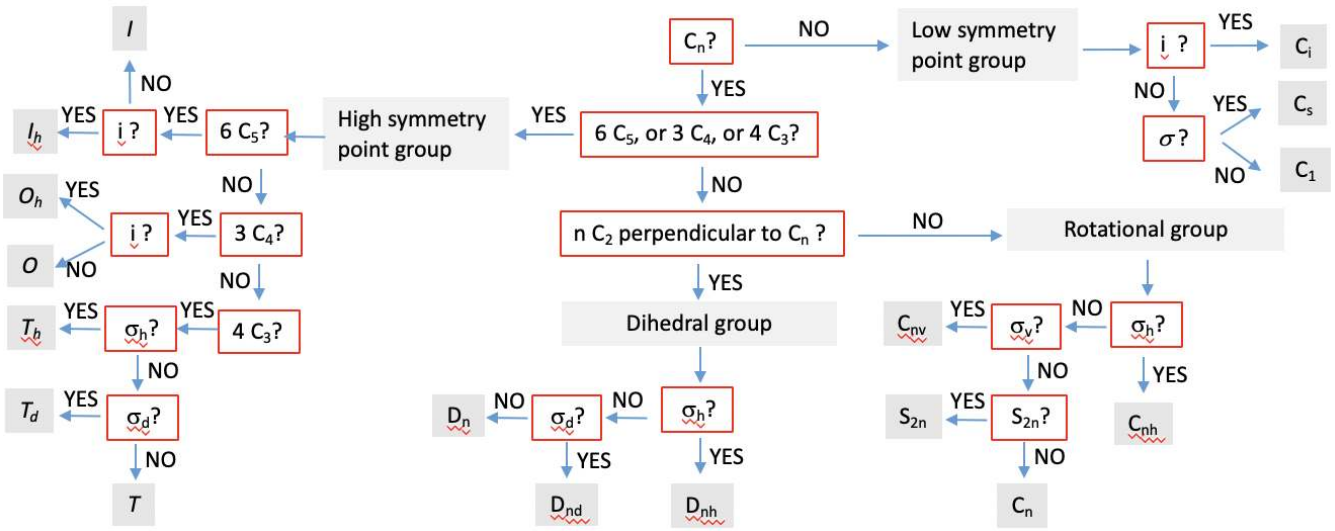


Figure 2.2.86 Guide for determination of point groups

You can first ask if there is at least one C_n present. If not, then the molecule must be in a low symmetry point group. If there is an inversion center, the point group is C_i. If not we can next ask, if there is a mirror plane. If yes it is C_s, and if not the point group is C_1. If a low symmetry point group can be ruled out, then we can ask next, if there is a high symmetry point group. This is the case when there are either $4C_3$, $3C_4$, or $6C_5$ rotational axes present, standing for tetrahedral, octahedral, and icosahedral symmetry, respectively. If there is an inversion center in case a C_5 is present, the point group is I_h. If not, it is I. Similarly, if there are $3C_4$ axes, and an inversion center, the point group must be O_h. If there is no inversion center the point group is O. If there are $4C_3$ axes, the point group must be T type. If there is a horizontal mirror plane in addition, then the point group must be T_h. If not, we can ask next is there are dihedral mirror planes. If yes, the point group is T_d, otherwise it is T. Now we have checked for all high symmetry point groups.

If a high-symmetry point groups can be ruled out, we ask if there are n C_2 axes in addition to the C_n principal axis. If this is so, then we must have a dihedral group of the D type. Next we ask, if there is a horizontal mirror plane. If yes, the point group must be D_{nh}. If not, we ask if there are dihedral mirror planes. If yes, the point group is D_{nd}. If there are no mirror planes at all, then the point group is D_n. If there are no n C_2 axes in addition to the C_n, the the group must be either a rotational group or an improper rotation group. We next ask, if there is a horizontal mirror plane. If yes, then the point group is of the type C_{nh}. If not, we ask if there are vertical mirror planes. If yes, then the point group is C_{nv}. If that is not the case, we ask if there is an S_{2n} in addition to the C_n. If yes, the point group is S_{2n}. If not, it is C_n.

Example: Dibromonaphtalene

Let us practice the point group guide by one example. Let us look at the dibromonaphtalene molecule (Fig. 2.2.87).

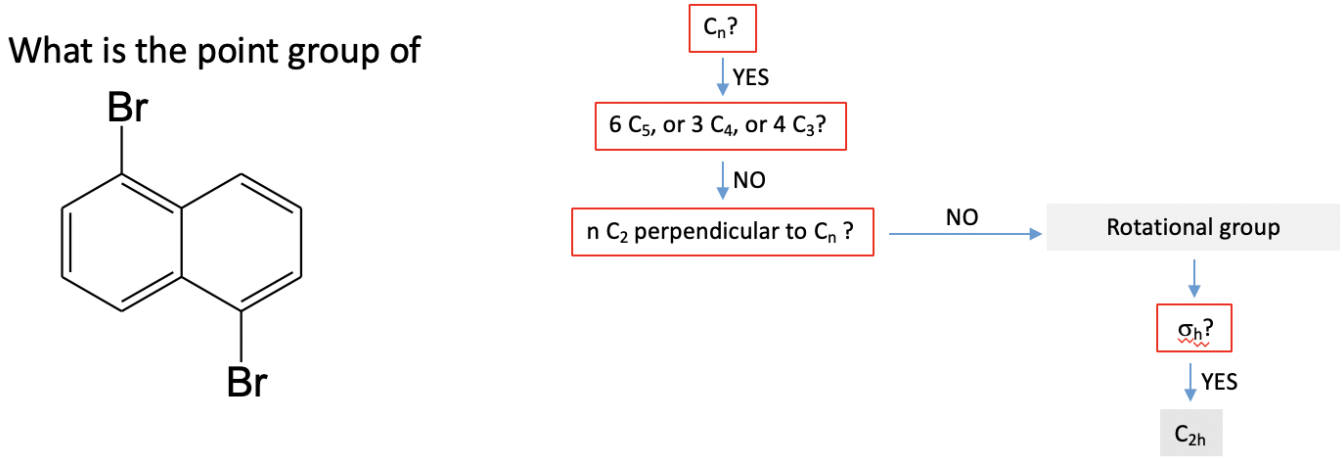


Figure 2.2.87 Guide for determining the point group of dibromonaphtalene

The first question we would ask is: Can you see at least one proper rotational axis? The answer is yes. There is a C_2 proper rotational axis that stands perpendicular to the plane of the molecule and goes through the center of the C-C bond that is shared by the two aromatic rings. Next we ask: Are the $6C_5$, $3C_4$ or $4C_3$ axes? That is clearly not the case, and thus we do not have a high symmetry point group. Next we can think about if the there are $2C_2$ axes in addition to the C_2 axes we already found. The answer is no, so the point group cannot be a dihedral group. Next, we would ask: Is there a horizontal mirror plane. This is indeed the case. There is a horizontal mirror plane in the plane of the molecule. It does not move any atoms around, but as we discussed before, a mirror does not need to do this to exist. This identifies the point group as C_{2h}.

Chiral Point Groups

A chiral point group is a point group that only has proper rotation operations in addition to the identity. This is equivalent to the statement that no improper rotations must exist in a chiral point group. This includes mirror planes and inversion centers because a mirror plane is the same as an S_1, and an inversion center is the same as an S_2. If a molecule belongs to a chiral point group, then it has a mirror image that cannot be superimposed with the original molecule. The two mirror images are called enantiomers. An example is the bromochlorofluoromethane. You can see two enantiomers separated by a dotted line (Fig. 2.2.88).

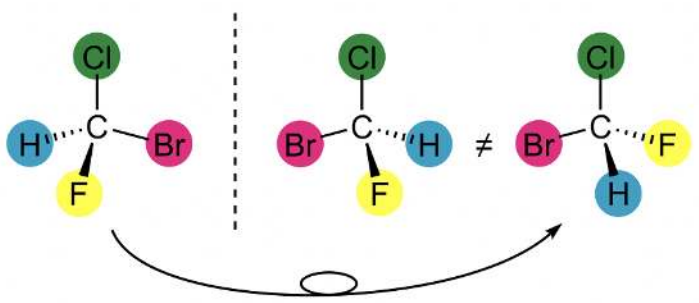


Figure 2.2.88 Chirality in bromochlorofluoromethane

The dotted line represents a mirror plane. Note that this mirror plane is not a mirror plane in the meaning of a symmetry element. You can see that the two molecules to the left and the right of the mirror plane are mirror images respective to each other. The molecules cannot be superimposed meaning that they are enantiomers. Note that the bromochlorofluoromethane molecule on the far right is not an enantiomer to the other two. It the same molecule as the enantiomer on the far left. We only need to rotate clockwise around the C-Cl axis to make the two molecules superimpose meaning that they are the same.

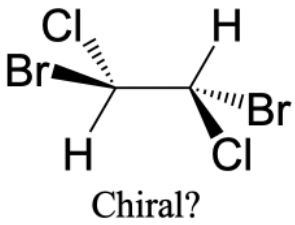


Figure 2.2.89 Dibromodichloroethane

It should be pointed out that the fact that a molecule has a carbon with four different substituents is not sufficient to make it a chiral molecule. The dibromodichloroethane molecule shown above (Fig. 2.2.89) has four different substituents around the carbon atom, but it is not chiral because there is an inversion center in the middle of the C-C bond.

Chiral High Symmetry Point Groups

Chiral groups not necessarily need to have low symmetry, in fact, the high symmetry rotational subgroups I, O, and T are chiral groups because they only have proper axes in addition to the identity (Fig. 2.2.90).

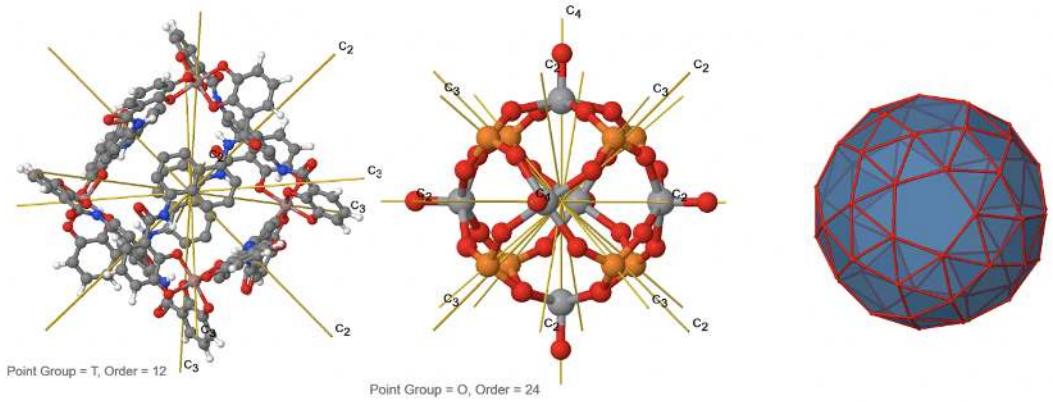


Figure 2.2.90 Objects belonging to chiral high symmetry point groups (T, O, and I from left to right).

Dr. Kai Landskron (Lehigh University). If you like this textbook, please consider to make a donation to support the author's research at Lehigh University: Click Here to Donate.

This page titled 2.2: Point Groups is shared under a not declared license and was authored, remixed, and/or curated by Kai Landskron.

- **2.2: Point Groups** by Kai Landskron is licensed CC BY 4.0.

2.3: Matrix Representations of Symmetry Operations and Character Tables

Matrix Representations of Symmetry Operations

Thus, far we have looked at symmetry operations qualitatively, and determined their nature by inspection. Now let us have a look how we can describe symmetry operations from a more mathematical point of view. Why do we do this? We do this to be able to understand so-called character tables which we will later need to apply symmetry to molecular orbital theory. Generally, symmetry operations can be described by matrices. When a matrix representing a symmetry operation is multiplied with coordinates of an object, then this gives the new coordinates of the object after the symmetry operation was carried out. Therefore let us briefly review matrices, and matrix multiplications in particular. A matrix is nothing but an array of numbers arranged into rows and columns. When we multiply to matrices, we must multiply each row with each column of the matrix. When the first matrix A_{ik} has i rows and k columns and the second matrix B_{kj} has k rows and j columns, then the product matrix C_{ij} has i rows and j columns. A requirement for a matrix multiplication is that the number of columns of the first matrix is the same as the number of the rows of the second column. Otherwise, one can just not multiply each row with each column of the two matrices.

A_{ik} = initial matrix with i rows and k columns
B_{kj} = initial matrix with k rows and j columns

↓

C_{ij} = product matrix with i rows and j columns

$$C_{ij} = \sum A_{ik} \times B_{kj}$$

Figure 2.3.1 Review on multiplying matrices

Let us do this by a few examples.

Example 1 of Matrix Multiplication

In the first example we multiply two 2x2 matrices, meaning that they both have two rows and two columns (Fig. 2.3.2). First, we need to check if the two matrices can be multiplied. We can see that the number columns of the first matrix is 2, and the number of rows of the second matrix is also 2. Therefore, we can multiply the two matrices.

$$\underset{\substack{i=2\\k=2}}{\begin{bmatrix}1 & 5\\ 2 & 6\end{bmatrix}} \times \underset{\substack{k=2\\j=2}}{\begin{bmatrix}7 & 3\\ 4 & 8\end{bmatrix}} = \begin{bmatrix}(1)(7)+(5)(4) & (1)(3)+(5)(8)\\ (2)(7)+(6)(4) & (2)(3)+(6)(8)\end{bmatrix} = \underset{\substack{i=2\\j=2}}{\begin{bmatrix}27 & 43\\ 38 & 54\end{bmatrix}}$$

Figure 2.3.2 Example 1 of matrix multiplication

The product matrix is expected to be also a 2x2 matrix. Now we need to multiply the first row of the first matrix with the first column of the second matrix, and that means that we to multiply 1x7 and 5x4. The sum of 1x7+5x4=27 gives us the first character of the first row of the product matrix. Next, we multiply the first row of the first matrix with the second column of the second matrix. So we have to multiply 1x3 and 5x8. The sum of the two products gives the second character of the first row of the product matrix. Because the second matrix has no additional column, there is no further column with which the first row of the first matrix could be multiplied. Therefore, we now go to the second row of the first matrix, and multiply it with the first column of the second matrix. This gives the products 2x7 and 6x4. When added together, then this gives 38, and this is now the first character of the second row of the product matrix. Lastly, we multiply the second row of the first matrix with the second row of the second matrix. This gives 2x3 and 6x8 which gives 54 when added together. This is the second character in the second row of the product matrix.

Example 2 of Matrix Multiplication

In the next example, we multiply a 1x3 matrix with a 3x3 matrix (Fig. 2.3.3). This is possible because the number of the columns of the second matrix is 3, and the number of rows of the second matrix is also 3.

$$\underset{\substack{i=1\\k=3}}{[1\ 2\ 3]} \times \underset{\substack{k=3\\j=3}}{\begin{bmatrix} 1 & 0 & 0 \\ 0 & -1 & 0 \\ 0 & 0 & 1 \end{bmatrix}} =$$

$$(1)(1) + (2)(0) + (3)(0) \quad (1)(0) + (2)(-1) + (3)(0) \quad (1)(0) + (2)(0) + (3)(1)$$

$$= \underset{\substack{i=1\\j=3}}{[1\ -2\ \ 3]}$$

Figure 2.3.3 Example 2 of matrix multiplication

The product matrix would be expected to have one row and three columns. The first matrix has only one row, so we multiply it with the three columns of the second matrix. Multiplying the first row of the first matrix with the first column of the second matrix gives (1)(1) + (2)(0) + (3)(0) = 1. This is the first character in the first, and only row in the product matrix. The multiplication of the first row of the first matrix with the second column of the second matrix is (1)(0) + (2)(-1) + (3)(0) = -2 which is the second character of the first row of the product matrix. The multiplication of the first row of the first matrix with the third column of the second matrix gives (1)(0) + (2)(0) + (3)(1) = 3. This is the third character of the first row of the product matrix. Overall, the product matrix is [1 -2 3].

Example 3 of Matrix Multiplication

In the last example let us multiply a 3x3 matrix with a 3x1 matrix (Fig. 2.3.4). Again, the number of the columns of the first matrix is the same as the number of the rows of the second matrix, they are both 3. Thus, we can multiply the two matrices.

$$\begin{bmatrix} 1 & 0 & 0 \\ 0 & -1 & 0 \\ 0 & 0 & 1 \end{bmatrix} \times \begin{bmatrix} 1 \\ 2 \\ 3 \end{bmatrix} = \begin{bmatrix} 1 \\ -2 \\ 3 \end{bmatrix}$$

Figure 2.3.4 Example 3 of matrix multiplication

Multiplying the first row of the first matrix with the first, and in this case only column of the second matrix gives 1x1 + 0x2 + 0x3 = 1. This is the first and only character of the first row of the product matrix. The second matrix has only one column, therefore we multiply the second row of the first matrix with the only column of the second matrix in the next step. This gives 0x1 + (-1)x2 + 0x3 = -2. This the character of the second row of the product matrix. Lastly, we multiply the third row of the first matrix with the column of the second matrix. This gives 0x1 + 0x2 + 1x3 = 3. This is the character of the third row of the product matrix.

Applying Matrix Multiplications to Symmetry Operations

So what do symmetry operations have to do with the multiplication of matrices? The answer is that a symmetry operation can be described as a matrix, and the multiplication of this matrix with the matrix that represents the coordinates of the position of the points in an object, will give the new coordinates of the object after the symmetry operation has been carried out (Fig. 2.3.5).

[new coordinates] = [transformation matrix][old coordinates]

Figure 2.3.5 Relationships between symmetry operations and matrices

Example H_2O

A matrix that represents a symmetry operation is a 3x3 matrix and the matrix that describes coordinates is a 3x1 matrix. When two are multiplied then this gives a 3x1 matrix that describes the new coordinates of the object. For example, let us look at the water molecule H_2O.

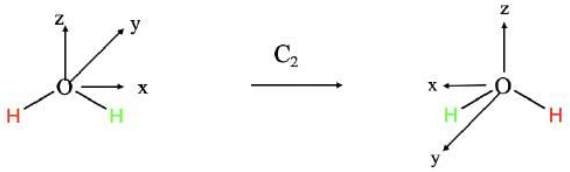


Figure 2.3.6 Transformation of coordinates in H_2O upon application of the C_2 symmetry operation

We can define a coordinate system in the water molecule so that the molecule is within the xz plane, whereby the z-axis is chosen so that it bisects the H-O-H bond angle. The y-axis would stand perpendicular and point into the board plane (Fig. 2.3.6). Any point within the water molecule, would have coordinates x,y,z that are defined by vectors $\vec{x}$, $\vec{y}$, $\vec{z}$ that point to these coordinates. For example, the center of a particular hydrogen atoms would have specific coordinates that would be described by three vectors that when added up, would point to the center of the hydrogen atom. Now let us think how the coordinates will change as we carry out a specific symmetry operations. For instance, take the C_2 symmetry operation that is carried out around the z-axis. How will the rotation change, the x,y, and z coordinates, respectively?

The x-coordinate is defined by a vector pointing into x-direction. As we rotate this vector 180° around the z-axis, it will retain its length but will point into the opposite direction (Fig. 2.3.6). Hence, we can say that the coordinate x has changed its algebraic sign, and is now –x. Now what about the y-coordinate? A vector pointing into y-direction will also be rotated around 180°, and point into the opposite direction. That means it is –y after the execution of the symmetry operation. Finally, how will the z-coordinate change? Because we rotate around z, there will not be any change to the z-vector, and thus the new coordinate z will be identical to the old coordinate z. If we represent the three vectors of the old coordinates by a 3x1 matrix $\vec{x}$, $\vec{y}$, $\vec{z}$, the new coordinates of the matrix $\vec{x}'$, $\vec{y}'$, $\vec{z}'$ are represented by the matrix $-\vec{x}$,$-\vec{y}$, $\vec{z}$. The matrix that when multiplied with the matrix for the old coordinates gives the matrix for the new coordinates, would be the matrix that would represent the symmetry operation C_2. In the case of the C_2 symmetry operation the matrix has the form below (Fig. 2.3.7).

$$\begin{bmatrix} -1 & 0 & 0 \\ 0 & -1 & 0 \\ 0 & 0 & 1 \end{bmatrix}$$

Figure 2.3.7 C_2 symmetry operation for H_2O in matrix form

We can show that this matrix correctly represents the symmetry operation C_2 by applying the multiplication rules for matrices. Multiplying the first row of the matrix for C_2 with the only column of the matrix for the old coordinates would give $(-1 \times \vec{x}) + (0 \times \vec{y}) + (0 \times \vec{z}) = -\vec{x}$ for the first character of the product matrix. Multiplying the second row of the matrix representation of C_2 with the only column of the matrix for the old coordinates gives $(0 \times \vec{x}) + (-1 \times \vec{y}) + (0 \times \vec{z}) = -\vec{y}$ for the second character of the product matrix. Multiplication of the third row of the matrix for C_2 with the column of the matrix for the old coordinates gives $(0 \times \vec{x}) + (0 \times \vec{y}) + (1 \times \vec{z}) = \vec{z}$ This proves that the matrix correctly represents the symmetry operation C_2.

$$\begin{bmatrix} -1 & 0 & 0 \\ 0 & -1 & 0 \\ 0 & 0 & 1 \end{bmatrix} \times \begin{bmatrix} \vec{x} \\ \vec{y} \\ \vec{z} \end{bmatrix} = \begin{bmatrix} \vec{x}' \\ \vec{y}' \\ \vec{z}' \end{bmatrix} = \begin{bmatrix} -\vec{x} \\ -\vec{y} \\ \vec{z} \end{bmatrix}$$

Figure 2.3.8 The symmetry operation C_2 in matrix form transforming the coordinates in H_2O

We can develop the matrix representation for the σ(xz) reflection operation along the same line we did for the C_2 operation. Let us first think about how the vectors representing the coordinate changes as the reflection operation is carried out. The vectors $\vec{x}$ and $\vec{z}$ do not change because they are within the xz mirror plane. However, the $\vec{y}$vector changes its direction as it is reflected to the other side of the mirror plane. Thus, the y-coordinate changes its algebraic sign.

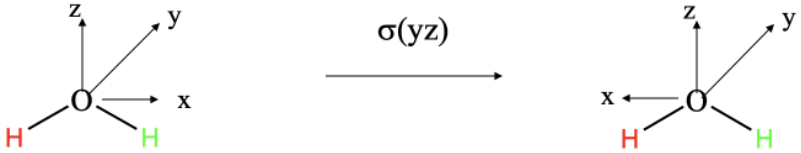


Figure 2.3.9 Transformation of coordinates of H_2O upon the application of the σ_{xz} symmetry operation

The matrix representing the new coordinates therefore has the form $\vec{x}$, - $\vec{y}$, $\vec{z}$. The matrix that when multiplied with the matrix of the old coordinates, gives the matrix of the new coordinates must be the matrix representing the symmetry operation σ_{xz}. It has the form below (Fig. 2.3.10).

$$\begin{bmatrix} 1 & 0 & 0 \\ 0 & -1 & 0 \\ 0 & 0 & 1 \end{bmatrix}$$

Figure 2.3.10 σ_{xz} symmetry operation in H_2O in matrix form

We could again show using the multiplication rules for matrices that multiplication of this matrix with the matrix for the old coordinates gives the matrix for the new coordinates (Fig. 2.3.11).

$$\begin{bmatrix} \vec{x}' \\ \vec{y}' \\ \vec{z}' \end{bmatrix} = \begin{bmatrix} 1 & 0 & 0 \\ 0 & -1 & 0 \\ 0 & 0 & 1 \end{bmatrix} \times \begin{bmatrix} \vec{x} \\ \vec{y} \\ \vec{z} \end{bmatrix} = \begin{bmatrix} \vec{x} \\ -\vec{y} \\ \vec{z} \end{bmatrix}$$

Figure 2.3.11 the symmetry operation for σ_{xz} in matrix form transforming the coordinates of H_2O.

We can apply the same process for the σ(yz) symmetry operation. The σ(yz) mirror plane contains the coordinates y and z, and thus their vectors do not change upon the application of the symmetry operation. However, the vector $\vec{x}$ changes its direction upon reflection at the yz plane, and thus the algebraic sign of the x-coordinate changes (Fig. 2.3.12).

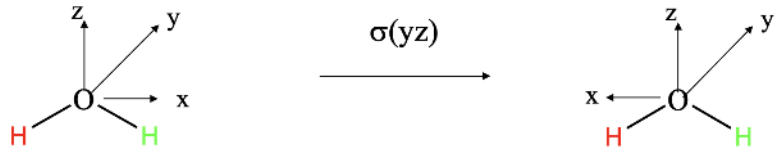


Figure 2.3.12 Transformation of the coordinates in H_2O upon the application of the σ_{yz} symmetry operation

The matrix for the new coordinates is thus -$\vec{x}$, $\vec{y}$, $\vec{z}$. In this case the matrix that when multiplied with the matrix of the old coordinates $\vec{x}$, $\vec{y}$, $\vec{z}$ gives the matrix with the new coordinates -$\vec{x}$, $\vec{y}$, $\vec{z}$ has the form below (Fig. 2.3.13).

$$\begin{bmatrix} -1 & 0 & 0 \\ 0 & 1 & 0 \\ 0 & 0 & 1 \end{bmatrix}$$

Figure 2.3.13 σ_{yz} symmetry operation in H_2O in matrix form

We could again use the multiplication rules for matrices to show that the above matrix is the correct matrix representation of the symmetry operation σ(yz), Fig. 2.3.14.

$$\begin{bmatrix} \vec{x}' \\ \vec{y}' \\ \vec{z}' \end{bmatrix} = \begin{bmatrix} -1 & 0 & 0 \\ 0 & 1 & 0 \\ 0 & 0 & 1 \end{bmatrix} \times \begin{bmatrix} \vec{x} \\ \vec{y} \\ \vec{z} \end{bmatrix} = \begin{bmatrix} -\vec{x} \\ \vec{y} \\ \vec{z} \end{bmatrix}$$

Figure 2.3.14 The multiplication of the σ_{yz} operation in matrix form with the coordinates of H_2O produces the new coordinates for H_2O

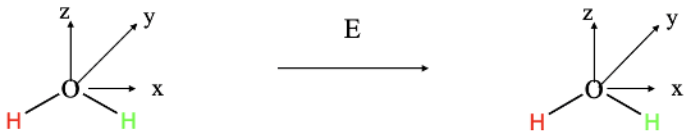


Figure 2.3.15 Transformation of the coordinates of H_2O by the E symmetry operation

Lastly, we can also determine the matrix representation of the identity operation (Fig. 2.3.15). It has the form below (Fig. 2.3.16).

$$\begin{bmatrix} 1 & 0 & 0 \\ 0 & 1 & 0 \\ 0 & 0 & 1 \end{bmatrix}$$

Figure 2.3.16 E symmetry operation in H_2O in matrix form

Like previously, we could use the multiplication rules to show that this matrix produces the correct matrix for the new coordinates. Since the identity does nothing to an object (Fig. 2.3.15), the new coordinates are the same as the old coordinates (Fig. 2.3.17).

$$\begin{bmatrix} \vec{x}' \\ \vec{y}' \\ \vec{z}' \end{bmatrix} = \begin{bmatrix} 1 & 0 & 0 \\ 0 & 1 & 0 \\ 0 & 0 & 1 \end{bmatrix} \times \begin{bmatrix} \vec{x} \\ \vec{y} \\ \vec{z} \end{bmatrix} = \begin{bmatrix} \vec{x} \\ \vec{y} \\ \vec{z} \end{bmatrix}$$

Figure 2.3.17 Multiplication of the symmetry operation E for H_2O with the coordinates of H_2O produces the correct, new coordinates for H_2O

Reducible and Irreducible Representations

Let us look closer at the four matrices that we just derived (Fig. 2.3.18).

$$\begin{bmatrix} 1 & 0 & 0 \\ 0 & 1 & 0 \\ 0 & 0 & 1 \end{bmatrix} \quad \begin{bmatrix} -1 & 0 & 0 \\ 0 & -1 & 0 \\ 0 & 0 & 1 \end{bmatrix} \quad \begin{bmatrix} -1 & 0 & 0 \\ 0 & 1 & 0 \\ 0 & 0 & 1 \end{bmatrix} \quad \begin{bmatrix} 1 & 0 & 0 \\ 0 & -1 & 0 \\ 0 & 0 & 1 \end{bmatrix}$$

Figure 2.3.18 The four matrices for the symmetry operations in the point group C_{2v}

It is noteworthy that all characters are zero, except those on a diagonal that goes from the top left corner in the matrix to the bottom right corner. This diagonal is called the trace of the matrix. With good justification we can say that the characters on the trace of the matrix tell us what the symmetry operation does with a coordinate. If it is a -1 the algebraic sign of the coordinate changes, if it is +1, it does not. If we write the characters of the trace of the matrices that belong to a specific coordinate on a line underneath the symmetry operations, we get what is called an irreducible representation for the specific coordinate (Fig. 2.3.19).

	E	C_2	σ_{yz}	σ_{xz}	"character"
x	1	-1	-1	1	irreducible representation
y	1	-1	1	-1	
z	1	1	1	1	
Γ	3	-1	1	1	Reducible Representation

Figure 2.3.19 The irreducible and reducible representations associates with the coordinates in H_2O

For example, for the x-coordinate the characters of the traces of the matrices for the symmetry operations E, C_2, σ_{yz}, σ_{xz}, are 1, -1, -1, and 1, respectively. For the y-coordinate the characters would be 1, -1, 1, and -1, and for the z- coordinate they are 1, 1, 1, and 1. The use of an irreducible representation is that it tells us directly in a concise form what the symmetry operations do to a specific coordinate. The sum of two or more irreducible representations is a so-called reducible representation. If we sum up the three irreducible representations of Fig. 2.3.19, then this gives a reducible representation with the characters 1+1+1=3, (-1)+(-1)+1=-1, (-1)+1+1=1, and 1+(-1)+1=1. We will see about the use of reducible representations in a little bit.

Symmetry Types of Irreducible Representations

The specific characters in an irreducible representation determine the symmetry type of the irreducible representation. It is denoted by a capital letter with subscripts and/or superscripts. For example the irreducible representation for the x-coordinate is of the type B_1 (Fig. 2.3.20)

	E	C_2	σ_v (xz)	σ_v' (yz)
B_1	1	-1	1	-1
B_2	1	-1	-1	1
A_1	1	1	1	1

Figure 2.3.20 Symmetry types of of the irreducible representations associated with the coordinates of H_2O

B means that the symmetry is anti-symmetric with regard to the principal axis (Fig. 2.3.21).

"B" means *anti-symmetric* with regard to rotation about the principle axis.

Figure 2.3.21 The definition of the B irreducible representation

Anti-symmetric means that the algebraic sign of the coordinate changes as we rotate. In this case the principal axis is the C_2 axis. We can see that the algebraic sign changes because the character of the irreducible representation for the x-coordinate underneath C_2 is -1. The subscript 1 means that the representation is symmetric to a C_2 perpendicular to the principal axis, or if lacking to a vertical σ_v (Figure 2.3.22)

Subscript 1 means the representation is *symmetric* to a C_2 perpendicular to the principal axis or, if lacking, to a vertical plane σ_v.

Figure 2.3.22 The definition of the subscript 1 in an irreducible representation

In this case, we do not have a C_2 perpendicular to the C_2 which is our principal axis, but we have two vertical mirror planes. Symmetric means that the coordinate does not change its algebraic sign as the symmetry operation is carried out. We can see that this is true for the reflection with the lower number of primes which comes first in our considerations. It is indicated by the character +1 underneath the symmetry operation.

The irreducible representation of the y-coordinate has the symmetry type B_2 (Fig.2.3.20) The symmetry type is again B, because the character underneath C_2 is -1. The subscript is 2 in this case, and this means that the representation is *antisymmetric* to a C_2 perpendicular to the principal axis or, if lacking to a vertical plane σ_v (Fig. 2.3.23)

Subscript 2 means the representation is *antisymmetric* to a C_2 perpendicular to the principal axis or, if lacking to a vertical plane σ_v.

Figure 2.3.23 The definition of the subscript 2 in the irreducible representation

We can see that the σ_v(xz) is anti-symmetric as indicated by the character -1 in the irreducible representation. Lastly, let us look at the symmetry type of the irreducible representation for the z-coordinate which is A_1 (Fig. 2.3.20) A means symmetric with regard to rotation around the principle axis (Fig. 2.3.24).

"A" means *symmetric* with regard to rotation about the principle axis.

Figure 2.3.24 The definition of the A irreducible representation

We can confirm the symmetric situation for the rotation around z by verifying that the character underneath the principal axis C_2 is +1.

Symmetry Types of Orbitals

Irreducible representations are more powerful than only telling you the symmetry type of a specific coordinate in a point group. More generally, they can tell the symmetry type of a mathematical function in a specific point group. Remember, that orbitals are mathematically wave functions. Thus, it should be possible to assign orbitals to a symmetry type within a given point group. Let us look for example, at the 2s and the 2p orbitals of the oxygen atom in the water molecule. Let us consider the 2s orbital first, and determine what the symmetry operations do with it. We can see that no symmetry operation changes the 2s orbital in any way, thus all characters of the irreducible representation that belongs to the orbital should be +1. We can see that this is only the case for the irreducible representation with the symmetry type A_1. Therefore we can say that the 2s orbital of the O-atom in the water molecule has the symmetry type A_1 (Fig. 2.3.25).

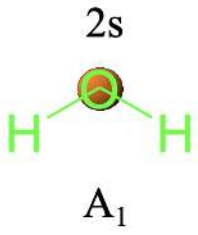


Figure 2.3.25 The 2s orbital of the O-atom in the water molecule has the symmetry type A_1

Next, let us determine the symmetry type of the $2p_z$ orbital. The $2p_z$ orbital is oriented along the z-axis around which we rotate. When carrying a C_2 operation we can see that this operation does not make any changes to the orbital. The same is true for the two reflection operations. Again, we can see that the symmetry operations do not change the $2p_z$ orbital in any way, and therefore it also must belong to the symmetry type A_1 (Fig. 2.3.26)

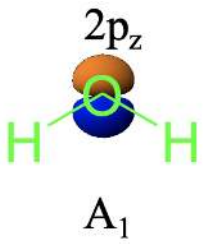


Figure 2.3.26 The $2p_z$ orbital of the O-atom in the water molecule has the symmetry type A_1

For the $2p_x$ orbital the situation is different though (Fig. 2.3.27). We can see that rotating around the C_2 axis changes the algebraic sign of the orbital. This means that the $2p_x$ orbital should belong to a symmetry type which has a character of -1 for the C_2 operation. We can see that this can be the B_1 or the B_2 symmetry type, but not A_1. This rules out the A_1 symmetry type. We still need to decide if the symmetry type is B_1 or B_2. For B_1 reflection at the σ_v(xz) mirror plane would need to be symmetric, and for B_2 it would need to be anti-symmetric. We can see that the orbital does not change when we carry out the σ_v (xz) reflection, and thus the symmetry type must be B_1.

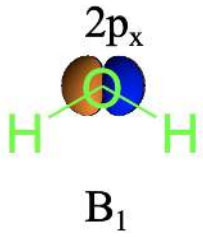


Figure 2.3.27 The $2p_x$ orbital of the O-atom in the water molecule having the symmetry type B_1

Lastly let us determine the symmetry type of the $2p_y$ orbital (Fig. 2.3.28). The $2p_y$ orbital is oriented perpendicular to the paper plane, the blue lobe points to the front, and the orange one, hardly visible points to the back. We can see that when we rotate around 180° the orange lobe points to the front, and the blue one points to the back. That means that the wave function of the orbital has changed its algebraic sign. Therefore, it must be of B symmetry type. Which one is it? B_1 or B_2? We can see that in this case the σ_v(xz) does change the algebraic sign of the wave function because the front lobe of the orbital gets reflected to the back, and the lobe in the back gets reflected to the front. Thus, it is antisymmetric with respect to σ_v(xz) and thus it must belong to the symmetry type B_2.

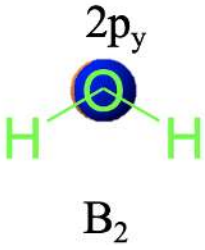


Figure 2.3.28 The $2p_y$ orbital of the O-atom in the water molecule having the symmetry type B_2

We could have determined the symmetry types of the orbitals also from a more mathematical perspective. Remember when we discussed the atomic orbitals we saw that the wave function of a p_z orbital is a linear function of the z-coordinate (Fig. 2.3.29). Therefore it has the same symmetry type as the z coordinate, namely A_1. A p_y orbital is a linear function of y, therefore it has the same symmetry type as the coordinate y: B_2. A p_x orbital is only a function of x, therefore its symmetry type is that of the coordinate x: B_1. The 2s orbital is not a function of any coordinate. Because of that it must belong to the symmetry type in which all characters are +1 which is the A_1 symmetry type in the point group C_{2v}.

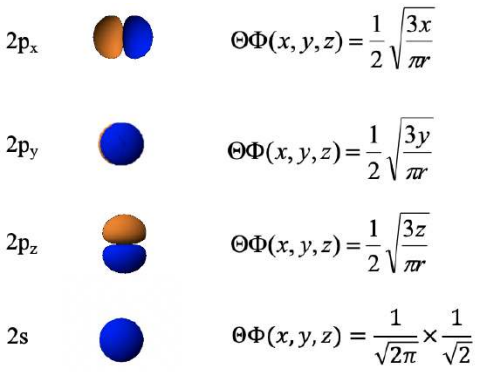


Figure 2.3.29 The angular wave functions of the 2s and 2p orbitals in cartesian coordinates.

By the same means we can also determine the symmetry type of the d orbitals of the O atom in H_2O. They are not occupied, and not involved in the bonding, but nonetheless they are possible states for the electrons. Let us determine them using the table below (Fig. 2.3.30)

			xz	yz
C_{2v}	E	C_2	σ_v	σ_v'
A_1	1	1	1	1
A_2	1	1	-1	-1
B_1	1	-1	1	-1
B_2	1	-1	-1	1

Figure 2.3.30 Character table for the point group C_{2v}

Does the $3d_{z^2}$ – orbital change when the symmetry operations are carried out (Fig. 2.3.31)? No, it does not! Therefore, it has the symmetry type A_1.

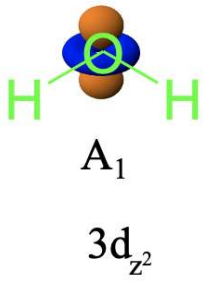


Figure 2.3.31 The $3d_{z^2}$ orbital of the O atom of the water molecule has the symmetry type A_1

What about the $3d_{xz}$? The $3d_{xz}$ orbital changes its algebraic sign when the C_2 operation is carried out, but not when the reflections are carried out. Therefore, it is of B_1 symmetry type (Fig. 2.3.32).

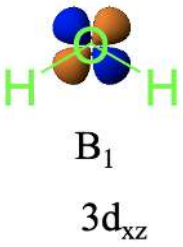
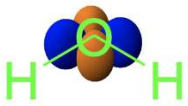


Figure 2.3.32 The $3d_{xz}$ orbital of the O atom of the water molecule has the symmetry type B_1

The $3d_{x^2-y^2}$-orbital also does not change when the symmetry operations are executed, thus it is of symmetry type A_1 (Fig. 2.3.33)

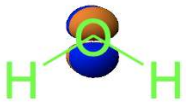


A_1

$3d_{x^2-y^2}$

Figure 2.3.33 The $3d_{x^2-y^2}$ orbital of the O atom of the water molecule has the symmetry type A_1

For the d_{yz} orbital rotation and the $\sigma_v(xz)$ reflection changes the algebraic sign, therefore it is B_2 (Fig. 2.3.24).

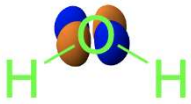


B_2

$3d_{yz}$

Figure 2.3.34 The $3d_{yz}$ orbital of the O atom of the water molecule has the symmetry type B_2

For the $3d_{xy}$ we can see that rotation does not change the orbital, but the $\sigma_v(xz)$ reflection does. This means that the symmetry type must be A_2 (Fig. 2.3.35).



A_2

$3d_{xy}$

Figure 2.3.35 The $3d_{xy}$ orbital of the O atom of the water molecule has the symmetry type A_2

This is a new symmetry type which also belongs to the point group C_{2v}. No single coordinate is of this symmetry type, but mathematical functions that are the product of the coordinates x and y, such as the $3d_{xy}$ orbital are. Similarly, because the $3d_{z^2}$ orbital is a function of z^2 and the $3d_{z^2}$ has the symmetry type A_1 any function of z^2 has this symmetry type. Analogously, any function which is the product of the x and the z coordinate belongs to the symmetry type B_1, any function which is a function of x^2-y^2 belongs to the symmetry type A_1, and any function which is a product of y and z belongs to the symmetry type B_2.

Character Tables

There is only a finite number of irreducible representations and symmetry types in a specific point group.

Generally, all the irreducible representations that are possible in a specific point group define the so-called *character table* of the point group Fig. 2.3.36).

Definition: Character Table

A complete set of irreducible representations in a point group defines its character table

Character tables describe what the symmetry operations of a point group do with a mathematical function. You can see the complete character table of the point group C_{2v} below (Fig. 2.3.36).

Symmetry operations that are conjugate are grouped in a class (column).

C_{2v}	E	C_2	$\sigma_v(xz)$	$\sigma_v'(yz)$	Linear function	Square function
A_1	1	1	1	1	z	x^2, y^2, z^2
A_2	1	1	-1	-1	R_z	xy
B_1	1	-1	1	-1	x, R_y	xz
B_2	1	-1	-1	1	y, R_x	yz

Figure 2.3.36 Character table for the point group C_{2v}

It is made of several rows and columns. In the first column you can find the point group symbol to the very left, and then the symbols for the different symmetry types of the irreducible representations the point group has. Then, there are several columns with symmetry operations in the first row, and the characters for the irreducible representations below. Each of these columns is called a class. Symmetry operations that are conjugate are grouped into the same column, or the same class. For the point group C_{2v}, each operation gets its own column and that means that they are all non-conjugate. But this is not always true, in many other point groups there are several symmetry operations that are conjugate, and listed in the same column. We have already discussed qualitatively that conjugate operations transform the coordinates of an object in a similar way. Now we have a more exact definition which is that whenever the characters for the operations in their irreducible representations are the same, they belong to the same class.

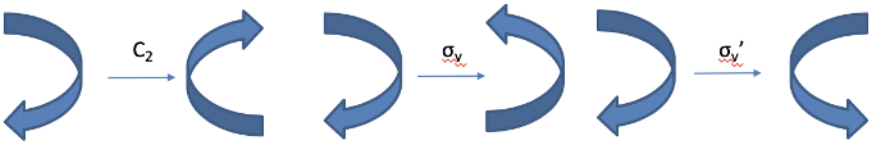


Figure 2.3.37 Transformation of a rotational vector rotating around z by the symmetry operations in the C_{2v} point group

The sum of characters underneath the identity operation E defines the dimension of the point group. For C_{2v} the dimension of the point group is 1+1+1+1=4. The order (h) of the point group is just the sum of all symmetry operations in the point group. For C_{2v} the order is 4. In the two far right columns of the character table you can find the mathematical functions that belong to the different irreducible representations. In the second column from the right linear and rotational functions are listed, and in the far right column square functions are listed. For example, the letter z is in the row associated with the symmetry type A_1. This means that any linear function of the z-coordinate has the symmetry type A_1. The letters x and y are in rows for the symmetry type B_1 and B_2 respectively. This means that any linear function of x and y has the symmetry type B_1 and B_2 respectively.

You can also see the symbols R_z, R_x, and R_y in the same column. These symbols stand for rotational functions around the z, x, and y axis respectively. R_z is in the row of the symmetry type A_2, which means that any rotational function of z has the symmetry type A_2. How can we understand that? Consider a rotational vector around z that indicates clockwise rotation (Fig. 2.3.37). If we rotate this vector by 180° counter-clockwise it will not change its direction, it will still point clock-wise, and thus the character underneath C_2 in the character table should be a 1. This rules out that the symmetry is B type, it must be either A_1 or A_2 type. We can further see that when we reflect this vector at the two vertical mirror planes, it reverses its direction, now pointing counter-clockwise. Therefore, the characters underneath the two mirror planes should be both -1. This means that the symmetry type must be A_2. If we did the same exercise with the R_x and the R_y rotational vectors we could show that they belong to the symmetry types B_2 and B_1 respectively. In the last column the square functions are listed. The row in which the function is located gives you the information about the symmetry type of the square function. For example any function of x^2, y^2, or z^2 has the symmetry type A_1, a function that is a product of x and y has the symmetry type A_2 and so forth.

Matrix Representations of Symmetry Operations in C_{3v}

Now let us go from the point group C_{2v} to the point group C_{3v} and determine the matrix representations of the symmetry operations. We will see that for this, and more generally for any point group with rotational axes with an order higher than 2, a symmetry degeneracy is possible, which means that two or even all three coordinates belong to the same symmetry type. The coordinates do not change independently upon the execution of a symmetry operation, they are linked to each other. Let us look at the ammonia molecule that belongs to the point group C_{3v}.

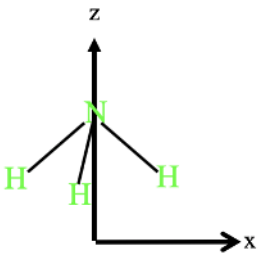
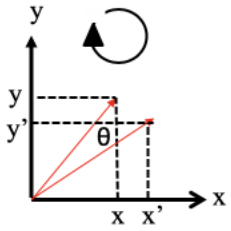


Figure 2.3.38 A suitable representation of the coordinate system in the ammonia molecule belonging to the C_{3v} point group

We can define the coordinate system so that the x-axis points to the right, the z-axis point to the to top , and the y-axis stands perpendicular to the paper plane (Fig. 2.3.38). The ammonia molecule is oriented so that its pyramid points into z-direction, and one of the three N-H bonds is within the xz plane.

Now let us see how the coordinates change when we rotate the molecule by an arbitrary general angle θ around the z-axis. In the diagram shown below, we now look along the z-axis, and the xy plane is within the paper plane (Fig. 2.3.39).



$$x' = x\cos\theta - y\sin\theta$$
$$y' = x\sin\theta + y\cos\theta$$

Figure 2.3.39 Transformation of x and y coordinates by rotation of the molecule of ammonia around an arbitrary angle θ

We can see that the rotation changes both the x and and the y coordinate together, but leaves the z-coordinate unaffected. According to trigonometry the new x-coordinate x' is x' = x cos θ - y sin θ. The new coordinate y' is y' = x sin θ + y cos θ.

The matrix representation of a symmetry operation that rotates around an arbitrary angle must be able to convert the old coordinates x,y,z into the new coordinates below (Fig. 2.3.40).

$$\begin{matrix} x\cos\theta - y\sin\theta \\ x\sin\theta + y\cos\theta \\ 1 \end{matrix}$$

Figure 2.3.40 The new coordinates (matrix form) of the NH_3 molecule after the rotation around an arbitrary angle θ

The matrix which is able to do this has the form below (Fig. 2.3.41)

$$\begin{matrix} \cos\theta & -\sin\theta & 0 \\ \sin\theta & \cos\theta & 0 \\ 0 & 0 & 1 \end{matrix}$$

Figure 2.3.41 Matrix representation for the rotation operation around an arbitrary angle θ

We could again use the multiplication rules for matrices to show that this matrix is the correct matrix.

The matrix that we just developed rotates around a general angle θ. What does this matrix look like in the point group C_{3v} where we rotate around 120° and 240°? Well, all we need to do is to insert the values of 120° and 240° for θ into the matrix. The sinus of 120° is -√3/2, and the sinus of 240° is √3/2. The cosinus of 120° and 240° are both -1/2 (Fig. 2.3.42).

$$\begin{matrix} \sin 120° = -\frac{\sqrt{3}}{2} & \sin 240° = \frac{\sqrt{3}}{2} \\ \cos 120° = -\frac{1}{2} & \cos 240° = -\frac{1}{2} \end{matrix} \quad \text{(clockwise)}$$

Figure 2.3.42 The values of sinus and cosinus for a 120° and 240° clockwise rotation

Note that these are the values for clockwise rotation. Because the C_3 operations rotate anti-clockwise, we must use the values for the 240° rotation for the C_3^1 and the values for the 120° rotation for the C_3^2 operation. Considering this, the matrix for the C_3^2 operation and the matrix for the C_3^1 operation are the matrices shown below (Fig. 2.3.43).

$$C_3^2 = \begin{matrix} -\frac{1}{2} & -\frac{\sqrt{3}}{2} & 0 \\ \frac{\sqrt{3}}{2} & -\frac{1}{2} & 0 \\ 0 & 0 & 1 \end{matrix} \qquad C_3^1 = \begin{matrix} -\frac{1}{2} & \frac{\sqrt{3}}{2} & 0 \\ -\frac{\sqrt{3}}{2} & -\frac{1}{2} & 0 \\ 0 & 0 & 1 \end{matrix}$$

Figure 2.3.43 The matrices for the C_3^2 operation and the C_3^1 operation

We can see there is a significant difference to the all the matrices we saw before. There are non-zero characters not only on the trace of the matrix, but also on other positions within the matrix, in particular in the first two rows which represent the x and the y coordinates. This is a consequence of the fact that the x and the y coordinates are no longer independent in C_{3v}, they change in a dependent way. We say that they are degenerate.

Now can we determine the remaining symmetry operations in C_{3v}. There are three conjugate vertical mirror planes to consider. The first mirror plane stands within the xz plane and passes through the N-H bond that is within the xz plane. The matrix for it is simple. It has the form below (Fig. 2.3.44).

$$1\text{st } \sigma_v' = \begin{matrix} 1 & 0 & 0 \\ 0 & -1 & 0 \\ 0 & 0 & 1 \end{matrix}$$

Figure 2.3.44 The matrix for the first mirror plane in the C_{3v} point group

It is straightforward to understand why the matrix has this form. Because the mirror plane is in the xz plane the coordinates x and z are not affected by the reflection at this plane. Therefore there are two +1 characters on the trace of the matrix in the rows for the x and the z coordinates, respectively, and all other characters in these rows are 0. The character in the second row on the trace of the matrix is -1 because the algebraic sign of the y-coordinate changes as we reflect at the xz plane. However, the other two mirror planes are not co-planar with any two coordinates, and for these planes the x and the y coordinates are dependent again. The matrix for the second mirror plane and the matrix for the third one are shown below (Fig. 2.3.45).

$$2\text{nd } \sigma_v' = \begin{matrix} \frac{1}{2} & -\frac{\sqrt{3}}{2} & 0 \\ -\frac{\sqrt{3}}{2} & -\frac{1}{2} & 0 \\ 0 & 0 & 1 \end{matrix}$$

$$3\text{rd } \sigma_v' = \begin{matrix} \frac{1}{2} & \frac{\sqrt{3}}{2} & 0 \\ \frac{\sqrt{3}}{2} & -\frac{1}{2} & 0 \\ 0 & 0 & 1 \end{matrix}$$

Figure 2.3.45 The matrices for the second mirror plane and the matrix for the third mirror plane in C_{3v}

We will not derive them in detail here. It is enough for us to understand here that these matrices have more complex forms with non-zero values outside the trace of the matrix because of the degeneracy of the x and y coordinates. Lastly, we should not forget the identity. Because the identity does nothing with an object, its matrix is always the matrix below in any point group (Fig. 2.3.46).

$$E = \begin{matrix} 1 & 0 & 0 \\ 0 & 1 & 0 \\ 0 & 0 & 1 \end{matrix}$$

Figure 2.3.46 The identity matrix for any point group

Because we know now the matrix representations of the symmetry operations we can understand the character table for the point group C_{3v} (Fig. 2.3.47)

C_{3v}	E	$2C_3$	$3\sigma_v$	Linear function	Square function
A_1	1	1	1	z	x^2+y^2, z^2
A_2	1	1	-1	R_z	
E	2	-1	0	(x,y)	(x^2-y^2, xy) (xz, yz)

means “double degeneracy”

Figure 2.3.47 The character table for the point group C_{3v}

The character table has three classes for the three groups of non-conjugate symmetry operations. In the first class there is only the identity. You can see that the second class contains the C_3^1 and the C_3^2 operations, summarized as $2C_3$. The third class contains the 3 conjugate σ_v operations. In the point group C_{3v} there are three irreducible representations. The first two have the symmetry types A_1 and A_2 respectively, the third of is of type E. The last one is new to us. It stands for “double degeneracy”, and this symmetry type exists due to the double-degeneracy of the x and the y coordinate. You can see that the character table explicitly states that x and y are double-degenerate when you look into the last column of the character table. The letters x and y are in parentheses separated by a comma. The parentheses indicate the degeneracy of these two coordinates. More generally, any two functions that are linear functions of x or y are degenerate in C_{3v}. You can see that there are also other functions that are degenerate. For instance functions of x^2-y^2 and xy are degenerate. Also functions of xz and yz are degenerate.

You can see that the characters in the irreproducible representation of the E symmetry type are also unusual. Previously, we only encountered the characters 1 and -1. However, the character underneath the identity is 2, and the character in the class for the vertical mirror planes is 0. How can we understand these characters? The answer has to do with the double-degeneracy of the x and y coordinates. Because of this double-degeneracy, the characters in the irreducible representations are the sum of the characters on the trace of the matrices for the x and y coordinate. Let us check what they are. You can see the three matrices representing the three classes of the symmetry operations below (Fig. 2.3.48).

$$\begin{array}{c} \\ x \\ y \\ z \end{array} \quad \begin{array}{c} E \\ \begin{pmatrix} 1 & 0 & 0 \\ 0 & 1 & 0 \\ 0 & 0 & 1 \end{pmatrix} \end{array} \quad \begin{array}{c} 2C_3 \\ \begin{pmatrix} -1/2 & \sqrt{3}/2 & 0 \\ \sqrt{3}/2 & -1/2 & 0 \\ 0 & 0 & 1 \end{pmatrix} \end{array} \quad \begin{array}{c} 3\sigma_v \\ \begin{pmatrix} 1 & 0 & 0 \\ 0 & -1 & 0 \\ 0 & 0 & 1 \end{pmatrix} \end{array}$$

Figure 2.3.48 The three matrices representing the three classes of symmetry operations

For the identity the sum of the two characters is 1+1=2 which explains the character 2 in the irreducible representation E. For the matrix representing the C_3 operations the characters on the trace of the matrix for x and y are -1/2. When summed up -1/2 + (-1/2) gives -1 which explains the character -1 in the irreducible representation. Lastly for the matrix representing the vertical mirror planes the characters on the trace of the matrix for the x and y coordinates are 1 and -1, respectively. -1+1=0 which explains the character 0 in the irreducible representation of the symmetry type E.

The z coordinate has the symmetry type A_1 which is straightforward to understand because the characters for z on the trace of the matrices for the three different classes of symmetry operations are all 1. You can also see from the character table that there is again an irreducible representation to which no coordinate belongs to. It is the one with the symmetry type A_2. In C_{3v} only rotational functions around z have that symmetry type.

Symmetry Types of Degenerate Irreducible Representations

There are not only double-degenerate irreducible representations, denoted by a symbol E, there can also be triply-degenerate ones, indicated by a symbol T. In this case all three coordinates x, y, and z are degenerate. Triple-degeneracy does not appear in the point group C_{3v}, but in other point groups, in particular the high-symmetry point groups (Fig. 2.3.49).

“E” indicates that the representation is doubly-degenerate.
“T” indicates that the representation is triply-degenerate (x,y,z are dependent).

Figure 2.3.49 The definition of "E" and "D" irreducible representations

Both the E and T symbols can carry subscripts and primes that have specific meanings. The prime (‘) and (“) double prime in the symmetry representation label indicates “symmetric” or “anti-symmetric” with respect to σ_h, e.g. E` or E``(Fig. 2.3.50).

The prime (‘) and (“) double prime in the symmetry representation label indicates
“symmetric” or “anti-symmetric” with respect to σ_h. E.g. E` or E``

Figure 2.3.50 The definition of prime (') and (") in irreducible representations

The subscripts g and u stand for the German words “gerade” and “ungerade” and a g and a u indicates “symmetric” or “anti-symmetric” with respect to inversion, *i*, respectively (Fig. 2.3.51).

The subscripts g (gerade) and u (ungerade) in the symmetry representation label
indicates “symmetric” or “anti-symmetric” with respect to inversion, *i*.
Example T_g or E_u

Figure 2.3.51 The definition of g (gerade) and u (ungerade) in irreducible representations

For example, there can be symmetry types like T_g or E_u. There are other subscripts possible, and we do not need to go through them exhaustively. It is enough to understand that they indicate a certain symmetry property in a symmetry type.

Character Tables and Degenerated Orbitals

One of the most useful properties of character tables are that one can identify degenerate orbitals very easily. For example, a quick look into the character table of the point group C_{3v} reveals that the $2p_x$ and the $2p_y$ orbital in NH_3 must be degenerate (Fig. 2.3.52).

C_{3v}	E	$2C_3$	$3\sigma_v$	Linear function	Square function
A_1	1	1	1	z	x^2+y^2, z^2
A_2	1	1	-1	R_z	
E	2	-1	0	(x,y)	(x^2-y^2, xy) (xz, yz)

Degenerate orbitals are always grouped in parenthesis

Figure 2.3.52 Character table of the C_{3v} point group

This is because the $2p_x$ orbital is a linear function of x, and the $2p_y$ orbital is a linear function of y, and linear functions of x and y are listed in parentheses in the double-degenerate irreducible representation of the type E. This double-degeneracy could also be derived by inspecting the orbitals in the NH_3 molecule, but this is not as easy as looking up the character table. You can see the $2p_x$ and the $2p_y$ orbitals in the ammonia molecule below (Fig. 2.3.53).

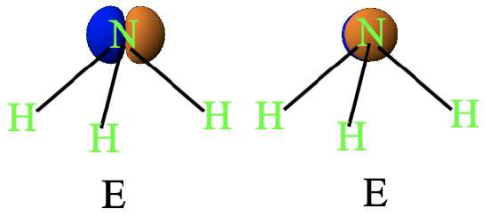


Figure 2.3.53 The $2p_x$ and $2p_y$ orbitals in ammonia

The two orbitals stand perpendicular to each other, but the NH_3 molecule has C_3 rotational symmetry. Therefore, why would the two orbitals be symmetry-degenerate? If they are degenerate, then there must be at least one symmetry operation that can interconvert the two orbitals. From the above depiction it not obvious what symmetry operation this could be.

Identifying the Double Degeneracy of $2p_x$ and $2p_y$ in NH_3

We can do a little trick to see that a reflection operation is the one that can interconvert the two orbitals. The trick is to rotate the coordinate system by 45°. You can see the ammonia molecule in the bird’s perspective below (Fig. 2.3.54).

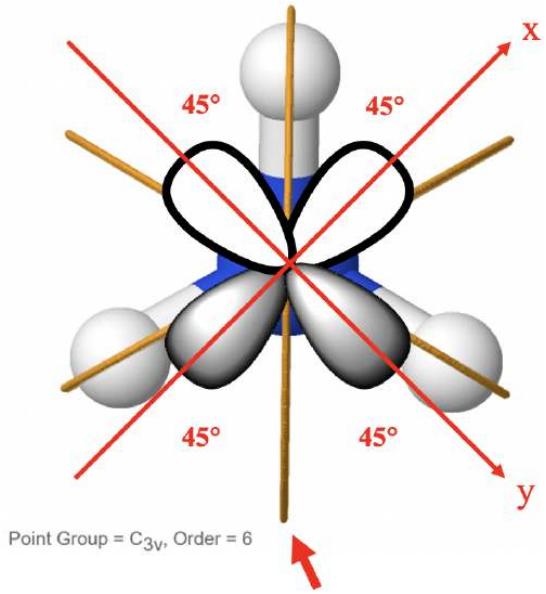


Figure 2.3.54 Ammonia in the bird's perspective with an arrow indicating the reflection plane that interconverts $2p_x$ and $2p_y$

This means that we look perpendicular to the base of the pyramid. You can see the NH_3 molecule with its three mirror planes above. Now we can choose our coordinate system so that the x and the y axes are rotated 45° with respect to one of the mirror planes. By definition, the $2p_x$ orbital must be oriented along the x-axis, and the $2p_y$ orbital must be oriented along the y-axis. You can see that one of the mirror planes, namely the one that oriented vertically, is able to interconvert the two orbitals. Upon reflection, the left and the right lobes of both orbitals will swap up their positions, so that after the symmetry operation is complete, the 2p orbitals are interconverted. Overall we can see that proving the degeneracy of two orbitals by inspection can be tricky. A quick look into the character table can tell us much more easily if two orbitals are degenerate.

Dr. Kai Landskron (Lehigh University). If you like this textbook, please consider to make a donation to support the author's research at Lehigh University: Click Here to Donate.

This page titled 2.3: Matrix Representations of Symmetry Operations and Character Tables is shared under a not declared license and was authored, remixed, and/or curated by Kai Landskron.

- **2.3: Matrix Representations of Symmetry Operations and Character Tables** by Kai Landskron is licensed CC BY 4.0.

2.4: Concept Review Questions Chapter 2

Concept Review Questions

Section 1

1. What is the definition of symmetry, a symmetry operation, and a symmetry element?

2. There are five basic types of symmetry operations. Name them.

3. Of these five types of operations, two are not independent (i.e. they can be expressed by two of the three others). Name the two operations and explain why they are not independent.

4. What is the definition of the identity operation?

5. What is the definition of a proper rotational axis, and a proper rotation operation?

6. What is the definition of a mirror plane and a reflection operation?

7. What is the definition of an improper rotational axis and a rotation-reflection operation?

8. What is the definition of an inversion center and an inversion operation?

9. What is a principal axis?

10. What is the definition of a horizontal, vertical, and dihedral mirror plane, respectively?

11. What are the rules for giving axes and mirror planes primes?

12. How often do you have to carry out a proper rotation (order n), a reflection, an inversion, and a rotation-reflection (order n), respectively until you have reached the identity?

Section 2

1. What is a Platonic Solid?

2. Name the possible platonic solids.

3. Draw an icosahedron according to the rules that you have learned in class.

4. Which are the three low symmetry point groups? Which symmetry elements do they contain?

5. Name all high symmetry point groups.

6. What is a rotational subgroup?

7. What symmetry properties does a rotational point group have?

8. What symmetry properties does a dihedral point group have?

9. What different types of rotational point groups do you know?

10. What types of dihedral point group do you know?

Section 3

1. What is a matrix?

2. What are the multiplication rules for matrices?

3. Explain why transformation matrices represent symmetry operations?

4. What is an irreducible representation?

5. What is a reducible representation?

6. What is meant by an A and B symmetry type of an irreducible representation?

7. Explain briefly, why there are non-zero entries on positions other than those on the trace of the matrix for C_3 symmetry operations?

8. The x and y coordinates are dependent for C_3 rotations around the z axis in the point group C_{3v}. Explain.

9. The irreducible representation of the type E contains characters other than +1 and -1. Explain how these characters are generated?

10. Two orbitals are degenerate when a symmetry operation can interconvert them. Show how the double degeneracy of the $2p_x$ and the $2p_y$ orbitals in the point group C_{3v} can be demonstrated using this principle.

Dr. Kai Landskron (Lehigh University). If you like this textbook, please consider to make a donation to support the author's research at Lehigh University: Click Here to Donate.

2.4: Concept Review Questions Chapter 2 is shared under a not declared license and was authored, remixed, and/or curated by LibreTexts.

- **Concept Review Questions Chapter 2** by Kai Landskron is licensed CC BY 4.0.

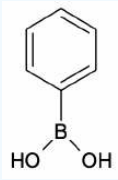
2.5: Homework Problems Chapter 2

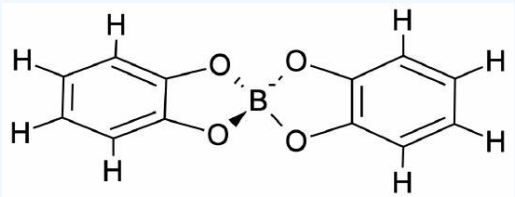
Homework Problems

Section 2

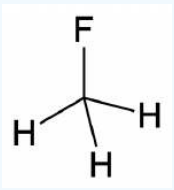
Exercise 1

Determine all symmetry elements and all unique symmetry operations of the following molecules:

a) 

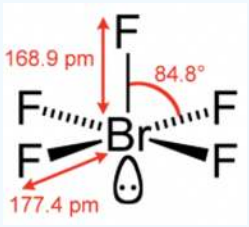
b) 

Note: The boron is tetrahedrally coordinated by O.

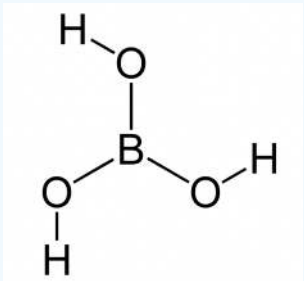
c) 

d) ethane (staggered conformation)

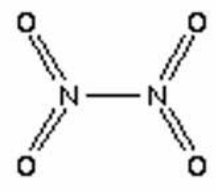
e) bromine tetrafluoride



f) Boric acid



g) Dinitrogen tetroxide



h) $PtCl_4^{2-}$ (square planar)

i) bromobenzene

j) SF_4

k) ClF_3

l) CO_2

m) benzene

Answer

a) Elements: E, C_2, σ_v, σ_v'

Operations: E, C_2, σ_v, σ_v'

b) Elements: E, S_4 C_2, $2\sigma_v$

Operations: E, S_4^1, S_4^3 C_2, $2\sigma_v$

c) Elements: E, C_3, $3\sigma_v$

Operations: E, C_3^1, C_3^2, $3\sigma_v$

d) Elements: E, C_3, 3 C_2, i, S_3, $3\sigma_d$

Operations: E, C_3^1, C_3^2, i, 3 C_2^1, S_6^1, S_6^5, $3\sigma_d$

e) Elements: E, C_4, C_2, 2 σ_v, 2 σ_v'

Operations: E, C_4^1 C_4^3, C_2^1, $2\sigma_v$, 2 σ_v'

f) Elements: E, C_3, σ_h, S_3

Operations: E, C_3^1, C_3^2, σ_h, S_3^1, S_3^5

g) Elements: E, C_2, C_2', C_2'', i, σ_h, $2\sigma_v$

Operations: E, C_2^1, $C_2'^1$, $C_2''^1$, i, σ_h, $2\sigma_v$

h) Elements: E, C_4, C_2, $2C_2'$. $2C_2''$, i, S_4, σ_h, $2\sigma_v$, $2\sigma_d$

Operations: E, C_4^1, C_4^3, C_2^1, $2C_2'^1$, 2 $C_2''^1$, i, S_4^1, S_4^3, σ_h, $2\sigma_v$, $2\sigma_d$

i) Elements: E, C_2 σ_v, σ_v'

Operations: E, C_2^1, σ_v, σ_v'

j) Elements: E, C_2 σ_v, σ_v'

Operations: E, C_2^1, σ_v, σ_v'

k) Elements: E, C_2 σ_v, σ_v'

Operations: E, C_2^1, σ_v, σ_v'

l) Elements: E, C_∞, ∞C_2, $\infty\sigma_v$, σ_h, S_∞, i

Operations: E, ∞C_∞, ∞C_2^1, $\infty\sigma_v$, σ_h, ∞S_∞, i

m) Elements: E, C_6, C_3, C_2, $6C_2'$, σ_h, $6\sigma_v$, i, S_6, S_3

Operations: E, C_6^1, C_6^5, C_3^1, C_3^2, C_2^1, $6C_2'^1$, σ_h, $6\sigma_v$, i, S_6^1, S_6^5, S_3^1, S_3^5.

Exercise 2

When is a molecule chiral?

a) It has no mirror planes

b) It is has no inversion center

c) It has no principal axis

d) It has no rotation reflections (improper rotations)

Answer

d) It has no rotation reflections (improper rotations)

Exercise 3

If a molecule has a principal axis C_n , and n additional C_2 axes standing perpendicular to C_n then it belongs to

a) A dihedral point group

b) A rotational point group

c) A low symmetry point group

d) A high symmetry point group

Answer

a) A dihedral point group

Exercise 4

Which of the following molecules are chiral:

a) CH_4

b) $CHCl_3$

c) HCFClBr

d) HOF

e) BHFCl

Answer

c) HCFClBr

Exercise 5

Determine the point groups of the molecules at symmetry.otterbein.edu/challenge/index.html until you feel that you can determine point groups effortlessly

Section 3

Exercise 1

Can the following matrices be multiplied and if so what is the product matrix?

a) $\begin{bmatrix} 2 & 1 & 0 \\ 5 & 9 & 1 \\ 2 & 2 & 3 \end{bmatrix} \begin{bmatrix} 0 & 3 & 1 \\ 4 & 1 & 2 \\ -1 & -1 & 3 \end{bmatrix}$

b) $\begin{bmatrix} 3 & 1 & 0 \end{bmatrix} \begin{bmatrix} 4 \\ 2 \\ 1 \end{bmatrix}$

c) $\begin{bmatrix} 1 & 2 & 3 & 4 \\ 4 & 3 & 2 & 1 \end{bmatrix} \begin{bmatrix} 1 & 4 \\ 2 & 3 \\ 3 & 2 \\ 4 & 1 \end{bmatrix}$

d) $\begin{bmatrix} 2 & -1 \\ 1 & 1 \end{bmatrix} \begin{bmatrix} 1 & 5 & 8 \\ 2 & 2 & 4 \\ 1 & 8 & 1 \end{bmatrix}$

Answer

a) $$\begin{bmatrix}2&1&0\\5&9&1\\2&2&3\end{bmatrix}\begin{bmatrix}0&3&1\\4&1&2\\-1&-1&3\end{bmatrix}=\begin{bmatrix}2\times0+1\times4+0\times(-1)&2\times3+1\times1+0\times(-1)&2\times1+1\times2+0\times3\\5\times0+9\times4+1\times(-1)&5\times3+9\times1+1\times(-1)&5\times1+9\times2+1\times3\\2\times0+2\times4+3\times(-1)&2\times3+2\times1+3\times(-1)&2\times1+2\times2+3\times3\end{bmatrix}=\begin{bmatrix}4&7&4\\35&23&26\\5&5&15\end{bmatrix}$$

b) $$\begin{bmatrix}3&1&0\end{bmatrix}\begin{bmatrix}4\\2\\1\end{bmatrix}=\begin{bmatrix}3\times4+1\times2+0\times1\end{bmatrix}=\begin{bmatrix}14\end{bmatrix}$$

c) $$\begin{bmatrix}1&2&3&4\\4&3&2&1\end{bmatrix}\begin{bmatrix}1&4\\2&3\\3&2\\4&1\end{bmatrix}=\begin{bmatrix}1\times1+2\times2+3\times3+4\times4&1\times4+2\times3+3\times2+4\times1\\4\times1+3\times2+2\times3+1\times4&4\times4+3\times3+2\times2+1\times1\end{bmatrix}=\begin{bmatrix}30&20\\20&30\end{bmatrix}$$

d) $$\begin{bmatrix}2&-1\\1&1\end{bmatrix}\begin{bmatrix}1&5&8\\2&2&4\\1&8&1\end{bmatrix}$$

These two matrices cannot be multiplied.

Exercise 2

Determine the irreducible representations for the following orbitals in the point group D_{2h}.

The z axis is defined as the axis of the principal C_2 axis. C_2' is defined as the axis rotating around y. σ_v is defined as the xz plane.

	E	C_2	C_2'	C_2''	i	σ_h	σ_v	σ_v'
a) 2s								
b) $2p_x$								
c) $2p_y$								
d) $2p_z$								
e) $3d_{z2}$								
f) $3d_{x2-y2}$								
g) $3d_{xy}$								
h) $3d_{yz}$								
i) $3d_{xz}$								

Answer

	E	C_2	C_2'	C_2''	i	σ_h	σ_v	σ_v'
a) 2s	1	1	1	1	1	1	1	1
b) $2p_x$	1	-1	-1	1	-1	1	1	-1
c) $2p_y$	1	-1	1	-1	-1	1	-1	1
d) $2p_z$	1	1	-1	-1	-1	-1	1	1
e) $3d_{z2}$	1	1	1	1	1	1	1	1
f) $3d_{x2-y2}$	1	1	1	1	1	1	1	1
g) $3d_{xy}$	1	1	-1	-1	1	1	-1	-1
h) $3d_{yz}$	1	-1	-1	1	1	-1	-1	1
i) $3d_{xz}$	1	-1	1	-1	1	-1	1	-1

Exercise 3

Determine the matrix representations of the symmetry elements of the following point groups:

a) D_2

Define principal C_2 axis as the axis running along z. C_2' runs along x.

b) C_3

If we define the principal C_3 axis running along the z axis:

Answer

a)

$$E: \begin{matrix}1&0&0\\0&1&0\\0&0&1\end{matrix} \qquad C_2: \begin{matrix}-1&0&0\\0&-1&0\\0&0&1\end{matrix} \qquad C_2': \begin{bmatrix}1&0&0\\0&-1&0\\0&0&-1\end{bmatrix}$$

$$C_2'': \begin{matrix}-1&0&0\\0&1&0\\0&0&-1\end{matrix}$$

b)

$$E: \begin{matrix}1&0&0\\0&1&0\\0&0&1\end{matrix} \qquad C_3^1: \begin{matrix}-\frac{1}{2}&-\frac{\sqrt{3}}{2}&0\\\frac{\sqrt{3}}{2}&-\frac{1}{2}&0\\0&0&1\end{matrix} \qquad C_3^2: \begin{matrix}-\frac{1}{2}&\frac{\sqrt{3}}{2}&0\\-\frac{\sqrt{3}}{2}&-\frac{1}{2}&0\\0&0&1\end{matrix}$$

Dr. Kai Landskron (Lehigh University). If you like this textbook, please consider to make a donation to support the author's research at Lehigh University: Click Here to Donate.

2.5: Homework Problems Chapter 2 is shared under a not declared license and was authored, remixed, and/or curated by LibreTexts.

- **Homework Problems Chapter 2** by Kai Landskron is licensed CC BY 4.0.

CHAPTER OVERVIEW

3: Review of Chemical Bonding

Learning Objectives

- Be able to draw Lewis dot structures, assign formal charges, predict molecular geometries (including bond angles), and calculate bond orders for molecules, including hypervalent molecules and ions.
- Describe hypervalent molecules using no-bond resonance.
- Understand and articulate how predictions of molecular structure and bonding can be experimentally verified.
- Learn to construct hybrid orbitals from s and p atomic orbitals.
- Use the isoelectronic principle to design new molecules and solids.
- Rationalize bond strength and chemical reactivity using bond polarity arguments.
- Interrelate bond length and bond strength.

There is no topic more fundamental to Chemistry than the nature of the chemical bond, and the introduction you find here will provide you with an overview of the fundamentals and a basis for further study.

3.1: Prelude to Chemical Bonding

3.2: Valence Bond Theory- Lewis Dot Structures, the Octet Rule, Formal Charge, Resonance, and the Isoelectronic Principle

3.3: The Shapes of Molecules (VSEPR Theory) and Orbital Hybridization

3.4: Bond Polarity and Bond Strength

3.5: Discussion Questions

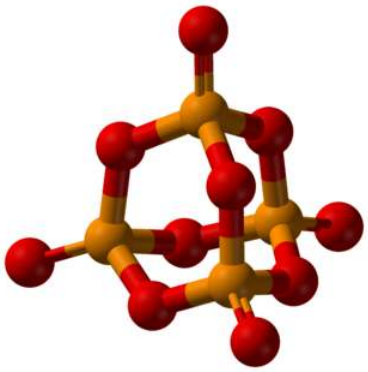
3.6: Problems

3.7: References

3: Review of Chemical Bonding is shared under a CC BY-SA license and was authored, remixed, and/or curated by LibreTexts.

3.1: Prelude to Chemical Bonding

Molecules (and extended solids) are built from atoms that form chemical bonds. Theories of bonding seek to explain why molecules and solids form, what their structures are, why some are more stable than others, and how they react. As we will learn in Chapter 2, quantum mechanics gives us the most realistic picture of chemical bonding via molecular orbital (MO) theory. However, the MO description of bonding is conceptually difficult and mathematically intensive. This chapter will review less rigorous (but still useful) models such as Lewis dot structures and valence shell electron-pair repulsion (VSEPR) theory. When combined with a qualitative quantum mechanical description of bonding through the concepts of orbital hybridization and resonance, these simple models can help us understand a great deal about the structures, stabilities, and reactions of inorganic molecules.



Ball-and-stick representation of chemical bonding in the molecules P_4O_{10} and P_4S_{10}.

The theory of chemical bonding has a long history, dating back to ancient Greece and the atomists Democritus, Leucippus, and the Epicureans. They postulated the existence of immutable atoms moving through the void, and envisioned the physical properties of materials as arising from the kinds and shapes of atoms. In his epic poem *De rerum natura* (On the Nature of Things), the Roman poet Lucretius (c. 99 BC – c. 50 BC), drawing on his Epicurean beliefs, describes some atoms and chemical bonding in the following way:

> *What seems to us the hardened and condensed*
> *Must be of atoms among themselves more hooked,*
> *Be held compacted deep within, as 'twere*
> *By branch-like atoms -- of which sort the chief*
> *Are diamond stones, despisers of all blows*
> *And stalwart flint and strength of solid iron*
> *And brazen bars, which, budging hard in locks,*
> *Do grate and scream. But what are liquid, formed*
> *Of fluid body, they indeed must be*
> *Of elements more smooth and round -- because*
> *Their globules severally will not cohere.*

Lucretius' poem is enjoyable reading and contains some remarkable insights into the microscopic world, given the tools available at the time. Modern analytical methods show that he was off base with his ideas about hooks and spheres, however. We will revisit the nature of chemical bonding in the substances Lucretius mentions (diamond, silicates, iron, brass, and water) in the context of modern chemical theories to understand why they have the special properties they do.

3.1: Prelude to Chemical Bonding is shared under a CC BY-SA license and was authored, remixed, and/or curated by LibreTexts.

- **1.1: Prelude to Chemical Bonding** by Chemistry 310 is licensed CC BY-SA 4.0. Original source: https://en.wikibooks.org/wiki/Introduction_to_Inorganic_Chemistry.

3.2: Valence Bond Theory- Lewis Dot Structures, the Octet Rule, Formal Charge, Resonance, and the Isoelectronic Principle

Atoms and Molecules

Atomism, because it was dismissed by Aristotle, enjoyed a long sleep in scientific discourse until it was reconsidered by Galileo, Decartes, and Gassendi in the 1600s. Dalton postulated the modern atomic theory in 1808 based on his observation that elements such as hydrogen and oxygen combined in specific ratios (the Law of Definite Proportions), but the atomic theory remained contentious throughout most of the 19th century. Thompson, Rutherford, Bohr, and others around the turn of the 20th century established that matter was indeed composed of atoms that contained heavy nuclei and light electrons, and that atoms could exist in excited states that could be interpreted as excitations of their electrons to different energy levels. However the atomic theory did not provide a ready explanation for the bonded states of atoms in molecules.

In 1916, still more than a decade before modern quantum theory would adequately describe the shapes of atomic orbitals, Lewis proposed the octet theory based on the empirically observed rules of valence, i.e., the combining ratios of atoms in molecules.[1] This theory, in hindsight, can be rationalized for s- and p-block elements by observing that main-group atoms can use their four valence orbitals (s, p_x, p_y, and p_z) to accommodate up to eight electrons, some or all of which may be shared with other atoms. In Lewis' model, the valence electrons of an atom were situated at the corners of a cube, and the cubes could share edges or faces to complete their octets. Lewis developed a shorthand notation for these structures based on dots that represented the valence electrons, as illustrated in Fig. **3.2.1**. A pair of electrons shared between atoms constitutes a chemical bond, and can also be represented as a line joining the atoms. Four electrons shared between atoms, represented by two lines, is a double bond, and so forth. Any pairs of electrons not involved in bonding form "lone pairs" that belong to one atom only and are thus not involved in bonding.

The Lewis picture is powerful in its simplicity. It can be readily used to rationalize or predict the combining ratios of atoms, to sort plausible and unlikely structures for molecules (including large ones), and to rationalize the acid-base properties of many molecules. It is important to remember that the model is built on a shaky, pre-quantum mechanical description of atoms and so with it, we will make mistakes. Nevertheless it is useful to see how far we can go with the Lewis model.

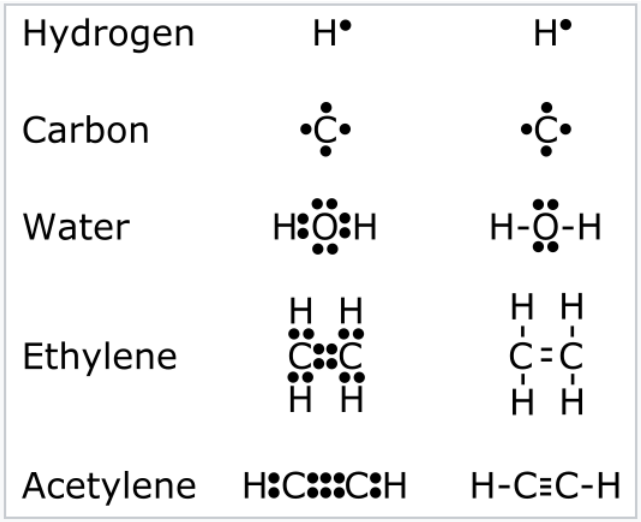


Figure **3.2.1**: Examples of Lewis dot diagrams showing chemical bonds between carbon, hydrogen, and oxygen, and non-bonding electron pairs.

Constructing the octet valence bond picture for a molecule

We can construct an octet picture for any molecule using the **N-V method:**

Number of electrons *needed* to make separate octets around all atoms = **N**

(N = 8 for non-H atoms, N = 2 for H)

Number of *valence* electrons = **V** (add up using group numbers; don't forget to add or subtract for charges on ions)

Number of *shared* electrons = **S** = N-V; and therefore the number of bonds = S/2

Fill in lone pairs everywhere else to complete octets

Example: nitrate anion, NO_3^-

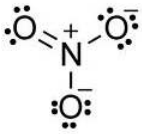
N = 4 atoms x 8 electrons = 32

V = 5 + 6 + 6 + 6 + 1 = 24 (N + O + O + O + charge)

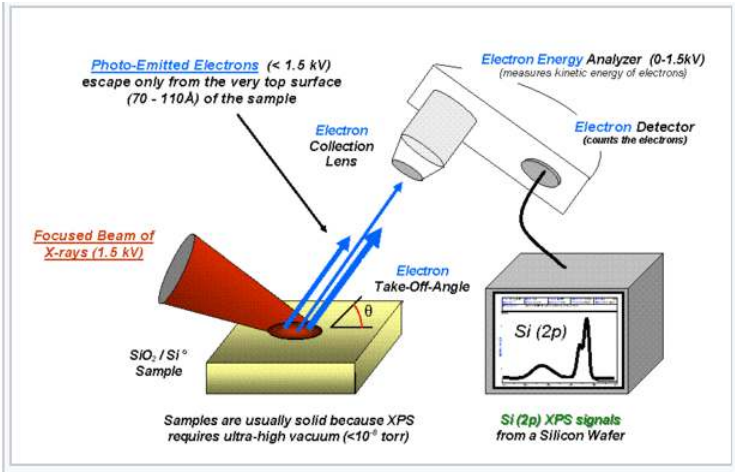
S = 32-24 = 8 shared electrons = **4 bonds**

The number of lone pairs is obtained by difference: (V-S)/2 = (24-8)/2 = 8

Now draw the molecule, starting with the four bonds and adding eight lone pairs to complete the octets:



Count the shared and unshared electrons around each atom in the nitrate ion and you will see that all atoms are **octet** and that the total number of valence electrons (V) is 24. If you do the N-V calculation according to the rules above, you should always get an octet structure.



The charges on atoms in a molecule (or an extended solid such as SiO_2) can be estimated from X-ray photoelectron spectra (XPS). Energetic X-rays ionize atoms by kicking out electrons from their core orbitals. By conservation of energy, the kinetic energy (KE) of an emitted electron is related to its binding energy (BE) and the energy of the incoming X-ray photon (hv) by BE = hv - KE. Electrons are harder to remove from positively charged atoms (higher BE), and easier to remove from negatively charged atoms (lower BE), relative to the neutral element.

The **formal charge** distribution is assigned by dividing the shared (bonding) electrons equally between atoms. Thus, the singly bonded O atoms each possess 7 electrons, and because O is in group 6, their formal charge is -1. The doubly bonded O has a formal charge of zero. The N atom has a formal charge of +1 because it "owns" 4 valence electrons and is in group 5.

Note that the **formal charge** is **not** the same thing as the **oxidation number** (or **oxidation state**). In the nitrate ion, the oxidation state of nitrogen is +5 and the oxidation state of oxygen is -2. The formal charge is typically closer to the "real" charge on the atom (as measured, e.g., by X-ray photoelectron spectroscopy). Oxidation states are a useful bookkeeping device for keeping track of

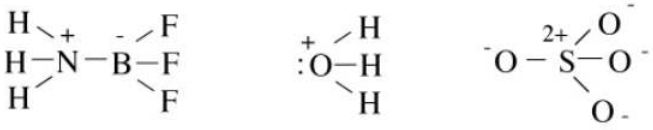
oxidation-reduction reactions, as we will discuss in Chapter 4. Like oxidation states, the formal charges on the atoms in a molecule or ion must *add up to its overall charge*.

We can similarly draw the Lewis structure for ammonia as shown below:



When we divide the shared electrons equally between the atoms, we see that the N atom has five electrons and each H atom has one. These are the same as their group numbers, and thus, all the formal charges in the ammonia molecule are zero.

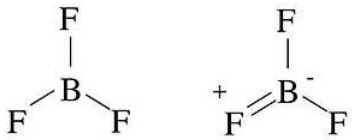
Octet structures of the Lewis acid-base adduct NH_3BF_3, the hydronium ion H_3O^+, and the sulfate anion SO_4^{2-} are shown below. In this case (and in many Lewis structures we will draw), we leave off the implied lone pairs around the peripheral atoms. Try calculating the number of bonds in each of these molecules using the N-V method, and fill in the lone pairs that are not explicitly drawn in.



In cases where more than one valence bond structure is possible, we can use formal charges to decide which structures should be more or less stable. The rules are:

- The formal charges on atoms are minimized in stable structures, zero being the best case.
- Negative formal charges should be placed on the most electronegative atom(s).
- Positive formal charges should be placed on the least electronegative atom(s).
- It is unfavorable to place like charges (++ or --) on neighboring atoms in a molecule.

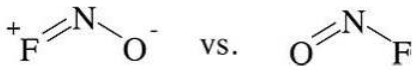
Examples of these rules are shown below for alternative structures of BF_3 and ONF.

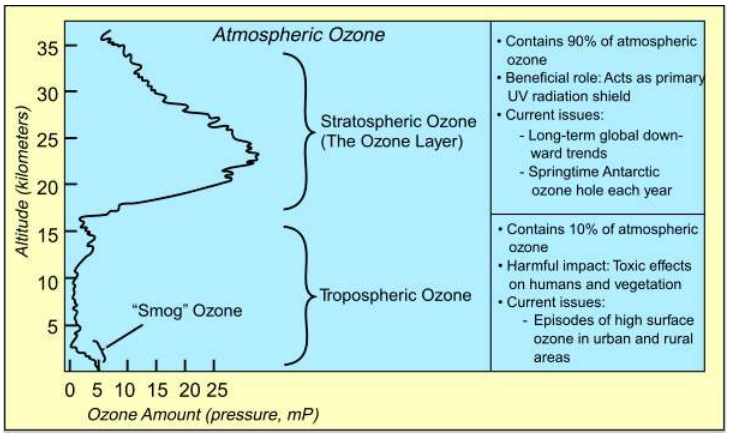


In the BF_3 case, the structure on the left is non-octet, because there are only six electrons (three bonds) in the valence shell of B. Such structures are said to be *electron deficient*. An octet structure (right) can be drawn, but it places a positive formal charge on F, the most electronegative atom in the molecule. Thus, neither structure is completely "happy," but the formal charge rules tell us that the electron-deficient structure on the left is more stable. The electron deficiency of BF_3makes it a powerful Lewis acid.

In the case of ONF, the structure on the left is unfavorable for two reasons. First, it places a positive formal charge on F, the most electronegative atom. Second, there is another possible structure (right) that has zero formal charge, which is preferable to one with

non-zero charge. This means that the structure on the right, with a double bond between N and O, is more reasonable.

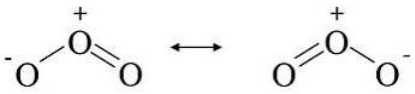




Life outside of the ocean owes its existence to the presence of ozone (O_3) in the stratosphere. Ozone absorbs the ultraviolet light in the solar spectrum, which otherwise would cause catastrophic damage to DNA and other biological molecules. Because ozone is produced photochemically from O_2, which is itself generated by photosynthesis, the spectroscopic signature of ozone in the atmosphere of distant planets is one possible way to look for extraterrestrial life.

Resonance structures

The ozone (O_3) molecule has two equivalent octet structures, shown below:



In both cases, the Lewis dot diagram suggests that there are three kinds of oxygen atoms in the molecule, with +1, 0, and -1 formal charges. These structures also suggest that ozone should have one single and one double bond. Experimentally (by electron diffraction), however, we find that the molecule is symmetric, with both O-O bond lengths the same. The real (instantaneous) structure is the average of the two forms, as shown below. In the classical Lewis picture of the molecule, we can rationalize resonance by observing that electrons, being thousands of times lighter than the nuclei of atoms, move very fast on the timescale of molecular vibrations. Thus, in the time it takes for the oxygen atoms to adjust their positions, the electrons can move back and forth many times. In the quantum mechanical MO picture (Chapter 2), we will see that resonance involves electrons that are fully

delocalized over the atoms in the molecule. We represent resonance structures with a double-headed arrow to signify that the only difference between the Lewis structures is the distribution of electrons.

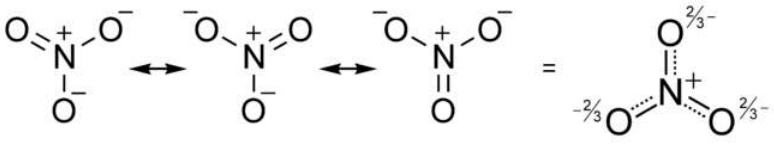


Susan Solomon discovered the heterogeneous catalytic mechanism whereby ozone is decomposed by chlorofluorocarbons (freons), creating the Antarctic ozone hole. Her work formed the basis of the U.N. Montreal Protocol, an international agreement to protect the ozone layer by regulating damaging chemicals.

In the instantaneous structure of ozone, the formal (-) charge is shared between the two terminal oxygen atoms and therefore each one has a formal charge of -1/2. The O-O bonds are the average of a single and a double bond, i.e., each O-O bond order is 1.5.

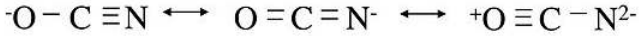


Similarly, the nitrate anion has three resonance structures, and experimentally (by X-ray crystallography of nitrate salts) we find that all the N-O bonds in the ion are the same. In this case, in the averaged structure, each O atom has a formal charge of -2/3 and the N-O bond order is 4/3 (=1.33...).



Inequivalent resonance structures

The rules of resonance also apply to inequivalent structures, which in general will have different energies from each other. In this case the structure of the molecule represents a weighted average of the low energy structures. A good example is the cyanate ion, OCN^-. We can write three inequivalent octet structures for the molecule:

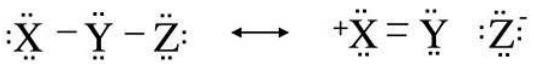


The first two are reasonable resonance structures, although we suspect the one on the left is the best because it puts the negative formal charge on the most electronegative atom. The last one is clearly a bad resonance structure, because the formal charges are

high and there is a positive charge on the oxygen atom. The real structure is thus a weighted average of the first two.

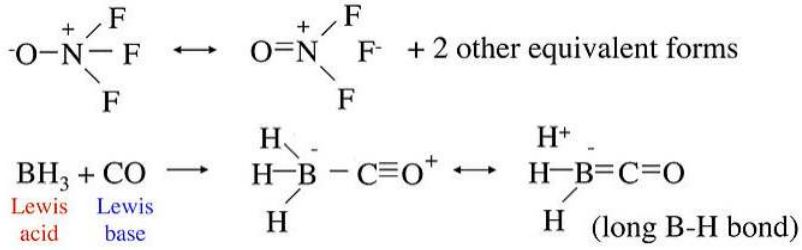
No-bond resonance

An interesting and useful kind of inequivalent resonance structure is one in which there is a bond order of *zero* between two of the atoms. This concept of **no-bond resonance** is important in understanding the bonding in many halogen- and hydrogen-containing compounds. The idea is illustrated below for the generic molecule X-Y-Z, where Z might be an electronegative halogen atom such as F. By moving the bonding electrons from the Y-Z bond onto the Z atom, and moving a lone pair from X into the X-Y bond, we generate the resonance structure shown on the right in which all atoms remain octet, but there is no bond between Y and Z.

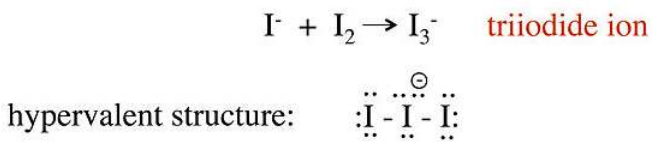


It is important to recognize in this example that the no-bond form is only one resonance structure, and therefore the Z atom is still bound to Y. If the two resonance structures in this example have the same energy, we would expect the X-Y bond order to be 1.5 and the Y-Z bond order to be 0.5. Therefore the Y-Z bond should be longer than it is in a compound where the bond order is one, and it should be relatively easy to break the Y-Z bond.

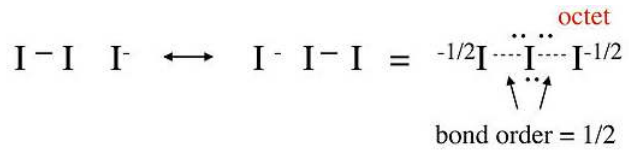
Some molecular examples of no-bond resonance are shown below. In the molecule ONF_3, the N-F bond is unusually long relative to the N-F bond in NF_3, in which the bond order is 1. This can be explained by the no-bond resonance forms shown on the right. Similarly, in the Lewis acid-base adduct formed by combining BH_3 with CO, we can explain the long B-H bonds using no-bond resonance forms that place a partial positive charge on the H atoms.



No-bond resonance is often used to provide an octet bonding picture for so-called **hypervalent compounds**, which are compounds that appear to have more than 8 valence electrons in the bonding shell of the central atom. For example, we can consider two different valence bond structures for the triiodide ion, I_3^-, which is formed by reaction of I^- with I_2 in water:

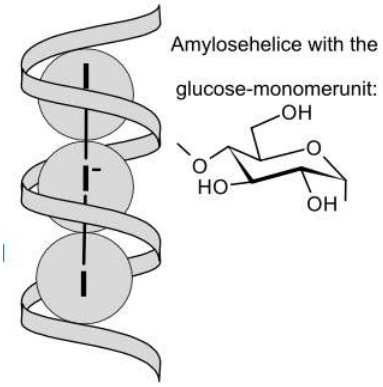


In this structure, the central iodine atom has 10 electrons in its valence shell, in violation of the octet rule. Raman spectra of the triiodide ion show that the I-I bond is weaker than the I-I single bond in I_2, suggesting that this picture is not an accurate description of the bonding. A better representation of I_3^- can be obtained with no-bond resonance structures, as shown below. We will see that this picture is consistent with the MO description of I_3^- in Chapter 2:

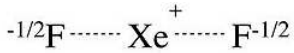




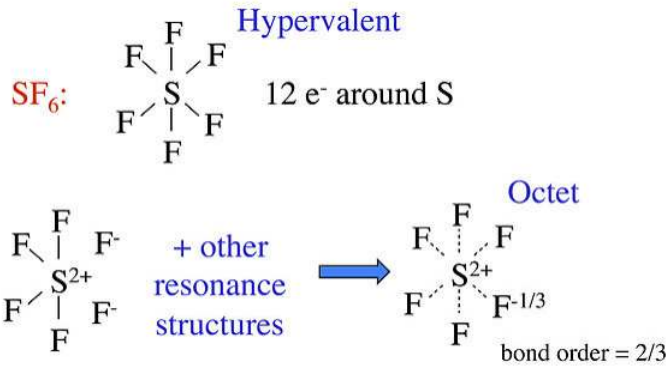
The deep blue color of starch-iodine solutions results from the complexation of linear polyiodide ions (I_n^-) by the starch (amylose) left-handed helix. The interior of the helix is hydrophobic. In electron donor solvents such as ethanol and water, I_2 and salts of I_3^- have a brown color, the result of a charge transfer interaction between the solvent and solute.[2][3]

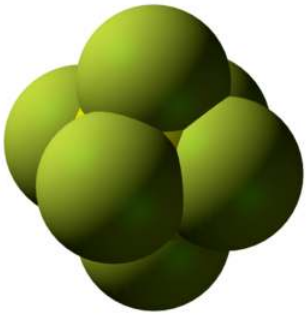


We can draw a similar picture for the XeF_2 molecule, which has the same number of valence electrons as I_3^-. This picture is consistent with XPS data, which show a partial negative charge on the F atoms, as well as vibrational spectra, which show that the Xe-F bond is weaker in XeF_2 than it is in the singly-bonded cation $Xe\text{-}F^+$.



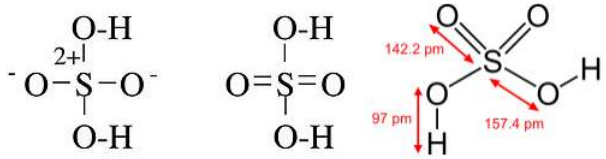
Other well known examples of hypervalent compounds are PF_5, $P(CH_3)_5$, and SF_6, as well as oxyacids such as H_2SO_4 and $HClO_4$. The hypervalent structure is often drawn for these molecules, with the explanation that d-orbitals on the central atom contribute to the bonding in dsp^3 and d^2sp^3 hybrids for 5- and 6-coordinate molecules, respectively. However, realistic molecular orbital calculations show that the phosphorus and sulfur 3d orbitals are too high in energy to contribute significantly to bonding in PF_5 and SF_6. For these molecules, we can use no-bond resonance to make reasonable octet structures that predict polar bonds between the central atom and F.





Space-filling model of sulfur hexafluoride. SF_6 is surprisingly unreactive with water, relative to other compounds that contain S-F bonds. The tight packing of F atoms around S prevents nucleophilic attack by water.

In other cases, such as $P(CH_3)_5$, the octet structure is unreasonable because it suggests a polar bond between P and C, with a partial negative charge on C. Further, in the case of oxyacids such as H_2SO_4 and $HClO_4$, X-ray crystallographic data establish that the S-O and Cl-O bonds are shorter for the oxygen atoms not bonded to hydrogen, which is more consistent with the hypervalent picture:

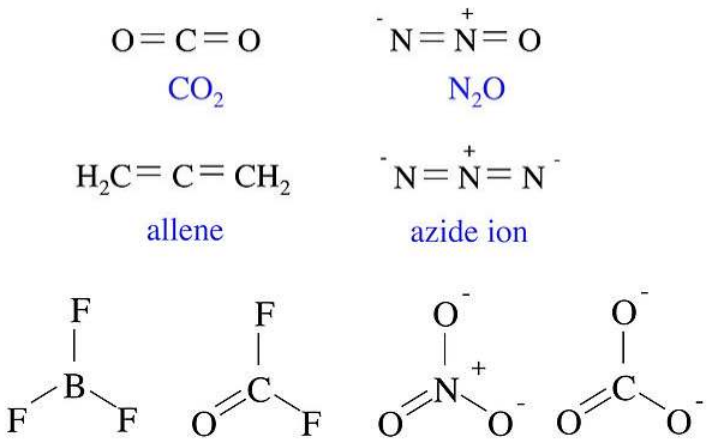


The question of whether hypervalency and the octet rule are really useful descriptions of the bonding in these compounds has been considered in a number of computational studies, which have used increasingly accurate quantum mechanical calculations to determine the number of electrons associated with the central atom. In a 2002 study, Gillespie and Silvi[4] found that the population of the valence shell is greater than eight for compounds with electropositive ligands, such as $P(CH_3)_5$, and less than eight for compounds such as PF_5. They concluded that these valence electron shell populations depend primarily on the coordination numbers and electronegativities of the central atoms and their ligands, and that there is no fundamental difference between the bonding in hypervalent and non-hypervalent (Lewis octet) molecules. This reminds us that the octet rule is not a law of nature, but rather an empirical rule that is useful within certain limits.

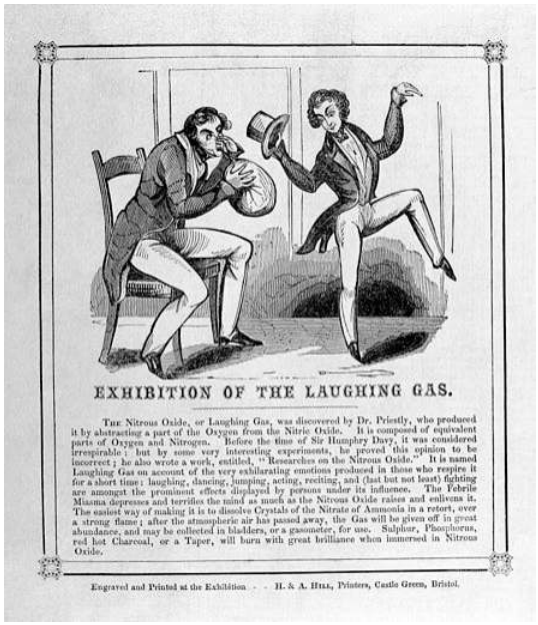
The isoelectronic principle

In calculating the octet structures of molecules using the N-V method, we needed to know only the number of atoms and the number of electrons, not the identities of the atoms themselves. This means that we will get the same answer (and the same set of octet and resonance structures) for *any* molecule or ion that contains (a) the same number of non-hydrogen atoms, and (b) the same total number of valence electrons. Such molecules are said to be *isoelectronic*. This is a powerful conclusion because, once we have determined the electronic structure of one molecule, we can write down the same solution for *all other molecules* that are isoelectronic. For example, we noted above that I_3^- and XeF_2, which both have 22 valence electrons, have the same valence bond structure. We can further expect that isoelectronic molecules will have the same shapes and, very often, similar physical properties.

The four molecules and ions below all contain three non-hydrogen atoms and 16 valence electrons. All of them are linear molecules with two double bonds. The four molecules and ions shown below them all contain four non-hydrogen atoms and 24 valence electrons. These four have a trigonal planar shape. While BF_3 is a member of this isoelectronic series, we do not write it in the resonance form that contains a B=F double bond, because that would put a positive formal charge on F.



Similarly we can show that CH_4, NH_3, NH_4^+, H_2O, H_3O^+, HF, F^-, and OH^- are all isoelectronic with one non-H atom and eight valence electrons. In the next section we will see that this gives rise to nearly identical electronic shapes for these molecules.



Nitrous oxide (N_2O), or laughing gas, is isoelectronic with CO_2. The two molecules have the same shape (linear) and similar physical properties. CO_2 sublimes at -78 °C, whereas N_2O melts at -91 °C and boils at -88 °C.

Isoelectronic solids

The isoelectronic principle works not just for molecules but for extended solids as well. One technologically important set of isoelectronic solids are the p-block semiconductors. The group 14 element Si is the most widely used semiconductor for electronics, but, as we will discuss later, it is not a good light emitter. Light-emitting diodes (LEDs), which are used in lasers, high efficiency lighting, and display technologies, are made from compounds that are isoelectronic with Si and Ge, especially GaAs, GaP, AlAs, and GaN (all contain four valence electrons per atom). CdTe and $CuIn_{1-x}Ga_xSe_2$ (CIGS) are promising solar cell materials that also have the same number of valence electrons per atom. Like Si and Ge, these compounds have tetrahedrally bonded structures in the solid state and absorb light across most of the solar spectrum, as we will discuss in more detail in Chapters 8 and 10.

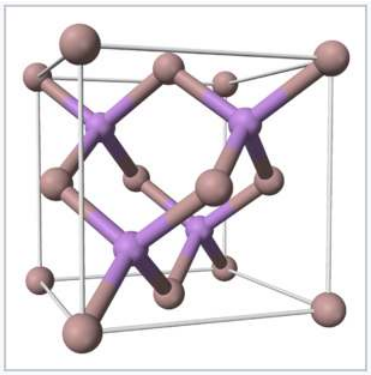


Figure **3.2.2**: The tetrahedral bonding in crystals of GaAs, CdTe, $CuIn_{1-x}Ga_xSe_2$ and other semiconductors is similar to that in isoelectronic Si and Ge.

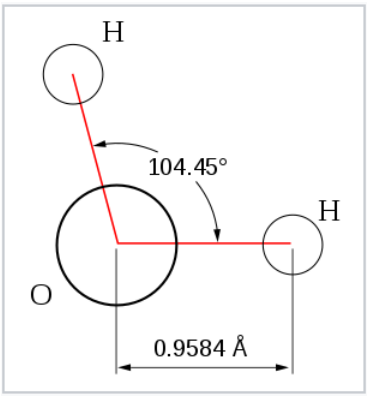
The isoelectronic principle is also a powerful tool in materials research, because it provides guidance about where to look for new materials with similar and perhaps improved properties. For example, the discovery that 8.5% efficient thin layer solar cells could be made with the compound $CsSnI_3$[5] stimulated the exploration of many isoelectronic ABX_3 compounds with the same perovskite crystal structure. Very recently thin film solar cells based on light absorbers in this structural family $(MA)PbI_{3-x}Cl_x$ and $FA_xMA_{1-x}PbBr_yI_{3-y}$ (MA^+ = methylammonium, $CH_3NH_3^+$; FA^+ = formamidinium, $HC(NH_2)_2^+$) have been reported with efficiencies as high as 22%.[6][7][8]

3.2: Valence Bond Theory- Lewis Dot Structures, the Octet Rule, Formal Charge, Resonance, and the Isoelectronic Principle is shared under a CC BY-SA license and was authored, remixed, and/or curated by LibreTexts.

- **1.2: Valence Bond Theory- Lewis Dot Structures, the Octet Rule, Formal Charge, Resonance, and the Isoelectronic Principle** by Chemistry 310 is licensed CC BY-SA 4.0. Original source: https://en.wikibooks.org/wiki/Introduction_to_Inorganic_Chemistry.

3.3: The Shapes of Molecules (VSEPR Theory) and Orbital Hybridization

The Valence Shell Electron Pair Repulsion (VSEPR) theory is a simple and useful way to predict and rationalize the shapes of molecules. The theory is based on the idea of minimizing the electrostatic repulsion between electron pairs, as first proposed by Sidgwick and Powell in 1940,[9] then generalized by Gillespie and Nyholm in 1957,[10] and then broadly applied over the intervening 50+ years.[11]



Geometry of the water molecule

To use the VSEPR model, one begins with the Lewis dot picture to determine the number of lone pairs and bonding domains around a central atom. Because VSEPR considers all bonding domains equally (i.e., a single bond, a double bond, and a half bond all count as one electron domain), one can use either an octet or hypervalent structure, provided that the number of lone pairs (which should be the same in both) is calculated correctly. For example, in either the hypervalent or octet structure of the I_3^- ion above, there are three lone pairs on the central I atom and two bonding domains. We then follow these steps to obtain the **electronic geometry**:

- Determine the number of lone pairs on the central atom in the molecule, and add the number of bonded atoms (a.k.a. bonding domains)
- This number (the *steric number*) defines the electronic shape of the molecule by minimizing repulsion. For example a steric number of three gives a trigonal planar electronic shape.
- The angles between electron domains are determined primarily by the electronic geometry (e.g., 109.5° for a steric number of 4, which implies that the electronic shape is a tetrahedron)
- These angles are adjusted by the hierarchy of repulsions: (lone pair - lone pair) > (lone pair - bond) > (bond - bond)

The **molecular geometry** is deduced from the electronic geometry by considering the lone pairs to be present but invisible. The most commonly used methods to determine molecular structure - X-ray diffraction, neutron diffraction, and electron diffraction - have a hard time seeing lone pairs, but they can accurately determine the lengths of bonds between atoms and the bond angles.

The table below gives examples of electronic and molecular shapes for steric numbers between 2 and 9. We are most often concerned with molecules that have steric numbers between 2 and 6.

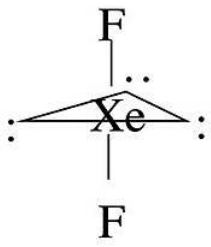
Bonding electron pairs	Lone pairs	Electron domains (Steric #)	Shape	Ideal bond angle (example's bond angle)	Example	Image
2	0	2	linear	180°	CO_2	Linear-3D-balls.png
3	0	3	trigonal planar	120°	BF_3	Trigonal-3D-balls.png
2	1	3	bent	120° (119°)	SO_2	Bent-3D-balls.png
4	0	4	tetrahedral	109.5°	CH_4	AX4E0-3D-balls.png
3	1	4	trigonal pyramidal	109.5° (107°)	NH_3	Pyramidal-3D-balls.png
2	2	4	bent	109.5° (104.5°)	H_2O	Bent-3D-balls.png
5	0	5	trigonal bipyramidal	90°, 120°, 180°	PCl_5	Trigonal-bipyramidal-3D-balls.png
4	1	5	seesaw	180°, 120°, 90° (173.1°, 101.6°)	SF_4	Seesaw-3D-balls.png
3	2	5	T-shaped	90°, 180° (87.5°, < 180°)	ClF_3	T-shaped-3D-balls.png
2	3	5	linear	180°	XeF_2	Linear-3D-balls.png
6	0	6	octahedral	90°, 180°	SF_6	AX6E0-3D-balls.png
5	1	6	square pyramidal	90° (84.8°), 180°	BrF_5	Square-pyramidal-3D-balls.png
4	2	6	square planar	90°, 180°	XeF_4	Square-planar-3D-balls.png
7	0	7	pentagonal bipyramidal	90°, 72°, 180°	IF_7	Pentagonal-bipyramidal-3D-balls.png
6	1	7	pentagonal pyramidal	72°, 90°, 144°	$XeOF_5^-$	Pentagonal-pyramidal-3D-balls.png
5	2	7	planar pentagonal	72°, 144°	XeF_5^-	Pentagonal-planar-3D-balls.png
8	0	8	square antiprismatic		XeF_8^{2-}	Square-antiprismatic-3D-balls.png
9	0	9	tricapped trigonal prismatic		ReH_9^{2-}	AX9E0-3D-balls.png

From the Table, we see that some of the molecules shown as examples have bond angles that depart from the ideal electronic geometry. For example, the H-N-H bond angle in ammonia is 107°, and the H-O-H angle in water is 104.5°. We can rationalize this in terms of the last rule above. The lone pair in ammonia repels the electrons in the N-H bonds more than they repel each other. This lone pair repulsion exerts even more steric influence in the case of water, where there are two lone pairs. Similarly, the axial F-S-F angle in the "seesaw" molecule SF_4 is a few degrees less than 180° because of repulsion by the lone pair in the molecule.

Geometrical isomers

For some molecules in the Table, we note that there is more than one possible shape that would satisfy the VSEPR rules. For example, the XeF_2 molecule has a steric number of five and a trigonal bipyramidal geometry. There are three possible

stereoisomers: one in which the F atoms occupy axial sites, resulting in linear molecule, one in which the F atoms occupy one equatorial and one axial site (resulting in a 90° bond angle), and one in which the F atoms are both on equatorial sites, with a F-Xe-F bond angle of 120°.



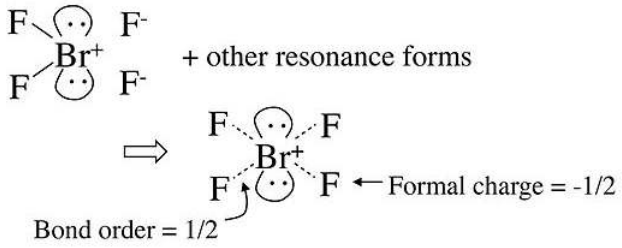
The observed geometry of XeF_2 is linear, which can be rationalized by considering the orbitals that are used to make bonds (or lone pairs) in the axial and equatorial positions. There are four available orbitals, s, p_x, p_y, and p_z. If we choose the z-axis as the axial direction, we can see that the p_x and p_y orbitals lie in the equatorial plane. We assume that the spherical s orbital is shared equally by the five electron domains in the molecule, the two axial bonds share the p_z orbital, and the three equatorial bonds share the p_x and p_y orbitals. We can then calculate the bond orders to axial and equatorial F atoms as follows:

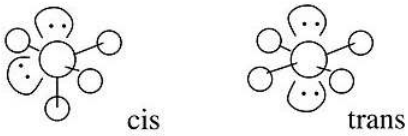
$$axial: \ \tfrac{1}{5} + \tfrac{1}{2}p_z = 0.7 \ bond (formal \ charge = -0.3)$$

$$equatorial: \ \tfrac{1}{5}s + \tfrac{1}{3}p_x + \tfrac{1}{3}p_y = 0.867 \ bond (formal \ charge = -0.122)$$

Because fluorine is more electronegative than a lone pair, it prefers the axial site where it will have more negative formal charge. In general, by this reasoning, lone pairs and electropositive ligands such as CH_3 will always prefer the equatorial sites in the trigonal bipyramidal geometry. Electronegative ligands such as F will always go to the axial sites.

In the case of the BrF_4^- anion, which is isoelectronic with XeF_4 in the Table, the electronic geometry is octahedral and there are two possible isomers in which the two lone pairs are *cis* or *trans* to each other. In this case, lone pair - lone pair repulsion dominates and we obtain the *trans* arrangement of lone pairs, giving a square planar molecular geometry.





Orbital hybridization

The observation of molecules in the various electronic shapes shown above is, at first blush, in conflict with our picture of atomic orbitals. For an atom such as oxygen, we know that the 2s orbital is spherical, and that the $2p_x$, $2p_y$, and $2p_z$ orbitals are dumbell-shaped and point along the Cartesian axes. The water molecule contains two hydrogen atoms bound to oxygen not at a 90° angle, but at an angle of 104.5°. Given the relative orientations of the atomic orbitals, how do we arrive at angles between electron domains of 104.5°, 120°, and so on? To understand this we will need to learn a little bit about the quantum mechanics of electrons in atoms and molecules.

The atomic orbitals ψ represent solutions to the **Schrödinger wave equation**,

$$E\psi = \hat{H}\psi \tag{3.3.1}$$

Here E is the energy of an electron in the orbital, and $\hat{H}$ is the Hamiltonian operator.

By analogy with classical mechanics, the Hamiltonian is commonly expressed as the sum of operators corresponding to the kinetic and potential energies of a system in the form

$$\hat{H} = \hat{T} + \hat{V} \tag{3.3.2}$$

where $\hat{V} = V(\mathbf{r}, t)$ is the potential energy, and

$$\hat{T} = \frac{\hat{\mathbf{p}} \cdot \hat{\mathbf{p}}}{2m} = \frac{\hat{p}^2}{2m} = -\frac{\hbar^2}{2m}\nabla^2, \tag{3.3.3}$$

is the kinetic energy operator in which m is the mass of the particle and the momentum operator is:

$$\hat{p} = -i\hbar\nabla, \text{where} \nabla = \frac{\delta}{\delta x} + \frac{\delta}{\delta y} + \frac{\delta}{\delta z} \tag{3.3.4}$$

Here $\hbar$ is h/2π, where h is Planck's constant, and the Laplacian operator ∇^2 is:

$$\nabla^2 = \frac{\delta^2}{\delta x^2} + \frac{\delta^2}{\delta y^2} + \frac{\delta^2}{\delta z^2} \tag{3.3.5}$$

Although this is not the technical definition of the Hamiltonian in classical mechanics, it is the form it most commonly takes in quantum mechanics. Combining these together yields the familiar form used in the Schrödinger equation:

$$\hat{H} = \hat{T} + \hat{V} = \frac{\hat{\mathbf{p}} \cdot \hat{\mathbf{p}}}{2m} + V(\mathbf{r}, t) = -\frac{\hbar^2}{2m}\nabla^2 + V(\mathbf{r}, t) \tag{3.3.6}$$

For hydrogen-like (one-electron) atoms, the Schrödinger equation can be written as:

$$E\psi = -\frac{\hbar^2}{2\mu}\nabla^2\psi - \frac{Ze^2}{4\pi\epsilon_0 r}\psi \tag{3.3.7}$$

where **Z** is the nuclear charge, e is the electron charge, and **r** is the position of the electron. The radial potential term on the right side of the equation is due to the Coulomb interaction, i.e., the electrostatic attraction between the nucleus and the electron, in which ε_0 is the dielectric constant (permittivity of free space) and

$$\mu = \frac{m_e m_n}{m_e + m_n} \tag{3.3.8}$$

is the 2-body reduced mass of the nucleus of mass m_n and the electron of mass m_e. To a good approximation, $\mu \approx m_e$.



Erwin Schrödinger as a young scientist

This is the equation that Erwin Schrödinger famously derived in 1926 to solve for the energies and shapes of the s, p, d, and f atomic orbitals in hydrogen-like atoms. It was a huge conceptual leap for both physics and chemistry because it not only explained the quantized energy levels of the hydrogen atom, but also provided the theoretical basis for the octet rule and the arrangement of elements in the periodic table.

The Schrödinger equation can be used to describe chemical systems that are more complicated than the hydrogen atom (e.g., multi-electron atoms, molecules, infinite crystals, and the dynamics of those systems) if we substitute the appropriate potential energy

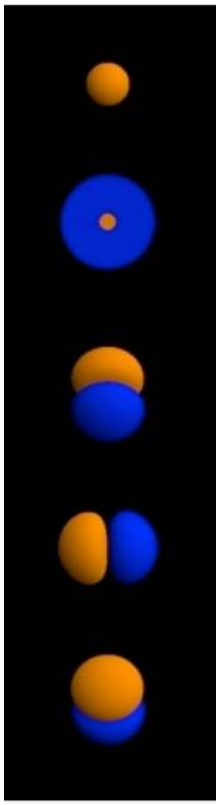
function V(r,t) into the Hamiltonian. The math becomes more complicated and the equation must be solved numerically in those cases, so for our purposes we will stick with the simplest case of time-invariant, one-electron, hydrogen-like atoms.

Without going into too much detail about the Schrödinger equation, we can point out some of its most important properties:

$$E\psi = -\frac{\hbar^2}{2\mu}\nabla^2\psi - \frac{Ze^2}{4\pi\epsilon_0 r}\psi \tag{3.3.9}$$

- The equation derives from the fact that the total energy (E) is the sum of the kinetic energy (KE) and the potential energy (PE). These three quantities are represented mathematically as **operators** in the equation.
- On the left side of the equation, the total energy operator (E) is a scalar that is multiplied by the wavefunction ψ. ψ is a function of the spatial coordinates (x,y,z) and is related to the probability that the electron is at that point in space.
- The first term on the right side of the equation represents the kinetic energy (KE). The kinetic energy operator is proportional to ∇^2 (the Laplacian operator) which takes the second derivative (with respect to three spatial coordinates) of ψ. Thus, the Schrödinger equation is a **differential equation**.
- The second term on the right side of the equation represents the Coulomb potential (PE), i.e. the attractive energy between the positively charged nucleus and the negatively charged electron.
- The solutions to the Schrödinger equation are a set of **energies** E (which are scalar quantities) and **wavefunctions** (a.k.a. **atomic orbitals**) ψ, which are functions of the spatial coordinates. You will sometimes see the energies referred to as *eigenvalues* and the orbitals as *eigenfunctions*, because mathematically the Schrödinger equation is an eigenfunction-eigenvalue equation. Although ψ is a function of the coordinates, E is not. So an electron in a $2p_z$ orbital has the same total energy E (= PE + KE) no matter where it is in space.
- These E values and their associated wavefunctions ψ are catalogued according to their **quantum numbers** *n*, *l*, and m_l. That is, there are many solutions to the differential equation, and each solution (ψ(xyz) and E) has a unique set of quantum numbers. Some sets of orbitals are **degenerate**, meaning that they have the same energy (e.g., $2p_x$, $2p_y$, and $2p_z$).
- The solutions ψ(xyz) to the Schrödinger equation (e.g., the 1s, 2s, $2p_x$, $2p_y$, and $2p_z$ orbitals) represent **probability amplitudes** for finding the electron at a particular point (x,y,z) in space. A probability amplitude can have either **+ or - sign**. We typically represent the different signs by shading or by + and - signs on the two lobes of a 2p orbital.
- The square of the probability amplitude, ψ^2, is always a positive number and represents the **probability** of finding the electron at a point x,y,z in space. Because the total probability of finding the electron somewhere is 1, the wavefunction must be **normalized** so that the integral of ψ^2 over the spatial coordinates (from -∞ to +∞) is 1.

- The solutions to the Schrödinger equation are **orthogonal**, meaning that the product of any two (integrated over all space) is zero. For example the product of the 2s and $2p_x$ orbitals, integrated over the spatial coordinates from -∞ to +∞, is zero.



The shapes of the first five atomic orbitals: 1s, 2s, $2p_x$, $2p_y$, and $2p_z$. The colors denote the sign of the wave function.

Orbital hybridization involves making *linear combinations* of the atomic orbitals that are solutions to the Schrödinger equation. Mathematically, this is justified by recognizing that the Schrödinger equation is a *linear* differential equation. As such, any sum of solutions to the Schrödinger equation is also a valid solution. However, we still impose the constraint that our hybrid orbitals must be **orthogonal** and **normalized**.

Rules for orbital hybridization:

- Add and subtract atomic orbitals to get hybrid orbitals.
- We get the same number of orbitals out as we put in.
- The energy of a hybrid orbital is the weighted average of the atomic orbitals that make it up.
- The coefficients are determined by the constraints that the hybrid orbitals must be orthogonal and normalized.

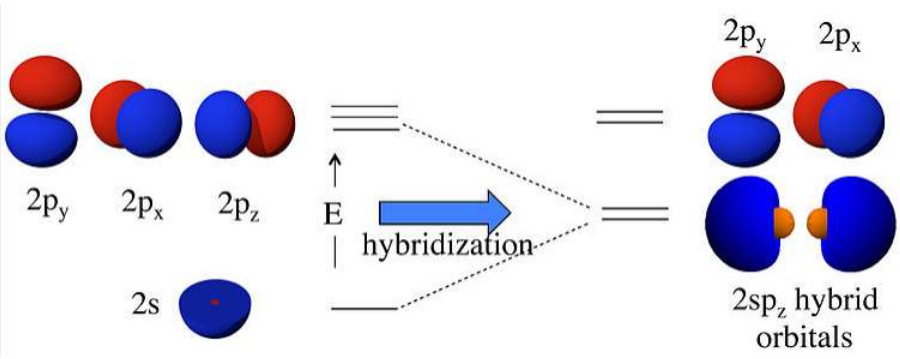
For **sp hybridization**, as in the BeF_2 or CO_2 molecule, we make two linear combinations of the 2s and $2p_z$ orbitals (assigning z as the axis of the Be-F bond):

$$\psi_1 = \frac{1}{\sqrt{2}}(2s) + \frac{1}{\sqrt{2}}(2p_z) \tag{3.3.10}$$

$$\psi_2 = \frac{1}{\sqrt{2}}(2s) - \frac{1}{\sqrt{2}}(2p_z) \tag{3.3.11}$$

Here we have simply added and subtracted the 2s and 2pz orbitals; we leave it as an exercise for the interested student to show that both orbitals are normalized (i.e., $\int \psi_1^2 d\tau = \int \psi_2^2 d\tau = 1$) and orthogonal (i.e., $\int \psi_1 \psi_2 d\tau = 0$) .

What this means physically is explained in the figure below. By combining the 2s and $2p_z$ orbitals we have created two new orbitals with large lobes (high electron probability) pointing along the z-axis. These two orbitals are degenerate and have an energy that is halfway between the energy of the 2s and $2p_z$ orbitals.



Linear combinations of the 2s and $2p_z$ atomic orbitals make two $2sp_z$ hybrids. The $2p_x$and $2p_y$ orbitals are unchanged.

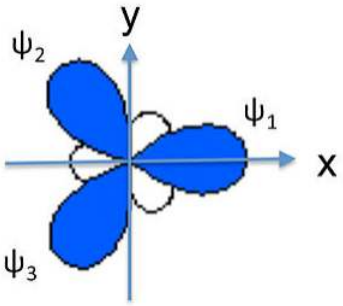
For an isolated Be atom, which has two valence electrons, the lowest energy state would have two electrons spin-paired in the 2s orbital. However, these electrons would not be available for bonding. By **promoting** these electrons to the degenerate $2sp_z$ hybrid orbitals, they become unpaired and are prepared for bonding to the F atoms in BeF_2. This will occur if the **bonding energy** (in the promoted state) exceeds the promotion energy. The **overall bonding energy**, i.e., the energy released by combining a Be atom in its ground state with two F atoms, is the difference between the bonding and promotion energies.

We can similarly construct **sp^2 hybrids** (e.g., for the BF_3 molecule or the NO_3^- anion) from one 2s and two 2p atomic orbitals. Taking the plane of the molecule as the xy plane, we obtain three hybrid orbitals at 120° to each other. The three hybrids are:

$$\psi_1 = \frac{1}{\sqrt{3}}(2s) + \frac{\sqrt{2}}{\sqrt{3}}(2p_x) \tag{3.3.12}$$

$$\psi_2 = \frac{1}{\sqrt{3}}(2s) - \frac{1}{\sqrt{6}}(2p_x) + \frac{1}{\sqrt{2}}(2p_y) \tag{3.3.13}$$

$$\psi_3 = \frac{1}{\sqrt{3}}(2s) - \frac{1}{\sqrt{6}}(2p_x) - \frac{1}{\sqrt{2}}(2p_y) \tag{3.3.14}$$



These orbitals are again degenerate and their energy is the weighted average of the energies of the 2s, $2p_x$, and $2p_y$ atomic orbitals.

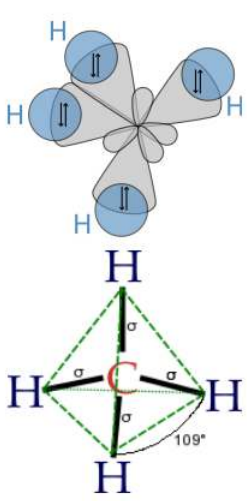
Finally, to make a sp^3 hybrid, as in CH_4, H_2O, etc., we combine all four atomic orbitals to make four degenerate hybrids:

$$\psi_1 = \frac{1}{2}(2s + 2p_x + 2p_y + 2p_z) \tag{3.3.15}$$

$$\psi_2 = \frac{1}{2}(2s - 2p_x - 2p_y + 2p_z) \tag{3.3.16}$$

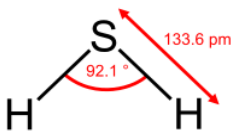
$$\psi_3 = \frac{1}{2}(2s + 2p_x - 2p_y - 2p_z) \tag{3.3.17}$$

$$\psi_4 = \frac{1}{2}(2s - 2p_x + 2p_y - 2p_z) \tag{3.3.18}$$



The lobes of the **sp^3 hybrid** orbitals point towards the vertices of a tetrahedron (or alternate corners of a cube), consistent with the tetrahedral bond angle in CH_4 and the nearly tetrahedral angles in NH_3 and H_2O. Similarly, we can show that we can construct the trigonal bipyramidal electronic shape by making sp and sp^2 hybrids, and the octahedral geometry from three sets of sp hybrids. The picture that emerges from this is that the atomic orbitals can hybridize as required by the shape that best minimizes electron pair repulsions.

Interestingly however, the bond angles in PH_3, H_2S and H_2Se are close to 90°, suggesting that P, S, and Se primarily use their p-orbitals in bonding to H in these molecules. This is consistent with the fact that the energy difference between s and p orbitals stays roughly constant going down the periodic table, but the bond energy *decreases* as the valence electrons get farther away from the nucleus. In compounds of elements in the 3rd, 4th, and 5th rows of the periodic table, there thus is a *decreasing tendency to use s-p orbital hybrids in bonding*. For these heavier elements, the bonding energy is not enough to offset the energy needed to promote the s electrons to s-p hybrid orbitals.



3.3: The Shapes of Molecules (VSEPR Theory) and Orbital Hybridization is shared under a CC BY-SA license and was authored, remixed, and/or curated by LibreTexts.

- **1.3: The Shapes of Molecules (VSEPR Theory) and Orbital Hybridization** by Chemistry 310 is licensed CC BY-SA 4.0. Original source: https://en.wikibooks.org/wiki/Introduction_to_Inorganic_Chemistry.

3.4: Bond Polarity and Bond Strength

Linus Pauling introduced the concept of electronegativity 1932 in order to explain the extra stability of molecules with polar bonds. [12] The electronegativity of an atom, represented by the Greek letter χ, can be defined as the tendency of an atom to draw electrons to itself in a chemical bond. On the Pauling scale, the electronegativity difference between two atoms A and B was defined in terms of the dissociation energies E_d of the A-A, B-B, and A-B bonds:

$$\chi_A - \chi_B = \sqrt{E_d(AB) - [E_d(AA) + E_d(BB)]/2} \tag{3.4.1}$$

where the energies are expressed in electron volts.

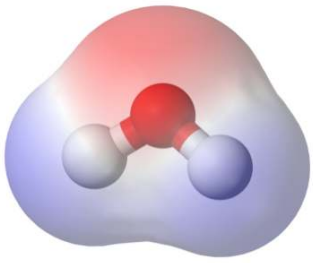
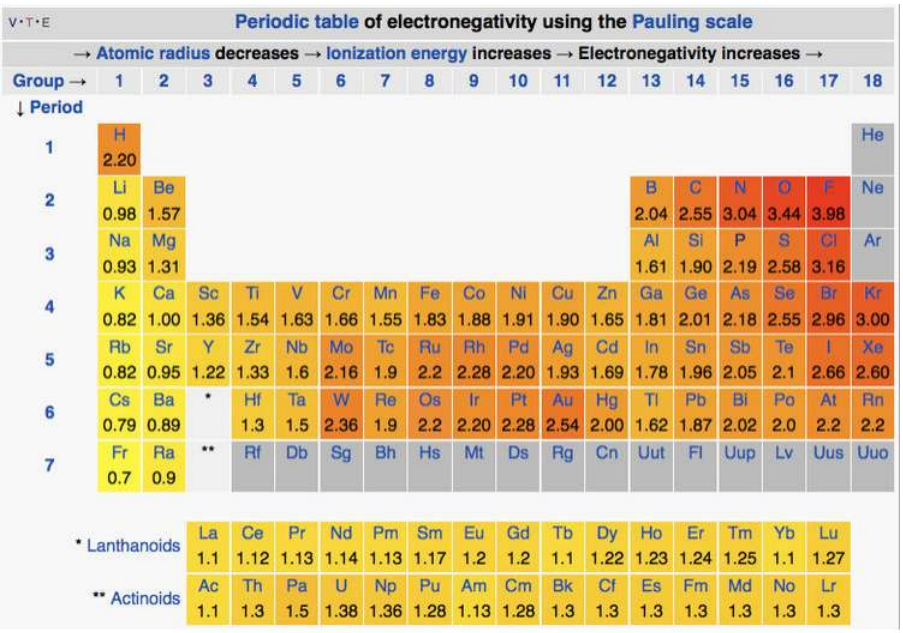


Figure **3.4.1**: A water molecule, a commonly used example of polarity. The two charges are present with a negative charge in the middle (red), and a positive charge at the ends (blue).

This definition, while directly relevant to the strength of chemical bonds, requires thermochemical input data from many compounds, some of which were not available at the time. Mulliken[13][14] and later Pearson[15] developed a scale of electronegativities based on the average of the electron affinity and ionization energy of the free A and B atoms, which they correlated with thermochemical data and the Pauling scale.

On the Pauling scale, the least electronegative elements are the alkali metals (χ = 0.7-1.0) and the most electronegative are oxygen (3.5) and fluorine (4.0) at the upper right of the periodic table. Carbon and hydrogen have intermediate electronegativities (2.6 and 2.2 on the Pauling scale, respectively). The general trend (see table below) is that electronegativities increase going up and to the right in the periodic table. There are some interesting exceptions to this behavior, most notably two islands of high electronegatvity at the bottom of the transition series, peaking at tungsten (χ = 2.4) and gold (χ = 2.5). The first of these can be explained by the very high metal-metal bond energy of elements such as Mo and W, which can use all six of their valence electrons in bonding, as we will discuss in Chapter 6. The second however occurs with more weakly bonded noble metals such as Pt and Au, and is responsible for their low position in the activity series,[16] as well as their extraordinary properties as catalysts.

Table of Pauling electronegativities



Periodic table of electronegativity using the Pauling scale

→ Atomic radius decreases → Ionization energy increases → Electronegativity increases →

Group →	1	2	3	4	5	6	7	8	9	10	11	12	13	14	15	16	17	18
↓ Period																		
1	H 2.20																	He
2	Li 0.98	Be 1.57											B 2.04	C 2.55	N 3.04	O 3.44	F 3.98	Ne
3	Na 0.93	Mg 1.31											Al 1.61	Si 1.90	P 2.19	S 2.58	Cl 3.16	Ar
4	K 0.82	Ca 1.00	Sc 1.36	Ti 1.54	V 1.63	Cr 1.66	Mn 1.55	Fe 1.83	Co 1.88	Ni 1.91	Cu 1.90	Zn 1.65	Ga 1.81	Ge 2.01	As 2.18	Se 2.55	Br 2.96	Kr 3.00
5	Rb 0.82	Sr 0.95	Y 1.22	Zr 1.33	Nb 1.6	Mo 2.16	Tc 1.9	Ru 2.2	Rh 2.28	Pd 2.20	Ag 1.93	Cd 1.69	In 1.78	Sn 1.96	Sb 2.05	Te 2.1	I 2.66	Xe 2.60
6	Cs 0.79	Ba 0.89	*	Hf 1.3	Ta 1.5	W 2.36	Re 1.9	Os 2.2	Ir 2.20	Pt 2.28	Au 2.54	Hg 2.00	Tl 1.62	Pb 1.87	Bi 2.02	Po 2.0	At 2.2	Rn 2.2
7	Fr 0.7	Ra 0.9	**	Rf	Db	Sg	Bh	Hs	Mt	Ds	Rg	Cn	Uut	Fl	Uup	Lv	Uus	Uuo

* Lanthanoids	La 1.1	Ce 1.12	Pr 1.13	Nd 1.14	Pm 1.13	Sm 1.17	Eu 1.2	Gd 1.2	Tb 1.1	Dy 1.22	Ho 1.23	Er 1.24	Tm 1.25	Yb 1.1	Lu 1.27
** Actinoids	Ac 1.1	Th 1.3	Pa 1.5	U 1.38	Np 1.36	Pu 1.28	Am 1.13	Cm 1.28	Bk 1.3	Cf 1.3	Es 1.3	Fm 1.3	Md 1.3	No 1.3	Lr 1.3

The polarity of bonds is determined by electronegativity differences. As a guideline we define bonds as:

- **ionic** if $\Delta\chi > 2.0$
- **polar** if $2.0 > \Delta\chi > 0.5$
- **nonpolar** if $0.5 > \Delta\chi$

The polarity of bonds helps us understand non-covalent forces between molecules, such as hydrogen bonding and dipole-dipole interactions. It also helps us interpret the reactivity of molecules. For example, the Si-H bond (χ_{Si} = 1.8, χ_H = 2.1) is more hydride-like than the C-H bond (χ_C = 2.5, χ_H = 2.1). Therefore silanes react with acids to make H_2, whereas phosphines (χ_P = 2.1) and hydrocarbons do not. Similarly, electrophilic substitution reactions occur more readily on Si-H and P-H compounds than they do on C-H compounds.

There is also a correlation between the strength of a chemical bond and the bond length, longer bonds being weaker because of weaker orbital overlap. Pauling introduced an empirical formula relating bond length to bond strength. For a given pair of atoms (for example, two carbon atoms):

$$D(n) = D(1) - 0.6\log_{10}(n) \tag{3.4.2}$$

where D(n) represents the bond length in Å and n is the bond order. D(1) in this case would be the length of a C-C single bond, which we can obtain from the average bond length in alkanes (1.54 Å). Using this formula we can predict that the bond lengths in ethylene (C=C double bond) and acetylene (C≡C triple bond) should be 1.36 and 1.25 Å, respectively, which are close to the experimental values of 1.33 and 1.20 Å. In a related form the Pauling formula can be used to calculate bond lengths when the single bond length D(1) is not available:

$$D(n) = D(m) - 0.6\log_{10}(n/m) \tag{3.4.3}$$

Here n and m represent two different bond orders between the same kinds of atoms. This tells, for example, that the difference in length between a triple and double bond, D(2)-D(3), should be - 0.6 $\log_{10}(2/3)$ = 0.11 Å. Some bond lengths and bond energies are anomalous. For example, the F-F bond length in F_2 is 1.43 Å, which is 0.15 Å *longer* than twice the covalent radius of the F atom (0.64 Å). The F-F bond is also quite weak (bond dissociation energy = 155 kJ/mol) relative to the Cl-Cl bond (242 kJ/mol). By putting the extra bond length into the Pauling formula, we calculate that the bond order in the F_2 molecule is only 0.6, i.e., substantially weaker than a F-F single bond. The physical reason for this is that the F-F bond is "stretched" by repulsion of the lone pairs on the F atoms. This crowding is caused by the fact that the [He] $1s^2$ core orbital, as well as the valence orbitals of the fluorine atoms, are contracted by the high nuclear charge. The Cl_2 atom, with its larger [Ne] ($1s^22s^22p^6$) core, in contrast, has a "normal" single bond length (1.98 Å) that is twice the covalent radius of the Cl atom (0.99 Å). A similar lone pair repulsion effect

explains the anomalously long and weak N-N and O-O single bonds in hydrazine (H_2N-NH_2) and hydrogen peroxide (HO-OH), which are both highly reactive molecules.

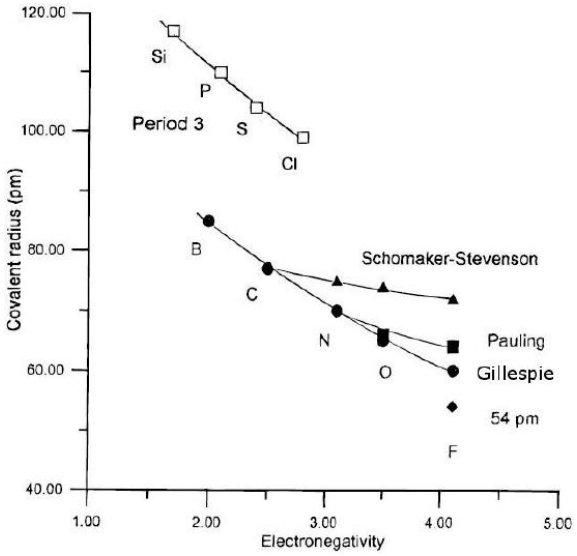


Figure **3.4.2**: Trends in covalent radii for p-block elements. The covalent radius of F has been difficult to determine because of electron pair repulsion effects. Early reports (Shomaker and Stevenson, Pauling) overestimated the size of the F atom.[17][18] [19]Accurate quantum chemical calculations place the F single-bond covalent radius at about 0.64 Å.[20] (Public Domain; N4nojohn via Wikipedia)

The important roles of electronegativity differences and lone pair repulsion are evident when comparing trends in bond strengths. The table below shows the average single-bond enthalpies of p-block elements with H and F. H makes stronger bonds with 2nd row elements (C, N, O, F) than with third row elements (Si, P, S, Cl) because the 2p valence electrons are closer to the nucleus and thus make stronger bonds than electrons in 3p orbitals. The bonds to H also follow the expected trend of increasing bond strength with increasing electronegativity difference. Bonds between second row elements (C, N, O, F) and F are however anomalously weak because of lone pair repulsion. For this reason, the Si-F bond is substantially stronger than the C-F bond, whereas the C-H bond is much stronger than the Si-H bond. The strong Si-F bond is the reason that HF etches glass (to produce the SiF_6^{2-} anion), and the strong C-H bond is an important factor in the stability of hydrocarbons and other organic molecules.

Average E-H and E-F bond enthalpies (kJ/mol)

C-H 413	N-H 391	O-H 483	H-F 567
Si-H 323	P-H 322	S-H 339	H-Cl 431
C-F 485	N-F 272	O-F 190	F-F 155
Si-F 565	P-F 490	S-F 327	Cl-F 253

The anomalously weak bond in F_2 is responsible for the high electronegativity of fluorine, as well as the legendary reactivity of elemental fluorine gas, which reacts explosively with hydrogen and powdered metals. Because of the instability of elemental fluorine and the polar nature of its bonds with more electropositive elements, fluorine compounds tend to be very stable. For example, the noble gases Xe and Kr react with fluorine to make covalent compounds, whereas other halogens do not react. Fluorocarbon compounds contain strong C-F bonds and have high thermal and chemical stability. Perfluorocarbons such as Teflon (poly(tetrafluoroethylene), -(CF_2CF_2)n-, PTFE) are also highly hydrophobic. The extraordinary hydrophobicity of perfluorocarbons arises from the fact that -CF_2- and -CF_3 groups are "fatter" than -CH_2- and -CH_3 groups; dissolving them in water is therefore more disruptive to the hydrogen bonding network than is dissolving a hydrocarbon. [21]

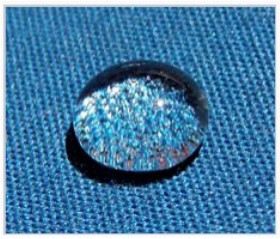


Figure **3.4.2**: Fabric treated with fluorosurfactant

3.4: Bond Polarity and Bond Strength is shared under a CC BY-SA license and was authored, remixed, and/or curated by LibreTexts.

- **1.4: Bond Polarity and Bond Strength** by Chemistry 310 is licensed CC BY-SA 4.0. Original source: https://en.wikibooks.org/wiki/Introduction_to_Inorganic_Chemistry.

3.5: Discussion Questions

Group essay project:

Join a group of classmates from your inorganic chemistry course. Each group should have 3 or 4 students. Arrange a time to meet for an hour or so. Prior to the meeting, read part I (pp. 1367-1391) as well as the summary at the end of Linus Pauling's article (J. Am. Chem. Soc. 1931, 53, 1367-1400) on the nature of the chemical bond.

This paper was published only a few years after Schrödinger developed the quantum mechanical theory of atomic orbitals and is considered one of the most important papers in the history of modern chemistry. At the meeting, discuss the following questions: (1) What was understood about chemical bonding in molecules before Pauling published this work? (2) What new concepts did the paper introduce that we still use today? (3) Why were these ideas important? and (4) What, if anything, did Pauling get wrong, and why?

Together with your classmates, write a 1-2 page essay addressing these questions. Please include the names of all students in your group on the first page; all of you will receive the same grade on this assignment. Anonymous excerpts from a few of these essays will be shared with the class.

In-class discussion questions from this chapter:

- What are inequivalent resonance structures? Illustrate with some new examples not covered above.
- Explain no-bond resonance and hypervalency, using some new examples.
- What are the limitations of valence bond theory for molecules that contain an odd number of electrons? Illustrate with one or two examples.

3.5: Discussion Questions is shared under a CC BY-SA license and was authored, remixed, and/or curated by LibreTexts.

- **1.5: Discussion Questions** by Chemistry 310 is licensed CC BY-SA 4.0. Original source: https://en.wikibooks.org/wiki/Introduction_to_Inorganic_Chemistry.

3.6: Problems

1. Write octet structures (including formal charges, bond order, and molecular shape) for SeO_3^{2-}, SeF_4, XeF_4, $HClO_3$ (= $HOClO_2$), NO_3^-, and ClO_2^+.

2. Write octet structures (including formal charges, bond order, and molecular shape) for Al_2Cl_6, $SnCl_3^-$, BrF_4^-, HOClO, SO_3, and NO_2^+.

3. Show using resonance why the S-O bond is slightly shorter in SO_2F_2 than in SO_2.

4. Give the formulas for five stable molecules and/or ions that are isoelectronic with ammonia.

5. Name three well known molecules or ions that are isoelectronic with (a) O_3, (b) BF, (c) CO_3^{2-}, and (d) N_3^-.

6. Name three well known molecules or ions that are isoelectronic with (a) CN^-, (b) H_2O, (c) BF_3, and (d) CO_2.

7. The N-N bond distance is 1.10 Å in N_2. Using the Pauling bond length – bond strength formula, D(n) = D(1) - 0.6 log(n), calculate the bond distance in the N_2^+ cation.

8. In hydroxylamine, H_2NOH, the N-O bond distance is 1.46 Å. Using the Pauling bond length - bond strength formula, estimate the N-O bond distances in NO_2 and NO_3^-.

9. While PF_5 and SF_6 are stable molecules, NF_5 and OF_6 are unknown. Can you draw octet structures for these compounds? Why would these molecules be unstable?

10. Consider the compounds NH_3 and PH_3. The H-N-H bond angle in ammonia is 108° (close to the tetrahedral angle, 109.5°), but the analogous angle in PH_3 is 93°. Why is the angle in PH_3 closer to 90° than it is to the tetrahedral angle?

11. Two hypothetical structures for the $N_2F_3^+$ ion are $[N\text{-}NF_3]^+$ and $[F\text{-}N\text{-}NF_2]^+$. Which one is more stable? Explain. (Note: lines in the formulas can represent either single or multiple bonds)

12. Krypton difluoride, KrF_2, decomposes at dry ice temperature to Kr and F_2. However, several salts of the $[KrF]^+$ ion are relatively stable. Draw valence bond pictures for KrF_2 and $[KrF]^+$, showing lone pairs, possible resonance structures, formal charges, bond orders, and bond angles. Why is $[KrF]^+$ more stable than KrF_2?

13. Consider the molecule ClF_3O_2 (with Cl the central atom). How many isomers are possible? Which is the most stable?

14. The Br-F bond distance in the interhalogen compound BrF is 1.76 Å. Use this information to estimate the average bond lengths in BrF_3 and BrF_5.

15. The B-H bond distances are about the same in BH_3 and BH_4^-. however, the B-F bond distance in BF_3 is shorter than that in the BF_4^- ion. Explain.

16. The N-N bond dissociation energy in hydrazine ($H_2N\text{-}NH_2$) is 159 kJ/mol. The dissociation energy of the N-N triple bond in N_2 is 941 kJ/mol, i.e., much greater than three times the N-N single bond dissociation energy in hydrazine. Explain why the N-N bond in hydrazine is so weak, and why this effect is not seen in N_2.

17. Show that a set of three sp^2 hybrid orbitals satisfies the following criteria: (a) any two orbitals in the sp^2 set are orthogonal, and (b) the orbitals are properly normalized.

18. Quantum mechanically, the momentum (p) of a particle traveling in a specific direction (e.g., the x direction) can be obtained by operating on its wavefunction ψ with the **momentum operator**:

$$\hat{p}\psi = p\psi, \text{ where } \hat{p} = -i\hbar\frac{\delta}{\delta x} \tag{3.6.1}$$

Knowing the correct form of this operator was the key to Schrödinger's formulation of the Hamiltonian operator, $\hat{H} = \frac{\hat{p}^2}{2m} + V$, which operates on a wavefunction to give the total energy. The momentum operator must also be consistent with the **de Broglie relation**, $p = \frac{h}{\lambda}$, which relates the momentum to the particle wavelength.

By analogy to electromagnetic waves, Schrödinger knew that a wavelike particle (such as an electron) traveling in free space in the x-direction could be described by the wavefunction:

$$\psi(x,t) = Ae^{i(kx-\omega t+\varphi)} \tag{3.6.2}$$

where the **wavenumber** k is inversely related to the particle's **de Broglie wavelength** λ by $k = \frac{2\pi}{\lambda}$. Here A is a normalization constant, ω is the frequency of the wave, and φ represents its phase.

Show using the momentum operator $\hat{p}$ that the value of the momentum p we obtain for a free particle from $\hat{p}\psi = p\psi$ is consistent with the de Broglie relation, $p = \frac{h}{\lambda}$.
(Hint: k, ω, and φ are independent of x)

19. Which S-N bonds in the cyclic $S_4N_3^+$ ion would you predict to be the shortest? The atomic connectivity in the ring is: -S-S-N-S-N-S-N-. [*Hint:* determine the number of π-bonds in the molecule by electron counting and then find the most stable resonance structures].

20. F has a higher electronegativity than Cl, and F_2 is a much stronger oxidizing agent than Cl_2, despite the fact that the electron affinity of fluorine (-328 kJ/mol) is weaker than that of chlorine (-349 kJ/mol). Explain this apparent contradiction.

21. (a) Explain why C-H, N-H, and O-H bonds in chemical compounds are stronger than Si-H, P-H, and S-H bonds, respectively. (b) Explain why C-F, N-F, and O-F single bonds follow the opposite trend, namely, they are weaker than Si-F, P-F, and S-F single bonds, respectively.

3.6: Problems is shared under a CC BY-SA license and was authored, remixed, and/or curated by LibreTexts.

- **1.6: Problems** by Chemistry 310 is licensed CC BY-SA 4.0. Original source: https://en.wikibooks.org/wiki/Introduction_to_Inorganic_Chemistry.

3.7: References

1. G. N. Lewis, "The atom and the molecule," J. Am. Chem. Soc. 1916, 38, 762-785
2. W. Saenger, "The structure of the blue starch-iodine complex," Naturwissenschaften 71, 31-36 (1984).
3. R. D. Hancock and B. J. Tarbet, "The other double helix - the fascinating chemistry of starch," J. Chem. Ed. 77, 988-992 (2000).
4. R. J. Gillespie and B. Silvi, "The octet rule and hypervalence: two misunderstood concepts," Coord. Chem. Rev. 233-234, 53-62 (2002).
5. I. Chung, B. Lee, J. He, R. P. H. Chang and M. G. Kanatzidis, All-solid-state dye-sensitized solar cells with high efficiency, Nature 485, 486-489 (2012). doi:10.1038/nature11067
6. S.D. Stranks, G. E. Eperon, G. Grancini, C. Menelaou, M. J. P. Alcocer, T. Leijtens, L. M. Herz, A. Petrozza, and H. J. Snaith, Electron-Hole Diffusion Lengths Exceeding 1 Micrometer in an Organometal Trihalide Perovskite Absorber, Science 342, 341-344 (2013). DOI: 10.1126/science.1243982
7. G. Xing, N. Mathews, S. Sun, S. S. Lim, Y. M. Lam, M. Grätzel, S. Mhaisalkar, and T. C. Sum, Long-Range Balanced Electron- and Hole-Transport Lengths in Organic-Inorganic CH3NH3PbI3, Science 342, 344-347 (2013). DOI: 10.1126/science.1243167
8. J.-P. Correa-Baena, A. Abate, M. Saliba, W. Tress, T. J. Jacobsson, M. Grätzel, and A. Hagfeldt, The rapid evolution of highly efficient perovskite solar cells, Energy Environ. Sci., 10, 710-727 (2017). DOI: 10.1039/C6EE03397K
9. N. V. Sidgwick and H. M. Powell, Proc. Roy. Soc. A176, 153 (1940),
10. R. J. Gillespie and R. S. Nyholm, Quart. Rev. Chem. Soc., 11, 339 (1957).
11. R. J. Gillespie, "Fifty years of the VSEPR model," Coord. Chem. Rev. 252, 1315-1327 (2008). DOI: 10.1016/j.ccr.2007.07.007
12. Pauling, L. (1932). "The Nature of the Chemical Bond. IV. The Energy of Single Bonds and the Relative Electronegativity of Atoms". *J. Am. Chem. Soc.* **54** (9): 3570–3582. doi:10.1021/ja01348a011.
13. Mulliken, R. S. (1934). "A New Electroaffinity Scale; Together with Data on Valence States and on Valence Ionization Potentials and Electron Affinities". *J. Chem. Phys.***2** (11): 782–793. doi:10.1063/1.1749394. Bibcode: 1934JChPh...2..782M.
14. Mulliken, R. S. (1935). "Electronic Structures of Molecules XI. Electroaffinity, Molecular Orbitals and Dipole Moments". J. Chem. Phys. **3** (9): 573–585. doi:10.1063/1.1749731. Bibcode: 1935JChPh...3..573M.
15. Pearson, R. G. (1985). "Absolute electronegativity and absolute hardness of Lewis acids and bases". J. Am. Chem. Soc. **107** (24): 6801. doi:10.1021/ja00310a009.
16. B. Hammer and J. K. Norskov, "Why gold is the noblest of all the metals," *Nature***376,** 238 - 240 (2002. doi:10.1038/376238a0
17. Schomaker, Verner; Stevenson, D. P. (1941). "Some Revisions of the Covalent Radii and the Additivity Rule for the Lengths of Partially Ionic Single Covalent Bonds *". *Journal of the American Chemical Society* **63**: 37–40. doi:10.1021/ja01846a007.
18. Pauling, L. The Nature of the Chemical Bond, 3rd ed.; Cornell University Press: Ithaca, NY, 1960; p. 224.
19. Robinson, Edward A.; Johnson, Samuel A.; Tang, Ting-Hua; Gillespie, Ronald J. (1997). "Reinterpretation of the Lengths of Bonds to Fluorine in Terms of an Almost Ionic Model". *Inorganic Chemistry* **36** (14): 3022–3030. doi:10.1021/ic961315b. PMID 11669953.
20. Pyykkö, Pekka; Atsumi, Michiko (2009). "Molecular Double-Bond Covalent Radii for Elements Li–E112". *Chemistry: A European Journal* **15** (46): 12770–12779. doi:10.1002/chem.200901472.
21. V. H. Dalvi and P. J. Rossky, Molecular origins of fluorocarbon hydrophobicity, Proc. Natl. Acad. Sci. USA 107,13603–13607 (2010). DOI: 10.1073/pnas.0915169107.

3.7: References is shared under a CC BY-SA license and was authored, remixed, and/or curated by LibreTexts.

- **1.7: References** by Chemistry 310 is licensed CC BY-SA 4.0. Original source: https://en.wikibooks.org/wiki/Introduction_to_Inorganic_Chemistry.

CHAPTER OVERVIEW

4: Molecular Orbital Theory

Learning Objectives

- Be able to construct molecular orbital diagrams for homonuclear diatomic, heteronuclear diatomic, homonuclear triatomic, and heteronuclear triatomic molecules.
- Understand and be able to articulate how molecular orbitals form – conceptually, visually, graphically, and (semi)mathematically.
- Interrelate bond order, bond length, and bond strength for diatomic and triatomic molecules, including neutral and ionized forms.
- Use molecular orbital theory to predict molecular geometry for simple triatomic systems
- Rationalize molecular structure for several specific systems in terms of orbital overlap and bonding.
- Understand the origin of aromaticity and anti-aromaticity in molecules with π-bonding.

Valence bond (VB) theory gave us a qualitative picture of chemical bonding, which was useful for predicting the shapes of molecules, bond strengths, etc. It fails to describe some bonding situations accurately because it ignores the wave nature of the electrons. Molecular orbital (MO) theory has the potential to be more quantitative. With it we can also get a picture of where the electrons are in the molecule, as shown in the image at the right. This can help us understand patterns of bonding and reactivity that are otherwise difficult to explain.

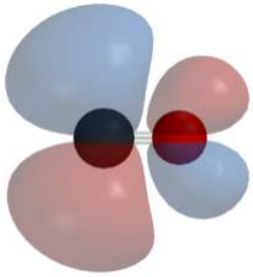
4.1: Prelude to Molecular Orbital Theory
4.2: Constructing Molecular Orbitals from Atomic Orbitals
4.3: Orbital Symmetry
4.4: σ, π, and δ orbitals
4.5: Diatomic Molecules
4.6: Orbital Filling
4.7: Periodic Trends in π Bonding
4.8: Three-center Bonding
4.9: Building up the MOs of More Complex Molecules- NH_3, P_4
4.10: Homology of σ and π orbitals in MO diagrams
4.11: Chains and Rings of π-Conjugated Systems
4.12: Discussion Questions
4.13: Problems
4.14: References

4: Molecular Orbital Theory is shared under a CC BY-SA license and was authored, remixed, and/or curated by LibreTexts.

4.1: Prelude to Molecular Orbital Theory

Valence bond (VB) theory gave us a qualitative picture of chemical bonding, which was useful for predicting the shapes of molecules, bond strengths, etc. It fails to describe some bonding situations accurately because it ignores the wave nature of the electrons. Molecular orbital (MO) theory has the potential to be more quantitative. With it we can also get a picture of where the electrons are in the molecule, as shown in the image at the right. This can help us understand patterns of bonding and reactivity that are otherwise difficult to explain.

Although MO theory in principle gives us a way to calculate the energies and wavefunctions of electrons in molecules very precisely, usually we settle for simplified models here too. These simple models do not give very accurate orbital and bond energies, but they do explain concepts such as resonance (e.g., in the ferrocene molecule) that are hard to represent otherwise. We can get more accurate energies from MO theory by computational "number crunching." While MO theory is more correct than VB theory and can be very accurate in predicting the properties of molecules, it is also rather complicated even for fairly simple molecules. For example, you should have no trouble drawing the VB pictures for CO, NH_3, and benzene, but we will find that these are increasingly challenging with MO theory.



The lowest unoccupied molecular orbital of the carbon monoxide molecule is a π antibonding orbital that derives from the 2p orbitals of carbon (left) and oxygen (right)

4.1: Prelude to Molecular Orbital Theory is shared under a CC BY-SA license and was authored, remixed, and/or curated by LibreTexts.

- **2.1: Prelude to Molecular Orbital Theory** by Chemistry 310 is licensed CC BY-SA 4.0. Original source: https://en.wikibooks.org/wiki/Introduction_to_Inorganic_Chemistry.

4.2: Constructing Molecular Orbitals from Atomic Orbitals

Molecular orbital theory involves solving (approximately) the Schrödinger equation for the electrons in a molecule. To review from Chapter 1, this is a differential equation in which the first and second terms on the right represent the kinetic and potential energies:

$$E\psi = -\frac{\hbar^2}{2\mu}\nabla^2\psi + V\psi \tag{4.2.1}$$

While the Schrödinger equation can be solved analytically for the hydrogen atom, the potential energy function V becomes more complicated - and the equation can then only be solved numerically - when there are many (mutually repulsive) electrons in a molecule. So as a first approximation we will assume that the s, p, d, f, etc. orbitals of the atoms that make up the molecule are good solutions to the Schrödinger equation. We can then allow these wavefunctions to interfere constructively and destructively as we bring the atoms together to make bonds. In this way, we use the atomic orbitals (AO) as our basis for constructing MO's.

LCAO-MO = **linear combination of atomic orbitals.** In physics, this is called this the tight binding approximation.

We have actually seen linear combinations of atomic orbitals before when we constructed hybrid orbitals in Chapter 1. The basic rules we developed for hybridization also apply here: orbitals are added with scalar coefficients (c) in such a way that the resulting orbitals are **orthogonal** and **normalized**. The difference is that in the MO case, the atomic orbitals come from different atoms.

The linear combination of atomic orbitals always gives back the *same number of molecular orbitals.* So if we start with two atomic orbitals (e.g., an s and a p_z orbital as shown in Fig. **4.2.1**), we end up with two molecular orbitals. When atomic orbitals add in phase, we get constructive interference and a lower energy orbital. When they add out of phase, we get a node and the resulting orbital has higher energy. The lower energy MOs are *bonding* and higher energy MOs are *antibonding*.

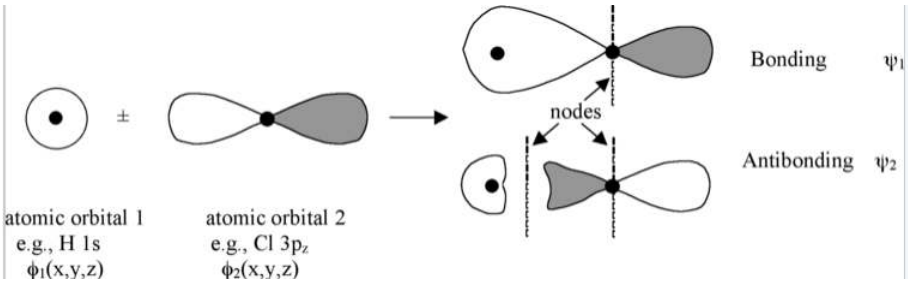


Figure **4.2.1**: Sigma bonding and antibonding combinations of an s and p orbital

Molecular orbitals are also called **wavefunctions** (ψ), because they are solutions to the Schrödinger equation for the molecule. The atomic orbitals (also called basis functions) are labeled as φ's, for example, φ_{1s} and φ_{3pz} or simply as $\varphi_1$and φ_2.

In principle, we need to solve the Schrödinger equation for all the orbitals in a molecule, and then fill them up with pairs of electrons as we do for the orbitals in atoms. In practice we are really interested only in the MOs that derive from the valence orbitals of the constituent atoms, because these are the orbitals that are involved in bonding. We are especially interested in the **frontier orbitals**, i.e., the highest occupied molecular orbital (the **HOMO**) and the lowest unoccupied molecular orbital (the **LUMO**). Filled orbitals that are much lower in energy (i.e., core orbitals) do not contribute to bonding, and empty orbitals at higher energy likewise do not contribute. Those orbitals are however important in photochemistry and spectroscopy, which involve electronic transitions from occupied to empty orbitals. The fluorescent dyes that stain the cells shown in Fig. **4.2.2** absorb light by promoting electrons in the HOMO to empty MOs and give off light when the electrons drop back down to their original energy levels.

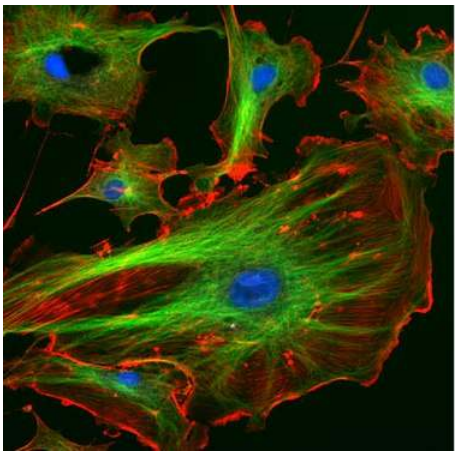


Figure **4.2.2**: Different components of endothelial cells are stained by blue, green, and red fluorescent dyes. For each dye the color of emitted light corresponds to the energy given off when an electron drops from the LUMO to the HOMO of the molecule.

As an example of the LCAO-MO approach we can construct two MO's (ψ_1 and ψ_2) of the HCl molecule from two AO's $\varphi_1$and φ_2 (Fig. 2.1.1). To make these two linear combinations, we write:

$$\Psi_1 = c_1\varphi_1 + c_2\varphi_2 \tag{4.2.2}$$

and

$$\Psi_2 = c_1\varphi_1 - c_2\varphi_2 \tag{4.2.3}$$

The coefficients c_1 and c_2 will be equal (or nearly so) when the two AOs from which they are constructed are the same, e.g., when two hydrogen 1s orbitals combine to make bonding and antibonding MOs in H_2. They will be unequal when there is an energy difference between the AOs, for example when a hydrogen 1s orbital and a chlorine 3p orbital combine to make a polar H-Cl bond.

Nodes:

The wavefunctions φ and ψ are **amplitudes** that are related to the probability of finding the electron at some point in space. They have lobes with (+) or (-) signs, which we indicate by shading or color. Wherever the wavefunction changes sign we have a node. As you can see in Fig. **4.2.1**, nodes in MOs result from destructive interference of (+) and (-) wavefunctions. Generally, the more nodes, the higher the energy of the orbital.

In the example above we have drawn a simplified picture of the Cl $3p_z$ orbital and the resulting MOs, leaving out the radial node. Recall that 2p orbitals have no radial nodes, 3p orbitals have one, as illustrated in Fig. **4.2.3**. 4p orbitals have two radial nodes, and so on. The MOs we make by combining the AOs have these nodes too.



Figure **4.2.3**: Nodal structure of 2p and 3p orbitals

Normalization:

We square the wave functions to get probabilities, which are always positve or zero. So if an electron is in orbital φ_1, the probability of finding it at point xyz is the square[1] of φ_1(x,y,z). The total probability does not change when we combine AOs to make MOs, so for the simple case of combining φ_1 and φ_2 to make $\psi_1$and ψ_2,

$$\Psi_1^2 + \Psi_2^2 = \varphi_1^2 + \varphi_2^2 \tag{4.2.4}$$

Overlap integral:

The spatial overlap between two atomic orbitals φ_1 and φ_2 is described by the overlap integral S,

$$S_{12} = \int \varphi_1 * \varphi_2 d\tau \tag{4.2.5}$$

where the integration is over all space $d\tau = dxdydz$.

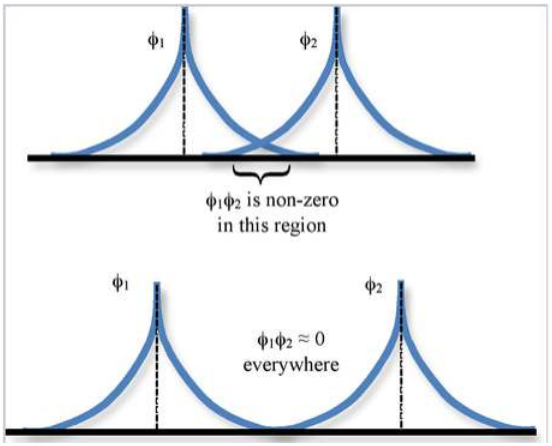


Figure **4.2.4**: The wavefunctions of atomic orbitals decrease exponentially with distance. Orbital overlap is non-zero when two atoms are close together, as illustrated for 1s orbitals in the upper figure. The lower figure shows orbitals that are too far away to interact. In this case both S and β are close to zero.

Energies of bonding and antibonding MOs:

The energies of bonding and antibonding orbitals depend strongly on the distance between atoms. This is illustrated in Fig. 2.1.5 for the hydrogen molecule, H_2. At very long distances, there is essentially no difference in energy between the in-phase and out-of-phase combinations of H 1s orbitals. As they get closer, the in-phase (bonding) combination drops in energy because electrons are shared between the two positively charged nuclei. The energy reaches a minimum at the equilibrium bond distance (0.74 Å) and then rises again as the nuclei get closer together. The antibonding combination has a node between the nuclei so its energy rises continuously as the atoms are brought together.

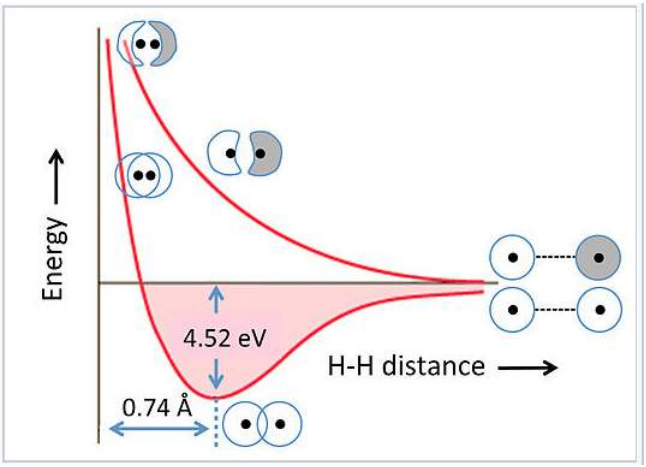


Figure **4.2.5**: Energy as a function of distance for the bonding and antibonding orbitals of the H_2 molecule

At the equilibrium bond distance, the energies of the bonding and antibonding molecular orbitals (ψ_1, ψ_2) are lower and higher, respectively, than the energies of the atomic basis orbitals φ_1 and φ_2. This is shown in Fig. **4.2.6** for the MO's of the H_2 molecule.

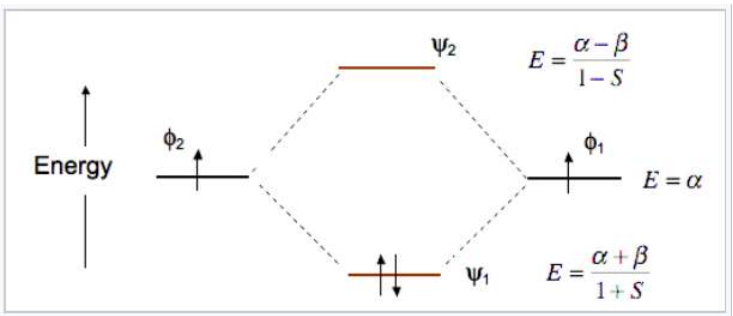


Figure **4.2.6**: Molecular orbital energy diagram for the H_2 molecule

The energy of an electron in one of the atomic orbitals is α, the **Coulomb integral**.

$$\alpha = \int \varphi_1 H \varphi_1 d\tau \tag{4.2.6}$$

where **H** is the **Hamiltonian operator**. Essentially, α represents the *ionization energy* of an electron in atomic orbital φ_1 or φ_2.

The energy difference between an electron in the AO's and the MO's is determined by the **exchange integral β**,

$$\beta = \int \varphi_1 H \varphi_2 d\tau \tag{4.2.7}$$

β is an important quantity, because it tells us about the bonding energy of the molecule, and also the difference in energy between bonding and antibonding orbitals. Calculating β is not straightforward for multi-electron molecules because we cannot solve the Schrödinger equation analytically for the wavefunctions. We can however make some approximations to calculate the energies and wavefunctions numerically. In the Hückel approximation, which can be used to obtain approximate solutions for π molecular orbitals in organic molecules, we simplify the math by taking S=0 and setting H=0 for any p-orbitals that are not adjacent to each other. The extended Hückel method,[2] developed by Roald Hoffmann, and other semi-empirical methods can be used to rapidly obtain relative orbital energies, approximate wavefunctions, and degeneracies of molecular orbitals for a wide variety of molecules and extended solids. More sophisticated ab initio methods are now readily available in software packages and can be used to compute accurate orbital energies for molecules and solids.

We can get the coefficients c_1 and c_2 for the hydrogen molecule by applying the normalization criterion:

$$\Phi_1 = (\varphi_1 + \varphi_2)/(\sqrt{2(1+S)})(\text{bonding orbital}) \tag{4.2.8}$$

and

$$\Phi_2 = (\varphi_1 - \varphi_2)/(\sqrt{2(1-S)})(\text{antibonding orbital}) \tag{4.2.9}$$

In the case where S≈0, we can eliminate the 1-S terms and both coefficients become 1/√2

Note that the bonding orbital in the MO diagram of H_2 is stabilized by an energy β/1+S and the antibonding orbital is destabilized by β/1-S. That is, the antibonding orbital goes up in energy more than the bonding orbital goes down. This means that H_2 ($\psi_1^2\psi_2^0$) is energetically more stable than two H atoms, but He_2 with four electrons ($\psi_1^2\psi_2^2$) is *unstable* relative to two He atoms.

Bond order: In any MO diagram, the bond order can be calculated as ½ (# of bonding electrons - # of antibonding electrons). For H_2 the bond order is 1, and for $He_2$the bond order is zero.

Heteronuclear case (e.g., HCl) - Polar bonds

Here we introduce an electronegativity difference between the two atoms making the chemical bond. The energy of an electron in the H 1s orbital is higher (it is easier to ionize) than the electron in the chlorine $3p_z$ orbital. This results in a larger energy difference between the resulting molecular orbitals ψ_1 and ψ_2, as shown in Fig. **4.2.7**. The bigger the electronegativity difference between atomic orbitals (the larger Δα is) the more "φ_2 character" the bonding orbital has, i.e., the more it resembles the Cl $3p_z$ orbital in this case. This is consistent with the idea that H-Cl has a polar single bond: the two electrons reside in a bonding molecular orbital that is primarily localized on the Cl atom.

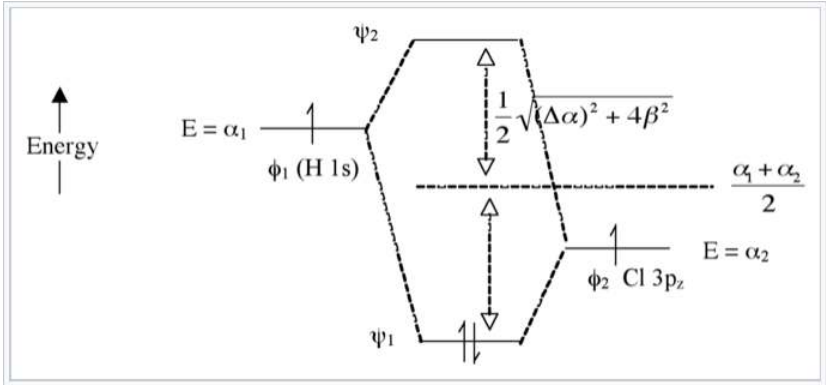


Figure 4.2.7: Molecular orbital energy diagram for the HCl molecule

The antibonding orbital (empty) has more H-character. The bond order is again 1 because there are two electrons in the bonding orbital and none in the antibonding orbital.

Extreme case - Ionic bonding (NaF): very large Δα

In this case, there is not much mixing between the AO's because their energies are far apart (Fig. 4.2.8). The two bonding electrons are localized on the F atom , so we can write the molecule as Na^+F^-. Note that if we were to excite an electron from ψ_1 to ψ_2 using light, the resulting electronic configuration would be $(\psi_1^1\psi_2^1)$ and we would have Na^0F^0. This is called a charge transfer transition.

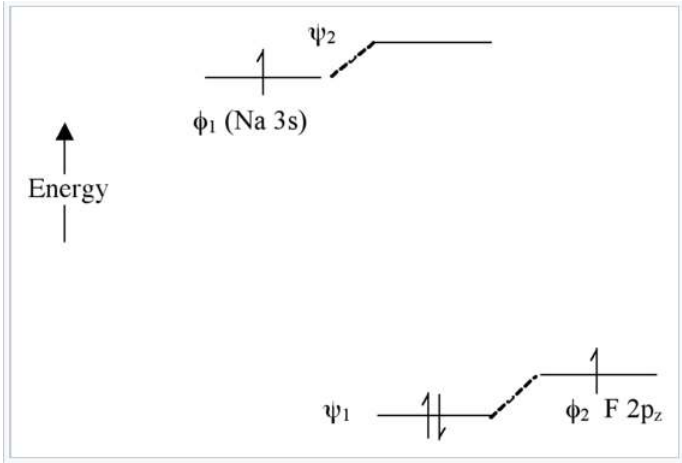


Figure 4.2.8: Molecular orbital energy diagram illustrating ionic bonding in the NaF molecule

Summary of molecular orbital theory so far:

• **Add and subtract** AO wavefunctions to make MOs. Two AOs → two MOs. More generally, the *total number of MOs equals the number of AO basis orbitals*.

• We showed the simplest case (only two basis orbitals). More accurate calculations use a much larger basis set (more AOs) and solve for the matrix of c's that gives the lowest total energy, using mathematically friendly approximations of the potential energy function that is part of the Hamiltonian operator H.

• **More nodes → higher energy** MO

• **Bond order** = ½ (# of bonding electrons - # of antibonding electrons)

• **Bond polarity** emerges in the MO picture as orbital "character."

• AOs that are **far apart in energy** do not interact much when they combine to make MOs.

4.2: Constructing Molecular Orbitals from Atomic Orbitals is shared under a CC BY-SA license and was authored, remixed, and/or curated by LibreTexts.

- **2.2: Constructing Molecular Orbitals from Atomic Orbitals** by Chemistry 310 is licensed CC BY-SA 4.0. Original source: https://en.wikibooks.org/wiki/Introduction_to_Inorganic_Chemistry.

https://chem.libretexts.org/@go/page/344435

4.3: Orbital Symmetry

The MO picture for a molecule gets complicated when many valence AOs are involved. We can simplify the problem enormously by noting (without proof here) that orbitals of different symmetry with respect to the molecule do not interact. The symmetry operations of a molecule (which can include rotations, mirror planes, inversion centers, etc.), and the symmetry classes of bonds and orbitals in molecules, can be rigorously defined according to **group theory**. Here we will take a simple approach to this problem based on our intuitive understanding of the symmetry of three-dimensional objects as illustrated in Fig. **4.3.1**.



Figure **4.3.1**: Example of σ symmetry.

AO's must have the same **nodal symmetry** (as defined by the molecular symmetry operations), or their overlap is zero.

For example, in the HCl molecule, there is a unique symmetry axis →, which is typically defined as the Cartesian z-axis, as shown in Fig. **4.3.2**.

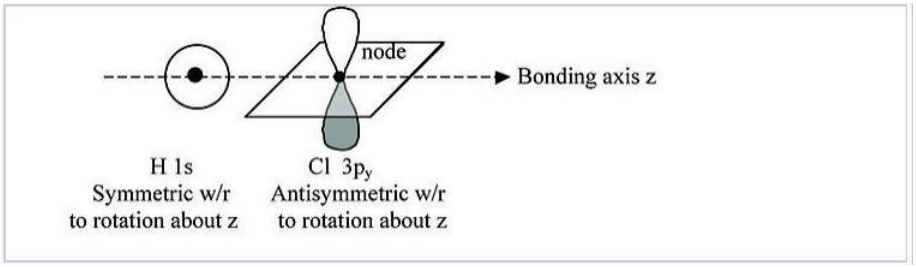


Figure **4.3.2**: Orbitals of σ and π symmetry do not interact.

We can see from this figure that the H 1s orbital is unchanged by a 180° rotation about the bond axis. However, the same rotation inverts the sign of the Cl $3p_y$wavefunction. Because these two orbitals have different symmetries, the Cl $3p_y$ orbital is **nonbonding** and doesn't interact with the H 1s. The same is true of the Cl $3p_x$orbital. The p_x and p_y orbitals have π symmetry (nodal plane containing the bonding axis) and are labeled π_{nb} in the MO energy level diagram, Fig. **4.3.3**. In contrast, the H 1s and Cl $3p_z$ orbitals both have σ symmetry, which is also the symmetry of the clay pot shown in Fig. **4.3.1**. Because these orbitals have the same symmetry (in the point group of the molecule), they can make the bonding and antibonding combinations shown in Fig. **2.1.1**.

The MO diagram of HCl that includes all the valence orbitals of the Cl atom is shown in Fig. **4.3.3**. Two of the Cl valence orbitals ($3p_x$ and $3p_y$) have the wrong symmetry to interact with the H 1s orbital. The Cl 3s orbital has the same (σ) symmetry as H 1s, but it is much lower in energy so there is little orbital interaction. The energy of the Cl 3s orbital is thus affected only slightly by forming the molecule. The pairs of electrons in the π_{nb} and σ_{nb} orbitals are therefore **non-bonding**.

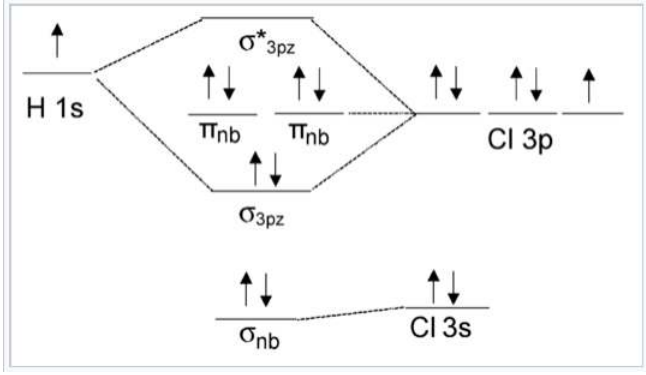


Figure **4.3.3**: Energy level diagram of the HCl molecule showing MOs derived from the valence AOs.

Note that the MO result in Fig. **4.3.3** (1 bond and three pairs of nonbonding electrons) is the same as we would get from valence bond theory for HCl. The nonbonding orbitals are localized on the Cl atom, just as we would surmise from the valence bond picture.

In order to differentiate it from the σ bonding orbital, the σ antibonding orbital, which is empty in this case, is designated with an asterisk.

4.3: Orbital Symmetry is shared under a CC BY-SA license and was authored, remixed, and/or curated by LibreTexts.

- **2.3: Orbital Symmetry** by Chemistry 310 is licensed CC BY-SA 4.0. Original source: https://en.wikibooks.org/wiki/Introduction_to_Inorganic_Chemistry.

4.4: σ, π, and δ orbitals

Inorganic compounds use s, p, and d orbitals (and more rarely f orbitals) to make bonding and antibonding combinations. These combinations result in **σ, π,** and **δ** bonds (and antibonds).

You are already familiar with σ and π bonding in organic compounds. In inorganic chemistry, π bonds can be made from p- and/or d-orbitals. δ bonds are more rare and occur by face-to-face overlap of d-orbitals, as in the ion $Re_2Cl_8^{2-}$. The fact that the Cl atoms are eclipsed in this anion is evidence of δ bonding.

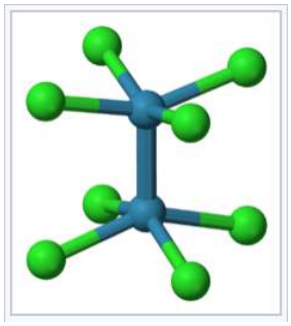
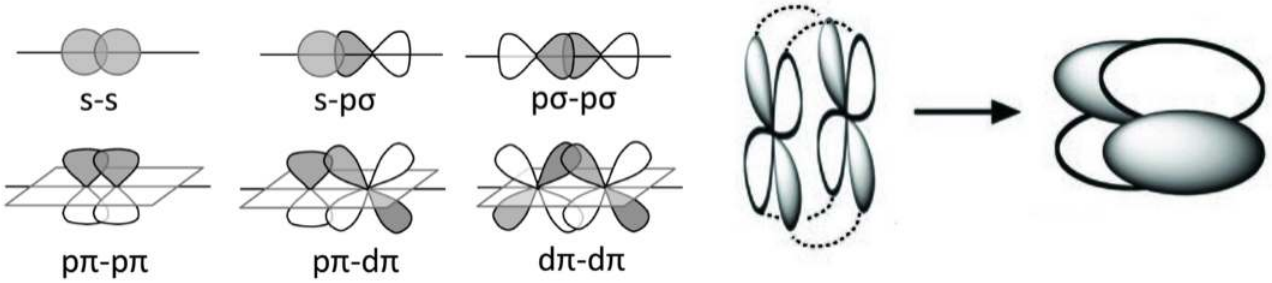
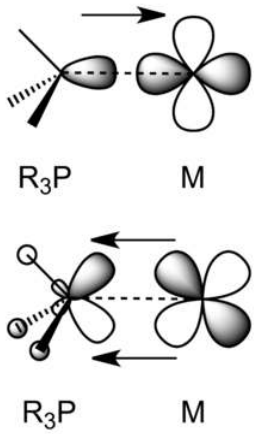


Figure **4.4.1**: The octachlorodirhenate(III) anion, $[Re_2Cl_8]^{2-}$, which has a quadruple Re-Re bond.[3]

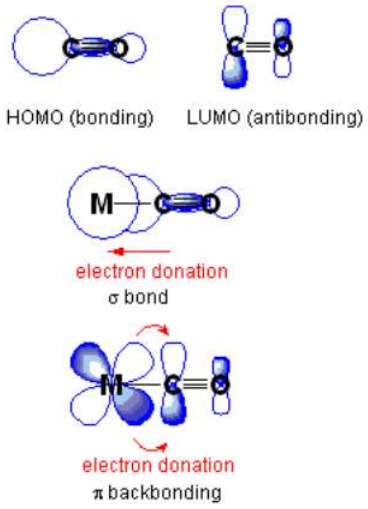
Some possible σ (top row), π (bottom row), and δ bonding combinations (right) of s, p, and d orbitals are sketched below. In each case, we can make bonding or antibonding combinations, depending on the signs of the AO wavefunctions. Because pπ-pπ bonding involves sideways overlap of p-orbitals, it is most commonly observed with second-row elements (C, N, O). π-bonded compounds of heavier elements are rare because the larger cores of the atoms prevent good π-overlap. For this reason, compounds containing C=C double bonds are very common, but those with Si=Si bonds are rare. δ bonds are generally quite weak compared to σ and π bonds. Compounds with metal-metal δ bonds occur in the middle of the transition series.



Transition metal d-orbitals can also form σ bonds, typically with s-p hybrid orbitals of appropriate symmetry on ligands. For example, phosphines (R_3P:) are good σ donors in complexes with transition metals, as shown below.



pπ-dπ bonding is also important in transition metal complexes. In metal carbonyl complexes such as $Ni(CO)_4$ and $Mo(CO)_6$, there is sideways overlap between filled metal d-orbitals and the empty π-antibonding orbitals (the LUMO) of the CO molecule, as shown in the figure below. This interaction strengthens the metal-carbon bond but weakens the carbon-oxygen bond. The C-O infrared stretching frequency is diagnostic of the strength of the bond and can be used to estimate the degree to which electrons are transferred from the metal d-orbital to the CO π-antibonding orbital.



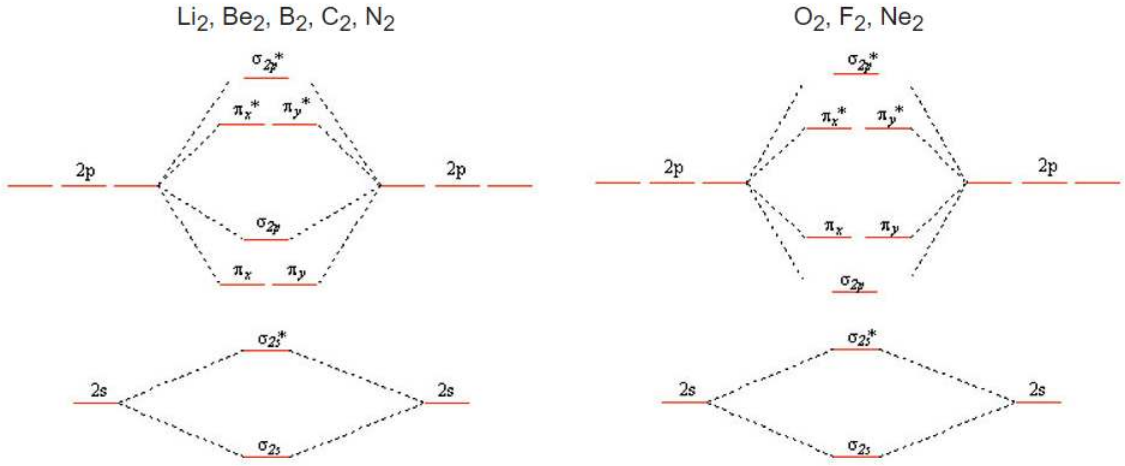
The same kind of backbonding occurs with phosphine complexes, which have empty π orbitals, as shown at the right. Transition metal complexes containing halide ligands can also have significant pπ-dπ bonding, in which a filled pπ orbital on the ligand donates electron density to an unfilled metal dπ orbital. We will encounter these bonding situations in Chapter 5.

4.4: σ, π, and δ orbitals is shared under a CC BY-SA license and was authored, remixed, and/or curated by LibreTexts.

- **2.4: σ, π, and δ orbitals** by Chemistry 310 is licensed CC BY-SA 4.0. Original source: https://en.wikibooks.org/wiki/Introduction_to_Inorganic_Chemistry.

4.5: Diatomic Molecules

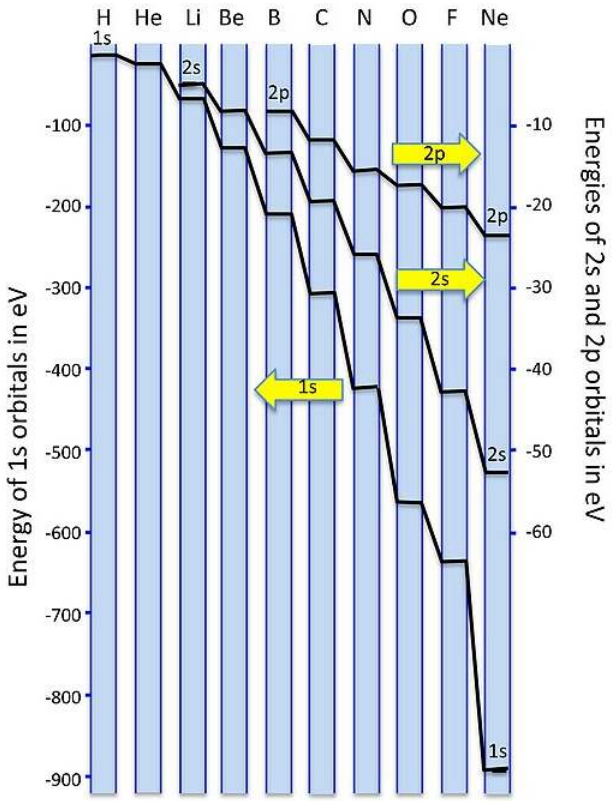
Valence bond theory fails for a number of the second row diatomics, most famously for O_2, where it predicts a diamagnetic, doubly bonded molecule with four lone pairs. O_2 does have a double bond, but it has two unpaired electrons in the ground state, a property that can be explained by the MO picture. We can construct the MO energy level diagrams for these molecules as follows



We get the simpler diatomic MO picture on the right when the 2s and 2p AOs are well separated in energy, as they are for O, F, and Ne. The picture on the left results from mixing of the σ_{2s} and σ_{2p} MO's, which are close in energy for Li_2, Be_2, B_2, C_2, and N_2. The effect of this mixing is to push the σ_{2s}* down in energy and the σ_{2p}up, to the point where the pπ orbitals are below the σ_{2p}. Asymmetric diatomic molecules and ions such as CO, NO, and NO^+ also have the ordering of energy levels shown on the left because of sp mixing. A good animation of the molecular orbitals in the CO molecule can be found on the University of Liverpool **Structure and Bonding** website.

Why don't we get sp-orbital mixing for O_2 and F_2? The reason has to do with the energies of the orbitals, which are not drawn to scale in the simple picture above. As we move across the second row of the periodic table from Li to F, we are progressively adding protons to the nucleus. The 2s orbital, which has finite amplitude at the nucleus, "feels" the increased nuclear charge more than the 2p orbital. This means that as we progress across the periodic table (and also, as we will see later, when we move down the periodic table), the **energy difference between the s and p orbitals increases**. As the 2s and 2p energies become farther apart in energy, there is less interaction between the orbitals (i.e., less mixing).

A plot of orbital energies is shown below. Because of the very large energy difference between the 1s and 2s/2p orbitals, we plot them on different energy scales, with the 1s to the left and the 2s/2p to the right. For elements at the left side of the 2nd period (Li, Be, B) the 2s and 2p energies are only a few eV apart. The energy difference becomes very large - more than 20 electron volts - for O and F. Since single bond energies are typically about 3-4 eV, this energy difference would be very large on the scale of our MO diagrams. For all the elements in the 2nd row of the periodic table, the 1s (core) orbitals are very low in energy compared to the 2s/2p (valence) orbitals, so we don't need to consider them in drawing our MO diagrams.



4.5: Diatomic Molecules is shared under a CC BY-SA license and was authored, remixed, and/or curated by LibreTexts.

- **2.5: Diatomic Molecules** by Chemistry 310 is licensed CC BY-SA 4.0. Original source: https://en.wikibooks.org/wiki/Introduction_to_Inorganic_Chemistry.

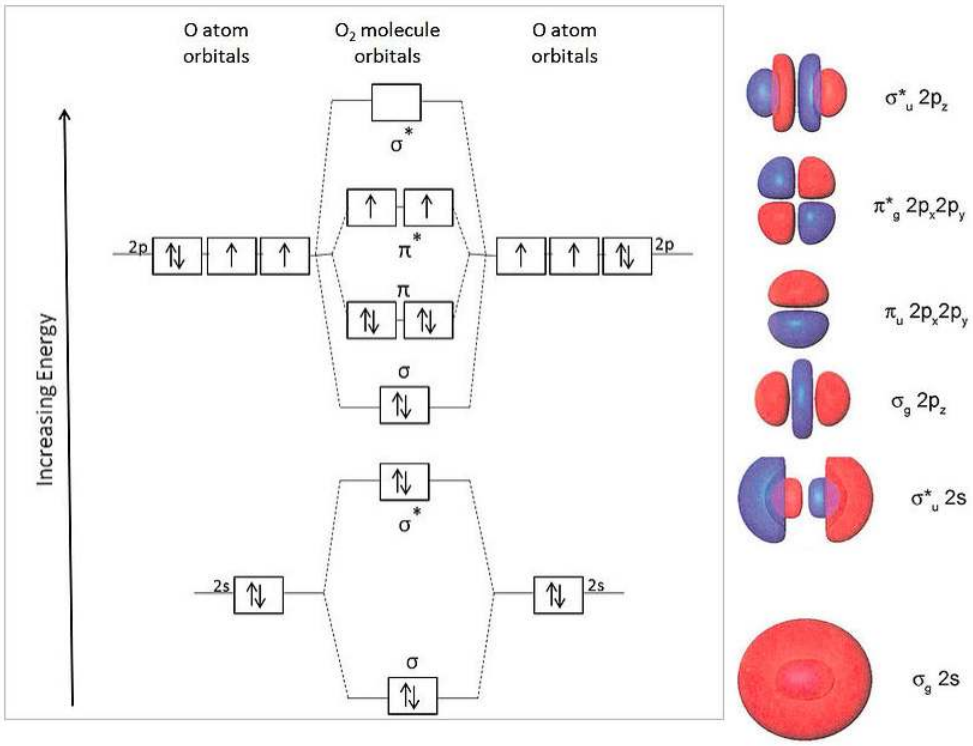
4.6: Orbital Filling

MO's are filled from the bottom according to the **Aufbau principle** and **Hund's rule**, as we learned for atomic orbitals.

Question: what is the quantum mechanical basis of Hund's rule?

> Consider the case of two degenerate orbitals, such as the π or π* orbitals in a second-row diatomic molecule. If these orbitals each contain one electron, their spins can be parallel (as preferred by Hund's rule) or antiparallel. The Pauli exclusion principle says that no two electrons in an orbital can have the same set of quantum numbers (n, l, m_l, m_s). That means that, in the parallel case, the Pauli principle prevents the electrons from ever visiting each other's orbitals. In the antiparallel case, they are free to come and go because they have different m_s quantum numbers. However, having two electrons in the same orbital is energetically unfavorable because like charges repel. Thus, the parallel arrangement, thanks to the Pauli principle, has lower energy.

For O_2 (12 valence electrons), we get the MO energy diagram below. The shapes of the molecular orbitals are shown at the right.



This energy ordering of MOs correctly predicts **two unpaired electrons** in the π* orbital and a net **bond order of two** (8 bonding electrons and 4 antibonding electrons). This is consistent with the experimentally observed paramagnetism of the oxygen molecule.

Other interesting predictions of the MO theory for second-row diatomics are that the C_2 molecule has a bond order of 2 and that the B_2 molecule has two unpaired electrons (both verified experimentally).

We can also predict (using the O_2, F_2, Ne_2 diagram above) that NO has a bond order of 2.5, and CO has a bond order of 3.

The symbols "g" and "u" in the orbital labels, which we only include in the case of centrosymmetric molecules, refer to their symmetry with respect to inversion. *Gerade* (g) orbitals are symmetric, meaning that inversion through the center leaves the orbital unchanged. *Ungerade* (u) means that the sign of the orbital is reversed by the inversion operation. Because g and u orbitals have different symmetries, they have zero overlap with each other. As we will see below, factoring orbitals according to g and u symmetry simplifies the task of constructing molecular orbitals in more complicated molecules, such as butadiene and benzene.

The orbital shapes shown above were computed using a *one-electron model* of the molecule, as we did for hydrogen-like AOs to get the shapes of s, p, and d-orbitals. To get accurate MO energies and diagrams for *multi-electron* molecules (i.e. all real

molecules), we must include the fact that electrons are “correlated,” i.e. that they avoid each other in molecules because of their negative charge. This problem cannot be solved analytically, and is solved approximately in numerical calculations by using density functional theory (DFT). We will learn about the consequences of electron correlation in solids (such as superconductors) in Chapter 10.



Red giant stars are characterized by the presence of C_2 molecules in their atmospheres. Since C_2 has a net bond order of two, it reacts rapidly as it cools from the gas phase to make other forms of carbon such as **fullerenes**, **graphite**, and **diamond**, all of which have four bonds for every two carbon atoms.

4.6: Orbital Filling is shared under a CC BY-SA license and was authored, remixed, and/or curated by LibreTexts.

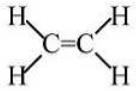
- **2.6: Orbital Filling** by Chemistry 310 is licensed CC BY-SA 4.0. Original source: https://en.wikibooks.org/wiki/Introduction_to_Inorganic_Chemistry.

4.7: Periodic Trends in π Bonding

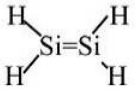
As we noted in Section 2.3, *pπ-bonding almost always involves a second-row element.*

We encounter π-bonding from the sideways overlap of p-orbitals in the MO diagrams of second-row diatomics (B_2…O_2). It is important to remember that π-bonds are weaker than σ bonds made from the same AOs, and are especially weak if they involve elements beyond the second row.

Example:



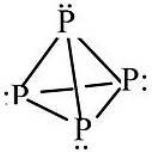
Ethylene: Stable molecule, doesn't polymerize without a catalyst.



Silylene: Never isolated, spontaneously polymerizes. Calculations indicate 117 kJ/mol stability in the gas phase relative to singly-bonded (triplet) $H_2Si\text{-}SiH_2$.

The large Ne core of Si atoms inhibits sideways overlap of 3p orbitals → weak π-bond.

Other examples: **P_4 vs. N_2**





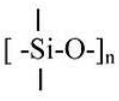
P cannot make π-bonds with itself, so it forms a tetrahedral molecule with substantial ring strain. This allotrope of P undergoes spontaneous combustion in air. Solid white phosphorus very slowly converts to red phosphorus, a more stable allotrope that contains sheets of pyramidal P atoms, each with bonds to three neighboring atoms and one lone pair.

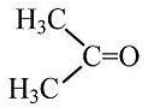


White phosphorus (P_4) is a soft, waxy solid that ignites spontaneously in air, burning with a bright flame and generating copious white P_4O_{10} smoke. The sample shown here is photographed under water to prevent the oxidation reaction

N can make π-bonds, so N_2 has a very strong triple bond and is a relatively inert diatomic gas.

$(CH_3)_2SiO$ vs. $(CH_3)_2CO$

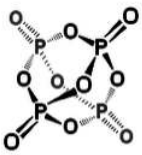




"RTV" silicone polymer (4 single bonds to Si) vs. acetone (C=O double bond). Silicones are soft, flexible polymers that can be heated to high temperatures (>300 °C) without decomposing. Acetone is a flammable molecular liquid that boils at 56 °C.



Silicone polymers $(R_2SiO)_n$ are used in non-stick cookware like these muffin cups, in Silly Putty, soft robotics, and many other applications.



Exceptions:

2nd row elements can form reasonably strong π-bonds with the *smallest* of the 3rd row elements, P, S, and Cl. Thus we find S=N bonds in sulfur-nitrogen compounds such as S_2N_2 and $S_3N_3^-$, P=O bonds in phosphoric acid and P_4O_{10} (shown above), and a delocalized π-molecular orbital in SO_2 (as in ozone).

4.7: Periodic Trends in π Bonding is shared under a CC BY-SA license and was authored, remixed, and/or curated by LibreTexts.

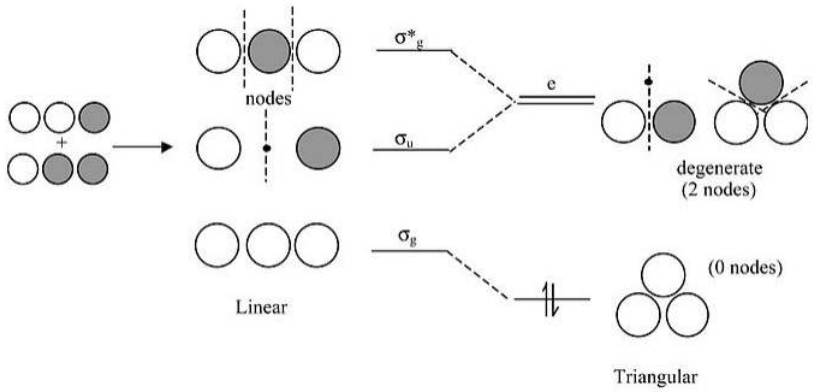
- **2.7: Periodic Trends in π Bonding** by Chemistry 310 is licensed CC BY-SA 4.0. Original source: https://en.wikibooks.org/wiki/Introduction_to_Inorganic_Chemistry.

4.8: Three-center Bonding

Many (but not all) of the problems we will solve with MO theory derive from the MO diagram of the H_2 molecule (Fig. **2.1.5**), which is a case of two-center bonding. The rest we will solve by analogy to the H_3^+ ion, which introduces the concept of three-center bonding.

We can draw the H_3^+ ion (and also H_3 and H_3^-) in either a **linear** or **triangular** geometry.

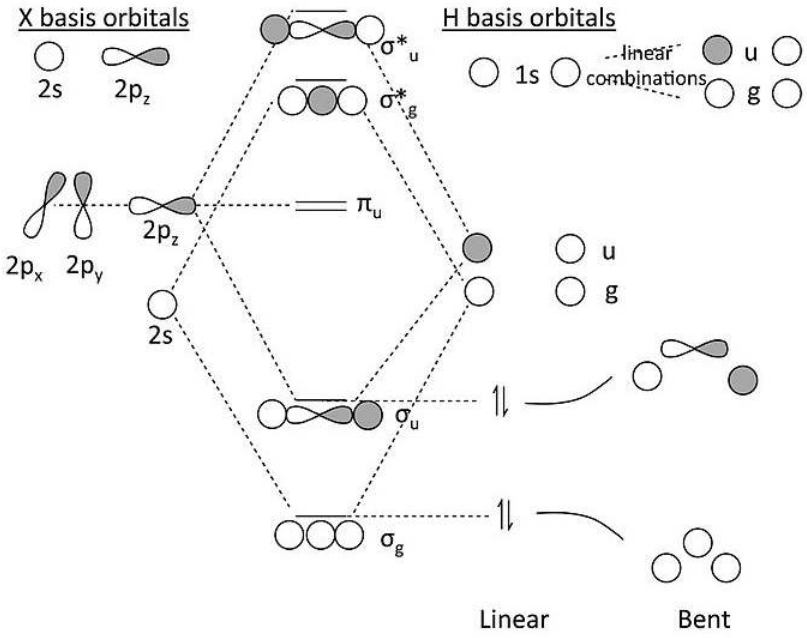
Walsh correlation diagram for H_3^+:



A few important points about this diagram:

- For the linear form of the ion, the highest and lowest MO's are symmetric with respect to the inversion center in the molecule. Note that the central 1s orbital has **g symmetry**, so by symmetry it has **zero overlap** with the **u combination** of the two 1s orbitals on the ends. This makes the σ_u orbital a **nonbonding** orbital.
- In the triangular form of the molecule, the orbitals that derive from σ_u and σ^*_g become degenerate (i.e., they have identically the same energy by symmetry). The term symbol "e" means **doubly degenerate**. We will see later that "t" means triply degenerate. Note that we drop the "g" and "u" for the triangular orbitals because a triangle does not have an inversion center.
- The **triangular form is most stable** because the two electrons in H_3^+ have lower energy in the lowest orbital. Bending the molecule creates a third bonding interaction between the 1s orbitals on the ends.

MO diagram for XH_2 (X = Be, B, C…):



Some key points about this MO diagram:

- In the linear form of the molecule, which has inversion symmetry, the 2s and 2p orbitals of the X atom factor into three symmetry classes:

  $2s = \sigma_g$

  $2p_z = \sigma_u$

  $2p_x, 2p_y = \pi_u$

- Similarly, we can see that the two H 1s orbitals make two linear combinations, one with σ_g symmetry and one with σ_u symmetry. They look like the bonding and antibonding MO's of the **H_2 molecule** (which is why we say we use that problem to solve this one).
- The π_u orbitals must be **non-bonding** because there is no combination of the H 1s orbitals that has π_u symmetry.
- In the MO diagram, we make bonding and antibonding combinations of the σ_g's and the σ_u's. For BeH_2, we then populate the lowest two orbitals with the four valence electrons and discover (not surprisingly) that the molecule has **two bonds** and can be written **H-Be-H**. The correlation diagram shows that a bent form of the molecule should be **less stable**.

An interesting story about this MO diagram is that it is difficult to predict a priori whether CH_2 should be linear or bent. In 1970, Charles Bender and Henry Schaefer, using quantum chemical calculations, predicted that the ground state should be a bent triplet with an H-C-H angle of 135°.[4] The best experiments at the time suggested that methylene was a linear singlet, and the theorists argued that the experimental result was wrong. *Later experiments proved them right!*

"A theory is something nobody believes, except the person who made it. An experiment is something everybody believes, except the person who made it." – Einstein

---

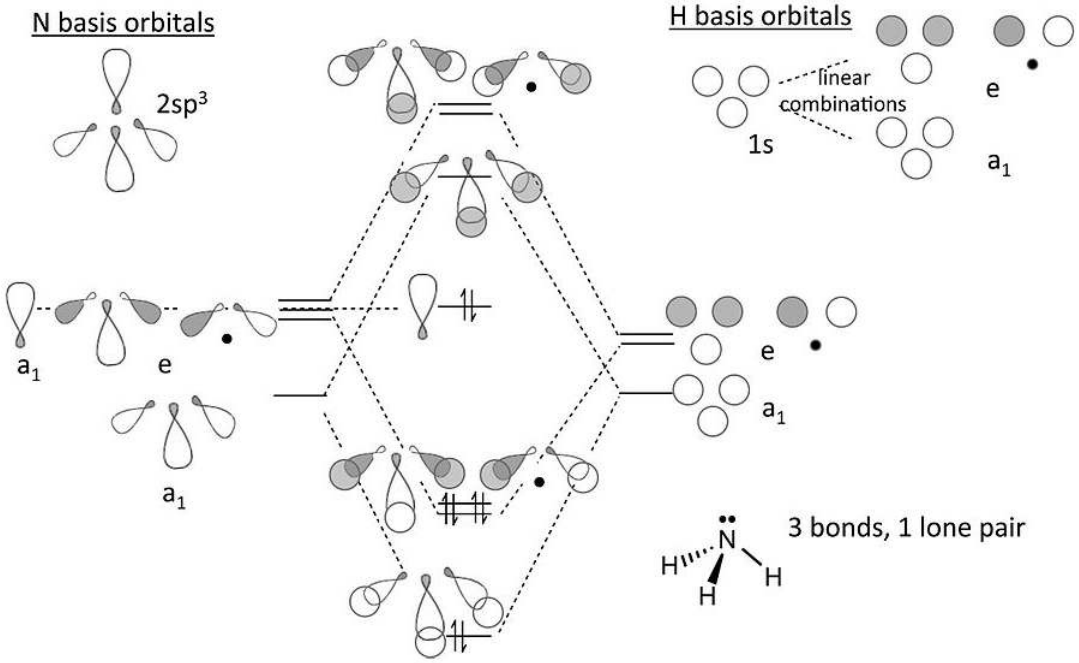
4.8: Three-center Bonding is shared under a CC BY-SA license and was authored, remixed, and/or curated by LibreTexts.

- **2.8: Three-center Bonding** by Chemistry 310 is licensed CC BY-SA 4.0. Original source: https://en.wikibooks.org/wiki/Introduction_to_Inorganic_Chemistry.

4.9: Building up the MOs of More Complex Molecules- NH_3, P_4

MO diagram for NH_3

We can now attempt the MO diagram for NH_3, building on the result we obtained with triangular H_3^+.

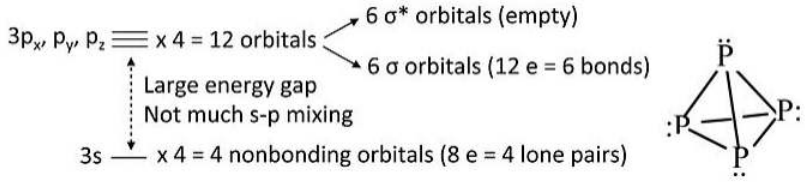


Notes on the MO diagram for ammonia:

- Viewed end-on, a p-orbital or an sp_x hybrid orbital looks just like an s-orbital. Hence we can use the solutions we developed with s-orbitals (for H_3^+) to set up the σ bonding and antibonding combinations of nitrogen sp^3 orbitals with the H 1s orbitals.
- We now construct the sp^3 hybrid orbitals of the nitrogen atom and orient them so that one is "up" and the other three form the triangular base of the tetrahedron. The latter three, by analogy to the H_3^+ ion, transform as one totally symmetric orbital ("a_1") and an e-symmetry pair. The hybrid orbital at the top of the tetrahedron also has a_1 symmetry.
- The three hydrogen 1s orbitals also make one a_1 and one (doubly degenerate) e combination. We make bonding and antibonding combinations with the nitrogen orbitals of the same symmetry. The remaining a_1 orbital on N is non-bonding. The dotted lines show the correlation between the basis orbitals of a_1 and e symmetry and the molecular orbitals
- The result in the 8-electron NH_3 molecule is **three N-H bonds** and **one lone pair** localized on N, the **same as the valence bond picture** (but much more work!).

P_4 molecule and P_4^{2+} ion:

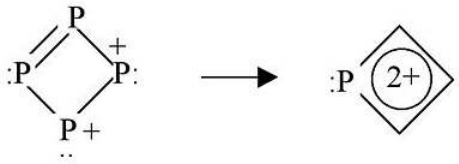
By analogy to NH_3 we can construct the MO picture for one vertex of the P4 tetrahedron, and then multiply the result by 4 to get the bonding picture for the molecule. An important difference is that there is relatively little s-p hybridization in P_4, so the lone pair orbitals have more s-character and are lower in energy than the bonding orbitals, which are primarily pσ.



Take away 2 electrons to make P_4^{2+}

Highest occupied MO is a bonding orbital → *break one bond, 5 bonds left*

Square form relieves ring strain, (60° → 90°)



2 π electrons

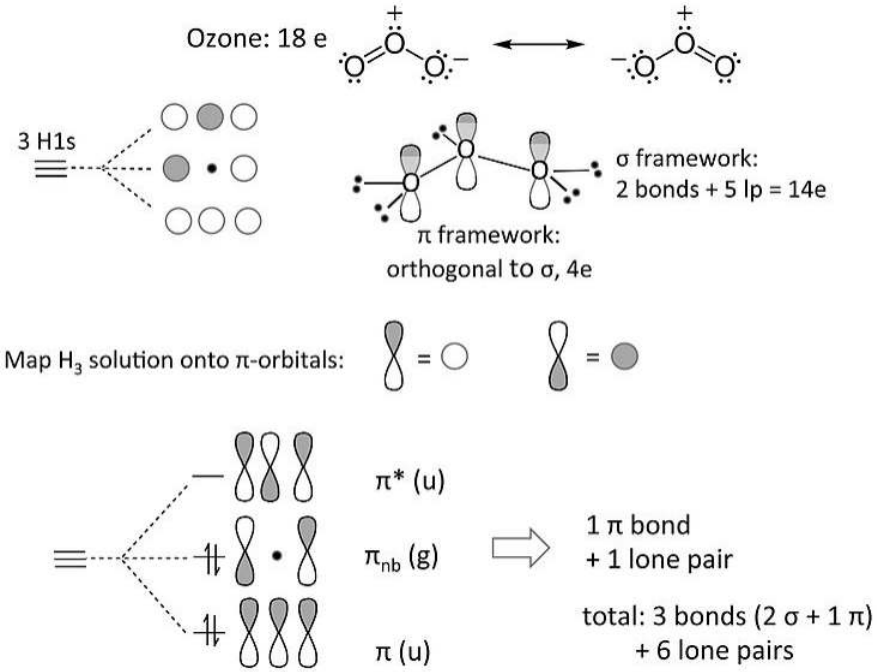
aromatic (4n + 2 rule)

4.9: Building up the MOs of More Complex Molecules- NH_3, P_4 is shared under a CC BY-SA license and was authored, remixed, and/or curated by LibreTexts.

- **2.9: Building up the MOs of More Complex Molecules- NH_3, P_4** by Chemistry 310 is licensed CC BY-SA 4.0. Original source: https://en.wikibooks.org/wiki/Introduction_to_Inorganic_Chemistry.

4.10: Homology of σ and π orbitals in MO diagrams

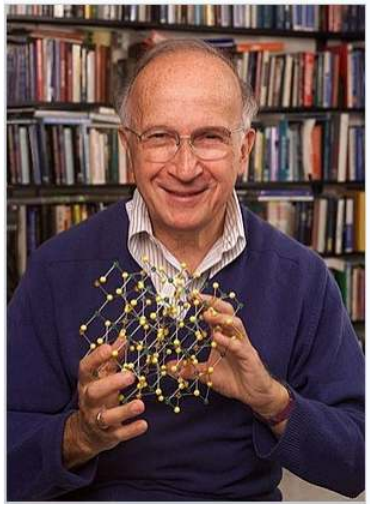
The **ozone molecule** (and related 18e molecules that contain three non-H atoms, such as NO_2^- and the allyl anion $[CH_2\text{-}CH\text{-}CH_2]^-$) is an example of **3-center 4-electron** π-bonding. Our MO treatment of ozone is entirely analogous to the 4-electron H_3^- anion. We map that solution onto this one as follows:



The nonbonding π-orbital has a node at the central O atom. This means that the non-bonding electron pair in the π-system is shared by the two terminal O atoms, i.e., that the formal charge is shared by those atoms. This is consistent with the octet resonance structure of ozone.

This trick of mapping the solution for a set of s-orbitals onto a π-bonding problem is a simple example of a broader principle called the **isolobal analogy**. This idea, developed extensively by Roald Hoffmann at Cornell University, has been used to understand bonding and reactivity in organometallic compounds.[5] In the isolobal analogy, symmetry principles (as illustrated above in the

analogy between H_3^- and ozone) are used to construct MO diagrams of complex molecules containing d-frontier orbitals from simpler molecular fragments.



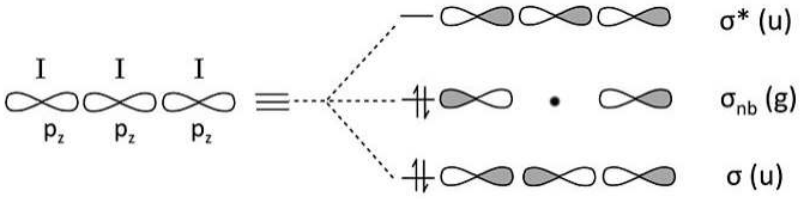
Professor Roald Hoffmann's ideas about orbital symmetry have helped explain the bonding and reactivity of organic and organometallic molecules, and also the structures and properties of extended solids.

The triiodide ion. An analogous (and seemingly more complicated) case of 3-center 4-electron bonding is $\mathbf{I_3^-}$. Each I atom has 4 valence orbitals (5s, $5p_x$, $5p_y$, $5p_z$), making a total of 12 frontier orbitals, and the I_3^- anion has 22 electrons.

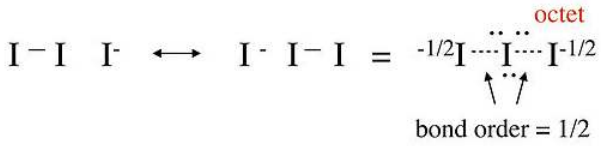
We can simplify the problem by recalling two periodic trends:

- The s-p orbital splitting is large, relative to the bond energy, after the second row of the periodic table. Thus, the 5s orbital is low in energy and too contracted to make bonds with its neighbors.
- π-overlap of 5p orbitals is very weak, so the $5p_x$ and $5p_y$ orbitals will also be non-bonding.

This leaves only the three $5p_z$ orbitals to make bonding/nonbonding/antibonding combinations. Again, the problem is entirely analogous to ozone or H_3^-.



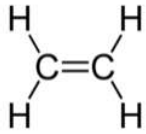
Counting orbitals we obtain 9 lone pairs from the nonbonding 5s, $5p_x$, and $5p_y$ orbitals, as well as one bond and one lone pair from the $5p_z$ orbital combinations above. The total of 10 nonbonding pairs and one bond accounts for the 22 electrons in the ion. The non-bonding $5p_z$ pair is localized on the terminal I atoms, giving each a -1/2 formal charge. This MO description is entirely consistent with the octet no-bond resonance picture of I_3^- that we developed in Chapter 1.



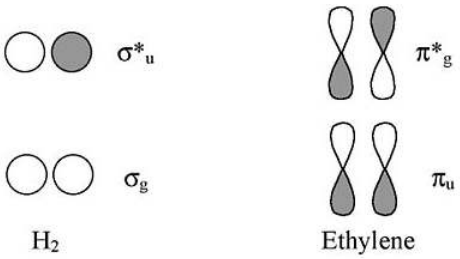
4.10: Homology of σ and π orbitals in MO diagrams is shared under a CC BY-SA license and was authored, remixed, and/or curated by LibreTexts.

- **2.10: Homology of σ and π orbitals in MO diagrams** by Chemistry 310 is licensed CC BY-SA 4.0. Original source: https://en.wikibooks.org/wiki/Introduction_to_Inorganic_Chemistry.

4.11: Chains and Rings of π-Conjugated Systems

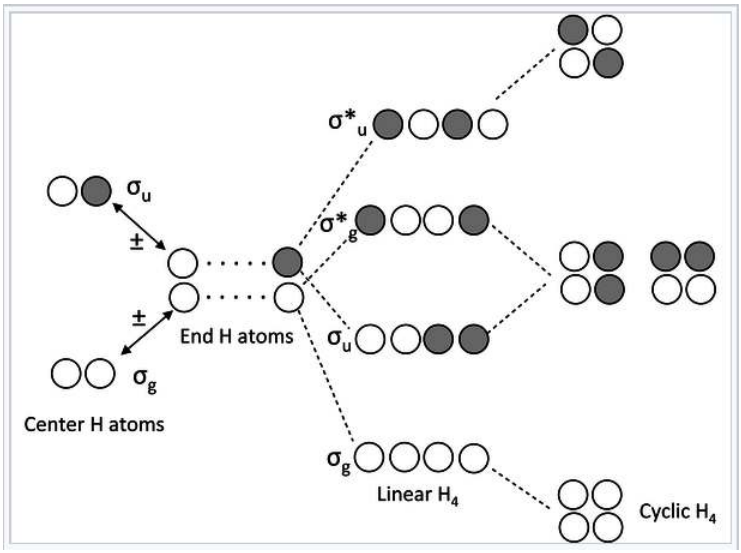


Ethylene: The π system is analogous to σ-bonding in H_2



Viewed from the top or bottom, the ethylene π-orbitals look like the H_2 σ orbitals. Thus we can map solutions from chains and rings of H atoms onto chains and rings of π-orbitals (as we did for the three-orbital case of O_3).

Chains and rings of four H atoms or π-orbitals (H_4 or butadiene):

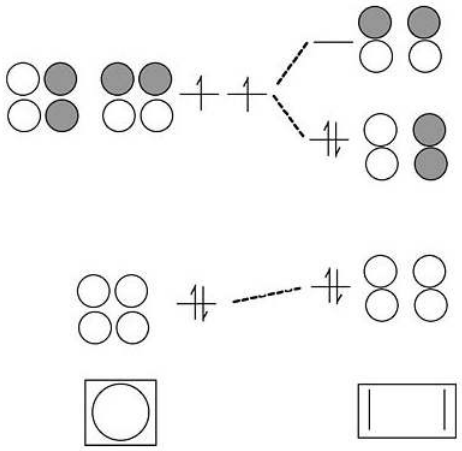


MO diagram for H4 or butadiene

A few notes about this MO diagram:

- In the linear form of the molecule, the combination of AOs makes a *ladder* of evenly spaced energy levels that alternate g – u – g – u …. Each successive orbital has one more node. This is a general rule for linear chains of σ or π orbitals with even numbers of atoms.
- In the cyclic form of the molecule, there is one non-degenerate orbital at the bottom, one at the top, and a ladder of doubly degenerate orbitals in between. This is also a general rule for cyclic molecules with even numbers of atoms. This is the origin of the **4n+2 rule** for aromatics.
- H_4 has four valence electrons, and by analogy butadiene has four π-electrons. These electrons fill the lowest two MOs in the linear form of the molecule, corresponding to two conjugated π-bonds in butadiene (H_2C=CH-CH=CH_2).
- In the cyclic form of the molecule, the degenerate orbitals are singly occupied. The molecule can break the degeneracy (and lower its energy) by distorting to a puckered rectangle. This is a general rule for **anti-aromatic** cyclic molecules (4n rule). Thus

cyclobutadiene should be anti-aromatic and have two single and two double bonds that are not delocalized by resonance.

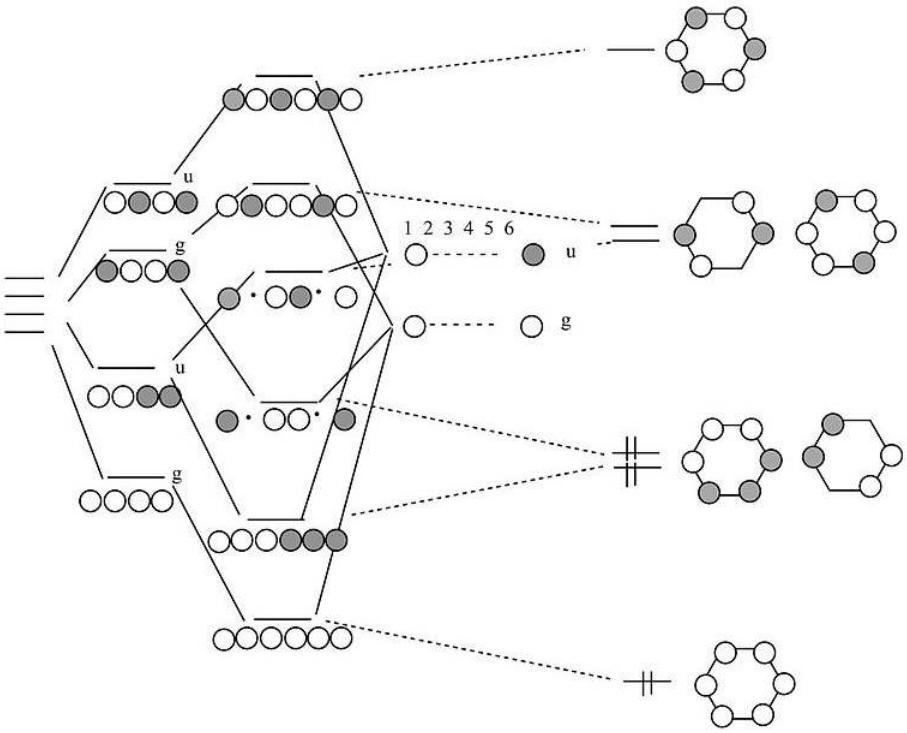


Cyclobutadiene is actually a very unstable molecule because it polymerizes to relieve ring strain. Sterically hindered derivatives of the molecule do have the puckered rectangular structure predicted by MO theory.

Benzene π-orbitals:

How do we get from a 4-atom to 6-atom chain?

By analogy to the process we used to go from a 2-atom chain to a 4-atom chain, we now go from 4 to 6. We start with the orbitals of the 4-atom chain, which form a ladder of g and u orbitals. Then we make g and u combinations of the two atoms that we are adding at the ends. By combining g's with g's and u's with u's, we end up with the solutions for a string of 6 atoms. Closing these orbitals into a loop gives us the π molecular orbitals of the benzene molecule. The result is three π bonds, as we expected. Benzene fits the 4n+2 rule (n=2) and is therefore aromatic.



Here we have used the isolobal analogy to construct MO diagrams for π-bonded systems, such as ethylene and benzene, from combinations of s-orbitals. It raises the interesting question of whether the aromatic 4n+2 rule might apply to s-orbital systems, i.e., if three molecules of H_2 could get together to form an aromatic H_6molecule. In fact, recent studies of hydrogen under ultra-high pressures in a diamond anvil cell show that such structures do form. A solid hydrogen phase exists that contains sheets of distorted six-membered rings, analogous to the fully connected 2D network of six-membered rings found in graphite or graphene.[6]

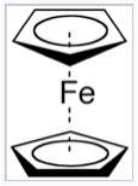
It should now be evident from our construction of MO diagrams for four- and six-orbital molecules that we can keep adding atomic orbitals to make chains and rings of 8, 10, 12... atoms. In each case, the g and u orbitals form a ladder of MOs. At the bottom rung of the ladder of an N-atom chain, there are no nodes in the MO, and we add one node for every rung until we get to the top, where there are N-1 nodes. Another way of saying this is that the *wavelength* of an electron in orbital x, counting from the bottom (1,2,3...x,...N), is 2Na/x, where a is the distance between atoms. We will find in Chapters 6 and 10 that we can learn a great deal about the electronic properties of metals and semiconductors from this model, using the infinite chain of atoms as a model for the crystal.

4.11: Chains and Rings of π-Conjugated Systems is shared under a CC BY-SA license and was authored, remixed, and/or curated by LibreTexts.

- **2.11: Chains and Rings of π-Conjugated Systems** by Chemistry 310 is licensed CC BY-SA 4.0. Original source: https://en.wikibooks.org/wiki/Introduction_to_Inorganic_Chemistry.

4.12: Discussion Questions

- Derive the molecular orbital diagrams for linear and bent H_2O.
- Explain why the bond angles in H_2O and H_2S are different.
- We have derived the MO diagrams for the pi-systems of four- and six-carbon chains and rings. Repeat this exercise for a 5-carbon chain and 5-carbon ring (e.g., the cyclopentadienide anion), starting from the MO pictures for H_2 and H_3. This tricky problem helps us understand the electronic structure of ferrocene, and was the subject of a Nobel prize in 1973.



Ferrocene

4.12: Discussion Questions is shared under a CC BY-SA license and was authored, remixed, and/or curated by LibreTexts.

- **2.12: Discussion Questions** by Chemistry 310 is licensed CC BY-SA 4.0. Original source: https://en.wikibooks.org/wiki/Introduction_to_Inorganic_Chemistry.

4.13: Problems

1. The ionization energy of a hydrogen atom is 1312 kJ/mol and the bond dissociation energy of the H_2^+ molecular ion is 256 kJ/mol. The overlap integral S for the H_2^+molecular ion is given by the expression $S = (1 + R/a_0 + R^2/3a_0^2)\exp(-R/a_0)$, where R is the bond distance (1.06 Å) and a_0 is the Bohr radius, 0.529 Å. What are the values of α and β (in units of kJ/mol) for H_2^+?

2. Compare the bond order in H_2^+ and H_2 using the molecular orbital energy diagram for H_2. The bond dissociation energy of the H_2 molecule is 436 kJ/mol. Explain why this energy is less than twice that of H_2^+.

3. What is the bond order in HHe? Why has this compound never been isolated?

4. Would you expect the Be_2 molecule to be stable in the gas phase? What is the total bond order, and how many net σ and π bonds are there?

5. Give a plausible explanation for the following periodic trend in F-M-F bond angles for gas-phase alkali difluoride (MF_2) molecules. (Hint - it has something to do with a trend in s- and p-orbital energies; see Chapter 1, section 1.2)

Compound	F-M-F angle (degrees)
BeF_2	180
MgF_2	158
CaF_2	140
SrF_2	108
BaF_2	100

6. The most stable allotrope of nitrogen is N_2, but the analogous phosphorus molecule (P_2) is unknown. Explain.

7. Using molecular orbital theory, show why the H_3^+ ion has a triangular rather than linear shape.

8. Use MO theory to determine the bond order and number of unpaired electrons in (a) O_2^-, (b) O_2^+, (c) gas phase BN, and (d) NO^-. Estimate the bond lengths in $O_2^-$and O_2^+ using the Pauling formula, and the bond length in the O_2 molecule (1.21 Å).

10. Compare the results of MO theory and valence bond theory for describing the bonding in (a) CN^- and (b) neutral CN. Is it possible to have a bond order greater than 3 in a second-row diatomic molecule?

11. The C_2 molecule, which is a stable molecule only in the gas phase, is the precursor to fullerenes and carbon nanotubes. Its luminescence is also responsible for the green glow of comet tails. Draw the molecular orbital energy diagram for this molecule. Determine the bond order and the number of unpaired electrons.

12. Use the Pauling formula to estimate the bond order in C_2 from the bond distance, 1.31 Å. The C-C single bond distance in ethane is 1.54 Å. Does your calculation agree with your answer to problem 11? What bond order would valence bond theory predict for C_2?

13. Draw the MO diagram for the linear $[FHF]^-$ ion. The only orbitals you need to worry about are the frontier orbitals, i.e., the H 1s and the two F sp_z hybrid orbitals that lie along the bonding (z) axis. What is the order of the HF bonds? What are the formal charges on the atoms?

14. The cyclooctatetraene (cot) molecule (picture a stop sign with four double bonds) has a puckered ring structure. However in $U(cot)_2$, where the oxidation state of uranium is 4+ and the cot ligand has a formal charge of 2-, the 8-membered rings are planar. Why is cot^{2-} planar?

4.13: Problems is shared under a CC BY-SA license and was authored, remixed, and/or curated by LibreTexts.

- **2.13: Problems** by Chemistry 310 is licensed CC BY-SA 4.0. Original source: https://en.wikibooks.org/wiki/Introduction_to_Inorganic_Chemistry.

4.14: References

1. More precisely, in the case of a complex wavefunction φ, the probability is the product of φ and its complex conjugate φ*
2. Hoffmann, R. (1963). "An Extended Hückel Theory. I. Hydrocarbons.". *J. Chem. Phys.* **39** (6): 1397–1412. doi:10.1063/1.1734456. Bibcode: 1963JChPh..39.1397H.
3. Cotton, F. A.; Harris, C. B. Inorg. Chem., 1965, 4 (3), 330-333. DOI|10.1021/ic50025a015
4. C. F. Bender and H. F. Schaefer III, New theoretical evidence for the nonlinearity of the triplet ground state of methylene, J. Am. Chem. Soc. 92, 4984–4985 (1970).
5. Hoffmann, R. (1982). "Building Bridges Between Inorganic and Organic Chemistry (Nobel Lecture)". *Angew. Chem. Int. Ed.* **21** (10): 711–724. doi:10.1002/anie.198207113.
6. I. Naumov and R. J. Hemley, Acc. Chem. Res. 47, 3551–3559 (2014) dx.doi.org/10.1021/ar5002654.

4.14: References is shared under a CC BY-SA license and was authored, remixed, and/or curated by LibreTexts.

- **2.14: References** by Chemistry 310 is licensed CC BY-SA 4.0. Original source: https://en.wikibooks.org/wiki/Introduction_to_Inorganic_Chemistry.

CHAPTER OVERVIEW

5: Coordination Chemistry I - Structures and Isomers

5.1: History

5.2: Nomenclature

5.3: Coordination Numbers and Structures

5.4: Isomerism

5.5: Concept Review Questions Chapter 5

5.6: Homework Problems Chapter 5

Dr. Kai Landskron (Lehigh University). If you like this textbook, please consider to make a donation to support the author's research at Lehigh University: Click Here to Donate.

This page titled 5: Coordination Chemistry I - Structures and Isomers is shared under a not declared license and was authored, remixed, and/or curated by Kai Landskron.

5.1: History

Coordination Chemistry

Now let us direct our focus toward actual coordination chemistry, also often called complex chemistry. In the following, we will apply the previously learned concepts about atomic theory, symmetry, molecular orbital theory, and acid-base chemistry to coordination compounds. Let us first ask: How are coordination compounds, or complexes defined? They are typically Lewis-acid base adducts between a metal atom or a metal ion as the Lewis acid and one or more ligands as a Lewis base. These ligands can be inorganic ligands such as halogenide ions, water, and ammonia molecules, or organic ligands like amines or alcohols. Coordination compounds are known since the antique due to their often intense color, and are used as a pigment or dye, for example Prussian Blue ($KFe[Fe(CN)_6]$ or tetrammine copper, both of which are intensely blue. You can see a few examples of coordination compounds below, namely the hexahydrate of copper (II) sulfate which is blue, iron (III) chloride, which is yellow, and nickel sulfate which is greenish-blue. Because of their intense color they have also attracted the attention of modern chemists from the early on, but the chemical bonding in these compounds remained a mystery for a relatively long time. The bonding in these compounds seemed more complex, hence the name complex compounds.



Figure 5.1.1 $Cu(SO_4)$ x 5 H_2O (Attribution: No machine-readable author provided. Yuvalif assumed (based on copyright claims). / Public domain https://commons.wikimedia.org/wiki/F...er-Sulfate.JPG), $FeCl_3$ x 6 H_2O (Attribution: Benjah-bmm27 / Public domain https://commons.wikimedia.org/wiki/F...ate-sample.jpg) and $NiSO_4$ x 6 H_2O (Attribution: Benjah-bmm27 / Public domain https://commons.wikimedia.org/wiki/F...ate-sample.jpg), respectively

History on Coordination Compounds

What was the problem with the bonding in coordination compounds? Their empirical formulas could be easily determined by element analysis, but the results could not be explained with the concept of valence. In the early days of modern chemistry it was believed that the number of bonds in a compound could not exceed the valence. For example, in the compound of the formula $Co(NH_3)_6Cl_3$ the valence of Co would be +3, therefore cobalt could not make more than three bonds. Assuming that the Co^{3+} ion would make three bonds to the 3 Cl^- ions, how would one involve the six NH_3 molecules in the bonding?



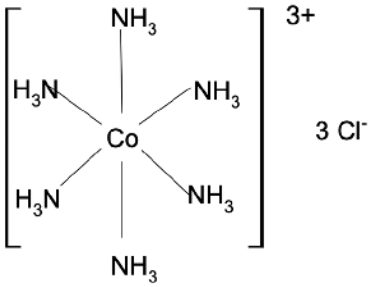
Figure 5.1.2 Alfred Werner (1866-1919) (Attribution: ETH Zürich / CC BY-SA (https://creativecommons.org/licenses/by-sa/3.0) https://commons.wikimedia.org/wiki/F...ortr_09965.jpg)

The chemist who solved this mystery was Alfred Werner. He correctly suggested that the number of bonds would not be restricted to the valence, but that more bonds would be allowed. It would be possible that the six NH_3 molecules bind directly to Co^{3+}

forming a so-called complex cation. They would be in the so-called first coordination sphere around the Co. The three chloride ions would then be bound loosely to the complex cation balancing the charge of the complex cation. They would be in the second coordination sphere.

Formula Writing in Coordination Chemistry

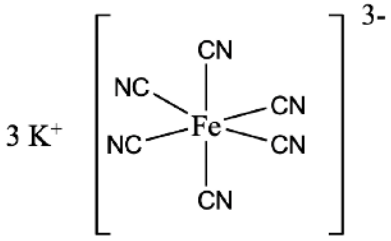
How can we write a formula of a coordination compound that contains complex ions?



$[Co(NH_3)_6]Cl_3$

Figure 5.1.3 Example of complex cation notation

For complex cations we write the element symbol for the metal ion first followed by the formula for the ligands. If there is more than one ligand, then we will place the ligands in parentheses, and indicate their number by a subscript behind the parentheses. The entire complex cation is placed in brackets. The formula for the anion in the second coordination sphere is placed behind the brackets and the number of anions is indicated by a subscript (Fig. 5.1.3).



$K_3[Fe(CN)_6]$

Figure 5.1.4 Example of a formula for a complex with a complex anion

For complex anions, we write the formula for the counter cation first, followed by the complex anion in brackets. You can see two examples above (Fig. 5.1.3 and 5.1.4). We have complex cations of Co with six NH_3 ligands coordinated to it in the first coordination sphere. Three Cl^- ions are in the second coordination sphere. Hence the formula is $[Co(NH_3)_6]Cl_3$. The second example is the coordination compound with the complex anion having a 3- charge in which six cyanide anions bind to a central Fe^{3+} ion. The K^+ ion in the second coordination sphere compensates the charge of the complex anion. Hence the formula is $K_3[Fe(CN)_6]$.

Dr. Kai Landskron (Lehigh University). If you like this textbook, please consider to make a donation to support the author's research at Lehigh University: Click Here to Donate.

This page titled 5.1: History is shared under a not declared license and was authored, remixed, and/or curated by Kai Landskron.

- **5.1: History** by Kai Landskron is licensed CC BY 4.0.

5.2: Nomenclature

Classification of Ligands

Let us look a little closer at ligands and see how we can classify them. One way is to categorize them into monodentate and multi-dentate ligands.

Monodentate ligands have only one point of attachment to the metal ion.

Definition: Monodentate ligand

Monodentate ligands have only one point of attachment to the metal ion

Examples for such ligands are halogenide ligands, ammonia as ligand, and water as ligand. The molecules often have different names when acting as ligands, and you must know these names. For example, water as a ligand is called an aqua ligand, ammonia as a ligand is called an ammine ligand, chloride as a ligand is called a chloro ligand.

Ligands with more than one point of attachment are called multidentate ligands, or chelate ligands.

Definition: Multidentate ligands

Multi-dentate ligands have two or more points of attachment to the metal ion

Complexes with chelate ligands are called chelate complexes. Greek prefixes indicate how many points of attachment the ligand has (Fig. 5.2.1).

2: bi-dentate
3: tri-dentate
4: tetra-dentate
5: penta-dentate
6: hexa-dentate

Figure 5.2.1 Greek prefixes indicating how many points of attachment the chelating ligand has

If there are two, then we have a bidentate ligand, when there are three, we have a tridentate ligand. We use the prefixes tetra, penta, and hexa to indicate four, five, and six points of attachment, respectively. Multi-dentate ligands with more than six points of attachment are rare.

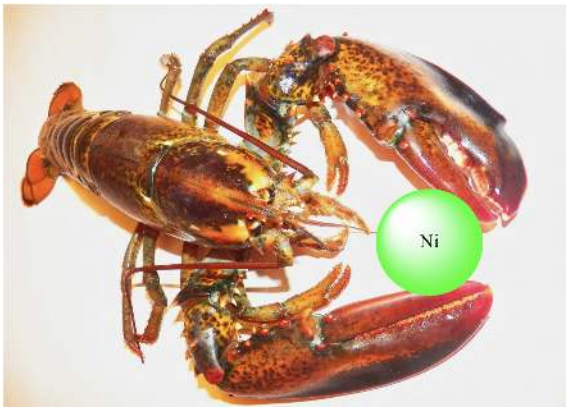
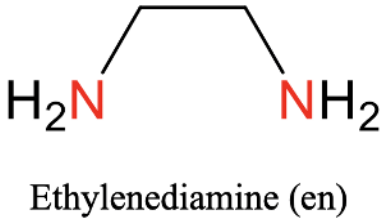


Figure 5.2.2 Visual representation of the origin of the word chelate (Attribution: Junior Libby https://www.publicdomainpictures.net...503683515x.jpg)

The name chelate ligand comes from the Greek word chela, meaning great claw of the lobster. We can see that our lobster in Figure 5.2.2 happily chelates a Ni^{2+} ion with its two great claws!

Common Bidentate Ligands

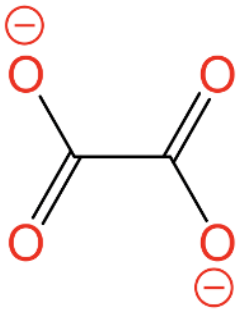
A few common bidentate ligands are shown below.



Ethylenediamine (en)

Figure 5.2.3 The ethylenediamine (en) ligand. Donor atoms are denoted red.

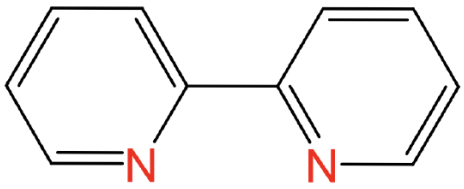
The first one is ethylene diamine. It has two nitrogen donor atoms that can bind to the metal, and they are separated by an ethylene group (Fig. 5.2.3).



Oxalate (ox)

Figure 5.2.4 The oxalate (ox) ligand. Donor atoms are denoted red.

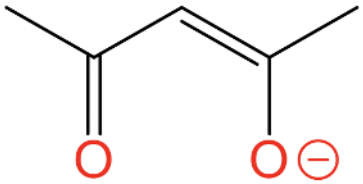
Another common ligand is the oxalate ligand. It has two O donor atoms separated by two carbon atoms. There are two negative charges that are delocalized over the four O atoms (Fig. 5.2.4).



bipyridyl (bipy)

Figure 5.2.5 The Bipyridyl (bipy) ligand. Donor atoms are denoted red.

As a third example you can see the bipyridyl ligand having two N donor atoms as part of two aromatic rings. The two N atoms are separated by two carbon atoms (Fig. 5.2.5).



acetylacetonate (acac)

Figure 5.2.6 Acetylacetonate (acac). Donor atoms are denoted red.

Lastly, there is the acetyl acetonate ligand with two O donor atoms separated by three C atoms (Fig. 5.2.6). The acetyl acetonate carries a negative charge that is delocalized between the two O atoms. In this case the donor atoms are separated by three carbons.

Common ligands often have specific abbreviations. They are often used in the formulas of coordination compounds with these ligands. For example, the ethylene diamine ligand is abbreviated *en*, the oxalate ligand is abbreviated *ox*, the bipyridyl ligand is abbreviated *bipy*, and the acetyl acetonate ligand is abbreviated *acac*. There are not only bidentate ligands with O and N donor atoms, but also with others such as P and S.

Rings in Complexes with Chelate Ligands

In most chelating ligands the donor atoms are separated by two or three other atoms, mostly carbon atoms. This is because in this case the chelate ligands can form five- and six-membered rings with the metal ion (Fig. 5.2.7).

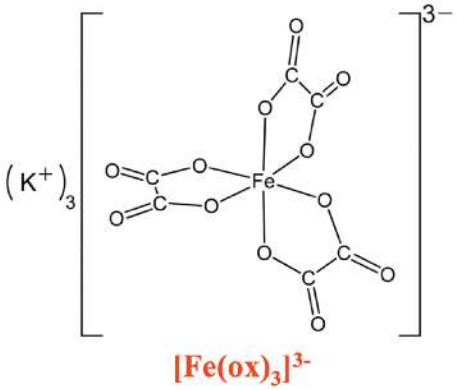


Figure 5.2.7 Trioxolato iron complex (Attribution: Benjah-bmm27 / Public domain https://commons.wikimedia.org/wiki/F...oxalate-2D.png)

You can see that the trioxolato iron complex above has three five-membered rings containing one Fe, two O, and two C atoms. These ring sizes are particularly stable because they have the least ring strain. As a consequence, the respective chelate complexes are particularly stable.

Tridentate Ligands

Here are a couple of examples for tridentate ligands.

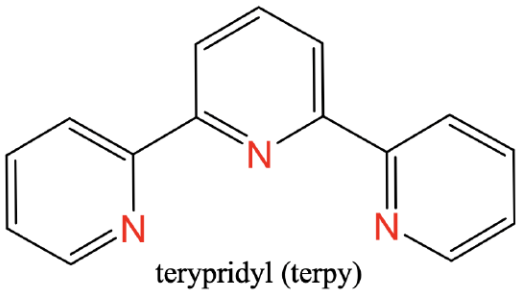


Figure 5.2.8 Terypridyl (terpy). Donor atoms are denoted red.

The first one is terpyridyl, abbreviated “Terpy”(Fig. 5.2.8), the second one is bisethylenetriamine, abbreviated “tris” (Fig. 5.2.9).

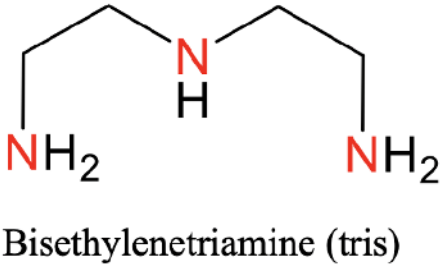


Figure 5.2.9 Bisethylenetriamine (tris). Donor atoms are denoted red.

Both of them have three N-donor atoms separated by two carbon atoms. In the “tris”-ligand there are two ethylene groups between the N atoms, in the case of the “terpy”-ligand the N-atoms are part of three aromatic rings (Fig. 5.2.8. and Fig. 5.2.9)

Tetradentate Ligands

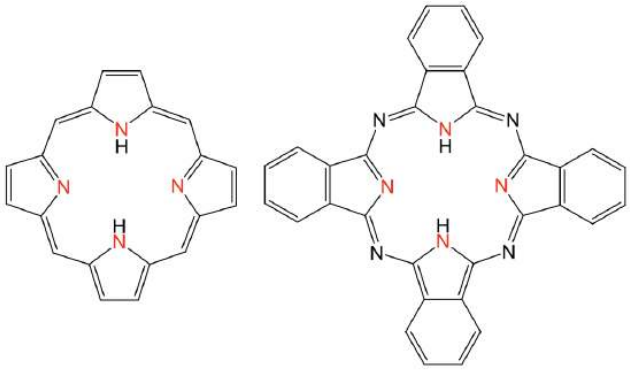


Figure 5.2.10 Porphyrine (left) and Phtalocyanine (right). Donor atoms are denoted red.

Two common tetradentate ligands are porphyrine and phtalocyanine (Fig. 5.2.9 and 5.2.10). Both are co-called macrocyclic ligands because they are large cycles. They both have four N-donor atoms pointing inside of the cycle. The phtalocyanine ligand has four additional N atoms connecting the five-membered rings via imine-linkages. Further the phtalocyanine has four benzene rings fused to the four five-membered rings. The porphyrine ligand is very important in biological systems. For example, it is part of the protein hemoglobin. In this case a an Fe^{2+} ion sits in the center of the porphyrin ring. It is also a component of chlorophyll in which case an Mg^{2+} ion sits in the center of the ring. Phtalocyanine ligands are important as components of dyes.

Hexadentate Ligand, EDTA

A very common hexadentate ligand is the ethylenediamine tetraacetic acid (EDTA) ligand. You can see its structure below (Fig. 5.2.11).

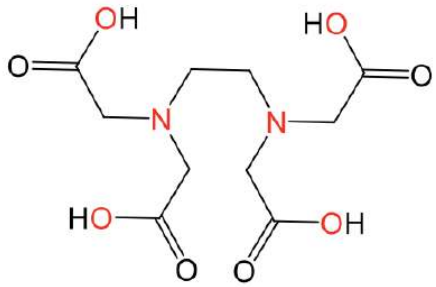
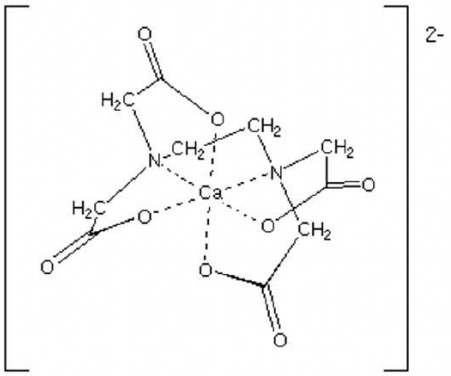


Figure 5.2.11 Structure of EDTA (donor atoms are denoted red)

It has two N-donor atoms separated by an ethylene group. Each N-atom is further connected to two acetyl groups. The overall four acetyl groups carry four O-donor atoms. Overall, there are six donor atoms. The six donor atoms can coordinate octahedrally to a metal ion such as a Ca^{2+} ion (Fig. 5.2.12).



EDTA complex with Ca^{2+}

Figure 5.2.12 EDTA complex with Ca^{2+}

In coordinated form the EDTA ligand is deprotonated, and the O donor atoms carry a negative charge. Therefore an EDTA complex with a divalent cation such as Ca^{2+} has a 2- charge.

Nomenclature of Complexes

Now let us develop a nomenclature for coordination chemistry so that we can communicate them in an educated manner. One important aspect is that we name the number of ligands. To indicate the number of a particular ligand we use Greek prefixes (Fig. 5.2.13).

2	di
3	tri
4	tetra
5	penta
6	hexa
7	hepta
8	octa

Figure 5.2.13 Greek prefixes associated with the number of ligands in a coordination compound.

These are the same prefixes we got to know when we discussed multidentate ligands. If there are two ligands we use the prefix di, if there are three we use the prefix tri- and so fourth.

Nomenclature of Complexes with Anionic Coordination Spheres

We can now develop the full name of a coordination compound. Let us consider compounds with complex anions first. We can name them according to three steps.

In the first step we name the counter cation. We do not account for the number of counter cations in the name.

Next, we determine the name and the number of ligands. If the ligand is anionic it gets the suffix “o”. Note that sometimes for ease of pronunciation abbreviations are used. For example a Cl^- is a chloro-ligand, and not a chlorido ligand. You must memorize these shorter forms. Generally, when an anion ends with “ide”, the “ide” is omitted, and replaced by “o”.

The third step is to name the metal ion and add the suffix “ate” to the name. You can either add the oxidation number of the metal in roman numerals or the charge of the complex anion in parentheses after the name of the metal. The first nomenclature is called the “Stock” system, the latter the “Ewing-Bassett” system. Note that if the element symbol of the metal is derived from a latin name then the latin name is used. For example if silver is the metal then the complex anion is an argentate, if lead is the metal the

complex anion is a plumbate. Also here abbreviations are often used to make pronunciation easier. If the name ends with “um” that ending is replaced by “ate”.

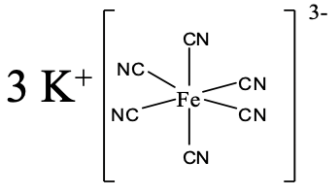


Figure 5.2.14 Example of a complex with a complex anion

An example for coordination compounds with a complex anion is shown above (Fig. 5.2.14). What is its name? There are three K^+ cations, so the name starts with potassium. We realize next, that there are six cyanide anions as ligands, so the name continues “hexacyano”. The name of the metal is iron, but we use the latin name ferrum, and replace the ending “um” with the ending “ate”. The oxidation number of the iron is +3. We can see that from the fact that the complex ion has a 3- charge, and the six cyano ligands have a 1- charge each. If we used the Stock system we would therefore place the roman numerals for +3 in parentheses behind the name. If we used the Ewing-Bassett system, we would place the (3-) for the negative charge of the complex behind the name. So overall it would be either a potassium hexacyanoferrate (III) or a potassium hexacyanoferrate (3-).

Exercises

How would you name the following two compounds?



Figure 5.2.17 Example 1

Let us look at the first example (Fig. 5.2.17). First, we need to name the cation. What is it? It is just “hydrogen”. Next we need to determine the name and number of ligands. We have six chloro ligands, so the name continues with “hexachloro”. The name of metal is platinum. We replace the ending “um” by “ate”. In the Stock system the roman numeral would be (IV) because the oxidation state of the Pt is +4. We can see this from the fact that the complex anion has a 2- charge, and the six chloro ligands have a 1- charge each. We must add +4 to -6 to get to -2. Therefore, in the Stock system, the name would be hydrogen hexachloroplatinate (IV), and in the Ewing-Bassett system it would be hydrogen hexachloroplatinate (2-).

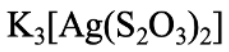


Figure 5.2.18 Example 2

The second example (Fig. 5.2.18) has three K^+ cations, so the name starts with potassium. What is the name of the ligand? The name of the anion is thiosulfate. In this case we replace the ending “e” by the ending “o”. We have two ligands, so it is a “dithiosulfato”. The metal is silver, but we use the latin name “argentum”, and replace the ending “um” by the ending “ate”. So it is an “argentate” . Fusing the parts together gives “potassium dithiosulfato argentate”. The oxidation number of Ag is +1, the charge at the anion is -3. So put either (I) in roman numerals or 3- in parentheses behind the name.

Nomenclature of Complexes with Cationic Coordination Spheres

Now let us name complexes with complex cations. We name the complex cation first, and then the anion. Then, we determine the name and the number of the ligands and prefixes accordingly. If there is an anionic ligand we give it the suffix “o” again. Then, we name the metal. In this case, we always use English names. We place the oxidation number in roman numerals or the charge of the complex cation behind the name, depending on whether we want to use the Stock or the Ewing-Bassett system.

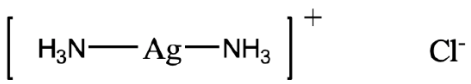


Figure 5.2.19 Example of a complex with a complex cation

For example, how would you name the complex depicted above (Fig. 5.2.19)? There are two NH_3 ligands which are neutral. We have to consider that NH_3 as a ligand is called an “ammine” ligand. Note that it is spelled with two “m” in the middle. So the name

starts “diammine”. The name of the metal is silver, and the oxidation state of silver is +1. This is because the complex has a 1+ charge and the ammine ligands are neutral. The anion is a chloride anion.

Diamminesilver(I) chloride

Figure 5.2.20

Therefore, the name in the Stock system would be “diamminesilver(I) chloride (Fig. 5.2.20).

Diamminesilver(1+) chloride

Figure 5.2.21

In the Ewing-Bassett system it would be “Diamminesilver (1+) chloride” (Fig. 5.2.21)

Exercises

What would be the names of the two compounds listed below.

$$[Pt(NH_3)_4]\ Cl_2$$

Figure 5.2.22 Example 1

The first example, Fig. 5.2.22, has four NH_3 ligands, so the name starts with tetraammine. Platinum is the metal, so the name continues “platinum”. The oxidation state of Pt is +2 because the complex cation has a 2+ charge, and the ligands are charge-neutral. The name of the anion is “choride”. So overall it is a “tetraammineplatinum(II) chloride” according to the Stock system or a “tetrammineplatinum(2+) chloride according to the Ewing-Bassett system.

$$[Ni(H_2O)_6]\ Cl_2$$

Figure 5.2.23 Example 2

The second compound (Fig. 5.2.23) has six water ligands, therefore the name starts with “hexaaqua” followed by the name of the metal with is “nickel”. The oxidation state of Ni is 2+ because the charge at the complex cation is +2, and the ligands are charge-neutral. The name of the anion is “chloride”. Therefore, the name is either hexaaaqua nickel (II) chloride or “hexaaquanickel (2+) chloride.

Nomenclature of Complexes with Cationic and Anionic Coordination Spheres

There is also the possibility that a coordination compound is made of a complex cation and a complex anion. In this case, the rules discussed previously hold, the only new thing to learn is that we name the complex cation first and the complex anion second.

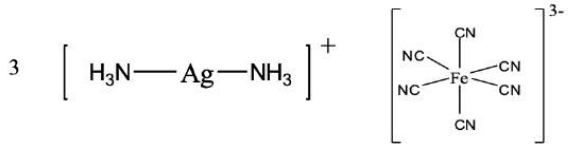


Figure 5.2.24 Coordination compound made of both a complex cation and complex anion

In the compound depicted (Fig. 5.2.24) we have a diammine silver (I) cation and a hexacyanoferrate (III) anion.

Diamminesilver(I) hexacyanoferrate (III)
or
Diamminesilver(1+) hexacyanoferrate(3-)

$$[Ag(NH_3)_2]_2\ [Fe(CN)_6]$$

Figure 5.2.24

Hence the name is diammine silver (I) hexacyanoferrate (III) in the Stock system or diammine silver(1+) hexacyanoferrate (3-), Fig. 5.2.24.

Nomenclature of Complexes with More Than One Ligand of the Same Kind

What if there are different ligands in a coordination compound? In this case, we name the ligands in alphabetical order, and give each ligand a prefix according to its number.

$$[Co(NH_3)_4Cl_2]NO_3$$

Figure 5.2.26 Example 1

For example: What is the name of $[Co(NH_3)_4Cl_2]NO_3$, Fig. 5.2.26? This is a compound with a complex cation containing ammine and chloro ligands. Because “a” comes before “c” in the alphabet we have to name the ammine ligand first. There are four ammine ligands and two chloro ligands. Therefore, we use the prefixes “tetra” in front of “ammine” and “di” in front of “chloro”. So the name starts “tetraamminedichloro”. Then, we name the metal which is cobalt. The oxidation number of cobalt is +3 because there are four charge-neutral ammine ligands, two anionic chloro ligands, and the charge at the complex cation is +1. +3 -2 = +1. So in the Stock system the compound is called tetramminedichlorocobalt(III) nitrate, in the Ewing-Basset system it is called tetramminedichlorocobalt(1+) nitrate.

$$[Pt(NH_3)BrCl(H_2O)]SO_4$$

Figure 5.2.27 Example 2

Let us do one more example, Fig. 5.2.27. In the compound $[Pt(NH_3)BrCl(H_2O)]SO_4$ there is a complex cation with four different ligands: an “ammine” ligand, a “bromo”-ligand, a "chloro"-ligand, and an "aqua" ligand. What is the order of them? According to the alphabet, “ammine” comes first, “aqua” is second, “bromo” is third, and “chloro” is fourth. They do not get a prefix because there is just one of them for each. The metal is platinum, and its oxidation state is +4 because the complex cation has a 2+ charge, and there are two neutral ligands, namely the aqua and the ammine ligands, and two anionic ones, namely the bromo and the chloro ligands: +4 - 2 = +2.

Ammineaquabromochloroplatinum(IV)sulfate
or
ammineaquabromochloroplatinum(2+)sulfate

Figure 5.2.28

Therefore, the name is ammineaquabromochloroplatinum(IV)sulfate in the Stock system, and ammineaquabromochloroplatinum(2+)sulfate in the Ewing-Bassett system, 5.2.28.

Nomenclature of Complexes with Complicated Ligands in a Coordination Sphere

So far we only considered relatively simple ligands that were either monoatomic, or contained a few atoms only. However, many ligands, in particular chelating ligands, contain more atoms, and have more complex names. These names may already contain prefixes that we use to number ligands. For example the ethylenediamine ligand is a chelating ligand with a longer name that already contains the prefix “di”. In such cases, to avoid ambiguity, we put the ligand name in parentheses, and place a somewhat different prefix in front of it to account for the number of the ligands.

“Tris” instead of “tri”
“tetrakis instead of “tetra”
“pentakis” instead of “penta”
etc.

Figure 5.2.29 Prefixes used for complicated ligands

Instead of “di” we use “bis”, instead of “tri” we use “tris”, instead of “tetra” we use “tetrakis”, instead of “penta” we use “pentakis”, and so on, Fig. 5.2.29.

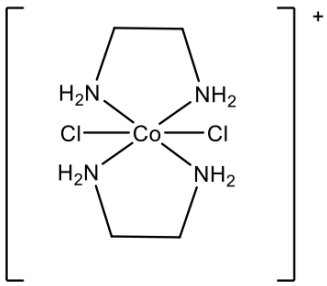


Figure 5.2.30 Example of a complex cation with more complicated ligands.

For example, what is the name of the complex cation depicted above (Fig. 5.2.30)? We first need to realize that there are two different ligands: chloro ligands and ethylenediamine ligands. We need to name the chloro ligands first, because they come first in the alphabet. Because there are two chloro ligands we use the prefix “di”. The ethylenediamine ligand is placed in parentheses, and the prefix “bis” is used instead of “di”. The metal is cobalt in the oxidation state +3 because the complex cation has a 1+ charge, and there are two chloro ligands with a 1- charge each, and two charge-neutral ethylenediamine ligands: +3 -2 = +1.

Dichlorobis(ethylenediamine)cobalt(III)
Dichlorobis(ethylenediamine)cobalt(1+)

Figure 5.2.31

Therefore, the name is dichlorobis(ethylenediamine)cobalt(III) in the Stock system and dichlorobis(ethylenediamine)cobalt(1+) in the Ewing-Bassett system (Fig. 5.2.31).

Nomenclature of Complexes with Bridging Ligands

Ligands cannot only be terminal, they can also bridge two metal centers. To indicate that a ligand is a bridging ligand we give it a prefix μ. Bridging ligands are named before terminal ligands, and the name of the molecular fragments with the terminal ligands and metal ions is placed in parentheses after the name of the bridging ligand.

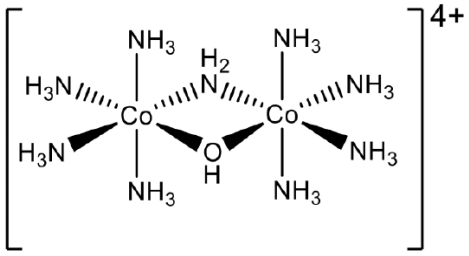


Figure 5.2.32 Complex with bridging ligands

So what is the name of the complex cation depicted above (Fig. 5.2.32)? We can see that there are two different bridging ligands, one is a hydroxo-ligand OH^-, and the other is called an amido ligand NH_2^-. These bridging ligands bridge two identical molecular fragments containing a Co atom and four ammine ligands each. The two bridging ligands need to be named first, and we have to name them according to alphabetic order. Hence, the name starts “ μ-amido- μ-hydroxo”. Then, we need to name the two fragments which are bridged. Because there is one Co and four NH_3 ligands, the name of the fragment is “tetraamminecobalt”. Because this is a more complex name we need to put it into parentheses. There are two fragments, therefore we need to use the prefix “bis”. The oxidation state of Co is +3. This is because there are two anionic ligands, the hydroxo, and the amido ligand which have both a 1- charge. The other ligands are neutral. The complex cation carries a 4+ charge: +6-2=+4. Because there are two Co atoms, they have an oxidation number of +6/2=+3.

μ-amido-*μ*-hydroxobis(tetraamminecobalt)(III)

Figure 5.2.33

Hence, the overall name according to the Stock system is “ μ-amido-μ-hydroxobis(tetraamminecobalt)(III)”, Fig. 5.2.33.

μ-amido-*μ*-hydroxobis(tetraamminecobalt)(4+)

Figure 5.2.34

In the Ewing-Bassett system it is μ-amido- μ-hydroxobis(tetraamminecobalt)(4+), Fig. 5.2.34. Now we have completed the chapter on nomenclature.

Dr. Kai Landskron (Lehigh University). If you like this textbook, please consider to make a donation to support the author's research at Lehigh University: Click Here to Donate.

This page titled 5.2: Nomenclature is shared under a not declared license and was authored, remixed, and/or curated by Kai Landskron.

- **5.2: Nomenclature** by Kai Landskron is licensed CC BY 4.0.

5.3: Coordination Numbers and Structures

Coordination Numbers (CN) and Structures of Complexes

Coordination compounds have many different structures or shapes, and therefore it is important that we are able to categorize the structures of coordination compounds, understand why a particular structure forms, and why certain structures are more common than others.

A central parameter that determines the structure is the coordination number. A coordination number is the number of points of attachment between the ligands and the metal.

Definition: Coordination Number

The coordination number is the number of points of attachment between the ligands and the metal

What are the main factors that are associated with the coordination number? Some of them are associated with the metal ion, and some of them are associated with the ligands. The shape and the size of a ligand greatly influences the coordination number. Generally, the bulkier the ligand the smaller than coordination number. With regard to the metal ion, the size of the metal ion plays an important role. The larger the metal ion, the more ligands fit around it, and the coordination number increases. In addition, the electron configuration of the metal ion plays a role. For certain electron configurations certain coordination numbers are preferred because these coordination numbers stabilize electron energies. Lastly, there are intermolecular interactions to consider. In solid state they occur between neighbored complexes, in solution they occur between the complex and solvent molecules. This can lead to different coordination numbers and structures in the solid state, and in solution, respectively.

Main Factors Determining CNs

1. Shape and size of ligands
2. Size of metal ion
3. Electron configuration of metal ion
4. Intermolecular interactions (solution vs. solid state)

As you can see, there are many factors that influence the coordination number, and the shape of the complexes. These factors are sometimes opposing, which makes the prediction of structures difficult. Nonetheless, there are a number of rules that allow for a fair accuracy in structure prediction, and we will go through these rules in the following.

Low Coordination Numbers (CN)

CN = 1

The coordination number 1 is very rare. When there is one point of attachment, then there are usually reactive coordination sites at the metal ion that lead to cluster formation. This reduces the energy and increases the coordination number. For example, in methyl lithium (MeLi) the Li appears to have the coordination number 1 because you may think that there is only a single, covalent Li-C bond. However, there is actually a tetrahedral cluster Li_4Me_4.

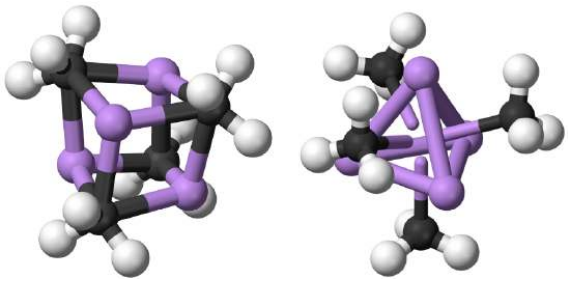


Figure 5.3.1 Two different views on the structure of MeLi tetrameric cluster (Attribution: Benjah-bmm27 / Public domain https://commons.wikimedia.org/wiki/F...2-3D-balls.png)

The four Li atoms build a tetrahedron and the methyl groups are placed above the faces of the tetrahedron (Fig. 5.3.1). One can also think of MeLi as a near cubic molecule in which the Li atoms occupy every other vertice of the cube, and methyl groups the remaining vertices of the cube (Fig. 5.3.2). The cluster formation avoids the coordination number 1, and stabilizes the methyl lithium. In addition to a tetrameric cluster there is also a hexameric cluster for Me-Li known.

.

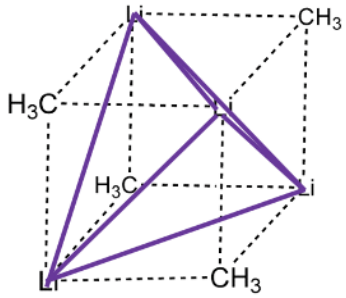


Figure 5.3.2 Structure in methyllithium inscribed into a cube. (https://commons.wikimedia.org/wiki/File:MeLi.png)

The coordination number 1 is only possible when a large metal ion is surrounded by a very bulky ligand that suppresses cluster formation, and there is no coordination of solvent molecules to the metal.

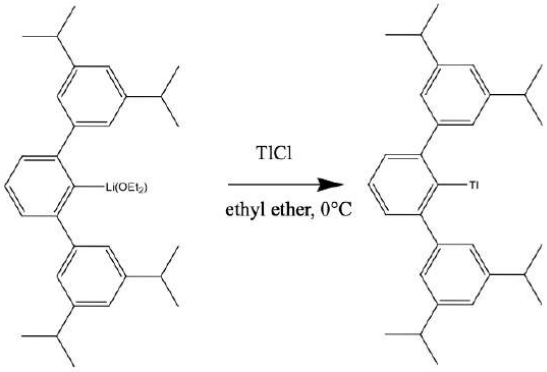


Figure 5.3.3 2,6,-$Trip_2C_6H_3Tl$ (Attribution: Niemeyer, M., and Power, P. P., J. Angew. Chem., Int. Ed., 1998, 37, 1277.)

An example the the cluster 2,6,-$Trip_2C_6H_3Tl$. (Trip = 2,4,6, i-$Pr_3C_6H_2$), Fig. 5.3.3. It has a Tl^+ coordinated to a bowl-shaped, bulky ligand via a Tl-C bond. The Tl fits exactly into the bowl-shaped cavity in the ligand, thereby preventing cluster formation. The compound can be prepared from its lithium derivative and thallium chloride in diethyl ether at 0°C.

CN = 2

The coordination number 2 is also rare, but already a lot more common than the coordination number 1. Generally, d^{10} metal ions have a tendency to make structures with CN=2. These structures are linear structures. An example of a d^{10} ion is Ag^+. Why is it d^{10}? Ag is located in group 11, so it has 11 valence electrons. If we remove one, there are ten. The energy of the Ag^+ ion is minimized when the 4d-subshell is full, and the 5s-subshell is empty. Ag^+ makes many linear structures with ligands, example ammine ligands or cyano ligands. In an oversimplified picture, we may explain the structure using VSEPR arguments assuming there is an sp-hybridization of the 5s and one 5p orbital, and the two electron lone pairs at the two ligands get donated into the sp-hybridized orbitals. What other d^{10}-ions can you think of? There would be the higher and lower homologue of the Ag^+ ion, the Cu^+, and the Au^+ ion.

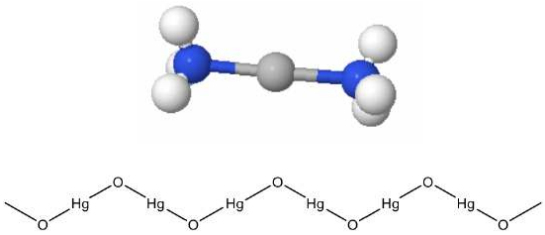


Figure 5.3.4 Linear structures formed with a coordination number of 2: $[Ag(NH_3)_2]^+$ and HgO (Attribution: https://chem.libretexts.org/@api/deki/files/18507/2.bmp?revision=2&size=bestfit&width=243&height=134 http://creativecommons.org/licenses/by-nc-sa/3.0/us/)

They make linear complexes such as $CuCl_2^-$ and $Au(CN)_2^-$. Hg^{2+} is also a d^{10} ion that often makes linear complexes, for example $Hg(CN)_2^-$. This linear coordination is not only found in molecular compounds but also in extended solids. For example, HgO and HgS make zig-zag chains of linearly coordinated Hg^{2+} (Fig. 5.3.4). The bending of the chain occurs at the oxide anions, because of the electron lone pairs at O. Other metal ions but d^{10} ions make linear structures only when the ligands are very bulky. These examples are rare.

CN = 3

The coordination number 3 is also rare for coordination compounds. They are most common for d^{10} ions, especially when the ligands are bulky. In most cases the trigonal planar structure, or a structure close to that is adopted.

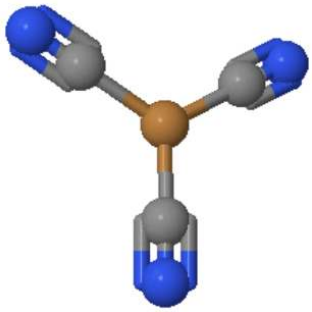


Figure 5.3.5 The $Cu(CN)_3^{2-}$ anion (Attribution: https://chem.libretexts.org/@api/deki/files/18508/3.bmp?revision=1 http://creativecommons.org/licenses/by-nc-sa/3.0/us/)

An example is the $Cu(CN)_3^{2-}$ anion in which Cu^+ is surrounded by three cyanide anions in a trigonal planar fashion (Fig. 5.3.5).

CN = 4

The coordination number 4 is a very common coordination number. It is actually the second-most common coordination number, only surpassed by the coordination number 6. The by far most common structure associated with the coordination number 4 is the tetrahedral structure. Why? It is because the ligands have the greatest distance from each other, and the smallest steric repulsion. Generally, smaller ions and/or larger ligands favor the coordination number 4 over the coordination number 6.

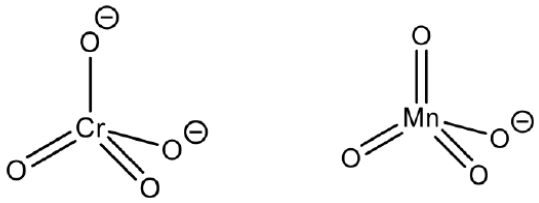


Figure 5.3.6 Permanganate anion and the chromate anion

This is the case in the permanganate anion and the chromate anion, for example. Here, the oxidation state of Mn and Cr are +7 and +6 respectively, making the ionic radius very small.

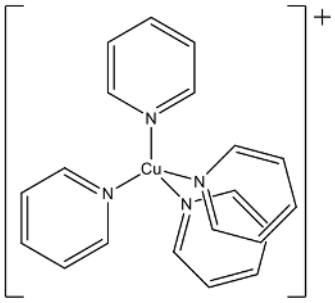


Figure 5.3.7 The tetrakis(pyridyl) copper(1+) ion

Another example is the tetrakis(pyridyl) copper(1+) ion. Here, the ligands are fairly bulky. The tetrahedral structure is particularly common for d^0 and d^{10} ions, and mostly favored over the octahedral structure. All examples above have either d^0 or d^{10} ions. Cr(VI) and Mn(VII) are d^0 and Cu(I) is d^{10} thus fulfilling this requirement as well.

The second-most common structure after the tetrahedral structure is the square planar structure. It is only common for ions with d^8 electron configuration. What are common d^8 ions? Examples are the ions Ni^{2+}, Pd^{2+}, and Pt^{2+}. We can find these elements in group 10 of the periodic table. Therefore, they must have ten valence electrons in the neutral state. Because of the 2+ charge, two electrons are removed leaving eight electrons. All eight electrons are in the d-valence subshell, therefore the ions are called d^8 ions.

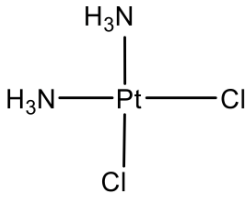


Figure 5.3.8 Cis-platinum

The arguably most well known square planar complex is cis-platinum. It has two chloro and two ammine ligands attached to Pt in cis-position. It is known as anti-cancer drug.

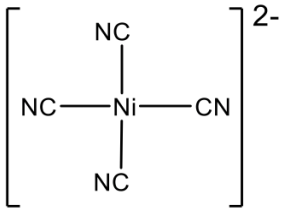


Figure 5.3.9 $Ni(CN)_4^{2-}$

$Ni(CN)_4^{2-}$ is another example of a group 10 square planar complex.

Can you think of other d^8 ions? The group 11 elements Cu, Ag, and Au have eleven valence electrons in the neutral state. In this case we need to remove three electrons to get to eight electrons, meaning that Cu^{3+}, Ag^{3+}, and Au^{3+} are d^8 ions. Cu and Ag are not very stable in the oxidation state +3, therefore examples of square planer Cu(III) and Ag(III) are fairly rare.

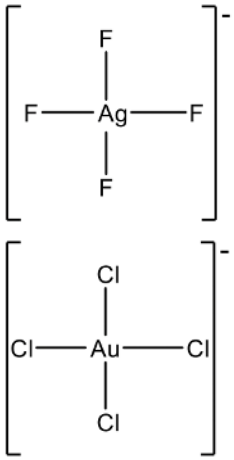


Figure 5.3.10 Structures of AgF_4^- and $AuCl_4^-$, respectively

Examples are AgF_4^- and CuF_4^-, Fig. 5.3.10. However Au^{3+} is more common and there is a relatively large number of Au(III) complexes, e.g. $AuCl_4^-$.

Because group 12 elements are not stable in the oxidation state 4, there are no group 12 d^8 ions. However group 9 d^8 ions are known. In this case the ions must be in the oxidation state +1 in order to have eight d electrons. Cobalt is not stable in the oxidation state +1, but Rh and Ir are, and square planar Rh(I) and Ir(I) complexes are common.

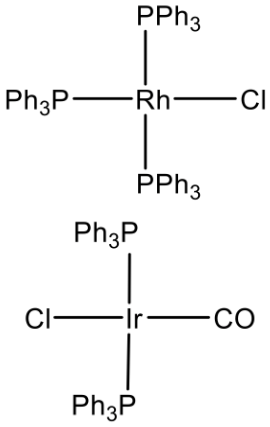


Figure 5.3.11 Structures of $Rh(PPh_3)_3Cl$ and $Ir(CO)(PPh_3)_2Cl$.

For example Rh makes a $Rh(PPh_3)_3Cl$ complex (Fig. 5.3.11). It is a common hydrogenation catalyst. Vasca's complex $Ir(CO)(PPh_3)_2Cl$ is another example (Fig. 5.3.11). It has the property to reversibly bind oxygen.

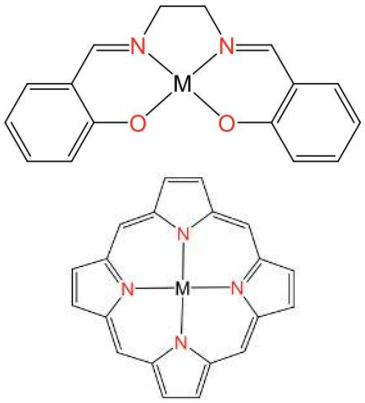


Figure 5.3.12 A generic salen complex (top) and a porphyrin complex (bottom). M = metal.

The square planar coordination is possible also with metal ions other than d^8 ions, but only when the ligand forces the metal ion into this coordination. Ligands that do this are for example the porphyrin ligand and the salen ligand. They are tetradentate ligands with donor atoms that form a square forcing the metal ion to adopt a square-planar coordination (Fig. 5.3.12).

A last possibility is the seesaw structure. It is know for main group elements, but not for transition metal elements.

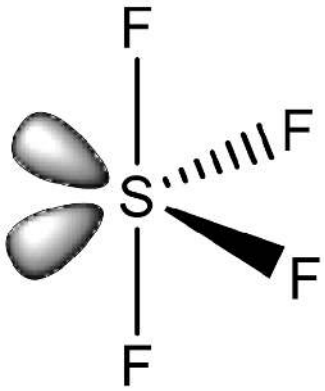


Figure 5.3.13 Structure of SF_4

An example is SF_4 (Fig. 5.3.13). The seesaw structure is derived from the octahedral structure whereby two adjacent corners of the octahedron are occupied by electron lone pairs. Formally one could consider a compound like SF_4 as a coordination compound in which four F^- ligands bind to an S^{4+} cation. However, this view is commonly not adopted, and the S-F bonds are not viewed as dative covalent bonds.

CN = 5

For the coordination number 5, the two most common structures are the trigonal bipyramid and the square pyramid. They are about equally common because they have very similar energies. Which one is preferred, depends on the particular circumstances, the nature of the metal, the ligands, the solvent, etc. Many molecules have structures in between, mostly described as distorted trigonal bipyramids. Distortion is even more common in solid state due to packing effects. Packing effects minimize the void space in the crystal.

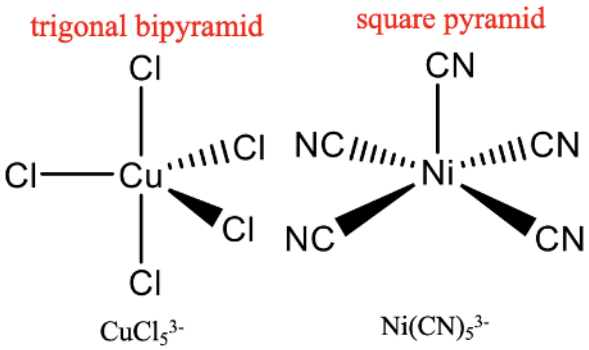


Figure 5.3.14 Structures of $CuCl_5^{3-}$ and $Ni(CN)_5^{3-}$, respectively

An example for a trigonal bipyramidal structure is $CuCl_5^{3-}$, an example for a square-pyramidal structure is $Ni(CN)_5^{3-}$ (Fig. 5.3.14). The pentagon, another conceivable structure, is not known. Five-coordinate compounds are known for the full range of transition metals. A difference compared to the structures with the coordination numbers 2 to 4 is, that in the structures with the coordination number 5 not all ligands are symmetry-equivalent. For the trigonal bipyramidal shape we distinguish between axial and equatorial ligands. In square-pyramidal complexes, the fifth ligand at the tip of the pyramid is symmetrically different to the other four at the base of the pyramid.

Because the energy difference between the trigonal bipyramidal and the square pyramidal structure is small, and there is only a small activation barrier between the two structures, they are often fluxional. This means that they can dynamically interconvert.

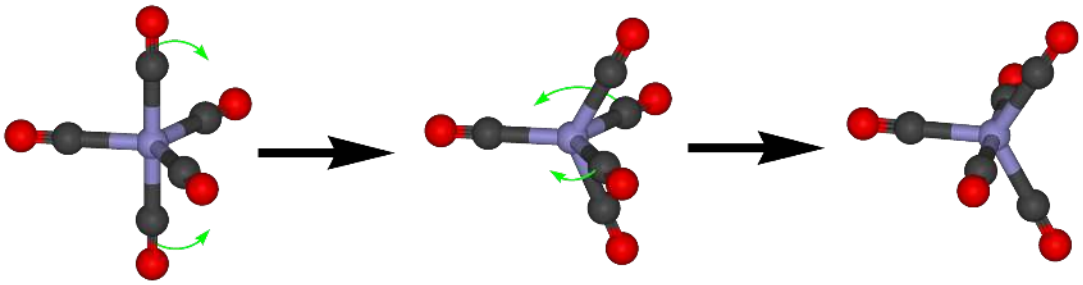


Figure 5.3.15 Berry pseudo rotation illustrated for the iron pentacarbonyl molecule. (Attribution: Benjah-bmm27 / Public domain https://commons.wikimedia.org/wiki/F...-mechanism.png)

This interconversion occurs according to a mechanism called the Berry pseudo rotation. In the Berry pseudo-rotation one 120° bond angle between two ligands in equatorial position increases until it is eventually 180°. The initial 180° angle between two ligands in axial position decreases until it is 120°. This means that the two previously equatorial ligands are now axial ligands, and the two axial ligands are now equatorial ligands. As the Berry pseudo rotations occurs, the complex moves from a trigonal bipyramidal structure through a square-pyramidal intermediate to another trigonal bipyramidal structure. The Berry pseudo rotation happens often very fast, therefore in many measurements the five ligands appear identical. For example, the PF_5 molecule shows only one signal in the ^{19}F NMR because the movement of F atoms from the equatorial to the axial position and vice versa is too fast for the NMR time scale. At low temperatures, the Berry pseudo rotation may be slow enough so that axial and equatorial positions can be resolved. In compounds with larger ligands the pseudo rotation may also be slow enough so that axial and equatorial positions are resolved in the NMR.

CN = 6

The most common coordination number is the coordination number 6. This coordination number exists for all transition metal electron configurations from d^0 to d^{10}. We can explain this by the fact that many metal ions have the right size to support six ligands around them, and there are many ligands that have the right size to surround a metal ion in the coordination number 6. The by far most common shape for the coordination number 6 is the octahedral shape. It is the shape for which the ligands have the largest distance from each other thereby minimizing steric repulsion. A second reason is that the orientation of atomic orbitals supports the octahedral shape, as many orbitals point along the x,y, and z axes, in particular the p orbitals, and the d_{z^2} as well as the $d_{x^2-y^2}$.

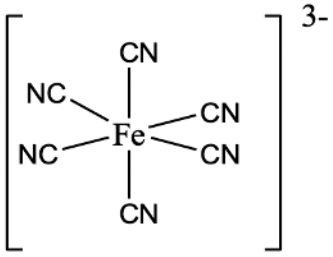


Figure 5.3.16 Structure of the hexacyanoferrate(3-) anion

An example is the hexacyanoferrate(3-) anion in which six cyano ligands surround the metal ion octahedrally (Fig. 5.3.16).

Distortions of Complexes with CN = 6

Octahedral complexes can distort in two basic ways. The first common distortion is the so-called tetragonal distortion. Tetragonal distortion can be achieved either via elongating an octahedron along two opposite vertices, or compressing the octahedron along two opposite vertices.

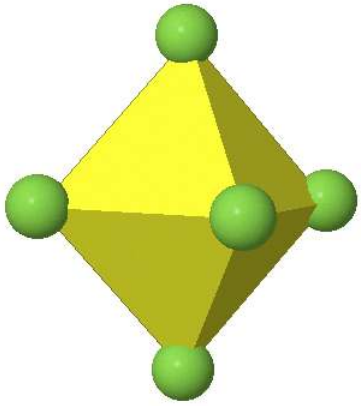


Figure 5.3.17 Tetragonal distortion (elongated octahedron) (Attribution:Chemtube3d.com)

In the first case, two opposite vertices are further away from the center of the octahedron compared to the other four corners (Fig. 5.3.17).

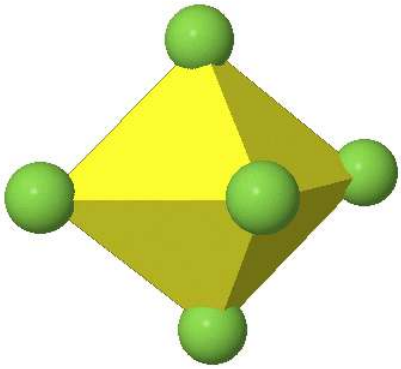


Figure 5.3.18 Tetragonal distortion (compressed octahedron) (Attribution:Chemtube3d.com)

In the compressed octahedron two opposite corners are closer to the center compared to the four other corners (Fig. 5.3.18). Both the elongated and the compressed octahedron have the same symmetry, meaning they belong to the same point group. Which point group is it? We still have a C_4 principal axis, but one only. It goes through the corners of the two opposite vertices along which we distorted. There is a horizontal mirror plane perpendicular to the C_4 axis, as well as an inversion center. Thus, the point group must be D_{4h}. In tetragonally distorted octahedra all faces are equivalent, but the distances of the ligands from the center of the octahedron are not the same.

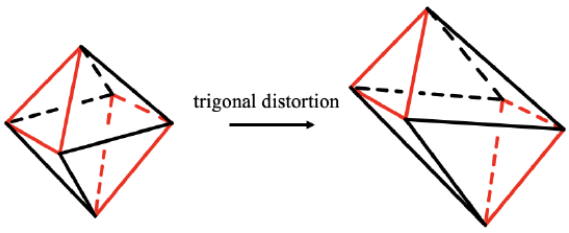


Figure 5.3.19 Trigonal distortion of an octahedron

When you elongate or compress the octahedron along to opposite faces you create a trigonal antiprism (5.3.19). It is called antiprism because the two opposite regular triangular faces, shown here in red are oriented in staggered fashion. This type of distortion is called trigonal distortion. The point group of a trigonal antiprism is D_{3d}. The C_3 axis goes through the two opposite regular triangular faces of the antiprism. There are three C_2 axes standing perpendicular, and going through the centers of the six remaining distorted triangular faces. There are three vertical mirror planes also that bisect the angle between the C_2 axes. In a trigonal antiprism the faces are not all equal, but the distance of the vertices are all the same.

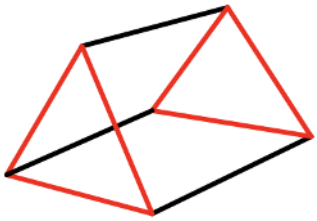


Figure 5.3.20 Trigonal prism

When we rotate one of the two opposite triangular faces of an antiprism by 60°, the two faces become eclipsed and a trigonal prism results (Fig. 5.3.20). Trigonal prismatic compounds are mostly observed when there are three bidentate ligands connecting the top and bottom triangular faces. What is the point group? It is D_{3h}. There is a C_3 axes going through the two opposite triangles. 3 C_2 axes are going through the centers of the three rectangles, and there is a horizontal mirror plane perpendicular to the C_3 axis. Does an elongation or compression along the two opposite triangular faces change the symmetry? Think about it. No, it does not change it.

CN = 7

Coordination numbers higher than 6 are considered high coordination numbers. They are significantly less common than the coordination numbers, 4, 5, and 6. A simple explanation is that large coordination numbers require a very large cation or a very small anion of the combination of both to avoid steric repulsion. These conditions are statistically less likely. In addition, large coordination numbers are not so favorable from the stand point of orbital orientation.

Let us first look at the coordination number 7 in more detail. There are three structures possible which are about equally common in nature.

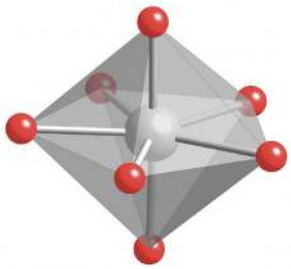


Figure 5.3.21 Pentagonal bipyramid, ZrF_7^{3-} (Attribution: chemtube3d.com https://www.chemtube3d.com/images/ga...s/I607ST22.jpg)

The first one is the pentagonal bipyramid of which ZrF_7^{3-} is an example (Fig. 5.3.21).

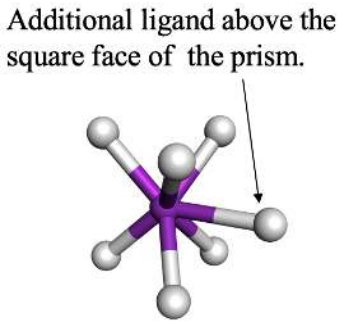


Figure 5.3.22 Trigonal prism, TaF_7^{2-} (Attribution: J3D3 / CC BY-SA (https://creativecommons.org/licenses/by-sa/3.0) https://commons.wikimedia.org/wiki/F...CapRightps.png)

The second one is the capped trigonal prism. TaF_7^{2-} is an example for it (Fig. 5.3.22). The seventh ligand is placed above a square face of the prism, not a triangular face. Can you imagine why? Think about it for a moment. The answer is that the square face is larger than the triangular face, and thus there is less steric repulsion.

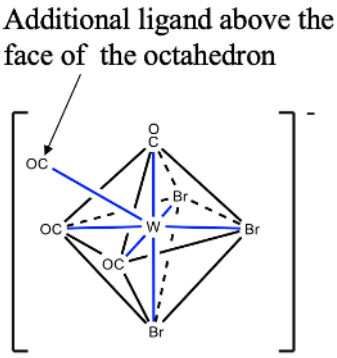


Figure 5.3.23 Capped octahedron, tribromotetracarbonyltungstate(IV)

The third structure is the capped octahedron. An example is the tribromotetracarbonyltungstate(IV). In this compound three bromo ligands and three carbonyl ligands occupy the vertices of two opposite faces in the octahedron. The fourth carbonyl ligand is placed above the triangular face with the carbonyl ligands. You can see that like for the coordination number 5, the ligands are not symmetrically equivalent.

CN = 8

Now, let us go to the coordination number 8. What shapes could you imagine that adopt the coordination number 8? The most symmetric, and simple shape is the cube (Fig. 5.3.24).

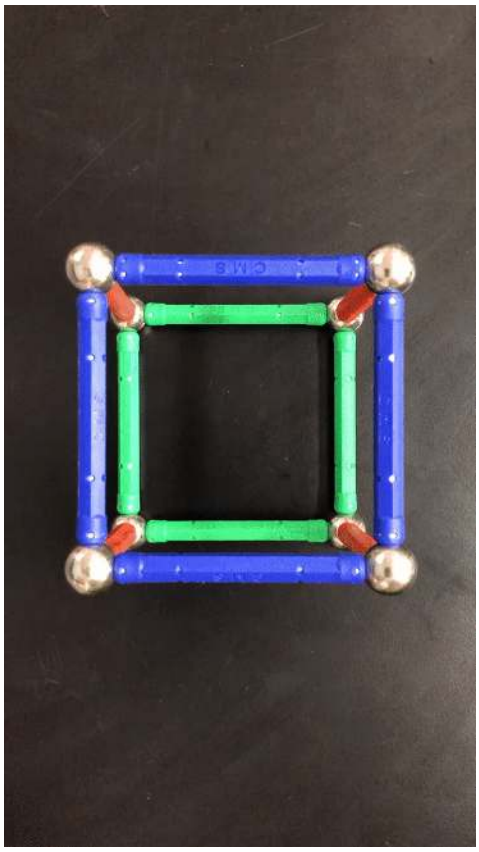


Figure 5.3.24 Transformation of a cube into a square antiprism. No cubic complexes are known.

However, complexes with cubic shapes are not observed. This is because there is another related structure which is energetically more favorable. It is the square antiprism (Fig.5.3.25). In a square antiprism, two opposite square faces are oriented in staggered fashion relative to each other. Relative to the cube one face of the cube is rotated by 45° relative to the opposite face, and the two opposite square faces are interconnected with each other to form triangular faces. The square antiprism is preferred over the square prism because the vertices where the ligands sit have a greater distance to each other compared to the cube.

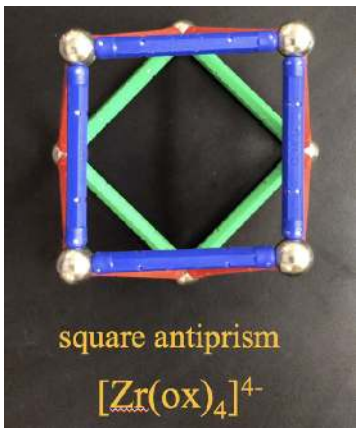


Figure 5.3.25 Square antiprism. The tetraoxolato zirconate(4-) anion has square anti-prismatic shape.

An example of a coordination compound that makes a square antiprism is the tetraoxolato zirconate(4-) anion.

A structure related to the square antiprism is the dodecahedron. Note that we are not talking about the dodecahedron that is a platonic solid here. We can derive the dodecahedron by squeezing on the two opposite corners of the two squares. This distorts and bends a square to form two additional triangular faces. This produces the dodecahedron (Fig. 5.3.26).

A video of the square antiprism to dodecahedron transformation can be accessed through the link below:

https://www.youtube.com/watch?v=A8G7...ature=youtu.be

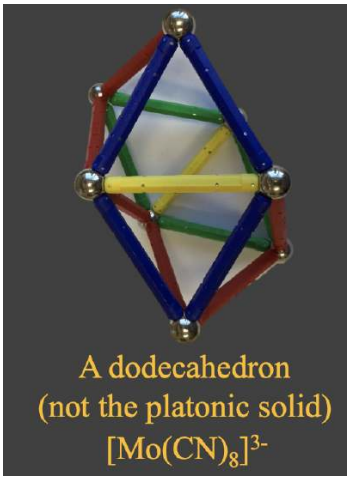


Figure 5.3.26 Dodecahedron. The octacyanomolybdate (3-) anion is an example for this shape.

An example for this shape is the complex octacyanomolybdate (3-), (Fig. 5.3.26). As you can see from the examples, all metal ions are large metal ions, and the ligands a small, confirming that structures with large coordination numbers are favored by large metal ions and small ligands.

CN = 9

Finally, let us think about shapes associated with the coordination number 9.

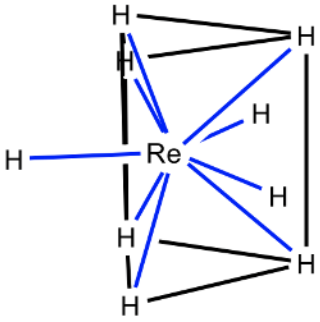


Figure 5.3.27 Tricapped prism of the nonahydridorhenate anion.

One possible shape is the tricapped trigonal prism for which the nonahydridorhenate is an example (Fig. 5.3.27). Here three additional ligands are placed above the three rectangular faces of the trigonal prism. Unsurprisingly, the ligands are small, and the metal ion is large.

Another example is the tricapped antiprism. The nonaammine lanthanum(3+) cation is an example. In this case the three additional ligands are placed above three triangular faces of an antiprism. The coordination number 9 is not the upper limit for coordination numbers. Coordination numbers up to 16 have been observed, but they are rare.

Dr. Kai Landskron (Lehigh University). If you like this textbook, please consider to make a donation to support the author's research at Lehigh University: Click Here to Donate.

This page titled 5.3: Coordination Numbers and Structures is shared under a not declared license and was authored, remixed, and/or curated by Kai Landskron.

- **5.3: Coordination Numbers and Structures** by Kai Landskron is licensed CC BY 4.0.

5.4: Isomerism

This section will be about isomerism in coordination compounds. You may know isomerism already from your organic chemistry classes. Here, we will apply isomerism to coordination chemistry. Some forms of isomerism in organic and coordination chemistry are the same, but there are some forms of isomerism that only occur in coordination chemistry.

Let us first briefly review the definition of isomerism: Isomerism is when two or more compounds have identical empirical formulas but different structures.

Definition: Isomerism

When two or more compounds have identical empirical formulas but different structures they are called isomers.

We distinguish between two basic types of isomerisms: Constitutional isomerism and stereoisomerism. What is the difference? In constitutional isomerism the bonds are not between the same atoms.

Definition: Constitutional Isomers

In constitutional isomers the bonds are not between the same atoms.

In stereoisomerism, the bonds are between the same atoms, but ligands are at different coordination sites.

Definition: Stereoisomers

In stereoisomers, the bonds are between same atoms, but the ligands are at different coordination sites.

Forms of Constitutional Isomerism

Hydrate Isomerism

First, let us look more closely at hydrate isomerism. In hydrate isomerism, in one isomer a water ligand is in the first coordination sphere, and in the other isomer it is in the second coordination sphere. A water molecule in the second coordination sphere is only defined for the solid state, but not in solution. This is because in solution the water molecule would become part of the solvent. Here are a few examples for hydrate isomers.

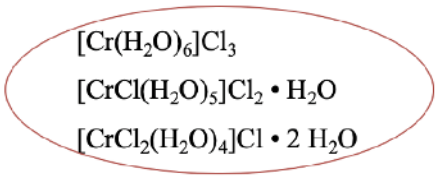


Figure 5.4.1 Two hydrate isomers of the complex $[Cr(H_2O)_6]Cl_3$

In the complex $[Cr(H_2O)_6]Cl_3$ there are six aqua ligands in the first coordination sphere (Fig. 5.4.1). In one hydrate isomer, there are only five water molecules in the first coordination sphere, the sixth one is in the second coordination sphere. One chloride anion has moved from the second to the first coordination sphere. There is a third hydrate isomer which has four aqua ligands in the first coordination sphere and two water molecules in the second coordination sphere. Two chloro ligands are now in the first coordination sphere, and one in the second coordination sphere. More hydrate isomers would be possible theoretically, but for some reason nature does not make them.

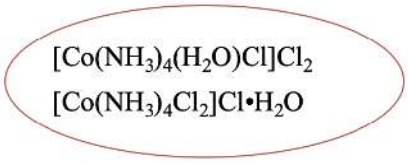


Figure 5.4.2 The hydrate isomers of the complex $[Co(NH_3)_4(H_2O)Cl]Cl_2$

Another example is $[Co(NH_3)_4(H_2O)Cl]Cl_2$. It has a hydrate isomer in which one aqua ligand has moved to the second coordination sphere, and one chloride anion has moved from the second to the first coordination sphere (Fig. 5.4.2).

Ionization Isomerism

A second form of isomerism is the ionization isomerism. In this case an ion moves from the first to the second coordination sphere and/or vice versa.

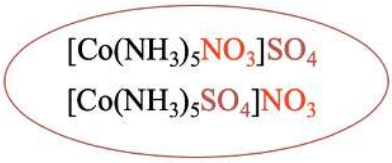


Figure 5.4.3 Two ionization isomers of the complex $[Co(NH_3)_5NO_3]SO_4$

For example, in the compound $[Co(NH_3)_5NO_3]SO_4$ there is a nitrate ion in the first coordination sphere, and a sulfate ion in the second coordination sphere (Fig. 5.4.3). There is an ionization isomer to this compound, in which the sulfate ion is now in the first coordination sphere, and the nitrate is in the second coordination sphere.

Coordination Isomerism

Another form of constitutional isomerism is coordination isomerism. In this isomerism, ligands are bound to different metal ions. Naturally, this implies that this form of isomerism can only exist if at least one isomer has two distinguishable metal ions.

For example, the compound $Pt(NH_3)_2Cl_2$ has two different coordination isomers. At first glance, they do not seem to be isomers at all. However, we can verify that they have the same empirical formula than the first compound (Fig. 5.4.4).

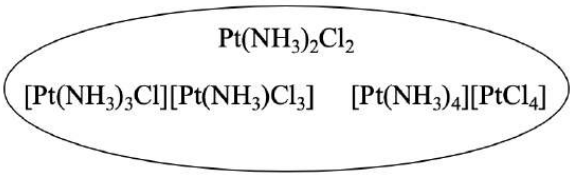


Figure 5.4.4 Two different coordination isomers for the complex $Pt(NH_3)_2Cl_2$

$[Pt(NH_3)_3Cl][Pt(NH_3)Cl_3]$ has two Pt atoms, four NH_3 units and four Cl atoms. That makes $Pt_2(NH_3)_4Cl_4$. This formula can be divided by 2 to to give $Pt(NH_3)_2Cl_2$. We can now easily see that the two compounds are isomers. The third isomer also has two Pt atoms, four NH_3 units, and four chloro atoms, so it must be an isomer as well.

Why are they coordination isomers? This is because in the first complex all ligands are bound to the same metal atom, whereas in the other two the ligands are bound to different metal atoms. In these compounds, one Pt atom belongs to a complex cation, and the other one to a complex anion. In the second isomer, three ammine ligands and one chloro ligand are bound to the first Pt atom, and one ammine and three chloro ligands are bound to the second Pt atom. In the third isomer, four ammine ligands are bound to the first platinum atom, and four chloro ligands belong to the second platinum atom.

Coordination isomerism is also possible for metal ions of different elements.

$$[Co(en)_3]Cr(CN)_6] \text{ and } [Cr(en)_3][Co(CN)_6]$$

Figure 5.4.5 Example of two coordination isomers with metal ions of different elements

In the example shown (Fig. 5.4.5), the first isomer has ethylenediamine bound to Co and cyanide bound to Cr, whereas in the second isomer ethylenediamine is bound to Cr and the cyano ligand is bound to Co.

$$[Pt(NH_3)]_4[PtCl_6] \text{ and } [Pt(NH_3)_4Cl_2][PtCl_4]$$

Pt(II) Pt(IV) Pt(IV) Pt(II)

Figure 5.4.6 Two coordination isomers with metal ions in different oxidation states (Oxidation states noted below each coordination sphere)

Further, in coordination isomers metal ions can be in different oxidation states. We can see that in the two depicted isomers there are complex cations, and complex anions with Pt in in different oxidation states (Fig. 5.4.6). In the first isomer Pt(II) makes the complex cation having four ammine ligands attached to it. Pt(IV) is part of the complex anion being surrounded by six chloro ligands. In the second isomer Pt(IV) forms the complex cation having four ammine and two chloro ligands in the first coordination sphere, and Pt(II) forms the complex anion having four chloro ligands.

Linkage isomerism

Linkage isomerism, also called ambidentate isomerism, is an isomerism that can be observed for ligands that have more than one reactive end. In two linkage isomers, the ligands will bind with different ends to the metal. Which end is reactive depends on the effective HOMO-LUMO interactions. Soft donor atoms tend to bind to soft metals, and hard donor atoms tend to bind to hard metals. Also the solvent can play a big role.

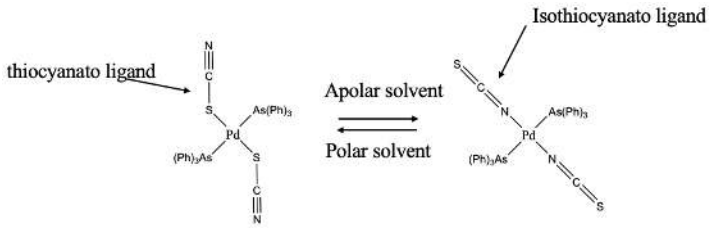


Figure 5.4.7 Two ambidentate isomers of thiocyanate

An example of an ambidentate ligand is the thiocyanate anion (Fig. 5.4.7). It can bind either with the sulfur or with the nitrogen end to a metal ion. When it binds with the S-end it is called the thiocyanato-ligand, when it binds with the N-end it is called the isothiocyanato ligand. Which atom binds to the metal can depend on the solvent. In the example shown, thiocyanate binds with S to Pd in polar solvents, but with N in apolar solvents. We could try to rationalize why. A possibility is that in polar solvents the more electronegative N atom can engage in hydrogen bonding which is not possible in apolar solvents. Steric arguments could also play a role. You can see that the triphenyl arsine ligands are fairly bulky. When the ligand binds with the nitrogen, then it binds in linear fashion avoiding steric interference with one of the arsine ligands. So it may be that in apolar solvents steric interactions dominate the behavior, while in polar solvents solvent-ligand interactions are in control.

It is even possible that two, same ambidentate ligands bind with opposite ends to the metal in one and the same molecule.

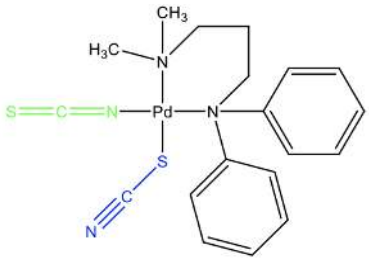


Figure 5.4.8 An example of two, same ambidentate ligands binding with opposite ends to the metal in one and the same molecule.

An example is the complex shown (Fig. 5.4.8). In this molecule, there is a thiocyanato and an isocyanato ligand binding to Pd. What arguments would we have to explain this ambidentate isomerism? Think about it for a moment. We can see that the two methyl groups are far less bulky than the two phenyl groups. When thiocyanate binds with the S-atom, then it can bend away from the two bulky phenyl groups. The second thiocyanate anion binds with the N atom because there is no significant interference between the methyl groups and the linear isothiocyanate ligand. This behavior indicates that thermodynamically, the Pd-N interaction is stronger, but only a little bit stronger because other factors such as steric interference can easily reverse the behavior.

Thio- and isothiocyanato ligands are not the only examples of ambidentate ligands.

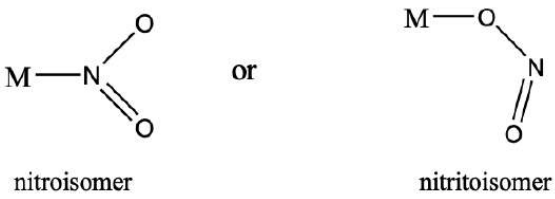


Figure 5.4.9 Two linkage isomers of the nitrite anion

Another example is the nitrite anion. It can either bind with the N- end or the O-end to a metal. In the first case it is called a nitroisomer, in the latter it is called a nitrito isomer (Fig. 5.4.9). Nitritoisomers are usually more stable.

Stereoisomers (Configuration Isomers)

Now let us discuss the second major type of isomerism: Stereisomerism. As mentioned previously, in stereoisomerism the bonds are between the same atoms, but the positions at which the ligands bind, the coordination sites, are different. There are two basic types of stereoisomerism: diastereomerism, and enantiomerism (Fig. 5.4.10).

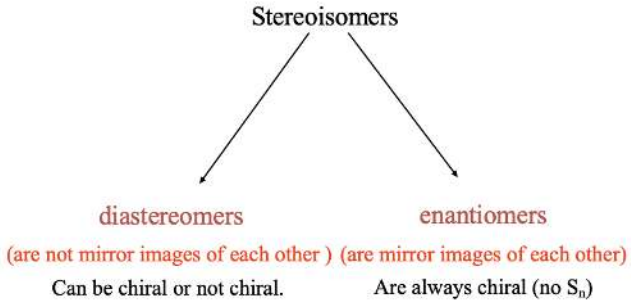


Figure 5.4.10 Types of stereoisomerism

In diastereomerism, the diastereomers are not mirror images to each other.

Definition: Diastereomers

Diastereomers are stereoisomers that are not mirror images of each other. They can be chiral or not chiral.

In enantiomerism, the enantiomers are mirror images to each others. Enantiomers are always chiral molecules.

Definition: Enantiomers

Stereoisomers that are mirror images of each other. They are always chiral.

Diastereomers can be chiral, but do not have to be chiral. Remember, a molecule is chiral when it does not have an improper rotational axis.

Example - Diastereomers and Enantiomers

Let us take an example from organic chemistry to illustrate the difference between enantiomerism and diastereomerism.

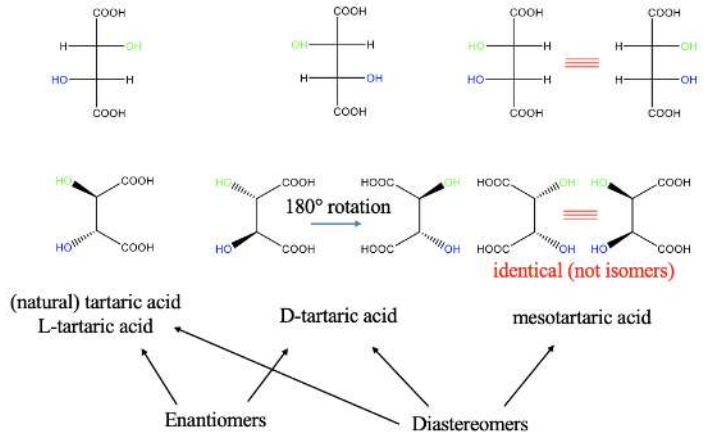


Figure 5.4.11 Example of diastereomers and enantiomers

Above (on the top left of Fig. 5.4.11) you see the Fischer projection an isomer of a compound called tartaric acid, it is called L-tartraric acid. The first OH group from the top points to the left, and the second one points to the right. This is the natural form of tartaric acid. The real structure of L-tartaric acid is depicted below (bottom left). You can see the the OH group that points to the right in the Fischer projection points toward us, while the other one, that points to the left in the Fischer projection, points away from us.

In the D-tartaric acid isomer, the first OH group in the Fischer projection points to the left, and the second one points to the right. For the real structure this means that the first OH-group points away from us, and the second one points toward us. These two isomers are mirror images to each other, and thus they are enantiomers. You may not immediately see in the real structure that the two are mirror images, but you can see it when you rotate the molecule around the C-C bond axis so that the carboxylic acid groups point to the the left (Fig. 5.4.11). Can you see it now?

There is a third isomer which is the so-called mesotartraric acid. We can draw its Fischer projection with both OH groups pointing to the right side (Fig. 5.4.11). In the real structure now both hydroxo groups point to the front. Is this molecule a mirror image of one of the two previous molecules? No, it is not! Therefore, it is a diasteromer relative to the other two. At first glance it seems that we can draw another molecule which is the mirror image of the mesotatraric acid. It would have two hydroxo groups pointing to the left in the Fischer projection, and two hydroxo groups pointing away from us in the real structure. However, the two molecules can be rotated so that they superimpose, and therefore they are not isomers, but identical molecules.

Cis-Trans Isomerism

Let us now discuss some common forms of stereoisomerism. The cis-trans isomerism is one very common stereoisomerism. It occurs when two, same ligands are in adjacent or opposite positions. For example, in a square planar complex two ligands can be adjacent or in opposite positions. When in adjacent position, the bond angle is 90° and we have a cis-isomer, when in opposite position, the bond angle is 180° and we have a trans-isomer.

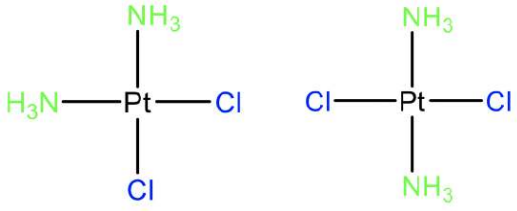


Figure 5.4.12 Cis-platinum and trans-platinum, respectively

The probably most well known example of a cis-isomer in coordination chemistry is cis-platinum which is an anti-cancer drug (Fig. 5.4.12). Its trans-isomers does not have these pharmaceutical properties showing that cis-trans isomerism can have a profound impact on the properties of a molecule. Overall cis-trans isomerism in Pt(II) complexes have been most intensely studied, but cis-trans isomerism is also known for other d^8 metal ions in square planar complexes. We can also ask if cis- and trans isomers are

diastereomers or enantiomers. Let us look at the example of cis- and trans-platinum to answer this question. Clearly, these two isomers are not mirror images to each other, so they must be diasteromers. Generally, cis- and trans- isomers are diastereomers.

Cis-trans isomerism extends beyond square planar complexes, and is also known for other shapes, for example, the trigonal bipyramidal shape, and the octahedral shape. In the cis-isomer of an octahedral complex two ligands occupy positions on the same face of the octahedron, whereas in the trans-isomer they occupy opposite position of the octahedron.

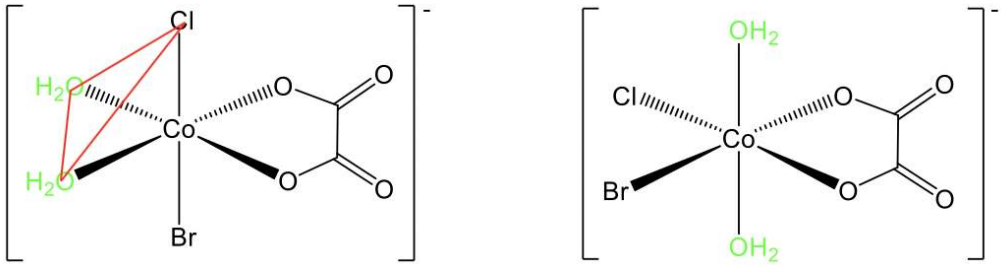


Figure 5.4.13 Cis and trans isomers of the diaquabromochlorooxalato cobalt(1-) complex, respectively

For example, in the complex diaquabromochlorooxalato cobalt(1-) there are cis and trans isomers known (Fig. 5.4.13). In the trans-isomer the two aqua-ligands stand in opposite position, and there is a 180° angle between them. In the cis-isomer they are in adjacent position, and the angle is 90°. We can see that the two ligands are on the same triangular face of the octahedron, shown in red.

Are there rules that can help us to decide if a cis- or a trans- complex will form? As you might suspect, the largest ligands usually go in trans-position due to steric repulsion arguments. Bidentate ligands usually form the cis-isomer because bidentate ligands are usually designed to make five- or six-membered rings with the metal ion. Are cis-trans isomers chiral? If the ligands are simple, then they are usually not, but if they are more complicated, then they can be. In this context it needs to be said that ideal structures are rarely observed. For example, a square planar complex is rarely an ideal square plane e.g. because the bond angles may be somewhat distorted from the 90° angle due to the fact that the ligands have unequal steric requirements. A slight distortion actually can remove one or many symmetry elements, leading to chirality, however, such small deviations are usually ignored.

Fac-mer Isomerism

Another common type of stereoisomerism in coordination chemistry is fac-mer isomerism. Fac stands for facial and mer stands for meridional. In a fac-isomer the same ligands are on a common face of a polyhedral complex, in the mer isomer they are on a plane that bisects the polyhedron. This kind of isomerism is very common for octahedral complexes, but not restricted to those.

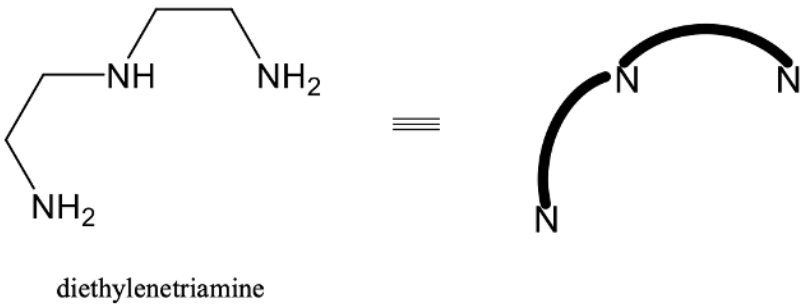


Figure 5.4.14 Fac- (left) and mer-isomers (right) of the triammine trichloro cobalt(III) complex.

For example the complex triammine trichloro cobalt(III) has a fac- and a mer-isomer. You can see that in the fac-isomer the identical ligands are on two opposite triangular faces of the octahedron. In the mer-isomers they lie on two planes that bisect the octahedron. We can again ask if they are diastereomers or enantiomers? The answer is: They are not mirror images to each other, so they are not enantiomers, but diastereomers.

Fac-mer Isomerism with Tridentate Ligands

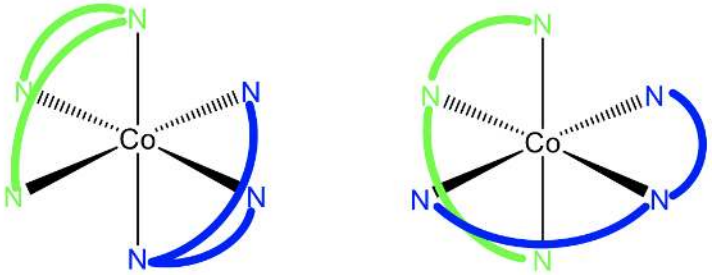
Fac-mer isomerism is also common for octahedral complexes with tridentate ligands, for example the ligand diethylenetriamine (Fig. 5.4.15).



diethylenetriamine

Figure 5.4.15 Diethylenetriamine

In this ligand two NH_2 groups and one NH group are interconnected by two ethylene units. For clarity reasons, in complexes with this ligand, often only the N donor atom of the NH_2 and NH groups is depicted, and the ethylene diammine units are simplified as bent lines interconnecting the N-atoms. We will use this simplification in the following (Fig. 5.4.16).



fac-isomer mer-isomer

Figure 5.4.16 Fac-mer isomers of the bis(diethylenetriamine) cobalt complex.

Here is an example of bis(diethylenetriamine) cobalt complexes that are fac-mer isomers (Fig. 5.4.16). One ethylenediamine ligand is shown in green, the other one is shown in blue. You can see that the left isomer is the fac-isomer with all three donor atoms of a ligand placed on the same face of the octahedron. On the right side is the mer-isomer, with all donor atoms of the same ligand placed on planes that bisect the octahedron. Also in this case the two isomers are not mirror images and are diasteromers to each other.

Triethylenetetramine Complexes

There is isomerism similar to fac-mer isomerism in octahedral complexes with the tetradentate ligand triethylenetetramine (Fig. 5.4.17).

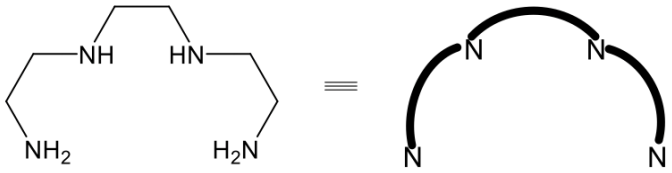


Figure 5.4.17 Triethylenetetramine

In this ligand, two NH and two NH_2 groups are bridged by four ethylene groups. We can again depict the ligand in a simplified way by just showing the N donor atoms, and by simplification of the ethylene groups as bent lines.

One possibility to realize an octahedral complex with triethylenetetraamine ligands is to orient all three rings in the same plane, we can also say we have an octahedral complex with three coplanar rings. This is shown below (Fig.5.4.18).

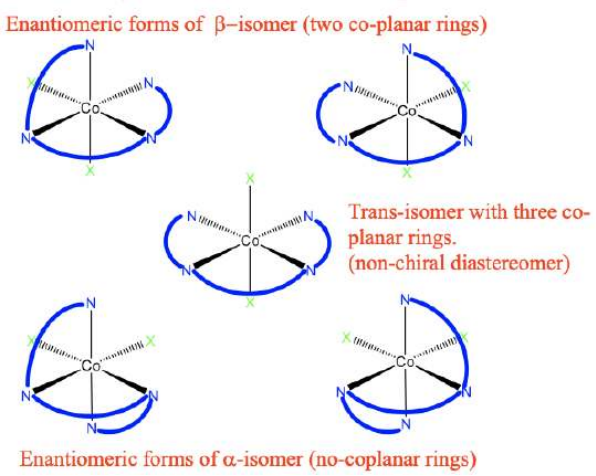


Figure 5.4.18 Octahedral complex with triethylenetertraamine ligands

The three ethylenediamine units make three five-membered rings which are co-planar to each other. The N-atoms occupy overall four vertices of the octahedron. There are two other generic ligands X located at to opposite vertices of the octahedron. Therefore, this isomer is called the trans-isomer.

We can ask if this molecule is chiral? The answer is no, because there is a mirror plane which is co-planar with the three five-membered rings. In addition to this trans-isomer, there are also two cis-isomers, one is called the α-isomer, the other one is called the β-isomer. In the β-isomer, there are now only two co-planar rings, the third one is now out of plane. The two ligands X are in cis-position relative to each other. Is the trans-isomer a diastereomer or enantiomer to the β -isomer? They are clearly not mirror images to each other, therefore they must be diasteromers. Is this β-isomer chiral? Yes, it is! There is no improper rotational axis. Therefore, an enantiomer must exist, and this enantiomer must be a mirror image of the β-form. Here it is! Naturally, it must also have two co-planar rings, and two ligands X in cis-position. It is therefore also considered a β-isomer.

Now let us discuss the α-isomerism. In an α-isomer no two ligands are co-planar any more. This isomer is a diasteromer to the trans- and the β-form because the isomers are not mirror images. Also the α-isomer is chiral. Therefore, there must be another α-isomer which is the mirror image to the first α-isomer. It is shown in the bottom right of **Figure 5.4.18**.

Nomenclature for Propeller Complexes

Complexes with two or more non-coplanar rings that are non-adjacent are always chiral and are called “propeller complexes”. There is a special nomenclature for propeller complexes that we will briefly discuss in the following.

Let us first understand why these complexes are propeller complexes? They are called like that because the non-coplanar rings are oriented relative to each other similarly to propeller blades. A propeller must have at least two blades, but can also have more than that. We distinguish between so-called left handed propellers and right-handed propellers. A left-handed propeller has the property to move away from you in a medium like air or water when rotated counter-clockwise.

Definition: Left-Handed Propeller

Counterclockwise rotation moves a left-handed propeller away

A right handed propeller moves away from you when rotated clock-wise.

Definition: Right-Handed Propeller

Clockwise rotation moves a right-handed propeller away

The tip of one blade of a left-handed propeller describes a left-handed helix as it moves away, the tip of a blade of a right-handed propeller describes are right-handed helix as it moves away.

Determining the Handedness of "Propeller Compexes"

How can we determine the handedness of a propeller molecule? Let us determine it using the example of the tris(oxalato) ferrate(III) anion. Fig. 5.4.19.

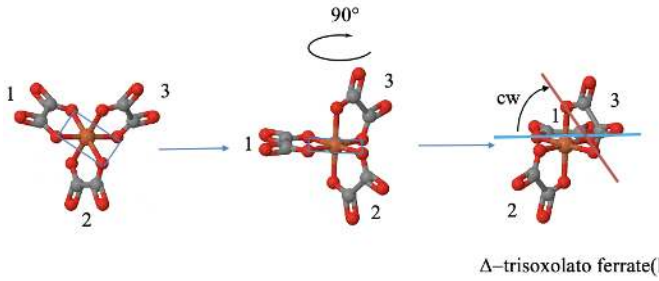


Figure 5.4.19 The tris(oxalato) ferrate(III) anion. The molecule is rotated in two steps so that ring 1 is oriented horizontally, and points to the back. The horizontal blue line needs to be rotated counter-clockwise to make it parallel to the brown line.

It is a three-bladed propeller molecule because it has three five-membered rings between the three oxolato ligands and the iron center. Each ring is considered a blade. None of the rings are co-planar and none of them are adjacent, meaning that the rings do not share a donor atom.

In order to determine the handedness, we can first rotate the molecule so that one of the rings is oriented horizontally and points to the back. Unless we have a three-dimensional model, we need to do this in our mind. Once that is accomplished we can draw a horizontal line between the two donor atoms of that ring. Next we can draw a line between two donor atoms of another ring. If necessary, we extend the line so that the line crosses the horizontal line. Next, we determine the smallest angle between the two lines, and rotate the horizontal line until it becomes parallel to the other line. We can do this just in our mind. If we need to rotate anti-clockwise, the propeller is considered left-handed, we call it a Λ -isomer. If we need to rotate clock-wise, the the propeller is right-handed, we call it Δ-isomer.

Determining Handedness for Propeller Molecules Requiring More Than One Label

In some cases coordination compounds have multiple non-adjacent, non-coplanar ring combinations, and the handedness must be determined for each combination. Examples are octahedral EDTA complexes.

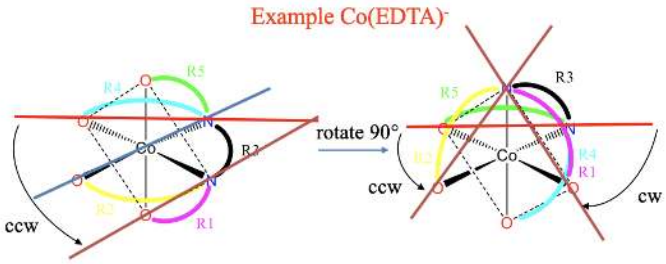


Figure 5.4.20 An octahedral EDTA Co complex. Rotation around the blue line moves the green ring into horizontal position, pointing to the back.

In those complexes there are overall five different rings which we can label R1 to R5. You can see the different rings in different colors (Fig. 5.4.20) For clarity we have abbreviated the linkers between the donor atoms by bent lines in different colors. Each color represents a different linker making a different ring.

We realize that ring R3 is shared with all other rings, therefore it is adjacent to all other rings and does not need to be considered. R1 is adjacent to R2, and R3, but not adjacent and not co-planar with R4 and R5. Therefore we need to consider the R1-R4 and R1-R5 combinations. Further, R2 is coplanar with R3 and R4, and adjacent to R3, but is not coplanar and not adjacent to R5. Therefore, we need to consider the R2-R5 combination as well. R4 and R5 are adjacent, so we do not need to consider this combination. We have found all combinations we need.

We now need to rotate the complex so that one relevant ring is oriented horizontally and points to the back. We can for example choose the ring R4. Luckily, is already correctly oriented. Next, we can connect the donor atoms of the ring R4 to produce a

horizontal line. Now let us draw a line between the donor atoms of the ring R1. We see that we need to rotate the horizontal line counter-clockwise to make it parallel to this line, thus the R1-R4 ring combination is a **Λ**-configuration.

We can next determine the R1-R5 handedness by first reorienting the molecule so that R5 points to the back. R1 could also be chosen. However, R5 is part of two relevant ring combinations, and so we can kill two birds with one stone if we choose R5. We can move ring R5 to the back by rotating 90° counter-clockwise around the blue axis shown in Fig. 5.4.20. It goes through an O atom, the cobalt atom, and an N atom. This axis stands perpendicular to the square indicated by dotted lines. The square has four donor atoms on the four vertices, and these donor atoms move 90° counter-clockwise as the rotation is carried out. The orientation of the rings follow the movement of the donor atoms. The O-donor atom of the ring R5 moves so that R5 is now horizontal, and points to the back. Next we can interconnect the donor atoms of R5, and the donor atoms of R1 by lines. We can see that the horizontal line must be rotated clockwise so that it becomes parallel with the other one. Therefore, the R1-R5 configuration is a **Δ**-configuration.

For the determination of the combination R2-R5 the complex does not need to be reoriented again. We can directly draw a line through the donor atoms of R2, and determine the direction of rotation. This time we need to rotate counter-clockwise again, meaning the R2-R5 combination is in **Λ**-configuration.

Overall, we have a ΛΔΛ-(ethylenediamine tetracetato)cobaltate(III). Note that the order of designation is arbitrary, we could have named the molecule a ΛΛΔ-complex or a ΔΛΛ-complex also.

Exercise

Let us practice this by one more example.

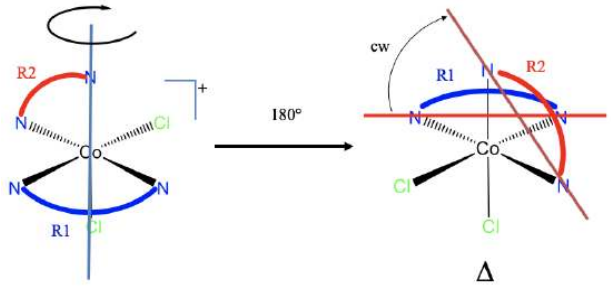


Figure 5.4.21 Example to determine handedness

What is the handedness of the complex shown? First of all: Does it meet the criteria for a propeller complex? The answer is yes. There are two rings, R1 and R2, and they are both not coplanar, and non-adjacent.

To determine handedness we need to first move the molecule so that one ring is oriented horizontally and points to the back. We could choose any of them, but it seems easier to rotate the ring R1 that points to the front and is oriented horizontally by 180° around an axis that is defined by one N and on Cl atom (shown in blue in Fig. 5.4.21)), and is oriented vertically. This rotation moves one of the donor atoms of the other ring by 180°, which defines the new orientation of the ring. Now we can draw a horizontal line through the donor atom of ring 1, and a line through the donor atoms of ring R2. We can see that we must rotate clock-wise, and the propeller complex is right-handed.

Ring Conformations

In addition to isomerism, also conformism has an influence on the structure of a coordination compound. There may be two or more conformers possible for a particular isomer. As an example, let us consider a ring between a metal ion and an ethylenediamine ligand (Fig. 5.4.22).

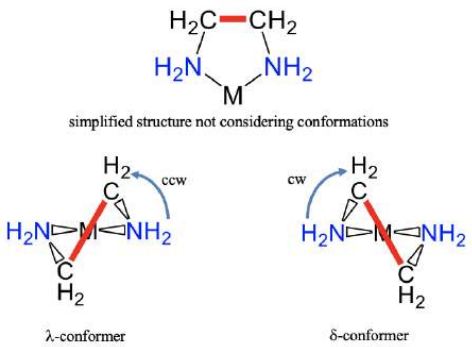


Figure 5.4.22 Ring structure between a metal ion and an ethylene diamine ligand

In contrast to simplified depictions often used, it is not planar, because of the sp^3-hybridization of the carbon and nitrogen atoms. There are two different conformations possible that differ in the orientation of the C-C bond within the ring. They are shown above (Fig. 5.4.22). In the conformation shown left we must rotate a thought horizontal line going through the two nitrogen donor atoms counterclockwise so that it becomes parallel to the C-C bond. For the other conformer, we need to rotate the thought horizontal line clockwise. We call the first conformer the **λ**-conformer, and the second one the **δ**-conformer. In this case we use lower case letters to indicate conformerism and not isomerism.

Dr. Kai Landskron (Lehigh University). If you like this textbook, please consider to make a donation to support the author's research at Lehigh University: Click Here to Donate.

This page titled 5.4: Isomerism is shared under a not declared license and was authored, remixed, and/or curated by Kai Landskron.

- **5.4: Isomerism** by Kai Landskron is licensed CC BY 4.0.

5.5: Concept Review Questions Chapter 5

Chapter 5

Section 1 & Section 2

1. Explain how the name “chelate” ligand originates.

Section 3

1. What are the main factors determining coordination numbers?

2. Is the coordination number 1 common? Explain.

3. For which electron configuration are the coordination numbers 2 and 3 common?

4. What is the structure of methyl lithium?

5. What electron configuration is common for square planar shapes?

6. What is the most common shape for the coordination number 4?

7. Which are the most common shapes for the coordination number 5?

8. What is the Berry pseudo rotation? Describe its mechanism.

9. What are the most common shapes of coordination compounds with the coordination number 7? What are the point groups associated with these shapes.

10. Explain briefly, why molecular coordination compounds with cubic shapes are not known, while square anti-prisms are relatively common.

11. Explain why coordination compounds with high coordination numbers (7 and larger) are not very common.

12. Name an example of a coordination compound with the coordination number 9.

Section 4

1. What is the difference between a constitutional isomer and a stereoisomer.

2. Name four types of constitutional isomerism.

3. What is the definition of hydrate isomerism?

4. Why is hydrate isomerism only possible in solid state?

5. What is the definition of ionization isomerism?

6. What is the definition of coordination isomerism?

7. What is the definition of linkage (ambidentate) isomerism?

8. What is the difference between a diasteromer and an enantiomer?

9. What is the definition of cis-trans isomerism?

10. What is the definition of fac-mer isomerism?

11. What is the definition of a propeller complex?

12. What is the definition of a left-handed/right-handed propeller?

Dr. Kai Landskron (Lehigh University). If you like this textbook, please consider to make a donation to support the author's research at Lehigh University: Click Here to Donate.

5.5: Concept Review Questions Chapter 5 is shared under a not declared license and was authored, remixed, and/or curated by LibreTexts.

- **Concept Review Questions Chapter 5** by Kai Landskron is licensed CC BY 4.0.

5.6: Homework Problems Chapter 5

Homework Problems

Exercise 1

Name the following compounds:

a. $[(NH_3)_5Cr\text{-}O\text{-}Cr(NH_3)_5]^{4+}$
b. $Na[Fe(NH_3)_3Cl_3]$
c. $VOCl_3$
d. Na_2PdCl_4
e. $[Ni(NH_3)_3(NMe_3)](PF_6)_2$

Answer

a) μ-oxo bis(pentaamminechromium (III)) (or 4+)

b) sodium triammine trichloroferrate (II) (or (1-))

c) trichlorooxo vandadium(V) (or (0))

d) sodium tetrachloropalladate (II) (or (2-))

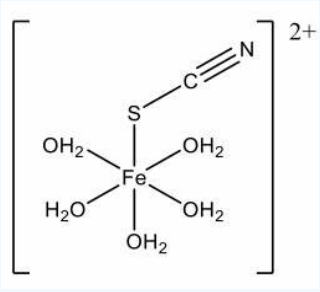
e) triammine (trimethylamine) nickel (II) hexafluorophosphate or triammine (trimethylamine) nickel (2+) hexafluorophosphate

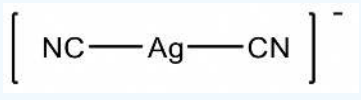
Exercise 2

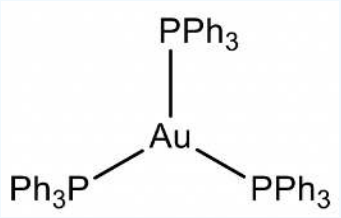
Write a plausible structural formula for

a. pentaaquathiocyanatoiron(III).
b. dicyanoargentate (I)
c. Tris(triphenylphosphine)gold(I)

Answer

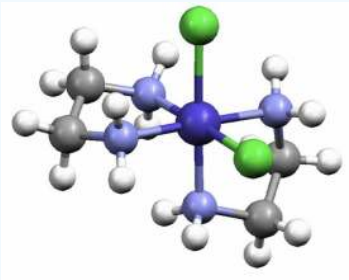
a) 

b) 

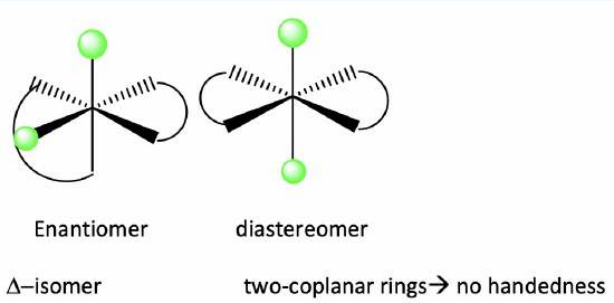
c) 

Exercise 3

What other stereoisomers can you draw for the complexes depicted below. Are they diasteromers or enantiomers? Determine the handedness of all isomers.

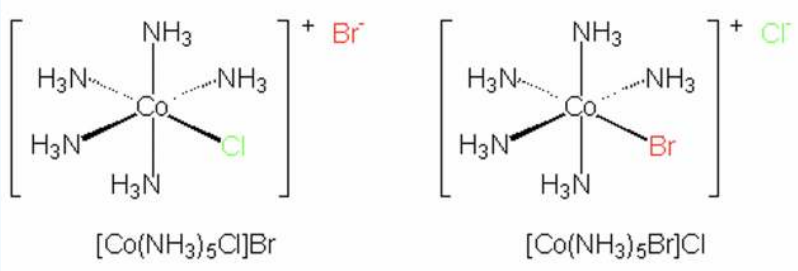


Answer



Exercise 4

What type of isomerism is present between the following molecules:



Answer

Ionization isomerism

Exercise 5

How many hydrate isomers are theoretically possible for $[Al(H_2O)_6]Cl_3$. Write down their formulas.

Answer

$[Al(H_2O)_5Cl]Cl_2 \times H_2O$

$[Al(H_2O)_4Cl_2]Cl \times 2\ H_2O$

$[Al(H_2O)_3Cl_3] \times 3\ H_2O$

Exercise 6

What isomerisms do you see between the following two compounds:

$[M(H_2O)_4Cl_2]Br_2$ and $[M(H_2O)_3ClBr_2]Cl$ x H_2O.

Answer

Hydrate isomerism and ionization isomerism

Exercise 7

What distortions are common for the octahedral shape?

Answer

Tetragonal and trigonal distortions

Exercise 8

Which coordination number and shape would you most likely expect for a complex between Ag^+ and $S_2O_3^{2-}$?

Answer

CN = 2, linear shape.

Exercise 9

Which of the following complexes are most likely square planar:

a. $AuCl_4^-$
b. $ZnCl_4^{2-}$
c. $TiCl_4$
d. $FeCl_4^{2-}$

Answer

a) $AuCl_4^-$

Dr. Kai Landskron (Lehigh University). If you like this textbook, please consider to make a donation to support the author's research at Lehigh University: Click Here to Donate.

5.6: Homework Problems Chapter 5 is shared under a not declared license and was authored, remixed, and/or curated by LibreTexts.

- **Homework Problems Chapter 5** by Kai Landskron is licensed CC BY 4.0.

CHAPTER OVERVIEW

6: Coordination Chemistry III - Bonding

6.1: 7.1 Bonding in Coordination Compounds

6.2: Concept Review Questions Chapter 7

6.3: Homework Problems Chapter 7

This page titled 6: Coordination Chemistry III - Bonding is shared under a not declared license and was authored, remixed, and/or curated by Kai Landskron.

6.1: 7.1 Bonding in Coordination Compounds

Bonding in Coordination Compounds

This chapter is devoted to bonding theories for coordination compounds. Let us first think about, what a good theory should be able to do in general. The answer is, that it should be able to make many correct explanations for experimental observations based on a few, sensible, assumptions. In addition, it should be able to predict experimental observations. The more the theory can explain and predict, and the fewer the necessary assumptions, the better the theory. What does this mean for a bonding theory? What would a good bonding theory for coordination compounds be able to do? It should certainly be able to explain and predict the number of bonds and the shape of a molecule. In addition, it should be able to explain the magnetism of molecules, in particular dia- and paramagnetism. Remember, a molecule is diamagnetic when it has no unpaired electrons. It is paramagnetic when there are unpaired electrons. A diamagnetic molecule is repelled by an external magnetic field. A paramagnetic molecule is attracted by an external magnetic field. It should further be able to explain the stability and reactivity of complexes, as well as the optical properties of complexes. Optical properties of compounds are linked to bonding because they are related to electronic states.

Valence Bond Theory

There are essentially three bonding concepts that are used to describe the bonding in coordination compounds. The first one is the valence bond theory. The valence bond concept was introduced by Linus Pauling in 1931 to explain covalent bonding in molecules of main group elements.

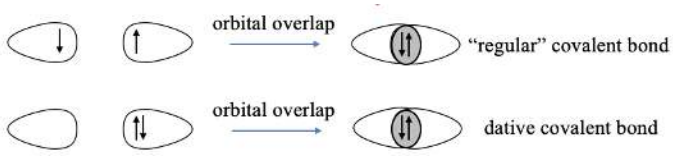


Figure 7.1.1 Electron sharing and valence bond theory

The basic idea is to overlap half-filled valence orbitals to form covalent bonds in which the two electrons are shared between the bonding partners (Fig. 7.1.1). These orbitals can either be atomic orbitals, or hybridized atomic orbitals. The concept works very well to explain the shapes of molecules of main group elements. The valence bond concept in its original form assumes that each bonding partner contributes one electron to the covalent bond. This is not consistent with the dative bonding in coordination compounds where it is assumed that one partner donates an electron pair and the other partner accepts it. To adapt valence bond theory to suit coordination compounds, Pauling suggested that a dative bond is formed via the overlap of a full valence orbital of the donor and an empty valence orbital of the acceptor. We will see that this concept can explain the shapes of coordination compounds in some cases, but overall it does not work very well. We will also see that valence bond theory can explain magnetism in some cases, but also here the valence bond theory has significant deficits. By its nature, valence bond theory cannot explain optical properties. Overall, valence bond theory is far more suitable for main group element molecules compared to transition metal complexes.

Crystal Field Theory

The second major theory is the crystal field theory. It is actually not a bonding theory because it is based on repulsive electrostatic interactions. It was originally developed to explain color in ionic crystals. Later, it was found that it can also explain colors in molecular coordination compounds, and is suitable to explain shapes and magnetism of complexes. However, because it is based on repulsive electrostatic interactions it cannot actually explain what holds the atoms in a molecule together. However, the crystal field theory is quite simple and convenient to use, and there is a lot of practicality to it.

Ligand Field Theory

The third theory is the ligand field theory. It is the most powerful theory, but also the most complicated one. Basically, it is molecular orbital theory applied to coordination compounds. It can make detailed statements about the number of bonds and shapes of molecules, and can explain the magnetism and optical properties of coordination compounds.

Valence Bond Theory for Coordination Compounds

Octahedral Complexes

Let us have a closer look at the valence bond theory, and assess valence bond theory for complexes by a number of examples.

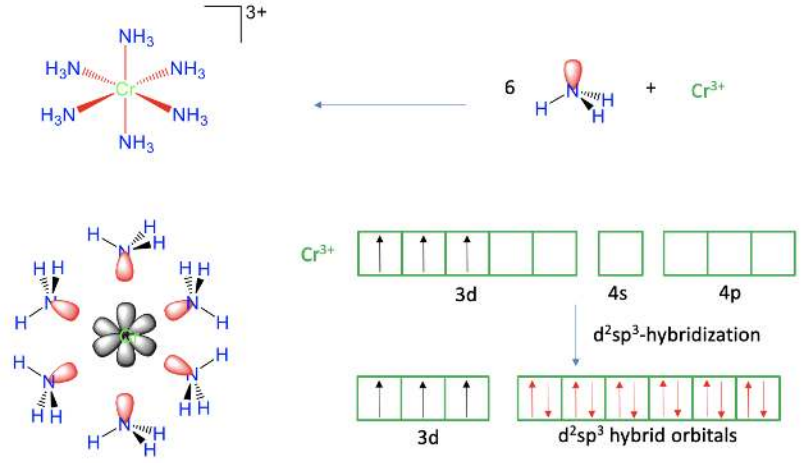


Figure 7.1.2 Valence bond theory applied to the hexaammine chromium (3+) cation

The first example is the hexaammine chromium (3+) cation (Fig. 7.1.2). From experiment we know that it has an octahedral shape, with six dative Cr-N bonds. Can valence bond theory explain the six bonds and the octahedral shape satisfactorily? In order to explain the six dative Cr-N bonds we would need to overlap six empty chromium valence orbitals with six filled valence orbitals of N. We can see that the six ammine ligands have one electron lone pair each that can serve as the valence orbitals. Does chromium have six empty valence orbitals? In order to assess this, we first need to know the oxidation state of the chromium. It is +3 because the ligands are all neutral when the bonds are cleaved heteroleptically, and the complex cation has a 3+ charge. Therefore, the chromium is a Cr^{3+} cation.

Next, we need to know the electron configuration of the Cr^{3+}. A neutral Cr atom has the electron configuration $4s^1 3d^5$. When a transition metal loses electrons to form a cation, it always loses its two valence electrons first, and then its d electrons. For chromium this means that we must remove the one 4s electron, and two of the five 3d-electrons. The three remaining 3d electrons are expected to be spin up in three different d orbitals according to Hund's rule. How many empty valence orbitals remain? These would be two 3d and the 4s orbitals. In addition, it would also be justified to consider the three 4p orbitals as valence orbitals because the 4p orbitals are energetically only slightly higher than the 4s orbital. That means that we would have the six valence orbitals that we would need to explain the six bonds. There is, however, a complication. The six bonds in the complex are not distinguishable, but the six valance orbitals in the Cr^{3+} ion are distinguishable, for example, the 3d orbitals have different shape and energy than the 4s orbital, which is different from the 4p orbitals. Therefore, if we overlapped these orbitals with the electron lone pairs at N, the bonds would not be equivalent, or indistinguishable. We would have difficulty to explain the highly symmetric octahedral shape of the molecule. To go around this issue, valence bond theory uses the concept of hybridization. In this concept we mathematically mix the wave functions of the valence orbitals to form hybridized orbitals. In our example we would mix the two empty d-orbitals, the 4s orbital, and the three 4p orbitals to form six so-called d^2sp^3 hybridized orbitals. They have the same shape and size, and their lobes point toward the corners of an octahedron. Therefore, we can now create overlap between these six orbitals, and the six electron lone pairs at N to form six equivalent, indistinguishable Cr-N bonds. We conclude that we have now satisfactorily explained the bonding and the shape of the complex.

Can we also explain its magnetism? From experiment we know that the complex is paramagnetic, and that there are three unpaired electrons. Does valence bond theory predict the same? Yes, it does. There are three unpaired electrons in the three half-filled d-orbitals.

Tetrahedral Complexes

Our next is example is a tetrahedral complex, the tetrahydroxo zincate (2-) complex anion, Fig. 7.1.3.

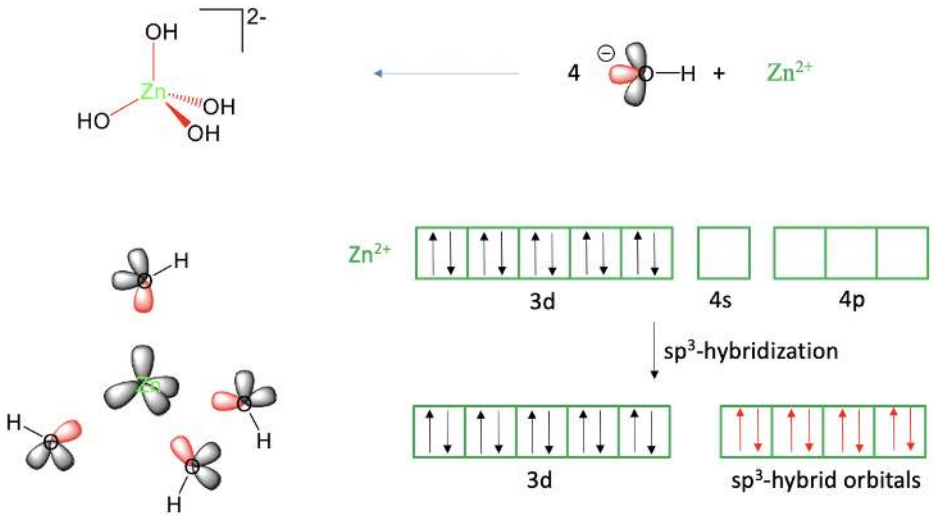


Figure 7.1.3 Valence bond theory applied to the tetrahydroxo zincate (2-) complex.

When viewing it as a Lewis-acid base complex with dative bonds it can be thought as an adduct of a Zn^{2+} and four hydroxide anions. One of the three electron lone pairs at the hydroxide ions would donate its electrons into empty Zn valence orbitals. That means we would need overall four empty Zn valence orbitals to explain the four Zn-O bonds. A neutral zinc atom has the electron configuration $4s^2\ 3d^{10}$. We can derive this from the fact that zinc is in group 12 of period 4 in the periodic table. A Zn^{2+} ion has two electrons less. Because we must remove s electrons before we remove d electrons, the Zn^{2+} has the electron configuration $3d^{10}$. Like in the previous example we can justifiably consider the 4p orbitals as additional valence orbitals. We can see that we have four empty orbitals available to make the four bonds, namely the 4s and the 4p orbitals, but these orbitals are not equivalent, and do not have the correct orientation to explain the tetrahedral shape of the complex. There is a 90° angle between the p-orbitals which is smaller than the 109.5° tetrahedral bond angle in the molecule. However, we can solve this problem by hybridizing the 4s and the three 4p orbitals to form four sp^3-hybridized orbitals. These hybrid orbitals have the property that their lobes point toward the corners of a tetrahedron. Thus, they are suitable to explain the tetrahedral shape of the molecule. We can place the ligands around the Zn^{2+} ion and approach the ligands on the bond axes to create orbital overlap between the empty sp^3-hybridized orbitals and one electron lone pair at the oxygen atom. This produces the tetrahedral tetrahydroxo zincate (2-) anion.

Can we also explain the magnetism of the molecule? What magnetism would valence bond theory predict? We can see that there are no unpaired electrons in any of the metal valence orbitals. Thus, the complex should be diamagnetic. This is also what we find experimentally. Thus, valence bond theory is able to explain the magnetism of this complex anion.

Square Planar Complex

Now let us see if the valence bond theory can also explain a square planar complex such as tetracyanonickelate (2-).

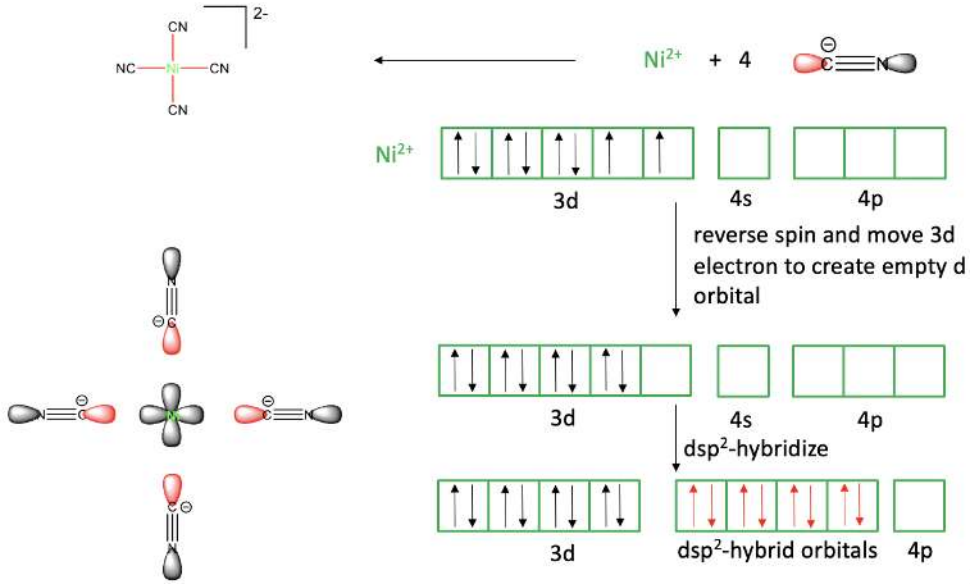


Figure 7.1.4 Valence bond theory applied to the tetracyanonickelate (2-) square planar complex

In the valence bond picture we view the Ni-CN bonds as dative bonds, and the complex is considered an adduct of Ni^{2+} and CN^-. To explain the four bonds, the Ni^{2+} ion would need to have four empty valence orbitals. Ni is a group 10 metal and a neutral Ni atom has the electron configuration $4s^2 3d^8$. To create a Ni^{2+} ion we must remove the two 4s electrons, and thus the Ni^{2+} has the electron configuration $3d^8$. Do we have four empty orbitals available? Yes, the 4s and the three 4p orbitals are empty but again they are not equivalent and thus not suitable to explain four equivalent Ni-C bonds. Can we hybridize these orbitals? Yes, we can, but the resulting four sp^3 hybridized orbitals would not be suitable to explain the square planar shape, only the tetrahedral shape. What valence bond theory suggests in this case is to reverse the spin of one of the unpaired d electrons and move it into the other half-filled d-orbital. This produces an empty d-orbital that we can now hybridize with the 4s and two of the 2p orbitals to four dsp^2-hybridized orbitals. These four orbitals have the property that their lobes point toward the vertices of a square, thus they are suitable to explain the square-planar shape. We can approach the ligands now on the bond axes to create orbital overlap between the empty dsp^2 Ni and the electron lone pairs of the ligands. We can also say that the ligands donate their electron lone pairs into the hybridized metal orbitals. This produces the four covalent bonds that we need and yields a molecule of a square planar shape.

We can see that the valence bond theory can still explain the square planar shape, but only with the help of the additional assumption that one of the d-electrons gets spin-reversed and moves into another d-orbital. An assumption a theory makes should always be reasonable, so let us critique how reasonable this assumption is. Firstly, is the spin-reversal reasonable? Spin-reversal is a quantum-mechanically forbidden process, and thus it is questionable to assume that it happens. Secondly, there is no good explanation for why the electron moves. The energy of two spin-paired electrons in the same orbital is actually higher than that of two spin-paired electrons in different orbitals. So overall, we see that valence bond theory has difficulties to explain the square planar shape. It must make assumptions that are not very plausible.

Octahedral d^5 High and Low Spin Orbital Complex

The valence bond theory has also difficulties to explain so-called high spin and low spin octahedral complexes. For example, it is known from magnetic measurements for $3d^5$ transition metal ions that they can make octahedral complexes with either one unpaired electron or five unpaired electrons, depending on the ligand. In the first case, the number of paired electrons in the d-orbitals is maximized, and we have a low-spin complex, in the other case the number of unpaired electrons is maximized, and we have a high spin complex. What approach does valence bond theory take to explain this phenomenon?

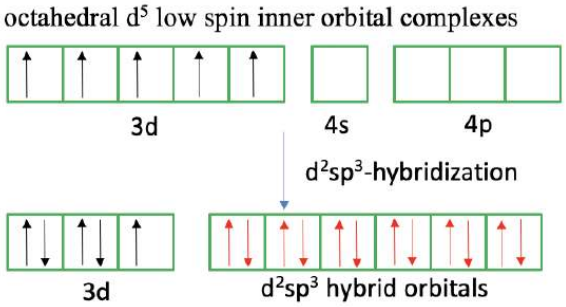


Figure 7.1.5 Valence bond theory applied to an octahedral d^5 low spin-complex

In the case of a low spin-complex, valence bond theory assumes a so-called inner orbital complex. Like in the square planar complex it is assumed that unpaired electrons reverse their spins and move into other half-filled d-orbitals so that spin-pairing is maximized. In the case of a d^5 ion, two electrons reverse their spin, and move into two other half-filled orbitals. This leaves one unpaired electron. We see that due to the movement of the two electrons two 3d-orbitals are empty now, and so are the 4s and the 4p orbitals. The six empty orbitals can now be combined to form d^2sp^3-hybridized orbitals that can explain the octahedral shapes. Approaching the ligands overlaps the electron lone pair at the ligand with the empty hybrid orbitals to form a dative, covalent bond. We can also say the ligands donate electron lone pairs to form six covalent bonds. We can again criticize that spin-reversal is forbidden and spin-pairing is energetically unfavorable making the approach valence bond theory takes to explain the low-spin complex unsatisfactory.

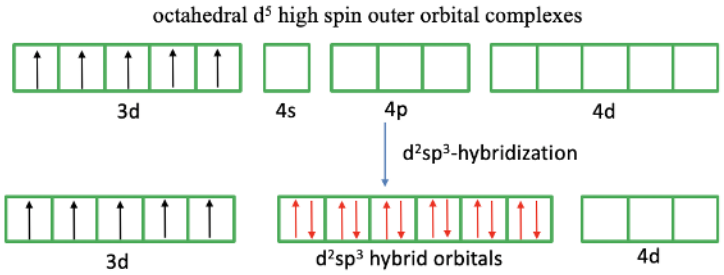


Figure 7.1.6 Valence bond theory applied to an octahedral d^5 high spin-complex

What about the $3d^5$ high spin complex (Fig. 7.1.6)? In this case we cannot pair spins to create empty d-orbitals because we need to explain five unpaired electrons. Now, valence bond theory makes another new assumption. It assumes that the outer 4d orbitals get involved in the bonding. These orbitals are empty and available for hybridization. We can therefore hybridize two 4d, the 4s, and the three 4p orbitals to form d^2sp^3 hybridized orbitals. In the last step we can approach the ligands, and the ligands can donate their electron lone pairs into the transition metal d-orbitals. Now we have explained the six bonds, the octahedral shape, and the five unpaired electrons.

We can again critique the valence bond approach. What justification is there to assume that the 4d orbitals are involved. The answer is: Very little. These orbitals are just too high in energy to be considered valence orbitals. It is not reasonable to assume that they are involved in the bonding. Therefore, again, we see that valence bond theory has difficulties to explain the properties of a complex. Valence bond theory also does not explain distortions of octahedral complexes due to the Jahn-Teller effect.

Octahedral d^7 High and Low Spin Orbital Complex

High-spin and low-spin complexes are not only observed for octahedral complexes of d^5-ions, but for example also for octahedral d^7 ion complexes. A low-spin complex has three unpaired electrons and a high-spin complex has one unpaired electron. We will see that valence bond theory has even greater troubles to explain these compounds.

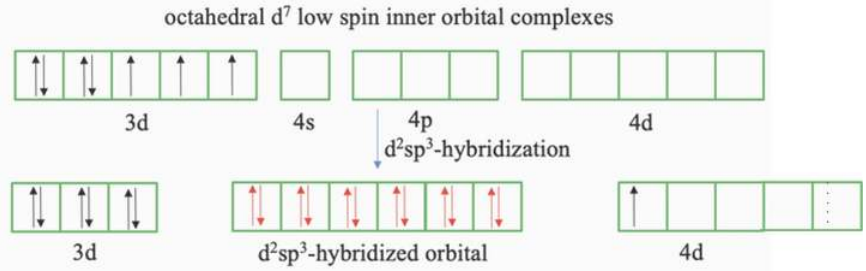


Figure 7.1.7 Valence bond theory applied to an octahedral d^7 low spin-complex

In a d^7 ion there are four paired and three unpaired electrons according to Hund's rule (Fig. 7.1.7). We can reverse the spin of one unpaired electron and pair it with an unpaired electron in another half-filled orbital to reduce the number of unpaired electrons to one. However, this gives us only one empty 3d orbital available for d^2sp^3-hybridization. In this case we cannot produce more empty 3d-orbitals by reversing the spin. Therefore, we must make again the questionable assumption that outer orbitals are involved in the bonding such as the 4d orbitals. Valence bond theory now suggests to move the unpaired electron from the 3d to the 4d orbital. This is simply done to create another empty 3d orbital that we need for d^2sp^3-hybridization. However, why would the 3d electron just go into another orbital of much higher energy? If we make this questionable assumption though, we have indeed six orbitals available for hybridization, and we can let the ligands donate an electron pair into the empty hybrid orbitals.

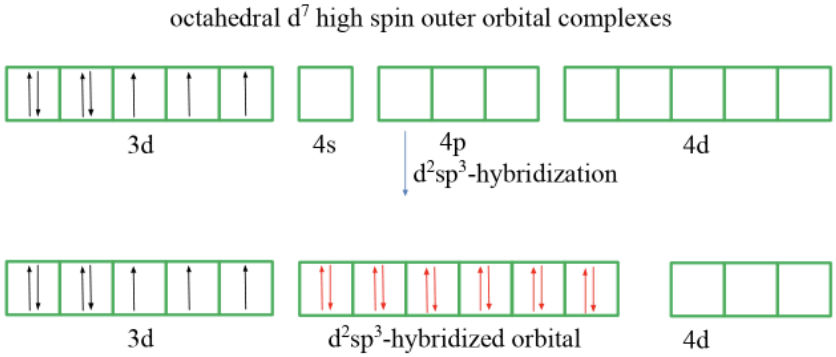


Figure 7.1.8 Valence bond theory applied to an octahedral d^7 high spin-complex

Finally, let us discuss an octahedral d^7 high-spin outer orbital complex (Fig. 7.1.8). In this case we cannot pair any spins in the 3d orbitals. Therefore we assume again that the 4d orbitals get involved in the bonding, and hybridize two of them with the 4s and the three 4p orbitals. The six ligands can then donate six electron pairs into the orbitals thereby creating six bonds and explaining the octahedral shape.

Overall, we see that in the valence bond theory we move around electrons as we please in order to explain shapes and magnetism of complexes without good justification. Therefore, the valence bond theory, while extremely valuable for main group compounds, is only of limited use for transition metal complexes.

Crystal Field Theory

Now let us discuss the second bonding theory for coordination compounds, the crystal field theory. It is actually not a bonding theory because it is based on repulsive electrostatic interactions. Nonetheless, it has many features of a bonding theory in the sense that it can explain many phenomena that a bonding can explain, in particular molecular shape, magnetism, and optical properties.

What are the principles of crystal field theory? Crystal field theory assumes that the electrons in the metal d-orbitals are surrounded by an electric field which is caused by the ligand electrons. This electric field is called the crystal field. The name crystal field comes from the fact that this principle was first applied to transition metal ions surrounded by anions in crystals, and was only later extended to transition metal ions surrounded by ligands in molecular coordination compounds. The assumption that ligands surrounding a transition metal ion produce an electric field makes sense because the ligands contain electrons that are associated with an electric field. It is further assumed that the crystal field raises the energy of the metal-d-orbitals because of electrostatic repulsion between the ligand electrons and the metal electrons.

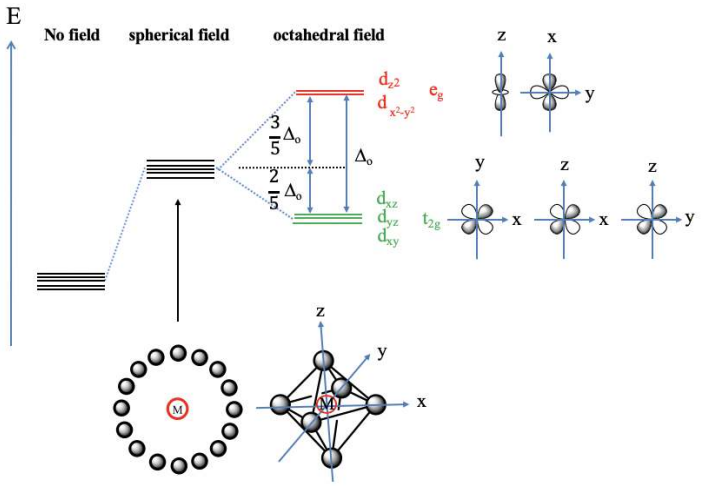


Figure 7.1.9 Crystal field theory demonstrated in the hypothetical spherical case, and the practical octahedral case

Let us first assume the hypothetical case that the ligand electrons surround the metal d-orbitals exactly spherically (Fig. 7.1.9, bottom left). In this case the electric field is completely isotropic, and this means that the energy of all five metal d-orbitals increases to the same extent. Now let us consider the practical case that the ligands surround the metal in octahedrally, which is the case in an octahedral complex. We can say we have an octahedral crystal field. The electric field will now not be spherical any more, it will be the strongest where the ligands are, namely on the vertices of the octahedron, and less strong elsewhere. The vertices of the octahedron lie on the x, y, and z axes of the coordinate system. Thus, the crystal field is the strongest on the axes, and less strong elsewhere. What consequence does this have on the metal d-orbital energies relative to the spherical crystal field? Orbitals that have their electron density mostly on the axes will experience a greater electrostatic repulsion from the crystal field, and therefore will be higher in energy. Orbitals that will have their electron density mostly elsewhere, meaning not on the axes, will experience smaller repulsion, and thus the energy will be smaller compared to the spherical crystal field. Which are the orbitals that have their electron density mostly on the axes? These are the d_{z^2} and the $d_{x^2-y^2}$ orbitals. The d_{z^2} orbital has its energy density mostly on the z-axis, the $d_{x^2-y^2}$ – orbital has its energy mostly on the x and the y axes. The energy of both orbitals is increased by exactly the same amount. This is not obvious given that the orbitals have very different shapes. To understand this, it helps to remember that when orbitals are symmetrically degenerate, they also must be energetically degenerate.

An octahedral complex belongs to the point group O_h and in the point group O_h the d_{z^2} and the $d_{x^2-y^2}$-orbitals are degenerate and have e_g symmetry. Therefore, the $d_{x^2-y^2}$ and the d_{z^2}-orbitals in an octahedral crystal field are also often just called the e_g-orbitals. The remaining d-orbitals, the d_{xy}, the d_{yz}, and the d_{xz} orbitals have their electron density mostly in between the axes, therefore their energy is lower compared to the spherical crystal field. The energy of all three orbitals is reduced by exactly the same amount. We can again understand this when considering that these orbitals are triple-degenerate in the point group O_h and have the symmetry type t_{2g}. For that reason the d_{xy}, the d_{yz}, and the d_{xz} in an octahedral crystal field are also often called the t_{2g}-orbitals. The energy difference between the t_{2g} and the e_g orbitals is called Δ_o. The energy of the t_{2g} orbitals is decreased by 2/5 Δ_o relative to the spherical crystal field, and the energy of the e_g-orbitals is increased by 3/5 Δ_o relative to the spherical crystal field. Where do the factors 2/5 and 3/5 come from? They are due to the law of the conservation of energy. The overall energy reduction due to the energy decrease of the t_{2g}-orbitals must be equal to the overall energy increase due to the energy increase of the e_g orbitals: $\Sigma E(t_{2g})=-\Sigma(E(e_g)$. Because there are three t_{2g} orbitals but only two e_g orbitals this equation only holds when the energy of the e_g orbitals is increased by 3/5 Δ_o and the energy of the t_{2g} orbitals is decreased by 2/5Δ_o, or 3 x 2/5 Δ_o = 2 x 3/5 Δ_o. Note that the energy of all orbitals will be greater in comparison to the case of no electrical field existing, but the energy is increased to a greater extent for the e_g-orbitals compared to the t_{2g} orbitals.

The Tetrahedral Crystal Field

What about a tetrahedral complex with a tetrahedral crystal field?

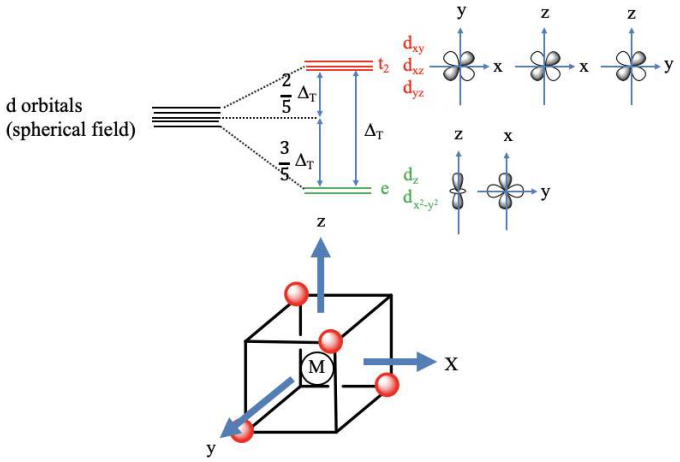


Figure 7.1.10 Crystal field theory for a tetrahedral complex

In this case, the ligands do not approach on the axes (Fig. 7.1.10). We can understand this when we consider that we can inscribe a tetrahedron in a cube. If we connect every other corner of a cube then we obtain a tetrahedron. We can define the coordinate system so that the three axes go through the centers of the square faces of the cube. We can see that the axes do not point toward the ligands, thus the ligands do not approach on the axes. Therefore, the orbitals that have their electron density mostly on the axes have a decreased energy relative to the spherical crystal field. These are the d_{z^2} and the $d_{x^2-y^2}$ orbitals. Their energy is the same despite the fact that they have quite different shape. We can explain this again with symmetry arguments. In the point group T_d the $d_{x^2-y^2}$ and the d_{z^2} – orbitals are double-degenerate and have the symmetry type *e*. Because they are symmetrically degenerate, they are also energetically degenerate. The energy of the d_{xy}, the d_{yz}, and the d_{xz} orbitals have most of their energy density in between the axes. Therefore, their energies are increased relative to the spherical crystal field. They are increased by the same amount because the orbitals are triply degenerated in the point group T_d and have the symmetry type t_2. The energy difference between the *e* and the t_2 orbitals is called Δ_t. The energy of the t_2 orbitals is decreased by 2/5 Δ_t. The energy of the e orbitals is increased by 3/5 Δ_t. This is again the due to the law of the conservation of energy. The total amount of decreased energy must equal the total amount of increased energy. The tetrahedral crystal field energy is smaller than that of the octahedral field because the octahedral field interacts more strongly with the d-orbitals compared to the tetrahedral field. One can calculate that it is actually just 4/9 of the octahedral field. This is mainly because the lobes of the t_2 orbitals to not point exactly toward the vertices of the tetrahedron, while the lobes of the e_g orbitals do point exactly toward the vertices of the octahedron.

Tetragonally Distorted Octahedral and Square Planar Crystal Fields

One nice feature of crystal field theory is that can can readily explain distortions such as the tetragonal distortion of octahedral complexes (Fig. 7.1.11).

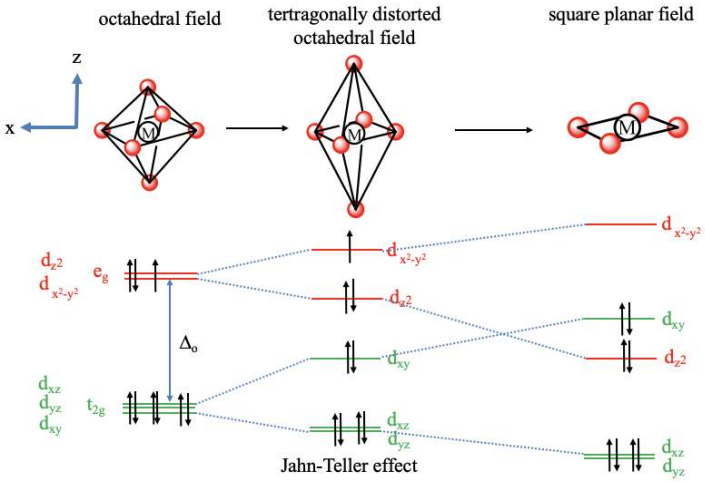


Figure 7.1.11 Tetragonal distortions in the octahedral crystal field leading to a square planar field.

In a tetragonally distorted complex there is a tetragonally distorted crystal field. In an elongated octahedron two ligands are further away from the metal than the four others. Let us assume these two ligands are on the z-axis. Then, the crystal field is weaker on the z-axis. To keep the overall crystal field constant we must bring the other four ligands closer to the metal center. That means that we compress along the x and the y-axis. What will happen to the energy of the orbitals as the octahedron distorts? Because we elongate in the z-direction, the d_{z^2} orbital, that has most electron density on the z-axis goes down in energy. Because we compress on the x and the y-axis, the energy of the $d_{x^2-y^2}$ orbital increases. What about the t_{2g} orbitals? The d_{xy} orbital goes up in energy because it has electron density in the xy plane, but not along the z-axis. The d_{xz} and d_{yz} decrease in energy because they have a significant electron density in z-direction, and the electron density in z-direction is the same for both orbitals. We can now also think about, if the crystal field theory can explain why tetragonal distortion occurs preferentially for certain electron configurations of the metal. For example, it is known that metal ions with d^9 electron configuration often make octahedral complexes with tetragonal distortions. For instance, the hexaaqua copper (2+) complex is an example of a tetragonally distorted complex with a Cu^{2+} ion that has a d^9 electron configuration. We can understand that the tetragonal distortion occurs when comparing the energy of the electrons in the undistorted vs the distorted octahedron. In the undistorted octahedron we have three electrons in the degenerated e_g orbitals. As we distort, we can move two electrons in the energetically lower d_{z^2}-orbital and fill the third one into the energetically higher $d_{x^2-y^2}$-orbital. Thus, overall the electrons have a lower energy explaining the distortion. This is an example of the Jahn-Teller effect. In general, the Jahn-Teller effect can occur when there are partially occupied degenerate orbitals. In this case a molecule can lower its energy through distortion. Note that not only partial occupation of the e_g-orbitals, but also partial occupation of the t_{2g}-orbitals can cause the Jahn-Teller effect, although the effect is typically smaller. For example in complexes with metal ions the d^4-electron configuration, all four electrons can be stabilized through Jahn-Teller distortion. It should also be noted that in addition to an elongation, there is also the possibility of compressing the octahedron along the z-axis. In this case the order of energy of the d_{z^2} and the $d_{x^2-y^2}$ orbital reverses, and the order of energy of the d_{xy}, as well as the d_{xz} and d_{yz} reverses as well.

Finally, let us look at the square planar crystal field in square planar complexes. To understand the square planar crystal field it helps to understand the square planar shape as an infinitely elongated octahedron. If we move the two ligands along the z-axis infinitely far away from the metal ion, then we have created a square planar structure. How will the orbital energies change compared to an elongated octahedron? The $d_{x^2-y^2}$ orbital will have an even higher energy due to the necessity to compensate for the decreased field associated with the ligands on the z-axis by further compressing along the x and the y-axis. The d_{z^2}-orbital is even further decreased in energy because the ligands along the z-axis are now completely gone. The d_{xy} orbital is increased in energy because of the enhanced field in the xy-plane. It is now higher than the d_{z^2}-orbital. The d_{xz} and the d_{yz} orbitals are further decreased in energy because they have significant electron density in z-direction.

Viewing the square planar shape as an extreme case of a tetragonally elongated octahedron also lets us understand why the square planar shape is so often adopted by d^8-metal complexes. We can see that the stabilization energy, and thus the tendency to distort is the greatest when two electrons are in the metal e_g orbitals. In this case two electrons lower their energy through distortion and no electron has an increased energy. Thus, we would understand that the distortion becomes so great, so that the octahedral complex eventually loses two ligands and adopts the square planar shape. This is a nice example how crystal field theory can explain shapes and the number of bonds in a complex without actually being a bonding theory.

High Spin and Low Spin Complexes

One of the greatest strength of crystal field theory is that it can explain high-spin and low spin octahedral complexes in a simple way. The basis for that is the assumption that different ligands produce crystal fields of different strengths and that the differently strong crystal fields produce different Δ_o values. This assumption is plausible because it can be expected that different ligands interact differently with a metal ion, for example, the bond length or the bond strength may be different. If the ligands produce a large crystal field then we would expect a large Δ_o, when the crystal field is small, then we would expect a small Δ_o. The size of the Δ_o determines if we get a high spin or a low spin complex. If the Δ_o is larger than the spin pairing energy, then a low spin complex is favored, if Δ_o is smaller than the spin-pairing energy, then the high spin complex is favored.

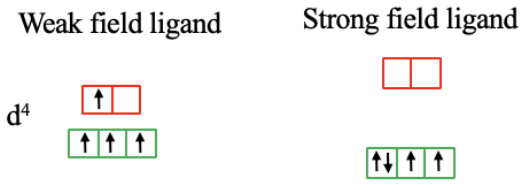


Figure 7.1.12 High and low spin d^4-metal complexes due to a weak and strong crystal field, respectively.

For example in a d^4-metal complex with small Δ_o all electrons are unpaired (Fig. 7.1.12, left). Three of them are in the t_{2g}-orbitals, and the fourth one is in the e_g-orbital. Now let us assume a different ligand that can produce a Δ_o that is large enough to overcome the spin pairing energy. In this case the fourth electron would pair the spin of one of the three electrons in the t_{2g}-orbitals (Fig. 7.1.12, right). We would obtain a low spin d^4-complex.

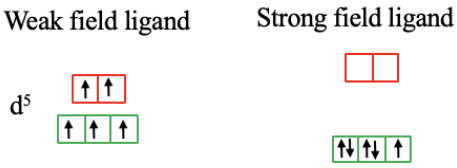


Figure 7.1.13 High and low spin d^5-metal complexes due to a weak and strong crystal field, respectively.

In the case of a d^5-metal high spin complex there are five unpaired electrons, and all orbitals are half-filled. If the the ligand produces a crystal field large enough, the spin pairing energy is overcome and there are two paired and one unpaired electron in the t_{2g} orbitals (Fig. 7.1.13).

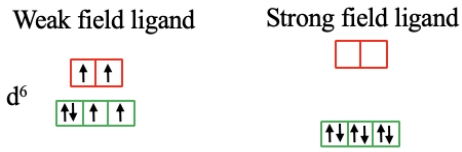


Figure 7.1.14 High and low spin d^6-metal complexes due to a weak and strong crystal field, respectively.

For a d^6-metal high spin complex with a weak crystal field there are two unpaired electrons in the t_{2g} and e_g orbitals respectively. In the case of a strong field ligand and a low spin complex all electrons are in the t_{2g} orbitals and all spins are paired (Fig. 7.1.14).

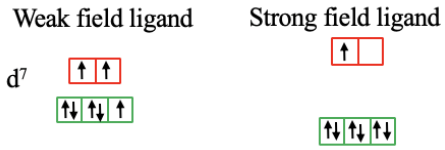


Figure 7.1.15 High and low spin d^7-metal complexes due to a weak and strong crystal field, respectively.

In the case of a d^7-high spin complex there are two electron pairs and one unpaired electron in the t_{2g} orbitals, and there are two unpaired electrons in the e_g orbitals. For the low-spin complex the spin pairing energy is overcome. However, one electron must remain unpaired in the e_g-orbitals because the t_{2g}-orbitals are fully occupied with six electrons. The number of unpaired electrons in high and low spin complexes predicted by crystal field theory is what is experimentally observed. Therefore we can state that crystal field theory can quite elegantly explain high and low spin complexes.

We can also understand why there are no d^1, d^2, d^3, d^8, d^9, and d^{10} low and high spin complexes. In the electron configurations d^1-d^3 all electrons are unpaired in the t_{2g} orbitals. Therefore, there is no electron that could be moved from an e_g to a t_{2g} orbital. For the configurations d^8-d^{10} all t_{2g} orbitals are necessarily full. Therefore, there is no possibility to move an electron from an e_g to a t_{2g} orbital regardless the crystal field strength.

Further, we can explain why there are no low spin tetrahedral complexes. We have learned previously that a tetrahedral crystal field has only 4/9 of the strength of an octahedral field. Because it is so much weaker, no ligand is able to produce a field strong enough to overcome the spin pairing energy. High spin and low spin complexes are possible though for square planar complexes.

Strong and Weak Field Ligands: The Spectrochemical Series

Crystal field theory cannot only explain magnetism well, it can also make statements about the optical properties of a coordination compound. A complex can absorb light when an electron is excited from a d orbital of lower energy to a d orbital of higher energy. The larger the Δ, the smaller the wavelength of the absorbed light. In the case of an octahedral complex, absorption of light would excite an electron from a t_{2g} to an e_g orbital.

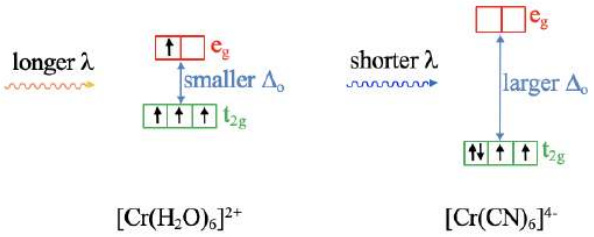


Figure 7.1.16 Octahedral $[Cr(H_2O)]_6^{2+}$ complex compared to an octahedral $[Cr(CN)_6]^{4-}$ complex

For example, an octahedral $[Cr(H_2O)]_6^{2+}$ complex has a smaller Δ_o compared to an octahedral $[Cr(CN)_6]^{4-}$ complex (Fig. 7.1.16), and thus the aqua complex absorbs light of longer wavelength compared to the cyano complex. Vice versa, measuring the absorption spectrum of the complexes, allows us to make statements about the relative crystal field strength of the ligands. By measuring the absorption spectrum of many complexes with a variety of ligands we can develop a so-called spectrochemical series that orders ligands according to their field strength.

$I^- < Cl^- < F^- < OH^- < H_2O < SCN^- < NH_3 < en < NO_2^- < CN^- < CO$

Weaker field	Stronger Field
Smaller Δ	Larger Δ
Longer λ	Smaller λ

Figure 7.1.17 Spectrochemical series for selected ligands.

You can see such a series containing a non-exhaustive number of ligands in Fig. 7.1.17. You can see that the iodo ligands is on the very left side, and is the weakest field ligand, the carbonyl ligand is on the very right hand side, and is the strongest field ligand. All others are in between. We can see for example, that an aqua ligand is a stronger field ligand compared to a fluoro ligand, but a weaker ligand than an ammine ligand. Generally, ligands at the lower end of the series produce weaker fields, smaller Δs, and absorb light light with longer wavelengths. Ligands at the upper end of the series produce stronger fields, create larger Δs, and absorb light of shorter wavelengths. However, crystal filed theory cannot explain different ligand strength. Why does one ligand produce a stronger field than another? To answer this question, we need the ligand field theory.

Ligand Field Theory

Ligand field theory is the most powerful bonding theory for coordination compounds. It is essentially molecular orbital theory applied to coordination compounds. It can explain covalent bonding in coordination compounds, it can explain their shapes, it can explain their magnetism, and their electronic spectra. It can also explain the stability of coordination compounds, in particular the 18e rule and their exceptions. It is, however, more complicated than other bonding theories.

Just like in molecular orbital theory we can apply symmetry adapted linear combination of atomic orbitals to construct molecular orbitals. However, slightly modified rules apply to optimize molecular orbital theory for coordination compounds. These modifications are useful due to the greater complexity of coordination compounds. In the first step we determine the point group of the molecule and assign axes in a useful way. In the second step, we determine the valence orbitals, also called frontier orbitals of the metal. For example, for a transition metal of the 4th period we would consider the 4s, the 4p, and the 3d orbitals as the frontier orbitals. Next, we determine the symmetry of these orbitals. We can do this by just looking into the character table of the respective point group. In the following we select the highest-energy ligand orbitals that are suitable for σ-bonding. For ligands that are molecules or polyatomic ions, these orbitals are the HOMOs suitable for σ-bonding. For simple ions like chloro-ligands these are the highest occupied atomic orbitals. Next, we group the selected ligand orbitals to form ligand group orbitals (LGOs), and determine their symmetry types. To do so, we determine the reducible representation, and then the irreducible representations of the LGOs. This gives us the symmetry types of the ligand group orbitals. We then combine metal frontier orbitals and ligand group

orbitals of the same symmetry type to form molecular orbitals. Now we have constructed all molecular orbitals suitable for σ-bonding, and can draw a molecular orbital diagram for the σ-bonding in the coordination compound.

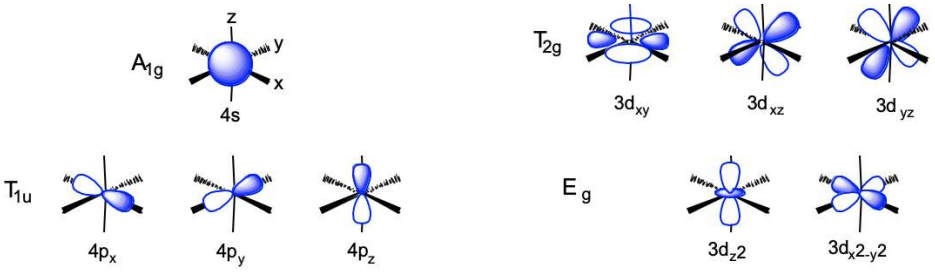
Next, we look for ligand orbitals that are suitable for π-bonding with the metal. We then determine the symmetry types of their ligand group orbitals. Ligand group orbitals and metal orbitals of the same symmetry will then be combined to form molecular orbitals. These MOs represent the π-bonding in the molecule. We add these molecular orbitals to the molecular orbital diagram. Finally, we check if there are ligand orbitals suitable for δ-bonding with the metal. If so, we also form ligands group orbitals for these, determine their symmetry types, and combine ligand group orbitals and metal orbitals of the same symmetry to form molecular orbitals. These orbitals will then also be added to the molecular orbital diagram.

Applicable rules for the construction of molecular orbital diagrams using ligand field theory

1. Determine point group of the complex and assign axes.
2. Determine which are the relevant metal frontier orbitals for bonding.
3. Determine symmetry types of these metal orbitals.
4. Select ligand HOMOs (suitable for σ-bonding) if the ligand is a molecule. If a simple ion, select the highest occupied atomic orbital.
5. Form ligand group orbitals (LGOs) from selected ligand orbitals and determine their symmetry types.
6. Combine metal orbitals and ligand group orbitals of appropriate symmetries to form molecular orbitals.
7. Select ligand orbitals for π and σ bonding if applicable, determine their symmetry and combine them with appropriate metal orbitals.

Ligand Field Theory for an Octahedral Complex of a 4th Period Transition Metal

Let us apply the ligand field theory to a 4th period octahedral transition metal complex first. According to the rules we must first determine the point group and define the coordinate system. The point group is obviously O_h.



O_h	E	$8C_3$	$6C_2$	$6C_4$	$3C_2(=C_4^2)$	i	$6S_4$	$8S_6$	$3\sigma_h$	$6\sigma_d$		
A_{1g}	1	1	1	1	1	1	1	1	1	1		$x^2+y^2+z^2$
A_{2g}	1	1	−1	−1	1	1	−1	1	1	−1		
E_g	2	−1	0	0	2	2	0	−1	2	0		$(2z^2-x^2-y^2, x^2-y^2)$
T_{1g}	3	0	−1	1	−1	3	1	0	−1	−1	(R_x, R_y, R_z)	
T_{2g}	3	0	1	−1	−1	3	−1	0	−1	1		(xy, xz, yz)
A_{1u}	1	1	1	1	1	−1	−1	−1	−1	−1		
A_{2u}	1	1	−1	−1	1	−1	1	−1	−1	1		
E_u	2	−1	0	0	2	−2	0	1	−2	0		
T_{1u}	3	0	−1	1	−1	−3	−1	0	1	1	(x, y, z)	
T_{2u}	3	0	1	−1	−1	−3	1	0	1	−1		

Figure 7.1.18 Character table for the O_h point group and frontier metal orbitals

We can define the coordinate system so that the ligands approach on the x, y, and z axes, respectively. Next, we need to see what the frontier orbitals are. These would be the 4s, the 4p, and the 3d orbitals (Fig. 7.1.18). What symmetry types do they have? We can see this by looking into the character table for the point group O_h. An s orbital always has the totally symmetric symmetry type which is always listed first in the character table. In the point group O_h this is the symmetry type A_{1g}. What about the 4p orbitals? We can see that the letters x,y, and z are in parentheses in the irreducible representation of the symmetry type T_{1u}. This means that the three 4p orbitals are triply degenerate and have the symmetry type T_{1u}. Finally, we need to determine the symmetry types of the 3d orbitals. We find xy, xz, and yz in parentheses in the irreducible representation of the symmetry type T_{2g}. Thus, these orbitals have the symmetry type T_{2g}. We further find $2z^2$-x^2-y^2 and x^2-y^2 in the line for the symmetry type E_g , thus the d_{z^2} and the $d_{x^2-y^2}$ orbitals are degenerate and have the symmetry type E_g. Remember here from the chapter about atomic structure that $2z^2$-x^2-y^2

mathematically describes a cone, and that the d_{z^2} orbital has a conical node. We have now found all the symmetry types of the frontier orbitals.

Next, we need to direct our attention to the ligand and find the highest occupied molecular or atomic orbital suitable for σ-bonding. Of course, it depends now what the ligand is.

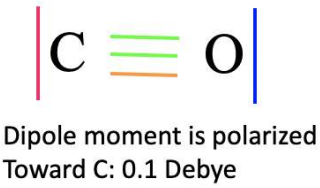


Figure 7.1.19 Lewis dot structure of carbon monoxide. σ-bond: orange. π-bonds: green. Electron lone pairs at C and O are red and blue respectively.

As an example let us choose the common and interesting carbonyl ligand (Fig. 7.1.19). To determine its HOMO suitable for σ-bonding with the metal, we will first need to know the molecular orbital diagram for the carbon monoxide molecule. The carbon monoxide molecule is a linear, polar molecule that belongs to the point group $C_{\infty v}$.

C_{4v}	E	$2C_4$	C_2	$2\sigma_v$	$2\sigma_d$		
A_1	1	1	1	1	1	z	x^2+y^2, z^2
A_2	1	1	1	-1	-1	R_z	
B_1	1	-1	1	1	-1		x^2-y^2
B_2	1	-1	1	-1	1		xy
E	2	0	-2	0	0	$(x,y)(R_x,R_y)$	(xz,yz)

Figure 7.1.20 C_{4v} character table.

The character table of this point group is somewhat hard to work with because of the infinite order of the principal axis, and the infinite number of vertical mirror planes. We will therefore use the subgroup C_{4v} instead (Fig. 7.1.20). A subgroup of a group is a group that results when we remove certain symmetry elements from the original group. We should remove symmetry elements so that degeneracies in the molecular orbitals are not overlooked, which can happen when you reduce the symmetry too much. The point group C_{4v} is the point group with the lowest symmetry we can choose without overlooking degeneracies. Essentially, this is because the atomic orbitals of C and O are only 2s and 2p, and the 2p-orbitals perpendicular to the C-O bond axis can be rotated by 90° to make the orbitals interconvert. This requires a rotational axis of the order 4. If we chose the point group C_{2v}, which has even lower symmetry, we would still be able to construct a molecular orbital diagram, but we would overlook that the $2p_x$ and the $2p_y$ orbitals are degenerate. We see that in the case of a diatomic linear molecule there is no central atom and no ligands. Therefore, we cannot apply the SALC method exactly as we previously learned it. Therefore, we treat the C and O atoms like central atom orbitals that interact with each other. To determine their symmetry types we can just look into the character table for C_{4v}. We find that the 2s orbitals and the $2p_z$ orbitals have the symmetry type A_1 and the $2p_x$ and the $2p_y$ orbitals are double-degenerate and have the symmetry type E (Fig. 7.1.20). Now we can just combine the atomic orbitals to form molecular orbitals.

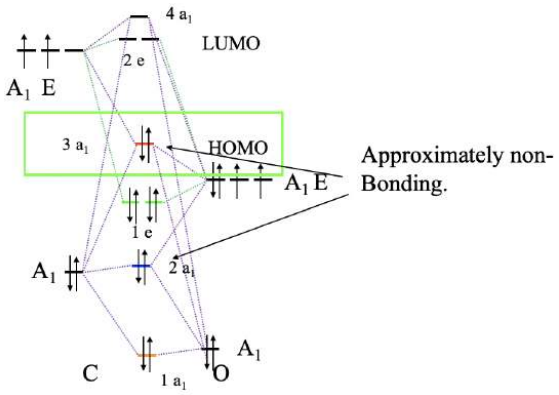


Figure 7.1.21 Molecular orbital diagram for the CO ligand. Orange, red, green and blue colors of MOs refer to the use of colors in the Lewis dot structure of Fig. 7.1.19

To construct a molecular orbital diagram we must consider that O is considerably more electronegative than C, and therefore, the 2s orbital of O is lower in energy compared to the 2s orbital of C. The 2p orbitals of O are lower in energy than those of C. Now we can label our orbitals with their symmetry types, and combine orbitals of the same symmetry type to form molecular orbitals (Fig. 7.1.21). We can start, for instance, with the orbitals of the A_1 symmetry type. There are two on each side, so we will have overall four. Our qualitative assumption would be that there should be a strongly bonding and a strongly anti-bonding orbital, and weakly bonding and a weakly anti-bonding orbital in addition. The strongly bonding one would have the lowest energy and be labeled $1a_1$, the weakly bonding one would have higher energy and is labeled $2a_1$, the weakly anti-bonding one has an even higher energy and is labeled $3a_1$, and the strongly anti-bonding one would have the highest energy of all the four, and has the label $4a_1$. The strongly anti-bonding orbital must be above the $2p_z$ orbital of C, and the strongly bonding one must be below the 2s orbital of O. We can write the $2a_1$ and the $3a_1$ orbital at energy levels so that the energy differences between all four a_1 orbitals are about the same. We can now also connect the MOs and AOs of a_1 symmetry with dotted lines. Now we can turn our attention to the orbitals with E symmetry. There are overall four orbitals of E symmetry, therefore, we expect two bonding double–degenerate orbitals with e-symmetry, and two anti-bonding double-degenerate orbitals with e-symmetry. The bonding MOs must be below the energy level of the 2p orbitals of O, and the two anti-bonding orbitals must be written above the energy levels of the 2p orbitals of C. We can now connect the atomic and molecular orbitals with dotted lines. Finally, we still need to fill in the electrons. There are four electrons coming from the carbon and six electrons coming from the oxygen, which gives ten electrons overall. This means that the $1a_1$, the $2a_1$, the $1e_1$ and the $3a_1$ molecular orbitals are full. This makes the $3a_1$ orbital the HOMO. It is suitable for σ-bonding with the metal because it has been created through σ-interactions between the $2p_z$ and the 2s orbitals of O and P respectively.

It is again interesting to compare the MO picture of the bonding in CO with the Lewis-dot structure (Fig. 7.1.19). In the Lewis dot structure we have a triple bond with six bonding electrons. They correspond to the bonding $1a_1$ and 1e electrons. In the Lewis dot structure all six electrons are energetically indistinguishable, but in the MO diagram we can clearly see that two electrons have a lower energy than the other four which are energetically degenerate. The $1a_1$ MO is a σ-orbital while the other two are π-orbitals because the $2p_x$ and the $2p_y$ orbitals interaction in π-fashion. The $2a_1$ and $3a_1$ orbitals can be approximated as non-bonding MOs representing the two electron lone pairs at C and O respectively. Because the $3a_1$ is slightly anti-bonding it has its electron density mostly at C, while the $2a_1$ is slightly bonding and therefore its counterpart is the electron lone pair at O. Interestingly the dipole moment of CO is slightly polarized toward C by 0.1 Debye despite the fact that O is the more electronegative atom. This can be attributed to the fact that the HOMO as a weakly anti-bonding orbital is primarily located at C, In addition, the $2a_1$ orbital is fairly close in energy to the 2s of C, therefore the 2s of C contributes significantly to this orbital. This leads to the fact that there is a significant amount of electron density located at C as well.

One a_{1g} ligand group orbital
(no node)

Two e_g orbitals
(two nodes)

Three t_{1u} orbitals
(one node)

Figure 7.1.22 Ligand group orbital symmetry types

In the next step, we need to group the six HOMOs to form ligand group orbitals, and determine their symmetry types. This is being done by first determining the reducible representation of the orbitals using the orbital swapping method, and then determining the number of irreducible representations of a given type using the reduction formula from group theory. We will not go through the details of the calculations here, because there is nothing really new to learn, but just discuss the outcome. The outcome is that there is one ligand group orbital with the symmetry type a_{1g}, two doubly degenerated ligand group orbitals with the symmetry type e_g, and three triply degenerated ligand group orbitals having the symmetry type t_{1u}. The a_{1g} orbital does not have a node because it is totally symmetric. The t_{1u} orbitals have one node, and the e_g-orbitals have two nodes (Fig. 7.1.22). This is not a result of the reduction formula, but one could show that by actually computing the ligand group orbitals using a formula called the projection operator (which we will not discuss in detail here).

Because we now know our the symmetry types of our metal frontier orbitals and our ligand group orbitals we can construct a qualitative molecular orbital diagram (Fig. 7.1.23). To do so we can plot the frontier orbitals on the left side of the molecular orbital diagram, and the ligand group orbitals on the right side of the molecular orbital diagram.

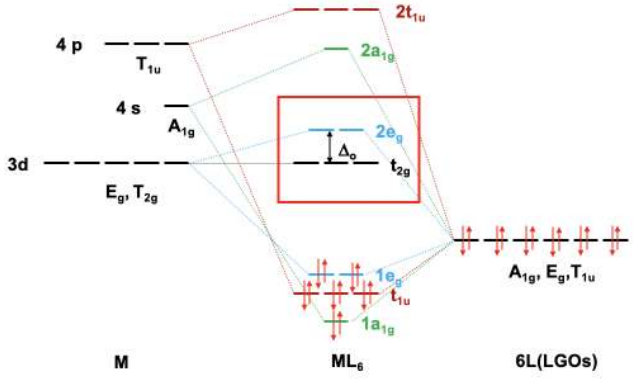


Figure 7.1.23 Qualitative molecular orbital diagram for an octahedral complex of a 4th period transition metal (σ-bonding only).

For a 4th row transition metal the sequence of energy is 3d<4s<4p. It makes sense to assume that the ligand group orbitals have about the same energy as the 3d orbitals of the metal, and we can plot them accordingly. Next, we can assign the orbitals their previously determined symmetry types. Then, we can start to combine orbitals of the same symmetry types to form molecular orbitals. We can start for instance with the orbitals having the symmetry type A_1. The 4s orbital has that symmetry type. Also one ligand group orbital is of this type. Therefore, we would expect one bonding and one anti-bonding molecular orbital. We can label them $1a_{1g}$ and $2a_{1g}$, respectively, and connect them with the A_{1g} atomic and ligand group orbitals by dotted lines. Next, for example, we can consider the E_g orbitals. There are two metal d orbitals and two ligand group orbitals of that symmetry. We therefore produce two doubly degenerate bonding, and two doubly degenerate anti-bonding molecular orbitals. We can label them $1e_g$ and $2e_g$ respectively. We can further see, that there are the three T_{1u} metal 4p orbitals that we can combine with the ligand T_{1u} orbitals. This gives three triple-degenerated bonding orbitals and three triple-degenerated anti-bonding orbitals with t_{1u} symmetry. Lastly, there are the metal T_{2g} orbitals. There are no ligand group orbitals with the same symmetry, and therefore the T_{2g} orbitals remain non-bonding. We have to write them with unchanged energy into the molecular orbital diagram.

Now we are finished with the construction of molecular orbitals, but still need to fill the electrons into them. We consider the metal-ligand bond a dative bond, with electron pairs being donated by the ligand's HOMO. Therefore, we consider all ligand group

orbitals to be full with electrons. That means that we have overall 6x2=12 electrons to consider. What about the metal electrons? Well, it depends now which metal ion we have. Let us assume here that we have a d^0 metal ion with no d electrons. That means that we overall have 12 electrons that we need to fill into the molecular orbitals according to energy. This fills the $1a_{1g}$, three t_{1u}, and the two $1e_g$ orbitals. Now let us assume that we would not have a d^0 metal ion, but a metal ion with d electrons. There could be up to ten d electrons. Where would they go? They would go into the five orbitals with the next highest energies. Which ones are these? Well, these are the t_{2g} and the $2e_g$ orbitals. The t_{2g} orbitals are the non-bonding metal d_{xz}, d_{xy}, and d_{yz} orbitals, therefore these orbitals are located only at the metal. The $2e_g$ orbitals are anti-bonding molecular orbitals that have been constructed from the d_{z^2} and the $d_{x^2-y^2}$ orbitals, and are similar in energy to the $d_{x^2-y^2}$ and d_{z^2} orbitals. We can therefore say that the t_{2g} and the $2e_g$ orbitals are the d orbitals under the influence of an octahedral ligand field. Due to the presence of the ligand field the energies of the metal d-orbitals split and the difference in energy is the octahedral ligand field energy Δ_o. Now we can see that there is an interesting analogy to the crystal field theory. Like the d-orbitals split in energy under an octahedral crystal field into t_{2g} and e_g orbitals, the d-orbitals split in energy in an octahedral ligand field into t_{2g} and e_g orbitals. Like in crystal field theory the energy of the d_{z^2} and the $d_{x^2-y^2}$ is raised. The energy of the other three d-orbitals is unaffected similar, but not exactly the same as the d_{xy}, d_{yz}, and the d_{xz} orbitals in an octahedral crystal field.

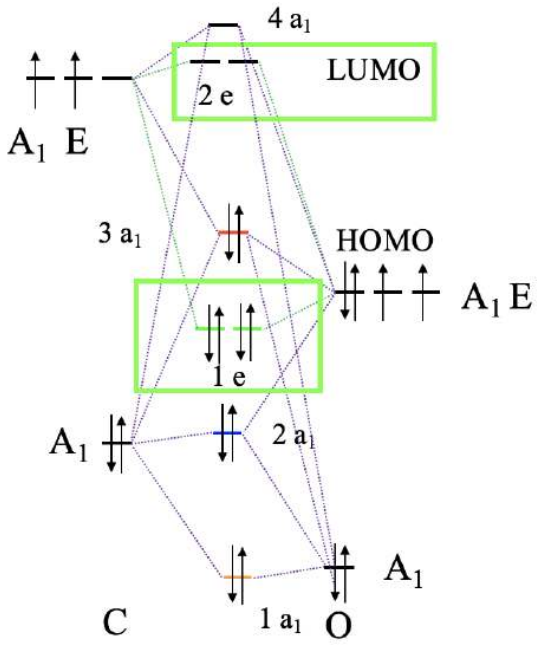


Figure 7.1.24 Molecular orbital diagram for CO ligand and relevant MOs for the π-bonding with the metal (green).

Now we have understood the σ-bonding in an octahedral complex, next let us consider the π-bonding. That means that we have to think about what orbitals of the ligand has the right symmetry for π-bonding with the metal. They should also have an energy similar to the metal orbitals so that significant covalent interaction can occur. We shall stick with our carbonyl ligand, thus we need to look into the molecular orbital diagram of the CO molecule again, and see if there are molecular orbitals suitable for π-bonding (Fig. 7.1.24). The CO molecule has the 1e and the 2e orbitals, that are bonding and anti-bonding π-orbitals, respectively. We can understand this when considering that they are constructed from the $2p_x$ and the $2p_y$ orbitals that overlap in π-fashion to make the π-bonding in the molecule. Each ligand has two 1e and two 2e orbitals which gives overall four orbitals. These orbitals are energetically similar to the HOMO, thus we can expect that they are energetically close enough to the energy of d-metal orbitals, and can get involved in bonding. We have six ligands meaning that we have 6x12=24 orbitals overall. The twelve 1e orbitals are bonding π-orbitals, and the twelve 2e orbitals are anti-bonding π*-orbitals.

Why are these orbitals suitable for π-bonding with metal d-orbitals? Let us look at their shape, and how they can overlap with a metal d-orbital (7.1.25).

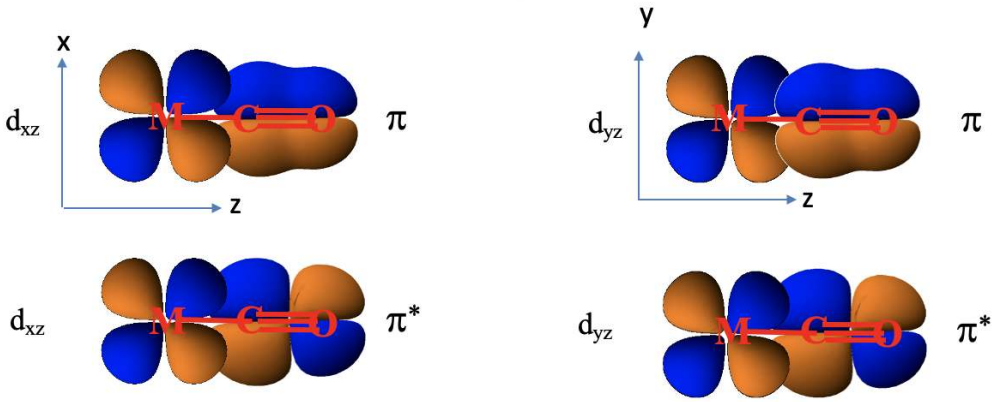


Figure 7.1.25 π-bonding in an octahedral carbonyl complex of a 4th period transition metal

Look for example at a 1e orbital constructed from two $2p_x$ orbitals, and how it is oriented relative to the metal-ligand bond axis which we shall define as the z-axis. Next, let us consider a metal d_{xz} orbital orbital. We can see that it is in plane with the 1e orbital, and that the overlap between the d_{xz} and the 1e orbital occurs in π-fashion. Now let us consider the analogous π*-orbital. We can see that it has an additional node, but it can also overlap with a d_{xz} orbital in π-fashion. The ligand does not only have π and π*-orbitals through overlap of two $2p_x$ orbitals, but also π and π*-orbitals that result from the overlap of two $2p_y$ orbitals. Those orbitals can overlap in π-fashion with a metal d_{yz} orbital. So far, we considered the interactions of a single ligand with the metal only. There are five other ligands, one also approaching from the z-axis, and the other four approaching from the x and y axes. They also have the π and π*-orbitals that interact with the d_{xz}, the d_{yz}, or the d_{xy} orbitals in π-fashion, depending on the direction of approach.

So what do we do with all these orbitals? We group the twelve bonding ones to form a set of ligand group orbitals, and group the twelve anti-bonding ones to form another set of ligand group orbitals. We determine the symmetry types of each set by first determining the reducible representation, and then the irreducible representations using the reduction formula. The result of this process is that the twelve bonding ligand group orbitals have T_{1g}, T_{2g}, T_{1u}, and T_{2u} symmetry. This means that there are three triple-degenerated ones that have T_{1g} symmetry, three other triple-degenerated ones that have T_{1u}, symmetry, three more triple-degenerated ones that have T_{1u} symmetry, and another three triple-degenerated ones that have T_{2u} symmetry. The twelve anti-bonding ligand group orbitals have the same symmetry types. Three have T_{1g} symmetry, three have T_{2g} symmetry, three have T_{1u} symmetry, and another three have T_{2u} symmetry.

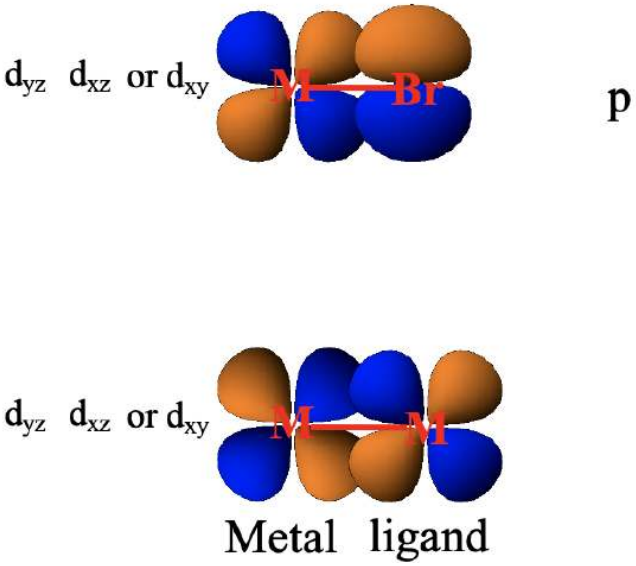


Figure 7.1.26 Other possibilities for π-interactions

It should be mentioned that there are a number of other orbitals that can make π-interactions when the ligand is not a CO ligand. For example halogenide ligands have p-orbitals that have suitable orientation to overlap with metal d-orbitals in π-fashion (Fig. 7.1.26). When there are complexes with metal-metal bonds then there is also the possibility of metal d-orbitals to overlap with other metal d-orbitals in π-fashion.

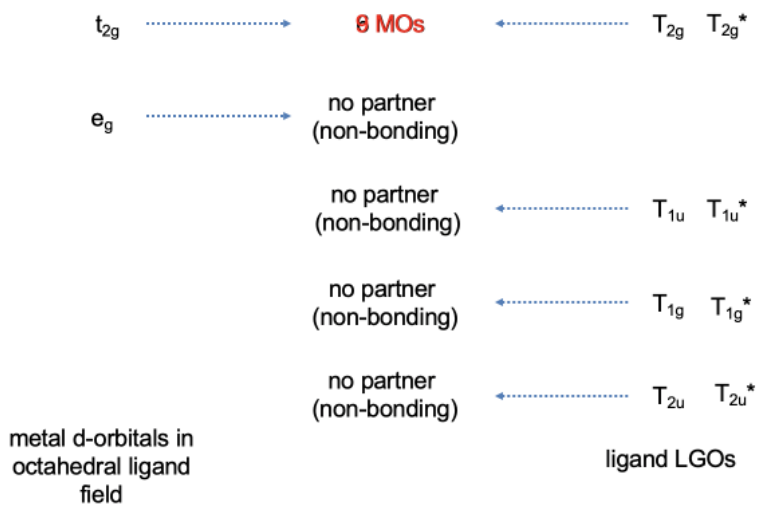


Figure 7.1.27 π-bonding MOs for the octahedral complex of a 4th period transition metal

Now that we have determined the symmetry types of the ligand group orbitals available for π-bonding, we need to select those ligand group orbitals that have suitable symmetry to form molecular orbitals with metal d-orbitals in the octahedral ligand field. These are the $2e_g$ and the t_{2g} MOs that resulted from the σ-interactions. For simplicity sake we will call the $2e_g$ molecular orbitals just the metal e_g orbitals. The t_{2g} MOs are identical to the metal T_{2g} atomic orbitals because the metal T_{2g} atomic orbitals remain exactly non-bonding with respect to σ-interactions. The ligand group orbitals have T_{1g}, T_{2g}, T_{1u}, and T_{2u} symmetry respectively. That means that we can combine the t_{2g} metal orbitals and the T_{2g} ligand group orbitals to form molecular orbitals. The metal e_g orbitals and the ligand T_{1g}, T_{1u}, and T_{2u} orbitals remain non-bonding because they do not find a partner (Fig. 7.1.27). The three bonding T_{2g} LGOs will form six MOs of the same symmetry type with the three metal t_{2g} orbitals. In addition, we need to consider that there are also three anti-bonding T_{2g}^* LGOs that were formed from the anti-bonding π-orbitals. They can also interact with the metal t_{2g} d-orbitals. Because the number of MOs of a given symmetry type is always the sum of the atomic orbitals + the LGOs of that symmetry type this adds three MOs to the six MOs giving overall nine t_{2g} MOs. There are also the T_{1u}^*, the T_{1g}^*, and the T_{2u}^* orbitals. They just remain non-bonding because they do not find a partner.

We can now think of two extreme cases for the combination of the metal t_{2g} with the ligand T_{2g} and T_{2g}^* orbitals. In the first case the T_{2g} LGOs are much closer in energy to the metal t_{2g} orbitals, and the T_{2g}* LGOs are energetically much higher than the metal t_{2g} orbitals. In this case we can neglect the covalent interactions between the T_{2g}^* orbitals and the metal t_{2g} orbitals, and the T_{2g}^* orbitals remain effectively non-bonding. We would consider only the interactions between the T_{2g} LGOs and the metal t_{2g} orbitals to form three bonding and three anti-bonding MOs of t_{2g} symmetry (Fig. 7.1.28). Now we need to consider the electrons. The bonding T_{2g} LGOs are full, and therefore there are overall six electrons to consider. These six electrons would go into the three bonding t_{2g} MOs. Now can also have up to ten metal d electrons. Six of them can be accommodated by the t_{2g} metal orbitals, the other four would be in the e_g orbitals. Upon the formation of the π-bond, the t_{2g} metal electrons will be in the anti-bonding t_{2g} orbitals. The e_g electrons will simply remain non-bonding. We can see that the π-interactions lower the energy of the ligand electrons, but increase the energy of the metal electrons. If we get a net stabilization of electron energies will depend on how many d electrons we have. As long as there are less than six d electrons we will see a stabilization, if there are more there will be an overall destabilization. We can also ask what impact the π-bonding has on the magnitude of the Δ_o. We can see that the π-bonding decreases the Δ_o. It is larger before the bonding compared to after the π-bonding.

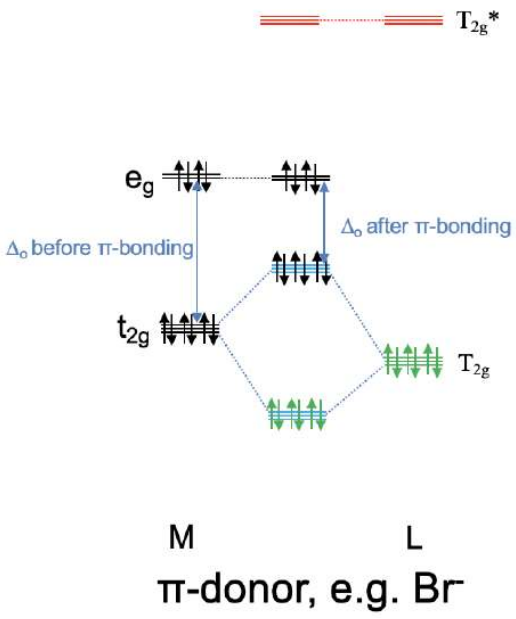


Figure 7.1.28 Influence of a π-donating ligand on Δ_o for the example of a d_{10} ion.

We call a ligand that has T_{2g} orbitals of similar energy to the metal t_{2g} orbitals, and T_{2g}^* orbitals of much higher energy compared to the metal t_{2g} orbitals a π-donating ligand, or a π-donor (Fig. 7.1.28). This is because before the π-bonding the ligand electrons are localized exclusively at the ligand, and after the π-bonding they are in the bonding t_{2g} MOs which are shared between the metal and the ligand. Thus, a partial electron transfer has occurred from the ligand to the metal. An example for π-donating ligands are halogenide ligands such as a bromo ligand.

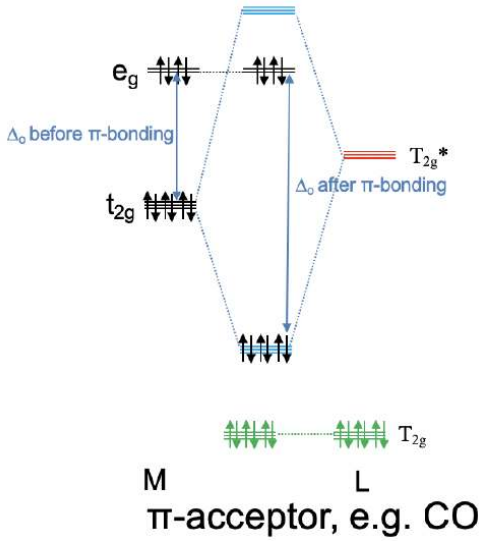


Figure 7.1.29 Influence of a π-acceptor ligand, e.g. CO, on Δ_o

Now let us consider the opposite case in which the anti-bonding T_{2g}^* ligand orbitals are energetically close to the metal t_{2g} orbitals and the bonding T_{2g} ligand orbitals are energetically too low in order to significantly interact with the metal t_{2g} orbitals. This means that the T_{2g}-orbitals remain practically non-bonding. The T_{2g}^* ligand group orbitals and the metal t_{2g} orbitals form three triply degenerated bonding molecular orbitals and three triply degenerated anti-bonding molecular orbitals. Because the T_{2g}^* ligand group orbitals are empty, no ligand electrons are filled into the new molecular orbitals. This means that up to six metal d electrons can be filled into the bonding molecular orbitals of t_{2g} symmetry. Any remaining d electrons in the e_g orbitals just remain in the e_g orbitals and do not change in energy. We can see that in contrast to the previous case, we can lower the energy of the metal d electrons through π-interactions. Because the bonding t_{2g} electrons are shared between the metal and the ligand, electron density has been transferred from the metal to the ligand. Therefore, a ligand that primarily utilizes its anti-bonding T_{2g}^*-orbitals for π-bonding is

called a π-acceptor ligand, it accepts d-electron density from the metal. An example for a π-acceptor ligand is the carbonyl ligand (Fig. 7.1.29). It is also important to understand the influence of a π-acceptor ligand on the size of Δ_o. Because the anti-bonding t_{2g} MO is higher in energy than the non-bonding e_g orbitals, the Δ_o is now defined by the energy difference between the bonding t_{2g} MOs and the e_g orbitals (Fig. 7.1.29). We can see that Δ_o is increased when π-acceptor interactions are taken into account.

We have now discussed the two extreme cases, however there are many ligands that are actually in between these two extremes, and there is a continuous spectrum from strongly π-donating, to weakly π-donating, to weakly π-accepting, to strongly π-accepting ligands. It is also possible that π-donor and π-acceptor effects cancel out. This is the case when the the T_{2g} and T_{2g}^*-ligand group orbitals are energetically about equidistant to the metal t_{2g} orbitals. Some ligands also do not have orbitals suitable for π-bonding at all, and there are neither π-donating nor π-accepting effects.

The effect of π-bonding on Δ_o can nicely explain the spectrochemical series. Because π-accepting ligands increase Δ_o, these complexes absorb light of shorter wavelength and of higher energy. π-donating ligands decrease Δ_o and and thus lead to the absorption of light having longer wavelengths. We see here that the ligand field theory is more powerful than the crystal field theory. The latter was not able to explain why different ligands produce different Δ_o values.

Ligand field theory is also able to nicely explain the magnetism of coordination compounds, and high and low spin complexes in particular. It is also able to explain why certain ligands tend to produce low spin complexes, while others tend to form high spin complexes. According to ligand field theory π-acceptors tend to make low spin complexes, and π-donors tend to make high-spin complexes. This is in accordance with experimental observation.

Octahedral Complexes and The 18 Electron Rule

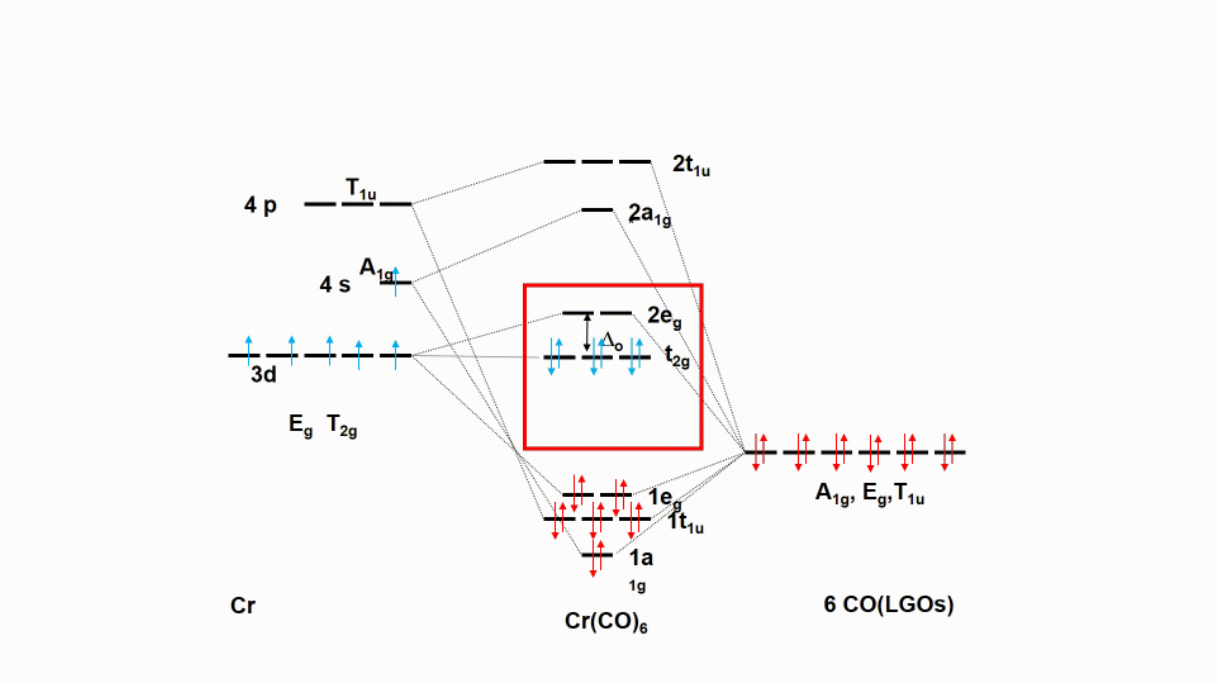


Figure 7.1.30 Qualitative MO diagram of the octahedral hexacarbonyl chromium complex under consideration of π-bonding.

Another great feature of ligand field theory is that it can explain the 18 electron rule, and exceptions from the 18 electron rule. For example, the octahedral hexacarbonyl chromium complex is an 18 electron complex. Let is construct a qualitative molecular orbital diagram and see if the MO diagram supports the stability of the complex. The MO diagram considering only the σ-interactions is shown in Fig. 7.1.30. We can see that all the twlelve ligand electrons are in the bonding molecular orbitals $1a_1$, $1t_u$, and $1e_g$. In addition the chromium has six valence electrons. These electrons remain non-bonding when considering σ-interactions only. However, this changes, when we consider π-interactions. The CO ligand is a strong π-acceptor ligand, therefore we consider only its T_{2g}^* π-ligand group orbitals for bonding. They must be located energetically above the LGOs for σ-bonding. The interaction of the metal t_{2g} orbitals creates three bonding t_{2g} MOs and the three anti-bonding ones. Because we can fill metal d electrons into the

bonding MOs the status of the d-electrons has changed from non-bonding to bonding. We can see now that all 18 electrons are in bonding MOs, and that no electron is in-non-bonding or anti-bonding MOs. When all electrons are in bonding MOs then this is the ideal situation for complex stability. This is explains why the 18 electron complex is stable. If we analyzed the MO diagrams of many other stable 18 electron complexes then we would also mostly find that all bonding MOs are filled, and all other MOs are empty. This explains the 18 electron rule.

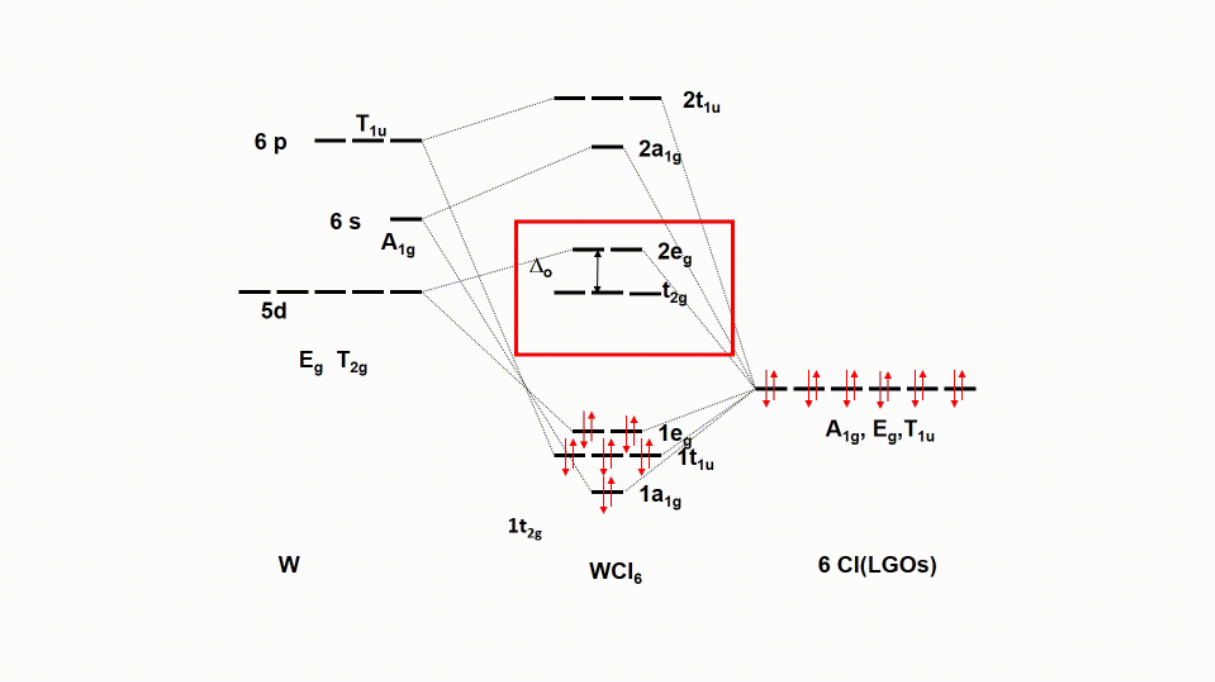


Figure 7.1.31 The qualitative molecular orbital diagram of WCl_6 under consideration of π-bonding.

Next, let us construct a qualitative molecular orbital diagram of WCl_6. This is not an 18 electron complex, it has only twelve electrons coming from the six chloro ligands. W is in the oxidation state +6 and is a d^0 species contributing no electons. Can ligand field theory explain this exception from the 18 electron rule? Let us again start with the MO diagram considering σ-bonding only. The twelve ligand electrons go into the bonding $1a_{1g}$, $1t_u$, and $1e_g$ orbitals. The non-bonding t_{2g} and the anti-bonding $2e_g$ orbitals remain empty due to the absence of metal d electrons. We can see that all bonding molecular orbitals are full and all others are empty, explaining the stability of the molecule, and thus the exception from the 18 electron rule. Now let us consider π-bonding in addition. A chloro ligand is a typical π-donor which uses its 3p electrons that are suitably oriented for π-bonding. Therefore, we only consider the T_{1g} ligand group orbitals for bonding here. These orbitals are full with electrons because a chloride anion has a full 3p subshell. The interaction of the T_{2g} LGOs with the metal t_{2g} orbitals creates a bonding t_{2g} MO and an anti-bonding t_{2g} MO. We can see that the ligand π-electrons now have a lower energy than without the π-interactions of the metal. Therefore, the π-bonding has further stabilized the complex. In a way, we can now even say that we have an 18 electron complex because when we add th 6 π electrons to the 12 σ electrons we get 18 bonding electrons overall. These additional 6 electrons are not accounted for in electron-counting because electron-counting treats the W-Cl bond as a single bond and only considers the σ-interactions between W and Cl.

Tetrahedral complex of a 4th period Transition Metal

Next, let us consider a tetrahedral complex and see if ligand field theory can explain it well. The point group for a tetrahedron is T_d, and we will need the character table of this point group (Fig. 7.1.32)

T_d	E	$8C_3$	$3C_2$	$6S_4$	$6\sigma_d$		
A_1	1	1	1	1			$x^2 + y^2 + z^2$
A_2	1	−1	1	−1			
E	2	−1	2	0			$(2z^2 - x^2 - y^2, x^2 - y^2)$
T_1	3	0	−1	1		(R_x, R_y, R_z)	
T_2	3	0	−1	−1		(x, y, z)	(xy, yz, xz)
Γ_σ	4	1	0	0		$A_1 + T_2$	
Γ_π	8	−1	0	0		$E + T_1 + T_2$	

Figure 7.1.32 Character table for the point group T_d

We choose the coordinate system like in the crystal field theory. We inscribe the tetrahedron into a cube by occupying every other vertice of the cube with a ligand (Fig. 7.1.34). Then, we let the axes run perpendicular to the faces of the cube. Next, we need to think about the symmetry types of the metal frontier orbitals. For a fourth period transition metal these are the 3d, the 4s, and the 4p orbitals. Looking into the character table of the point group T_d gives us their symmetry types (Fig. 7.1.32 and Fig. 7.1.33). The 4s orbital has the totally symmetric symmetry type A_1, We find the letters x,y, and z in parentheses in the irreducible representation of the type T_2, and this means that the 4p orbitals are triply degenerated and have the symmetry type T_2. The $3d_{xy}$, the $3d_{yz}$, and the $3d_{xz}$ orbitals are found in the same irreducible representation, are also triple-degenerated, and have T_2 symmetry. The $3d_{x^2-y^2}$ and the $3d_{z^2}$ orbitals have the symmetry type E according to the character table for T_d.

Metal orbitals:

4s	A_1
4p	T_2
$3d_{xy}$, $3d_{yz}$, $3d_{xz}$	T_2
$3d_{x^2-y^2}$ $3d_{z^2}$	E

Figure 7.1.33 Metal orbitals

Now we need to think about the ligands. Because we need to consider σ-bonding first, we have to find the HOMO of the ligand suitable for σ-bonding. We can choose again a carbonyl ligand as an example ligand, and in this case the HOMOs of the CO ligands would be used for σ-bonding. This is actually not immediately obvious. If we chose the coordinate system of the metal and ligands to be same same, then then the CO bond axis, which we previously defined as the z-axis, would not point toward the metal, and no σ-overlap with a metal orbital would be possible. Therefore, we must give each ligand a different coordinate system with the z-axes pointing toward the metal (Fig. 7.1.34). Only then, the CO molecule would point toward the metal, and would be oriented to make σ-bonding with the metal. Generally, when constructing MOs, the ligands should always be oriented to that bonding is maximized. This is usually the case when orbital overlap for σ-bonding is maximized.

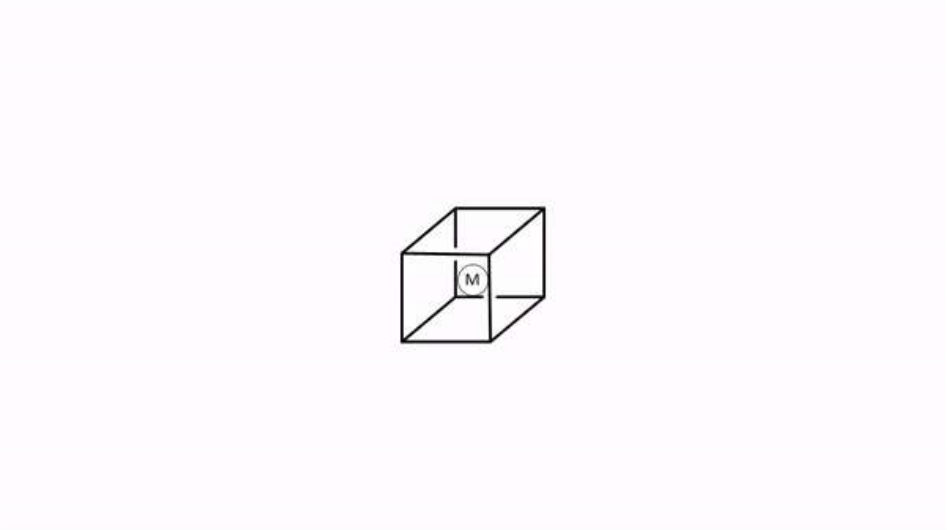


Figure 7.1.34 A tetrahedral complex inscribed in a cube with CO ligands each having its own coordinate system.

Because we have four ligands we will have four ligand HOMOs that we would group to form four ligand group orbitals. Which symmetry types do they have? In order to obtain the symmetry types we would need to determine the reducible representation first, and then the irreducible representations this reducible representation is composed of. We won't do this explicitly here and not go through the entire mathematical process, and only consider the results.

4 Ligand orbitals:

$$A_1 + T_2$$

Figure 7.1.35. Symmetry types for ligand group orbitals involved in σ-bonding

The result is that one ligand group orbital has the symmetry type A_1 and the other three have the symmetry type T_2 (Fig. 7.1.35).

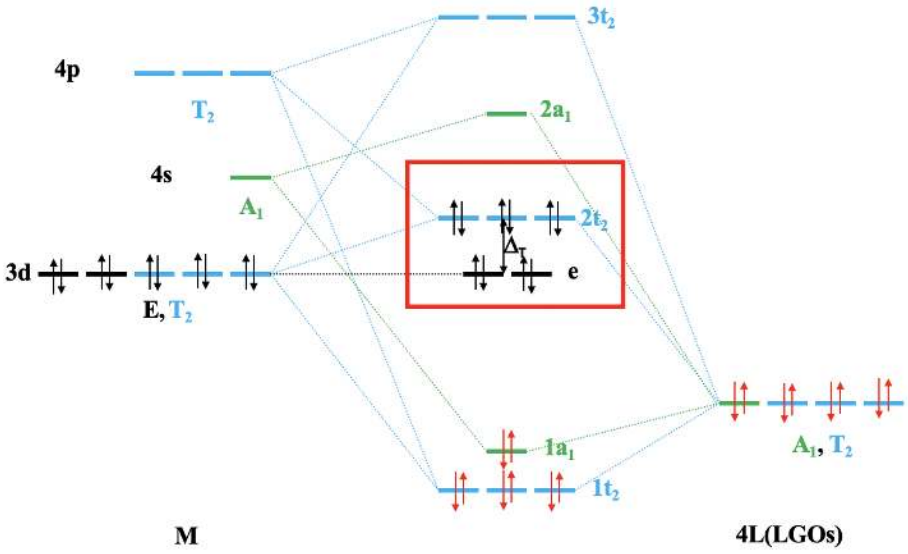


Figure 7.1.36 MO diagram reflecting the σ-bonding of a tetrahedral complex of a 4th period transition metal

We can now construct the molecular orbital diagram for σ-bonding (Fig. 7.1.36). First, we can plot the metal frontier orbitals according to the energy on the left side of the diagram, and label the orbitals according to their symmetry types. On the right side we plot the four ligand group orbitals, and label them according to their symmetry type. Their energy should be approximately that

of the metal d-orbitals. Now we can construct molecular orbitals by combining atomic and ligand group orbitals of the same symmetry type. The 4s orbital and one LGO have A_1 symmetry, and therefore we can combine them to form a bonding $1a_1$ and an anti-bonding $2a_1$ orbital. Next, let us direct our attention to the t_2 symmetry type. The 4p and three metal d orbitals have that symmetry type, and so have three LGOs. That is overall nine orbitals, so we must get nine MOs with t_2 symmetry. Because of triple-degeneracy, there must be three sets of triple-degenerate MOs. We can estimate that one set will be bonding, one will be approximately non-bonding, and one will be anti-bonding. We can label them $1t_2$, $2t_2$, and $3t_2$ respectively. The $2t_2$ is actually somewhat anti-bonding in nature. Now only the metal e-orbitals are left. They do not find a partner and remain non-bonding.

We still need to fill the electrons into the MOs. The four ligand HOMOs are considered full, which gives 4×2=8 electrons. The electrons occupy the bonding $1t_2$ and the $1a_1$ orbitals explaining the four dative metal-ligand bonds. All metal d electrons, which could be up to ten, would need to go into the e and/or the t_2-orbitals. The e-orbitals are the non-bonding d_{z^2} and $d_{x^2-y^2}$ orbitals, and the $2t_2$ orbitals are only weakly anti-bonding and have strong d-metal orbital character because they are have been constructed from the d_{xy}, the d_{yz}, and the d_{xz} orbitals, and are fairly similar in energy to those orbitals. We can therefore say that the the e and the 2_{t2} orbitals are the metal t_2 and e_g orbitals in a tetrahedral ligand field. The energy difference between the e and the $2t_2$ orbitals is the tetrahedral ligand field energy Δ_T. You see here again the relationship between ligand and crystal field theory. You can also see that ligand field theory can explain why crystal field theory works as a bonding theory even though it is not an actually bonding theory.

π-bonding in a tetrahedral complex

What is the π-bonding in a tetrahedral complex?

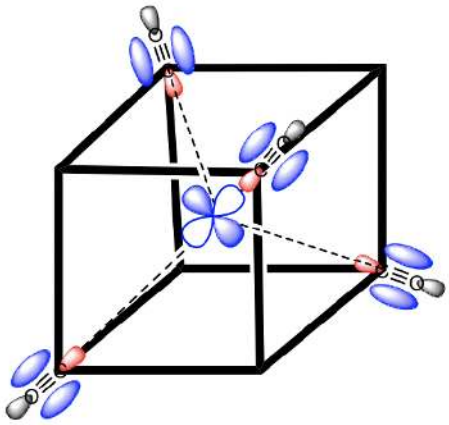


Figure 7.1.37 π-bonding in a tetrahedral complex

First, we need to decide if there are ligand orbitals that are suitably oriented to overlap with metal orbitals in π-fashion. We can see that no ligand orbital is overlapping with a metal d-orbital exactly in π-fashion, however, the e π and 2e π*-orbitals of the ligands still overlap so that at bonding interaction is created, and this orbital overall occurs similarly to π-overlap. Therefore, we can still approximate the bonding interactions as π-bonding. We need to consider though that because of smaller orbital overlap, the π-bonding in tetrahedral complexes is weaker than in octahedral complexes. How many ligand orbitals will we need to consider? Assuming that we will stick with CO as the ligand, there will be four per ligand, and thus there will be 4×4=16 overall. Of these, there will be eight bonding e π-orbitals and eight anti-bonding e π*-orbitals. We group the bonding ones to form a set of eight ligand group orbitals, and group the anti-bonding ones to form another set of eight anti-bonding ligand group orbitals. What will be their symmetry types? We can determine the reducible representations and irreducible representations to find this out. We are not going through the exact process here, but only look at the results. The result is that each set of ligand group orbitals has the two E-type orbitals, three T_1-type, and three T_2-type ligand group orbitals.

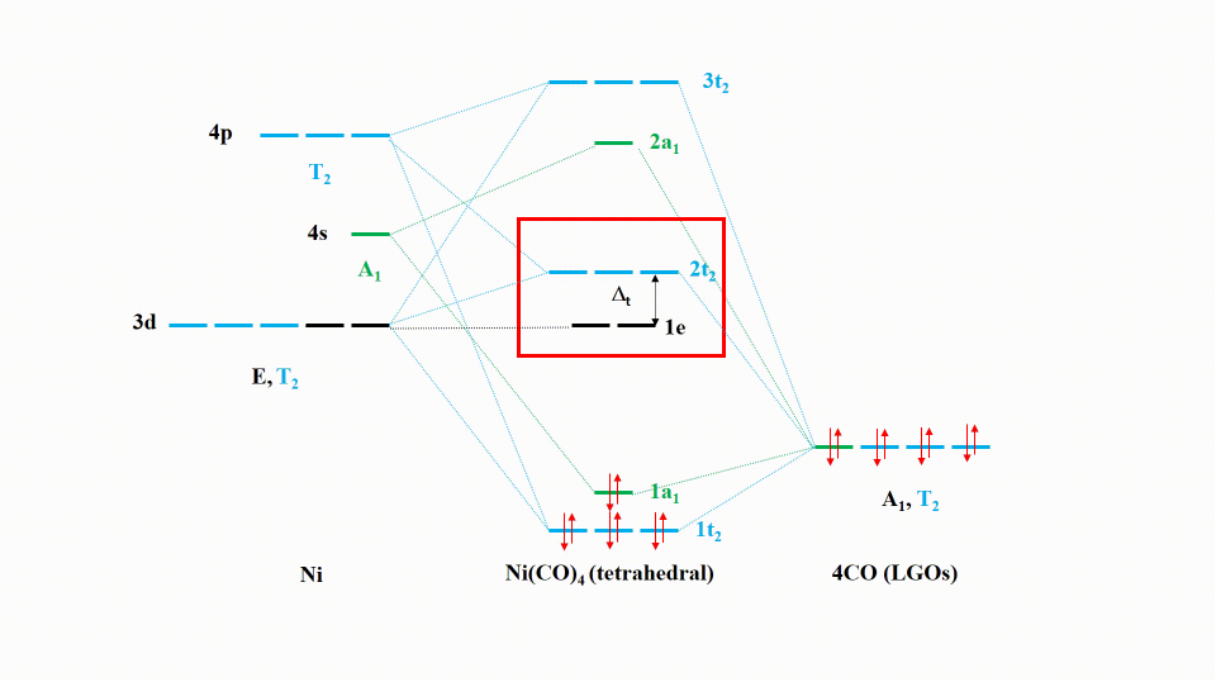


Figure 7.1.38 MO diagram of a tetrahedral complex of a 4th period transition metal (pi-bonding with pi-acceptor)

Since we now know the symmetry of the ligand group orbitals we can combine them with same-symmetry metal d-orbitals in the tetrahedral ligand field to form π-molecular orbitals. Let us do this for the example of nickel tetracarbonyl, a tetrahedral complex of Ni in the oxidation state 0 and four carbonyl ligand. We can use the MO diagram for σ-bonding which we constructed previously as a starting point, and modify it so that it accounts for π-bonding (Fig. 7.1.38).

First, we need to add the new ligand group orbitals to the MO diagram. We only need to consider the E and T_2 LGOs and not the T_1 LGOs because no metal orbital has t_1 symmetry. Next, we need to take into account that the CO ligand is a strong π-acceptor ligand. This means that we only need to consider the LGOs formed from the anti-bonding π*-orbitals. We must draw these orbitals above the LGOs for σ-bonding into the MO diagram because the LGOs for σ-bonding have been formed from the CO HOMOs while the anti-bonding LGOs for π-bonding have been formed from the CO LUMOs. We can now combine the π-LGOs and metal d-orbitals of the same symmetry to form π-MOs. We see that we can combine the e-type LGOs with the non-bonding e-type metal d_{z^2} and $d_{x^2-y^2}$ orbitals to form a pair of bonding MOs of e-symmetry, and an anti-bonding pair of e-symmetry, which we can label 1e and 2e, respectively. Now what is the effect on the T_2-type π-LGOs? We first need to realize that we have already three sets of triple-degenerated t_2-MOs generated through σ-interactions. The interaction of the T_2-LGOs with the σ-t_2-MOs must create another set of triply-degenerated orbitals so that the overall number of orbitals with t_2-symmetry remains the same. The interaction will occur mostly between the $2t_2$ MO and the T_2-LGOs because the $2t_2$ MOs have the most similar energy to the T_2-LGOs. This leads to the lowering of the energy of the $2t_2$ MOs, so that these formerly weakly anti-bonding orbitals become weakly bonding. The additionally created t_2-orbitals are weakly anti-bonding. We can label them $3t_2$. The former anti-bonding $3t_2$ –orbital will be re-labeled $4t_2$. We can double-check that we have constructed the t_2-MOs correctly by verifying that the number of T_2-LGOs, and that includes σ and π, plus the number of metal T_2 orbitals equals the number of t_2 molecular orbitals. We see that the number of metal T_2 orbitals + the number of T_2 LGOs is 6+6=12. The number of t_2 MOs is 4×3 which is also 12.

Finally, we still need to fill the electrons. As previously mentioned, the π-LGOs as empty and therefore the ligand does not contributed any electrons to the π-bonding. The Ni is in the oxidation state 0 and thus contributes 10 electrons because Ni is in the 10th group of the periodic table. Because a neutral Ni atom has the electron configuration $3d^8 4s^2$ we can draw eight electrons in to the 3d orbitals and two electrons into the 4s orbitals. The $1t_1$ and the $1a_1$ MOs are already full with ligand electrons due to σ-bonding. Thus, the metal electrons must go into the 2e and the $2t_2$ MOs. Both the e-orbitals and the $2t_2$-orbitals are bonding, and thus we can say that the metal d-electrons have been stabilized due to the π-acceptor nature of the ligand. We see here an analogy to

the octahedral ligand field. Like in the octahedral ligand field π-acceptor ligands tend to lower the energy of the metal d-electrons. We can also ask: What is the effect of a π-acceptor ligand on Δ_T? The answer is: Like Δ_o gets larger in the octahedral ligand field, Δ_T gets larger in a tetrahedral ligand field. However, the increase is much smaller compared to the octahedral field. Why? this is because in the octahedral ligand field, the energy of the e_g orbitals is not affected through the π-acceptor interactions, and only the t_{2g} orbitals are lowered in energy. In the case of the tetrahedral ligand field both the energy of the e and the t_2 orbitals get lowered, and the energy of the e-orbitals gets only slightly more lowered than the energy of the t_2 –orbitals. Therefore, the Δ_T only slightly increases. This fact can also serve as an additional explanation why tetrahedral complexes never make low-spin complexes, even with strong π-accepting ligands. The effect of the ligand on Δ_T is simply still too small because both the energy of the e and the t_2 orbitals have been lowered.

Finally, let us discuss the results in the context of the 18 electron rule. We can see that the number of electrons involved in σ-bonding are in bonding molecular orbitals. Thus, it is justified to say that the ligand field theory is able to explain the 18 electrons rule.

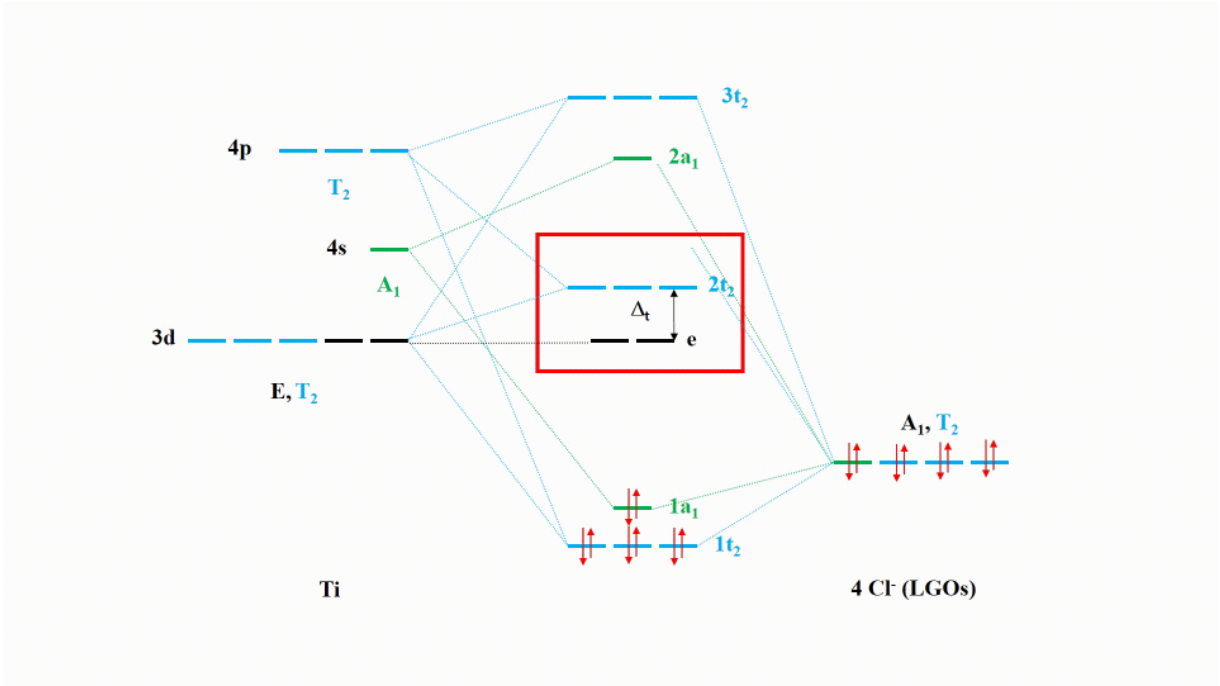


Figure 7.1.39 MO diagram of a tetrahedral complex of a 4th period transition metal (***π***-bonding with ***π***-donor)

Now let us think about how a π-donating ligand influences the magnitude of Δ_T. In this case we only need to consider the bonding E and T_2 ligand orbitals if the ligand has π-bonds. Those orbitals will be energetically below the LGOs for σ-bonding. If the ligand is a simple ion like chloride, then we would consider LGOs from the filled p-orbitals that that have suitable symmetry for π-overlap. Those LGOs would have the essentially the same energy as the σ-LGOs. Let us construct a qualitative MO diagram of $TiCl_4$ which has chloro ligands which are typical π-donating ligands. When constructing the MO diagram for π-bonding we can again start with the MO-diagram for σ-bonding, and then modify this diagram. We can first plot the filled π-T_2 and E_g LGOs with similar energy as the σ-LGOs on the right side of the diagram. The E ligand group orbitals will now interact with the e-metal orbitals. That interaction leads to a pair of bonding MOs of e-symmetry, and a pair of anti-bonding MOs of e-symmetry. This means that effectively, the formerly non-bonding e-metal orbitals become anti-bonding MOs, and move up in energy. The bonding e-type MO is created in addition and must have lower energy than the E-type π-LGOs. The interaction of the T_2-LGOs with the metal t_2-orbitals creates an additional set of bonding t_2-orbitals. The $2t_2$ orbitals move up in energy, and become more anti-bonding, as a consequence of that. We can just renumber the t_2 and the e MOs. Now we still need to fill the electrons into the MOs. The π-LGOs have overall eight electrons. These electrons will go into the newly formed bonding 1e and $1t_2$ molecular orbitals. We see that this leads to a stabilization of these electrons. This is an analogy to the octahedral ligand field. When we have a π-donor ligand,

then that the π-ligand electrons. What about the metal electrons. In $TiCl_4$ the Ti is in the oxidation state +4, therefore it is formally d^0, and it does not have any electrons. This explains the stability of the $TiCl_4$ as complex that does not obey the 18 electron rule. It has only 8 electrons, but the bonding situation is nonetheless ideal. All bonding MOs are full, and all others are empty. If the Ti had d electrons they would need to go into the 2e and the $3t_2$ orbitals which are both anti-bonding. This would destabilize the complex. In general π-donating ligands increase the energy of metal d-electrons, and this is another analogy to the octahedral ligand field. Now to the question, what is the effect of a π-donating ligand on Δ_T? Both the metal e and t_2 frontier orbitals have increased in energy but the e-orbitals more so than the t_2 orbitals. That means that the Δ_T has overall decreased. This is a further analogy to the octahedral ligand field. π-donating ligands lead to a smaller Δ_T.

Overall the ligand field theory can again provide an explanation for the spectrochemical series. π-donors lead to smaller Δ_T ligands, and thus the complex absorbs light of larger wavelengths, π-acceptors lead to larger Δ_T and those complexes absorb light of smaller wavelengths.

Square Planar Complex of a 4th Period Transition Metal

As a last example we will discuss now the molecular orbital diagram of a square planar complex. This will be the most complicated MO diagram we will discuss. The greater complexity stems from the lower symmetry in a square planar complex. It belongs to the point group D_{4h} whereas tetrahedral and octahedral complexes belong the high symmetry point groups T_d and O_h.

D_{4h}	E	$2C_4$ (z)	C_2	$2C'_2$	$2C''_2$	i	$2S_4$	σ_h	$2\sigma_v$	$2\sigma_d$	linear functions, rotations	quadratic functions
A_{1g}	+1	+1	+1	+1	+1	+1	+1	+1	+1	+1	-	x^2+y^2, z^2
A_{2g}	+1	+1	+1	-1	-1	+1	+1	+1	-1	-1	R_z	-
B_{1g}	+1	-1	+1	+1	-1	+1	-1	+1	+1	-1	-	x^2-y^2
B_{2g}	+1	-1	+1	-1	+1	+1	-1	+1	-1	+1	-	xy
E_g	+2	0	-2	0	0	+2	0	-2	0	0	(R_x, R_y)	(xz, yz)
A_{1u}	+1	+1	+1	+1	+1	-1	-1	-1	-1	-1	-	-
A_{2u}	+1	+1	+1	-1	-1	-1	-1	-1	+1	+1	z	-
B_{1u}	+1	-1	+1	+1	-1	-1	+1	-1	-1	+1	-	-
B_{2u}	+1	-1	+1	-1	+1	-1	+1	-1	+1	-1	-	-
E_u	+2	0	-2	0	0	-2	0	+2	0	0	(x, y)	-

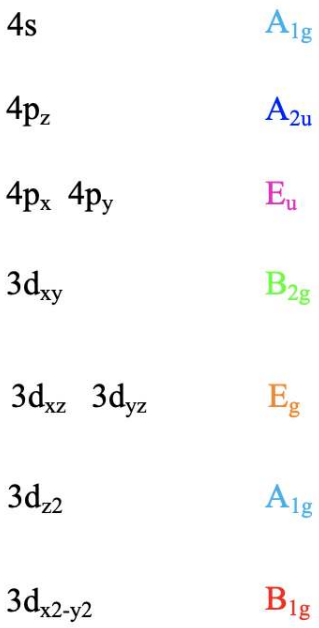


Figure 7.1.40 Character table for the D_{4h} point group and symmetry determination of the metal frontier orbitals.

The lower symmetry leads to a reduction in the degeneracy of the molecular orbitals. This creates more energy levels and hence a more complicated molecular orbital diagram. Let us think next about the definition of the axes. I would be sensible to define the xy plane as the plane of the molecule with the x and the y-coordinates going through the bonds. The z-axis would stand perpendicular to the plane of the molecule. What are the symmetry types of the metal frontier orbitals. Assuming a 4th period transition metal the 3d, the 4s, and the 4p orbitals would be the frontier orbitals. Looking into the character table of the point group D_{4h} (Fig. 7.1.10) shows that the symmetry of the 4s orbital is A_{1g}, the symmetry of the 4p orbitals is A_{2u} for the $4p_z$ orbital and e_u for the $4p_x$ and the $4p_y$ orbitals. The d orbitals have the symmetry types A_{1g}, B_{1g}, B_{2g}, and E_g for the $3d_{z^2}$, $d_{x^2-y^2}$, $3d_{xy}$, and $3d_{xz}/3d_{yz}$, respectively.

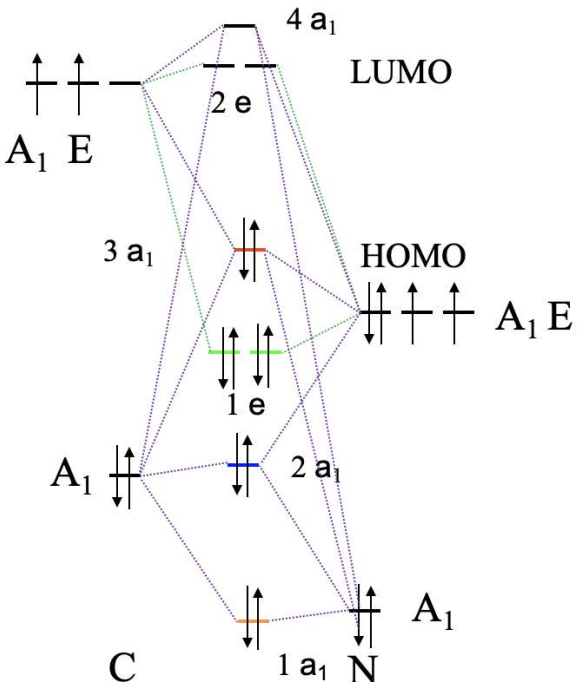


Figure 7.1.41 MO diagram of CN^-

Next, we to determine the ligand HOMOs suitable for σ-bonding. There are no square planar carbonyl complexes, therefore we will not choose the carbonyl ligand as a example ligand here. Instead we will use the related cyano ligand. The cyano ligand is isoelectronic with the carbonyl ligand. Formally, the O-atom in CO is replaced by N. Because N has one electron less than O, we must add one electron, giving the cyano ligand a 1- negative charge. Like in CO, the cyano ligand has a triple bond between C and N, and there is an electron lone pair at C, and one at N. The MO diagram is similar to that of CO, just the energy difference between C and N orbitals is somewhat smaller than that of the energy difference between C an O orbitals (Fig. 7.1.41). The number, symmetry, and energy order of the MOs of CN^- and CO is the same. Therefore, the CN^- has the same HOMOs suitable for σ-bonding, and we can select it for the construction of σ-MOs. Each ligand has one HOMO, therefore we have overall four HOMOs.

$$\Gamma_\sigma = A_{1g} + E_u + B_{1g}$$

Figure 7.1.42 LGOs for CN^-

We can group them to form LGOs and determine the symmetry types of the LGOs. The result is that there is on ligand group orbital with A_{1g} symmetry, there are two with E_u symmetry, and there is one with B_{1g} symmetry (Fig. 7.1.42).

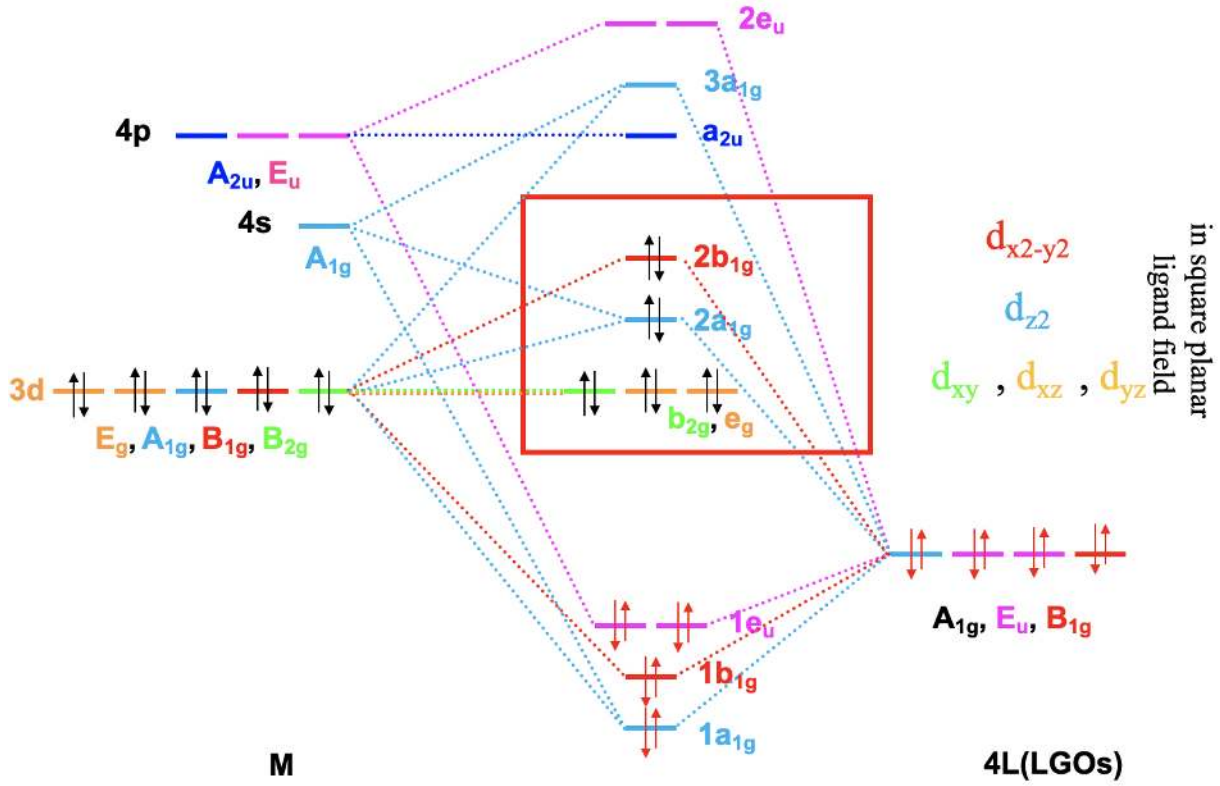


Figure 7.1.43 MO diagram for a square planar 4th period transition metal complex

We have now the all information necessary to construct a qualitative molecular orbital diagram for σ-bonding (Fig. 7.1.43). As usual we first plot the metal frontier orbitals on the left and the ligand group orbitals on the right side of the MO diagram, and label the symmetry types. Then, we need to combine metal frontier and ligand group orbitals of the same symmetry type to form molecular orbitals. We can for instance begin with the symmetry type A_{1g}. The 4s orbital and the $3d_{z^2}$ orbitals have this symmetry type, and so has one ligand group orbital. We will therefore get three molecular orbitals of that symmetry type, a bonding one, an approximately non-bonding one, and an anti-bonding molecular orbital. We plot them according to their expected energy into the MO diagram, and label the MOs $1a_{1g}$, $2a_{1g}$, and $3a_{1g}$, respectively. Next, we can look at the B_{1g} orbitals. The $3d_{x^2-y^2}$ orbital and one LGO of that symmetry type, and thus we can form a bonding and an anti-bonding MO from this combination. We can further see that we can combine the $4p_x$ and the $4p_y$ orbitals that have E_u symmetry with the remaining two LGOs of the same symmetry. This gives two double-degenerated bonding MOs of e_u symmetry, and two anti-bonding bonding ones of the same symmetry. Are there any orbitals with other symmetry types left? Yes, there are the metal d_{xy}, d_{xz}, and d_{yz} orbitals that have B_{2g}, and E_g symmetry, respectively, In addition, there is the p_z orbital that has a_{2u} symmetry. We can see that these metal orbitals do not find a partner. There is no LGO of these symmetry types. We therefore have to draw these orbitals as non-bonding orbitals into the MO diagram.

Now it is the time to fill the electrons into the molecular orbitals. The LGOs are occupied with electrons because they have been formed from the HOMOs of the ligand. Because we have four LGOs we have eight electrons to consider. These electron will therefore fill the $1a_1$, the $1b_{1g}$, and the $1e_u$ molecular orbitals. These orbitals are all bonding molecular orbitals. Thus, ligand field theory is able to explain the four bonds and the square planar shape of the molecule. Where would the metal d-electrons go? We could have up to ten d-electrons depending on the metal ion, and these ten electrons would go into the five MOs of the next higher energy. These are the non-bonding b_{2g} and e_g orbitals, the approximately-non-bonding $2a_{1g}$ orbital, and the anti-bonding $2b_{1g}$ orbital. We can consider these orbitals as the metal-d-orbitals in a square planar ligand field. The b_{2g} orbitals is the d_{z^2} orbital in the square planar ligand field, the e_g orbitals are d_{xz} and d_{yz} in a square planar ligand field, the $2a_{1g}$ orbital is the d_{z^2} orbital in a square planar ligand field and the $2b_{1g}$ orbital is the $d_{x^2-y^2}$ orbital in a square planar ligand field. We can see that these results are similar yet not completely analogous to those we obtained in the crystal field theory. Remember, that in the crystal field theory the $d_{x^2-y^2}$ orbital had also had the highest energy. However, the d_{z^2} was lower in energy than the d_{xy}, and the d_{xy} was not degenerate with the d_{xz} and the d_{yz} orbitals. The difference it due to the fact that in ligand field theory the d_{xy} orbital is considered non-bonding, not

interacting with the ligands at all, whereas in crystal field theory a strong electrostatic repulsion between the d_{xy} and the ligands is assumed because the d_{xy} orbital is in the plane of the molecule.

Square Planar Complex π-bonding

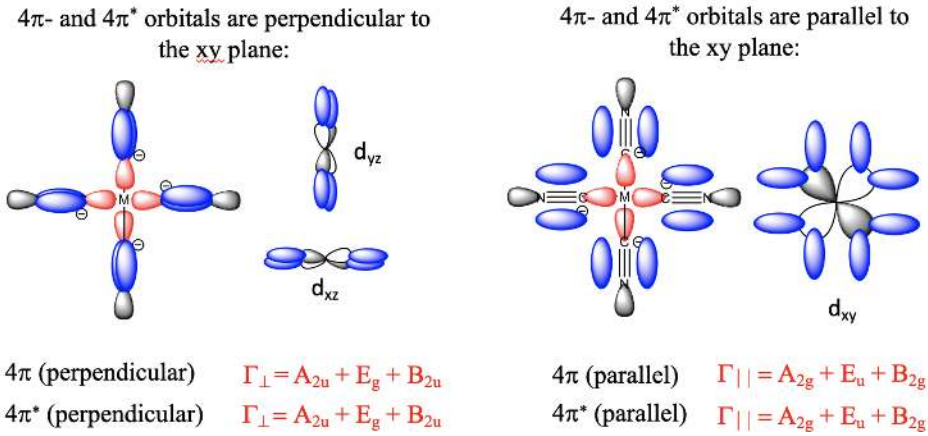


Figure 7.1.44 Square planar transition metal complexes: π-bonding

Now let us look at the π-bonding of a square planar transition metal complex (Fig. 7.1.44). If we assume a CN^- ligand, then the orbitals that have suitable symmetry to overlap with the metal frontier orbitals in π-fashion are the 1e and 2e π and π* orbitals from the MO diagram of CO. There are two π and two π* orbitals per ligand. Because we have four ligands there are overall eight π and eight π* orbitals. Now we need to consider that four of the π-orbitals are in the xy plane, while the other four are above and below the xy plane. We call the former the parallel orbitals, and the latter the perpendicular orbitals, because they are oriented parallel and perpendicular to the xy plane, respectively. We must distinguish them because they have a different symmetry and overlap differently with the metal d-orbitals. This is illustrated for the bonding π-orbitals in Fig. 7.1.44. The anti-bonding ones behave analogously. Therefore we group the orbitals to form four sets of ligand group orbitals $\pi_\perp$, $\pi_\parallel$, $\pi^*_\perp$, and $\pi^*_\parallel$. Our next task is to determine the symmetry types of these orbitals. We again omit the exact process, but only look at the results. Both the $\pi_\perp$ and the $\pi^*_\perp$ orbitals have one A_{2u}, two E_g and one B_{2u} ligand group orbitals. The $\pi_\parallel$ and $\pi^*_\parallel$ orbitals have one A_{2g}, two E_u, and one B_{2g} ligand group orbitals.

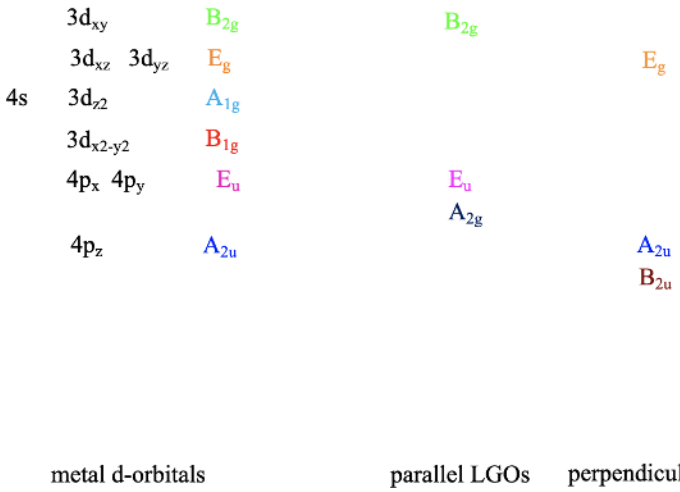


Figure 7.1.45 Symmetry types of metal frontier orbitals, parallel, and perpendicular LGOs for π-bonding

We now need to add the π-molecular orbitals to the molecular orbital diagram that we had constructed previously to account for σ-bonding. First, we need to consider which π-LGOs have the right symmetry to produce π-MOs with metal d-orbitals (Fig. 7.1.45). We can see that among the parallel LGOs the A_{1g} and the B_{1g} orbitals find partners, but not the E_u orbitals, For the perpendicular LGOs the E_g orbitals find partners, but not the A_{2u} and the B_{2u} orbitals. We therefore only need to consider the A_{1g}, the B_{1g} and the E_g LGOs. To make matters more complicated, to get a realistic MO diagram for a square planar complex with cyano ligands it is

necessary to consider the interactions of the 4s and the 4p orbitals with the π-LGOs as well. The symmetry of the 4s was A_{1g} and the symmetry of the 4p orbitals was A_{2u} and E_u, respectively. The 4s still does not find a partner, but the 4p orbitals do.

MO Diagram of a Square Planar Complex With a Cyano Ligand

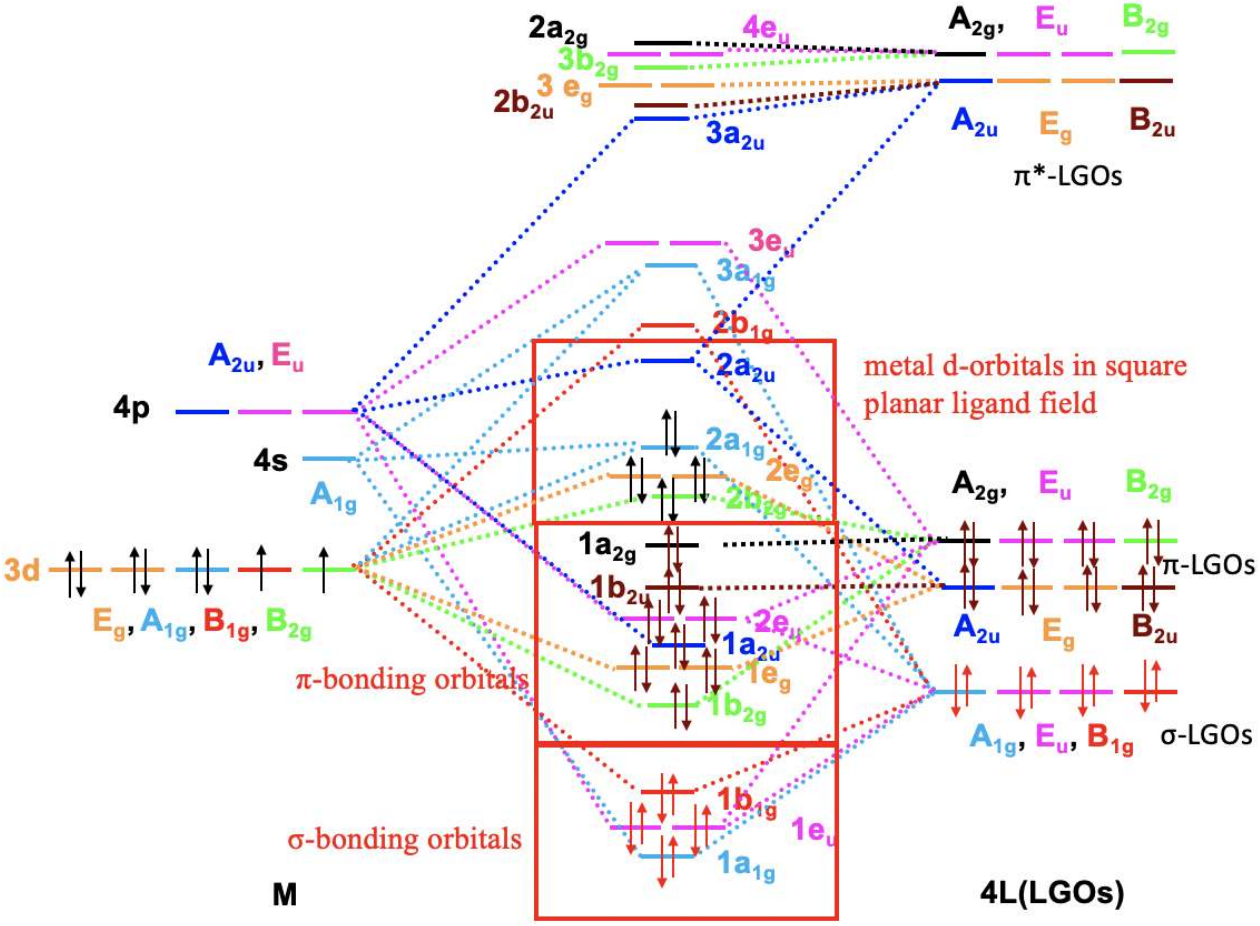


Figure 7.1.46 MO Diagram of a Square Planar Complex With a cyano Ligand under consideration of π-bonding.

Let us now construct the MO diagram of a square planar complex with a cyano ligand considering both σ and π-bonding for the example of the $Ni(CN)_4^{2-}$ complex anion. Because of the complexity of the diagram we will not modify the MO diagram for σ-bonding, like we did previously, but construct the complete MO diagram from scratch (Fig. 7.1.46). Like previously we can plot the metal 3d, 4s, and 4p orbitals on the left side of the diagram. On the right side of the diagram are now the LGOs for σ as well as π-bonding. For the $Ni(CN)_4^{2-}$ complex the σ-LGOs are energetically somewhat below the metal d-orbitals, the bonding π-LGOs have about the same energy as the metal d-orbitals, and the anti-bonding π*-LGOs have an energy significantly higher than the 4p orbitals. We can again construct MOs symmetry type by symmetry type until the MO diagram is complete. We can start with the symmetry type A_{1g}. We see there is only one σ-LGO that interacts with the 4s and the $3d_{z^2}$ which also have A_{1g} symmetry. That leads to a bonding, an approximately non-bonding, and anti-bonding a_{1g} MO which we can label $1a_{1g}$, $2a_{1g}$, and $3a_{1g}$, respectively. Next, we can for instance look at the B_{2g} orbitals. There is one d-orbital that has that symmetry, as well as two LGOs. The interaction is almost only with the bonding B_{2g} LGO because the energies are similar. This leads to a bonding and an anti-bonding π-MO with B_{2g} symmetry. The anti-bonding LGO is too high in energy and it does not significantly interact. Therefore we can draw it with the same energy into the MO-diagram. Now let us go to the B_{1g} orbitals. There is a metal d-orbital with B_{1g} symmetry, and a σ-LGO with B_{1g} symmetry. This produces a bonding and anti-bonding MO with B_{1g} symmetry. Now let us go to the E_g orbitals. There are two E_g metal d-orbitals, two E_g π-LGOs and two E_g π*-LGOs. Again, the π*-LGOs are too far off in energy, so that the bonding interaction is mostly between metal orbital the π-LGOs. This leads to a pair of bonding MOs and a pair of anti-bonding MOs. The π*-LGOs can be drawn with unchanged energy into the MO-diagram. The 4p orbitals of the metal have symmetry types, we have not considered yet: A_{2u} and E_u. Let us begin with the E_u orbitals. There are two σ-E_u LGOs, two π-E_u-LGOs and two π*-E_u LGOs. Overall we have four pairs of E_U-orbitals, and we would therefore expect four pairs of e_u-MOs. We

can make the approximation that there will be a bonding one, a weakly bonding one, a weakly anti-bonding one, and a strongly anti-bonding one. We can label them $1e_u$, $2e_u$, $3e_u$, and $4e_u$, respectively. The $4e_u$ has almost only contributions from the anti-bonding π^*-E_U LGOs due to energy arguments, therefore it is only connected to these via a dotted line, and not to the other E_u orbitals. Now to the A_{2u} orbitals: There is a π and a π^*-orbital of A_{2u} symmetry that can be combined with the 4p A_{2u} orbitals. This leads to three A_{2u} MOs overall, one bonding, one approximately non-bonding, and one anti-bonding one. Now we have used all metal d-orbitals. We notice that there are still some LGOs that we have not used. These are the π and π^* A_{2g} and the B_{2u} LGOs. They remain non-bonding can be drawn accordingly in the MO diagram.

We now need to fill the electrons into the MO-diagram. Firstly, there are the σ-electrons to consider. There are overall eight electrons stemming from the four occupied σ-LGOs. We can fill these eight electrons into the four MOs with the lowest energy. These are the $1a_1$, the $1e_u$ and the $1b_1$. These are all bonding MOs explaining the four σ-bonds within the complex. We can call these four orbitals the σ-bonding orbitals. Next we need to consider the electrons in the π-LGOs. There are overall eight of these orbitals containing 16 electrons. We must fill these electrons into the eight MOs of the next-higher energies. These are the $1b_{2g}$, the $1e_g$, the $1a_{2u}$, the $2e_u$, the $1b_{2u}$, and the $1a_{2g}$ orbitals. We see that these orbitals are either bonding or non-bonding, and thus overall the ligand π-electrons get stabilized due to the π-interactions with the ligand. We can call these orbitals the π-bonding molecular orbitals. Finally we need to look at the metal d-electrons. We assume Ni as the metal with Ni in the oxidation state +2 and d^8 electron configuration. We need to fill these eight electrons into the four next higher-energy MOs. This fills the $2b_{2g}$, the $2e_g$, and the $2a_{1g}$, orbitals which are either non-bonding or anti-bonding. This means that the metal electrons are overall destabilized. This behavior is consistent with the cyano-ligand acting as a π-donating ligand. We understand from this why square planar complexes prefer 16 over 18 electrons and disobey the 18 electron rule. If we had two more electrons then these would need to go into the energetically much higher $2a_{2u}$ orbitals. The energy gap between the $2a_{2u}$ and the $2a_{1g}$ orbital is significantly higher than that between the $1a_{1g}$, the $2b_{2g}$, and the $2e_g$ orbitals. Overall we can call the $2a_u$, the $2a_{1g}$, the $2e_g$, and the $2b_g$ orbitals the metal d-orbitals in a square planar ligand field. In a square planar ligand field we have three Δ_s. Δ_3 is the energy difference between the $2b_{2g}$ and the $2e_g$ orbitals, Δ_2 is the energy difference between the $2e_g$ and the $2a_{1g}$ orbitals, and Δ_1 is the energy between the $2a_{1g}$ and the $2a_{2u}$ orbitals. Δ_1 is much larger than the other two. It also almost always larger than the spin-pairing energy, therefore square planar complexes are almost always low-spin complexes.

Overall, we see that an MO diagram can become very complex even for a relatively simple molecule of relatively high symmetry. It should be noted that for MO diagrams as complex as this one, it is not possible any more determine the exact order of the energy levels just by qualitative inspection, and without exact computations. Nonetheless, you can see that it is possible to readily understand a complex MO diagram by following the symmetry-adapted linear combination of atomic orbitals approach. We just need to go through the symmetry types step by step and construct MOs by combining orbitals of the the same symmetry type until the process is completely. We have now reached the end of the chapter on ligand field theory.

Dr. Kai Landskron (Lehigh University). If you like this textbook, please consider to make a donation to support the author's research at Lehigh University: Click Here to Donate.

This page titled 6.1: 7.1 Bonding in Coordination Compounds is shared under a not declared license and was authored, remixed, and/or curated by Kai Landskron.

- **7.1: Bonding in Coordination Compounds** by Kai Landskron is licensed CC BY 4.0.

6.2: Concept Review Questions Chapter 7

Concept Review Questions

Section 1

1. What should a good theory be able to do?

2. What should a good bonding theory be able to do?

3. What is the major conceptual difference between valence bond theory of main group compounds with regular covalent bonds vs. coordination compounds with dative bonds?

4. Valence bond theory cannot explain optical properties of molecules. Explain why.

5. Explain the concept of crystal field theory.

6. Explain why the energy of the d_{z2} and the d_{x2-y2} orbitals in the octahedral crystal field is higher than that of the d_{xz}, the d_{yz}, and the d_{xy} orbitals.

7. Explain why the the d_{z2} and the d_{x2-y2} orbitals have the exactly the same energy in the octahedral crystal field.

8. Explain why the energy of the d_{xz}, the d_{yz}, and the d_{xy} orbitals are decreased by exactly 2/5 Δ_o.

9. Explain why the energy of the d_{xz}, the d_{xy}, and the d_{yz} orbitals are higher than the energy of d_{z2}, d_{x2-y2} orbitals in the tetrahedral crystal field.

10. Explain why the energies of the d_{xz}, the d_{xy}, and the d_{yz} orbitals are exactly the same in the tetrahedral crystal field.

11. Explain why the tetrahedral crystal field is smaller than the octahedral crystal field ($\Delta_T = 4/9\Delta_O$).

12. Which orbital energies increase and which ones decrease when an octahedral crystal field tetragonally distorts (elongated octahedra)? Explain why.

13. Explain why octahedral complexes of d^9 ions frequently distort tetragonally.

14. Explain the relationships between a tetragonally distorted octahedral crystal field and a square planar crystal field.

15. Explain why crystal field theory can explain why complexes with d^8 ions are often square planar.

16. Explain how crystal field theory explains high-spin and low-spin complexes.

17. Explain why crystal field theory can make statements about the electronic spectra of complexes.

18. What is meant by the spectrochemical series?

19. What is the relationship between molecular orbital theory and ligand field theory?

20. Describe the steps involved to construct a molecular orbital diagram in ligand field theory?

21. Why can ligand field theory explain the magnetic properties of coordination compounds?

22. Why is ligand field theory able to explain electronic spectra?

23. What are the relationships between crystal field theory and ligand field theory?

24. What is a π-donating ligand and what is a π-accepting ligand?

25. How do π-donating ligands change Δ_O in octahedral complexes? Explain briefly.

26. How do π-accepting ligands change Δ_O in octahedral complexes? Explain briefly.

27. How does ligand field theory explain the spectrochemical series?

28. How does ligand field theory explain that there are no low spin complexes for tetrahedral compounds?

29. What is the strength of π-bonding in tetrahedral complexes vs. octahedral complexes? Explain why.

Dr. Kai Landskron (Lehigh University). If you like this textbook, please consider to make a donation to support the author's research at Lehigh University: Click Here to Donate.

6.2: Concept Review Questions Chapter 7 is shared under a not declared license and was authored, remixed, and/or curated by LibreTexts.

- **Concept Review Questions Chapter 7** by Kai Landskron is licensed CC BY 4.0.

6.3: Homework Problems Chapter 7

Homework Problems

Section 1

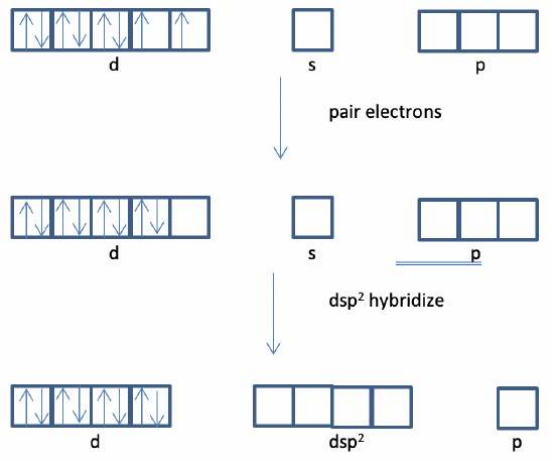
Exercise 1

Decide if valence bond theory is able to explain shapes of the following species. Explain your decision using appropriate electron box diagrams.

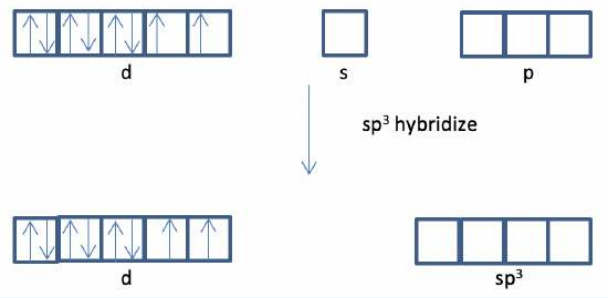
a. $PdCl_4^{2-}$ (square planar)
b. $NiCl_4^{2-}$ (tetrahedral)
c. $Cr(CO)_6$ (octahedral)
d. $ZnCl_4^{2-}$ (tetrahedral)
e. $Ag(NH_3)_2^{+}$ (linear)
f. $Au(PPh_3)_3^{+}$ (trigonal planar)
g. $Cu(NH_3)_4^{2+}$ (tetrahedral)

Answer

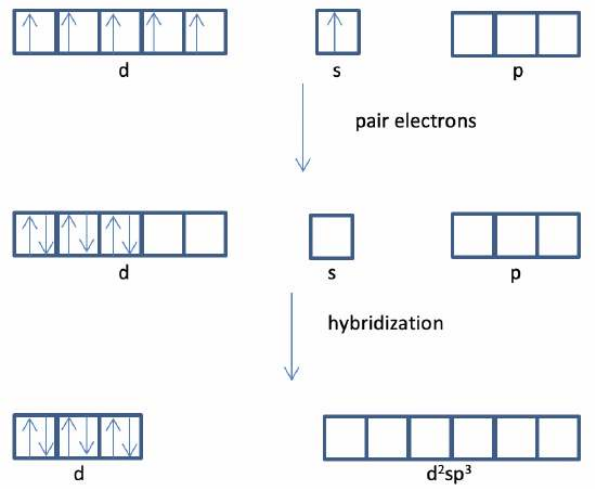
a) No. One would need to move an electron from one half-filled d-orbital into the other half-filled d-orbital. This would require to reverse the spin of the electron which is quantum-mechanically not allowed.



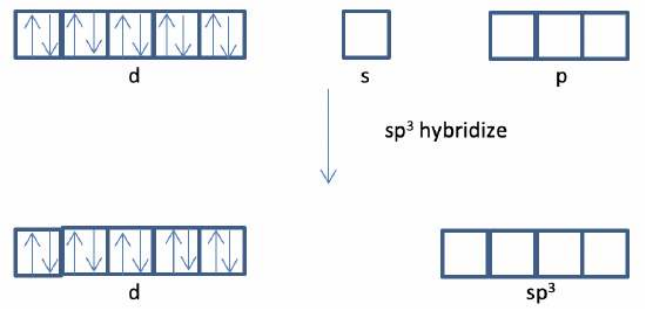
b) Yes, because s and p orbitals are empty and can be sp^3 hybridized:



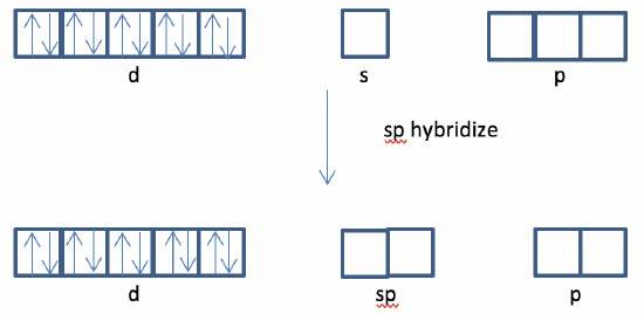
c) No, because one would need to move and spin-pair one s and two d electrons under spin-reversal.



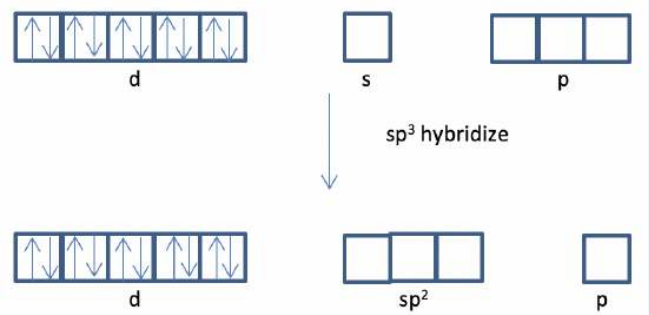
d) Yes, because empty s and p orbitals are available for hybridization



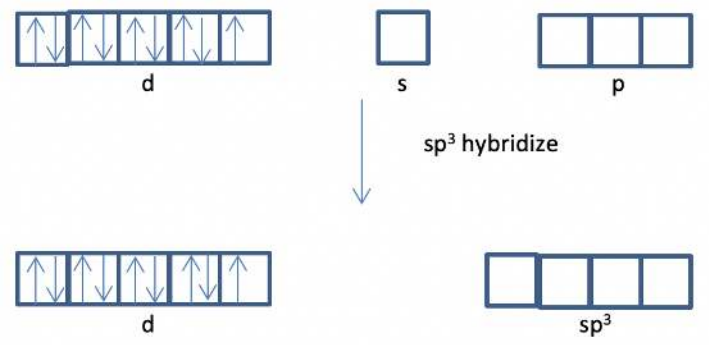
e) Yes, because empty s and p orbitals are available for sp hybridization which is able to explain linear shape.



f) Yes, because empty s and p orbitals are available for sp^2 hybridization which is able to explain trigonal planar shape.



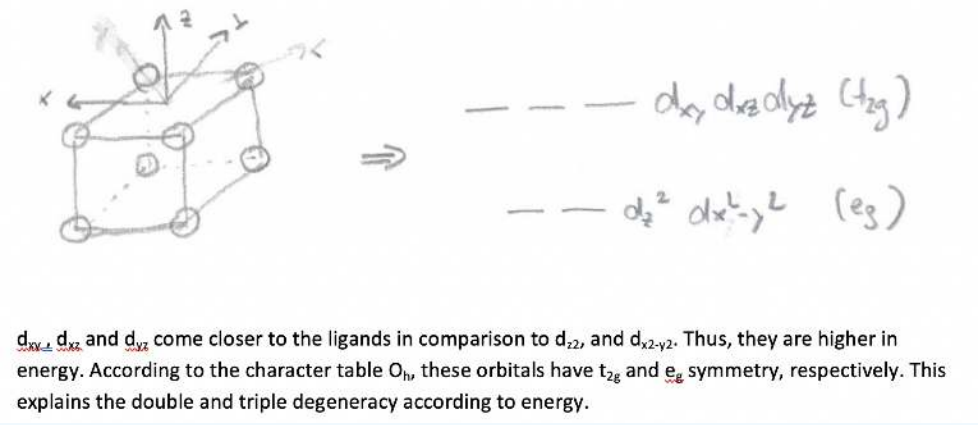
g) Yes, because empty s and p orbitals are available for sp^3 hybridization which is able to explain tetrahedral shape.



Exercise 2

We assume a hypothetical cubic crystal field. Predict how the energies of the metal d-orbitals split in this crystal field? Explain your decision briefly. What is the symmetry of these orbitals?

Answer



d_{xy}, d_{xz} and d_{yz} come closer to the ligands in comparison to d_{z2}, and d_{x2-y2}. Thus, they are higher in energy. According to the character table O_h, these orbitals have t_{2g} and e_g symmetry, respectively. This explains the double and triple degeneracy according to energy.

Exercise 3

The octahedral crystal field Δ_O for a d^4 metal complex is larger than the spin pairing energy. How many unpaired electrons would you expect in this complex?

Answer

I would expect two unpaired electrons.

Exercise 4

Verify by applying the symmetry adapted linear combination of atomic orbitals (SALC) method that the ligand group orbitals suitable for sigma bonding have the symmetry types A_g, E_g, and T_{1u} for an octahedral complex.

Answer

	E	C_3	C_2	C_4	C_2	i	S_4	S_6	σ_h	σ_d
Γ=	6	0	0	2	2	0	0	0	4	2

$\#A_g = 1/48\ (6x1x1 + 0 + 0 + 2x6x1 + 2x3x1 + 0 + 0 + 0 + 4x3x1 + 2x6x1) = 1$

$\#E_g = 1/48\ (6x1x2 + 0 + 0 + 0 + 2x3x2 + 0 + 0 + 0 + 4x3x2 + 0) = 1$

$\#T_{1u} = 1/48\ (6x1x3 + 0 + 0 + 2x6x1 + 2x3x(-1) + 0 + 0 + 0 + 4x3x1 + 2x6x1) = 1$

Because the overall number of LGOs must six, there will be no other LGOs with other symmetry types..

Exercise 5

Can the 4p orbitals of a period 4 transition metal also make pi-bonding with the ligands in an octahedral complex? Explain your decision briefly?

Answer

Yes, the 4p orbitals have T_{1u} symmetry which is suitable to make pi-bonding with the T_{1u} pi-ligand group orbitals.

Exercise 6

Which of the following ligands would you expect to be π-acceptors? Explain your decision briefly.

a) NO^+

b) H^-

c) Cl^-

d) CH_3^-

Answer

Only NO^+, because it is the only ligand that has π^*-orbitals.

Exercise 7

A general trigonal planar complex of the composition M(CN)3 is given. How many π- and π^* orbitals of the ligands will be involved in the π-bonding?

Answer

3*4=12 orbitals

Exercise 8

The energies of the metal d orbitals of the above complex are -24 eV. The energies of the π-orbitals of the ligand are -27 eV, the energies of the π*-orbitals are -10 eV. Would you expect the ligand to act as a π-donor or as a π-acceptor? Why?

Answer

It would act as a pi-donor, because the energy of the pi-orbitals is much closer to the energy of the metal d orbitals.

Exercise 9

Two octahedral complexes MX_6 and MY_6 are given. The energy of the ligand HOMOs suitable for sigma-bonding is about the same, but the orbital overlap between the metal and the ligand Y is significantly greater than the orbital overlap between the ligand X and the metal. For which complex would you expect a larger Δ_O?

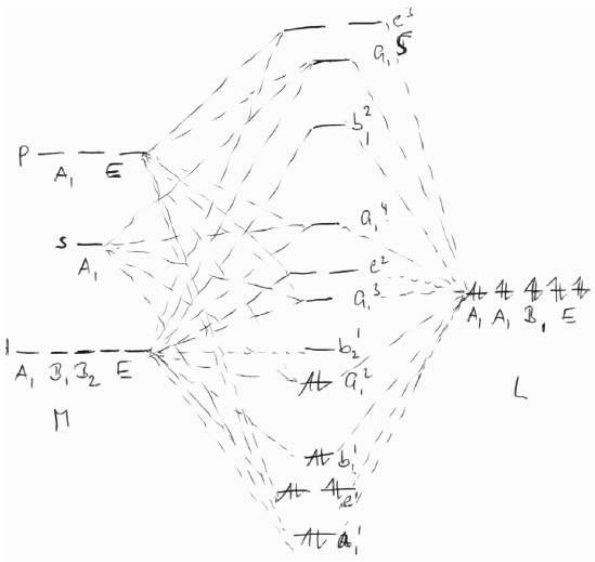
Answer

Δ_O will be greater for the orbitals with the ligand Y. This is because the stronger interactions raise the energy of the e_g^* orbitals, and thus the energy difference between these orbitals and the t_{2g} orbitals becomes larger.

Exercise 10

Construct a qualitative molecular orbital diagram of a square pyramidal complex using the symmetry adapted linear combination of atomic orbitals approach. Consider sigma-bonding only.

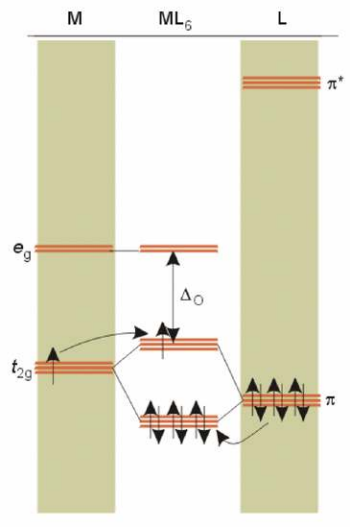
Answer



Exercise 11

Strong π-donating ligands lead to a decrease of the octahedral ligand field Δo. Illustrate this by sketching the relevant part of MO diagram.

Answer



Dr. Kai Landskron (Lehigh University). If you like this textbook, please consider to make a donation to support the author's research at Lehigh University: Click Here to Donate.

6.3: Homework Problems Chapter 7 is shared under a not declared license and was authored, remixed, and/or curated by LibreTexts.

- **Homework Problems Chapter 7** by Kai Landskron is licensed CC BY 4.0.

CHAPTER OVERVIEW

7: Metals and Alloys- Structure, Bonding, Electronic and Magnetic Properties

Learning Objectives

- Identify and assign unit cells, coordination numbers, asymmetric units, numbers of atoms contained within a unit cell, and the fraction of space filled in a given structure.
- Relate molecular orbital theory to the delocalization of valence electrons in metals.
- Understand the concepts of electron wavelength and density of states.
- Understand the consequences of the nearly free electron model for the band structure of metals and their conductivity.
- Explain why some metals are magnetic and others are diamagnetic, and how these phenomena relate to bonding and orbital overlap.
- Use the Curie-Weiss law to explain the temperature dependence of magnetic ordering.
- Acquire a physical picture of different kinds of magnetic ordering and the magnetic hysteresis loops of ferro- and ferrimagnets.

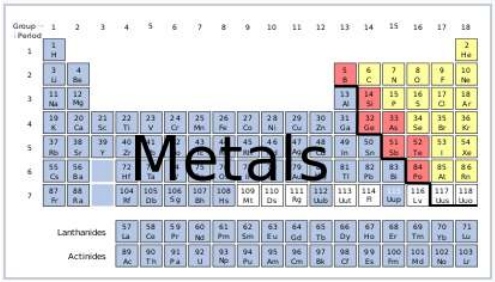
It should come as no surprise that the properties of extended solids are also connected to their structures, and so to understand what they do we should begin with their crystal structures. Most of the metals in the periodic table have relatively simple structures and so this is a good place to begin.

7.1: Prelude to Metals and Alloys
7.2: Unit Cells and Crystal Structures
7.3: Bravais Lattices
7.4: Crystal Structures of Metals
7.5: Bonding in Metals
7.6: Conduction in Metals
7.7: Atomic Orbitals and Magnetism
7.8: Ferro-, Ferri- and Antiferromagnetism
7.9: Hard and Soft Magnets
7.10: Discussion Questions
7.11: Problems
7.12: References

7: Metals and Alloys- Structure, Bonding, Electronic and Magnetic Properties is shared under a CC BY-SA license and was authored, remixed, and/or curated by LibreTexts.

7.1: Prelude to Metals and Alloys

In the chemistry of molecular compounds, we are accustomed to the idea that properties depend strongly on structure. For example we can rationalize the polarity of the water molecule based on its shape. We also know that two molecules with the same composition (e.g., ethanol and dimethyl ether) have very different properties based on the bonding arrangements of atoms. It should come as no surprise that the properties of extended solids are also connected to their structures, and so to understand what they do we should begin with their crystal structures. Most of the metals in the periodic table have relatively simple structures and so this is a good place to begin. We will see in Chapter 8 that the structures of more complex compounds are also in many cases related to the simple structures of metals and alloys.



Over 2/3 of the elements in the periodic table exist in their pure form as metals. All elemental metals (except the three - Cs, Ga, Hg - that are liquid) are crystalline solids at room temperature, and most have one of three simple crystal structures.

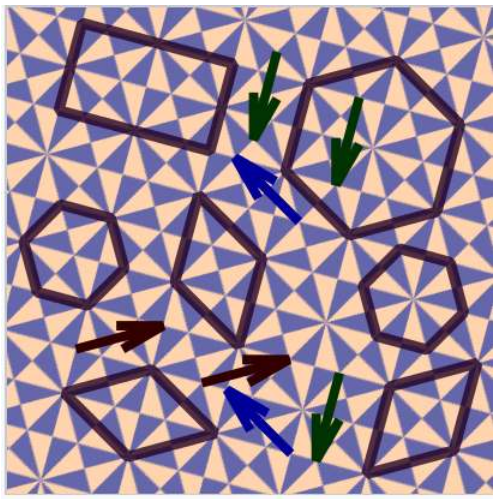
7.1: Prelude to Metals and Alloys is shared under a CC BY-SA license and was authored, remixed, and/or curated by LibreTexts.

- **6.1: Prelude to Metals and Alloys** by Chemistry 310 is licensed CC BY-SA 4.0. Original source: https://en.wikibooks.org/wiki/Introduction_to_Inorganic_Chemistry.

7.2: Unit Cells and Crystal Structures

Crystals can be thought of as repeating patterns, much like wallpaper or bathroom tiles, but in three dimensions. The fundamental repeating unit of the crystal is called the **unit cell**. It is a three dimensional shape that can be repeated over and over by unit translations to fill space (and leave minimal gaps) in the structure. Some possible unit cells are shown in the tiling pattern at the right, along with arrows that indicate **unit translation vectors**. In three dimensions, the hexagonal or rhombic unit cells of this pattern would be replaced by three dimensional boxes that would stack together to fill all space. As shown in the figure, the origin of the unit cell is arbitrary. The same set of boxes will fill all space no matter where we define the origin of the lattice. We will see that pure metals typically have very simple crystal structures with cubic or hexagonal unit cells. However the crystal structures of alloys can be quite complicated.

When considering the crystal structures of metals and alloys, it is not sufficient to think of each atom and its neighboring ligands as an isolated system. Instead, think of the entire metallic crystal as a network of atoms connected by a sea of shared valence electrons. The **electrons are delocalized** because there are **not enough of them** to fill each "bond" between atoms with an electron pair. For example, in the crystal structures of s-block and p-block metals, each atom has either 8 or 12 nearest neighbors, but the maximum number of s + p electrons is 8. Thus, there are not enough to put two electrons between each pair of atoms. Transition metals can also use their d-orbitals in bonding, but again there are never enough electrons to completely fill all the "bonds."



Possible unit cells in a periodic tile pattern. The arrows connect translationally equivalent points (lattice points) in the pattern.

The atoms in a metal lattice arrange themselves in a certain pattern which can be represented as a 3D box structure known as the **unit cell** which repeats across the entire metal.

Simple Cubic	Body Centered Cubic	Face Centered Cubic	Hexagonal Close Packed
Simple cubic.svg	Lattice body centered cubic.svg	Lattice face centered cubic.svg	Hexagonal close packed.png
1 atom/cell	2 atoms/cell	4 atoms/cell	2 atoms/cell

Metal atoms can be approximated as spheres, and therefore are not 100 % efficient in packing, the same way a stack of cannonballs has some empty spaces between the balls. Different unit cells have different packing efficiencies. The number of atoms that is included in the unit cell only includes the fractions of atoms *inside* of the box. Atoms on the corners of the unit cell count as ⅛ of an atom, atoms on a face count as ½, an atom in the center counts as a full atom. Using this, let's calculate the number of atoms in a simple cubic unit cell, a face centered cubic (fcc) unit cell, and a body centered cubic (bcc) unit cell.

Simple Cubic:

8 corner atoms × ⅛ = 1 atom/cell. The packing in this structure is not efficient (52%) and so this structure type is very rare for metals.

Body Centered Cubic, bcc:

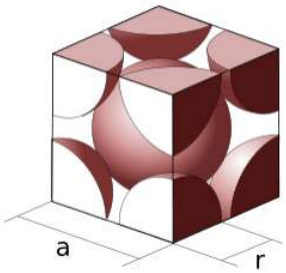
(8 corner atoms × ⅛) + (1 center atom × 1)= 2 atoms/cell. The packing is more efficient (68%) and the structure is a common one for alkali metals and early transition metals. Alloys such as brass (CuZn) also adopt these structures.

Face Centered Cubic, fcc (also called Cubic Close Packed, ccp):

(8 corner atoms × ⅛)+ (6 face atoms × ½)= 4 atoms/cell. This structure, along with its hexagonal relative (hcp), has the most efficient packing (74%). Many metals adopt either the fcc or hcp structure.

Hexagonal Close Packed, hcp:

Like the fcc structure, the packing density of hcp is 74%.

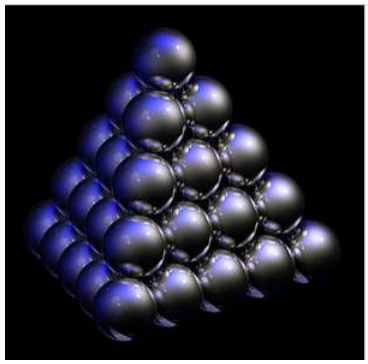


The unit cell of a bcc metal contains two atoms.

Calculating the packing fraction. The packing fractions of the crystal structures shown above can be calculated by dividing the volume of the atoms in the cell by the volume of the cell itself. The volume of the atoms in the cell is equal to the number of atoms/cell times the volume of a sphere, $(4/3)\pi r^3$. The volume of the cubic cells is found by cubing the side length. As an example, let's calculate the packing efficiency of a simple cubic unit cell. As we saw earlier in the section, a simple cubic unit cell contains one atom. The side length of the simple cubic unit cell is 2r, since the centers of each atom occupy the corners of the unit cell.

$$\text{Packing efficiency} = \frac{(1\ atom) \times (\frac{4}{3})\pi r^3}{(2r)^3} = 0.523 \tag{7.2.1}$$

The same method can be applied to bcc and fcc structures.



Face-centered cubic stack of cannonballs.

7.2: Unit Cells and Crystal Structures is shared under a CC BY-SA license and was authored, remixed, and/or curated by LibreTexts.

- **6.2: Unit Cells and Crystal Structures** by Chemistry 310 is licensed CC BY-SA 4.0. Original source: https://en.wikibooks.org/wiki/Introduction_to_Inorganic_Chemistry.

7.3: Bravais Lattices

Crystal lattices can be classified by their **translational** and **rotational symmetry**. In three-dimensional crytals, these symmetry operations yield 14 distinct lattice types which are called **Bravais lattices**. In these lattice diagrams (shown below) the dots represent lattice points, which are places where the whole structure repeats by translation. For example, in the body-centered cubic (**bcc**) structure of sodium metal, which is discussed below, we put one atom at the corner lattice points and another in the center of the unit cell. In the NaCl structure, which is discussed in Chapter 8, we place one NaCl formula unit on each lattice point in the face-centered cubic (**fcc**) lattice. That is, one atom (Na or Cl) would be placed on the lattice point and the other one would be placed halfway between. Similarly, in the cubic diamond structure, we place one C_2 unit around each lattice point in the fcc lattice.

The fourteen Bravais lattices fall into seven **crystal systems** that are defined by their rotational symmetry. In the lowest symmetry system (**triclinic**), there is no rotational symmetry. This results in a unit cell in which none of the edges are constrained to have equal lengths, and none of the angles are 90º. In the **monoclinic** system, there is one two-fold rotation axis (by convention, the b-axis), which constrains two of the angles to be 90º. In the **orthorhombic** system, there are three mutually perpendicular two-fold axes along the three unit cell directions. **Orthorhombic** unit cells have three unequal unit cell edges that are mutually perpendicular. **Tetragonal** unit cells have a four-fold rotation axis which constrains all the angles to be 90º and makes the a and b axes equivalent. The **rhombohedral** system has a three-fold axis, which constrains all the unit cell edges and angles to be equal, and the **hexagonal** system has a six-fold axis, which constrains the a and b lattice dimensions to be equal and the angle between them to be 120º. The **cubic** system has a three-fold axis along the body diagonal of the cube, as well as two-fold axes along the three perpendicular unit cell directions. In the cubic system, all unit cell edges are equal and the angles between them are 90º.

The translational symmetry of the Bravais lattices (the lattice **centerings**) are classified as follows:

- Primitive (P): lattice points on the cell corners only (sometimes called simple)
- Body-Centered (I): lattice points on the cell corners with one additional point at the center of the cell
- Face-Centered (F): lattice points on the cell corners with one additional point at the center of each of the faces of the cell
- Base-Centered (A, B, or C): lattice points on the cell corners with one additional point at the center of each face of one pair of parallel faces of the cell (sometimes called end-centered)

Not all combinations of the crystal systems and lattice centerings are unique. There are in total 7 × 6 = 42 combinations, but it can be shown that several of these are in fact equivalent to each other. For example, the monoclinic I lattice can be described by a monoclinic C lattice by different choice of crystal axes. Similarly, all A- or B-centred lattices can be described either by a C- or P-centering. This reduces the number of combinations to 14 conventional Bravais lattices, shown in the table below.

When the fourteen Bravais lattices are combined with the **32 crystallographic point groups**, we obtain the **230 space groups**. These space groups describe all the combinations of symmetry operations that can exist in unit cells in three dimensions. For two-dimensional lattices there are only 17 possible plane groups, which are also known as wallpaper groups.

Crystal family	Lattice system	Schönflies	14 Bravais Lattices			
			Primitive	Base-centered	Body-centered	Face-centered
Triclinic		C_i	Triclinic			
Monoclinic		C_{2h}	Monoclinic, simple	Monoclinic, centered		
Orthorhombic		D_{2h}	Orthorhombic, simple	Orthorhombic, base-centered	Orthorhombic, body-centered	Orthorhombic, face-centered
Tetragonal		D_{4h}	Tetragonal, simple		Tetragonal, body-centered	
Hexagonal	rhombohedral	D_{3d}	Rhombohedral			
	hexagonal	D_{6h}	Hexagonal			
Cubic		O_h	Cubic, simple		Cubic, body-centered	Cubic, face-centered

7.3: Bravais Lattices is shared under a CC BY-SA license and was authored, remixed, and/or curated by LibreTexts.

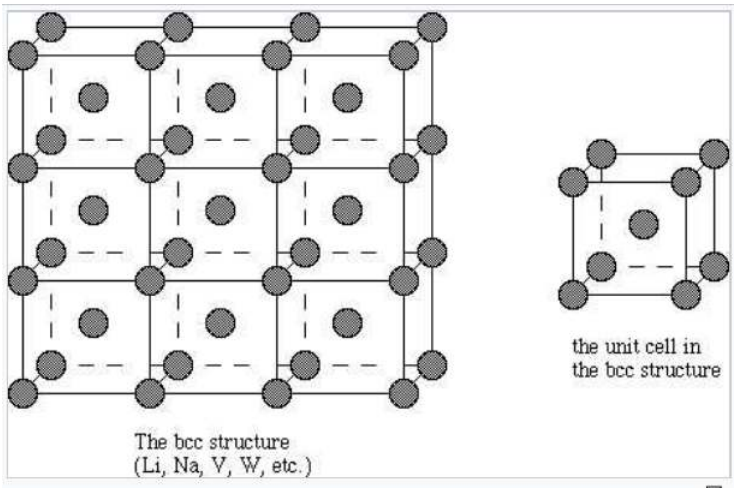
- **6.3: Bravais Lattices** by Chemistry 310 is licensed CC BY-SA 4.0. Original source: https://en.wikibooks.org/wiki/Introduction_to_Inorganic_Chemistry.

7.4: Crystal Structures of Metals

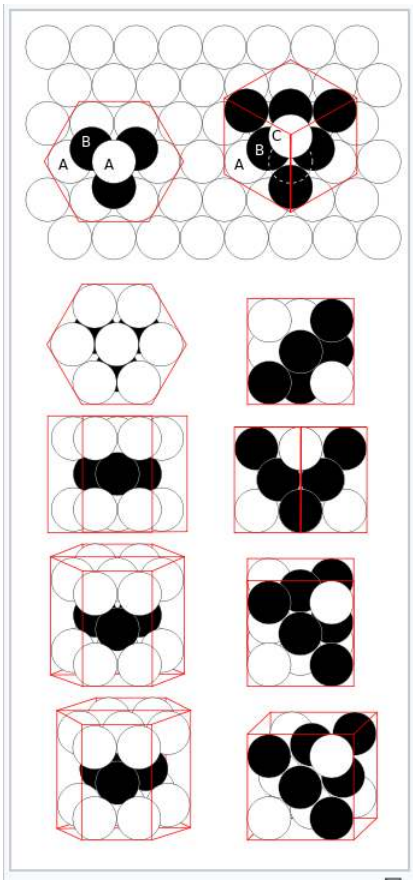
The Crystalline Nature of Metals

All metallic elements (except Cs, Ga, and Hg) are crystalline solids at room temperature. Like ionic solids, metals and alloys have a very strong tendency to crystallize, whether they are made by thermal processing or by other techniques such as solution reduction or electroplating. Metals crystallize readily and it is difficult to form a glassy metal even with very rapid cooling. Molten metals have low viscosity, and the identical (essentially spherical) atoms can pack into a crystal very easily. Glassy metals can be made,

however, by rapidly cooling alloys, particularly if the constituent atoms have different sizes. The different atoms cannot pack in a simple unit cell, sometimes making crystallization slow enough to form a glass.



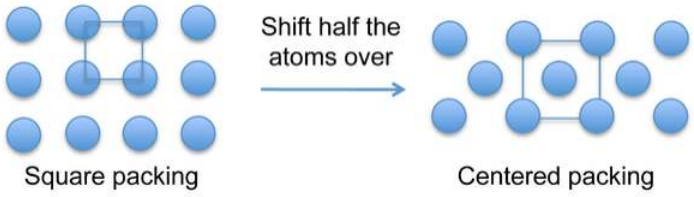
Body-centered cubic



hcp (left) and fcc (right) close-packing of spheres

Crystal structures

Most metals and alloys crystallize in one of three very common structures: body-centered cubic (bcc), hexagonal close packed (hcp), or cubic close packed (ccp, also called face centered cubic, fcc). In all three structures the coordination number of the metal atoms (i.e., the number of equidistant nearest neighbors) is rather high: 8 for bcc, and 12 for hcp and ccp. We can contrast this with the low coordination numbers (i.e., low valences - like 2 for O, 3 for N, or 4 for C) found in nonmetals. In the bcc structure, the nearest neighbors are at the corners of a cube surrounding the metal atom in the center. In the hcp and ccp structures, the atoms pack like stacked cannonballs or billiard balls, in layers with a six-coordinate arrangement. Each atom also has six more nearest neighbors from layers above and below. The stacking sequence is ABCABC... in the ccp lattice and ABAB... in hcp. In both cases, it can be shown that the spheres fill 74% of the volume of the lattice. This is the highest volume fraction that can be filled with a lattice of equal spheres.



Atoms in metallic crystals have a tendency to pack in dense arrangments that fill space efficiently. The simple square packing (above) upon which the simple cubic structure is based is inefficient and thus rare among metallic crystal structures. Body- or face-centered structures fill space more efficiently and more common.

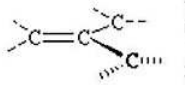
Periodic trends in structure and metallic behavior

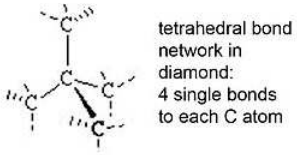
Remember where we find the metallic elements in the periodic table - everywhere except the upper right corner. This means that as we go down a group in the p-block (let's say, group IVA, the carbon group, or group VA, the nitrogen group), the properties of the elements gradually change from nonmetals to metalloids to metals. The carbon group nicely illustrates the transition. Starting at the top, the element carbon has two stable allotropes - graphite and diamond. In each one, the valence of carbon atoms is exactly satisfied by making four electron pair bonds to neighboring atoms. In graphite, each carbon has three nearest neighbors, and so there are two single bonds and one double bond. In diamond, there are four nearest neighbors situated at the vertices of a tetrahedron, and so there is a single bond to each one.

The two elements right under carbon (silicon and germanium) in the periodic table also have the diamond structure (recall that these elements cannot make double bonds to themselves easily, so there is no graphite allotrope for Si or Ge). While diamond is a good insulator, both silicon and germanium are semiconductors (i.e., metalloids). Mechanically, they are hard like diamond. Like carbon, each atom of Si and Ge satisfies its valence of four by making single bonds to four nearest neighbors.

The next element under germanium is tin (Sn). Tin has two allotropes, one with the diamond structure, and one with a slightly distorted bcc structure. The latter has metallic properties (metallic luster, malleability), and conductivity about 10^9 times higher than Si. Finally, lead (Pb), the element under Sn, has the ccp structure, and also is metallic. Note the trends in coordination number and conducting properties:

Element	Structure	Coord. no.	Conductivity
C	graphite, diamond	3, 4	semimetal, insulator
Si	diamond	4	semiconductor
Ge	diamond	4	semiconductor
Sn	diamond, distorted bcc	4, 8	semiconductor, metal
Pb	ccp	12	metal





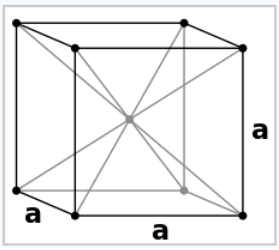
The elements C, Si, and Ge obey the octet rule, and we can easily identify the electron pair bonds in their structures. Sn and Pb, on the other hand, adopt structures with high coordination numbers. They *do not have enough valence electrons* to make electron pair bonds to each neighbor (this is a common feature of metals). What happens in this case is that the valence electrons become "smeared out" or delocalized over all the atoms in the crystal. It is best to think of the bonding in metals as a crystalline arrangement of positively charged cores with a "sea" of shared valence electrons gluing the structure together. Because the electrons are not localized in any particular bond between atoms, they can move in an electric field, which is why metals conduct electricity well. Another way to describe the bonding in metals is nondirectional. That is, an atom's nearest neighbors surround it in every direction, rather than in a few particular directions (like at the corners of a tetrahedron, as we found for diamond). Nonmetals (insulators and semiconductors), on the other hand, have directional bonding. Because the bonding is non-directional and coordination numbers are high, it is relatively easy to deform the coordination sphere (i.e., break or stretch bonds) than it is in the case of a nonmetal. This is why elements like Pb are much more malleable than C, Si, or Ge.

7.4: Crystal Structures of Metals is shared under a CC BY-SA license and was authored, remixed, and/or curated by LibreTexts.

- **6.4: Crystal Structures of Metals** by Chemistry 310 is licensed CC BY-SA 4.0. Original source: https://en.wikibooks.org/wiki/Introduction_to_Inorganic_Chemistry.

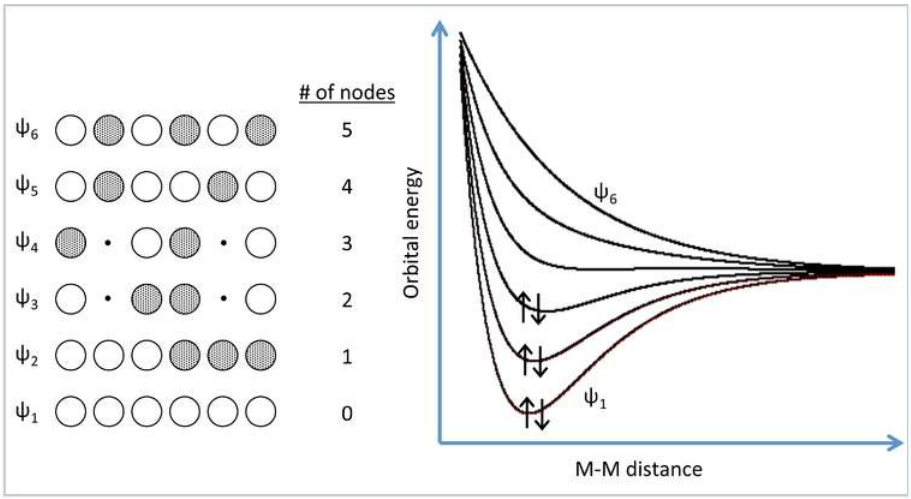
7.5: Bonding in Metals

The electron pair description of chemical bonds, which was the basis of the octet rule for p-block compounds, breaks down for metals. This is illustrated well by Na metal, the structure of which is shown at the left. Na has too few valence electrons to make electron pair bonds between each pair of atoms. We could think of the Na unit cell as having eight no-bond resonance structures in which only one Na-Na bond per cell contains a pair of electrons.



Sodium metal crystallizes in the body-centered cubic structure, in which each atom has eight nearest neighbors. Since the electronic configuration of Na is $[Ar]3s^1$, there are only two valence electrons per unit cell that are shared among eight Na-Na bonds. This means that the Na-Na bond order is 1/8 in Na metal.

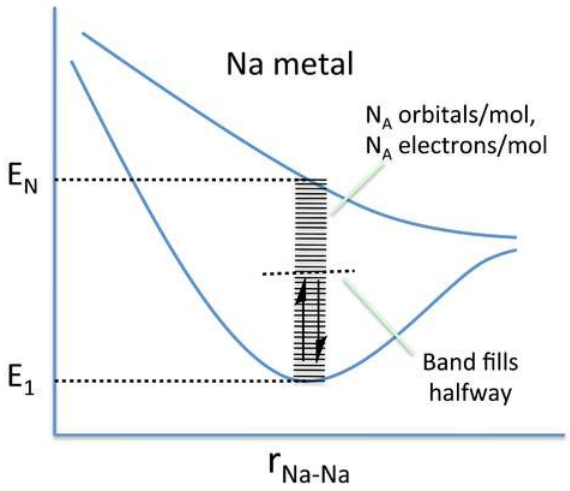
A more realistic way to describe the bonding in metals is through **band theory**. The evolution of energy bands in solids from simple MO theory (Chapter 2) is illustrated at the right for a chain of six Na atoms, each of which has one 3s valence orbital and contributes one valence electron. In general, **n** atomic orbitals (in this case the six Na 3s orbitals) will generate **n** molecular orbitals with **n-1** possible nodes. In Chapter 2, we showed that the energy versus internuclear distance graph for a two hydrogen atom system has a low energy level and a high energy level corresponding to the bonding and antibonding molecular orbitals, respectively. These two energy levels were well separated from each other, and the two electrons in H_2 energetically prefer the lower energy level. If more atoms are introduced to the system, there will be a number of additional levels between the lowest and highest energy levels.



MO picture for a linear chain of six Na atoms. Three of the six MOs can accommodate all six valence electrons. Adding more atoms to the chain makes more molecular orbitals of intermediate energy, which eventually merge into a continuous band of orbitals. For Na, the 3s band is always half-filled because each MO can accommodate two electrons.

In band theory, the atom chain is extrapolated to a very large number - on the order of 10^{22} atoms in a crystal - so that the different combinations of bonding and anti-bonding orbitals create "bands" of possible energy states for the metal. In the language of physics, this approach of building the bands from discrete atomic orbitals is called the "tight-binding" approximation. The number of atoms is so large that the energies can be thought of as a continuum rather than a series of distinct levels. A metal will only

partially fill this band, as there are fewer valence electrons than there are energy states to fill. In the case of Na metal, this results in a half-filled 3s band.



Nearly free electron model

In metals, the valence electrons are delocalized over many atoms. The total energy of each electron is given by the sum of its kinetic and potential energy:

$$E = KE + PE$$
$$E \approx p^2/2m + V$$

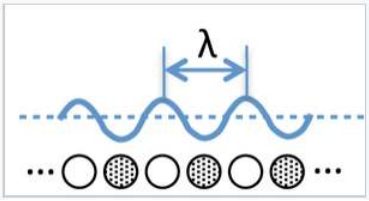
where **p** is the momentum of the electron (a vector quantity), m is its mass, and V is an average potential that the electron feels from the positive cores of the atoms. This potential holds the valence electrons in the crystal but, in the free electron model, is essentially uniform across the crystal.

Electron wavelength and wavenumber

What are the consequences of this model for band theory? For a hypothetical infinite chain (i.e., a 1D crystal) of Na atoms, the molecular orbitals at the bottom of the 3s band are fully bonding and the *wavelength* of electrons (2x the distance between nodes) in these orbitals is very long. At the top of the band, the highest orbital is fully antibonding and the wavelength is 2 times the distance between atoms (2a), since there is one node per atom. Remember that the **wavelength of an electron (λ)** is inversely proportional to its momentum p, according to the de Broglie relation **λ = h/p**.

For a (nearly) free electron, the kinetic energy can be expressed in terms of its wavelength, using $KE = p^2/2m$ and the de Broglie relation:

$$KE = \frac{p^2}{2m} = \frac{h^2}{2m\lambda^2} \tag{7.5.1}$$



We can think of the wavelength of an electron in a molecular orbital as twice the distance between nodes. If there are N atoms in a linear chain, the wavelength of the nth orbital is given by λ = 2Na/n, where a is the distance between atoms.

At this point, it is convenient to define the **wavenumber** of the electron as **k**, which has units of inverse length and is inversely proportional to λ. **k** is also directly proportional to the momentum **p**. Like **p**, **k** is a vector quantity. In a 1D crystal, **k** can be either

positive or negative, corresponding to an electron moving to the left or right along the chain.

$$k = \frac{2\pi}{\lambda} = \frac{2\pi p}{h} \text{ where h is Planck's constant} \tag{7.5.2}$$

The most important property of **k** is that it is *directly proportional to the number of nodes* **n** in a molecular orbital within the band. For a 1D crystal of sodium atoms that contains **N** unit cells, each separated by a distance a, a molecular orbital with n nodes has a wavelength λ = 2Na/n and the wavenumber k = πn/Na. We can see from this definition that k = 0 at the bottom of the band (where λ is infinite) and k = π/a at the top of the band where the MO contains **N** nodes and λ = 2a.

Energies of orbitals in a metallic crystal

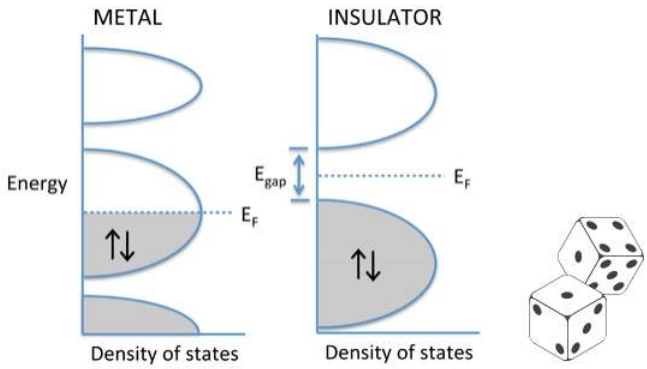
Electrons with long wavelengths do not "feel" the individual atoms in the lattice and so they behave as if they are *nearly free* (but confined to the crystal). Near the bottom of the band, the electron energy increases *parabolically* with the number of nodes (KE $\propto$ $\mathbf{n}^2$), since the momentum **p** is directly proportional to **n**. Because **p** is also directly proportional to **k**, we can write:

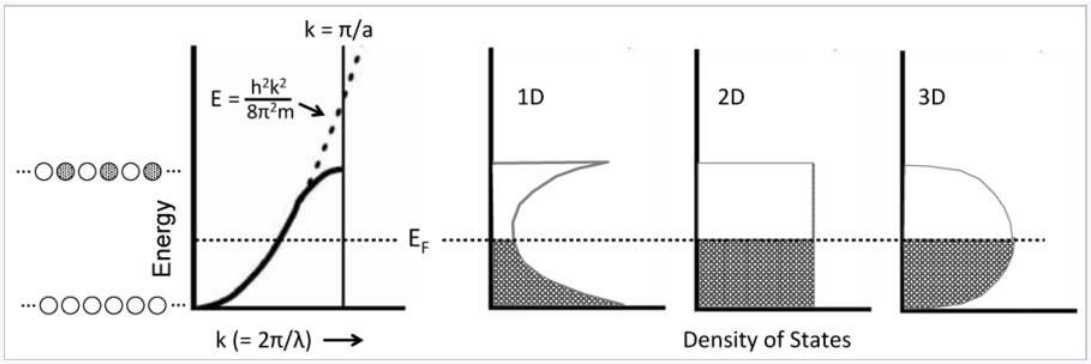
$$KE = \frac{p^2}{2m} = \frac{h^2k^2}{8\pi^2 m} \tag{7.5.3}$$

This parabolic relationship is followed as long as the electron wavelength is long compared to the distance between atoms. Near the top of the band, the wavelength becomes shorter and the electrons start to feel the positively charged atomic cores. In particular, the electrons prefer to have the maxima in their wavefunctions line up with the atomic cores, which is the most electrostatically favorable situation. The electron-atom attraction lowers the energy and causes the E vs. k curve to deviate from the parabolic behavior of a "free" electron as shown in the figure below.

Density of States (DOS)

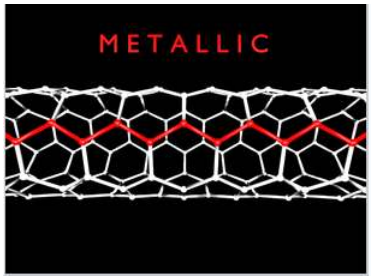
The density of states is defined as the number of orbitals per unit of energy within a band. Because of the parabolic relation between E and k, the density of states for a 1D metallic crystal is highest near the bottom and top of the energy band where the slope of the E vs. k curve is closest to zero. The shape of the DOS curve is different in crystals of higher dimensionality as shown in the figure in the left, because statistically there are more ways to make an orbital with N/2 nodes than there are with zero or N nodes. The situtation is analogous to the numbers you can make by rolling dice. With one die, the numbers 1-6 have equal probability. However, with two dice there is only one way to make a two (snake eyes) or a twelve (boxcars), but many ways to make a seven (a winner!).





Electrons in metals follow a parabolic dispersion curve, where the energy increases with the square of the wavenumber, k. Near the top of the band, the dispersion curve deviates from the parabolic dotted line. Because there is one MO for each value of k, the number of orbitals per unit energy (the density of states, DOS) is highest at the bottom and top of the band for a 1D chain of atoms. The density of states is constant with energy for a 2D crystal, and has a maximum in the middle of the band for a 3D crystal. At low temperature, all the MOs below the Fermi level E_F are occupied, and all the MOs above it are empty.

While most of the time we will talk about 3D crystals that have their maximum DOS near the middle of the energy band, there are examples of quasi-1D systems, such as carbon nanotubes. Metallic carbon nanotubes have strong optical absorption bands that correspond to transitions between the two regions of high DOS (the van Hove singularities) near the bottom and top of the bands.



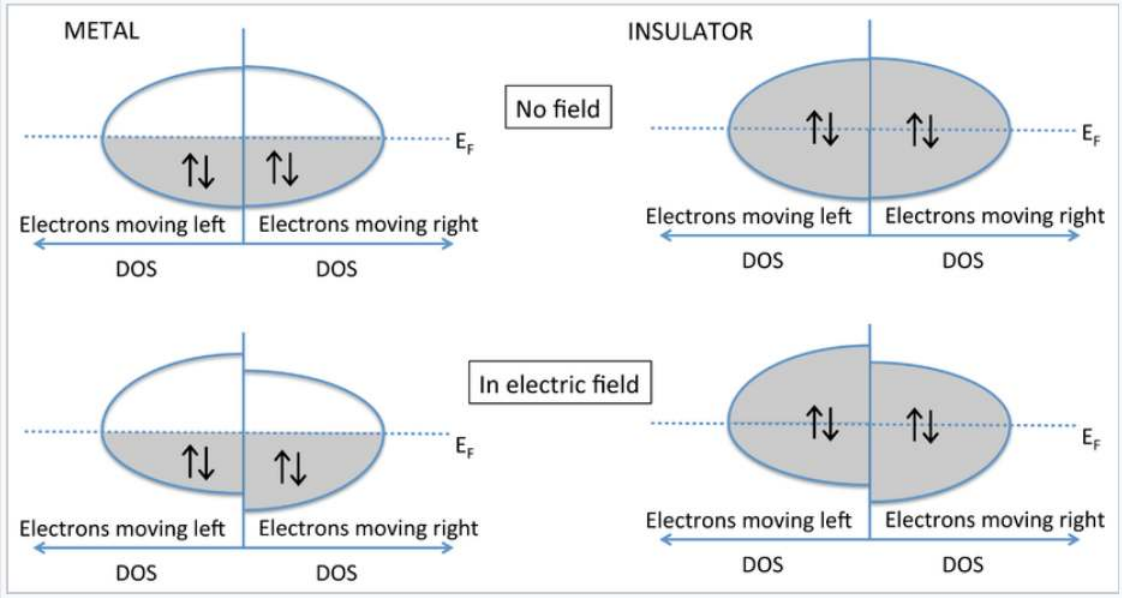
Single-walled carbon nanotubes with "armchair" chirality are metallic and have characteristic sharp absorption bands in the infrared. Prof. Millie Dresselhaus (below) did foundational research on the electronic properties of carbon nanotubes and other low-dimensional conductors.



Metals, semiconductors, and insulators

The degree to which bands fill determines whether a crystalline solid is a metal, semiconductor, or insulator. If the highest occupied molecular orbitals lie within a band - i.e., if the Fermi level E_F cuts through a band of orbitals - then the electrons are free to change their speed and direction in an electric field and the solid is metallic. However, if the solid contains just enough electrons to completely fill a band, and the next highest set of molecular orbitals is empty, then it is a semiconductor or insulator. In this case, there is an energy gap between the filled and empty bands, which are called the valence and conduction bands, respectively. Although the distinction is somewhat arbitrary, materials with a large gap (> 3 eV) are called insulators, and those with smaller gaps are called semiconductors. We will learn more about the properties of semiconductors in Chapter 10.

Why don't insulators conduct electricity? The energy vs. DOS diagram below shows what happens when an electric field is applied to a metal or an insulator. In this case we have changed the diagram to show explicitly the energies of electrons moving left and right. These energies are the same in the absence of an electric field. Once we apply a field (e.g., by putting a voltage across a metal wire), the electrons moving in the direction of the field have lower energy than those moving in the opposite direction. In the case of the metal, the populations of electrons moving with and against the electric field are different, and there is a net flow of current. Note that this can happen only when the Fermi level cuts through a partially filled band. With a semiconductor or insulator, the valence band is filled and the conduction band is empty. Applying an electric field changes the energies of electrons traveling with and against the field, but because the band is filled, the same number are going in both directions and there is no net current flow.



E vs. DOS diagrams comparing the behavior of metals and insulators in an applied electric field.

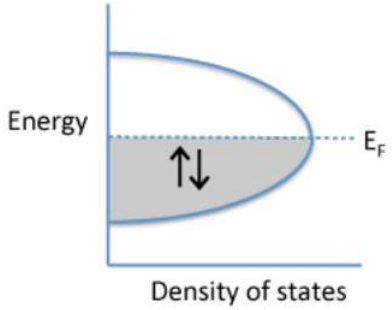
Note that in this picture, all the molecular orbitals extend over the entire crystal. The valence electrons are *delocalized,* even in the case of a semiconductor or insulator. However, there can be no net movement of electrons unless the band is partially filled.

7.5: Bonding in Metals is shared under a CC BY-SA license and was authored, remixed, and/or curated by LibreTexts.

- **6.5: Bonding in Metals** by Chemistry 310 is licensed CC BY-SA 4.0. Original source: https://en.wikibooks.org/wiki/Introduction_to_Inorganic_Chemistry.

7.6: Conduction in Metals

In metals, the valence electrons are in molecular orbitals that extend over the entire crystal lattice. As we will learn in Chapter 7, metals are almost always crystalline and the individual crystal grains are typically micron size. This means that the spatial extent of the orbitals is *very large* compared to the size of the atoms or the unit cell. The diagram at the left shows a generic plot of electron energy vs. density of states for a metal such as Na, Cu, or Ag. In these cases, there are N orbitals for N electrons, and each orbital can accommodate two electrons. Therefore the Fermi level, which corresponds to the energy of the highest occupied MO at zero temperature, is somewhere in the middle of the band of orbitals. The energy level spacing between orbitals is very small compared to the thermal energy kT, so we can think of the orbitals as forming a continuous band.



Classically, if the electrons in this band were free to be thermally excited, we would expect them to have a specific heat of 3R per mole of electrons. However, experimentally we observe that C_p is only about 0.02 R per mole. This suggests that *only about 1%* of the electrons in the metal can be thermally excited at room temperature. However, essentially *all* of the valence electrons are free to move in the crystal and contribute to electrical conduction. To understand this apparent paradox, we need to recall that the electrons exist in *quantized energy levels.*

Because of quantization, electrons in metals have a Fermi-Dirac distribution of energies. In this distribution, most of the electrons are spin-paired, although the individual electrons in these pairs can be quite far apart since the orbitals extend over the entire crystal. A relatively small number of electrons at the top of the Fermi sea are unpaired by thermal excitation. This is the origin of the Pauli paramagnetism of metals.

How fast are electrons traveling in a typical metal? Because of the bell shape of the E vs. DOS curve, most of the electrons have $E \approx E_F$. At the midpoint energy (E_F) of the band, the MO's have one node for every two atoms. We can calculate the de Broglie wavelength as twice the distance between nodes and thus:

$\lambda = \mathbf{4a}$ at the midpoint of the band.

where **a** is the interatomic spacing. Since a typical value of **a** is about 2 Å, we obtain the **de Broglie wavelength λ ≈ 8 Å**.

Using the de Broglie relation p = h/λ, we can write:

$$\mathbf{p = \frac{h}{\lambda} = m_e v_F} \tag{7.6.1}$$

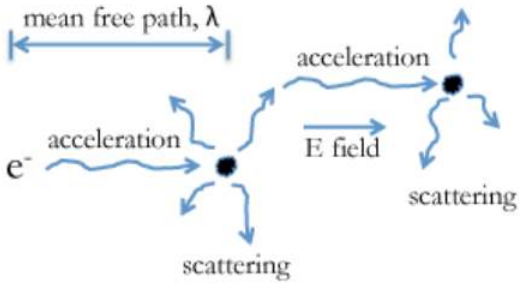
where $\mathbf{m_e}$ is the mass of the electron and $\mathbf{v_F}$ is the velocity of electrons with energy E_F.

Solving for $v_F = \frac{h}{m_e \lambda}$ we obtain $\mathbf{v_F = \frac{(6.62\times10^{-34} Js)}{(9.1\times10^{-31} kg)(8\times10^{-10} m)} = 1.0 \times 10^6 m/s}$

Experimental values of v_F are 1.07 x 10^6 and 1.39 x 10^6 m/s for Na and Ag, respectively, so our approximations are pretty good.

How fast are electrons moving in metals? Really, really fast!! **1,000,000 meters per second!** This is about 1/300 the speed of light, and about 3000 times the speed of sound in air (3 x 10^2 m/s).

However, the **drift velocity** of electrons in metals - the speed at which electrons move in applied electric field - is quite slow, on the order of 0.0001 m/s, or .01 cm/s. You can easily outrun an electron drifting in a metal, even if you have been drinking all night and have been personally reduced to a very slow crawl.



In order to understand the great disparity between the Fermi velocity and the drift velocity of electrons in metals, we need to consider a picture for the scattering of electrons, and their acceleration in an electric field, as shown at the left. If we apply a voltage across a metal (e.g., a metal wire), the electrons are subjected to an electric field **E**, which is the voltage divided by the length of the wire. This electric field exerts a force on the electron, causing it to accelerate. However, the electron is frequently scattered, mostly by phonons (lattice vibrations). Each time the electron is scattered its acceleration starts all over again. The time between scattering events is **τ** and the distance the electrons travel between scattering events is the **mean free path**, **λ**. (Note that this is NOT the same λ as the de Broglie wavelength, they just unfortunately have the same symbol!)

We can write the force on the electron as:

$$\mathbf{F = eE = m_e a = \frac{m_e v_{drift}}{\tau}} \tag{7.6.2}$$

In this equation, **a** is the acceleration in the electric field, $\mathbf{m_e}$ is the mass, and v_{drift} is the **drift velocity** of the electron.

Experimentally, the mean free path is typically obtained by measuring the scattering time. For an electron in Cu metal at 300 K, the scattering time τ is about 2 x 10^{-14} s. From this we can calculate the mean free path as:

$$\mathbf{\lambda = v_{avg}\tau \approx v_F\tau = (1 \times 10^6 m/s)(2 \times 10^{-14}) = 40nm} \tag{7.6.3}$$

The mean free path (40 nm = 400 Å) is quite long compared to the interatomic spacing (2 Å). To put it in perspective, if the interatomic spacing were scaled to the length of a football (0.3 m), the mean free path would be over half the length of the football field (60 m). Thus an electron travels a fairly long way between scattering events and scarcely notices the atomic structure of the metal in which it is traveling.

To summarize, electrons are traveling in metals at the Fermi velocity v_F, which is very, very fast (10^6 m/s), but the flux of electrons is the same in all directions. That is, they are *going nowhere fast*. In an electric field, a very small but directional *drift velocity* is superimposed on this fast random motion of valence electrons.



For ordinary metals, the mean free path of a valence electron (λ) is quite long relative to the interatomic spacing, represented in this analogy as the length of a football.

We can calculate the drift velocity of electrons as the acceleration in the electric field times the scattering time:

From F = ma, we obtain the acceleration (a) as:

$$\mathbf{a = \frac{F}{m_e} = \frac{eE}{m_e}} \tag{7.6.4}$$

And thus,

$$\mathbf{v_{drift} = a\tau = \frac{eE\tau}{m_e}} \tag{7.6.5}$$

If we divide both sides of this equation by the magnitude of the electric field (**E**), we obtain the **mobility (μ)**:

$$\mu = \frac{\mathbf{v_{drift}}}{\mathbf{E}} = \frac{e\tau}{\mathbf{m_e}} \tag{7.6.6}$$

μ has units of velocity/field = cm/s / V/cm = cm^2/Vs

An important consequence of the calculation of v_{drift} is **Ohm's Law**, V = iR. From the equations above, we can see that the drift velocity increases linearly with the applied electric field. The drift velocity (cm/s) is proportional to the current (i, coul/s), and the electric field (E, V/cm) is proportional to the voltage (V):

$$\mathbf{Current\ (i) = nev_{drift} \times area} \tag{7.6.7}$$

$$\mathbf{Voltage\ (V) = E \times length} \tag{7.6.8}$$

Here **n** is the density of valence electrons (#/cm^3) and **e** is the charge of the electron (coul). Combining these equations with our equation for v_{drift} we obtain:

$$V = i(\frac{m_e}{ne^2\tau})\frac{(}{length}area) = iR \tag{7.6.9}$$

Thus, V = iR, where R is the combination of the two terms in parentheses. The first of these is the **resistivity**, ρ, and the second is a geometrical factor.

The **conductivity (σ)** of a metal, which is the inverse of ρ, is proportional to μ, which in turn is proportional to τ (and λ):

$$\sigma = ne\mu = \frac{ne^2\tau}{m_e} \tag{7.6.10}$$

We can use this equation to work out the conductivity of a specific metal (Cu), for which n = 8.5 x 10^{22} cm^{-3} and τ = 2 x 10^{-14} s. Putting in the numbers for m_e and e, we obtain σ = 7 x 10^5 Ω^{-1} cm^{-1} for Cu, in good agreement with the measured value (6 x 10^5 $\Omega^{-1}cm^{-1}$).

7.6: Conduction in Metals is shared under a CC BY-SA license and was authored, remixed, and/or curated by LibreTexts.

- **6.6: Conduction in Metals** by Chemistry 310 is licensed CC BY-SA 4.0. Original source: https://en.wikibooks.org/wiki/Introduction_to_Inorganic_Chemistry.

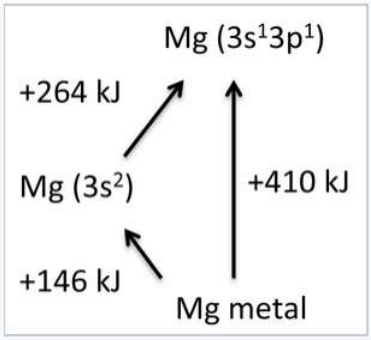
7.7: Atomic Orbitals and Magnetism

The MO picture we developed in Section 6.4 helps us rationalize the electrical conductivity of Na ($3s^1$), but what about Mg, which (as an atom in the gas phase) has a $3s^2$ electronic configuration? The two valence electrons are spin-paired in atomic Mg, as they are in the helium atom ($1s^2$). When the 3s orbitals of Mg combine to form a band, we would expect the band to be completely filled, since Mg has two electrons per orbital. By this reasoning, solid Mg should be an insulator. But Mg has all the properties of a metal: high electrical and thermal conductivity, metallic luster, malleability, etc. In this case the 3s and 3p bands are sufficiently broad (because of strong orbital overlap between Mg atoms) that they form a continuous band. This band, which contains a total of four orbitals (one 3s and three 3p) per atom, is only partially filled by the two valence electrons.



Mg crystals

Another way to think about this is to consider the **hybridization** of the 3s and 3p electrons in Mg. Hybridization requires promotion from the $3s^23p^0$ ground state of an Mg atom to a $3s^13p^1$ excited state. The **promotion energy** (+264 kJ/mol) is more than offset by the **bonding energy** (-410 kJ/mol), the energy released when gaseous atoms in the excited state condense to form the metallic solid. The heat of vaporization, or the cohesive energy of a metal, is the difference between the bonding energy and the promotion energy. Experimentally, we can measure the vaporization energy (+146 kJ/mol) and the promotion energy and use them to calculate the bonding energy. From this we learn that each s or p electron is worth about 200 kJ/mol in bonding energy. The concepts of promotion energy and bonding energy are very useful in rationalizing periodic trends in the bond strengths and magnetic properties of metals, which are described below.

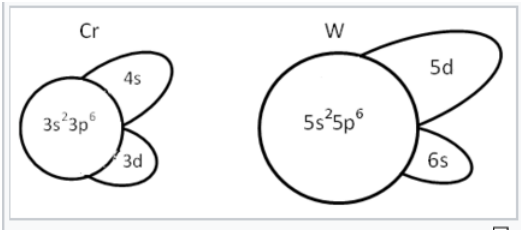


The cohesive energy of Mg metal is the difference between the bonding and promotion energies. The ground state of a gas phase Mg atom is $[Ar]3s^2$, but it can be promoted to the $[Ar]3s^13p^1$ state, which is 264 kJ/mol above the ground state. Mg uses two electrons per atom to make bonds, and the sublimation energy of the metal is 146 kJ/mol.

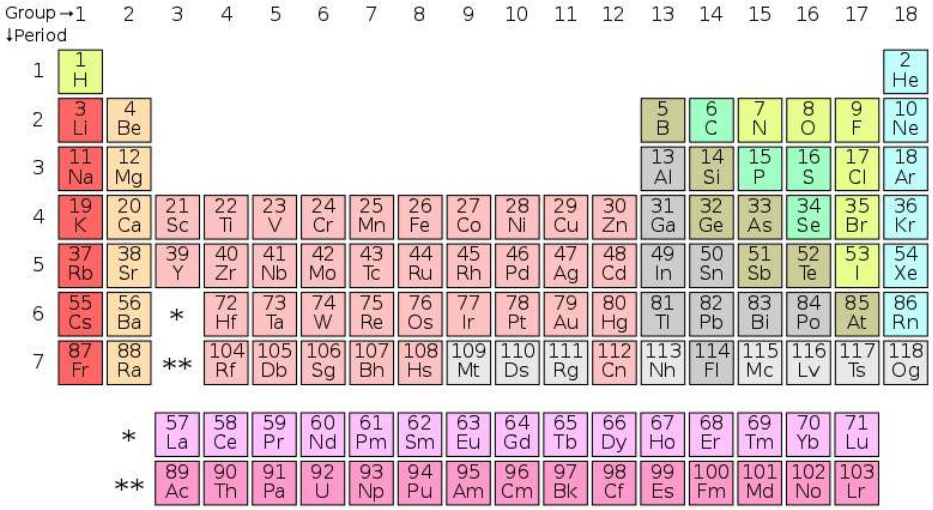
Periodic trends in d-electron bonding

While electrons in s and p orbitals tend to form strong bonds, d-electron bonds can be strong or weak. There are two important periodic trends that are related to orbital size and orbital overlap. As we move *across the periodic table* (Sc - Ti - V - Cr - Fe), the *d orbitals contract* because of increasing nuclear charge. Moving *down the periodic table* (V - Nb - Ta), the *d orbitals expand* because of the increase in principal quantum number. These trends explain the distinct behavior of the 3d elements relative to those in the 4d and 5d series. In the 3d series, the contraction of orbitals affects the ability of the d electrons to contribute to bonding. Past V in the first row of the transition metals, the 3d electrons become much less effective in bonding because they overlap weakly

with their neighbors. Weak overlap of 3d orbitals gives narrow d-bands and results in the emergence of magnetic properties as discussed below.

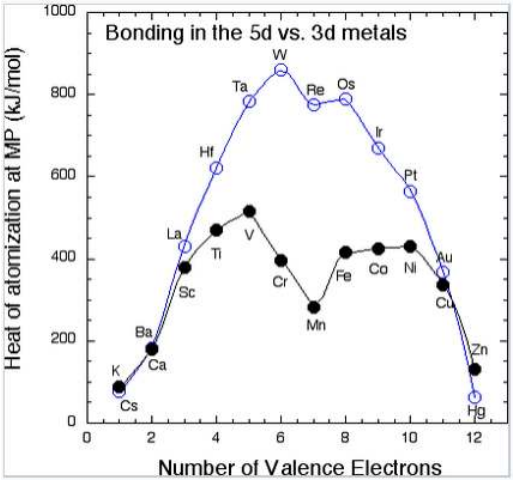


Schematic representation of the sizes of different orbitals of Cr and W. In the first transition series, shielding of the 3d orbitals is poor. Therefore the 4s and 4p orbitals are more effective in bonding than the 3d. In the third transition series, the situation is reversed. The increased nuclear charge is felt most strongly by the 6s, which takes on the character of an inert electron pair. The 5d orbitals are well shielded by the complete n=4 shell so they have good orbital overlap with neighboring atoms.



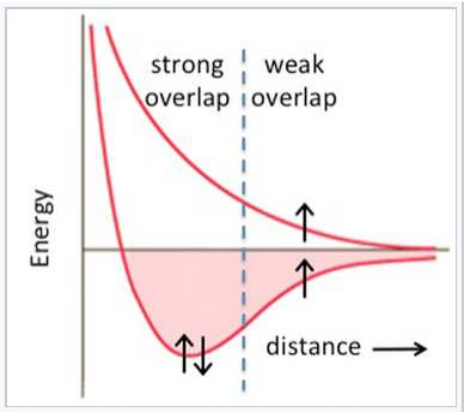
In the **4d and 5d series**, a plot of cohesive energy vs. number of valence electrons (below left) has a "volcano" shape that is peaked at the elements Mo and W ($5s^1 4d^5$ and $6s^1 5d^5$, respectively). The number of bonding electrons, and therefore the bonding energy, increases steadily going from Rb to Mo in the 4d series, and from Cs to W in the 5d series. Mo and W have the most bonding energy because they can use all six of their valence electrons in bonding without promotion. Elements past Mo and W have more d electrons, but some of them are spin paired and so some promotion energy is needed to prepare these electrons for bonding. For example, Pt metal must be promoted from the $6s^1 5d^9$ atomic ground state to $6s^1 5d^7 6p^2$ in order to make six bonds per atom, and the energy cost of promoting electrons from the 5d to the 6p orbitals is reflected in the net bonding energy. Because of their strong

bonding energy, elements in the middle of the 4d and 5d series have very high melting points. We do not see magnetism in the 4d or 5d metals or their alloys because orbital overlap is strong and the bonding energy exceeds the electron pairing energy.



The heat of vaporization (the cohesive energy) of metals in the 3d and 5d series, measured at the melting point of the metal.

The **3d elements** (Sc through Zn) are distinctly different from the 4d and 5d elements in their bonding (and consequently in their magnetic properties). In the 3d series, we see the expected increase in cohesive energy going from Ca ($4s^2$) to Sc ($4s^23d^1$) to Ti ($4s^23d^2$) to V ($4s^23d^3$), but then something very odd happens. The 3d series has a "crater" in the cohesive energy plot where there was a peak in the 5d series. The cohesive energy actually *decreases* going from V to Mn, even though the number of valence electrons is increasing. We can explain this effect by remembering that the 3d orbitals are progressively contracting as more protons are added to the nucleus. For elements beyond V, the orbital overlap is so poor that the 3d electrons are no longer effective in bonding, and the valence electrons begin to unpair. At this point the elements become **magnetic**. Depending on the way the spins order, metals and alloys in this part of the periodic table can be ferromagnetic (spins on neighboring atoms aligned parallel, as in the case of Fe or Ni) or antiferromagnetic (spins on neighboring atoms antiparallel, as in the case of Mn). We have seen the trade-off between orbital overlap and magnetism before (in Chapter 5) in the context of paramagnetic transition metal complexes. It is worth recalling that this behavior is predicted in the energy vs. distance diagram of the hydrogen atom (from Chapter 2). At short interatomic distances (or with strong overlap between atomic orbitals), the spins of the electrons pair and a bond is formed. Unpairing the electrons becomes favorable at larger interatomic distances where the overlap between orbitals is poor.



With strong overlap between orbitals of neighboring atoms, the bonding energy exceeds the pairing energy and electrons spin-pair. With weaker overlap, bonding is weak and spins unpair, resulting in magnetic behavior.

Interestingly, many alloys of the **4f elements** (the lanthanides) are also magnetic because the 4f orbitals, like the 3d orbitals, are poorly shielded from the nuclear charge and are ineffective in bonding. Strong permanent magnets often contain alloys of Nd, Sm, or Y, usually with magnetic 3d elements such as Fe and Co.

Because the 4f orbitals are contracted and not very effective in bonding, other physical properties of the lanthanides can also be affected. For example, it has been proposed that oxides of the 4f elements have weak surface interactions with polar molecules such as water because of f-orbital contraction. Experimentally, CeO_2, Er_2O_3, and Ho_2O_3 are observed to be hydrophobic, whereas main group and early transition metal oxides (e.g., Al_2O_3, SiO_2, TiO_2) are quite hydrophilic.[1]

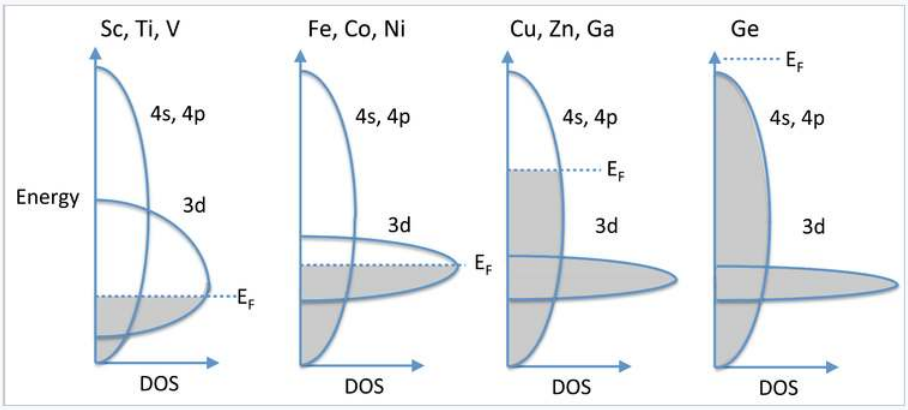
Late transition metal alloys

Although the bonding in the 5d series follows a "normal" volcano plot, the situation is a bit more complex for alloys of Re, Os, Ir, Pt, and Au. There is strong overlap between the 5d orbitals, but because these elements contain more than five d-electrons per atom, they cannot make as many bonds as 4d or 5d elements with half-filled d-shells such as Mo or W. This progressive filling of the d-band explains the steady decrease in bonding energy going from Os to Au. Pt and Au are both soft metals with relatively low heats of vaporization. However, these metals (especially Ir, Pt, and Au) can combine with early transition metals to form stable alloys with very negative heats of formation and high melting points. For example, ZrC and Pt react to form a number of stable alloys (ZrPt, Zr_9Pt_{11}, Zr_3Pt_4, $ZrPt_3$)[2] plus carbon. This reactivity is unusual because we normally think of Pt as a "noble" (i.e., unreactive) metal, and because ZrC is a very stable, refractory metal carbide. The favorable combination of early and late transition metals has been interpreted as arising from a d-electron "acid-base" interaction.[3] For example, in $HfPt_3$, Hf is the "acid" with an electron configuration of $6s^25d^2$, while Pt is the "base" with the electron configuration of $6s^15d^9$. They combine to create a stable "salt" product with a filled 5d electron configuration without promoting any electrons to higher orbitals. The implication is that Pt donates d-electrons to the "d-acid," Zr or Hf. However, electronic structure calculations on model compounds show that much of the bonding energy in ZrPt and $ZrPt_3$ arises from electron transfer from Zr to Pt (not the other way around) and the polarity of the resulting metal-metal bonds.[4] Regardless of the source of their stability, some early-late transition metal alloys are of particular interest for use in catalysis. For example, the alloy $ScPt_3$ is a good catalyst for oxygen reduction in fuel cells. Even though Sc is an active metal that is easily oxidized, it is stabilized in the aqueous acid environment of the fuel cell by its strong interaction with Pt.[5]

Filling of the 3d and 4s,4p bands

In the 3d series, we see magnetic behavior for elements and alloys between Cr and Ni. Past Ni, the elements (Cu, Zn, Ga,...) are no longer magnetic and they are very good electrical conductors, implying that their valence electrons are highly delocalized. We can understand this behavior by considering the overlap of 4s, 4p, and 3d orbitals, all of which are close in energy. The 4s and 4p have strong overlap and form a broad, continuous band. On the other hand, the 3d electrons are contracted and form a relatively narrow band. Progressing from the early 3d elements (Sc, Ti, V), we begin to fill the 3d orbitals, which are not yet so contracted that they cannot contribute to bonding. Thus, the valence electrons in Sc, Ti, and V are all spin-paired, except for a small number near the Fermi level that give rise to a weak Pauli paramagnetism. Moving across the 3d series to the magnetic elements (Fe, Co, Ni), the d-orbitals are now so contracted that their electrons unpair and we see cooperative ordering of spins (ferromagnetism and antiferromagnetism). Referring to the band diagram at the right, the 3d band is only partially filled and the Fermi level cuts through it. For Cu, Zn, and Ga, the 3d orbitals are even more contracted and the 3d band is thus more narrow, but now it is completely filled and the Fermi level is in the 4s,4p band. The strong orbital overlap in these bands results in spin pairing and a high degree of

electron delocalization. Consequently, metals in this part of the periodic table (Cu, Ag) are diamagnetic and are among the best electrical conductors at room temperature. Finally, at Ge, the 4s,4p band is completely filled and the solid is a semiconductor.



Progressive filling of the 3d and 4s,4p bands going across the periodic table from Sc to Ge.

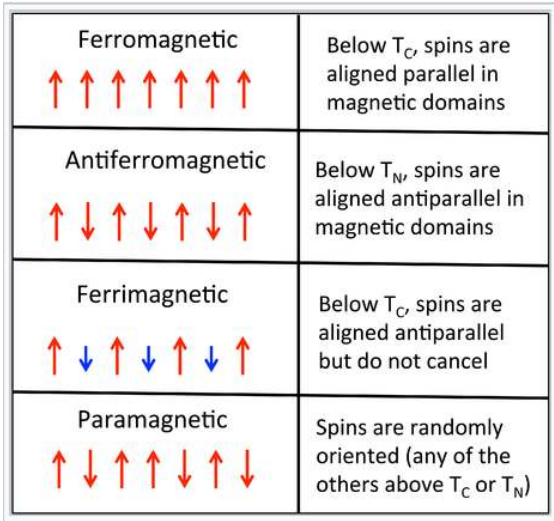
Materials are classified as diamagnetic if they contain no unpaired electrons. Diamagnetic substances are very weakly repelled from an inhomogeneous magnetic field. As we learned in Chapter 5, molecules or ions that have unpaired spins are paramagnetic and are attracted to a magnet, i.e., they move towards the high field region of an inhomogeneous field. This attractive force results from the alignment of spins with the field, but in the case of paramagnetism each molecule acts independently. In metals, alloys, oxides, and other solid state compounds, the unpaired spins interact strongly with each other and can order spontaneously, resulting in the cooperative magnetic phenomena described below.

7.7: Atomic Orbitals and Magnetism is shared under a CC BY-SA license and was authored, remixed, and/or curated by LibreTexts.

- **6.7: Atomic Orbitals and Magnetism** by Chemistry 310 is licensed CC BY-SA 4.0. Original source: https://en.wikibooks.org/wiki/Introduction_to_Inorganic_Chemistry.

7.8: Ferro-, Ferri- and Antiferromagnetism

The magnetism of metals and other materials are determined by the orbital and spin motions of the unpaired electrons and the way in which unpaired electrons align with each other. All magnetic substances are **paramagnetic** at sufficiently high temperature, where the thermal energy (kT) exceeds the interaction energy between spins on neighboring atoms. Below a certain critical temperature, spins can adopt different kinds of ordered arrangements.



A pictorial description of the ordering of spins in ferromagnetism, antiferromagnetism, ferrimagnetism, and paramagnetism

Let's begin by considering an individual atom in the bcc structure of iron metal. Fe is in group VIIIb of the periodic table, so it has eight valence electrons. The atom is promoted to the $4s^1 3d^7$ state in order to make bonds. A localized picture of the d-electrons for an individual iron atom might look like this:



Since each unpaired electron has a spin moment of 1/2, the total spin angular momentum, **S**, for this atom is:

$S = 3\frac{1}{2} = \frac{3}{2}$ (in units of h/2π)

We can think of each Fe atom in the solid as a little bar magnet with a spin-only moment **S** of 3/2. The spin moments of neigboring atoms can align in parallel (↑ ↑), antiparallel (↑ ↓), or random fashion. In bcc Fe, the tendency is to align parallel because of the positive sign of the exchange interaction. This results in **ferromagnetic** ordering, in which all the spins within a magnetic domain (typically hundreds of unit cells in width) have the same orientation, as shown in the figure at the right. Conversely, a negative exchange interaction between neighboring atoms in bcc Cr results in **antiferromagnetic** ordering. A third arrangement, **ferrimagnetic** ordering, results from an antiparallel alignment of spins on neighboring atoms when the magnetic moments of the neighbors are unequal. In this case, the spin moments do not cancel and there is a net magnetization. The ordering mechanism is like that of an antiferromagnetic solid, but the magnetic properties resemble those of a ferromagnet. Ferrimagnetic ordering is most common in metal oxides, as we will learn in Chapter 7.

Magnetization and susceptibility

The **magnetic susceptibility**, **χ**, of a solid depends on the ordering of spins. Paramagnetic, ferromagnetic, antiferromagnetic, and ferrimagnetic solids all have $\chi > 0$, but the magnitude of their susceptibility varies with the kind of ordering and with temperature. We will see these kinds of magnetic ordering primarily among the **3d** and **4f** elements and their alloys and compounds. For example, Fe, Co, Ni, $Nd_2Fe_{14}B$, $SmCo_5$, and YCo_5 are all ferromagnets, Cr and MnO are antiferromagnets, and Fe_3O_4 and $CoFe_2O_4$ are ferrimagnets. Diamagnetic compounds have a weak *negative* susceptibility ($\chi < 0$).

Definitions

- H = applied magnetic field (units: Henry (H))
- B = induced magnetic field in a material (units: Tesla (T))
- M = magnetization, which represents the magnetic moments within a material in the presence of an external field H.

Magnetic susceptibility $\chi = M/H$

Usually, χ is given in *molar* units in the *cgs system*:

χ_M = molar susceptibility (units: cm^3/mol)

Typical values of χ_M:

Compound	Type of Magnetism	χ at 300K (cm^3/mol)
SiO_2	Diamagnetic	-3×10^{-4}
Pt metal	Pauli paramagnetic	$+2 \times 10^{-4}$
$Gd_2(SO_4)_3 \cdot 8H_2O$	Paramagnetic	$+5 \times 10^{-2}$
Ni-Fe alloy	Ferromagnetic	$+10^4 - 10^6$

To correlate χ with the number of unpaired electrons in a compound, we first correct for the small diamagnetic contribution of the core electrons:

$$\chi^{corr} = \chi^{obs} - \chi^{diamagnetic\ cores} \tag{7.8.1}$$

Susceptibility of paramagnets

For a paramagnetic substance,

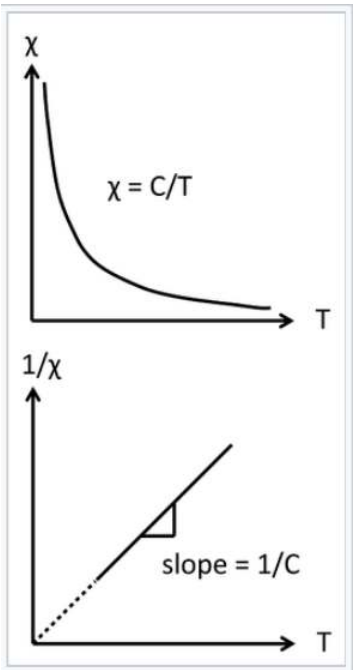
$$\chi_M^{corr} = \frac{C}{T} \tag{7.8.2}$$

The inverse relationship between the magnetic susceptibility and T, the absolute temperature, is called **Curie's Law**, and the proportionality constant C is the **Curie constant**:

$$C = \frac{N_A}{3k_B}\mu_{eff}^2 \tag{7.8.3}$$

Note that C is not a "constant" in the usual sense, because it depends on μ_{eff}, the **effective magnetic moment** of the molecule or ion, which in turn depends on its number of unpaired electrons:

$$\mu_{eff} = \sqrt{n(n+2)}\mu_B \tag{7.8.4}$$



Curie law behavior of a paramagnet. A plot of 1/χ vs. absolute temperature is a straight line, with a slope of 1/C and an intercept of zero.

Here μ_B is the Bohr magneton, a physical constant defined as $\mu_B = eh/4\pi m_e = 9.274 \times 10^{-21}$ erg/gauss (in cgs units).

In cgs units, we can combine physical constants,

$$\frac{N_A}{3k_B}\mu_B^2 = .125 \tag{7.8.5}$$

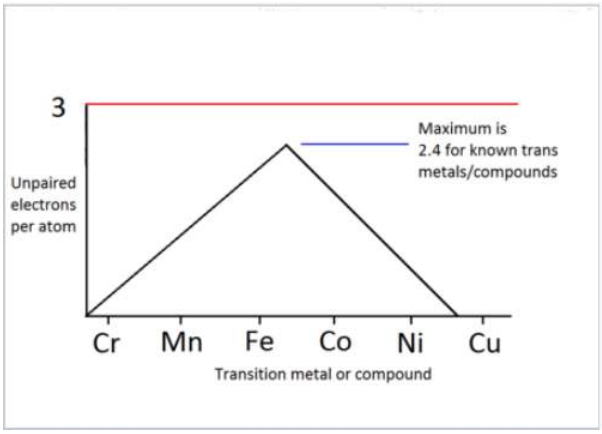
Combining these equations, we obtain

$$\chi_M^{corr} = \frac{.125}{T}\left(\frac{\mu_{eff}}{\mu_B}\right)^2 \tag{7.8.6}$$

These equations relate the molar susceptibility, a bulk quantity that can be measured with a magnetometer, to μ_{eff}, a quantity that can be calculated from the number of unpaired electrons, n. Two important points to note about this formula are:

- The magnetic susceptibility is inversely proportional to the absolute temperature, with a proportionality constant C (Curie's Law)

- So far we are talking only about paramagnetic substances, where there is no interaction between neighboring atoms.



Number of unpaired electrons per atom, determined from Curie constants of transition metals and their 1:1 alloys.

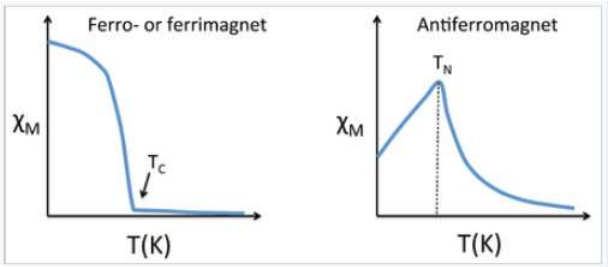
Returning to the isolated Fe atom with its three unpaired electrons, we can measure the Curie constant for iron metal (above the temperature of its transition to a paramagnetic solid) and compare it to the calculation of μ_{eff}. Since n = 3, we calculate:

$$\mu_{eff} = \sqrt{(3)(5)}\mu_B = 3.87\mu_B \tag{7.8.7}$$

The plot at the right shows the number of unpaired electrons per atom, calculated from measured Curie constants, for the magnetic elements and 1:1 alloys in the 3d series. The plot peaks at a value of 2.4 spins per atom, slightly lower than we calculated for an isolated iron atom. This reflects that fact that there is some pairing of d-electrons, i.e., that they do contribute somewhat to bonding in this part of the periodic table.

Susceptibility of ferro-, ferri-, and antiferromagnets

Below a certain critical temperature, the spins of a solid paramagnetic substance order and the susceptibility deviates from simple Curie-law behavior. Because the ordering depends on the short-range exchange interaction, this critical temperature varies widely. Metals and alloys in the 3d series tend to have high critical temperatures because the atoms are directly bonded to each other and the interaction is strong. For example, Fe and Co have critical temperatures (also called the Curie temperature, T_c, for ferromagnetic substances) of 1043 and 1400 K, respectively. The Curie temperature is determined by the strength of the magnetic exchange interaction and by the number of unpaired electrons per atom. The number of unpaired electrons peaks between Fe and Co as the d-band is filled, and the exchange interaction is stronger for Co than for Fe. In contrast to ferromagnetic metals and alloys, paramagnetic salts of transition metal ions typically have critical temperatures below 1K because the magnetic ions are not directly bonded to each other and thus their spins are very weakly coupled in the solid state. For example, in gadolinium sulfate, the paramagnetic Gd^{3+} ions are isolated from each other by SO_4^{2-} ions.

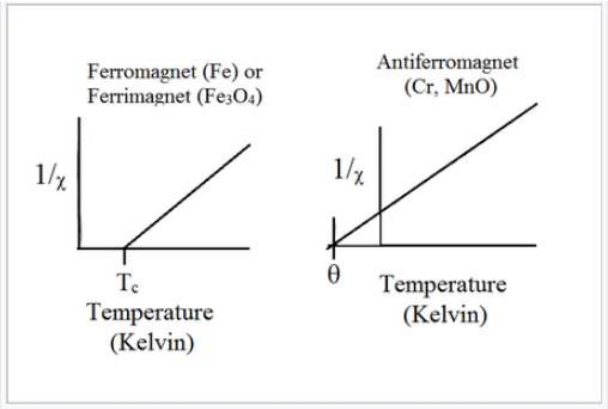


Magnetic susceptibility vs temperature (Kelvin) for ferrimagnetic, ferromagnetic, and antiferromagnetic materials

Above the critical temperature T_C, **ferromagnetic** compounds become paramagnetic and obey the **Curie-Weiss law:**

$$\chi = \frac{C}{T - T_c} \tag{7.8.8}$$

This is similar to the Curie law, except that the plot of $1/\chi$ vs. T is shifted to a positive intercept T_C on the temperature axis. This reflects the fact that ferromagnetic materials (in their paramagnetic state) have a greater tendency for their spins to align in a magnetic field than an ordinary paramagnet in which the spins do not interact with each other. Ferrimagnets follow the same kind of ordering behavior. Typical plots of χ vs. T and $1/\chi$ vs. T for ferro-/ferrimagnets are shown above and below.



Plots of $1/\chi$ vs. T for ferromagnets, ferrimagnets, and antiferromagnets.

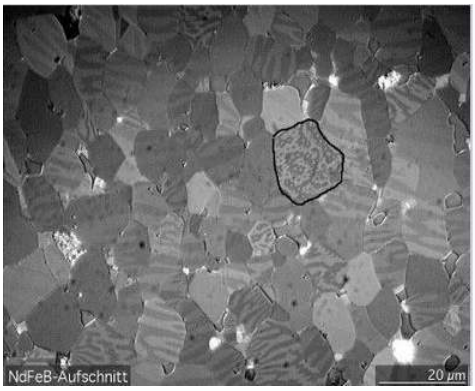
Antiferromagnetic solids are also paramagnetic above a critical temperature, which is called the Néel temperature, T_N. For antiferromagnets, χ reaches a maximum at T_N and is smaller at higher temperature (where the paramagnetic spins are further disordered by thermal energy) and at lower temperature (where the spins pair up). Typically, antiferromagnets retain some positive susceptibility even at very low temperature because of canting of their paired spins. However the maximum value of χ is much lower for an antiferromagnet than it is for a ferro- or ferrimagnet. The Curie-Weiss law is also modified for an antiferromagnet, reflecting the tendency of spins (in the paramagnetic state above T_N) to resist parallel ordering. A plot of $1/\chi$ vs. T intercepts the temperature axis at a negative temperature, $-\theta$, and the Curie-Weiss law becomes:

$$\chi = \frac{C}{T + \theta} \tag{7.8.9}$$

Ordering of spins below T_C

Below T_C, the spins align spontaneously in ferro- and ferrimagnets. Complex magnetization behavior is observed that depends on the history of the sample. For example, if a ferromagnetic material is cooled in the absence of an applied magnetic field, it forms a mosaic structure of magnetic domains that each have internally aligned spins. However, neighboring domains tend to align the opposite way in order to minimize the total energy of the system. This is illustrated in the figure at the left for a Nd-Fe-B magnet. The sample consists of 5-10 μm wide crystal grains that can be easily distinguished by the sharp boundaries in the image. Within

each grain are a series of lighter and darker stripes (imaged by using the optical Kerr effect) that are ferromagnetic domains with opposite orientations. Averaged over the whole sample, these domains have random orientation so the net magnetization is zero.



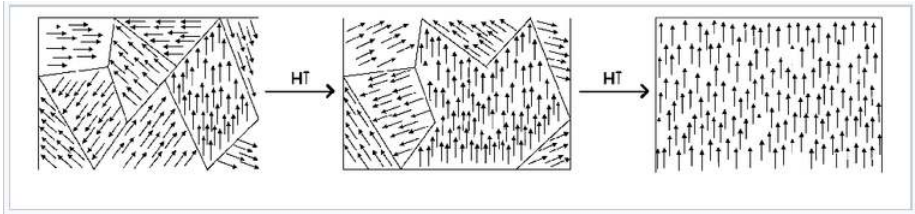
Microcrystalline grains within a piece of $Nd_2Fe_{14}B$ (the alloy used in neodymium magnets) with magnetic domains made visible with a Kerr microscope. The domains are the light and dark stripes visible within each grain.

When a sample like this one is magnetized (i.e., exposed to a strong magnetic field), the domain walls move and the favorably aligned domains grow at the expense of those with the opposite orientation. This transformation can be seen in real time in the Kerr microscope. The domain walls are typically hundreds of atoms wide, so movement of a domain wall involves a cooperative tilting of spin orientation (analogous to "the wave" in a sports stadium) and is a relatively low energy process.



The movement of domain walls in a grain of silicon steel is driven in this movie by increasing the external magnetic field in the "downward" direction, and is imaged using a Kerr microscope. White areas are domains with their magnetization directed up, dark areas - which eventually comprise the entire grain - are domains with their magnetization directed down.

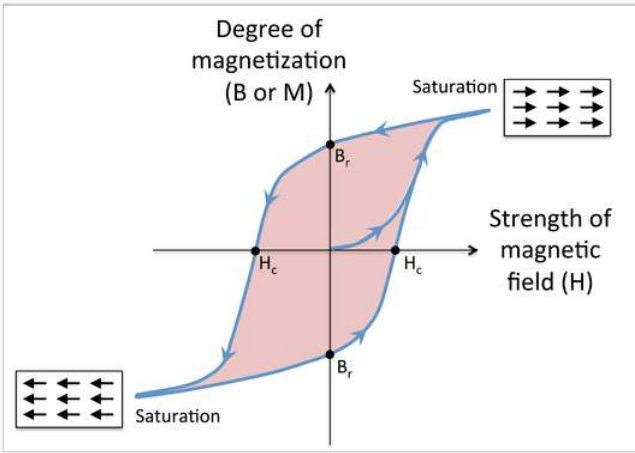
The process of magnetization moves the solid away from its lowest energy state (random domain orientation), so magnetization involves input of energy. When the external magnetic field is removed, the domain walls relax somewhat, but the solid (especially in the case of a "hard" magnet) can retain much of its magnetization. If you have ever magnetized a nail or a paper clip by using a permanent magnet, what you were doing was moving the walls of the magnetic domains inside the ferromagnet. The object thereafter retains the "memory" of its magnetization. However, annealing a permanent magnet destroys the magnetization by returning the system to its lowest energy state in which all the magnetic domains cancel each other.



Rotation of orientation and increase in size of magnetic domains in response to an externally applied magnetic field.

Magnetic hysteresis. Cycling a ferro- or ferrimagnetic material in a magnetic field results in hysteresis in the magnetization of the material, as shown in the figure at the left. At the beginning, the magnetization is zero, but it begins to rise rapidly as the magnetic field is applied. At high field, the magnetic domains are aligned and the magnetization is said to be saturated. When the field is removed, a certain **remanent magnetization** (indicated as the point $\mathbf{B_r}$ on the graph) is retained, i.e., the material is magnetized. Applying a field in the opposite direction begins to orient the magnetic domains in the other direction, and at a field $\mathbf{H_c}$ (the **coercive field**), the magnetization of the sample is reduced to zero. Eventually the material reaches saturation in the opposite direction, and when the field is removed again, it has remanent magnetization Br, but in the opposite direction. As the field continues to reverse, the magnet follows the hysteresis loop as indicated by the arrows. The area of colored region inside the loop is

proportional to the magnetic work done in each cycle. When the field cycles rapidly (for example, in the core of a transformer, or in read-write cycles of a magnetic disk) this work is turned into heat.



Magnetization of a ferro- or ferrimagnet vs. applied magnetic field H. Starting at the origin, the upward curve is the initial magnetization curve. The downward curve after saturation, along with the lower return curve, form the main loop. The intercepts Hc and Br are the coercivity and remanent magnetization.

7.8: Ferro-, Ferri- and Antiferromagnetism is shared under a CC BY-SA license and was authored, remixed, and/or curated by LibreTexts.

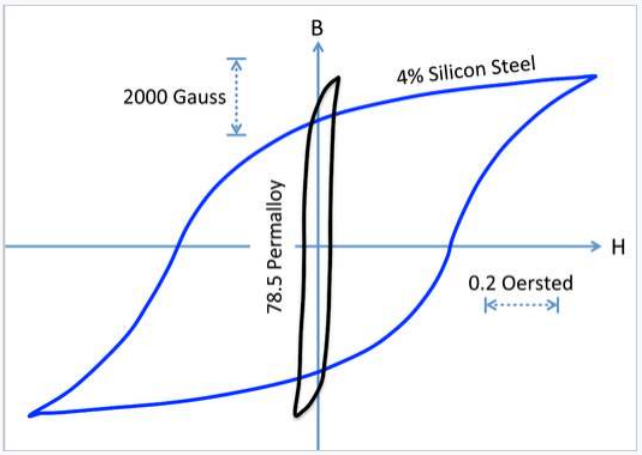
- **6.8: Ferro-, Ferri- and Antiferromagnetism** by Chemistry 310 is licensed CC BY-SA 4.0. Original source: https://en.wikibooks.org/wiki/Introduction_to_Inorganic_Chemistry.

7.9: Hard and Soft Magnets

Whether a ferro- or ferrimagnetic material is a **hard** or a **soft magnet** depends on the strength of the magnetic field needed to align the magnetic domains. This property is characterized by $\mathbf{H_c}$, the coercivity. Hard magnets have a high coercivity (H_c), and thus retain their magnetization in the absence of an applied field, whereas soft magnets have low values.

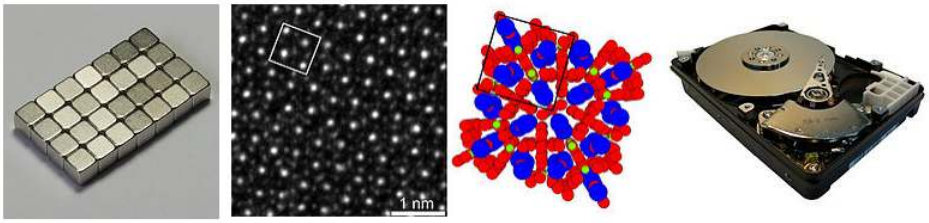
The figure at the right compares hysteresis loops for hard and soft magnets. Recall that the energy dissipated in magnetizing and demagnetizing the material is proportional to the area of the hysteresis loop. We can see that soft magnets, while they can achieve a high value of B_{sat}, dissipate relatively little energy in the loop. This makes **soft magnets** preferable for use in **transformer cores**, where the field is switched rapidly. **Permalloy**, an alloy consisting of about 20% Fe and 80% Ni, is a soft magnet that has very high magnetic permeability μ (i.e., a large maximum slope of the B vs. H curve) and a very narrow hysteresis loop.

Some materials, such as iron metal, can exist as either hard or soft magnets. Whether bcc iron is a hard or soft magnet depends on the crystal grain size. When crystal grains in iron are sub-micron size, and comparable to the size of the magnetic domains, then the magnetic domains are pinned by crystal grain boundaries. When the magnetic domains are pinned a stronger coercive magnetic field needs to be applied to cause them to re-align. When iron is annealed, the crystal grains grow and the magnetic domains become more free to align with applied magnetic fields. This decreases the coercive field and the material becomes a soft magnet.



Hysteresis loops comparing a hard magnet (iron-silicon steel) to a soft magnet (permalloy) on the same scale. H_c for permallloy is 0.05 Oe, about 10 times lower than that of the hard magnet. The remanent magnetizations of the two materials are comparable.

Hard magnets such as CrO_2, γ-Fe_2O_3, and cobalt ferrite ($CoFe_2O_4$) are used in magnetic recording media, where the high coercivity allows them to retain the magnetization state (read as a logical 0 or 1) of a magnetic bit over long periods of time. Hard magnets are also used in disk drives, refrigerator magnets, electric motors and other applications. Drive motors for hybrid and electric vehicles such as the Toyota Prius use the hard magnet $Nd_2Fe_{14}B$ (also used to make strong refrigerator magnets) and require 1 kilogram (2.2 pounds) of neodymium.[6]. A high-resolution transmission electron microscope image of $Nd_2Fe_{14}B$ is shown below and compared to the crystal structure with the unit cell marked.



7.9: Hard and Soft Magnets is shared under a CC BY-SA license and was authored, remixed, and/or curated by LibreTexts.

- **6.9: Hard and Soft Magnets** by Chemistry 310 is licensed CC BY-SA 4.0. Original source: https://en.wikibooks.org/wiki/Introduction_to_Inorganic_Chemistry.

7.10: Discussion Questions

- Discuss the relationship between the trends in bonding energy of the transition metals and their magnetic properties.
- Draw the hcp unit cell in sections and show how you would calculate (a) the number of atoms in the unit cell and (b) the fraction of space filled by equal spheres.

7.10: Discussion Questions is shared under a CC BY-SA license and was authored, remixed, and/or curated by LibreTexts.

- **6.10: Discussion Questions** by Chemistry 310 is licensed CC BY-SA 4.0. Original source: https://en.wikibooks.org/wiki/Introduction_to_Inorganic_Chemistry.

7.11: Problems

1. C-centered Bravais lattices exist in the monoclinic and orthorhombic systems but not in the tetragonal system. That is because the C-centered tetragonal lattice is equivalent to one of the other Bravais lattices. Which one is it? Show with a drawing how that lattice is related to the C-centered tetragonal lattice. How many atoms are in the unit cell of that lattice?

2. Which of the following sequences of close packed layers fills space most efficiently? Explain your answer.

(a) ABACCABA...

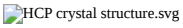
(b) ABABAB...

(c) AABBAABB...

(d) ABACABAC...

3. Calculate the fraction of space that is occupied by packing spheres in the (a) simple cubic, (b) body-centered cubic structure, (c) face-centered cubic (cubic close packed) structures. Assume that nearest neighbor spheres are in contact with each other.

4. The hexagonal close packed (hcp) structure is shown below. If the radius of the spheres is R, what is the vertical distance between layers in units of R? What fraction of space is filled by the spheres in the hcp lattice?



5. Consider a one-dimensional chain of sodium atoms that contains N atoms, where N is a large number. The distance between atoms in the chain is the lattice constant **a**. In the highest occupied molecular orbital of the chain, what is the distance between nodes (in units of **a**)?

6. Starting from the left side of the periodic table, the melting and boiling points of the elements first increase, and then decrease. For example, the order of boiling points is Rb < Sr < Y < Zr < Nb < Mo > Tc ≈ Ru > Rh > Pd > Ag. Briefly explain the reason for this trend.

7. Going across the periodic table from left to right starting from potassium, the bonding energies and heats of vaporization increase in the order K < Ca < Sc < Ti < V, but then decrease going from V to Mn (V > Cr > Mn). The heats of vaporization of V, Cr, and Mn are much less than those of Nb, Mo, and Tc, respectively. Explain these trends.

8. Some alloys of early and late transition metals (e.g., $ZrPt_3$) have much higher enthalpies of vaporization (per metal atom) than either pure metal. Why are such alloys unusually stable, relative to the pure metals?

9. Graphite is a semimetal composed of sheets of fused benzene rings. There are no bonds between sheets, only van der Waals interactions. What is the C-C bond order in graphite? Show why the C-C distance (1.42 Å) is different from that of benzene (1.40 Å).

10. Fe, Co, and Ni are ferromagnetic, whereas Ru, Ir, and Pt are diamagnetic. Explain why magnetic metals are found only among the 3d and 4f elements. Why are Sc and Ti, which are also 3d elements, diamagnetic?

11. The Curie temperature of cobalt is 1127•C, which is higher than that of Fe (770•C) or Ni (358•C). Why does Co have the highest Curie temperature?

12. Iron metal comes in magnetically “soft” and “hard” forms. Briefly explain the structural differences between them and draw magnetic hysteresis curves for each, indicating on your curves the coercive field and the remanent magnetization.

13. Aluminum metal has the fcc structure, a lattice constant of 4.046 Å, three valence electrons per atom, and an electron scattering time (at room temperature) of 11.8 fs. Use these values to calculate the room temperature resistivity (in ohm-cm) of Al metal.

7.11: Problems is shared under a CC BY-SA license and was authored, remixed, and/or curated by LibreTexts.

- **6.11: Problems** by Chemistry 310 is licensed CC BY-SA 4.0. Original source: https://en.wikibooks.org/wiki/Introduction_to_Inorganic_Chemistry.

7.12: References

1. G. Azimi et al., *Nature Materials* **12**,315–320 (2013), doi:10.1038/nmat3545
2. Stalick, J. K.; Waterstrat, R. J. J. Alloys Compounds 430, 123-131 (2007).
3. Brewer, L.; Wengert, P. R. Metall. Trans. 1973, 4, 83.
4. Wang, H.; Carter, E. A.; J. Am. Chem. Soc. 1993, 115, 2357-2362.
5. Greeley, J. et al., Alloys of platinum and early transition metals as oxygen reduction electrocatalysts, Nature Chem. 1, 552 - 556 (2009)
6. www.reuters.com/article/2009/08/31/us-mining-toyota-idUSTRE57U02B20090831

7.12: References is shared under a CC BY-SA license and was authored, remixed, and/or curated by LibreTexts.

- **6.12: References** by Chemistry 310 is licensed CC BY-SA 4.0. Original source: https://en.wikibooks.org/wiki/Introduction_to_Inorganic_Chemistry.

CHAPTER OVERVIEW

8: Metals and Alloys - Mechanical Properties

Learning Objectives

- Understand the structure of dislocations and grain boundaries and their role in controlling the mechanical properties of solids.
- Explain why the mechanical properties of bcc metals and alloys differ from those with close packed structures.
- Explain the effects of work hardening and annealing on structure and mechanical properties.
- Explain the mechanical properties of steel in terms of its phase behavior.
- Understand the structure and mechanical properties of amorphous metals.

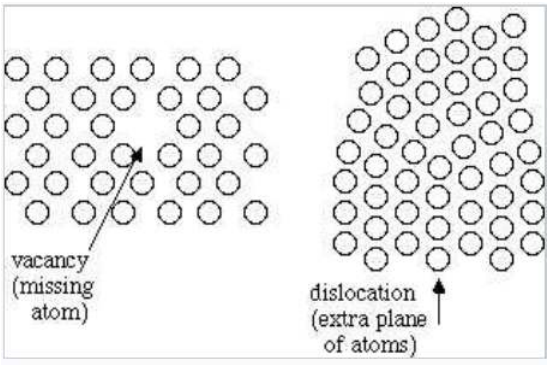
How much do the mechanical properties of metals and alloys vary with processing? The answer is, a great deal.

8.1: Defects in Metallic Crystals
8.2: Work Hardening, Alloying, and Annealing
8.3: Malleability of Metals and Alloys
8.4: Iron and Steel
8.5: Amorphous Alloys
8.6: Discussion Questions
8.7: Problems
8.8: References

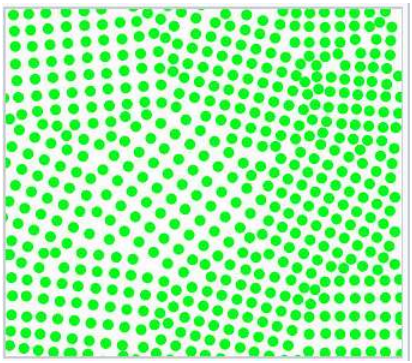
8: Metals and Alloys - Mechanical Properties is shared under a CC BY-SA license and was authored, remixed, and/or curated by LibreTexts.

8.1: Defects in Metallic Crystals

“Crystals are like people, it is the defects in them which tend to make them interesting!” - *Colin Humphreys.*



Metals, by virtue of their non-directional bonding, are more energetically tolerant of **defects** than are covalent network or ionic solids. Because there is no strong preference for one atomic position over another, the energy of a metallic crystal is not greatly impaired by the vacancy of a single atom or by the dislocation of a group of atoms. These kinds of "mistakes" in the packing of metal atoms within crystals are collectively called defects. The deformability of metals is the direct result of defects in the crystal structure. Defects in metals such as Al and Fe are responsible for the three orders of magnitude difference between the yield stress of annealed polycrystalline samples (i.e., normal articles of commerce) and perfect single crystals.



Grains and grain boundaries in a polycrystalline material

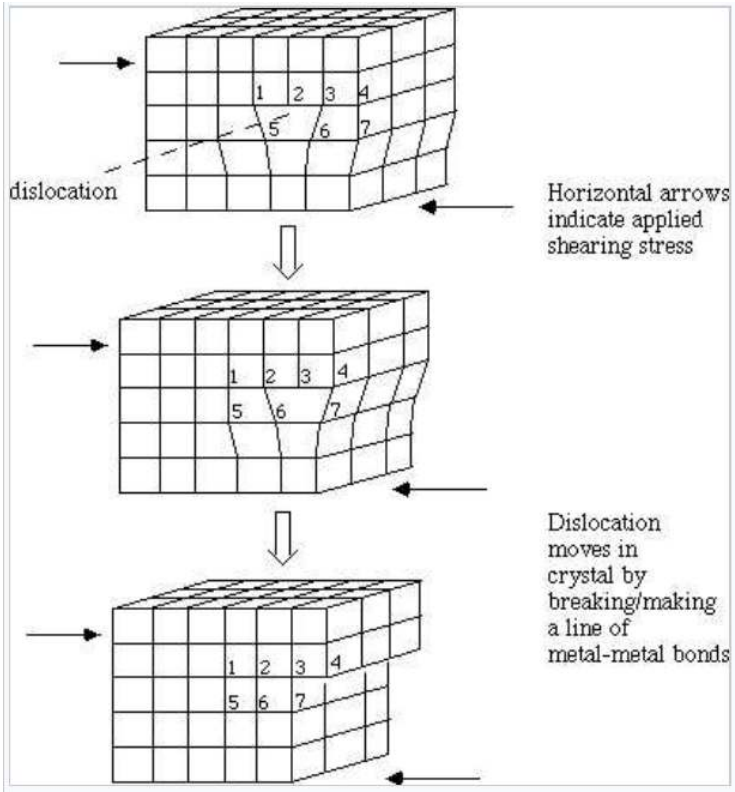
8.1: Defects in Metallic Crystals is shared under a CC BY-SA license and was authored, remixed, and/or curated by LibreTexts.

- **7.1: Defects in Metallic Crystals** by Chemistry 310 is licensed CC BY-SA 4.0. Original source: https://en.wikibooks.org/wiki/Introduction_to_Inorganic_Chemistry.

8.2: Work Hardening, Alloying, and Annealing

One of the questions we would like to ask is, why are the yield stresses of normal (polycrystalline) metal samples so much lower (by a factor of 1000) than they are in perfect single crystals? The answer has to do with the motion of dislocations. Consider the picture below, which shows planes of metal atoms near a dislocation (the individual atoms are numbered to help you see which bonds are broken and which are formed). The arrows indicate force applied under shear stress. Notice how the dislocation moves by breaking/making metal-metal bonds.

The key point here is that we can induce plastic deformation (shear) by breaking only one line of metal-metal bonds at a time along the dislocation line. This involves far less force than breaking an entire plane of bonds, as we would need to do to shear a perfect crystal. In a given polycrystalline sample, there are many dislocation lines that run perpendicular to all possible shear directions, so their motion can be used to "tear" the metal apart. Turbine rotors on large jets are made of very expensive **single crystal** nickel-titanium alloys, so that these shearing deformations can be avoided.[1]



We can see that motion of dislocations is basically bad news if we want a metal to be strong and hard (e.g., if we want a structural material, or a knife that can hold a decent edge). There are several ways we can overcome (to some extent) this problem:

1. Use **single crystals** and anneal out all the dislocations (expensive - especially with large items like turbine blades, and impossible with very large items like airplane wings or bridges).

2. **Work hardening** of the metal - this moves all dislocations to grain boundaries (the dislocation essentially becomes part of the grain boundary). Since a grain boundary is a planar defect, it is much less responsive to stress than a line defect.

3. Introduce **impurity atoms** (that is alloying elements) or impurity phases that "pin" the motion of defects. An impurity atom stops the motion because it is a different size, or makes stronger bonds, than the other metal atoms; the line defect has a hard time moving away from rows of such atoms. An impurity phase (like Fe_3C in iron) makes extra grain boundaries that can stop the motion of defects. This effect is analogous to the graphite fibers in fiber-reinforced cross-linked polymers (used, e.g., in tennis rackets) that stop the propagation of cracks.

A simple illustration of work hardening can be done with a piece of copper wire. When struck many times with a hammer, the copper wire becomes stiffer, and it is possible to hang a weight from it. Dislocations move to the crystal grain boundaries during work hardening, effectively halting their motion and at the same time making the individual crystal grains smaller. Because the crystal grains are now smaller, the amount of grain boundary area has increased, and with it the free energy of the material. Annealing reverses the process by lowering the free energy. When the wire is annealed in a flame (heated so that atoms can move and rearrange), the crystal grains grow, and the dislocations reappear. The copper again becomes ductile, and bends easily. Cold-working (work hardening) of metals is important for strengthening structural materials (e.g., iron beams) and for making brittle, hard edges (this is why blacksmiths hammer on knives and swords when they are making them. If you have ever watched them, they do the same thing to horseshoes, when they cool down, to make them stiff).



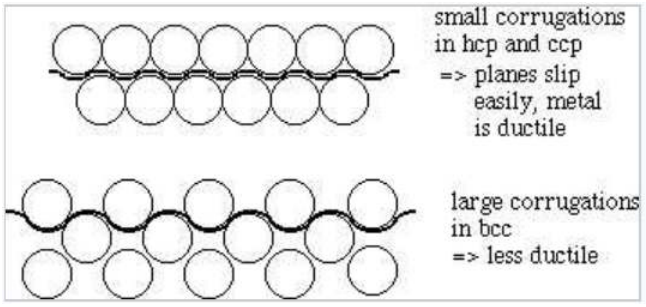
Blacksmith, 1606

8.2: Work Hardening, Alloying, and Annealing is shared under a CC BY-SA license and was authored, remixed, and/or curated by LibreTexts.

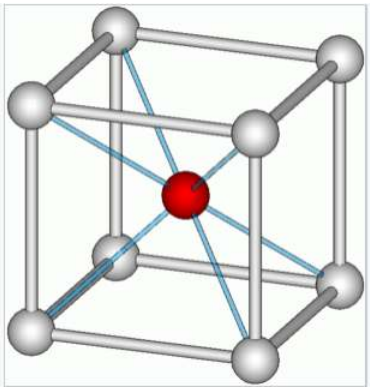
- **7.2: Work Hardening, Alloying, and Annealing** by Chemistry 310 is licensed CC BY-SA 4.0. Original source: https://en.wikibooks.org/wiki/Introduction_to_Inorganic_Chemistry.

8.3: Malleability of Metals and Alloys

Metals with close-packed structures (HCP and FCC) such as copper, gold, silver, zinc, magnesium, etc. are in general more malleable than those with the BCC structure (tungsten, vanadium, chromium, etc.). Why? In the close-packed structure, there is relatively little corrugation between sheets of metal atoms. This means that these planes can slip past each other relatively easily. In the BCC structure, there are no close-packed planes, and much greater corrugation between atoms at different levels. This makes it much harder for one row to slide past another.



This effect explains the hardness of alloys like brass (CuZn, which has the BCC structure), which are made by combining two soft metals (Cu and Zn, which are respectively FCC and HCP as pure metals, are both soft and ductile). Bronzes - originally made as alloys of copper and arsenic, but later as alloys of copper and tin - are harder than either of the constituent metals for the same reason.



The history of bronzes and brass dates to pre-historic times, with the earliest brasses made by smelting copper-zinc ores. In the Bronze Age, possession of these hard alloys provided a tactical advantage in warfare (see image at right), that was later supplanted when the technology for smelting iron was developed.



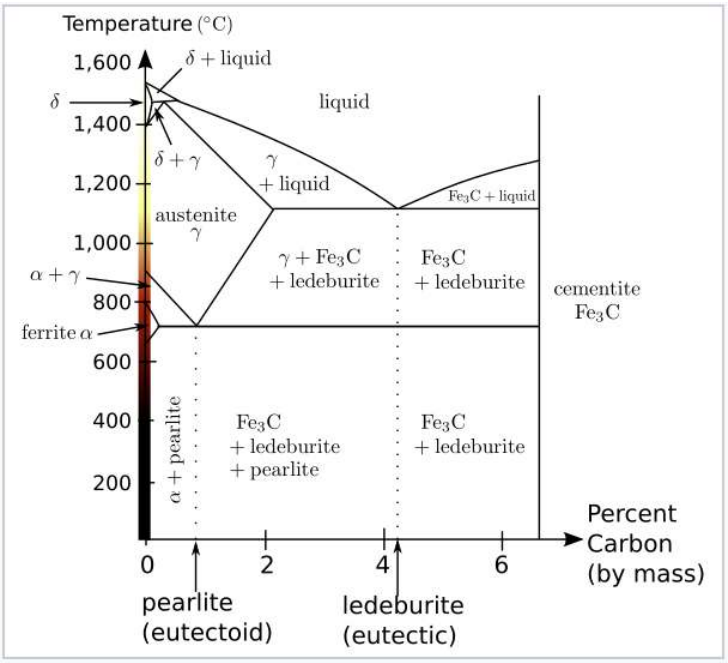
Bronze age weapons from Romania.

8.3: Malleability of Metals and Alloys is shared under a CC BY-SA license and was authored, remixed, and/or curated by LibreTexts.

- **7.3: Malleability of Metals and Alloys** by Chemistry 310 is licensed CC BY-SA 4.0. Original source: https://en.wikibooks.org/wiki/Introduction_to_Inorganic_Chemistry.

8.4: Iron and Steel

One other very important place where the difference between the hardness of a BCC and a close-packed metal is important is in steelmaking. Between room temperature and 912°C, iron has the BCC structure, and is a tough, hard metal ("tough as nails"). Above 912°C, pure iron switches over to the FCC (austenite) structure, which is much more ductile. So hot iron can be bent and worked into a variety of shapes when it is very hot but still solid (it melts at 1535°C). Rapid quenching of hot iron - e.g., when the blacksmith plunges a red hot piece directly into cold water - cools it to room temperature, but doesn't allow time for the FCC --> BCC phase transition to occur; therefore, such pieces are still relatively malleable and can be shaped.



The iron–iron carbide (Fe–Fe_3C) phase diagram. Below 912 °C, pure iron exists as the alpha phase, ferrite, which has the BCC structure. Between 912 and 1,394 °C, pure iron exists as the gamma phase, austenite, which has the FCC structure. Carbon is more soluble in the FCC phase, which occupies area "γ" on the phase diagram, than it is in the BCC phase. The percent carbon determines the type of iron alloy that is formed upon cooling from the FCC phase, or from liquid iron: alpha iron, carbon steel (pearlite), or cast iron.

Carbon is added (about 1% by weight) to iron to make "carbon steel", which is a very hard material. Carbon is rather soluble in the FCC phase of iron, but not in the BCC phase. Therefore, when the ductile FCC phase cools and turns into BCC ("tempering" the steel, which means cooling it slowly enough so the FCC to BCC transformation can occur), the iron can no longer dissolve the excess carbon. The carbon forms layers or grains of an extra phase, Fe_3C ("cementite" - a very hard material) which are layered or dotted throughout the matrix of BCC iron grains. The effect of all these little grains of Fe_3C is to stop the motion of dislocations, making for a harder but (with higher carbon content) increasingly brittle material. This is why knives and swords are quenched from the FCC phase, cold worked into the appropriate shapes, and then heated up again and tempered (before they are sharpened)

when they are made. Cast iron objects (frying pans, radiators, etc) have a higher carbon content and are therefore very strong, but tend to fracture rather than bend because of the larger fraction of the brittle Fe_3C phase in the alloy.

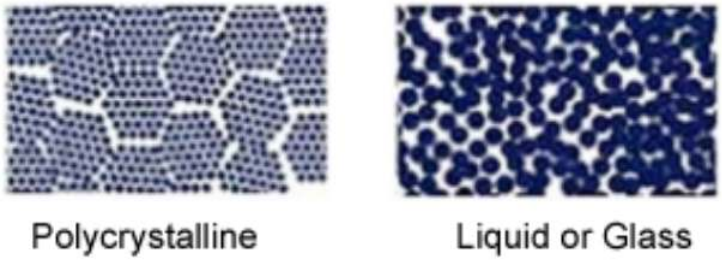


Upon cooling, high carbon steels phase segregate into a mixture of bcc iron (light gray) and Fe3C (dark gray) microscopic grains.

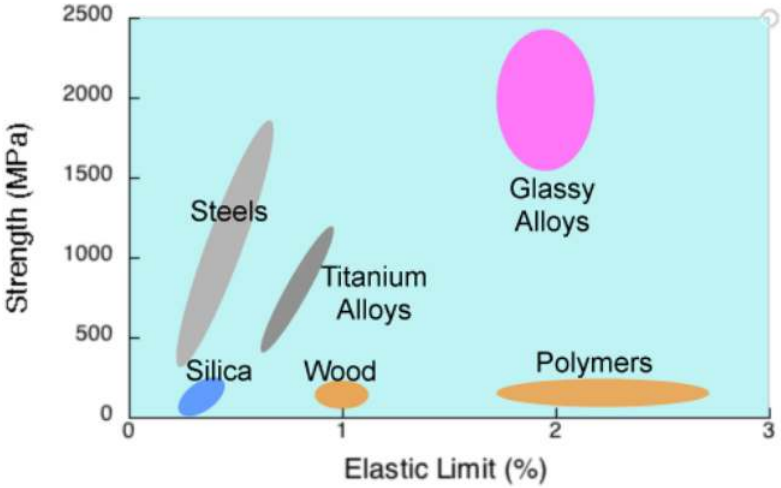
8.4: Iron and Steel is shared under a CC BY-SA license and was authored, remixed, and/or curated by LibreTexts.

- **7.4: Iron and Steel** by Chemistry 310 is licensed CC BY-SA 4.0. Original source: https://en.wikibooks.org/wiki/Introduction_to_Inorganic_Chemistry.

8.5: Amorphous Alloys



Alloys of metals with more complex stoichiometries can be made in amorphous form by slower cooling from the melt. These alloys have been prepared and studied since the 1960s, and since the 1990s amorphous alloys have been discovered that can be prepared in bulk form at cooling rates on the order of 1 deg/s, similar to the cooling rates of other kinds of glasses.



Currently amorphous metals (marketed under the tradenames Vitreloy and Liquidmetal) are used commercially in golf clubs, watches, USB flash drives, and other applications where very high elasticity, yield strength, and/or wear resistance are needed.

Year	Alloy	Cooling Rate (K/s)
1960	$Au_{75}Si_{24}$	10^6 - thin films & ribbons[3]
1969	Pd-Cu-Si	100-1000
1980s	La-Al-Cu & others	1-100
1990s	Zr-Ti-Cu-Ni-Be	~1 (similar to oxide glasses)

8.5: Amorphous Alloys is shared under a CC BY-SA license and was authored, remixed, and/or curated by LibreTexts.

- **7.5: Amorphous Alloys** by Chemistry 310 is licensed CC BY-SA 4.0. Original source: https://en.wikibooks.org/wiki/Introduction_to_Inorganic_Chemistry.

8.6: Discussion Questions

- Discuss the thermodynamics of work hardening and annealing in terms of the microscopic picture of defects in metallic crystals.
- In your pocket or purse, you may have a brass key, which is an alloy of Cu and Zn. How do the mechanical properties of this alloy depend on its structure, and why don't we make keys out of pure Cu or Zn?
- Cooling carbon steels along the eutectic lines (A and B) in the iron-carbon phase diagram above results in the formation of pearlite and ledeburite. How does the microstructure of these two iron alloys differ, and how does the microstructure affect their mechanical properties?

8.6: Discussion Questions is shared under a CC BY-SA license and was authored, remixed, and/or curated by LibreTexts.

- **7.6: Discussion Questions** by Chemistry 310 is licensed CC BY-SA 4.0. Original source: https://en.wikibooks.org/wiki/Introduction_to_Inorganic_Chemistry.

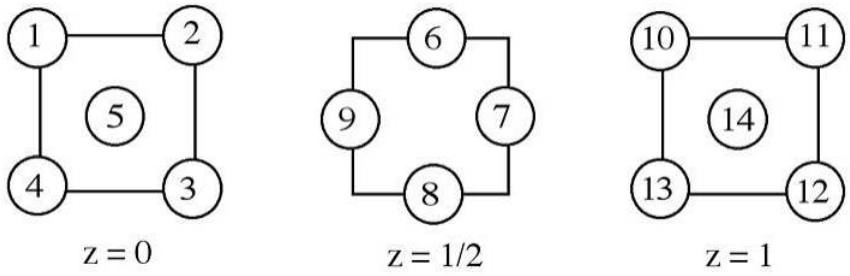
8.7: Problems

1. Show in a drawing how a planar dislocation moves through a solid under stress.

2. Why is a metal sample that has been annealed more malleable than one that has been work hardened? Explain which state of the metal has smaller crystal grains and why.

3. Explain (on the basis of structure) why alloys such as bronze make better structural materials than the constituent metals (copper and tin). How did the discovery of these alloys change civilization?

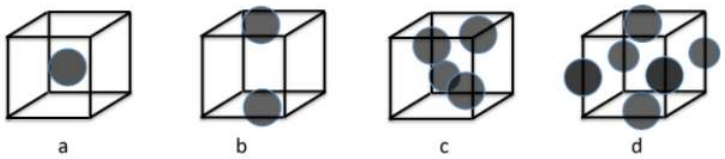
4. A layer sequence for an FCC = CCP metal is shown below. A body diagonal passes through the centers of atoms numbered 1 and 12. A close-packed plane perpendicular to this diagonal contains the centers of atoms numbered 3, 7, 8, 11, 13, and 14.



(a) Other close-packed planes of atoms parallel to this one pass through the cell. Segregate the remaining eight numbered atoms (not contained by this plane) into groups by the parallel plane that contains the center of the atom.

(b) Identify the other body diagonals by the numbered atoms that the diagonals pass through, and also identify one representative face diagonal by numbered atoms.

5. Identify the Bravais lattices that go with cubic unit cells (a) - (d). Remember that the origin of the unit cell is arbitrary.



8.7: Problems is shared under a CC BY-SA license and was authored, remixed, and/or curated by LibreTexts.

- **7.7: Problems** by Chemistry 310 is licensed CC BY-SA 4.0. Original source: https://en.wikibooks.org/wiki/Introduction_to_Inorganic_Chemistry.

8.8: References

1. P. Caron and T. Khan (1999), Evolution of Ni-based superalloys for single crystal gas turbine blade applications, Aerospace Science and Technology, 3, 513–523. http://dx.doi.org/10.1016/S1270-9638(99)00108-X
2. Libermann H. and Graham C. (1976). "Production Of Amorphous Alloy Ribbons And Effects Of Apparatus Parameters On Ribbon Dimensions". *IEEE Transactions on Magnetics* **12** (6): 921. doi:10.1109/TMAG.1976.1059201. Bibcode: 1976ITM....12..921L.
3. Klement, W.; Willens, R. H.; Duwez, POL (1960). "Non-crystalline Structure in Solidified Gold-Silicon Alloys". *Nature* **187** (4740): 869–870. doi:10.1038/187869b0. Bibcode: 1960Natur.187..869K.

8.8: References is shared under a CC BY-SA license and was authored, remixed, and/or curated by LibreTexts.

- **7.8: References** by Chemistry 310 is licensed CC BY-SA 4.0. Original source: https://en.wikibooks.org/wiki/Introduction_to_Inorganic_Chemistry.

CHAPTER OVERVIEW

9: Ionic and Covalent Solids - Structures

Learning Objectives

- Describe many crystal structures in terms of close-packed frameworks with systematic filling of octahedral and tetrahedral holes.
- Represent crystal structures by drawing them in sections.
- Rationalize, using chemical principles, why certain crystal structures are stable for certain compounds but not for others, as well as why certain structural and bonding motifs are preferred for certain compounds relative to others.
- Predict which crystal structures are most favorable for a given composition based on ionicity and periodic trends.
- Explain structure-dependent properties such as ferroelectricity and magnetic ordering based on crystal structures.
- Understand intercalation reactions in layered and open framework solids.
- Predict the preferred formation of normal or inverse spinels using arguments from transition metal chemistry (e.g. crystal field stabilization energies).

Inorganic solids often have simple crystal structures, and some of these structures are adopted by large families of ionic or covalent compounds. Examples of the most common structures include NaCl, CsCl, NiAs, zincblende, wurtzite, fluorite, perovskite, rutile, and spinel. We will develop these structures systematically from the close packed and non-close packed lattices shown below. Some layered structures, such as $CdCl_2$ and CdI_2, can be thought of as relatives of simple ionic lattices with some atoms "missing."

9.1: Prelude to Ionic and Covalent Solids - Structures
9.2: Close-packing and Interstitial Sites
9.3: Structures Related to NaCl and NiAs
9.4: Tetrahedral Structures
9.5: Layered Structures and Intercalation Reactions
9.6: Bonding in TiS_2, MoS_2, and Pyrite Structures
9.7: Spinel, Perovskite, and Rutile Structures
9.8: Discussion Questions
9.9: Problems
9.10: References

9: Ionic and Covalent Solids - Structures is shared under a CC BY-SA license and was authored, remixed, and/or curated by LibreTexts.

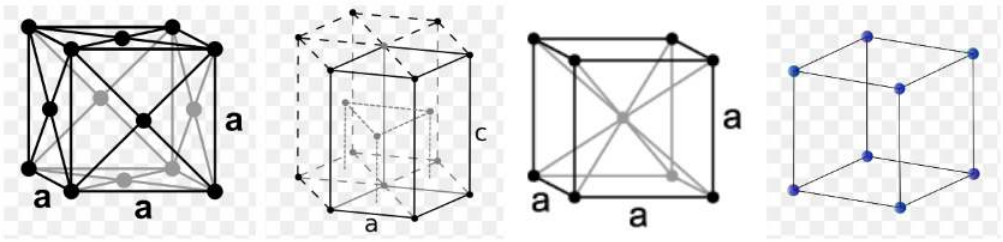
9.1: Prelude to Ionic and Covalent Solids - Structures

As we noted in our discussion of metal and alloy structures in Chapter 6, there is an intimate connection between the structures and the physical properties of materials. As we "graduate" from simple metal structures based on sphere packings to more complex structures, we find that this is still true. In this chapter we will try to systematize the structures of inorganic solids - metal oxides, halides, sulfides, and related compounds - and develop some rules for which structures to expect based on electronegativity differences, hard-soft acid-base rules, and other periodic trends. We will see that many of these structures are related to the sphere packings that we learned about in Chapter 6.



The morphology of twinned crystals of iron pyrite (FeS_2) is related to the underlying cubic symmetry of the unit cell. Like NaCl, the pyrite crystal structure can be thought of as a face-centered cubic array of anions (S_2^{2-}) with cations (Fe^{2+}) occupying all the octahedral holes.

Inorganic solids often have simple crystal structures, and some of these structures are adopted by large families of ionic or covalent compounds. Examples of the most common structures include NaCl, CsCl, NiAs, zincblende, wurtzite, fluorite, perovskite, rutile, and spinel. We will develop these structures systematically from the close packed and non-close packed lattices shown below. Some layered structures, such as $CdCl_2$ and CdI_2, can be thought of as relatives of simple ionic lattices with some atoms "missing."



Face-centered cubic (fcc) or cubic close-packed (ccp) | Hexagonal close-packed (hcp) | Body-centered cubic | Simple cubic

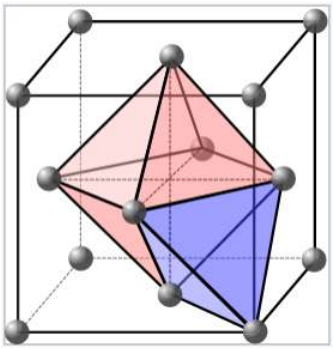
9.1: Prelude to Ionic and Covalent Solids - Structures is shared under a CC BY-SA license and was authored, remixed, and/or curated by LibreTexts.

- **8.1: Prelude to Ionic and Covalent Solids - Structures** by Chemistry 310 is licensed CC BY-SA 4.0. Original source: https://en.wikibooks.org/wiki/Introduction_to_Inorganic_Chemistry.

9.2: Close-packing and Interstitial Sites

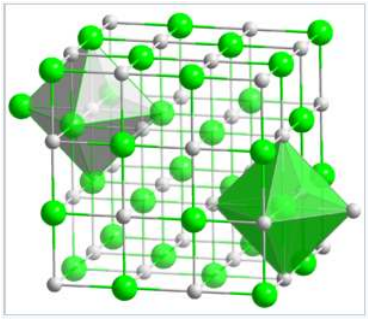
Many common inorganic crystals have structures that are related to cubic close packed (face-centered cubic) or hexagonal close packed sphere packings. These packing lattices contain two types of sites or "holes" that the interstitial atoms fill, and the coordination geometry of these sites is either **tetrahedral** or **octahedral**. An interstitial atom filling a tetrahedral hole is coordinated to four packing atoms, and an atom filling an octahedral hole is coordinated to six packing atoms. In both the hexagonal close packed and cubic close packed lattices, there is one octahedral hole and two tetrahedral holes per packing atom.

Question: Would anions or cations be better as packing atoms?
We might expect that anions, which are often larger than cations, would be better suited to the positions of packing atoms. While this is often true, there are many examples of structures in which cations are the packing atoms, and others in which the distinction is arbitrary. The NaCl structure is a good example of the latter.



One octahedral and one tetrahedral site in a face-centered cubic unit cell. Each cell contains four packing atoms (gray), four octahedral sites (pink), and eight tetrahedral sites (blue).

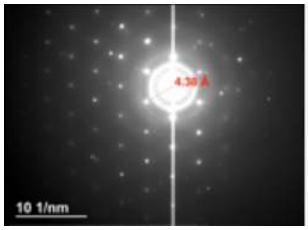
In the NaCl structure, shown on the right, the green spheres are the Cl^- ions and the gray spheres are the Na^+ ions. The octahedral holes in a face-centered cubic lattice can be found at fractional coordinates (1/2 1/2 1/2), (1/2 0 0), (0 1/2 0), and (0 0 1/2). There are four of these holes per cell, and they are filled by the chloride ions. The packing atoms (Na^+) have coordinates (0 0 0), (0 1/2 1/2), (1/2 1/2 0), and (1/2 0 1/2). Note that each of the Na^+ positions is related to a Cl^- position by a translation of (1/2 0 0). Another way of stating this is that the structure consists of **two interpenetrating fcc lattices**, which are related to each other by a translation of half the unit cell along any of the three Cartesian axes. We could have equivalently placed the Cl ions at the fcc lattice points and the Na ions in the octahedral holes by simply translating the origin of the unit cell by (1/2 0 0). Thus the distinction between packing and interstitial atoms in this case is arbitrary.



Crystal structure of NaCl. Both the Na^+ and Cl^- ions are octahedrally coordinated.

NaCl is interesting in that it is a three-dimensional checkerboard, and thus there are no NaCl "molecules" that exist in the structure. When this structure was originally solved (in 1913 by using X-ray diffraction) by W. L. Bragg, his interpretation met resistance by chemists who thought that precise integer stoichiometries were a consequence of the valency of atoms in molecules. The German chemist P. Pfeiffer noted in 1915 that ‘the ordinary notion of valency didn’t seem to apply’, and fourteen years later, the influential chemist H. E. Armstrong still found Bragg’s proposed structure of sodium chloride ‘more than repugnant to the common sense, not

chemical cricket'! Nevertheless, Bragg and his father, W. H. Bragg, persevered and used the then-new technique of X-ray diffraction to determine the structures of a number of other compounds, including diamond, zincblende, calcium fluoride, and other alkali halides. These experiments gave chemists their first real look at the atomic structure of solids, and laid the groundwork for X-ray diffraction experiments that later elucidated the structures of DNA, proteins, and many other compounds. For their work on X-ray diffraction the Braggs received the Nobel prize in Physics in 1915.

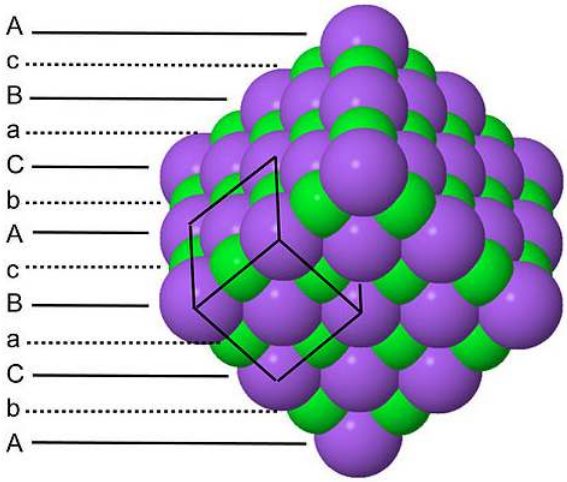


The lattice dimensions and positions of atoms in crystals such as NaCl are inferred from diffraction patterns.

Since each type of atom in the NaCl structure forms a face-centered cubic lattice, there are four Na and four Cl atoms per NaCl unit cell. It is because of this ratio that NaCl has a 1:1 stoichiometry. The shaded green and gray bipyramidal structures in the NaCl lattice show that the Na^+ ions are coordinated to six Cl^- ions, and vice versa. The NaCl structure can be alternatively drawn as a stacking of close-packed layer planes, AcBaCbAcBa... along the body diagonal of the unit cell. Here the uppercase letters represent the packing atoms, and the lower case letters are the interstitial atoms. This layered packing is illustrated below:

NaCl structure

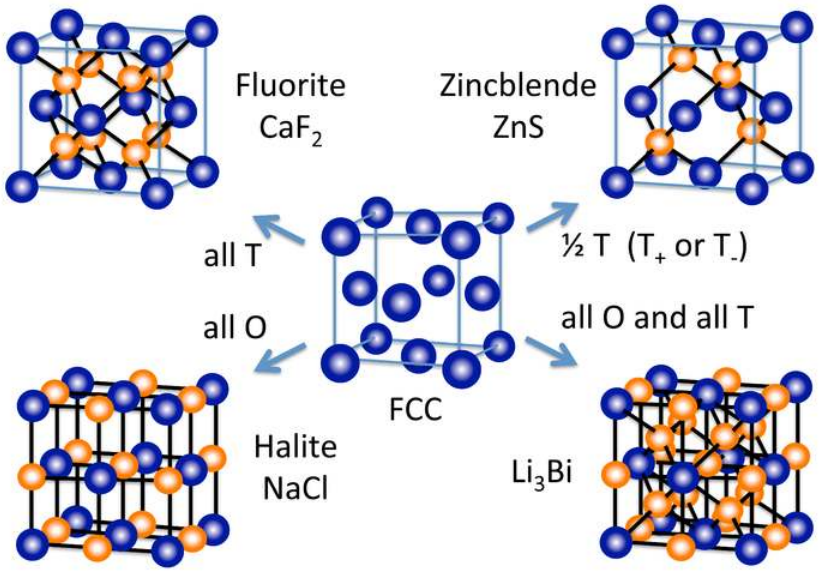
- ---------- A
- - - -c- - - -
- ---------- B
- - - -a- - - -
- ---------- C
- - - -b- - - -
- ---------- A
- - - -c- - - -
- ---------- B
- - - -a- - - -
- ---------- C
- - - -b- - - -
- ---------- A



Note that both the packing atoms and interstitials are stacked in the sequence A-B-C-A-B-C..., in keeping with the fact that each forms a cubic close-packed lattice.

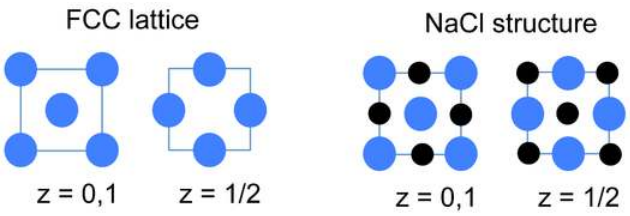
The NaCl structure is fairly common among ionic compounds:

- Alkali Halides (except CsCl, CsBr, and CsI)
- Transition Metal Monoxides (TiO, VO,..., NiO)
- Alkali Earth Oxides and Sulfides (MgO, CaO, BaS... except BeO and MgTe)
- Carbides and Nitrides (TiC, TiN, ZrC, NbC) -these are very stable refractory, interstitial alloys (metallic)



A number of other inorganic crystal structures are formed (at least conceptually) by filling octahedral and/or tetrahedral holes in close-packed lattices. The figure at the right shows some of the most common structures (fluorite, halite, zincblende) as well as a rather rare one (Li_3Bi) that derive from the fcc lattice. From the hcp lattice, we can make the NiAs and wurzite structures, which are the hexagonal relatives of NaCl and zincblende, respectively.

An alternative and very convenient way to represent inorganic crystal structures (especially complex structures such as Li_3Bi) is to draw the unit cell in slices along one of the unit cell axes. This kind of representation is shown at the left for the fcc lattice and the NaCl structure. Since all atoms in these structures have z-coordinates of either 0 or 1/2, only those sections need to be drawn in order to describe the contents of the unit cell. It is a useful exercise to draw some of the fcc compound structures (above) in sections.



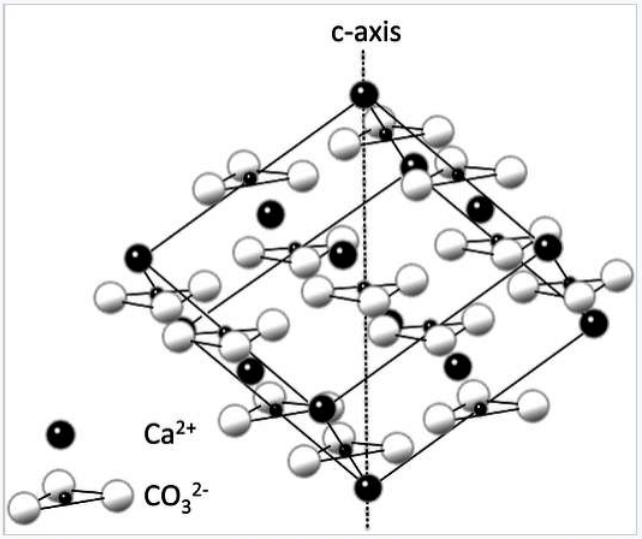
9.2: Close-packing and Interstitial Sites is shared under a CC BY-SA license and was authored, remixed, and/or curated by LibreTexts.

- **8.2: Close-packing and Interstitial Sites** by Chemistry 310 is licensed CC BY-SA 4.0. Original source: https://en.wikibooks.org/wiki/Introduction_to_Inorganic_Chemistry.

9.3: Structures Related to NaCl and NiAs

There are a number of compounds that have structures similar to that of NaCl, but have a lower symmetry (usually imposed by the geometry of the anion) than NaCl itself. These compounds include:

- FeS_2 (pyrite, "fools gold"): S_2^{2-} (disulfide) and Fe^{2+}
- CaC_2 (a salt-like carbide): Ca^{2+} and linear C_2^{2-} anions
- $CaCO_3$ (calcite, limestone, marble): Ca^{2+} and triangular CO_3^{2-}.



The rhombohedral unit cell of the calcite crystal structure. The hexagonal c-axis is shown.

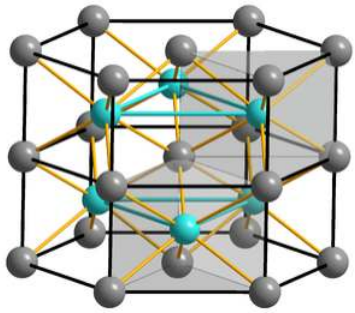
The **calcite** ($CaCO_3$) crystal structure is shown above. Triangular CO_3^{2-} ions fill octahedral holes between the Ca^{2+} ions (black spheres) in a distorted NaCl lattice. As in NaCl, each ion is coordinated by six of the other kind. From this image we can see why the $CaCO_3$ structure has a lower symmetry than that of NaCl. The fourfold rotation symmetry of the NaCl unit cell is lost when the spherical Cl^- ions are replaced by triangular CO_3^{2-} ions. Because of this symmetry lowering, transparent crystals calcite are birefringent, as illustrated below.



Calcite crystals are birefringent, meaning that their refractive indices are different along the two principal crystal directions. This gives rise to the phenomenon of double refraction.

NiAs structure

The NaCl structure can be described a face-centered cubic lattice with all of the octahedral holes filled. What if we start with a hexagonal-close packed lattice rather than a face-centered cubic lattice?



Nickel arsenide crystal structure. The Ni_6As trigonal prisms are shaded gray. One octahedron of six As atoms surrounding a Ni atom is shown in the center of the figure.

This is the structure adopted by **NiAs** and many other transition metal sulfides, phosphides, and arsenides. The cations are shown in gray while the anions are light blue in the figure at the right. The cations are in octahedral coordination, so each cation is coordinated to six anions. The anions are also coordinated to six cations, but they occupy trigonal prismatic sites. In terms of layer stacking, the NiAs structure is AcBcAcBc..., where the A and B sites (the hcp lattice) are occupied by the As atoms, and the c sites, which are eclipsed along the layer stacking axis, are occupied by Ni. Unlike the NaCl structure, where the anion and cation sites are interchangeable, NiAs has unique anion and cation sites. The layer stacking sequence for NiAs is shown below:

- ---------- A
- - - -c- - - -
- ---------- B
- - - -c- - - -
- ---------- A
- - - -c- - - -
- ---------- B
- - - -c- - - -

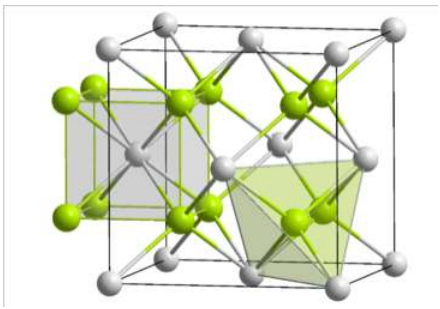
The NiAs structure cannot be adopted by ionic compounds because of the eclipsing cations, because the cation-cation repulsions would be internally destabilizing for an ionic compound. This structure is mainly adopted by covalent and polar covalent MX compounds, typically with "soft" X anions (S, Se, P, As,....) and low-valent transition metal cations. For example, some compounds with the NiAs structure are: MS, MSe, MTe (M=Ti, V, Fe, Co, Ni). Often these are nonstoichiometric or complex stoichiometries with ordered vacancies (Cr_7S_8, Fe_7S_8).

9.3: Structures Related to NaCl and NiAs is shared under a CC BY-SA license and was authored, remixed, and/or curated by LibreTexts.

- **8.3: Structures Related to NaCl and NiAs** by Chemistry 310 is licensed CC BY-SA 4.0. Original source: https://en.wikibooks.org/wiki/Introduction_to_Inorganic_Chemistry.

9.4: Tetrahedral Structures

In ccp and hcp lattices, there are two tetrahedral holes per packing atom. A stoichiometry of either M_2X or MX_2 gives a structure that fills all tetrahedral sites, while an MX structure fills only half of the sites. An example of an MX_2 structure is **fluorite**, CaF_2, whose structure is shown in the figure at the left. The packing atom in fluorite is Ca^{2+} and the structure is composed of three interpenetrating fcc lattices. It should be noted that the Ca^{2+} ion (gray spheres) as a packing atom defies our "rule" that anions are larger than cations and therefore must be the packing atoms. The fluorite structure is common for ionic MX_2 (MgF_2, ZrO_2, etc.) and M_2X compounds (Li_2O). In contrast, the hcp relative of the fluorite structure is quite rare because of unfavorable close contacts between like-charged ions.



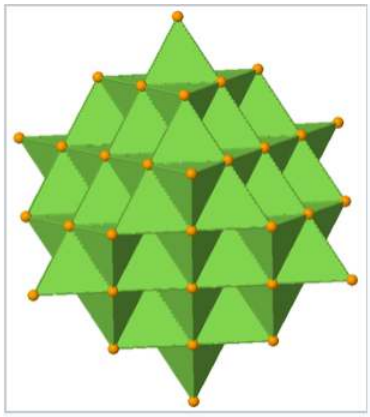
The fluorite (CaF_2) crystal structure showing the coordination environments of the Ca and F atoms

In terms of geometry, Ca^{2+} is in cubic coordination with eight F^- neighbors, and the fluoride ions are tetrahedrally coordinated by four Ca^{2+} ions. The 8:4 coordination geometry is consistent with the 1:2 Ca:F stoichiometry; in all crystal structures the ratio of the coordination numbers is the inverse of the stoichiometric ratio. The three interpenetrating fcc lattices have Ca at 0,0,0 , 1/2,1/2,0 , etc....F at 1/4,1/4,1/4 , 3/4,3/4,1/4 , etc... and F at 3/4,3/4,3/4 , 1/4,1/4/3/4 , etc.

Looking more closely at the tetrahedral sites in fluorite, we see that they fall into two distinct groups: T_+ and T_-. If a tetrahedron is oriented with a vertex pointing upwards along the stacking axis, the site is T_+. Likewise, a tetrahedron with a vertex oriented downward is T_-. The alternation of T_+ and T_- sites allows for efficient packing of ions in the structure. The layer stacking sequence in this structure (including fluoride ions in the T_+ and T_- sites) is:

- ---------- A
- - - -b- - - T_+
- - - -a- - - T_-
- ---------- B
- - - -c- - - T_+
- - - -b- - - T_-
- ---------- C
- - - -a- - - T_+
- - - -c- - - T_-
- ---------- A
- - - -b- - - T_+

- - - -a- - - T_-

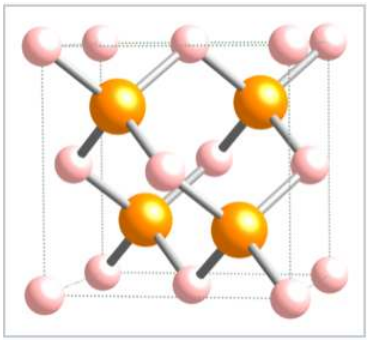


Polyhedral view of the fluorite crystal structure, showing T_+ and T_- Ca_4F tetrahedra. The Ca^{2+} ions are stacked ABCABC... along the body diagonal of the unit cell, which is the vertical direction in this image.

Tetrahedrally bonded compounds with a 1:1 stoichiometry (MX compounds) have only **half** of the tetrahedral sites (either the T_+ or T_- sites) filled. In this case, both the M and the X atoms are tetrahedrally coordinated. The **zincblende** and **wurtzite** structures are 1:1 tetrahedral structures based on fcc and hcp lattices, respectively. Both structures are favored by p-block compounds that follow the octet rule, and these compounds are usually semiconductors or insulators. The zincblende structure, shown below, can be thought of as two interpenetrating fcc lattices, one of anions and one of cations, offset from each other by a translation of 1/4 along the body diagonal of the unit cell. Examples of compounds with the zincblende structure include CuCl, CuI, ZnSe, HgS, BeS, CdTe, AlP, GaP, SnSb, CSi, and diamond. Additionally, the compound $CuInSe_2$ is zincblende in an ordered, doubled unit cell (the chalcopyrite structure). The solid solution compounds $CuIn_{1-x}Ga_xSe_2$ with this structure are among the most widely studied materials for use in efficient thin film photovoltaic cells. Using ZnS as a representative of zincblende, the coordination of both Zn and S atoms is tetrahedral. The layer sequence, which is AbBcCaAbBcC..., results in six-membered ZnS rings that have the same geometry as the "chair" version of cyclohexane. The chair conformation allows for a relatively long distance between opposite atoms in the ring and, as a result, it is more sterically favorable than the boat form. The sequence of close-packed layers in zincblende, filling only the T_+ sites and leaving the T_- sites empty, is shown below:

- ---------- A
- - - -b- - - T_+
- - - - - - T_-
- ---------- B
- - - -c- - - T_+
- - - - - - T_-
- ---------- C
- - - -a- - - T_+

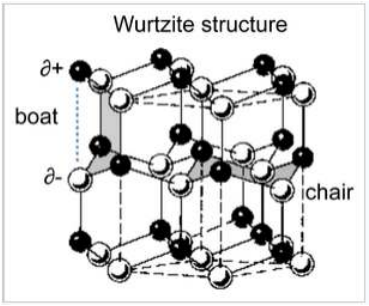
- - - - - - T_-



The zincblende unit cell

The wurtzite structure is a close relative of zinc blende, based on filling half the tetrahedral holes in the hcp lattice. Like zincblende, wurtzite contains planes of fused six-membered rings in the chair conformation. Unlike zincblende, however, the rings joining these planes contain six-membered "boat" rings. The boat aligns the anions so that they are directly above the cations in the structure, a less favorable situation sterically but a more favorable one in terms of electrostatics. As a result, the wurtzite structure tends to favor more polar or ionic compounds (e.g., ZnO, $NH_4^+F^-$) than the zincblende structure. As with zincblende, both ions are in tetrahedral (4:4) coordination and there are typically eight valence electrons in the MX compound. Examples of compounds with this structure include: BeO, ZnO, MnS, CdSe, MgTe, AlN, and NH_4F. The layered structure of wurtzite is AbBaAbB and the layer sequence with T_+ sites filled is illustrated below:

- ---------- A
- - - -b- - - T_+
- - - - - - T_-
- ---------- B
- - - -a- - - T_+
- - - - - - T_-
- ---------- A
- - - -b- - - T_+
- - - - - - T_-
- ---------- B

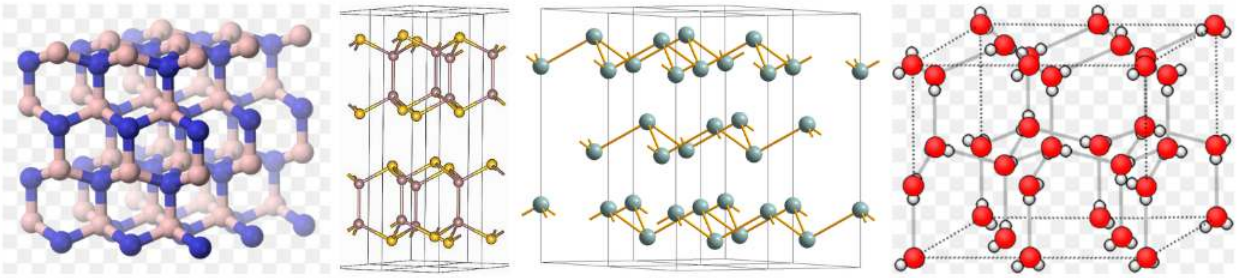


The chair and boat conformations of six-membered ZnS rings in the wurtzite structure.

An interesting consequence of the layer stacking in the wurtzite structure is that the crystals are polar. When cleaved along the c-axis (the stacking axis), crystals of ZnO, ZnS, and GaN have one negatively charged face and an opposite positively charged face. An applied electric field interacts with the crystal dipole, resulting in compression or elongation of the lattice along this direction. For this reason crystals of compounds in the wurtzite structure are typically piezoelectric.

Some compounds are diamorphic and can have either the zincblende or wurtzite structure. Examples of these compounds that have intermediate polarities include CdS and ZnS. SiO_2 exists in polymorphs (crystobalite and tridymite) that resemble zincblende and

wurtzite with O atoms midway between each of the Si atoms. The zincblende and wurtzite structures have efficient packing arrangements for tetrahedrally bonded networks and are commonly found in compounds that have tetrahedral bonding. Water, for example, has a tetrahedral hydrogen bonding network and is wurtzite-type. The undistorted wurtzite and zinc blende structures are typically found for AX compounds with eight valence electrons, which follow the octet rule. AX compounds with nine or ten electrons such as GaSe and GaAs crystallize in distorted variants of the wurtzite structure. In GaSe, the extra electrons form lone pairs and this creates layers in the structure, as can be seen in the figure below. To the right of GaSe, the structures of As, Sb, and SbAs show an ever further breakdown of the structure into layers as more valence electrons are added.



Wurtzite crystal structure | GaSe crystal structure | Crystal structure of Sb, SbAs, and gray As | Crystal structure of hexagonal ice

Hexagonal ice is the most stable polymorph of ice, which is obtained upon freezing at 1 atmosphere pressure. This polymorph (ice-I) has a hcp wurtzite-type structure. Looking at the structure shown at the right, we see that there are irregular arrangements of the O-H---O bonds. In the structure, hydrogen bonding enforces the tetrahedral coordination of each water molecule, resulting in a relatively open structure that is less dense than liquid water. For this reason, ice floats in water.

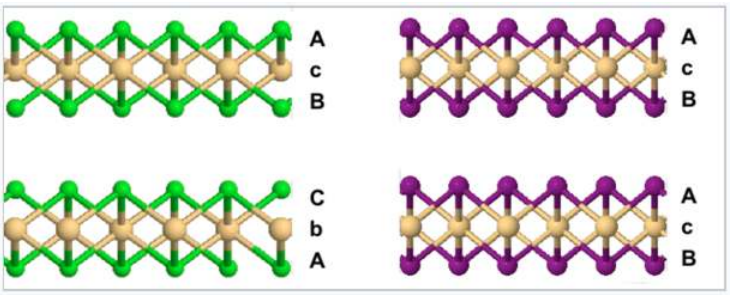
9.4: Tetrahedral Structures is shared under a CC BY-SA license and was authored, remixed, and/or curated by LibreTexts.

- **8.4: Tetrahedral Structures** by Chemistry 310 is licensed CC BY-SA 4.0. Original source: https://en.wikibooks.org/wiki/Introduction_to_Inorganic_Chemistry.

9.5: Layered Structures and Intercalation Reactions

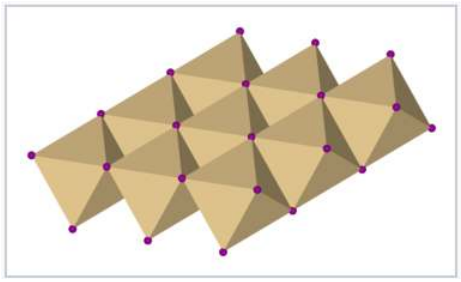
Layered structures are characterized by strong (and typically covalent) bonding between atoms in two dimensions and weaker bonding in the third. A broad range of compounds including metal halides, oxides, sulfides, selenides, borides, nitrides, carbides, and allotropes of some pure elements (B, C, P, As) exist in layered forms. Structurally, the simplest of these structures (for example binary metal halides and sulfides) can be described as having some fraction of the octahedral and/or tetrahedral sites are filled in the fcc and hcp lattices. For example, the $CdCl_2$ structure is formed by filling all the octahedral sites in alternate layers of the fcc lattice, and the CdI_2 structure is the relative of this structure in the hcp lattice.

In the **$CdCl_2$ structure**, the stacking sequence of anion layers is ABCABC...
In the **CdI_2 structure**, the anion stacking sequence is ABAB..., and all the cations are eclipsed along the stacking axis.



Comparison of the $CdCl_2$ (left) and CdI_2 (right) crystal structures

These are examples of **6-3 structures**, because the cations are coordinated by an octahedron of six anions, and the anions are coordinated by three cations to make a trigonal pyramid (like NH_3). Another way to describe these structures is to say that the MX_6 octahedra each share six edges in the MX_2 sheets.



Polyhedral drawing of one layer of the $CdCl_2$ or CdI_2 structure showing edge-sharing MX_6 octahedra

Because these structures place the packing atoms (the anions) in direct van der Waals contact, they are most stable for relatively **covalent** compounds. Otherwise, the electrostatic repulsion between contacting anions would destabilize the structure energetically. More ionic MX_2 compounds tend to adopt the fluorite (CaF_2) or rutile (TiO_2) structures, which are not layered.

Despite the fact that these two structure types are the same at the level of nearest and next-nearest neighbor ions, the CdI_2 structure is much more common than the $CdCl_2$ structure.

$CdCl_2$ structure:

MCl_2 (M = Mg, Mn, Fe, Co, Ni, Zn, Cd)

$NiBr_2$, NiI_2, $ZnBr_2$, ZnI_2

CdI_2 structure:

MCl_2 (M = Ti, V)

MBr_2 (M = Mg, Fe, Co, Cd)

MI_2 (M = Mg, Ca, Ti, V, Mn, Fe, Co, Cd, Ge, Pb, Th)

$M(OH)_2$ (M = Mg, Ca, Mn, Fe, Co, Ni, Cd)

MS_2 (M = Ti, Zr, Sn, Ta, Pt)

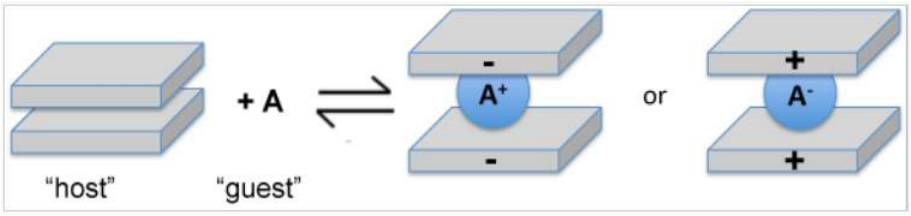
MSe_2 (M = Ti, Zr, Sn, V, Pt)

MTe_2 (M = Ti, Co, Ni, Rh, Pd, Pt)

Physically, layered compounds are **soft** and **slippery**, because the layer planes slide past each other easily. For example, graphite, MoS_2, and talc (a silicate) are layered compounds that are used widely as **lubricants** and lubricant additives.

An important reaction of layered compounds is **intercalation**. In intercalation reactions, guest molecules and ions enter the galleries that separate the sheets, usually with expansion of the lattice along the stacking axis. This reaction is typically reversible if it does not perturb the bonding within the sheets. Often the **driving force for intercalation is a redox reaction**, i.e., electron transfer between the host and guest. For example, lithium metal reacts with TiS_2, MoS_2, and graphite to produce $LiTiS_2$, Li_xMoS_2 ($x < 1$), and LiC_6. In these compounds, lithium is ionized to Li^+ and the sheets are negatively charged. Oxidizing agents such as Br_2, $FeCl_3$, and AsF_5 also react with graphite. In the resulting intercalation compounds, the sheets are positively charged and the intercalated species are anionic.

Intercalation reactions are especially important for electrochemical energy storage in **secondary batteries**, such as **lithium ion** batteries, **nickel-metal hydride** batteries, and **nickel-cadmium** batteries. The reversible nature of the intercalation reaction allows the electrodes to be charged and discharged up to several thousand times without losing their mechanical integrity. In lithium ion batteries, the negative electrode material is typically graphite, which is intercalated by lithium to make LiC_6. Several different oxides and phosphates containing redox active transition metal ions (Mn, Fe, Co, Ni) are used as the positive electrode materials.



Oxidative or reductive intercalation involves the placement of anions or cations between sheets.

Lithium ion batteries based on CoO_2 were first described in 1980[1] by John B. Goodenough's research group at Oxford. In batteries based on CoO_2, which has the CdI_2 structure, the positive electrode half-reaction is:

$$\mathrm{LiCoO_2 \leftrightharpoons Li_{1-x}CoO_2 + x\,Li^+ + xe^-} \tag{9.5.1}$$

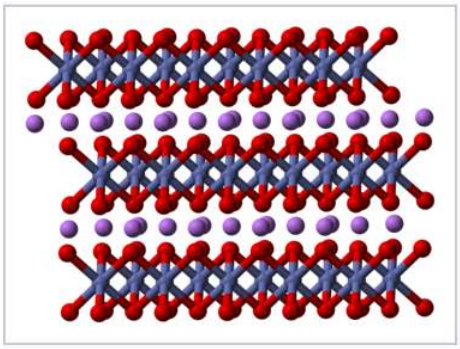
The negative electrode half reaction is:

$$\mathrm{x\,Li^+ + xe^- + x\,C_6 \leftrightharpoons x\,LiC_6} \tag{9.5.2}$$

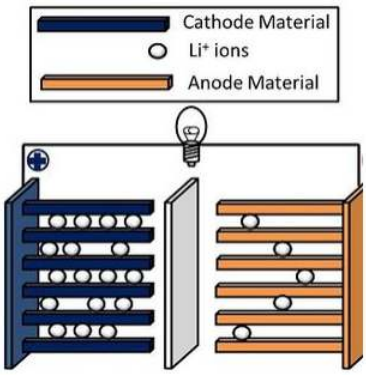
The battery is fully charged when the positive electrode is in the CoO_2 form and the negative electrode is in the LiC_6 form. Discharge involves the motion of Li^+ ions through the electrolyte, forming Li_xCoO_2 and graphite at the two electrodes.



Blue plaque erected by the Royal Society of Chemistry commemorating the development of cathode materials for the lithium-ion battery



Crystal structure of $LiCoO_2$[2]



The lithium ion battery is a "rocking chair" battery, so named because charging and discharging involve moving Li^+ ions from one side to the other. CoO_2 is one example of a positive electrode material that has been used in lithium ion batteries. It has a high energy density, but batteries based on CoO_2 have poor thermal stability. Safer materials include lithium iron phosphate ($LiFePO_4$), and $LiMO_2$ (M = a mixture of Co, Mn, and Ni). These batteries are used widely in laptop computers, portable electronics, cellular telephones, cordless tools, and electric and hybrid vehicles.

A similar intercalation reaction occurs in nickel-cadmium batteries and nickel-metal hydride batteries, except in this case the reaction involves the movement of protons in and out of the $Ni(OH)_2$ lattice, which has the CdI_2 structure:

$$\mathrm{NiO(OH) + H_2O + e^- \longrightarrow Ni(OH)_2 + OH^-} \tag{9.5.3}$$

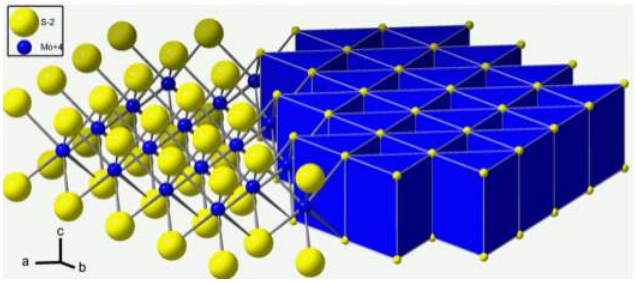
There are many layered compounds that cannot be intercalated by redox reactions, typically because some other stable product is formed. For example, the reaction of layered CdI_2 with Li produces LiI (NaCl structure) and Cd metal.

9.5: Layered Structures and Intercalation Reactions is shared under a CC BY-SA license and was authored, remixed, and/or curated by LibreTexts.

- **8.5: Layered Structures and Intercalation Reactions** by Chemistry 310 is licensed CC BY-SA 4.0. Original source: https://en.wikibooks.org/wiki/Introduction_to_Inorganic_Chemistry.

9.6: Bonding in TiS_2, MoS_2, and Pyrite Structures

Many layered dichalcogenides, such as TiS_2 and ZrS_2, have the CdI_2 structure. In these compounds, as we have noted above, the metal ions are octahedrally coordinated by S. Interestingly, the structures of MoS_2 and WS_2, while they are also layered, are different. In these cases, the metal is surrounded by a **trigonal prism** of sulfur atoms. NbS_2, TaS_2, $MoSe_2$, $MoTe_2$, and WSe_2 also have the trigonal prismatic molybdenite structure, which is shown below alongside a platy crystal of MoS_2.

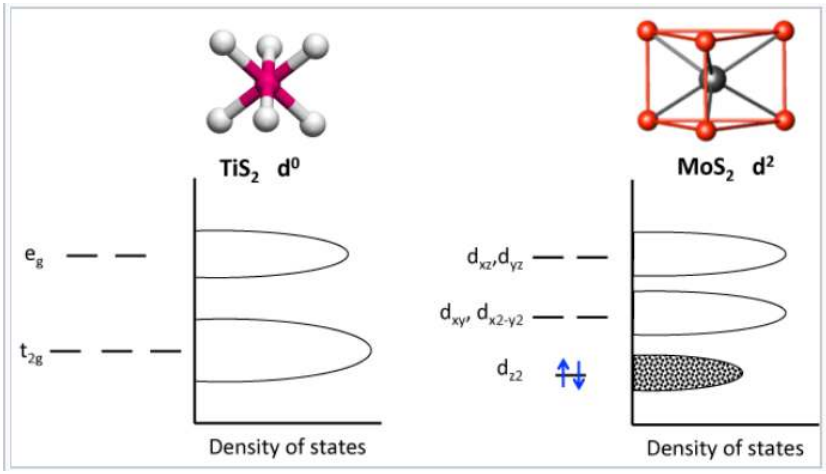




The coordination of the metal ions by a trigonal prism of chalcogenide ions is **sterically unfavorable** relative to octahedral coordination. There are close contacts between the chalcogenide ions, which are eclipsed in the stacking sequence **AbA/BaB/AbA/BaB**... (where "/" indicates the van der Waals gap between layers). What stabilizes this structure?

The molybdenite structure occurs most commonly in MX_2 compounds with a **d^1 or d^2 electron count**. The figure below compares the splitting of d-orbital energies in the octahedral and trigonal prismatic coordination environments:

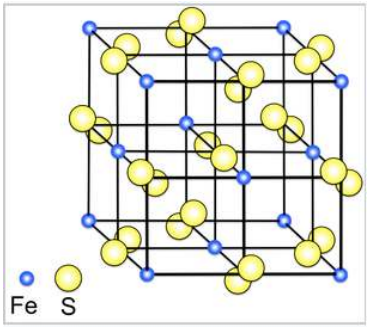
The trigonal prismatic structure is stabilized in MoS_2 by filling the lowest energy band, the d_{z2}. The d_{z2} orbital which points vertically through the triangular top and bottom faces of the trigonal prism, has the least interaction with the sulfide ligands and therefore the lowest energy. The d_{xz} and d_{yz} orbitals, which point at the ligands, have the highest energy. The d_{z2} orbital is lower in energy in this structure than the t_{2g} orbitals are in the octahedral structure of TiS_2.



d-orbital splittings and energy bands in TiS_2 and MoS_2. MoS_2 is a semiconductor with a 1.3 eV gap between its filled and empty bands.

Because it has an unfilled t_{2g} band, TiS_2 is relatively easy to reduce by intercalation with Li. For this reason, $LiTiS_2$ was one of the first intercalation compounds studied by Stanley Whittingham, who developed the concept of the non-aqueous lithium ion battery in the early 1970's.[3] Because it has a filled d_{z2} band, MoS_2 is harder to reduce, but it can be intercalated by reaction with the powerful reducing agent n-butyllithium to make Li_xMoS_2 ($x < 1$). Atoms in the van der Waals planes of these compounds are relatively unreactive, which gives MoS_2 its good oxidative stability and enables its application as a high temperature lubricant. Atoms at the edges of the crystals are however more reactive and in fact are catalytic. High surface area MoS_2, which has a high density of exposed edge planes, is used as a hydrodesulfurization catalyst and is also of increasing interest as an electrocatalyst for the reduction of water to hydrogen.

Layered metal dichalcogenides, including MoS_2, WS_2, and SnS_2, can form closed nanostructures that take the shape of multiwalled onions and multiwalled tubes. These materials were discovered by the group of Reshef Tenne in 1992, shortly after the discovery of carbon nanotubes. Since then nanotubes have been synthesized from many other materials, including vanadium and manganese oxides.



The pyrite (FeS_2) crystal structure. The structure is related to NaCl, with Fe^{2+} and S_2^{2-} ions occupying the cation and anion sites.

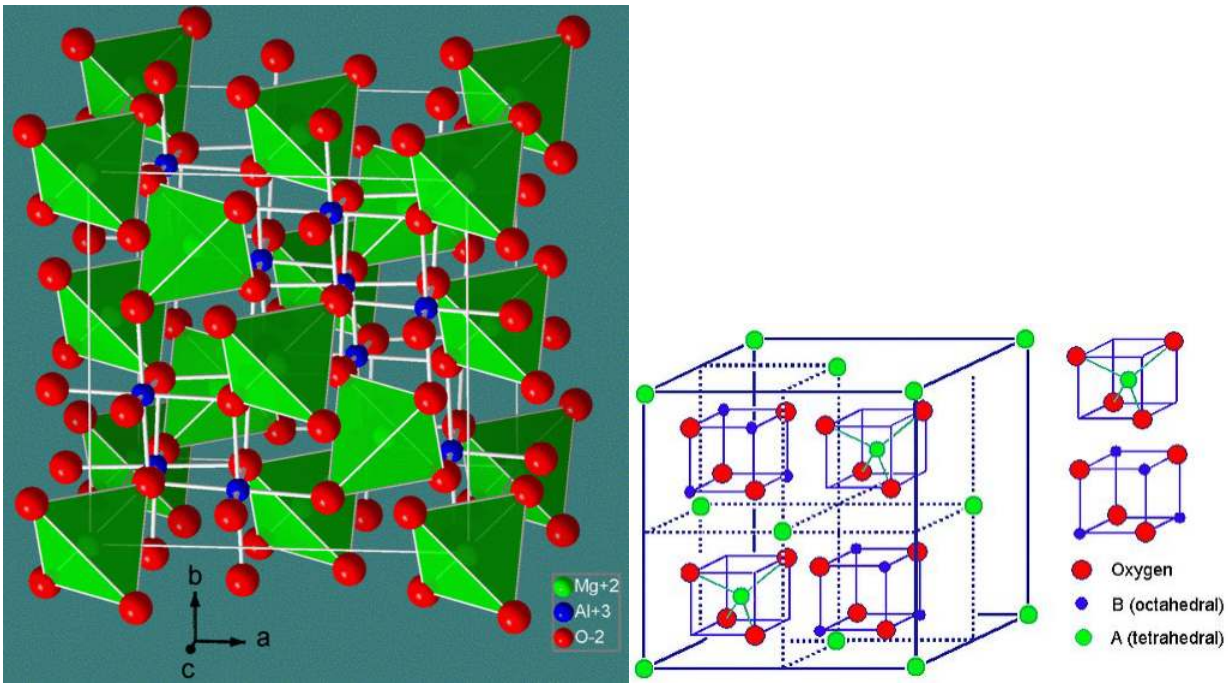
Although early (TiS_2) and late (PtS_2) transition metal disulfides have layered structures, a number of MS_2 compounds in the middle of the transition series, such as MnS_2, FeS_2 and RuS_2, have three-dimensionally bonded structures. For example, FeS_2 has the **pyrite structure**, which is related to the NaCl structure. The reason is that FeS_2 is not $Fe^{4+}(S^{2-})_2$, but is actually $Fe^{2+}(S_2^{2-})$, where S_2^{2-} is the disulfide anion (which contains a single bond like the peroxide anion O_2^{2-}). S^{2-} is too strong a reducing agent to exist in the same compound with Fe^{4+}, which is a strong oxidizing agent. Because FeS_2 is actually $Fe^{2+}(S_2^{2-})$, it is a 1:1 compound and adopts a 1:1 structure.

9.6: Bonding in TiS₂, MoS₂, and Pyrite Structures is shared under a CC BY-SA license and was authored, remixed, and/or curated by LibreTexts.

- **8.6: Bonding in TiS₂, MoS₂, and Pyrite Structures** by Chemistry 310 is licensed CC BY-SA 4.0. Original source: https://en.wikibooks.org/wiki/Introduction_to_Inorganic_Chemistry.

9.7: Spinel, Perovskite, and Rutile Structures

There are three more structures, which are derived from close-packed lattices, that are particularly important because of the material properties of their compounds. These are the **spinel** structure, on which ferrites and other magnetic oxides are based, the **perovskite** structure, which is adopted by ferroelectric and superconducting oxides, and the **rutile** structure, which is a common binary 6:3 structure adopted by oxides and fluorides.



The **spinel structure** is formulated MM'_2X_4, where M and M' are tetrahedrally and octahedrally coordinated cations, respectively, and X is an anion (typically O or F). The structure is named after the mineral $MgAl_2O_4$, and oxide spinels have the general formula AB_2O_4.

In the **normal spinel** structure, there is a close-packed array of anions. The A-site cations fill 1/8 of the tetrahedral holes and the B-site cations fill 1/2 of the octahedral holes. A polyhedral view of the normal spinel unit cell is shown at the left, and a simplified view (with the contents of the back half of the cell removed for clarity) is shown above. Each unit cell contains eight formula units and has a composition $A_8B_{16}O_{32}$.

Inverse spinels have a closely related structure (with the same large unit cell) in which the A-site ions and half of the B-site ions switch places. Inverse spinels are thus formulated $B(AB)O_4$, where the AB ions in parentheses occupy octahedral sites, and the other B ions are on tetrahedral sites. There are also mixed spinels, which are intermediate between the **normal** and **inverse** spinel structure.

Some spinel and inverse spinel AB combinations are:

$A^{2+}B^{3+}$, e.g., $MgAl_2O_4$ (normal spinel)

$A^{4+}B^{2+}$, e.g., $Pb_3O_4 = Pb^{II}(Pb^{II}Pb^{IV})O_4$ (inverse spinel)

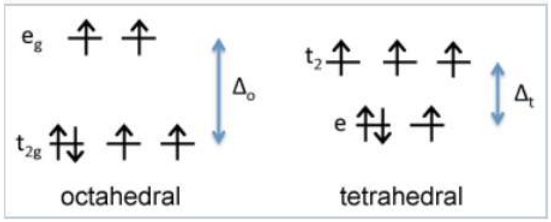
$A^{6+}B^{+}$, e.g., Na_2WO_4 (normal spinel)

Many magnetic oxides, such as Fe_3O_4 and $CoFe_2O_4$, are spinels.

Normal vs. inverse spinel structure

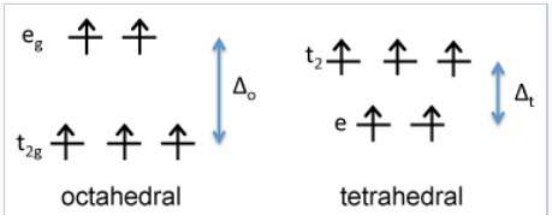
For transition metal oxide spinels, the choice of the normal vs. inverse spinel structure is driven primarily by the **crystal field stabilization energy** (CFSE) of ions in the tetrahedral and octahedral sites. For spinels that contain 3d elements such as Cr, Mn, Fe, Co, and Ni, the electron configuration is typically **high spin** because O^{2-} is a **weak field ligand**.

As an example, we can consider magnetite, Fe_3O_4. This compound contains one Fe^{2+} and two Fe^{3+} ions per formula unit, so we could formulate it as a normal spinel, $Fe^{2+}(Fe^{3+})_2O_4$, or as an inverse spinel, $Fe^{3+}(Fe^{2+}Fe^{3+})O_4$. Which one would have the lowest energy?



d-orbital energy diagram for Fe^{2+}

First we consider the crystal field energy of the **Fe^{2+}** ion, which is d^6. Comparing the tetrahedral and high spin octahedral diagrams, we find that the CFSE in an **octahedral** field of O^{2-} ions is $[(4)(\frac{2}{5}) - (2)(\frac{3}{5})]\Delta_o - P = \mathbf{0.4\Delta_o - P}$. In the **tetrahedral** field, the CFSE is $[(3)(\frac{3}{5}) - (3)(\frac{2}{5})]\Delta_t - P = \mathbf{0.6\Delta_t - P}$. Since Δ_o is about 2.25 times larger than Δ_t, the octahedral arrangement has a larger CFSE and is preferred for Fe^{2+}.



d-orbital energy diagram for Fe^{3+}

In contrast, it is easy to show that **Fe^{3+}**, which is d^5, would have a CFSE of zero in either the octahedral or tetrahedral geometry. This means that Fe^{2+} has a preference for the octahedral site, but Fe^{3+} has no preference. Consequently, we place Fe^{2+} on octahedral sites and **Fe_3O_4 is an inverse spinel**, $Fe^{3+}(Fe^{2+}Fe^{3+})O_4$.

Ferrites are compounds of general formula **$M^{II}Fe_2O_4$**. We can see that magnetite is one example of a ferrite (with M = Fe). Other divalent metals (M = Mg, Mn, Co, Ni, Zn) also form ferrites. Ferrites can be normal or inverse spinels, or mixed spinels, depending on the CFSE of the M^{II} ion. Based on their CFSE, Fe^{2+}, Co^{2+}, and Ni^{2+} all have a strong preference for the octahedral site, so those compounds are all inverse spinels. $ZnFe_2O_4$ is a normal spinel because the small Zn^{2+} ion (d^{10}) fits more easily into the tetrahedral site than Fe^{3+} (d^5), and both ions have zero CFSE. $MgFe_2O_4$ and $MnFe_2O_4$, in which all ions have zero CFSE and no site preference, are mixed spinels. **Chromite** spinels, **$M^{II}Cr_2O_4$**, are always **normal spinels** because the d^3 Cr^{3+} ion has a strong preference for the octahedral site.

Examples of normal and inverse spinel structures:

> **$MgAl_2O_4$** is a **normal spinel** since both Mg^{2+} and Al^{3+} are non-transition metal ions and thus CFSE = 0. The more highly charged Al^{3+} ion prefers the octahedral site, where it is surrounded by six negatively charged oxygen atoms.
>
> **Mn_3O_4** is a **normal spinel** since the Mn^{2+} ion is a high spin d^5 system with zero CFSE. The two Mn^{3+} ions are high spin d^4 with higher CFSE on the octahedral sites (3/5 Δ_O) than on the tetrahedral site (2/5 Δ_t ~ 1/5 Δ_O).
>
> **Fe_3O_4** is an **inverse spinel** since the Fe^{3+} ion is a high spin d^5 system with zero CFSE. Fe^{2+} is a high spin d^6 system with more CFSE on an octahedral site than on a tetrahedral one.
>
> **$NiFe_2O_4$** is again an **inverse spinel** since Ni^{2+} (a d^8 ion) prefers the octahedral site and the CFSE of Fe^{3+} (a d^5 ion) is zero.
>
> **$FeCr_2O_4$** is a **normal spinel** since Fe^{2+} is high spin d^6 ion with $CFSE = [4(\frac{2}{5}) - 2(\frac{3}{5})]\Delta_o = \frac{2}{5}\Delta_o$ on an octahedral site, and Cr^{3+} is a d^3 ion with CFSE = 3(2/5) Δ_O = 6/5 Δ_O. Hence it is more energetically favorable for Cr^{3+} to occupy both of the octahedral sites.

Co_3O_4 is a **normal spinel**. Even in the presence of weak field oxo ligands, Co^{3+} is a low spin d^6 ion with very high CFSE on the octahedral sites, because of the high charge and small size of the Co^{3+} ion. Hence the Co^{3+} ions occupy both octahedral sites, and Co^{2+} occupies the tetrahedral site.

Magnetism of ferrite spinels

Ferrite spinels are of technological interest because of their magnetic ordering, which can be ferrimagnetic or antiferromagnetic depending on the structure (normal or inverse) and the nature of the metal ions. Fe_3O_4, $CoFe_2O_4$, and $NiFe_2O_4$ are all inverse spinels and are ferrimagnets. The latter two compounds are used in magnetic recording media and as deflection magnets, respectively.

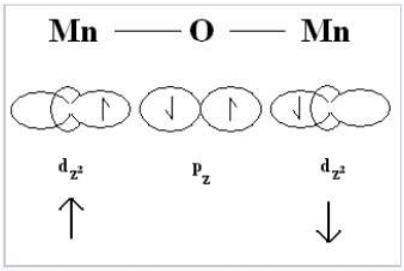
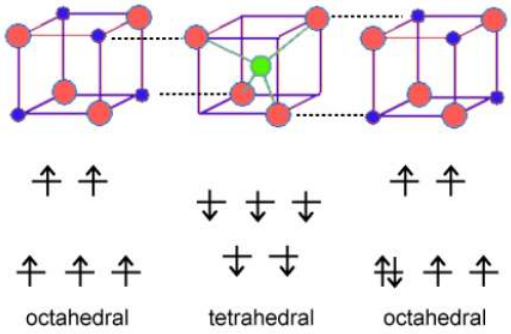


Illustration of antiferromagnetic superexchange between two transition metal cations through a shared oxygen atom.

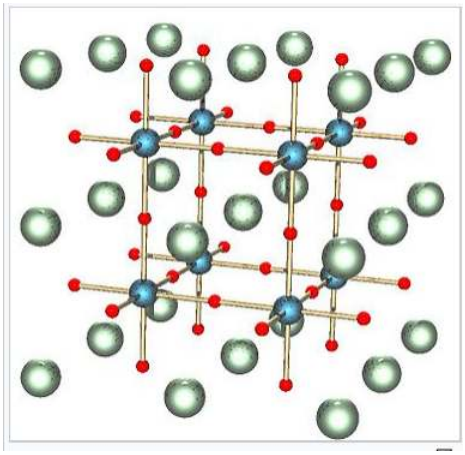
In order to understand the magnetism of ferrites, we need to think about how the unpaired spins of metal ions are coupled in oxides. If an oxide ion is shared by two metal ions, it can mediate the coupling of spins by superexchange as shown at the right. The coupling can be antiferromagnetic, as shown, or ferromagnetic, depending on the orbital filling and the symmetry of the orbitals involved. The **Goodenough-Kanamori rules** predict the local magnetic ordering (ferromagnetic vs. antiferromagnetic) that results from superexchange coupling of the electron spins of transition metal ions. For ferrites, the strongest coupling is between ions on neighboring **tetrahedral and octahedral sites**, and the ordering of spins between these two sites is reliably **antiferromagnetic**.



Because all the tetrahedral and octahedral sites in a spinel or inverse spinel crystal are coupled together identically, it works out that ions on the tetrahedral sites will all have one orientation (e.g., spin down) and ions on all the octahedral sites will have the opposite orientation (e.g., spin up). If the number of spins on the two sites is the same, then the solid will be antiferromagnetic. However, if the **number of spins is unequal** (as in the case of Fe_3O_4, $CoFe_2O_4$, and $NiFe_2O_4$) then the solid will be **ferrimagnetic**. This is illustrated above for Fe_3O_4. The spins on the Fe^{3+} sites cancel, because half of them are up and half are down. However, the four unpaired electrons on the Fe^{2+} ions are all aligned the same way in the crystal, so the compound is ferrimagnetic.

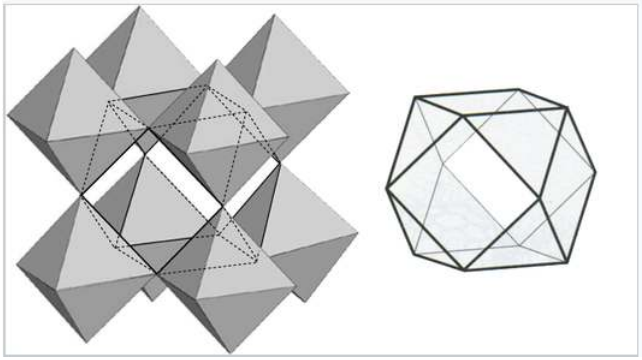
Perovskites are **ternary oxides** of general formula **ABO_3**. More generally, the perovskite formula is ABX_3, where the anion X can be **O, N, or halogen**. The A ions are typically large ions such as Sr^{2+}, Ba^{2+}, Rb^{+}, or a lanthanide 3+ ion, and the B ions are smaller transition metal ions such as Ti^{4+}, Nb^{5+}, Ru^{4+}, etc. The mineral after which the structure is named has the formula $CaTiO_3$.

The perovskite structure has simple cubic symmetry, but is related to the fcc lattice in the sense that the A site cations and the three O atoms comprise a fcc lattice. The B-site cations fill 1/4 of the octahedral holes and are surrounded by six oxide anions.



ABX_3 perovskite structure. A, B, and X are white, blue, and red, respectively.

The coordination of the A ions in perovsite and the arrangement of BO_6 octahedra is best understood by looking at the ReO_3 structure, which is the same structure but with the A-site cations removed. In the polyhedral representation of the structure shown at the right, it can be seen that the octahedra share all their vertices but do not share any octahedral edges. This makes the ReO_3 and perovskite structures flexible, like three-dimensional wine racks, in that the octahedra can **rotate and tilt cooperatively**. Eight such octahedra surround a large **cuboctahedral cavity**, which is the site of the A ions in the perovskite structure. Cations in these sites are coordinated by 12 oxide ions, as expected from the relationship between the perovskite and fcc lattices.



Polyhedral representation of the ReO_3 structure showing the large cuboctahedral cavity that is surrounded by 12 oxygen atoms

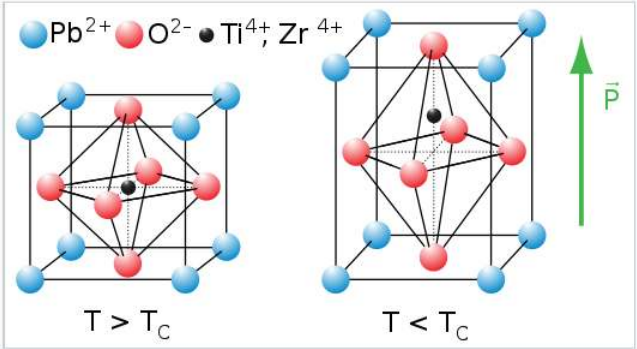
Because the A-site is empty in the ReO_3 structure, compounds with that structure can be reversibly **intercalated** by small ions such as **Li^+ or H^+**, which then occupy sites in the cuboctahedral cavity. For example, smart windows that darken in bright sunlight contain the **electrochromic** material WO_3, which has the ReO_3 structure. In the sunlight, a photovoltaic cell drives the reductive intercalation of WO_3 according to the reaction:

$$x\,H^+ + xe^- + WO_3 \leftrightharpoons H_xWO_3 \tag{9.7.1}$$

WO_3 is a light yellow compound containing d^0 W(VI). In contrast, H_xWO_3, which is mixed-valent W(V)-W(VI) = d^1-d^0, has a deep blue color. Such coloration is typical of mixed-valence transition metal complexes because their d-electrons can be excited to delocalized conduction band levels by red light. Because the electrochemical intercalation-deintercalation process is powered by a solar cell, the tint of the windows can adjust automatically to the level of sunlight.

Ferroelectric perovskites

The flexibility of the network of corner-sharing BO_6 octahedra is also very important in ferroelectric oxides that have the perovskite structure. In some perovsites with small B-site cations, such as Ti^{4+} and Nb^{5+}, the cation is too small to fit symmetrically in the BO_6 octahedron. The octahedron distorts, allowing the cation to move off-center. These distortions can be **tetragonal** (as in the example shown at the right), **rhombohedral**, or **orthorhombic**, depending on whether the cation moves towards a vertex, face, or edge of the BO_6 octahedron. Moving the cation off-center in the octahedron creates an **electric dipole**. In ferroelectrics, these dipoles align in neighboring unit cells through cooperative rotation and tilting of octahedra. The crystal thus acquires a net electrical polarization.



Tetragonal distortion of the perovskite unit cell in the ferroelectric oxide PZT, $PbTi_xZr_{1-x}$

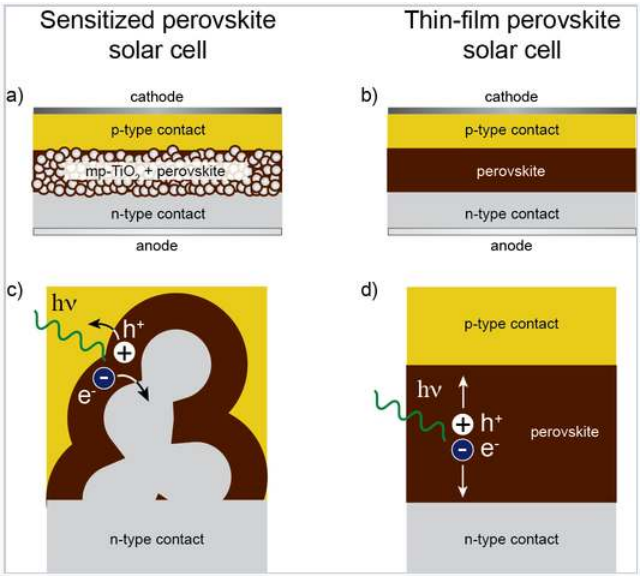
Ferroelectricity behaves analogously to **ferromagnetism**, except that the polarization is electrical rather than magnetic. In both cases, there is a **critical temperature (T_c)** above which the **spontaneous polarization** of the crystal disappears. Below T_c, the electric polarization of a ferroelectric can be switched with a coercive field, and hysteresis loop of polarization vs. field resembles that of a ferromagnet. Above T_c, the crystal is **paraelectric** and has a high dielectric permittivity.

Ferroelectric and paraelectric oxides (along with piezoelectrics and pyroelectrics) have a wide variety of applications as switches, actuators, transducers, and dielectrics for capacitors. **Ferroelectric capacitors** are important in memory devices (FRAM) and in the tuning circuits of cellular telephones. **Multiferroics**, which are materials that are simultaneously ferroelectric and ferromagnetic, are rare and are being now intensively researched because of their potential applications in electrically adressable magnetic memory.

Halide perovskites (ABX_3, X = Cl, Br, I) can be made by combining salts of monovalent A ions ($A^+ = Cs^+$, NH_4^+, RNH_3^+) and divalent metal salts such as $PbCl_2$ or PbI_2. These compounds have sparked recent interest as light absorbers for **thin film solar cells** that produce electricity from sunlight. Lead and tin halide perovskites can be grown as thin films from solution precursors or by thermal evaporation at relatively low temperatures. In some lead halide perovskites, the mobility of electrons and holes is very high, comparable to that of more expensive III-V semiconductors such as GaAs, which must be grown as very pure single crystals at high temperatures for use in solar cells. Because of their high carrier mobility, some lead halide perovskites are also electroluminescent and are of interest as inexpensive materials for light-emitting diodes (LEDs).

Tin and lead halide perovskites were first studied in the 1990s as materials for thin film electronics,[4] and more recently as light absorbers in dye-sensitized solar cells. Soon after the results on dye-sensitized perovskite cells were reported, it was discovered that halide perovskites could also be used in thin film solid state solar cells. The structures of these solar cells are shown schematically at the right. The highest reported solar power conversion efficiencies of perovskite solar cells have jumped from 3.8% in 2009 [5] to

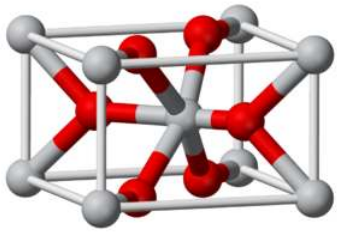
10.2% in 2012[6] and a certified 20.1% in 2014.[7]. The highest performing cells to date contain divalent lead in the perovskite B cation site and a mixture of methylammonium and formamidinium ions in the perovskite A cation site.



a) Solar cell architecture in which a lead halide perovskite absorber coats a layer of nanocrystalline anatase TiO_2. b) Thin-film solar cell, with a layer of lead halide perovskite sandwiched between two selective contacts. c) Charge generation and extraction in the sensitized architecture and d) in the thin-film architecture.

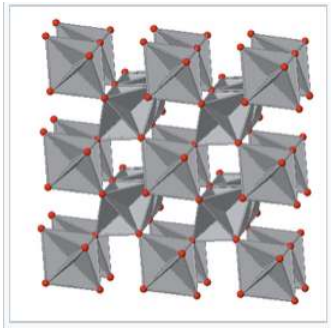
Despite their very impressive efficiency, perovskite solar cells are stable for relatively short periods of time and are sensitive to air and moisture. Current research is focused on understanding the degradation mechanisms of these solar cells and improving their stability under operating conditions.

The **rutile structure** is an important MX_2 (X = O, F) structure. It is a 6:3 structure, in which the cations are octahedrally coordinated by anions, and as such is intermediate in polarity between the CaF_2 (8:4) and SiO_2 (4:2) structures. The mineral rutile is one of the polymorphs of TiO_2, the others (anatase and brookite) also being 6:3 structures.



The rutile structure can be described as a distorted version of the NiAs structure with half the cations removed. Recall that compounds with the NiAs structure were typically metallic because the metal ions are eclipsed along the stacking axis and thus are in relatively close contact. In rutile, the MO_6 **octahedra share edges** along the tetragonal c-axis, and so some rutile oxides, such as

NbO_2, RuO_2 and IrO_2, are also **metallic** because of **d-orbital overlap** along that axis. These compounds are important as electrolyzer catalysts and catalyst supports because they combine high catalytic activity with good electronic conductivity.



View down the tetragonal c-axis of the rutile lattice, showing edge-sharing MO_6 octahedra.

Rutile TiO_2, because of its high refractive index, is the base pigment for white paint. It is a wide bandgap semiconductor that has also been extensively researched as an electrode for water splitting solar cells and as a photocatalyst (primarily as the anatase polymorph) for degradation of pollutants in air and water. Self-cleaning glass exploits the photocatalytic properties of a thin film of TiO_2 to remove oily substances from the glass surface and improve the wetting properties of the glass.

9.7: Spinel, Perovskite, and Rutile Structures is shared under a CC BY-SA license and was authored, remixed, and/or curated by LibreTexts.

- **8.7: Spinel, Perovskite, and Rutile Structures** by Chemistry 310 is licensed CC BY-SA 4.0. Original source: https://en.wikibooks.org/wiki/Introduction_to_Inorganic_Chemistry.

9.8: Discussion Questions

- Using the Liverpool 3D visualization website (http://www.chemtube3d.com/solidstate/_table.htm) determine the anion and cation coordination geometries in cadmium chloride and anatase. Describe the arrangement of octahedra (in terms of whether they share edges, faces, etc.) in these structures.
- Count the number of atoms in the Li_3Bi and ReO_3 unit cells, and determine the coordination environments of each of the ions.
- Silicon, germanium, and many other semiconductors adopt the diamond (or zincblende) structure. Assuming that all the atoms are the same size, calculate the volume fraction of the unit cell that is occupied by the atoms. How does the filling fraction of diamond compare to simple cubic and close-packed structures, and what does this tell us about the relationship between coordination number and density?
- Describe the structural basis of ferroelectricity in barium titanate.

9.8: Discussion Questions is shared under a CC BY-SA license and was authored, remixed, and/or curated by LibreTexts.

- **8.8: Discussion Questions** by Chemistry 310 is licensed CC BY-SA 4.0. Original source: https://en.wikibooks.org/wiki/Introduction_to_Inorganic_Chemistry.

9.9: Problems

1. For each of the following close packed layer sequences, indicate the name of the structure (structure type), the coordination environment of the cations (represented by lower case letters), and the coordination environment of the anions (upper case letters). Give two additional examples (apart from the structure type itself) of compounds with the same structure.

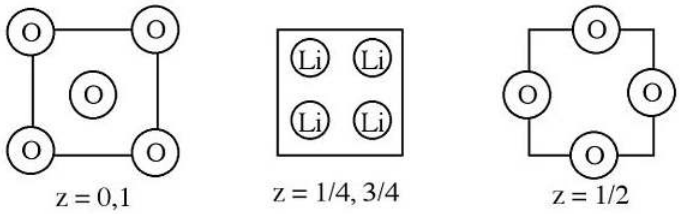
(a) AbBaAbBaAbB.....

(b) AaBbCcAaBbCc.....

(c) AcBaCbAcBaCb.....

(d) AcB | AcB | AcB |.... ("|" = van der Waals gap)

2. Below are sections of the lithium oxide unit cell.



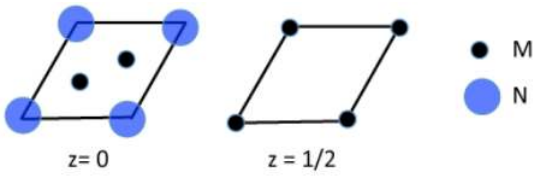
(a) Describe how to obtain (and do obtain) the empirical formula.

(b) What is the coordination number and geometry for each type of ion?

(c) Which atom is close-packed?

(d) What type and fraction of holes are filled by the other ion?

3. The hexagonal unit cell of a metal nitride is shown below in sections.



(a) What is the empirical formula of the compound?

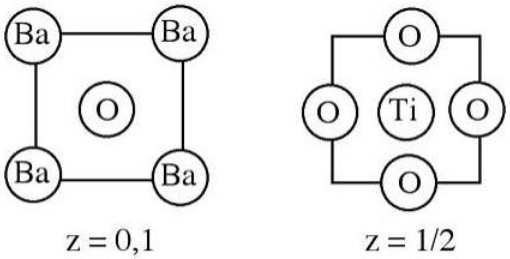
(b) How many M atoms are coordinated to each N atom?

(c) In what group of the periodic table would you expect to find M?

4. Draw the cubic Li_3Bi unit cell in sections.

5. If half the cesium is removed from the CsCl structure, such that each Cl atom is then tetrahedrally coordinated, what structure type is generated?

6. The crystal structure of barium titanate is shown below.



(a) What is the empirical formula of the compound?

(b) Which atoms (if any) are close packed?

(c) How many oxygen atoms coordinate (i) Ti^{4+} and (ii) Ba^{2+}?

(d) Why are the coordination numbers are different?

7. The structures of the disulfides (MS_2) show an apparently unusual trend, proceeding from left to right across the transition series. On the left side (TiS_2, ZrS_2, MoS_2, etc.), one finds layered structures, whereas in the middle (ReS_2, FeS_2, RuS_2) there are three-dimensional pyrite- and marcasite-type structures. On the right (PtS_2, SnS_2), there are again layered structures. Briefly explain these trends.

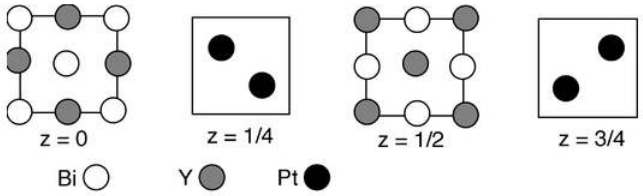
8. Explain why ionic compounds rarely have layered crystal structures.

9. Draw the zincblende structure in sections.

10. The zincblende structure is rarely found with very polar or ionic compounds. However, some polar and ionic compounds (BeO, NH_4F, etc.) have the wurtzite structure.

(a) Describe the similarities and the differences between the zincblende and wurtzite structures (in terms of coordination numbers, stacking sequence of cations and anions, etc.) (b) Why is wurtzite more ionic than zincblende?

11. A recent article by R. Cava and co-workers (*Nature Materials* 2010, *9*, 546-9) describes the unusual electronic properties of a Y-Pt-Bi alloy, the structure of which is shown in sections below:



(a) What is the stoichiometry of the compound?

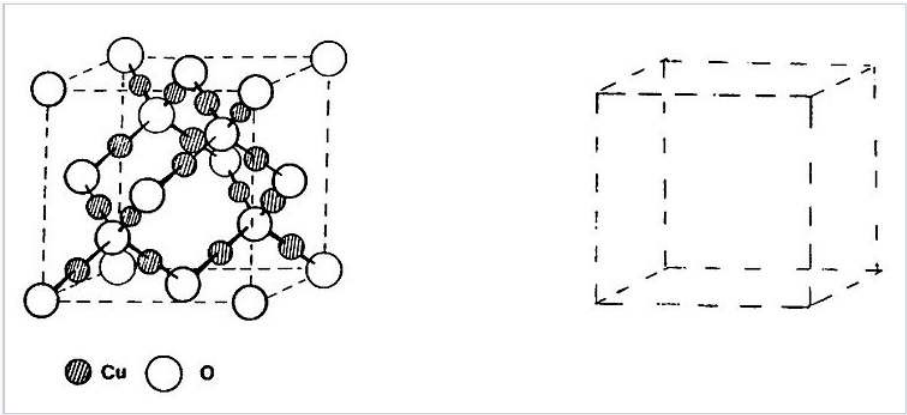
(b) How many Y and how many Pt atoms coordinate each Bi atom?

12. The fluorite structure, CaF_2, which is generated by filling all the tetrahedral holes in a FCC array, is a common MX_2 structure type.

(a) What is the coordination environment of F in a hypothetical relative of CaF_2, in which Ca forms a hcp array and F occupies all the tetrahedral sites?

(b) Suggest a reason why the structure described in (a) is very rare.

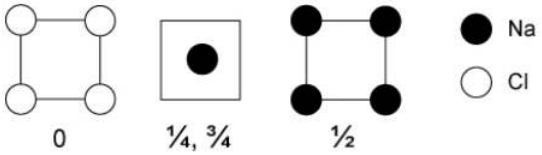
13. The cuprite (Cu_2O) structure is related to zincblende (or diamond) in that oxygen occupies both the Zn and S positions, with copper in between. This is shown schematically at the right. Actually, in cuprite there are *two* such interpenetrating networks with no bonds between them. Draw the second network in the empty cell. If you put the two halves together and take out the copper, what cubic packing lattice do you get? Is it a closest packing lattice? (*Hint #1:* start with an O atom at 1/2,1/2,1/2) (*Hint #2:* try this in pencil first)



14. Draw the rutile structure in sections of the unit cell, and verify that the stoichiometry is MX_2. What are the coordination numbers of Ti and O?

15. Stishovite is a high pressure form of SiO_2 found in meteorite craters. While normal SiO_2 has the quartz structure, in which each Si is coordinated by four O atoms, stishovite has the rutile structure. Would you expect the Si-O bond to be longer in stishovite, or in quartz? What is the bond order in each polymorph?

16. Na and Cl combine in a 1:1 ratio to make the ionic NaCl lattice. Interestingly, recent theoretical predictions (confirmed by high pressure synthesis and crystallography) have identified several other stoichiometries that form stable crystals at high pressure. These include Na_3Cl, Na_2Cl, Na_3Cl_2, $NaCl_3$, and several others.[8] The structure of one of these new sodium chlorides is shown below in sections.



a) What is the stoichiometry of this compound?

b) What are the coordination numbers of Na and Cl, and how do they compare to the coordination numbers in NaCl and Na metal?

c) Based on your answer to (b), explain why high pressure should stabilize this phase.

17. One of the new compounds discovered in the study described in problem 16 is $NaCl_3$. There are two polymorphs of this compound, one of which contains linear Cl_3^- ions. Accurate molecular orbital calculations indicate that the charge on the central Cl atom in these linear anions is close to zero. Draw a valence bond structure for the Cl_3^- ion that is consistent with these observations. Would you expect the Cl-Cl bond to be longer or shorter than the bond in Cl_2?

18. Some MX salts can exist in either the CsCl or NaCl structure. Use the Pauling formula to predict the M-X bond length in the CsCl structure of a compound that has a bond length of 3.5 Å in the NaCl structure. Would applying a high pressure stabilize the CsCl form, or the NaCl form of this compound? (*hint:* calculate the volume per formula unit)

19. Mn_3O_4 and Fe_3O_4 are both mixed-valence oxides. In both cases, there is one M^{2+} ion and two M^{3+} ions per formula unit (M = Fe, Mn).

(a) One of these is a normal spinel and one is an inverse spinel. Explain which is which, and why. (hint: think about CFSE's)

(b) For Mn_3O_4, what kind of magnetic ordering (ferri-, ferro-, or antiferromagnetic) would you expect, and why? You can assume that neighboring tetrahedral and octahedral ions in the structure are antiferromagnetically coupled.

(c) Sketch the approximate form of the χ vs. T and $1/\chi$ vs. T curves for Mn_3O_4. Label any special values of temperature on your graphs.

20. Predict whether each of the following should form a normal or inverse spinel: MgV_2O_4, VMg_2O_4, $NiGa_2O_4$, $ZnCr_2S_4$, $NiFe_2O_4$. Would kind of magnetic ordering (ferro-, ferri-, or antiferromagnetic) would you predict for $NiFe_2O_4$?

9.9: Problems is shared under a CC BY-SA license and was authored, remixed, and/or curated by LibreTexts.

- **8.9: Problems** by Chemistry 310 is licensed CC BY-SA 4.0. Original source: https://en.wikibooks.org/wiki/Introduction_to_Inorganic_Chemistry.

9.10: References

1. K. Mizushima, P.C. Jones, P.J. Wiseman, J.B. Goodenough (1980). "Li_xCoO_2(0<x<l): A New Cathode Material for Batteries of High Energy Density". *Materials Research Bulletin* **15**: 783–789. doi:10.1016/0025-5408(80)90012-4.
2. Yang Shao-Horn, Laurence Croguennec, Claude Delmas, E. Chris Nelson and Michael A. O'Keefe (July 2003). "Atomic resolution of lithium ions in $LiCoO_2$". *Nature Materials* **2** (7): 464–467. doi:10.1038/nmat922. PMID 12806387.
3. M. Stanley Whittingham "Lithium Batteries and Cathode Materials" Chem. Rev., 2004, vol. 104, pp. 4271–4302. DOI: 10.1021/cr020731c
4. Kagan, Cherie R.; Mitzi, David B.; Dimitrakopoulos, C. D. (1999). "Organic-inorganic hybrid materials as semiconducting channels in thin-film field-effect transistors". *Science* **286**: 945-947. doi:10.1126/science.286.5441.945.
5. Kojima, Akihiro; Teshima, Kenjiro; Shirai, Yasuo; Miyasaka, Tsutomu (6 May 2009). "Organometal Halide Perovskites as Visible-Light Sensitizers for Photovoltaic Cells". *Journal of the American Chemical Society* **131** (17): 6050–6051. doi:10.1021/ja809598r. PMID 19366264.
6. Chung, In; Lee, Byunghong; He, Jiaking; Chang, Robert P. H.; Kanatzidis, Mercouri G. (24 May 2012). "All-solid-state dye-sensitized solar cells with high efficiency". *Nature* **485**: 486-489. doi:10.1038/nature11067.
7. IEEE Spectrum, Perovskite Solar Cell Bests Bugbears, Reaches Record Efficiency, 7 January 2015
8. W. Zhang et al. (2013), "Unexpected Stable Stoichiometries of Sodium Chlorides." *Science*, vol. 342, no. 6165, pp. 1502-1505. doi: 10.1126/science.1244989

9.10: References is shared under a CC BY-SA license and was authored, remixed, and/or curated by LibreTexts.

- **8.10: References** by Chemistry 310 is licensed CC BY-SA 4.0. Original source: https://en.wikibooks.org/wiki/Introduction_to_Inorganic_Chemistry.

CHAPTER OVERVIEW

10: Ionic and Covalent Solids - Energetics

Learning Objectives

- Understand the geometric basis of radius ratio rules.
- Understand the chemical basis of structure maps and why they are better predictors of crystal structures than radius ratios.
- Use the Born-Mayer and Kapustinskii equations to calculate lattice energies of known and hypothetical compounds.
- Construct Born-Haber cycles using lattice energies and calculate unknown quantities in the cycles.
- Predict the stabilities of low and high oxidation states using lattice energies.
- Understand the quantum mechanical origin of the extra "resonance" stability of metals.
- Predict trends in the solubility and thermal stability of inorganic compounds using lattice energies.

In Chapter 8, we learned all about crystal structures of **ionic compounds**. A good question to ask is, *what makes a compound choose a particular structure?* In addressing this question, we will learn about the forces that hold crystals together and the relative energies of different structures. This will in turn help us understand in a more quantitative way some of the heuristic concepts we have learned about in earlier chapters, such as hard-soft acid-base theory.

10.1: Ionic Radii and Radius Ratios
10.2: Structure Maps
10.3: Energetics of Crystalline Solids- The Ionic Model
10.4: Born-Haber Cycles for NaCl and Silver Halides
10.5: Kapustinskii Equation
10.6: Discovery of Noble Gas Compounds
10.7: Stabilization of High and Low Oxidation States
10.8: Alkalides and Electrides
10.9: Resonance Energy of Metals
10.10: Prelude to Ionic and Covalent Solids - Energetics
10.11: The Strange Case of the Alkali Oxides
10.12: Lattice Energies and Solubility
10.13: Discussion Questions
10.14: Problems
10.15: References

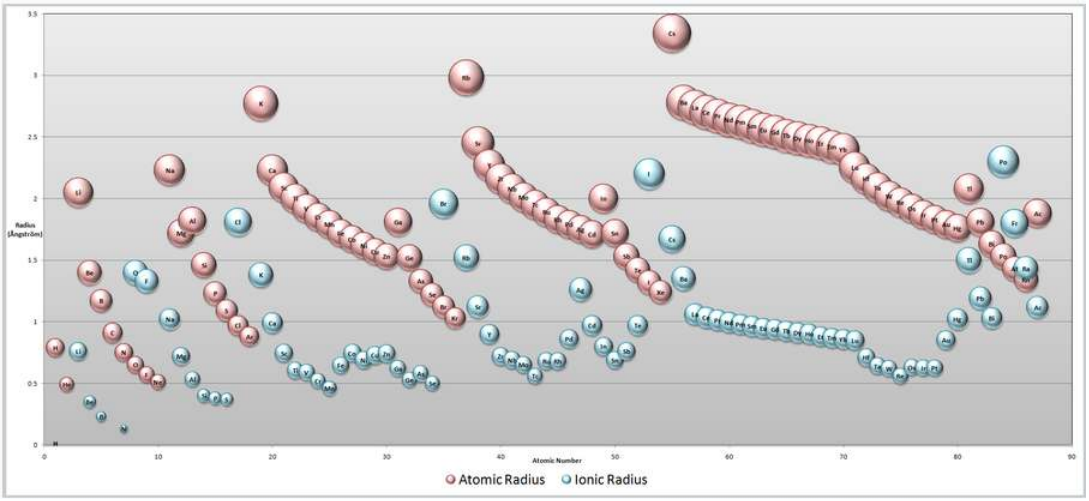
10: Ionic and Covalent Solids - Energetics is shared under a CC BY-SA license and was authored, remixed, and/or curated by LibreTexts.

10.1: Ionic Radii and Radius Ratios

Atoms in crystals are held together by electrostatic forces, van der Waals interactions, and covalent bonding. It follows that arrangements of atoms that can maximize the strength of these attractive interactions should be most favorable and lead to the most commonly observed crystal structures.

Radius ratio rules

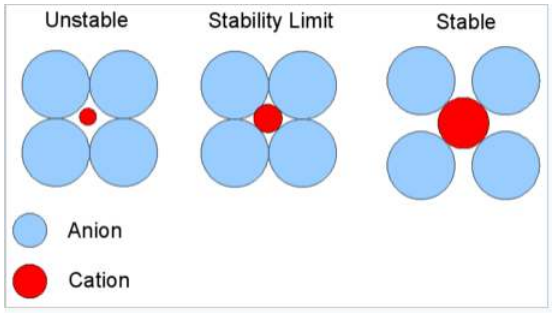
Early crystallographers had trouble solving the structures of inorganic solids using X-ray diffraction because some of the mathematical tools for analyzing the data had not yet been developed. Once a trial structure was proposed, it was relatively easy to calculate the diffraction pattern, but it was difficult to go the other way (from the diffraction pattern to the structure) if nothing was known *a priori* about the arrangement of atoms in the unit cell. It was (and still is!) important to develop some guidelines for guessing the coordination numbers and bonding geometries of atoms in crystals. The first such rules were proposed by Linus Pauling, who considered how one might pack together oppositely charged spheres of different radii. Pauling proposed from geometric considerations that the quality of the "fit" depended on the **radius ratio** of the anion and the cation.



Atomic and Ionic Radii. Note that cations are always smaller than the neutral atom (pink) of the same element, whereas anions are larger. Going from left to right across any row of the periodic table, neutral atoms and cations contract in size because of increasing nuclear charge. (click for larger image)

The basic idea of radius ratio rules is illustrated at the right. We consider that the anion is the packing atom in the crystal and the smaller cation fills interstitial sites ("holes"). Cations will find arrangements in which they can contact the largest number of anions. If the cation can touch all of its nearest neighbor anions, as shown at the right for a small cation in contact with larger anions, then the fit is good. If the cation is too small for a given site, that coordination number will be unstable and it will prefer a

lower coordination structure. The table below gives the ranges of cation/anion radius ratios that give the best fit for a given coordination geometry.



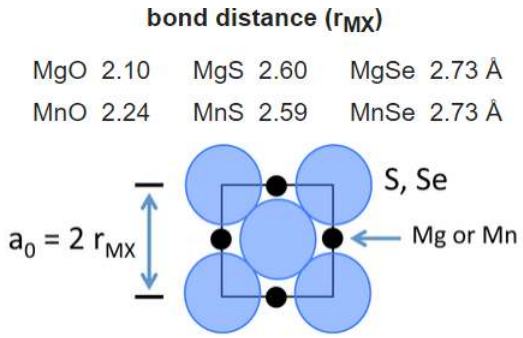
Critical Radius Ratio. This diagram is for coordination number six: 4 anions in the plane are shown, 1 is above the plane and 1 is below. The stability limit is at $r_C/r_A = 0.414$

Coordination number	Geometry	$\rho = r_{cation}/r_{anion}$
2	linear	0 - 0.155
3	triangular	0.155 - 0.225
4	tetrahedral	0.225 - 0.414
4	square planar	0.414 - 0.732
6	octahedral	0.414 - 0.732
8	cubic	0.732 - 1.0
12	cuboctahedral	1.0

There are unfortunately several challenges with using this idea to predict crystal structures:

- We don't know the radii of individual ions
- Atoms in crystals are not really ions - there is a varying degree of covalency depending electronegativity differences
- Bond distances (and therefore ionic radii) depend on bond strength and coordination number (remember Pauling's rule D(n) = D(1) - 0.6 log n)
- Ionic radii depend on oxidation state (higher charge => smaller cation size, larger anion size)

We can build up a table of ionic radii by assuming that the bond length is the sum of the radii ($r_+ + r_-$) if the ions are in contact in the crystal. Consider for example the compounds MgX and MnX, where X = O, S, Se. All of these compounds crystallize in the NaCl structure:



For the two larger anions (S^{2-} and Se^{2-}), the unit cell dimensions are the same for both cations. This suggests that the anions are in contact in these structures. From geometric considerations, the anion radius in this case is given by:

Extra close brace or missing open brace

and thus the radii of the S^{2-} and Se^{2-} ions are 1.84 and 1.93 Å, respectively. Once the sizes of these anions are fixed, we can obtain a self-consistent set of cation and anion radii from the lattice constants of many MX compounds.

How well does this model work? Let's consider the structures of tetravalent metal oxides (MO_2), using Pauling radii and the predictions of the radius ratio model:

Oxide MO_2	Radius ratio	Predicted coord. no.	Observed coord no. (structure)
CO_2	~0.1	2	2 (linear molecule)
SiO_2	0.32	4	4 (various tetrahedral structures)
GeO_2	0.43	4	4 (silica-like structures)
"	0.54	6	6 (rutile)
TiO_2	0.59	6	6 (rutile)
ZrO_2	0.68	6	7 (baddleyite)
"	0.77	8	8 (fluorite)
ThO_2	0.95	8	8 (fluorite)

Note that cations have different radii depending on their coordination numbers, and thus different radius ratios are calculated for Ge^{4+} with coordination numbers 4 and 6, and for Zr^{4+} with coordination numbers 6 and 8.

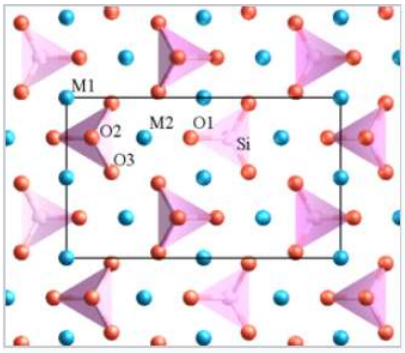
For this series of oxides, the model appears to work quite well. The correct coordination number is predicted in all cases, and borderline cases such as GeO_2 and ZrO_2 are found in structures with different coordination numbers. The model also correctly predicts the structures of BeF_2 (SiO_2 type), MgF_2 (rutile), and CaF_2 (fluorite).

What about the alkali halides NaCl, KBr, LiI, CsF, etc.? All of them have the NaCl structure except for CsCl, CsBr, and CsI, which have the CsCl (8-8) structure. In this case the radius ratio model fails rather badly. The Li^+ salts LiBr and LiI are predicted to have tetrahedral structures, and KF is predicted to have an 8-8 structure like CsCl. We can try adjusting the radii (e.g., making the cations larger and anions smaller), but the best we can do with the alkali halides is predict about half of their structures correctly. Since the alkali halides are clearly ionic compounds, this failure suggests that there is something very wrong with the radius ratio model, and its success with MO_2 compounds was coincidental.

In addition to the radius ratio rule, Linus Pauling developed other useful rules that are helpful in rationalizing and also predicting the structures of inorganic compounds. Pauling's rules[1] state that:

- Stable structures are **locally electroneutral**. For example, in the structure of the double perovskite Sr_2FeMoO_6, MO_6 (M = Fe^{2+}, Mo^{6+}) octahedra share all their vertices, and Sr^{2+} ions fill the cubooctahedral cavities that are flanked by eight MO_6 octahedra.[2] Each O^{2-} ion is coordinated to one Fe^{2+} and one Mo^{6+} ion in order to achieve local electroneutrality, and thus the FeO_6 and MoO_6 octahedra alternate in the structure.
- **Cation-cation repulsion** should be minimized. Anion polyhedra can share vertices (as in the perovskite structure) without any energetic penalty. Shared polyhedral edges, and especially shared faces, cause cation-cation repulsion and should be avoided. For example, in rutile, the most stable polymorph of TiO_2, the TiO_6 octahedra share vertices and two opposite edges, forming ribbons in the structure. In anatase TiO_2, each octahedron shares four edges so the anatase polymorph is less thermodynamically stable.

- **Highly charged cations** in anion polyhedra tend not to share edges or even vertices, especially when the coordination number is low. For example, in orthosilicates such as olivine (M_2SiO_4), there are isolated SiO_4^{4-} tetrahedra.



Structure of olivine. M (Mg or Fe) = blue spheres, Si = pink tetrahedra, O = red spheres.

As we will soon see, all of Pauling's rules are justified on the basis of lattice energy considerations. In ionic compounds, the arrangement of atoms that maximizes anion-cation interactions while minimizing cation-cation and anion-anion contacts is energetically the best.

10.1: Ionic Radii and Radius Ratios is shared under a CC BY-SA license and was authored, remixed, and/or curated by LibreTexts.

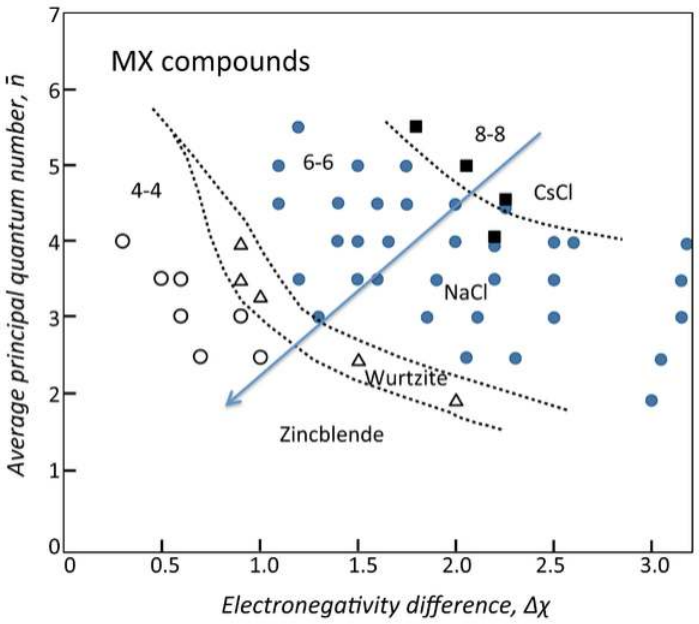
- **9.1: Ionic Radii and Radius Ratios** by Chemistry 310 is licensed CC BY-SA 4.0. Original source: https://en.wikibooks.org/wiki/Introduction_to_Inorganic_Chemistry.

10.2: Structure Maps

Structure maps, which plot structures against properties such electronegativity, are more consistent than radius ratio rules in correctly predicting coordination numbers and crystal structures. One of the early examples of this approach was published by Mooser and Pearson in 1959.[3]

A **Mooser-Pearson diagram** maps crystal structures according to the average principal quantum numbers of the atoms and their electronegativity difference. The basic ideas behind such a plot are:

- The greater the electronegativity difference, the more ionic is the compound. Higher ionicity results in higher coordination numbers because anions like to surround cations (and vice versa).
- Higher principal quantum numbers result in less s-p hybridization, less directional bonding, and therefore higher coordination number. We saw this trend before with the structures of elements in group IV: descending the group the coordination number increases progressively from 3-4 (carbon) to 12 (Pb).



The lines in the Mooser-Pearson diagram separate MX compounds with CsCl, NaCl, and tetrahedral (wurtzite and zincblende) structures. Note that wurtzite has higher ionicity than zincblende in the plot, consistent with our discussion of the "boat" and "chair" ring structures in Chapter 8. Diamorphic compounds tend to fall on the boundaries. On the whole, the Mooser-Pearson diagram makes far fewer errors in predicting structures than the radius ratio rule. There are similar diagrams for MX_2 structures, in which the order of ionicity is CaF_2 (8:4 coordination) > rutile (6:3) > silica structures (4:2).

10.2: Structure Maps is shared under a CC BY-SA license and was authored, remixed, and/or curated by LibreTexts.

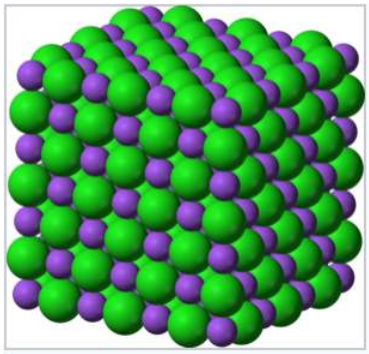
- **9.2: Structure Maps** by Chemistry 310 is licensed CC BY-SA 4.0. Original source: https://en.wikibooks.org/wiki/Introduction_to_Inorganic_Chemistry.

10.3: Energetics of Crystalline Solids- The Ionic Model

Many ionic compounds have simple structures. Because the forces holding the atoms together are primarily electrostatic, we can calculate the cohesive energy of the crystal lattice with good accuracy. Interesting questions to ask about these lattice energy calculations are:

- How accurate are lattice energy calculations?
- What do they teach us about the chemical bonds in ionic crystals?
- Can we use lattice energies to predict properties such as solubility, stability, and reactivity?
- Can we use lattice energies to predict the crystal structures of ionic compounds?

Let's start by looking at the forces that hold ionic lattices together. There are mainly two kinds of force that determine the energy of an ionic bond.



The NaCl crystal structure is the archetype for calculating lattice energies and computing enthalpies of formation from Born-Haber cycles.

1) **Electrostatic Force** of attraction and repulsion (Coulomb's Law): Two ions with charges z_+ and z_-, separated by a distance r, experience a force F:

$$\mathbf{F} = -\frac{e^2}{4\pi\varepsilon_0}\frac{z_+z_-}{r^2} \tag{10.3.1}$$

where

e = 1.6022×10^{-19} C

4 π ε_0 = 1.112×10^{-10} C²/(J m)

This force is attractive for ions of opposite charge.

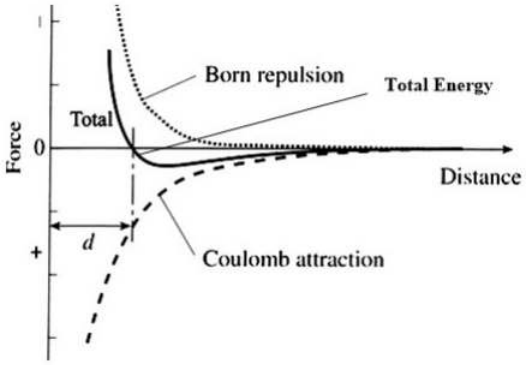
The electrostatic potential energy, E_{elec}, is then given by

$$\mathbf{E}_{elec}\int_{\infty}^{r} F(r)dr = \frac{e^2}{4\pi\varepsilon_0}\frac{z_+z_-}{r} \tag{10.3.2}$$

The sign of E_{elec} is negative for the attractive interaction between a cation and an anion. That is, the closer oppositely charged ions approach each other, the lower the potential energy.

2) **Closed-shell repulsion**. When electrons in the closed shells of one ion overlap with those of another ion, there is a repulsive force comes from the Pauli exclusion principle. A third electron cannot enter an orbital that already contains two electrons. This force is short range, and is typically modeled as falling off exponentially or with a high power of the distance r between atoms. For example, in the Born approximation, B is a constant and ρ is a number with units of length, which is usually empirically determined from compressibility data. A typical value of ρ is 0.345 Å.

$$\mathbf{E}_{repulsion} = Bexp(\frac{-r}{\rho}) \tag{10.3.3}$$



The energy of the ionic bond between two atoms is then calculated as the combination of net electrostatic and the closed-shell repulsion energies, as shown in the figure at the right. Note that for the moment we are ignoring the attractive van der Waals energy between ions, which we will explain below. For a pair of ions, the equilibrium distance between ions is determined by the minimum in the total energy curve. At this distance, the net force on each ion is zero.

Electrostatic energy of a crystal lattice

We can use these equations to calculate the lattice energy of a crystal by summing up the interactions between all pairs of ions. Because the closed-shell repulsion force is short range, this term is typically calculated only for interactions between neighboring ions. However, the Coulomb force is long range, and must be calculated over the entire crystal. This problem was first solved in 1918 by Erwin Madelung, a German physicist.[4]

Consider an ion in the NaCl structure labeled "O" in the diagram at the right. We can see that the nearest neighbor interactions (+ -) with ions labeled "1" are attractive, the next nearest neighbor interactions (- - and + +) are repulsive, and so on. In the NaCl structure, counting from the ion in the center of the unit cell, there are 6 nearest neighbors (on the faces of the cube), 12 next nearest neighbors (on the edges of the cube), 8 in the next shell (at the vertices of the cube), and so on. Their distances from ion "0" increase progressively: r_o, $\sqrt{2}\ r_o$, $\sqrt{3}\ r_o$, and so on, where r_o is the nearest neighbor distance.

We can now write the electrostatic energy at ion "O" as:

$$\mathbf{E}_{elec} = -6\frac{e^2}{4\pi\varepsilon_0}\frac{z_+z_-}{r_o} + 12\frac{e^2}{4\pi\varepsilon_0}\frac{z_+z_-}{\sqrt{2}r_o} - 8\frac{e^2}{4\pi\varepsilon_0}\frac{z_+z_-}{\sqrt{3}r_o} + ... \tag{10.3.4}$$

Factoring out constants and the nearest-neighbor bond distance r_o we obtain:

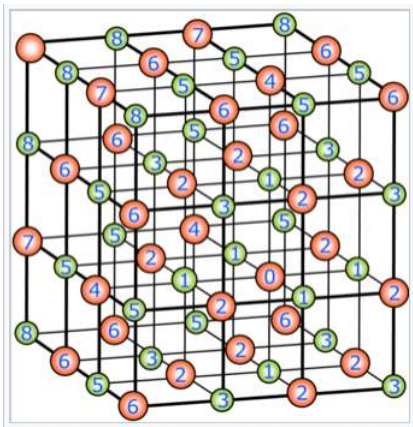
$$\mathbf{E}_{elec} = \frac{e^2}{4\pi\varepsilon_0}\frac{z_+z_-}{r_o}\left(6 - \frac{12}{\sqrt{2}} + \frac{8}{\sqrt{3}} - \frac{6}{\sqrt{4}} + ...\right) \tag{10.3.5}$$

Where the sum in parentheses, which is unitless, slowly converges to a value of A = 1.74756. Generalizing this formula for any three-dimensional ionic crystal we get a function:

$$\mathbf{E}_{elec} = \frac{e^2}{4\pi\varepsilon_0}\frac{z_+z_-}{r_o}NA \tag{10.3.6}$$

where N is Avogadro's number (because we are calculating energy per mole of ions) and A is called the *Madelung constant*. The **Madelung constant** depends only on the geometrical arrangement of the ions and so it varies between different types of crystal

structures, but within a given structure type it does not change. Thus MgO and NaCl have the same Madelung constant because they both have the NaCl structure



The Madelung constant is calculated by summing up electrostatic interactions with ion labeled 0 in the expanding spheres method. Each number designates the order in which it is summed. For example, ions labeled 1 represent the six nearest neighbors (attractive interaction), ions labeled 2 are the 12 next nearest neighbors (repulsive interaction) and so on. Note that if the sum is carried out over shells 1-2-3..., it converges very slowly, but there are mathematical methods for summing it which give a rapidly converging series.

The table below lists Madelung constants for some common structures. The **reduced Madelung constant** is obtained by normalizing the values to the number of ions in the formula unit. It can be seen from the table that the reduced Madelung constants are quite similar for different structures. This makes it hard to determine on the basis of electrostatic energy calculations which structure will be most stable for a given compound. It is interesting to note that the trend in reduced Madelung constants roughly follows the trend in ionicity (cf. the Mooser-Pearson diagram in Section 9.2). For example, wurtzite has a slightly higher Madelung constant than zincblende, consistent with our earlier conclusion that the wurtzite structure is favored by more polar compounds.

Structure	Madelung Constant, A	Reduced Madelung Constant, 2A/n
NaCl (halite)	1.7476	1.7476
CsCl	1.7627	1.7627
ZnS (zincblende)	1.6381	1.6381
ZnS (wurtzite)	1.6413	1.6413
CaF_2 (fluorite)	2.5194	1.6796
TiO_2 (rutile)	2.4080	1.6053
Al_2O_3 (corundum)	4.172	1.6688

Total lattice energy of a crystal

Having in hand a formula for the electrostatic energy, we can now add in the closed-shell repulsion term to obtain an equation that gives us the total lattice energy.

$$E_L = \frac{e^2}{4\pi\varepsilon_0}\frac{z_+z_-}{r_o}NA + NBexp(\frac{-r}{\rho}) \tag{10.3.7}$$

At the equilibrium bond distance, the forces on all the ions are zero, and we can use this fact to eliminate the constant B:

$$[\frac{dE}{dr}]_{r=r_o} = 0 \tag{10.3.8}$$

Expressed this way, E_L is a negative number (because z_+ and z_- have opposite signs). It represents the energy change for forming one mole of solid salt from one mole of the gaseous ions, separated initially at an infinite distance.



Lithium fluoride (shown here as a large single crystal in a beaker of water) is the only alkali halide that is not freely soluble in water. The lattice energy of LiF is the most negative of the alkali fluorides because Li^+ and F^- are both small ions and E_L is proportional to $1/r_0$.

10.3: Energetics of Crystalline Solids- The Ionic Model is shared under a CC BY-SA license and was authored, remixed, and/or curated by LibreTexts.

- **9.3: Energetics of Crystalline Solids- The Ionic Model** by Chemistry 310 is licensed CC BY-SA 4.0. Original source: https://en.wikibooks.org/wiki/Introduction_to_Inorganic_Chemistry.

10.4: Born-Haber Cycles for NaCl and Silver Halides

Now that we have an equation for the lattice energy of an ionic crystal, we can ask the question of how accurate it is. Remember, we made several approximations in arriving at this formula. We assumed that the lattice was completely ionic, we ignored the van der Waals attractive energy of the ions, and we assumed that there was no covalent contribution to the bonding.

Let's consider the lattice energy of table salt (NaCl)

$$Na^+_{(g)} + Cl^-_{(g)} \longrightarrow NaCl_{(s)}$$

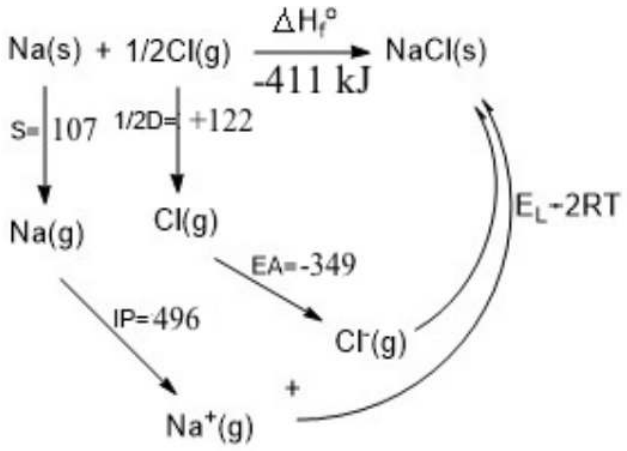
To calculate the lattice energy, we lump together the physical constants:

$$E_L(\frac{kJ}{mol}) = (1389.3)\frac{Aq_1q_2}{r_o}(1 - \frac{.345}{r_o}) \tag{10.4.1}$$

where r_o is expressed in Å. Now we can calculate the lattice energy for NaCl using r_o = 2.814 Å, as:

$$E_L = -(1389.3)\frac{1.7476}{2.814}(1 - \frac{.345}{2.814}) = -766.5\frac{kJ}{mol} \tag{10.4.2}$$

We can alternatively construct a **Born-Haber cycle** for the formation of NaCl from the elements and calculate the lattice energy as the "missing" term in the cycle.



S= Sublimation energy of Na(s)

IP= Ionization potential of Na(g)

D= Bond dissocation energy of Cl_2(g)

EA= Electron affinity of Cl(g)

E_L=Lattice energy of NaCl

R= Gas constant

T= Absolute temperature

From **Hess' Law:** $\Delta H_f = s + \frac{1}{2}D + IP + EA + E_L - 2RT = -396\frac{kJ}{mol}$

Here we have to subtract 2RT to convert our cycle of energies to a cycle of enthalpies, because we are compressing two moles of gas in making NaCl(s) and PΔV = ΔnRT, where Δn = -2.

Experimentally ΔH_f for NaCl is **-411 kJ/mol**

Because all the other numbers in the cycle are known accurately, the error in our calculation is only about 15 kJ (about 2% of E_L). The result is promising because we neglected the van der Waals term.

But....how did we get away with neglecting the van der Waals term?

This is because we used **energy minimization** to obtain the repulsion energy in the Born-Mayer equation. If we underestimate the attractive energy of the crystal lattice, the energy minimization criterion ensures that the repulsion energy is underestimated as well. The two errors partially compensate, so the overall error in the calculation is small.

We can do better by explicitly including the short-range van der Waals attractive energy between ions. The table below shows results of more detailed lattice energy calculations for ionic fluorides in which the van der Waals term is explicitly included. The errors in this case are only about 1% of E_L.

Compound	Calculated Lattice Energy (kJ/mol)	Experimental E_L from Born-Haber Cycle
MgF_2 (rutile structure)	-2,920	-2,908
CaF_2 (fluorite structure)	-2,586	-2,611
BaF_2 (fluorite structure)	-2,326	-2,368

Silver Halides

It is interesting to repeat this exercise for the silver halides, which have either the NaCl structure (AgF, AgCl, AgBr) or zincblende structure (AgI).

Silver Halide	Calculated	Cycle	Difference (kJ/mol)
AgF	-920	-954	34
AgCl	-833	-908	75
AgBr	-816	-900	84
AgI	-778	-883	105

Looking at the table, we see that the error is small for AgF and becomes progressively larger for the heavier silver halides. However we are still obtaining answers within about 12% error even for AgI. Should we interpret the good agreement with values calculated from the ionic model to mean that these compounds are ionic? Clearly, this description is inappropriate for AgI, where the electronegativity difference $\Delta\chi$ is only 0.6 (compare this value to 0.4 for a C-H bond, which we typically view as non-polar).



A drop of siver nitrate solution, when added to a dilute hydrochloric acid solution, results in the immediate formation of a white silver chloride precipitate. This reaction is used as a qualitative test for the presence of halide ions in solutions. The covalent bonding contribution to the lattice energies of AgCl, AgBr, and AgI makes these salts sparingly soluble in water.

Again, we can interpret the fortuitous agreement between the calculated and experimentally obtained energies in terms of compensating errors. Our lattice energy calculation *overestimates* the ionic contribution in the case of the heavier silver halides, but *underestimates* the covalent contribution. Of these compounds, only AgF is soluble in water and should be thought of as an ionic compound. The others are progressively more insoluble in water (K_{sp} is 10^{-10}, 10^{-13}, and 10^{-16} for AgCl, AgBr, and AgI), reflecting increasing covalency as $\Delta\chi$ decreases.

The moral of the story is that simple lattice energy calculations based on the ionic model work well, but *they do not necessarily imply that the compounds are ionic*!

10.4: Born-Haber Cycles for NaCl and Silver Halides is shared under a CC BY-SA license and was authored, remixed, and/or curated by LibreTexts.

- **9.4: Born-Haber Cycles for NaCl and Silver Halides** by Chemistry 310 is licensed CC BY-SA 4.0. Original source: https://en.wikibooks.org/wiki/Introduction_to_Inorganic_Chemistry.

10.5: Kapustinskii Equation

From the discussion above, it is clear that the lattice energy, E_L, of an ionic crystal can be calculated with reasonable accuracy if the structure is known. But how can we calculate E_L for a new or hypothetical compound of unknown structure? Recall that the reduced Madelung constant is about the same for different crystal structures. Russian chemist A. F. Kapustinskii recognized this fact and devised a formula that allows one to calculate E_L for any compound if we know the univalent radii of the constituent ions. [5]

The Madelung constant, A, is proportional to the number of ions (n) in formula unit, so dividing by the n gives similar values as shown in the table below:

A/n ~ invariant

Structure	A/n
NaCl	0.874
CsCl	0.882
Rutile	0.803
Fluorite	0.800

Kapustinskii noticed that the difference in ionic radii between M^+ and M^{2+} (the monovalent vs. divalent radius) largely compensates for the differences in A/n between monovalent (NaCl, CsCl) and divalent (rutile, CaF_2) structures. He thus arrived at a lattice energy formula using an average Madelung constant, corrected to monovalent radii. In the **Kapustinskii formula**, the lattice energy (kJ/mol) is given by:

$$E_L = \frac{1213.8 z_+ z_- n}{r_+ + r_-}\left(1 - \frac{0.345}{r_+ + r_-}\right) \tag{10.5.1}$$

Here the sum of the monovalent radii is used in place of r_o, the bond distance in the Born-Mayer equation. The beauty of this formula is that it requires no knowledge of the structure of the compound. Therefore it can be used, in combination with Born-Haber cycles, to predict the stability of unknown compounds. As we show below, this is a broadly useful tool in guiding syntheses and predicting the reactivity of inorganic solids.

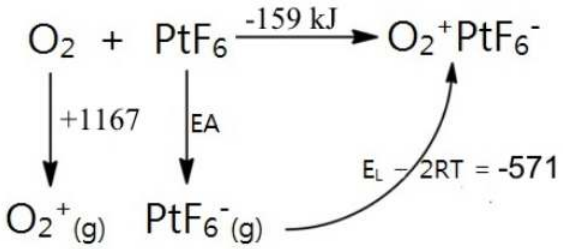
10.5: Kapustinskii Equation is shared under a CC BY-SA license and was authored, remixed, and/or curated by LibreTexts.

- **9.5: Kapustinskii Equation** by Chemistry 310 is licensed CC BY-SA 4.0. Original source: https://en.wikibooks.org/wiki/Introduction_to_Inorganic_Chemistry.

10.6: Discovery of Noble Gas Compounds

In 1962 at the University of British Columbia, Neil Bartlett was working with the powerful oxidizer PtF_6 and, because of an accidental leak in his vacuum line, noticed the compound's reaction with O_2 to generate a solid with formula "PtF_6O_2." The formula suggested Pt in the +10 oxidation state, which was clearly unreasonable because PtF_6 was known to be a more powerful oxidizer than either molecular fluorine (F_2) or molecular oxygen (O_2). Bartlett noticed that the X-ray powder diffraction pattern of the compound was similar to that of $Cs^+AsF_6^-$, a salt with the CsCl structure in which octahedral AsF_6^- ions occupy the chloride ion sites. This led Bartlett to propose a formulation of $O_2^+PtF_6^-$ for his new compound.[6] Magnetic susceptibility data subsequently confirmed the presence of the paramagnetic O_2^+ cation, which (see Chapter 2) has a bond order of 2.5. This formulation implies that PtF_6 was a strong enough oxidizing agent to oxidize molecular oxygen.

But just how strong an oxidizer is PtF_6? Its electron affinity could be estimated by using a Born-Haber cycle, filling in the lattice energy of $O_2^+PtF_6^-$ by means of Kapustinskii's formula:



The electron affinity (EA) for PtF_6 can be calculated as EA = -159 - 1167 + 571 = -751 kJ/mol. To put it in perspective, this is 417 kJ/mol more exothermic than the electron affinity of atomic fluorine (334 kJ). PtF_6 was by far the strongest oxidizer that had ever been made!



Crystals of xenon difluoride (XeF_2), which is made by photolysis of a gas mixture of Xe and F_2. XeF_2 is used as a selective etchant for SiO_2 in certain microelectronic fabrication processes. Prior to Neil Bartlett's discovery of the first xenon compound in 1962, it was believed that elements in group VIII (He, Ne, Ar, Kr, Xe) could not form chemical compounds. Since then chemists have discovered a rich family of noble gas compounds containing Xe, Kr, or Ar.

Bartlett recognized that Xe has ionization energy of +1170 kJ, which is very close to the ionization energy of O_2. Since Xe^+ should be about the same size as O_2^+, the lattice energy should be about the same with Xe^+ in the cation site of the $O_2^+PtF_6^-$ structure. Since all of the other terms in the Born-Haber cycle for the reaction of Xe with PtF_6 are the same, Bartlett concluded that $Xe^+PtF_6^-$, like $O_2^+PtF_6^-$, should be a stable compound. He purchased a lecture bottle of xenon gas and reacted the two compounds, producing an orange solid.[7] While the product initially formed in the reaction may in fact be $Xe^+PtF_6^-$, the Xe^+ free radical is a powerful Lewis acid and reacts further with excess PtF_6. The ultimate product of the reaction is formulated $[XeF^+][Pt_2F_{11}^-]$, a salt which contains Xe in the +2 oxidation state and Pt in the +5 oxidation state. This was an important discovery because it shattered the dogmatic notion, which derived from the octet rule, that elements in group VIII could not form bonds with other elements. The name of this group was changed from the "inert gases" to the "noble gases." Subsequently, many compounds of Xe and a few of Kr and even Ar (which is much harder to oxidize) were synthesized and characterized.

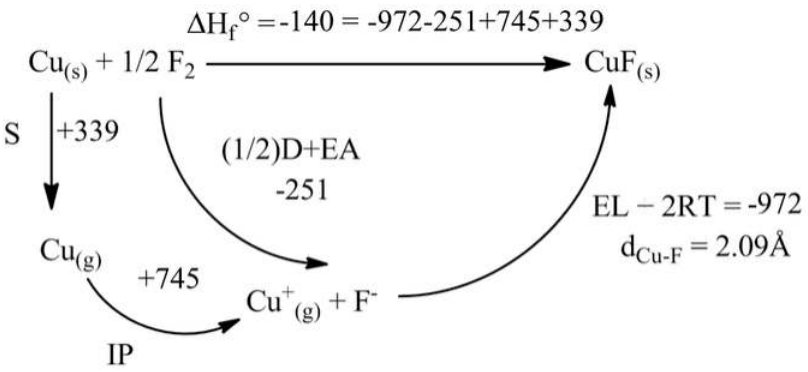
10.6: Discovery of Noble Gas Compounds is shared under a CC BY-SA license and was authored, remixed, and/or curated by LibreTexts.

- **9.6: Discovery of Noble Gas Compounds** by Chemistry 310 is licensed CC BY-SA 4.0. Original source: https://en.wikibooks.org/wiki/Introduction_to_Inorganic_Chemistry.

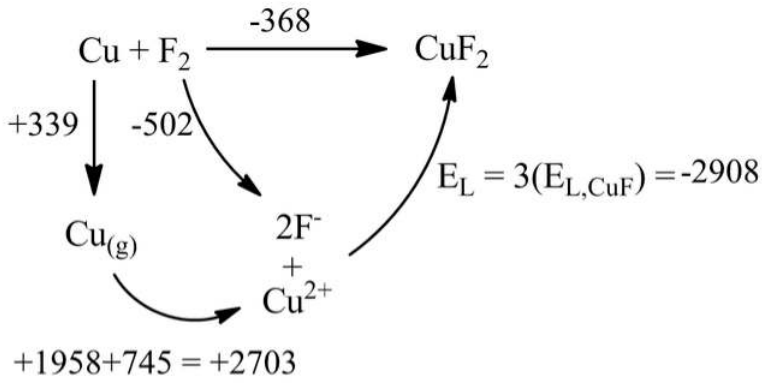
10.7: Stabilization of High and Low Oxidation States

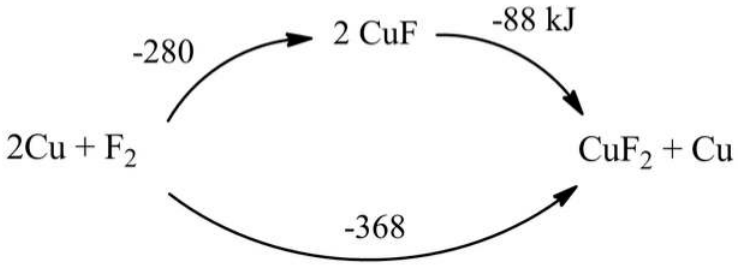
Lattice energies, in addition to guiding the discovery of unknown compounds, are useful in explaining the absence (i.e., the thermodynamic instability) of **non-existent compounds**.[8] For example, CuF and AuF are unknown compounds, whereas CuF_2, AuF_3, and AuF_5 are stable. In contrast AgF is a known, stable compound.

From the Born Haber cycle for CuF, the compound should be marginally stable (ΔH_f^o = -140 kJ/mol) with respect to the elements. Why then is CuF unknown?



To gain insight into this question, we first construct a Born-Haber cycle for the formation of CuF_2 from the elements. This compound is stable with respect to the elements by -368 kJ/mol.





Combining the two cycles we see that the **disproportionation** of CuF to Cu and CuF_2 is spontaneous. From similar cycles, we can also predict that the reaction $3AuF \rightarrow AuF_3 + 2Au$ should be spontaneous.

Why is the lowest oxidation state unstable for these fluorides? The key point is that the large difference in E_L values (2908-972=1926 kJ in the case of copper fluorides) drives their disproportionation reactions. Note that when we use the Kapustinskii equation, we calculate that E_L for CuF_2 is approximately **three times** that of CuF. We use the same univalent radii in both calculations, but Cu has a 2+ charge in CuF_2 (doubling the lattice energy relative to CuF), and contains 3/2 as many ions. The

product z_+z_-n is thus three times larger for CuF_2. The difference in E_L values will thus increase as E_L for the monovalent salt increases. We know that fluorides, having a small anion radius, will give larger E_L values than iodides, which have larger anions. Thus the disproportionation reaction becomes more favorable for CuF than it is for CuI.

The stability of the lower vs. higher oxidation state thus depends on the **size of the anion**. For example, in fluorides, CuF is unstable but CuF_2 is stable. However, in iodides, CuI is stable whereas CuI_2 is unstable. From this we can develop a broad conclusion: **small anions (O,F) tend to stabilize higher oxidation states, whereas large anions (S, Br, I...) stabilize lower oxidation states.** Note that this trend has to do with the **size** and not with the electronegativity of the anion. Coincidentally, F and O are electronegative elements, but it is really their small size that has consequences for the lattice energy and their stabilization of higher oxidation states.



Cuprous iodide (CuI) is a crystalline compound used in organic synthesis and cloud seeding. This compound can be made in the laboratory by reacting soluble Cu^{2+} salts with a solution of sodium or potassium iodide. Because CuI_2 is thermodynamicaly unstable, the reaction liberates I_2 and a CuI precipitate forms.

Remember that the **hard-soft acid-base rules** could be interpreted in terms of the dominance of ionic vs. covalent interactions. Here we have put the hard-hard interaction in quantitative terms, based on (electrostatic) lattice energies.

Ag appears to buck the periodic trend. Why is AgF stable? This is because the second IP is very high (2071 kJ vs. 1958 kJ for Cu, 1979 for Au). Thus both AgF and AgF_2 are known fluorides of Ag.

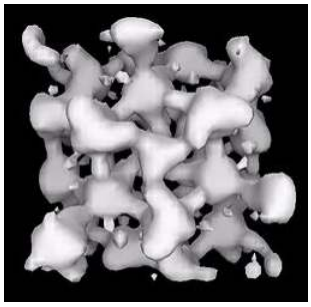
10.7: Stabilization of High and Low Oxidation States is shared under a CC BY-SA license and was authored, remixed, and/or curated by LibreTexts.

- **9.7: Stabilization of High and Low Oxidation States** by Chemistry 310 is licensed CC BY-SA 4.0. Original source: https://en.wikibooks.org/wiki/Introduction_to_Inorganic_Chemistry.

10.8: Alkalides and Electrides

Another interesting consequence of lattice energies involves the formation of certain salts containing Na^- and e^- anions. These compounds are known as **alkalides** and **electrides**, respectively.[9] Most of these compounds have been discovered by Prof. James Dye at Michigan State University.

The alkali metals have one electron in their valence shell. For example, the electronic configurations of Na and K are $[Ar]3s^1$ and $[Kr]4s^1$, respectively. Although we are accustomed to seeing these very electropositive elements give up their electrons when they make compounds with electronegative elements, they can also gain an electron to achieve a [noble gas]ns^2 configuration. This is possible with strong electron donors such as alkali metals, especially when the cation that is formed is stabilized by coordination to a crown ether. Typically, these compounds are synthesized by combining the alkali metal and the appropriate crown ether in liquid ammonia, and then evaporating the ammonia.



Cavities and channels in an electride

Electride salts are formed under similar conditions, except in this case the anion is simply an electron that exists in an anion "cavity" in the crystal. The crystal structures are clearly salt-like, with the cations (alkali cations stabilized by crown or cryptand ligands) alternating in the structure with electrons.

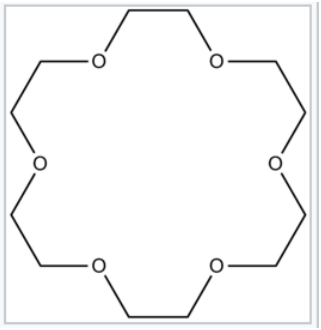
Alkalide Salt

$$2\,Na \xrightarrow{NH_3} Na^+(NH_3)^+ \; e^-(NH_3) \xrightarrow{18\,C_6} [Na(18\,C_6)]^+ \; Na^- \tag{10.8.1}$$

Electride Salt

$$2\,Cs \xrightarrow[18\,C_6]{NH_3} [Cs(18\,C_6)]^+ \; e^- \tag{10.8.2}$$

Complexing Na^+ (K^+, Rb^+, Cs^+) with crown ether ligands stabilizes the M^+ form of the metal ("salt" form). Because the metal cation with its ligand shell is rather large, the lattice energy of these salts is rather low.



18-Crown-6, a crown ether that strongly complexes Na^+ cations

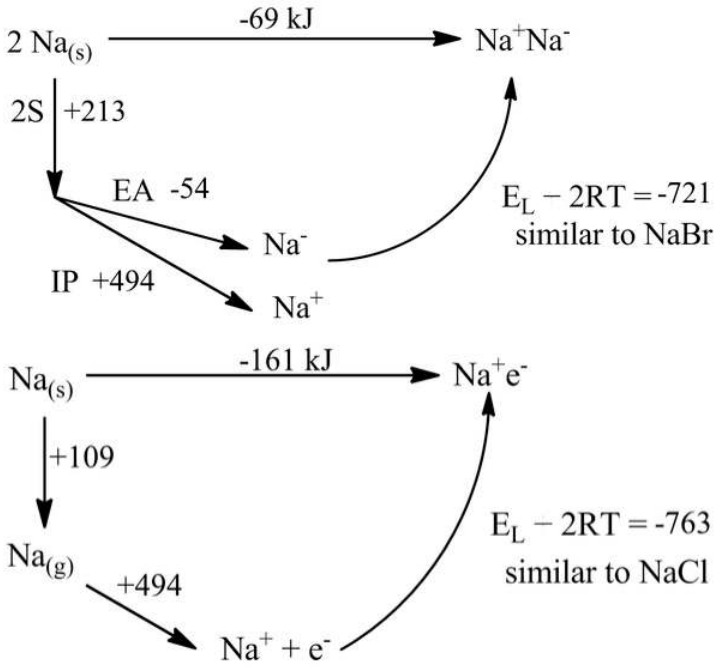
Solutions of electride salts are powerful reducing agents, as demonstrated by their use in the Birch reduction, in which aromatic compounds are hydrogenated to produce dienes. Electrides are also useful for reducing metal ions to metals. Evaporation of blue

electride solutions in anhydrous ammonia affords a mirror of Na. Such solutions slowly lose their color as the electrons reduce ammonia to the amide anion:

$$[Na(NH_3)_6]^+e^- + NH_3 \longrightarrow NaNH_2 + H_2$$

It is interesting to consider, in the context of lattice energies and Born-Haber cycles, what might happen without these ligands present. That is, we can ask the question of whether sodium metal would prefer to exist in the metallic form as Na(s), or to form the sodide salt Na^+Na^-, or the electride salt $Na^+ e^-$. Of course, we already know the answer to this question. Elemental sodium is clearly a metal (it is shiny, conducts electricity, and has a bcc crystal structure) and has never been observed in either of the "salt" forms. But how far away are these forms energetically?

We can calculate the energetics by assuming that the Na- ion is about the same size as Br^-, and that the e^- anion is about the same size as Cl^-. Then the lattice energies in the cycles become the same as those of NaBr and NaCl:



The rather surprising result from these calculations is that sodium would be marginally stable as a sodide salt and very stable (by 161 kJ) as an electride. All the terms in these simple cycles are known precisely. But we must be doing something wrong here, because Na(s) is clearly metallic.

The key, subtle point here is that Born-Haber cycles consider only the *potential energy* (rather than the total energy) of the substances in the cycle. Normally we can ignore the *kinetic energy* part of the total energy, but in this case we cannot because of the quantum mechanical effect of *resonance*.

10.8: Alkalides and Electrides is shared under a CC BY-SA license and was authored, remixed, and/or curated by LibreTexts.

- **9.8: Alkalides and Electrides** by Chemistry 310 is licensed CC BY-SA 4.0. Original source: https://en.wikibooks.org/wiki/Introduction_to_Inorganic_Chemistry.

10.9: Resonance Energy of Metals

The solution to the problem above must consider the quantum mechanical nature of the electron. The valence electrons in Na metal are in orbitals that are delocalized over the entire crystal. However in the Na^+ e^- "salt" form, the electrons are localized on specific anion sites. This localization imparts an additional kinetic energy (via the "**particle in a box**" effect) that adds to the total energy. From the quantum mechanical result for a particle in a one-dimensional box, we obtain

$$KE = \frac{h^2 n^2}{8mL^2} \tag{10.9.1}$$

where:

- h = Plank's constant = 6.626 x 10^{-34} J s
- n = energy level, assumed to be the lowest, n = 1
- m = electron mass = 9.109 x 10^{-31} kg
- L = size of the box

If we approximate the size of the electron "box" as 3 Å (3 x 10^{-10} m), we obtain:

$$KE = \frac{(6.626 \cdot 10^{-34})^2 (6.022 \cdot 10^{23})}{8 \cdot (9.1 \cdot 10^{-31})(3 \cdot 10^{-10})^2} = 4.04 \cdot 10^5 \frac{J}{mol} = +404 \frac{kJ}{mol} \tag{10.9.2}$$

This extra kinetic energy makes the Na^+e^- "salt" unstable relative to the electron-delocalized metal.

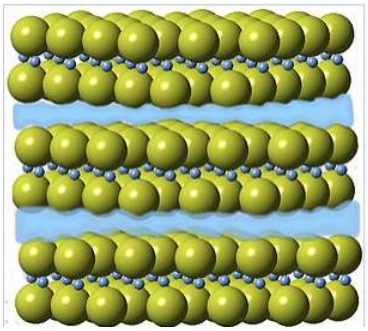


Sodium owes its metallic properties to the resonance stabilization of its delocalized valence electrons.

The calculation is not very accurate because the electron kinetic energy is not zero in the metal, and because the "box" size is not so well defined. However, it does illustrate that electron delocalization has a substantial effect in thermodynamically stabilizing metals. The situation is entirely analogous to the stabilization of aromatic molecules by electron delocalization. In molecules like benzene, resonance is also a quantum-mechanical kinetic energy effect. In general, the resonance stabilization energy is significantly larger in metals than it is in π-delocalized organic molecules. For example, the resonance energy of the six π-electrons in benzene is approximately 151 kJ/mol, less than half of the value we have calculated (per electron) in sodium metal.

Interestingly, several of the alkali metals (and other metallic elements) transform at ultrahigh pressures to optically transparent, insulating phases in which the valence electrons are localized.[10][11] These high pressure electride phases defy the general rule (which we will encounter in Chapter 10) that insulators transform to metals at sufficiently high density. They illustrate how the

stable structure of an element can depend on the trade-off between the lattice energy of an ionic electride structure and the resonance energy of an electron-delocalized metal.



Crystal structure of Ca_2N, with 2D electron layers shown schematically in blue.

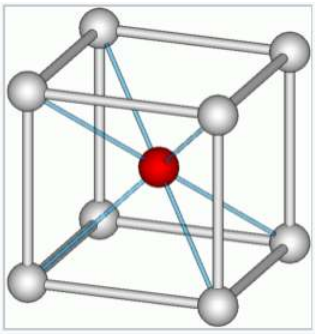
In addition to the salt-like electrides that are formed by complexing alkali metals with crown ether ligands, there are a number of recently discovered solid state nitrides and oxides, such as Ca_2N and $Ca_{24}Al_{28}O_{64}$, that are more properly formulated as electrides, i.e. as $[Ca_2N^+](e^-)$[12] and $[Ca_{24}Al_{28}O_{64}]^{4+}(e^-)_4$.[13] In these compounds the Ca, Al, O, and N atoms have their ordinary octet oxidation states (+2, +3, -2, and -3, respectively), and electrons act as anions, filling in cage-like voids or layers in the crystal. For example, Ca_2N adopts the anti-$CdCl_2$ structure, as shown at the right, with void spaces between layers that are occupied by a 2D gas of electrons. Like other layered materials, Ca_2N can be easily delaminated into thin nanosheets while retaining its structure and properties as an electride.[14] These compounds are powerful reducing agents and also have interesting activity as catalysts.[15]

10.9: Resonance Energy of Metals is shared under a CC BY-SA license and was authored, remixed, and/or curated by LibreTexts.

- **9.9: Resonance Energy of Metals** by Chemistry 310 is licensed CC BY-SA 4.0. Original source: https://en.wikibooks.org/wiki/Introduction_to_Inorganic_Chemistry.

10.10: Prelude to Ionic and Covalent Solids - Energetics

In Chapter 8, we learned all about crystal structures of **ionic compounds**. A good question to ask is, *what makes a compound choose a particular structure?* In addressing this question, we will learn about the forces that hold crystals together and the relative energies of different structures. This will in turn help us understand in a more quantitative way some of the heuristic concepts we have learned about in earlier chapters, such as hard-soft acid-base theory.



At ordinary pressures, the CsCl structure is adopted by only three of the alkali halides, CsCl, CsBr, and CsI. Under high pressure however, other alkali halides transform from the NaCl to the CsCl structure because of the higher Madelung constant of CsCl.

10.10: Prelude to Ionic and Covalent Solids - Energetics is shared under a CC BY-SA license and was authored, remixed, and/or curated by LibreTexts.

- **9.10: Prelude to Ionic and Covalent Solids - Energetics** by Chemistry 310 is licensed CC BY-SA 4.0. Original source: https://en.wikibooks.org/wiki/Introduction_to_Inorganic_Chemistry.

10.11: The Strange Case of the Alkali Oxides

The alkali oxides, made by reacting alkali metals (Li, Na, K, Rb, Cs) with oxygen, show an unusual trend. When lithium reacts with oxygen we obtain the binary oxide Li_2O, as expected from combining an element in group I with one in group VI. Curiously, the oxide that forms most readily when sodium metal is oxidized is not Na_2O, but is instead the peroxide Na_2O_2, which we can formulate as $(Na^+)_2(O_2^{2-})$. With potassium, rubidium, and cesium we obtain the superoxides MO_2, which contain the superoxide radical anion ($O_2^{-\cdot}$) and should be formulated as $(M^+)(O_2^-)$. While it is possible to make Na_2O, K_2O, Rb_2O, and Cs_2O by reaction of the appropriate metal nitrate (MNO_3) with elemental alkali metal M,[16] it is curious that these "normal valent" compounds do not form by direct reaction of the metal with oxygen.

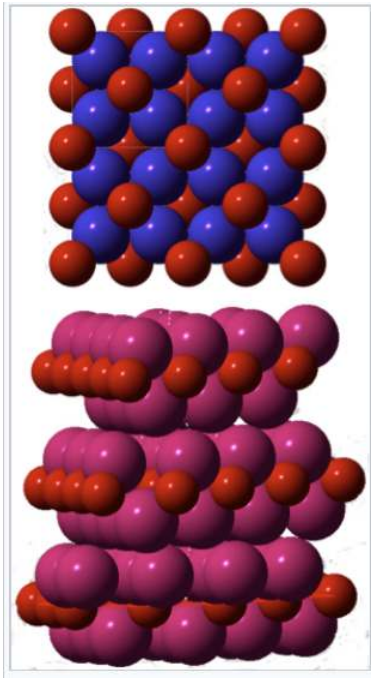


Sodium metal is oxided in air to sodium peroxide, Na_2O_2

Because the alkali metals are all very electropositive (χ = 0.8-1.0), and oxygen is very electronegative (χ = 3.5), we expect all the compounds we make by combining them to be reliably ionic. Consistent with this picture we find that Li_2O (along with Na_2O, K_2O, and Rb_2O) adopts the antifluorite structure (8:4 coordination - see problem 8.8.2), which we expect to find with relatively ionic M_2X compounds. Strangely however, Cs_2O crystallizes in the anti-$CdCl_2$ structure. This is odd because $CdCl_2$ has a layered structure that we normally associate with polar covalent MX_2 compounds (see section 8.4). In Cs_2O, six Cs^+ cations surround each O^{2-} anion in an octahedron. Each Cs^+ is coordinated to three O^{2-} ions, and the Cs^+ ions contact each other across a van der Waals gap. The juxtaposition of Cs^+ ions near each other is clearly electrostatically unfavorable, so why does Cs_2O prefer the anti-$CdCl_2$ structure to antifluorite?

The answer has to do with the crowding of alkali ions around oxygen, as illustrated for K_2O at the right. Because eight large K^+ ions surround each O^{2-} ion in the structure, the cations are essentially in contact. Indeed, the metal-oxygen bonds are "stretched" in Na_2O, K_2O, and Rb_2O relative to M-O bonds with the same bond order in other structures.[17] The situation is so extreme for Cs_2O that it finds an (electrostatically unfavorable) structure in which the coordination is lowered to 6:3. This packing problem is

relieved somewhat in the peroxides, where the coordination is still 8:4 but the anion is larger, and especially in the superoxides where the cation:anion ratio is 1:1 and the coordination is 6:6. Thus the larger alkali ions (K^+, Rb^+, Cs^+) tend to form superoxides.



Space-filling models of the crystal structures of K_2O (top) and Cs_2O (bottom). Oxygen atoms are red, potassium ions are blue, and cesium ions are magenta

Another way that we can rationalize this trend is through the energetics of forming the oxides, peroxides, and superoxides.

Let's calculate the enthalpy change (per mole of metal) for forming a metal oxide M_2O from the metal and oxygen:

$$M_{(s)} + \tfrac{1}{4}\ O_{2\ (g)} \longrightarrow \tfrac{1}{2}\ M_2O_{(s)}$$

We can use Hess' law to write this as a sum of reactions:

Reaction	ΔH
$M_{(s)} \longrightarrow M_{(g)} \longrightarrow M^+_{(g)}$	$\Delta_s + IE = \Delta_{f,M^+(g)}$
$\tfrac{1}{4}\ O_{2(g)} \longrightarrow \tfrac{1}{2}O_{(g)} \longrightarrow \tfrac{1}{2}\ O^{2-}$	$\tfrac{1}{4}\Delta H_d + \tfrac{1}{2}EA_1 + \tfrac{1}{2}EA_2 = \tfrac{1}{2}\Delta H_{f,O^{2-}(g)}$
$M^+_{(g)} + \tfrac{1}{2}O^{2-}_{(g)} \longrightarrow \tfrac{1}{2}M_2O_{(s)}$	$\tfrac{1}{2}E_{L,M_2O} - \tfrac{3}{2}RT$
Overall:	
$M_{(s)} + \tfrac{1}{4}O_{2(g)} \longrightarrow \tfrac{1}{2}M_2O_{(s)}$	$\Delta H_{f,M^+(g)} + \tfrac{1}{2}\Delta H_{f,O^{2-}(g)} + \tfrac{1}{2}E_{L,M_2O} - \tfrac{3}{2}RT$

To get the enthalpy change for the overall reaction (the heat of formation of 1/2 mole of M_2O) we will need the heats of formation of $M^+(g)$ and $O^{2-}(g)$, which are available from tabulated values, and E_L, which we can calculate from Kapustinskii's equation.

Similarly, we can write for the formation of the alkali peroxides:

$$M_{(s)} + \tfrac{1}{2}O_{2(g)} \longrightarrow \tfrac{1}{2}M_2O_{2(s)}$$

Reaction

Reaction	ΔH
$M_{(s)} \longrightarrow M_{(g)} \longrightarrow M^+_{(g)}$	$\Delta H_{(f,M^+(g)}$
$\frac{1}{2}\ O_{2\,(g)} \longrightarrow \frac{1}{2} {O_2}^{2-}{}_{(g)}$	$\frac{1}{2}\Delta H_{f,O_2^{2-}(g)}$
$M^+_{(g)} + \frac{1}{2}\ {O_2}^{2-}{}_{(g)} \longrightarrow \frac{1}{2}\ M_2O_{2\,(s)}$	$\frac{1}{2}E_{L,M_2O_2} - \frac{3}{2}RT$
Overall:	
$M_{(s)} + \frac{1}{2}O_{2\,(g)} \longrightarrow \frac{1}{2}M_2O_{2\,(s)}$	$\Delta H_{f,M^+(g)} + \frac{1}{2}\Delta H_{f,O_2^{2-}(g)} + \frac{1}{2}E_{L,M_2O_2} - \frac{3}{2}RT$

and for the superoxides:

$M_{(s)} + O_{2\,(g)} \longrightarrow MO_{2\,(s)}$

Reaction	ΔH
$M_{(s)} \longrightarrow M_{(g)} \longrightarrow M^+_{(g)}$	$\Delta H_{f,M^+(g)}$
$O_{2\,(g)} \longrightarrow {O_2}^-{}_{(g)}$	$\Delta H_{f,O_2^-(g)}$
$M^+_{(g)} + {O_2}^-{}_{(g)} \longrightarrow MO_{2\,(s)}$	$E_{L,MO_2} - 2RT$
Overall:	
$M_{(s)} + O_{2\,(g)} \longrightarrow MO_{2\,(s)}$	$\Delta H_{f,M^+(g)} + \Delta H_{(f,O_2^-(g)} + E_{L,MO_2} - 2RT$

For the gaseous anions and cations, we have the following heats of formation and ionic radii (CN=6):

Ion	ΔH_f, kJ	ionic radius, Å
Li^+	678	0.76
Na^+	602	1.02
K^+	506	1.38
Rb^+	485	1.52
Cs^+	473	1.67
O^{2-}	500	1.20
O_2^{2-}	519	1.59
O_2^-	-88	1.49

Now using Kapustinskii's equation, we can calculate the lattice energies for each compound; these have been converted to lattice enthalpies by subtracting 2 RT or 3 RT as appropriate:

$$\mathbf{E}_L = \frac{1213.8 z_+ z_- n}{r_+ + r_-}\left(1 - \frac{0.345}{r_+ + r_-}\right) \tag{10.11.1}$$

Metal	$\Delta H_L, M_2O$	$\Delta H_L, M_2O_2$	$\Delta H_L, MO_2$
Li	-3,065 kJ	-2,651 kJ	-918 kJ
Na	-2,776	-2,433	-838
K	-2,454	-2,178	-751
Rb	-2,345	-2,090	-721
Cs	-2,241	-2,007	-678

As expected, the lattice energies for M_2O and M_2O_2 are comparable, the latter being somewhat smaller in magnitude because of the larger size of the O_2^{2-} anion. The lattice energies of the superoxides, MO_2, are about 1/3 those of the corresponding peroxides because both the anion and cation are singly charged, and there are only two ions per formula unit.

Now, putting it all together, we can use the lattice energies and heats of formation of the individual ions to compare the heats of formation (per mole of metal) of each of the oxides:

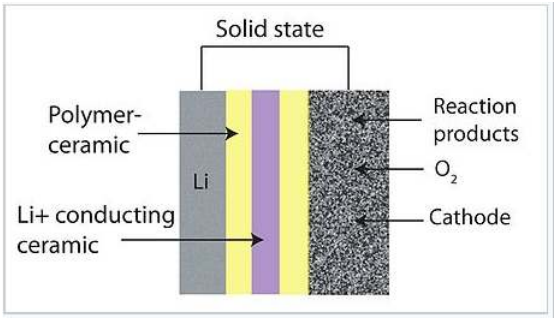
Metal	$1/2\ \Delta H_f, M_2O$	$1/2\ \Delta H_f, M_2O_2$	$\Delta H_f, MO_2$
Li	**-404** kJ	-388 kJ	-328 kJ
Na	-338	**-354**	-324
K	-271	-321	**-328**
Rb	-241	-300	**-324**
Cs	-53	-70	**-81**

We can see that for Li, the formation of Li_2O is favored over Li_2O_2 or LiO_2 because of the very favorable lattice energy of Li_2O. As the lattice energy becomes less negative with increasing cation size, the peroxide becomes the most stable at Na. For the heavier alkalis, M_2O becomes quite unstable and the superoxides MO_2 are the most stable. This is consistent with our observations of the chemistry of the group I oxides.

Metal-air batteries

The alkali oxides are quite interesting in the context of metal-air batteries because of their potential for extremely high energy storage on a mass basis. Such batteries have alkali metal (typically Li) or Zn anodes and utilize oxygen from the air at the cathode. Although lithium is the lightest and therefore the most energy-dense alkali metal, there are materials problems associated with the formation of Li dendrites when the battery is recharged, and also with the slow kinetics of the four-electron interconversion between $O_2(g)$ and 2 O^{2-} at the cathode. For this reason, superoxide batteries are currently being studied as alternatives. The one-electron cathode reaction $O_2 + e^- = O_2^-$ is kinetically fast, and potassium[18] and sodium[19] represent potentially viable alternatives

to lithium for the anode of these air-breathing batteries. Recently, it has been shown that LiO_2 can be kinetically stabilized by template growth on iridium nanoparticles, potentially opening the door to very high energy density lithium-air batteries.[20]



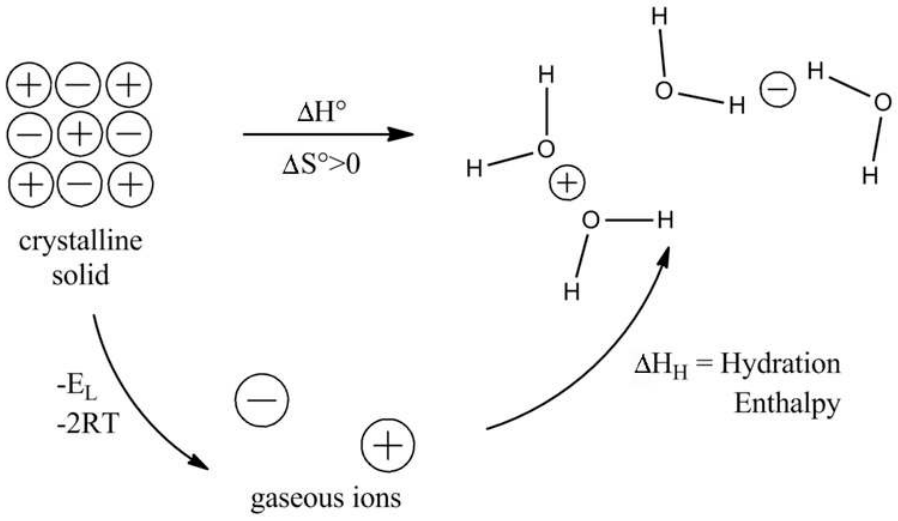
Schematic of an air-breathing lithium battery

10.11: The Strange Case of the Alkali Oxides is shared under a CC BY-SA license and was authored, remixed, and/or curated by LibreTexts.

- **9.11: The Strange Case of the Alkali Oxides** by Chemistry 310 is licensed CC BY-SA 4.0. Original source: https://en.wikibooks.org/wiki/Introduction_to_Inorganic_Chemistry.

10.12: Lattice Energies and Solubility

Lattice energies can also help predict compound solubilities. Let's consider a Born-Haber cycle for dissolving a salt in water. We can imagine this as the sum of two processes: (1) the vaporization of the salt to produce gaseous ions, characterized by the lattice enthalpy, and (2) the hydration of those ions to produce the solution. The enthalpy change for the overall process is the sum of those two steps. We know that the entropy change for dissolution of a solid is positive, so the solubility depends on the enthalpy change for the overall process.



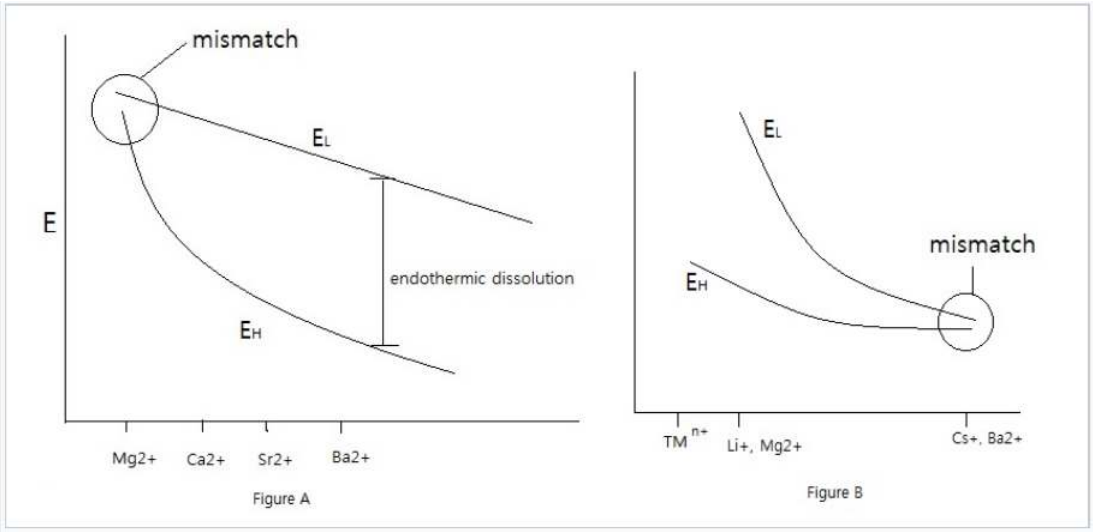
Here we need to consider the trends in both the lattice energy E_L and the hydration energy E_H. The lattice energy depends on the sum of the anion and cation radii ($r_+ + r_-$), whereas the hydration energy has separate anion and cation terms. Generally the solvation of small ions (typically cations) dominates the hydration energy because of the $1/r^2$ dependence.

$$E_L \alpha \frac{1}{r_+ + r_-} \tag{10.12.1}$$

$$E_H \alpha \frac{1}{r_+^2} + \frac{1}{r_-^2} \tag{10.12.2}$$

For salts that contain large anions, E_L doesn't change much as r_+ changes. That is because the anion dominates the $r_+ + r_-$ term in the denominator of the formula for E_L. On the other hand, E_H changes substantially with r_+, especially for small cations.

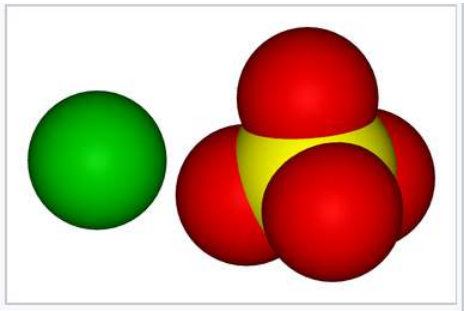
As a result, sulfate salts of small divalent cations, such as $MgSO_4$ (epsom salts), are soluble, whereas the lower hydration energy of Ba^{2+} in $BaSO_4$ makes that salt insoluble ($K_{sp} = 10^{-10}$).



Left: E_L diagram for sulfate salts. The large SO_4^{2-} ion is size-mismatched to small cations such as Mg^{2+}, which have large hydration energies, resulting soluble salts. With larger cations such as Ba^{2+}, which have lower E_H, the lattice energy exceeds the solvation enthalpy and the salts are insoluble.. Right: In the case of small anions such as F^- and OH^-, the lattice energy dominates with small cations such as transition metal ions (TM^{n+}), Mg^{2+}, and Li^+. Anion-cation size mismatch occurs with larger cations, such as Cs^+ and Ba^{2+}, which make soluble fluoride salts.

For small anions, E_L is more sensitive to r_+, whereas E_H does not depend on r_+ as strongly. For fluorides and hydroxides, LiF is slightly soluble whereas CsF is very soluble, and $Mg(OH)_2$ is insoluble whereas $Ba(OH)_2$ is very soluble.

Putting both trends together, we see that **low solubility** is most often encountered when the **anion and cation match well in their sizes**, especially when one or both are **multiply charged**.



Space-filling models showing the van der Waals surfaces of Ba^{2+} and SO_4^{2-}. The similarity in size of the two ions contributes to the low solubility of $BaSO_4$ in water.

Combining all our conclusions about solubility, we note the following trends:

1) Increasing **size mismatch** between the anion and cation leads to greater solubility, so CsF and LiI are the most soluble alkali halides.

2) Increasing **covalency** leads to lower solubility in the salts (due to larger E_L. For example, AgF, AgCl, AgBr, and AgI exhibit progressively lower solubility because of increasing covalency.

AgF > AgCl > AgBr > AgI

3) Increasing the **charge on the anion** lowers the solubility because the increase in E_L is large relative to the increase in E_H.

4) Small, polyvalent cations (having large E_H) make **soluble salts with large, univalent anions** such as I^-, NO_3^-, ClO_4^-, PF_6^-, and acetate.

Examples: Salts of transition metal and lanthanide ions

- Ln^{3+}: Nitrate salts are soluble, but oxides and hydroxides are insoluble.
- Fe^{3+}: Perchlorate is soluble, but sulfate is insoluble.

5) Multiple charged anions such as O^{2-}, S^{2-}, PO_4^{3-}, and SO_4^{2-} make insoluble salts with most M^{2+}, M^{3+}, and M^{4+} metals.

10.12: Lattice Energies and Solubility is shared under a CC BY-SA license and was authored, remixed, and/or curated by LibreTexts.

- **9.12: Lattice Energies and Solubility** by Chemistry 310 is licensed CC BY-SA 4.0. Original source: https://en.wikibooks.org/wiki/Introduction_to_Inorganic_Chemistry.

10.13: Discussion Questions

- Explain why lattice energy calculations are very accurate for NaCl and $CaCl_2$, but less accurate (by about 10%) for AgCl and $PbCl_2$. Does the Born-Mayer equation under- or overestimate the latter values?
- Fluorine is more electronegative than oxygen. However, for many transition metals, we can make higher oxidation states in oxides than we can in fluorides. For example, Mn(IV) is stable in an oxide (MnO_2), but MnF_4 is unstable relative to MnF_3 and fluorine.[21] Can you explain this in terms of lattice energies?

10.13: Discussion Questions is shared under a CC BY-SA license and was authored, remixed, and/or curated by LibreTexts.

- **9.13: Discussion Questions** by Chemistry 310 is licensed CC BY-SA 4.0. Original source: https://en.wikibooks.org/wiki/Introduction_to_Inorganic_Chemistry.

10.14: Problems

1. Use lattice energies to explain why $MgSO_4$ decomposes to magnesium oxide and SO_3 at a much lower temperature than does $BaSO_4$.

2. Solid MgO might be formulated as Mg^+O^- or $Mg^{2+}O^{2-}$. Use the thermochemical data below (some of which are irrelevant) and Kapustinskii's formula to determine which is more stable. The lattice constant for MgO (NaCl structure) is 4.213 Å. While the idea of an O^- ion might seem strange, note that the second electron affinity of O and the second ionization potential of Mg (in the table below) are both quite endothermic.

Reaction	ΔH^o, kJ/mol
Mg(s) = Mg(g)	148
$Mg(g) = Mg^+(g) + e^-$	739
$Mg^+(g) = Mg^{2+}(g) + e^-$	1,452
$O_2(g) = 2\ O(g)$	498
$O(g) + e^- = O^-(g)$	-141
$O^-(g) + e^- = O^{2-}(g)$	790

3. From the heat of formation of solid NH_4Cl (-315 kJ/mol) and gaseous NH_3 (-46), the bond dissociation energies of H_2 (436) and Cl_2 (244), the ionization potential of atomic hydrogen (1,311), and the electron affinity of atomic chlorine (-349), calculate the gas-phase proton affinity of NH_3. The lattice energy of NH_4Cl may be estimated from Kapustinskii's formula using $r_{N\text{-}Cl}$ = 3.50 Å.

4. Bottles of aqueous ammonia are often labeled “ammonium hydroxide.” We will test this idea by using a lattice energy calculation to determine whether the salt $NH_4^+OH^-$ can exist.

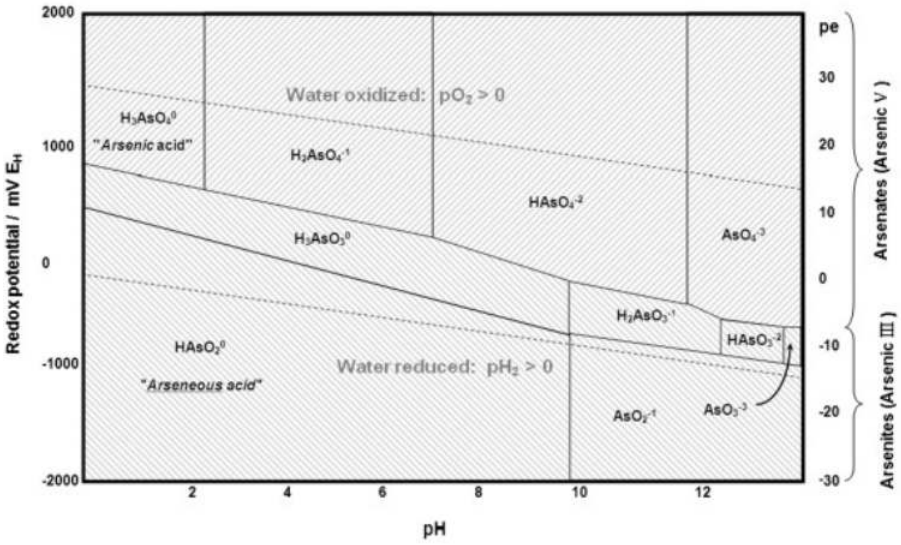
The heats of formation of gaseous OH- and H_2O are respectively -141 and -242 kJ/mol. Assuming that NH_4^+ is about the same size as Rb^+, and OH^- about the same size as F^-, using Kapustinskii's formula, ionic radii, and the NH_3 proton affinity calculated in problem 3, determine whether $NH_4^+OH^-$ should be a stable salt relative to NH_3 and H_2O. At what temperature should $NH_4^+Cl^-$ be unstable relative to NH_3 and HCl, if ΔH_f^o for HCl is -92 kJ/mol and ΔS^o ($\mathbf{NH_4Cl \longrightarrow NH_3 + HCl}$) = 280 J/mol K?

5. Lithium metal burns in nitrogen to make the nitride Li_3N. The heavier alkali metals (K, Rb, Cs) can form stable azides (MN_3), but not M_3N nitrides. Explain why this is so.

6. (a) Do you expect $BaSO_4$ or $MgSO_4$ to be more soluble in water? (b) Is LiF more soluble than $LiClO_4$? Explain.

7. Which polymorph of ZnS (zincblende or wurzite) would you expect to be more stable on the basis of electrostatic energy?

8. Arsenic contamination of ground water is a serious problem in Bangladesh, Chile, Argentina, and other parts of the world including the western United States. Arsenic poisoning been widespread in the Ganges river delta, where tube wells bring contaminated water up from 20-100 meters below the surface. One simple treatment that has been proposed is to precipitate the arsenic by aeration of the well water, which also contains high concentrations of Fe^{2+}. Referring to the Pourbaix diagram of arsenic below and the Pourbaix diagram of iron in Chapter 4, identify the iron and arsenic species that are present in aerated water at neutral pH. What insoluble compound precipitates to lower the concentration of arsenic? (Hint: which compound would have the largest lattice energy?)



10.14: Problems is shared under a CC BY-SA license and was authored, remixed, and/or curated by LibreTexts.

- **9.14: Problems** by Chemistry 310 is licensed CC BY-SA 4.0. Original source: https://en.wikibooks.org/wiki/Introduction_to_Inorganic_Chemistry.

10.15: References

1. Pauling, L. (1929). "The principles determining the structure of complex ionic crystals". *J. Am. Chem. Soc.* **51** (4): 1010–1026. doi:10.1021/ja01379a006.
2. K.-I. Kobayashi, T. Kimura, H. Sawada, K. Terakura, and Y. Tokura, Room-temperature magnetoresistance in an oxide material with an ordered double-perovskite structure, *Nature* (1998) **395**, 677-680. DOI:10.1038/27167
3. E. Mooser and W. B. Pearson, On the Crystal Chemistry of Normal Valence Compounds, Acta. Cryst. 12, 1015 (1959).
4. Madelung E (1918). "Das elektrische Feld in Systemen von regelmäßig angeordneten Punktladungen". *Phys. Zs.* **XIX**: 524–533.
5. A. F. Kapustinskii: *Lattice energy of ionic crystals*, *Quart. Rev. Chem. Soc.* Nr. 10, **1956**, pp. 283–294. DOI|10.1039/QR9561000283
6. Neil Bartlett and D. H. Lohmann (March 1962). "Dioxygenyl hexafluoroplatinate (V), $O_2^+[PtF_6]^-$". *Proceedings of the Chemical Society* (London: Chemical Society) (3): 115. doi:10.1039/PS9620000097.
7. Bartlett, N. (June 1962). "Xenon hexafluoroplatinate (V) $Xe^+[PtF_6]^-$". *Proceedings of the Chemical Society* (London: Chemical Society) (6): 218. doi:10.1039/PS9620000197.
8. W. E. Dasent, Non-Existent Compounds, *J. Chem. Educ.*, **1963**, *40*, p 130, DOI: 10.1021/ed040p130
9. Dye, J. L. (2003). "Electrons as Anions". *Science* **301** (5633): 607–608. doi:10.1126/science.1088103. PMID 12893933.
10. Ma, Y.; Eremets, M.; Oganov, A. R.; Xie, Y.; Trojan, I.; Medvedev, S.; Lyakhov, A. O.; Valle, M.; Prakapenka, V., "Transparent Dense Sodium," Nature 2009, 458, 182–183. doi:10.1038/nature07786
11. M.-S. Miao and R. Hoffmann, "High Pressure Electrides: A Predictive Chemical and Physical Theory," Acc. Chem. Res. 2014, 47, 1311–1317. DOI: 10.1021/ar4002922
12. K. Lee, et al., "Dicalcium nitride as a two-dimensional electride with an anionic electron layer," *Nature*, 2013, 494, 336–340. DOI:10.1038/nature11812
13. S. Matsuishi, et al., "High-Density Electron Anions in a Nanoporous Single Crystal: $[Ca_{24}Al_{28}O_{64}]^{4+}(e^-)_4$," *Science*, 2003, 301, 626-629. DOI: 10.1126/science.1083842
14. D. L. Druffel et al., "Experimental Demonstration of an Electride as a 2D Material," *J. Am. Chem. Soc.*, 2016, 138, 16089–16094. DOI: 10.1021/jacs.6b10114
15. Y. Inoue et al., "Highly Dispersed Ru on Electride $[Ca_{24}Al_{28}O_{64}]^{4+}(e^-)_4$ as a Catalyst for Ammonia Synthesis," ACS Catal., 2014, 4, 674–680. DOI: 10.1021/cs401044a
16. Holleman, A.F.; Wiberg, E., eds (2001). *Inorganic Chemistry*. San Diego: Academic Press. ISBN 978-0-12-352651-9.
17. N. K. McGuire and M. O'Keeffe, "Bond lengths in alkali metal oxides," *J. Solid State Chem.* **1984**, *54*, 49-53. DOI:10.1016/0022-4596(84)90129-4
18. X. Ren and Y. Wu, "A low-overpotential potassium–oxygen battery based on potassium superoxide," *J. Am. Chem. Soc.* **2013**, *135*, 2923–2926. DOI:10.1021/ja312059q
19. P. Hartmann, et al., "A rechargeable room-temperature sodium superoxide (NaO_2) battery," *Nature Materials* **2012**, *12*, 228–232. DOI:10.1038/nmat3486
20. Lu et al., "A lithium–oxygen battery based on lithium superoxide," *Nature* **2016**, *529*, 377-382. DOI:10.1038/nature16484
21. K. O. Christe, "Chemical synthesis of elemental fluorine," *Inorg. Chem.* **1986**, *25*,3721–3722. DOI: 10.1021/ic00241a001

10.15: References is shared under a CC BY-SA license and was authored, remixed, and/or curated by LibreTexts.

- **9.15: References** by Chemistry 310 is licensed CC BY-SA 4.0. Original source: https://en.wikibooks.org/wiki/Introduction_to_Inorganic_Chemistry.

CHAPTER OVERVIEW

11: Electronic Properties of Materials - Superconductors and Semiconductors

Learning Objectives

- Explain the physical basis of the Hubbard and Mott models of metal-insulator transitions.
- Understand why good superconductors derive from bad metals.
- Know the structures and the periodic trends in band gaps and colors of semiconductors.
- Obtain the band gap of an intrinsic semiconductor from the temperature dependence of the conductivity.
- Predict the doping type when impurities or defects are introduced into a semiconductor.
- Correlate the band picture and Fermi level with n- or p-type doping.
- Understand the physical principles of operation of diodes, LEDs, solar cells, and FETs.
- Explain the differences in structures and electronic properties of crystalline and amorphous semiconductors.

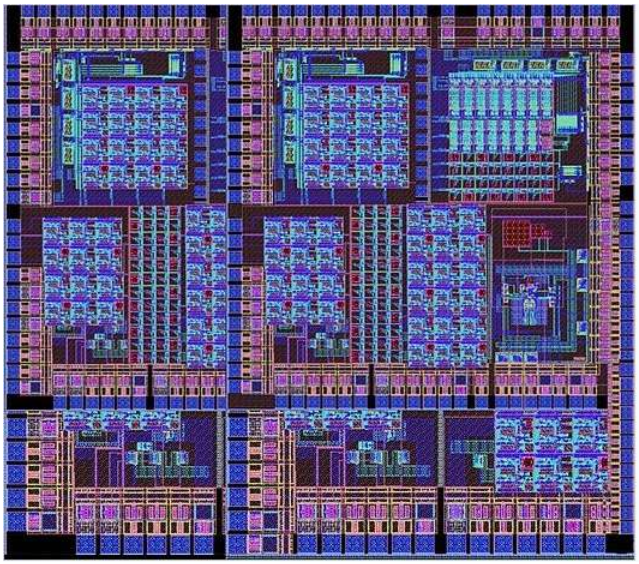
The band model (like MO theory) is based on a *one-electron* model. This was an approximation we made at the very beginning of our discussion of MO theory: we used hydrogen-like (one-electron) solutions to the Schrödinger equation to give us the shapes of s, p, d, and f atomic orbitals. In a one-electron atom, these orbitals are degenerate within a given shell, and the energy differences between, e.g., 2s and 2p orbitals arise only when we consider the energy of an electron in the field of other electrons in the atom. Moving from atoms to molecules, we made linear combinations to generate one-electron molecular orbitals (and, in solids, one-electron energy bands). But as in multi-electron atoms, life is not so simple for real molecules and solids that contain many electrons. Electrons repel each other and so their movement in molecules and in solids is ***correlated***.

11.1: Prelude to Electronic Properties of Materials - Superconductors and Semiconductors
11.2: Metal-Insulator Transitions
11.3: Superconductors
11.4: Periodic Trends- Metals, Semiconductors, and Insulators
11.5: Semiconductors- Band Gaps, Colors, Conductivity and Doping
11.6: Semiconductor p-n Junctions
11.7: Diodes, LEDs and Solar Cells
11.8: Amorphous Semiconductors
11.9: Discussion Questions
11.10: Problems
11.11: References

11: Electronic Properties of Materials - Superconductors and Semiconductors is shared under a CC BY-SA license and was authored, remixed, and/or curated by LibreTexts.

11.1: Prelude to Electronic Properties of Materials - Superconductors and Semiconductors

In Chapter 6 we developed an energy band picture for metals, starting from atomic orbitals and building up the molecular orbitals of the solid metallic crystal. This treatment gave us a useful picture of how electrons behave in metals, moving at very fast speed between scattering events, and migrating in an electric field at a slow drift velocity. It also taught us that a metal is something with a partially filled band, meaning that the Fermi level cuts through one of its bands of orbitals. An insulator or a semiconductor has a similar band picture, except that the bands are either completely full or completely empty. In this case the Fermi level lies in the gap between fully occupied and unoccupied bands. We will see in this chapter that the properties of semiconductors (along with their useful electronic applications) depend on the addition of small amounts of impurities ("dopants") that change the position of the Fermi level, resulting in conduction by electrons or "holes."



Modern integrated circuits contain billions of nanoscale transistors and diodes that are essential for logic and memory functions. Both kinds of devices rely on junctions between crystalline silicon regions that contain a few parts per million of boron or phosphorus impurities.

While the band picture works well for most crystalline materials, it does not tell us the whole story of conduction in solids. That is because the band model (like MO theory) is based on a *one-electron* model. This was an approximation we made at the very beginning of our discussion of MO theory: we used hydrogen-like (one-electron) solutions to the Schrödinger equation to give us the shapes of s, p, d, and f atomic orbitals. In a one-electron atom, these orbitals are degenerate within a given shell, and the energy differences between, e.g., 2s and 2p orbitals arise only when we consider the energy of an electron in the field of other electrons in the atom. Moving from atoms to molecules, we made linear combinations to generate one-electron molecular orbitals (and, in solids, one-electron energy bands). But as in multi-electron atoms, life is not so simple for real molecules and solids that contain many electrons. Electrons repel each other and so their movement in molecules and in solids is ***correlated***. While this effect is weak in a "good" metal such as sodium - where the wavefunctions are highly delocalized - it can be quite important in other materials such as transition metal oxides. Correlated electron effects give rise to **metal-insulator transitions** that are driven by small changes in temperature, pressure, or composition, as well as to **superconductivity** - the passage of current with zero resistance at low temperatures. In this chapter we will develop some simple models to understand these interesting and important electronic properties of solids.

11.1: Prelude to Electronic Properties of Materials - Superconductors and Semiconductors is shared under a CC BY-SA license and was authored, remixed, and/or curated by LibreTexts.

- **10.1: Prelude to Electronic Properties of Materials - Superconductors and Semiconductors** by Chemistry 310 is licensed CC BY-SA 4.0. Original source: https://en.wikibooks.org/wiki/Introduction_to_Inorganic_Chemistry.

11.2: Metal-Insulator Transitions

In Chapter 6 we learned that metals and insulators not only have different electrical properties but also have very different crystal structures. Metals tend to have high coordination numbers (typically 8 or 12) whereas insulators have low coordination numbers that can be rationalized as "octet" bonding arrangements. For example, in crystalline Si or Ge (diamond structure), each atom has four nearest neighbors. There are two electrons per bond, and thus each atom has eight electrons in its valence shell. Sn, the element below Ge, exists in two different forms, one (gray tin) with the diamond structure that is a brittle narrow-gap semiconductor, and the other (white tin) with a body-centered tetragonal structure that is a malleable metal. These two forms are very close in energy, and in fact metallic white tin transforms to the brittle semiconducting gray form at low temperature. Extremely cold weather in 18th century Europe caused many tin organ pipes to break and eventually turn to dust. This transformation has been called tin blight, tin disease, tin pest or tin leprosy. The dust is actually grey tin, which lacks the malleability of its metallic cousin white tin.

Under experimentally accessible temperatures and pressures, Si and Ge are always semiconducting (i.e., insulating), and Pb is always metallic. Why is Sn different? The reason has to do with orbital overlap. Theory tells us in fact that any (and all) insulators should become metallic at high enough pressure, or more to the point, at high enough density. For most insulators, however, the pressures required are far beyond those that we can achieve in the laboratory.



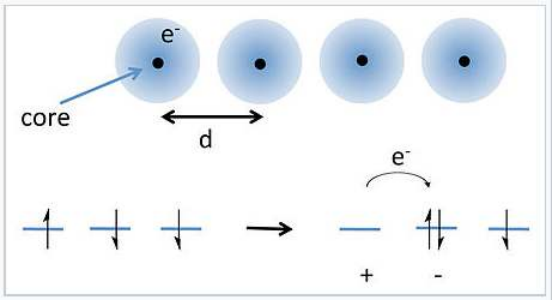
Figure **11.2.1**: Organ pipes destroyed by "tin blight"

How can we rationalize the transition of insulators to the metallic state? Indeed, how can we understand the existence of insulators at all?

The Hubbard Model

Let's consider a chain of a large number (N) of atoms as we did in Chapter 6. For convenience, we can say that these are atoms such as H, Na, or Cs that have one valence electron. The simple band model we developed earlier suggests that the chain should be metallic, because N atoms combine to make N orbitals, and the N valence electrons only fill the band of orbitals halfway. But this

conclusion doesn't depend on the density, which creates a paradox. If atoms in the chain are very far apart, we suspect that the electrons should localize on the atoms.

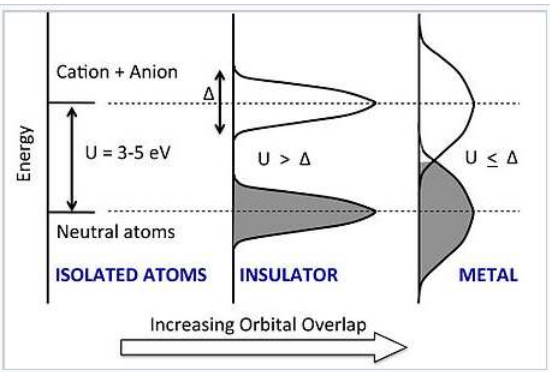


Electron hopping in a 1-D chain of atoms.

A solution to this problem was proposed by J. Hubbard in 1963.[1] Hubbard considered the energy required to transfer an electron from an atom to its nearest neighbor, as shown in the picture at the right. Because each atom already has one electron (with random spin), moving an electron over by one atom requires overcoming the energy of electron-electron repulsion to make a cation-anion pair. For well-separated atoms this energy (U) is given by:

$$U = IP - Ea - \frac{e^2}{4\pi\varepsilon_0 d} \tag{11.2.1}$$

where IP and EA are the ionization energy and electron affinity, ε_0 is the permittivity of free space, and the last term in the equation represents the coulombic attraction between the cation and the anion. For atoms such as alkali metals, U is on the order of 3–5 eV, which is much larger than the thermal energy kT. Thus we expect there to be very few anion-cation pairs at room temperature, and the chain of atoms should be insulating.

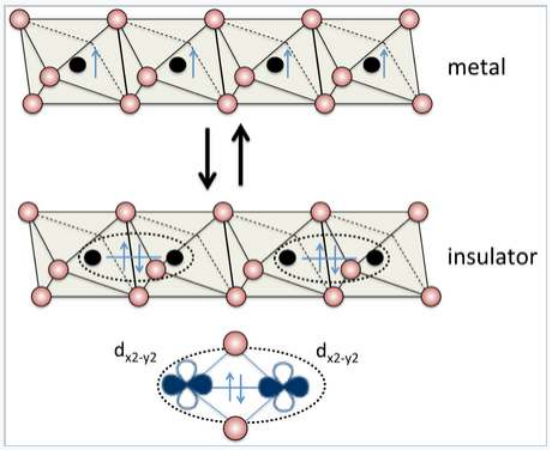


Energy vs. DOS for the chain of atoms as the density and degree of orbital overlap between atoms increases. Increasing overlap broadens the neutral atom and anion-cation states into bands, each of which has a bandwidth Δ. A transition to the metallic state occurs abruptly when Δ exceeds the Hubbard gap U.

What happens when we squeeze the atoms together? In the Hubbard model, as the distance between atoms decreases, the energies of both the neutral atom states and the anion-cation states broaden into bands, each of which has a band width Δ. The lower band can accommodate exactly *N* electrons (not *2N* as in the MO picture we developed earlier) because each orbital can only take one electron without spin-pairing. Thus for small Δ the lower band is full and the upper band is empty. However, as we continue to compress the chain, the orbital overlap becomes so strong that Δ ≈ U. At this point, the bands overlap and some of the electrons fill the anion-cation states. The chain then becomes conducting and the material is metallic.

Some materials, such as Sn and VO_2, happen to have just the right degree of orbital overlap to make the Hubbard transition occur by changing the temperature or pressure. Such materials can be very useful for electrical switching, as illustrated at the right for rutile structure VO_2. Most materials are far away from the transition, either on the metallic or insulating side. An interesting periodic trend that illustrates this concept can be seen among the transition metal monoxides, MO (M = Ti, V, Cr, Mn, Fe, Co, Ni),

all of which have the NaCl structure. TiO and VO are metallic, because the 3d orbitals have significant overlap in the structure. However, CrO, MnO, FeO, CoO, and NiO are all insulators, because the 3d orbitals contract (and therefore $\Delta < U$) going across the transition metal series. In contrast, the analogous sulfides (TiS, VS,....NiS) are all metallic. The sulfides have the NiAs structure, in which all the metal atoms are eclipsed along the stacking axis (the hexagonal c-axis). The short metal-metal distances along that axis result in strong orbital overlap, making $\Delta > U$.



Vanadium dioxide has the rutile structure, and in its undistorted form it is metallic, with one valence electron per V atom. Distortion of the lattice makes pairs of V atoms, resulting in an electronically insulating state. The metal-insulator transition can be driven reversibly by changing the temperature, pressure, or orbital occupancy. Electrical switching of this transition in VO_2 is being studied for applications in high performance thin film transistors[2]

The Mott Model

A simpler, less atomistic model of the metal-insulator transition was formulated by Neville Mott.[3] The Mott model considers the behavior of an electron in a material as a function of the density of all the other valence electrons. We know for a one-electron hydrogen-like atom (H, Na, Cs, etc.) the Schrödinger equation contains a potential energy term:

$$V(r) = -(\frac{e^2}{4\pi\varepsilon_0 r}) \tag{11.2.2}$$

This potential energy function gives rise to familiar ladder of allowed energy levels in the hydrogen atom. However, in a metal, this Coulomb potential must be modified to include the screening of nuclear charge by the other electrons in the solid. In this case there is a **screened Coulomb potential**:

$$V(r) = -(\frac{e^2}{4\pi\varepsilon_0 r})exp(-qr) \tag{11.2.3}$$

where q, which is the inverse of the **screening length**, is given by:

$$q^2 = 4m_e^2(\frac{3n}{\pi})^{\frac{1}{3}}(\frac{2\pi}{h}) \tag{11.2.4}$$

Here n is the density of atoms (or valence electrons), m_e is the electron mass, and h is Planck's constant. At distances much larger than the screening length q^{-1}, the electron no longer "feels" the charge on the nucleus. Mott showed that there is a critical density of electrons n_c above which the valence electrons are no longer bound by individual nuclei and are free to roam the crystal. This critical density marks the transition to the metallic state, and is given by the Mott criterion:

$$\mathbf{n_c^{\frac{1}{3}} a_H \approx 0.26} \tag{11.2.5}$$

In this equation, a_H is an effective Bohr radius for the valence electrons in the low-density limit, e.g. the average orbital radius of electrons in the 6s shell of a Cs atom when computing the value for Cs metal.



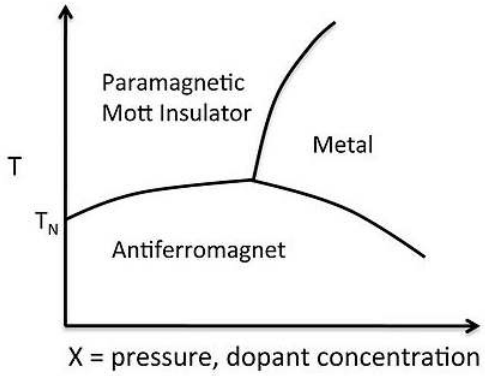
Solutions of lithium metal in liquid ammonia at low (top, ionic conductor) and higher (bottom, metal) Li concentration. From a video by Joshua Judkins

The important concept from the Mott model is that the metal-insulator transition depends very strongly on the **density of valence electrons.** This is consistent with the orbital overlap model of Hubbard, but also more general in the sense that it does not depend on a periodic structure of atoms. The Mott model is thus applicable to such diverse systems as metal atoms dissolved in liquid ammonia, metal atoms trapped in frozen gas matrices, and dopants in semiconductors.[4] In some systems, it is possible to continuously tune the density of valence electrons with rather striking results. For example, dissolving alkali metal (Li, Na, ...) in liquid ammonia (bp -33 ^oC) produces a blue liquid. The solvated alkali cations and negatively charged electrons impart ionic conductivity (as in a salt solution) but not electronic conductivity to the blue liquid ammonia solution. But as the concentration of electrons increases, a reflective, bronze-colored liquid phase forms that floats over the blue phase. This bronze phase is metallic and highly conducting. Eventually, with enough alkali metal added, the entire liquid is converted to the electronically conducting bronze phase.

The electrical switching of VO_2 between insulating and metallic phases (see above) can also be rationalized in terms of the Mott transition. Adding more electron density (by chemical or electric field doping) increases the concentration of valence electrons, driving the phase transition to the metallic state.

Thermodynamics and phase transitions

Thermodynamically, the metal-insulator transition is a **first-order phase transition**. In such a transition, the structure and properties change abruptly (think of the breakfast-to-lunch transition at McDonalds - there is just no way to get pancakes after, or hamburgers before 10:30 AM![5]). Thus in the case of Sn metal, the changes in structure (from four- to eight-coordination) and in electronic conductivity (insulator to metal) occur simultaneously. As in other first order phase transitions such as ice to water to steam, there is a latent heat associated with the transition and a discontinuity in derivative properties such as the heat capacity.



A typical phase diagram for a metal-insulator transition is shown at the right for V_2O_3. The octahedrally coordinated V^{3+} ion has a d^2 electron count, so there are two unpaired spins per atom, and at low temperature the spins in the lattice order antiferromagnetically. As we learned in Chapter 8, above the Néel temperature an antiferromagnet becomes a paramagnet, which is also a Mott insulator. Increasing the pressure, or doping with electrons (e.g., by substituting some d^3 Cr^{3+} for V^{3+}) pushes the electron density over the Mott transition, the spins pair, and the solid becomes metallic.

11.2: Metal-Insulator Transitions is shared under a CC BY-SA license and was authored, remixed, and/or curated by LibreTexts.

- **10.2: Metal-Insulator Transitions** by Chemistry 310 is licensed CC BY-SA 4.0. Original source: https://en.wikibooks.org/wiki/Introduction_to_Inorganic_Chemistry.

11.3: Superconductors

Superconductivity refers to the flow of electrical current in a material with zero resistance. Such materials are very important for use in electromagnets, e.g., in magnetic resonance imaging (MRI) and nuclear magnetic resonance (NMR) machines, because once the current starts flowing in the coils of these magnets it doesn't stop. Magnetic levitation using superconductors - which, below a critical field strength, are perfect diamagnets that are not penetrated by magnetic flux lines - is also potentially relevant to future technologies such as magnetically levitated trains.

The phenomenon of superconductivity, first discovered in Hg metal in 1911 by Onnes, continues to be only partially understood. It is of great interest to physicists as a macroscopic quantum phenomenon, and to chemists and materials scientists who try to make better superconductors (especially those that superconduct at higher temperatures) and devices derived from them, such as superconducting quantum interference devices (SQUIDs), which are extremely sensitive magnetometers.

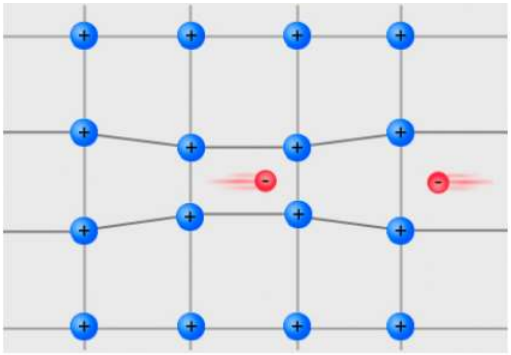


A magnet levitating above a high-temperature superconductor, cooled with liquid nitrogen. Persistent electric current flows on the surface of the superconductor, excluding the magnetic field of the magnet. This current effectively forms an electromagnet that repels the magnet.

Spin pairing and zero resistance

The transition from the metallic to the superconducting state is related to the quantum phenomena of Bose-Einstein condensation and superfluidity. Individual electrons have spin = 1/2, and as such are fermions (particles with half-integer spin). Because of the Pauli exclusion principle, no more than two fermions can occupy the same quantum state (such as an orbital in a molecule or a solid). The familiar consequence of this rule is the aufbau filling of orbitals with spin-paired electrons in each energy level. In contrast, particles with integer spins - which are called bosons - do not have this restriction, and any number of bosons can occupy the same quantized energy level.

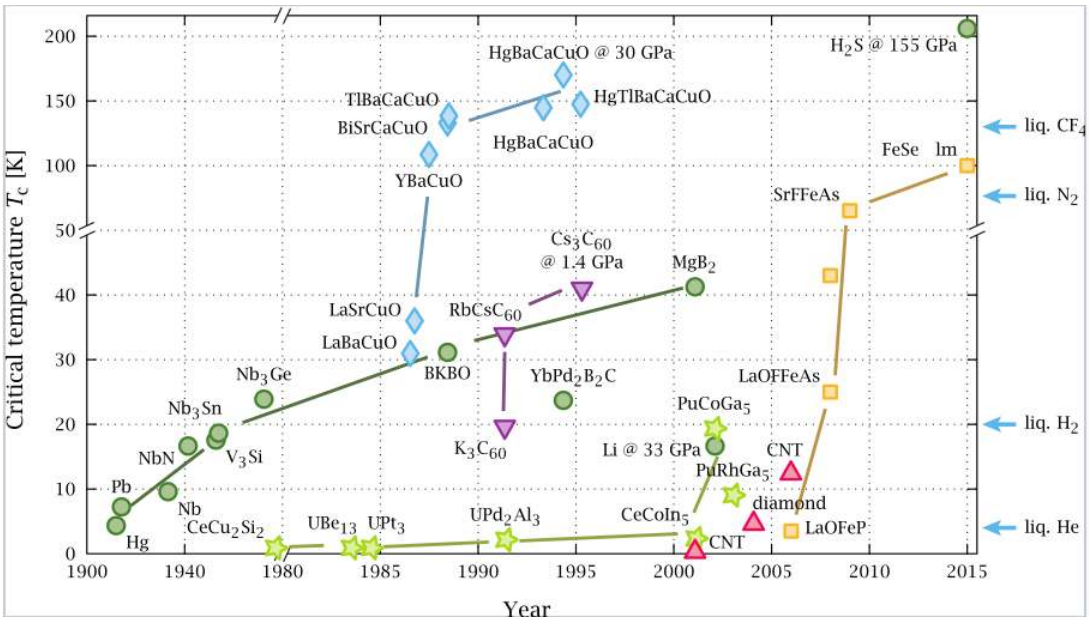
Superconductivity occurs when electrons spin pair into so-called Cooper pairs, which can travel through the lattice together. The electrons in a Cooper pair, although spin-paired, have a long-distance relationship: the spatial extent of a Cooper pair is a few nanometers in cuprate superconductors, and up to one micron in low T_c superconductors such as aluminum. Because its overall spin angular momentum is zero, a Cooper pair is a boson. When the temperature is low enough, the Cooper pairs "condense" into the lowest energy level. The second lowest energy level - which is typically a few meV above the ground state - is not accessible to them as long as the energy gap is larger than the thermal energy, kT. The scattering of electrons by the lattice then becomes forbidden by energy conservation because scattering dissipates energy, and the Cooper pairs cannot change their energy state. Thus the resistance (which arises from scattering, as we learned in Ch. 6) drops abruptly to zero below T_c. However, the Cooper pairs can be broken apart when they move fast, and thus superconductors turn back into normal metals (even below T_c) above some critical current density j_c. This phenomenon is also related to the critical magnetic field, H_c, that quenches superconductivity.



A trampoline for electrons

What causes electrons, which repel each other because of their negative charge, to pair up and travel together in superconductors? The mechanism - which must involve some kind of attractive interaction between electrons - is well understood for "conventional" superconductors which have relatively low transition temperatures, but is not yet known with certainty for high temperature oxide superconductors. In conventional, or BCS superconductors, the spin pairing is mediated by the lattice as shown in the figure at the left. A strong electron-lattice interaction causes a distortion in the lattice as an electron moves through. This elastic deformation is felt as an attractive force by a second electron moving in the opposite direction. This can be thought of as analogous to the interaction of two people jumping on a trampoline. The weight of the first person on the trampoline creates a "well" that attracts the second one, and they tend to move together (even if they don't like each other). Strange as this interaction seems, it is supported experimentally by isotope effects on T_c and by quantitative predictions of T_c values in conventional superconductors.

Bad metals make good superconductors. All superconductors are "normal" metals - with finite electrical resistance - above their critical transition temperature, T_c. If you ask where in the periodic table one might look for superconductors, the answer is surprising. The most conductive metals (Ag, Au, Cu, Cs, etc.) make the worst superconductors, i.e., they have the lowest superconducting transition temperatures, in many cases below 0.01 K. Conversely "bad" metals, such as niobium alloys, certain copper oxides, $K_xBa_{1-x}BiO_3$, MgB_2, FeSe, and alkali salts of C_{60}^{n-} anions, can have relatively high transition temperatures.

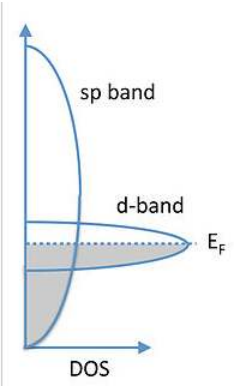


Timeline of superconducting materials, showing T_c vs. year of discovery.

We observe that most good superconductors appear in composition space very **near a metal-insulator transition**. In terms of our microscopic picture, orbital overlap in superconductors is poor, just barely enough to make them act as metals ($\Delta \approx U$) above T_c. In the normal state, superconductors with high T_c - which can be as high as 150 K - are typically "bad" metals. An important

characteristic of such metals is that the **mean free path** of electrons (in the normal state, above T_c) is on the order of the lattice spacing, i.e., **only a few Å**. In contrast, we learned in Ch. 6 that good metals such as Au, Ag, and Cu have electron mean free paths that are two orders of magnitude longer (ca. 40 nm). In a bad metal, the electron "feels" the lattice rather strongly, whereas in a good metal, the electrons are insensitive to small changes in the distance between metals atoms.

What does the band picture look like for a bad metal? The key point is that because orbital overlap is poor, the metal has a **high density of states** at the Fermi level. This is a universal property of high temperature superconductors and provides a clue of where to look for new and improved superconducting materials. Recall that transition elements in the middle of the 3d series (Cr, Fe, Co, Ni) were magnetic because of poor orbital overlap and weak d-d bonding. The elements below these - especially Nb, Ta, and W - have just barely enough d-d orbital overlap to be on the metallic side of the metal-insulator transition and to be "bad" metals. Carbides and nitrides of these elements are typically superconducting, with the carbon and nitrogen atoms serving to adjust the valence electron density, as illustrated in the table below.



Generic E vs. DOS for a bad metal.

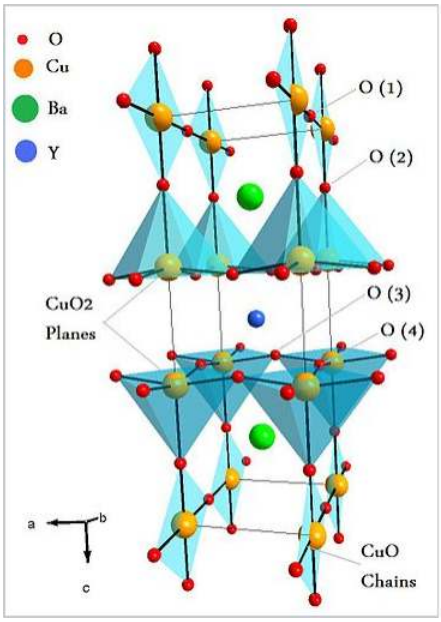
Compound	NbC	Mo_2N	TaC	VN	NbN	TaN	Nb_3Ge
T_c (K)	11.1	5.0	9.7	7.5	15.2	17.8	22.3

High T_c superconductors

In addition to having weak orbital overlap in the metallic state - which results in a high DOS at E_F - high temperature superconductors also typically contain elements in mixed oxidation states (for example, $Cu^{2+/3+}$ or $Bi^{3+/5+}$) that are close in energy to the O^{2-}/O^- couple in the lattice. At ambient pressure, cuprate superconductors have the highest known T_c values, ranging between about 35 and 150 K. The crystal structures of these materials are almost all variants of the perovskite lattice, as shown at the right for the 1-2-3 superconductor $YBa_2Cu_3O_{7-\delta}$. An ideal perovskite lattice would have formula ABO_3 = $A_3B_3O_9$. In $YBa_2Cu_3O_{7-\delta}$, Y and Ba occupy the A cation sites, Cu occupies the B sites, and two of the nine O atoms are missing.

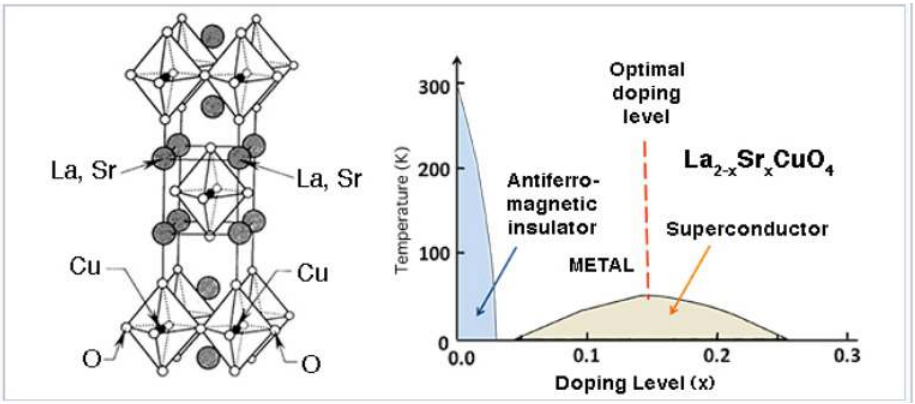
The $YBa_2Cu_3O_{7-\delta}$ lattice consists of mixed-valent copper(II/III) oxide sheets capped by oxygen atoms to form CuO_5 square pyramids. These sheets encapsulate the Y^{3+} cations. Copper(II) oxide ribbons that share the apical oxygen atoms of the square pyramids run in one direction through the structure. In $YBa_2Cu_3O_{7-\delta}$ and related materials, one component of the structure (here the Cu-O ribbons) acts as a **charge reservoir** to control the doping of the planar CuO_2 sheets, which are the elements of the structure

that carry the supercurrent. Cuprate superconductors with Bi, Tl, or Hg-containing charge reservoir layers and multiple, eclipsed CuO_2 sheets in the unit cell tend to have the highest T_c values.



Crystal structure of $YBa_2Cu_3O_{7-\delta}$ (YBCO), the first superconductor with T_c above the boiling point of liquid nitrogen.

The connection between the metal-insulator transtion and superconductivity is nicely illustrated in the phase diagram of $La_{2-x}Sr_xCuO_4$, the first cuprate superconductor, which was discovered in 1986 by Georg Bednorz and K. Alex Müller. This compound has a rather simple structure in which rocksalt La(Sr)O layers are intergrown with perovskite La(Sr)CuO_3 layers. Undoped La_2CuO_4 contains only Cu^{2+} ions and is an antiferromagnetic insulator. As a small amount of Sr^{2+} is substituted for La^{3+}, some of the Cu^{2+} is oxidized to Cu^{3+}, and the lattice is doped with holes. As the doping level increases, the antiferromagnetic phase undergoes a first-order phase transition to a "bad" metal, and at slightly higher doping density the superconducting phase appears. The proximity of the superconducting phase to the metal-insulator transition is a hallmark of cuprate superconductors. A maximum T_c of 35K is observed at x = 0.15. Doping at higher levels moves the Fermi level beyond the point of highest DOS in the d-band of Cu and the superconducting phase then gradually disappears. It is interesting to compare this phase diagram with that of V_2O_3 (above), which also undergoes an antiferromagnetic insulator to "bad" metal transition as it is doped.



Crystal structure and phase diagram of the cuprate superconductor $La_{2-x}Sr_xCuO_4$. (LSCO)

11.3: Superconductors is shared under a CC BY-SA license and was authored, remixed, and/or curated by LibreTexts.

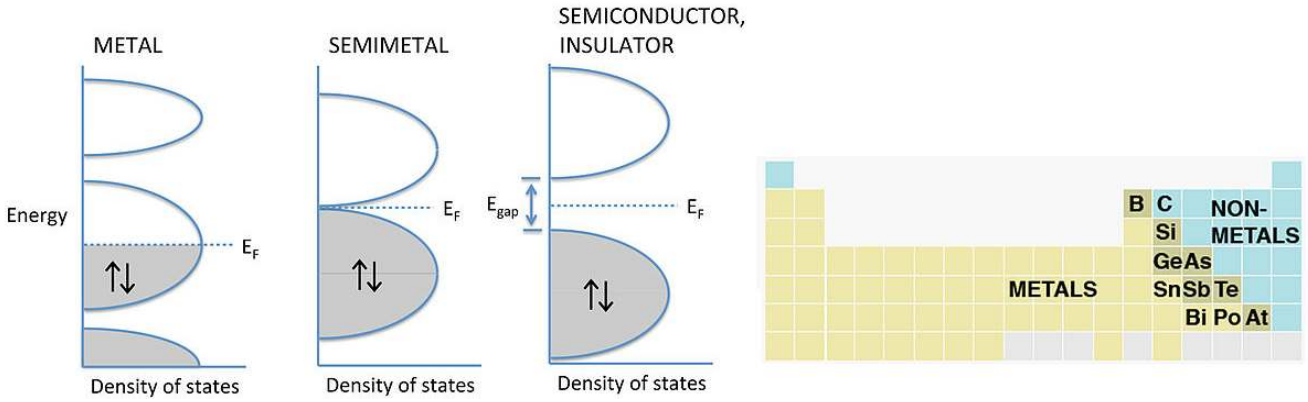
- **10.3: Superconductors** by Chemistry 310 is licensed CC BY-SA 4.0. Original source: https://en.wikibooks.org/wiki/Introduction_to_Inorganic_Chemistry.

11.4: Periodic Trends- Metals, Semiconductors, and Insulators

As we consider periodic trends in the electronic properties of materials, it is important to review some of the key bonding trends we have learned in earlier chapters:

- Going down the periodic table, atoms in solids tend to adopt structures with higher coordination numbers.
- The second row of the periodic table is special, with strong s-p hybridization and π-bonding between atoms.
- Electrons in higher quantum shells are less strongly bound, so the energy difference between bonding and antibonding orbitals becomes smaller for heavier atoms.

We also know that most of the elements in the periodic table are metals, but the elements in the top right corner are insulating under ordinary conditions (1 atm. pressure) and tend to obey the octet rule in their compounds.



At the transition between metals and non-metals in the periodic table we encounter a crossover in electronic properties, as well as in other properties such as the acidity of the oxides (see Ch. 3). The group of elements at the border is loosely referred to as the metalloids. Several of these elements (such as C, Sn, and As) can exist as different allotropes that can be metals, insulators, or something in between.

A more rigorous delineation of the electronic properties of these elements (and of many compounds) can be made by considering their band structures and the **temperature dependence of the electronic conductivity**. As we have previously discussed, metals have partially filled energy bands, meaning that the Fermi level intersects a partially filled band. With increasing temperature, metals become poorer conductors because lattice vibrations (which are called phonons in the physics literature) scatter the mobile valence electrons. In contrast, semiconductors and insulators, which have filled and empty bands, become better conductors at higher temperature, since some electrons are thermally excited to the lowest empty band. The distinction between insulators and semiconductors is arbitrary, and from the point of view of metal-insulator transitions, all semiconductors are insulators. We typically call an insulator a semiconductor if its band gap (E_{gap}) is less than about 3 eV. A semimetal is a material that has a band gap near zero, examples being single sheets of sp^2-bonded carbon (graphene) and elemental Bi. Like a narrow gap semiconductor, a semimetal has higher conductivity at higher temperature.

11.4: Periodic Trends- Metals, Semiconductors, and Insulators is shared under a CC BY-SA license and was authored, remixed, and/or curated by LibreTexts.

- **10.4: Periodic Trends- Metals, Semiconductors, and Insulators** by Chemistry 310 is licensed CC BY-SA 4.0. Original source: https://en.wikibooks.org/wiki/Introduction_to_Inorganic_Chemistry.

11.5: Semiconductors- Band Gaps, Colors, Conductivity and Doping

Semiconductors, as we noted above, are somewhat arbitrarily defined as insulators with **band gap energy ≤ 3.0 eV** (~290 kJ/mol). This cutoff is chosen because, as we will see, the conductivity of undoped semiconductors drops off exponentially with the band gap energy and at 3.0 eV it is very low. Also, materials with wider band gaps (e.g. $SrTiO_3$, E_{gap} = 3.2 eV) do not absorb light in the visible part of the spectrum

There are a number of places where we find semiconductors in the periodic table:

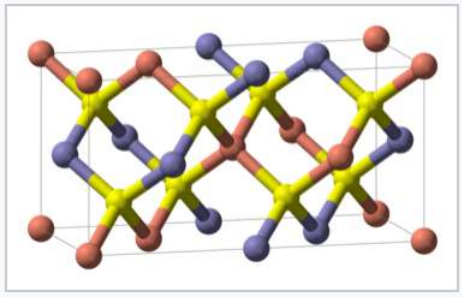
- Early transition metal oxides and nitrides, especially those with d^0 electron counts such as TiO_2, TaON, and WO_3
- Oxides of later 3d elements such as Fe_2O_3, NiO, and Cu_2O
- Layered transition metal chalcogenides with d^0, d^2 and d^6 electron counts including TiS_2, ZrS_2, MoS_2, WSe_2, and PtS_2
- d^{10} copper and sliver halides, e.g., CuI, AgBr, and AgI
- Zincblende- and wurtzite-structure compounds of the p-block elements, especially those that are isoelectronic with Si or Ge, such as GaAs and CdTe. While these are most common, there are other p-block semiconductors that are not isoelectronic and have different structures, including GaS, PbS, and Se.



A 2" wafer cut from a GaAs single crystal. GaAs, like many p-block semiconductors, has the zincblende structure.

The **p-block octet semiconductors** are by far the most studied and important for technological applications, and are the ones that we will discuss in detail.

Zincblende- and wurtzite-structure semiconductors have 8 valence electrons per 2 atoms. These combinations include 4-4 (Si, Ge, SiC,…), 3-5 (GaAs, AlSb, InP,…), 2-6 (CdSe, HgTe, ZnO,…), and 1-7 (AgCl, CuBr,…) semiconductors. Other variations that add up to an octet configuration are also possible, such as $Cu^{I}In^{III}Se_2$, which has the **chalcopyrite** structure, shown at the right.



The **chalcopyrite structure** is adopted by ABX_2 octet semiconductors such as $Cu^{I}In^{III}Se_2$ and $Cd^{II}Sn^{IV}P_2$. The unit cell is doubled relative to the parent **zincblende structure** because of the ordered arrangement of cations. Each anion (yellow) is coordinated by two cations of each type (blue and red).

How does the **band gap energy** vary with **composition**? There are two important trends

(1) Going **down a group** in the periodic table, the gap **decreases**:

C (diamond) > Si > Ge > α-Sn

E_{gap} (eV): 5.4 1.1 0.7 0.0

This trend can be understood by recalling that E_{gap} is related to the **energy splitting between bonding and antibonding orbitals**. This difference decreases (and bonds become weaker) as the principal quantum number increases.

(2) For isoelectronic compounds, **increasing ionicity** results in a **larger band gap**.

Ge < GaAs < ZnSe

0.7 1.4 2.8 eV

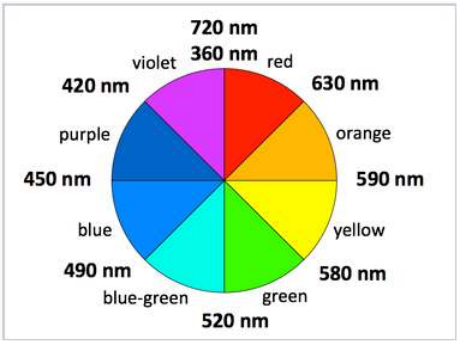
Sn < InSb < CdTe < AgI

0.0 0.2 1.6 2.8 eV

This trend can also be understood from a simple MO picture, as we discussed in Ch. 2. As the electronegativity difference Δχ increases, so does the energy difference between bonding and antibonding orbitals.

The band gap is a very important property of a semiconductor because it determines its color and conductivity. Many of the applications of semiconductors are related to band gaps:

- Narrow gap materials ($Hg_xCd_{1-x}Te$, VO_2, InSb, Bi_2Te_3) are used as infrared photodetectors and thermoelectrics (which convert heat to electricity).
- Wider gap materials (Si, GaAs, GaP, GaN, CdTe, $CuIn_xGa_{1-x}Se_2$) are used in electronics, light-emitting diodes, and solar cells.



Color wheel showing the colors and wavelengths of emitted light.

Semiconductor solid solutions such as $GaAs_{1-x}P_x$ have band gaps that are intermediate between the end member compounds, in this case GaAs and GaP (both zincblende structure). Often, there is a linear relation between composition and band gap, which is referred to as **Vegard's Law**. This "law" is often violated in real materials, but nevertheless offers useful guidance for designing materials with specific band gaps. For example, red and orange light-emitting diodes (LED's) are made from solid solutions with compositions of $GaP_{0.40}As_{0.60}$ and $GaP_{0.65}As_{0.35}$, respectively. Increasing the mole fraction of the lighter element (P) results in a larger band gap, and thus a higher energy of emitted photons.

Colors of semiconductors

The color of absorbed and emitted light both depend on the band gap of the semiconductor. Visible light covers the range of approximately 390-700 nm, or 1.8-3.1 eV. The **color of emitted light** from an LED or semiconductor laser corresponds to the band gap energy and can be read off the color wheel shown at the right.



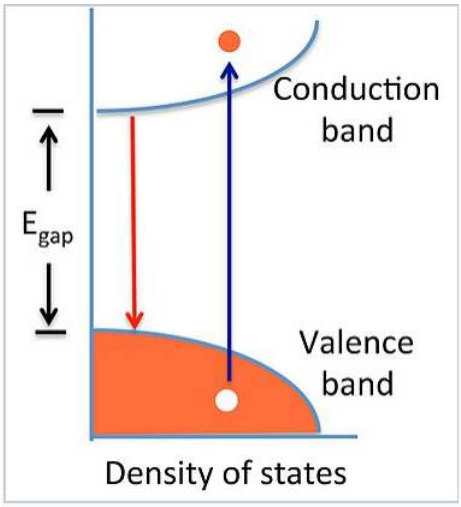
Fe_2O_3 powder is reddish orange because of its 2.2 eV band gap

The color of **absorbed light** includes the band gap energy, but also all colors of higher energy (shorter wavelength), because electrons can be excited from the valence band to a range of energies in the conduction band. Thus semiconductors with band gaps in the infrared (e.g., Si, 1.1 eV and GaAs, 1.4 eV) appear black because they absorb all colors of visible light. Wide band gap semiconductors such as TiO_2 (3.0 eV) are white because they absorb only in the UV. Fe_2O_3 has a band gap of 2.2 eV and thus absorbs light with $\lambda < 560$ nm. It thus appears reddish-orange (the colors of light reflected from Fe_2O_3) because it absorbs green, blue, and violet light. Similarly, CdS (E_{gap} = 2.6 eV) is yellow because it absorbs blue and violet light.

Electrons and holes in semiconductors

Pure (undoped) semiconductors can conduct electricity when electrons are promoted, either by heat or light, from the valence band to the conduction band. The promotion of an **electron** (e^-) leaves behind a **hole** (h^+) in the valence band. The hole, which is the absence of an electron in a bonding orbital, is also a mobile charge carrier, but with a positive charge. The motion of holes in the lattice can be pictured as analogous to the movement of an empty seat in a crowded theater. An empty seat in the middle of a row can move to the end of the row (to accommodate a person arriving late to the movie) if everyone moves over by one seat. Because the movement of the hole is in the opposite direction of electron movement, it acts as a positive charge carrier in an electric field.

The opposite process of excitation, which creates an electron-hole pair, is their recombination. When a conduction band electron drops down to recombine with a valence band hole, both are annihilated and energy is released. This release of energy is responsible for the emission of light in LEDs.



An electron-hole pair is created by adding heat or light energy E ≥ E_{gap} to a semiconductor (blue arrow). The electron-hole pair recombines to release energy equal to E_{gap} (red arrow).

At equilibrium, the creation and annihilation of electron-hole pairs proceed at equal rates. This dynamic equilibrium is analogous to the dissociation-association equilibrium of H^+ and OH^- ions in water. We can write a mass action expression:

$$n \times p = K_{eq} = n_i^2$$

where n and p represent the number density of electrons and holes, respectively, in units of cm^{-3}. The intrinsic carrier concentration, n_i, is equal to the number density of electrons or holes in an undoped semiconductor, where $n = p = n_i$.

Note the similarity to the equation for water autodissociation:

$$[H^+][OH^-] = K_w$$

By analogy, we will see that when we increase n (e.g., by doping), p will decrease, and vice-versa, but their product will remain constant at a given temperature.

Temperature dependence of the carrier concentration. Using the equations $K_{eq} = e^{(\frac{-\Delta G^o}{RT})}$ and $\Delta G^o = \Delta H^o - T\Delta S^o$, we can write:

$$n \times p = n_i^2 = e^{(\frac{\Delta S^o}{R})} e^{(\frac{-\Delta H^o}{RT})} \tag{11.5.1}$$

The entropy change for creating electron hole pairs is given by:

$$\Delta S^o = Rln(N_V) + Rln(N_V) = Rln(N_C N_V) \tag{11.5.2}$$

where N_V and N_C are the effective density of states in the valence and conduction bands, respectively.

and thus we obtain

$$n_i^2 = N_C N_V e^{(-\Delta H^o RT)} \tag{11.5.3}$$

Since the volume change is negligible, $\Delta H^o \approx \Delta E^o$, and therefore $\frac{\Delta H^o}{R} \approx \frac{E_{gap}}{k}$, from which we obtain

$$n_i^2 = N_C N_V e^{(\frac{-E_{gap}}{kT})} \tag{11.5.4}$$

and finally

$$\mathbf{n = p = n_i = (N_C N_V)^{\frac{1}{2}} e^{(\frac{-E_{gap}}{2kT})}} \tag{11.5.5}$$

For pure Si (E_{gap} = 1.1 eV) with N ≈ 10^{22}/cm^3, we can calculate from this equation a carrier density n_i of approximately 10^{10}/cm^3 at 300 K. This is about 12 orders of magnitude lower than the valence electron density of Al, the element just to the left of Si in the periodic table. Thus we expect the conductivity of pure semiconductors to be many orders of magnitude lower than those of metals.

Conductivity of intrinsic semiconductors

The conductivity (σ) is the product of the number density of carriers (n or p), their charge (e), and their mobility (μ). Recall from Chapter 6 that μ is the ratio of the carrier drift velocity to the electric field and has units of cm^2/Volt-second. Typically electrons and holes have somewhat different mobilities (μ_e and μ_h, respectively) so the conductivity is given by:

$$\sigma = ne\mu_e + pe\mu_h \tag{11.5.6}$$

For either type of charge carrier, we recall from Ch. 6 that the mobility μ is given by:

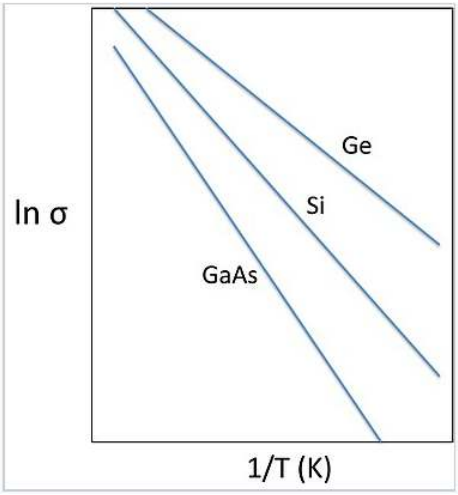
$$\mu = \frac{v_{drift}}{E} = \frac{e\tau}{m} \tag{11.5.7}$$

where e is the fundamental unit of charge, τ is the scattering time, and m is the effective mass of the charge carrier.

Taking an average of the electron and hole mobilities, and using n = p, we obtain

$$\sigma = \sigma_o e^{\left(\frac{-E_{gap}}{2kT}\right)},\ where\ \sigma_o = 2(N_C N_V)^{\frac{1}{2}} e\mu \tag{11.5.8}$$

By measuring the conductivity as a function of temperature, it is possible to obtain the activation energy for conduction, which is $E_{gap}/2$. This kind of plot, which resembles an Arrhenius plot, is shown at the right for three different undoped semiconductors. The slope of the line in each case is $-E_{gap}/2k$.



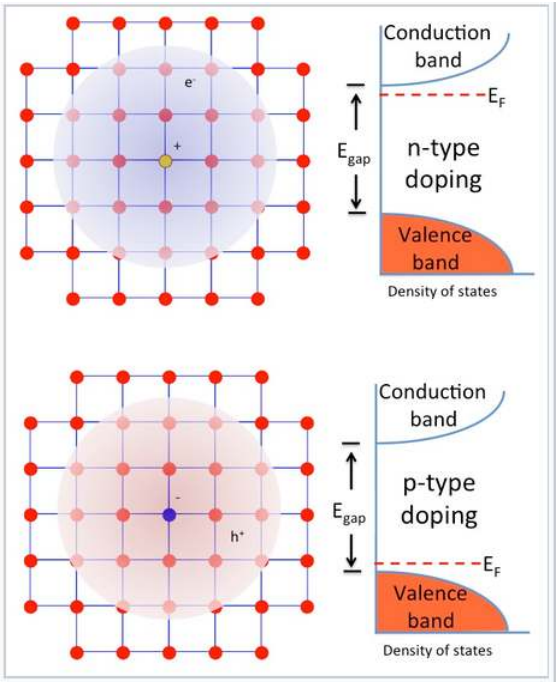
Plots of ln(σ) vs. inverse temperature for intrinsic semiconductors Ge (E_{gap} = 0.7 eV), Si (1.1 eV) and GaAs (1.4 eV). The slope of the line is $-E_{gap}/2k$.

Doping of semiconductors. Almost all applications of semiconductors involve controlled **doping**, which is the substitution of impurity atoms, into the lattice. Very small amounts of dopants (in the parts-per-million range) dramatically affect the conductivity of semiconductors. For this reason, very pure semiconductor materials that are carefully doped - both in terms of the concentration and spatial distribution of impurity atoms - are needed.

n- and p-type doping. In crystalline Si, each atom has four valence electrons and makes four bonds to its neighbors. This is exactly the right number of electrons to completely fill the valence band of the semiconductor. Introducing a phosphorus atom into the lattice (the positively charged atom in the figure at the right) adds an extra electron, because P has five valence electrons and only needs four to make bonds to its neighbors. The extra electron, at low temperature, is bound to the phosphorus atom in a hydrogen-like molecular orbital that is much larger than the 3s orbital of an isolated P atom because of the high dielectric constant of the semiconductor. In silicon, this "expanded" Bohr radius is about 42 Å, i.e., 80 times larger than in the hydrogen atom. The energy needed to ionize this electron – to allow it to move freely in the lattice - is only about 40–50 meV, which is not much larger

the thermal energy (26 meV) at room temperature. Therefore the Fermi level lies just below the conduction band edge, and a large fraction of these extra electrons are promoted to the conduction band at room temperature, leaving behind fixed positive charges on the P atom sites. The crystal is **n-doped**, meaning that the majority carrier (electron) is negatively charged.

Alternatively, boron can be substituted for silicon in the lattice, resulting in **p-type** doping, in which the majority carrier (hole) is positively charged. Boron has only three valence electrons, and "borrows" one from the Si lattice, creating a positively charged hole that exists in a large hydrogen-like orbital around the B atom. This hole can become delocalized by promoting an electron from the valence band to fill the localized hole state. Again, this process requires only 40–50 meV, and so at room temperature a large fraction of the holes introduced by boron doping exist in delocalized valence band states. The Fermi level (the electron energy level that has a 50% probability of occupancy at zero temperature) lies just above the valence band edge in a p-type semiconductor.



n- and p-type doping of semiconductors involves substitution of electron donor atoms (light orange) or acceptor atoms (blue) into the lattice. These substitutions introduce extra electrons or holes, respectively, which are easily ionized by thermal energy to become free carriers. The Fermi level of a doped semiconductor is a few tens of mV below the conduction band (n-type) or above the valence band (p-type).

As noted above, the doping of semiconductors dramatically changes their conductivity. For example, the intrinsic carrier concentration in Si at 300 K is about 10^{10} cm^{-3}. The mass action equilibrium for electrons and holes also applies to doped semiconductors, so we can write:

$$n \times p = n_i^2 = 10^{20} cm^{-6} \; at \; 300K \tag{11.5.9}$$

If we substitute P for Si at the level of one part-per-million, the concentration of electrons is about 10^{16} cm^{-3}, since there are approximately 10^{22} Si atoms/cm^3 in the crystal. According to the mass action equation, if n = 10^{16}, then p = 10^4 cm^{-3}. There are three consequences of this calculation:

- The density of carriers in the doped semiconductor (10^{16} cm^{-3}) is much higher than in the undoped material (~10^{10} cm^{-3}), so the conductivity is also many orders of magnitude higher.
- The activation energy for conduction is only 40–50 meV, so the conductivity does not change much with temperature (unlike in the intrinsic semiconductor)
- The minority carriers (in this case holes) do not contribute to the conductivity, because their concentration is so much lower than that of the majority carrier (electrons).

Similarly, for p-type materials, the conductivity is dominated by holes, and is also much higher than that of the intrinsic semiconductor.

Chemistry of semiconductor doping. Sometimes it is not immediately obvious what kind of doping (n- or p-type) is induced by "messing up" a semiconductor crystal lattice. In addition to substitution of impurity atoms on normal lattice sites (the examples given above for Si), it is also possible to dope with vacancies - missing atoms - and with interstitials - extra atoms on sites that are not ordinarily occupied. Some simple rules are as follows:

- For substitutions, adding an **atom to the right** in the periodic table results in **n-type** doping, and an atom to the **left** in **p-type** doping.

  For example, when TiO_2 is doped with Nb on some of the Ti sites, or with F on O sites, the result is n-type doping. In both cases, the impurity atom has one more valence electron than the atom for which it was substituted. Similarly, substituting a small amount of Zn for Ga in GaAs, or a small amount of Li for Ni in NiO, results in p-type doping.

- **Anion vacancies** result in **n-type** doping, and **cation vacancies** in **p-type** doping.

  Examples are anion vacancies in CdS_{1-x} and WO_{3-x}, both of which give n-type semiconductors, and copper vacancies in $Cu_{1-x}O$, which gives a p-type semiconductor.

- **Interstitial cations** (e.g. Li) donate electrons to the lattice resulting in **n-type** doping. Interstitial anions are rather rare but would result in p-type doping.

Sometimes, there can be both p- and n-type dopants in the same crystal, for example B and P impurities in a Si lattice, or cation and anion vacancies in a metal oxide lattice. In this case, the two kinds of doping **compensate** each other, and the doping type is determined by the one that is in higher concentration. A dopant can also be present on more than one site. For example, Si can occupy both the Ga and As sites in GaAs, and the two substitutions compensate each other. Si has a slight preference for the Ga site, however, resulting in n-type doping.

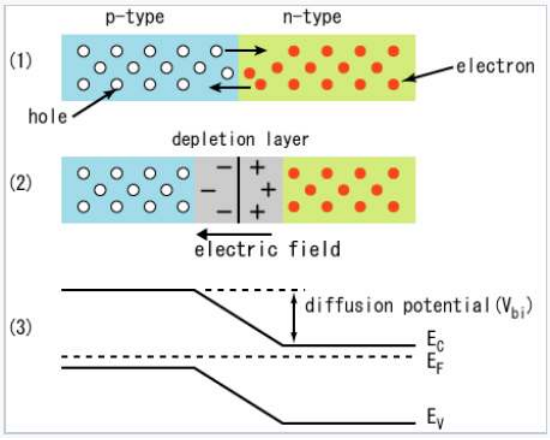
11.5: Semiconductors- Band Gaps, Colors, Conductivity and Doping is shared under a CC BY-SA license and was authored, remixed, and/or curated by LibreTexts.

- **10.5: Semiconductors- Band Gaps, Colors, Conductivity and Doping** by Chemistry 310 is licensed CC BY-SA 4.0. Original source: https://en.wikibooks.org/wiki/Introduction_to_Inorganic_Chemistry.

11.6: Semiconductor p-n Junctions

Semiconductor p-n junctions are important in many kinds of electronic devices, including diodes, transistors, light-emitting diodes, and photovoltaic cells. To understand the operation of these devices, we first need to look at what happens to electrons and holes when we bring p-type and n-type semiconductors together. At the junction between the two materials, mobile electrons and holes annihilate each other, leaving behind the fixed + and - charges of the electron donor and electron acceptor dopants, respectively. For example, on the n-side of a silicon p-n junction, the positively charged dopants are P^+ ions and on the p-side the negatively charged dopants are B^-. The presence of these uncompensated electrical charges creates an electric field, the **built-in field** of the p-n junction. The region that contains these charges (and a very low density of mobile electrons or holes) is called the **depletion region**.

The electric field, which is created in the depletion region by electron-hole recombination, repels both the electrons (on the n-side) and holes (on the p-side) away from the junction. The concentration gradient of electrons and holes, however, tends to move them in the opposite direction by diffusion. At equilibrium, the flux of mobile carriers is zero because the field-driven migration flux is equal and opposite to the concentration-driven diffusion flux.



When p-type and n-type semiconductors are joined, electrons and holes are annihilated at the interface, leaving a depletion region that contains positively and negatively charged donor and acceptor atoms, respectively. At equilibrium, the Fermi level (E_F) is uniform throughout the junction. E_F lies just above the valence band on the p-type side of the junction and just below the conduction band on the n-type side.

The width of the depletion layer depends on the screening length in the semiconductor, which in turn depends on the dopant density. At high doping levels, the depletion layer is narrow (tens of nanometers across), whereas at low doping density it can be as thick as 1 μm. The depletion region is the only place where the electric field is nonzero, and the only place where the bands bend. Elsewhere in the semiconductor the field is zero and the bands are flat.

In the middle of p-n junction, the Fermi level energy, E_F, is halfway between the valence band, VB, and the conduction band, CB, and the semiconductor is intrinsic ($n = p = n_i$)

11.6: Semiconductor p-n Junctions is shared under a CC BY-SA license and was authored, remixed, and/or curated by LibreTexts.

- **10.6: Semiconductor p-n Junctions** by Chemistry 310 is licensed CC BY-SA 4.0. Original source: https://en.wikibooks.org/wiki/Introduction_to_Inorganic_Chemistry.

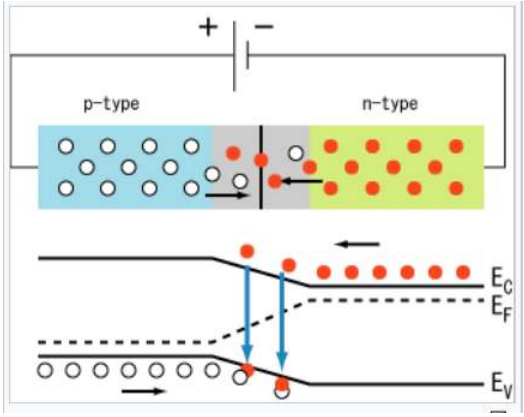
11.7: Diodes, LEDs and Solar Cells

Diodes are semiconductor devices that allow current to flow in only one direction. Diodes act as rectifiers in electronic circuits, and also as efficient light emitters (in LEDs) and solar cells (in photovoltaics). The basic structure of a diode is a junction between a p-type and an n-type semiconductor, called a p-n junction. Typically, diodes are made from a single semiconductor crystal into which p- and n- dopants are introduced.



Closeup of a diode, showing the square-shaped semiconductor crystal *(black object on left)* (John Maushammer, Wikipedia, CC-BY-SA)

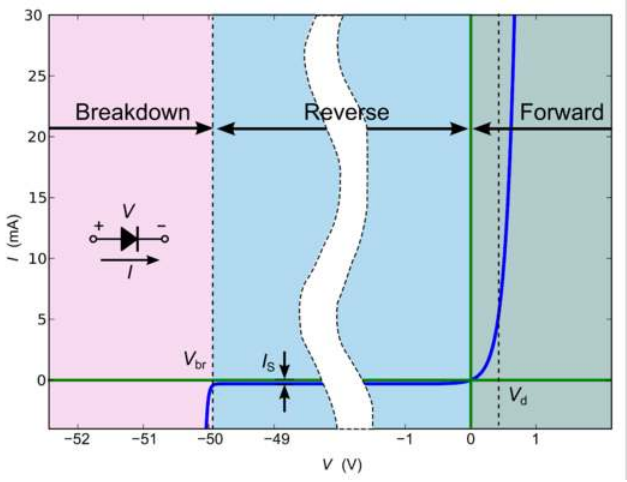
If the n-side of a diode is biased at positive potential and the p-side is biased negative, electrons are drawn to the n-side and holes to the p-side. This reinforces the built in potential of the p-n junction, the width of the depletion layer increases, and very little current flows. This polarization direction is referred to as "back bias." If the diode is biased the other way, carriers are driven into the junction where they recombine. The electric field is diminished, the bands are flattened, and current flows easily since the applied bias lowers the built-in potential. This is called "forward bias."



Electrons (red) and holes (white) in a forward-biased diode. (S-kei. Wikipedia, CC-BY-SA)

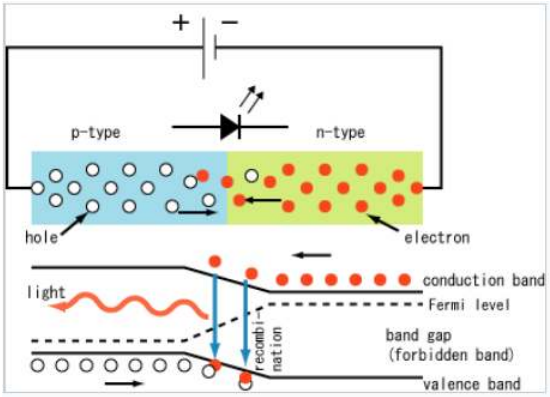
The figure on the left illustrates a forward-biased diode, through which current flows easily. As electrons and holes are driven into the junction (black arrows in lower left figure), they recombine (downward blue arrows), producing light and/or heat. The Fermi level in the diode is indicated as the dotted line. There is a drop in the Fermi level (equal to the applied bias) across the depletion layer. The corresponding diode i-V curve is shown on the right. The current rises exponentially with applied voltage in the forward

bias direction, and there is very little leakage current under reverse bias. At very high reverse bias (typically tens of volts) diodes undergo avalanche breakdown and a large reverse current flows.



Diode i-V curve

A **light-emitting diode** or **LED** is a kind of diode that converts some of the energy of electron-hole recombination into light. This radiative recombination process always occurs in competition with non-radiative recombination, in which the energy is simply converted to heat. When light is emitted from an LED, the photon energy is equal to the bandgap energy. Because of this, LED lights have pure colors and narrow emission spectra relative to other light sources, such as incandescent and fluorescent lights. LED lights are energy-efficient and thus are typically cool to the touch.



Light-emitting diode (LED). (S-kei. Wikipedia, CC-BY-SA)

Direct-gap semiconductors such as GaAs and GaP have efficient luminescence and are also good light absorbers. In direct gap semiconductors, there is no momentum change involved in electron-hole creation or recombination. That is, the electrons and holes originate at the same value of the momentum wavevector **k**, which we encountered in Ch. 6. **k** is related to the momentum (also a vector quantity) by **p** = h**k**/2π. In a direct-gap semiconductor, the top of the valence band and the bottom of the conduction band most typically both occur at **k** = 0. Since the momentum of the photon is close to zero, photon absorption and emission are strongly allowed (and thus kinetically fast). Polar semiconductors such as GaAs, GaN, and CdSe are typically direct-gap materials. **Indirect-gap** semiconductors such as Si and Ge absorb and emit light very weakly because the valence band maximum and conduction band minimum do not occur at the same point in k-space. This means that a lattice vibration (a phonon) must also be created or annihilated in order to conserve momentum. Since this "three body" (electron, hole, phonon) process has low probability, the radiative recombination of electrons and holes is slow relative to non-radiative decay - the thermalization of electron-hole

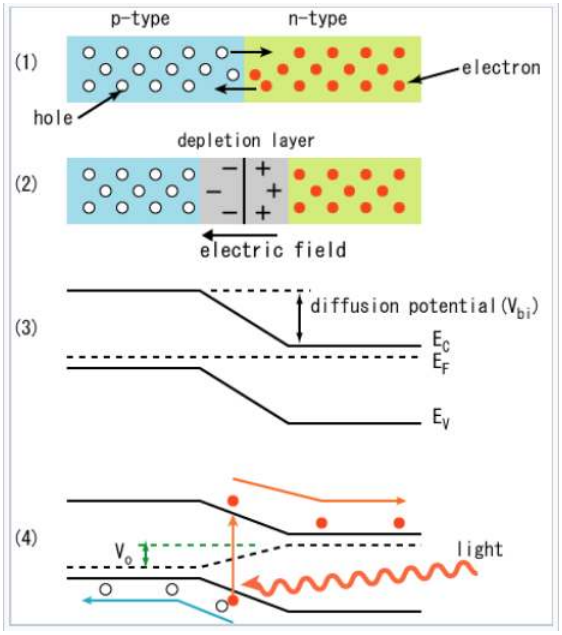
energy as lattice vibrations - in indirect-gap semiconductors. The momentum selection rule thus prevents light absorption/emission and there are no pure Si LEDs or Si-based lasers.



Prof. Shuji Nakamura holding a blue LED.

While red, orange, yellow, and green LEDs can be fabricated relatively easily from AlP-GaAs solid solutions, it was initially very difficult to fabricate blue LEDs because the best direct gap semiconductor with a bandgap in the right energy range is a nitride, GaN, which is difficult to make and to dope p-type. Working at Nichia Corporation in Japan, Shuji Nakamura succeeded in developing a manufacturable process for p-GaN, which is the basis of the blue LED. Because of the importance of this work in the development of information storage (Blu-Ray technology) and full-spectrum, energy-efficient LED lighting, Nakamura shared the 2014 Nobel Prize in Physics with Isamu Asaki and Hiroshi Amano, both of whom had made earlier contributions to the development of GaN diodes.

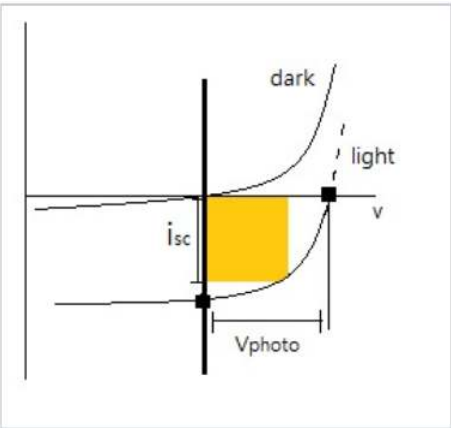
A **Solar cell**, or photovoltaic cell, converts light absorbed in a p-n junction directly to electricity by the photovoltaic effect. Photovoltaics is the field of technology and research related to the development of solar cells for conversion of solar energy to electricity. Sometimes the term solar cell is reserved for devices intended specifically to capture energy from sunlight, whereas the term photovoltaic cell is used when the light source is unspecified.



Photovoltaic effect in a semiconductor p-n junction. (S-kei. Wikipedia, CC-BY-SA)

Photocurrent in p-n junction solar cells flows in the diode reverse bias direction. In the dark, the solar cell simply acts as a diode. In the light, the photocurrent can be thought of as a constant current source, which is added to the i-V characteristic of the diode. The

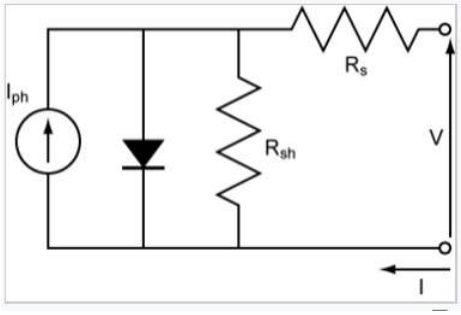
relationship between the dark and light current in a photovoltaic cell is shown in the diagram at the left.



Current-voltage characteristic of a solar cell in the dark and under illumination with band gap light. The short-circuit photocurrent is indicated as i_{sc}, and the open-circuit photovoltage is V_{photo}. The maximum power generated by the solar cell is determined by the area of the orange box.

The built-in electric field of the p-n junction separates e^- h^+ pairs that are formed by absorption of bandgap light in the depletion region. The electrons flow downhill, towards the n-type side of the junction, the holes flow uphill towards the p-side. If $h\nu \geq E_{gap}$, light can be absorbed by promoting an electron from the valence band to the conduction band. Any excess energy is rapidly thermalized. Light with $h\nu > E_g$ thus can store only E_g worth of energy in an e^- h^+ pair. If light is absorbed outside of depletion region, i.e., on the n- or p-side of the junction where there is no electric field, minority carriers must diffuse into the junction in order to be collected. This process occurs in competition with electron-hole recombination. Because impurity atoms and lattice defects make efficient recombination centers, semiconductors used in solar cells (especially indirect-gap materials such as Si, which must be relatively thick in order to absorb most of the solar spectrum) must be very pure. Most of the cost of silicon solar cells is associated with the process of purifying elemental silicon and growing large single crystals from the melt.

In the photodiode i-V curve above, V_{photo} is typically only about 70% of the bandgap energy E_{gap}. The photocurrent is limited by the photon flux, the recombination rate, and the re-emission of absorbed light.[6] The area of the orange rectangle indicates the power generated by the solar cell, which can be calculated as P = i x V. In good single crystal or polycrystalline solar cells made of Si, GaAs, CdTe, $CuIn_xGa_{1-x}Se_2$, or $(CH_3NH_3)PbI_3$ the quantum yield (the ratio of short circuit photocurrent to photon flux) is close to unity.

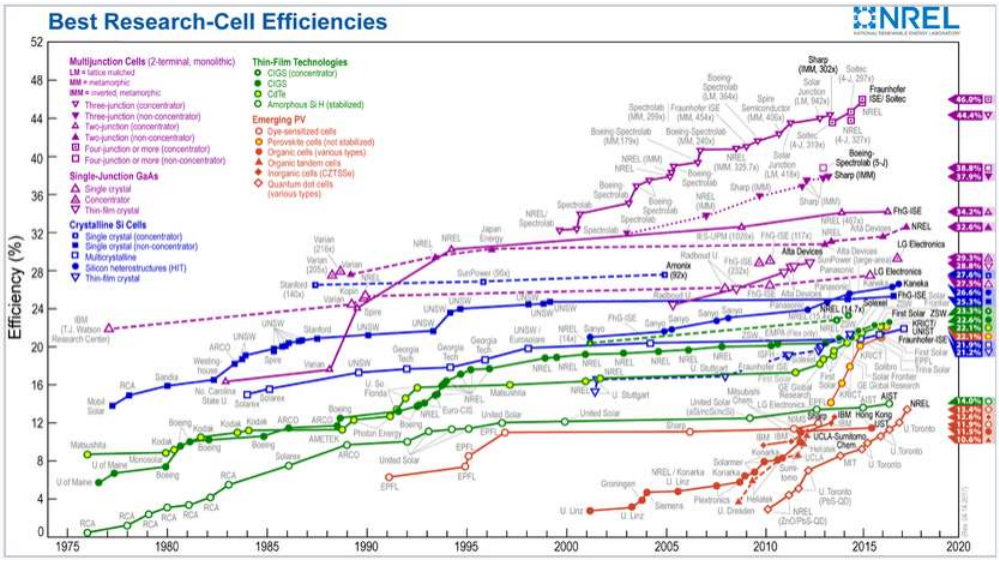


The equivalent circuit of a p-n junction solar cell, which results in the "light" i-V curve shown in the figure above. The solar cell is effectively a diode with a reverse-bias current source provided by light-generated electrons and holes. The shunt resistance (R_{sh}) in the equivalent circuit represents parasitic electron-hole recombination. A high shunt resistance (low recombination rate) and low series resistance (R_s) are needed for high solar cell efficiency.

Solar cells have many current applications. Individual cells are used for powering small devices such as electronic calculators. Photovoltaic arrays generate a form of renewable electricity, particularly useful in situations where electrical power from the grid is

unavailable such as in remote area power systems, Earth-orbiting satellites and space probes, remote radio-telephones and water pumping applications. Photovoltaic electricity is also increasingly deployed in grid-tied electrical systems.

The cost of installed photovoltaics (calculated on a per-watt basis) has dropped over the past decade at a rate of about 13% per year, and has already reached grid parity in Germany and a number of other countries.[7] Photovoltaic grid parity is anticipated in U.S. power markets in the 2020 timeframe.[8] A major driver in the progressively lower cost of photovoltaic power is the steadily increasing efficiency of solar cells, which is shown in the graphic at the right. Higher efficiency solar cells require less area to deliver the same amount of power, and this lowers the "balance of system" costs such as wiring, roof mounting, etc., which scale as the area of the solar panels. Progress towards higher efficiency reflects improved processes for making photovoltaic materials such as silicon and gallium arsenide, as well as the discovery of new materials. Silicon solar cells are a mature technology, so they are now in the flat part of the learning curve and are approaching their maximum theoretical efficiencies. Newer technologies such as organic photovoltaics, quantum dot solar cells, and lead halide perovskite cells are still in the rising part of the learning curve.

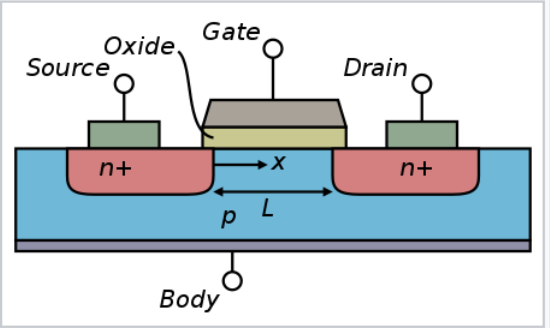


Reported timeline of solar cell energy conversion efficiencies since 1976 (National Renewable Energy Laboratory)

A **field effect transistor (FET)** is a transistor that uses an electric field to control the width of a conducting channel and thus the current in a semiconductor material. It is classified as unipolar transistor, in contrast to bipolar transistors.

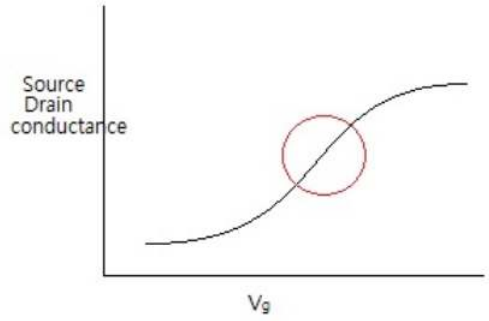
Field effect transistors function as current amplifiers. The typical structure of Si-based FETs is one in which two n-type regions (the source and the drain) are separated by a p-type region. An oxide insulator over the p-type region separates a metal gate lead from the semiconductor. This structure is called a metal-oxide-semiconductor FET (or MOSFET). When voltage is applied between source and drain, current cannot flow because either the n-p or the p-n junction is back-biased. When a positive potential is applied to the gate, however, electrons are driven towards the gate, and locally the semiconductor is "inverted" to n-type. Then the current flows easily between the n-type source and drain through the n-channel. The current flow between the source and drain is many

times larger than the current through the gate, and thus the FET can act as an amplifier. Current flow can also represent a logical "1," so FETs are also used in digital logic.



Cross section of an n-type MOSFET

In electronic devices such as microprocessors, field-effect transistors are kept in the off-state most of the time in order to minimize background current and power consumption. The FET shown above, which has n-type source and drain regions, is called an NMOS transistor. In a PMOS transistor, the source and drain regions are p-type and the gate is n-type. In **CMOS** (complementary metal-oxide semiconductor) integrated circuits, both NMOS and PMOS transistors are used. CMOS circuits are constructed in such a way that all PMOS transistors must have either an input from the voltage source or from another PMOS transistor. Similarly, all NMOS transistors must have either an input from ground or from another NMOS transistor. This arrangement results in low static power consumption.



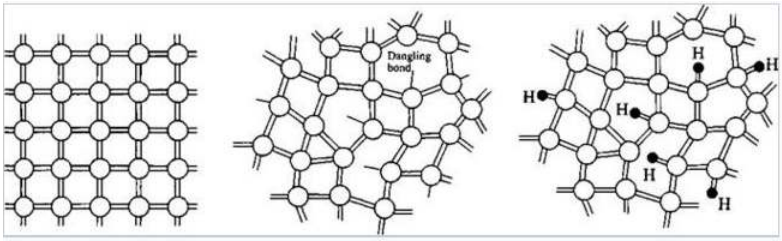
Transistors are most useful in the range of gate voltage (indicated by the red circle in the figure at the left) where the source-drain current changes rapidly. In this region it is possible to effect a large change in current between source and drain when a small signal is applied to the gate. An important figure of merit for FETs is the **subthreshold slope**, which is the slope a plot of log(current) vs. V_{gate}. An ideal subthreshold slope is one decade of current per 60 mV of gate bias. Typically, a decade change in source-drain current can be achieved with a change in gate voltage of ~70 mV. The performance of FETs as switches and amplifiers is limited by the subthreshold slope, which in turn is limited by the capacitance of the gate. It is desirable to have a very high gate capacitance, which requires a thin insulating oxide, but also to have a small leakage current, which requires a thick oxide. A current challenge in the semiconductor industry is to continue to scale FETs to even smaller nanoscale dimensions while maintaining acceptable values of these parameters. This is being done by developing new gate insulator materials that have higher dielectric constants than silicon oxide and do not undergo redox reactions with silicon or with metal gate leads. Only a few known materials (such as hafnium oxynitride and hafnium silicates) currently meet these stringent requirements.

11.7: Diodes, LEDs and Solar Cells is shared under a CC BY-SA license and was authored, remixed, and/or curated by LibreTexts.

- **10.7: Diodes, LEDs and Solar Cells** by Chemistry 310 is licensed CC BY-SA 4.0. Original source: https://en.wikibooks.org/wiki/Introduction_to_Inorganic_Chemistry.

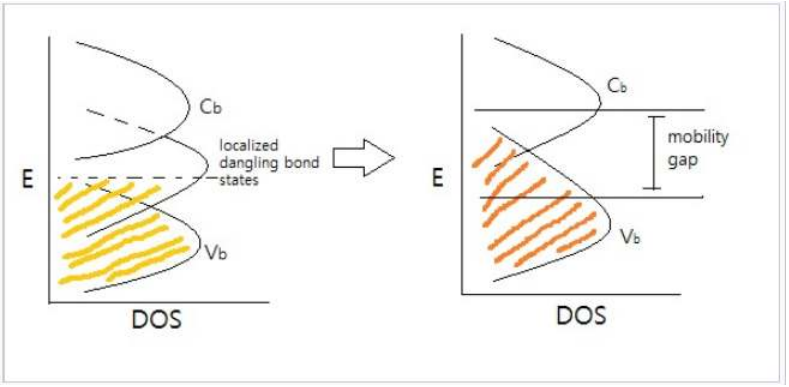
11.8: Amorphous Semiconductors

Amorphous semiconductors are disordered or glassy forms of crystalline semiconductor materials. Like non-conducting glasses, they are network structures with primarily covalent bonding. Crystalline silicon, which has the diamond structure, is an ordered arrangement of fused six-membered silicon rings, all in the "chair" conformation, as we saw in Ch. 8. The local bonding environment of the silicon atoms is tetrahedral. The silicon atoms in amorphous silicon (a-Si) are also predominantly tetrahedrally coordinated, but there is no long-range order in the structure. In addition to six-membered rings, there are five- and seven-membered rings, as well as some "dangling bond" sites in which Si atoms have only three nearest neighbors.



Schematic illustration of the structures of crystalline silicon (left), amorphous silicon (middle), and amorphous hydrogenated silicon (right)

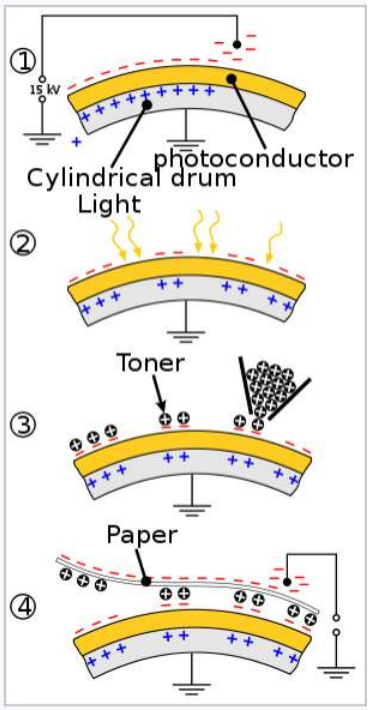
Two of the most widely studied amorphous semiconductors are a-Si and amorphous selenium, a-Se. Si and Se can both be made in glassy form, usually by sputtering or evaporation at relatively low temperature. In a-Se, as in a-Si, locally, most of the atoms have their "normal" valence, but there are many defects and irregularities in the structure. Dangling bonds in amorphous semiconductors have orbital energies in the middle of gap, and electrons in these states are effectively non-bonding. Because these dangling bond sites are far apart from each other, there is little orbital overlap between them, and they also exist over a range of energies. Electrons in these mid-gap states are therefore **localized**, a phenomenon known as Anderson localizaton. Amorphous Si is insulating because electrons the Fermi level (in the middle of the gap) are not mobile in the lattice. These localized states create a mobility gap, and only electrons in states that are strongly bonding or antibonding are delocalized. Therefore, unmodified a-Si is not very useful as a semiconductor. However, by hydrogenating the material as it is formed (typically in a plasma of H atoms), the under-coordinated Si atoms are bonded to hydrogen atoms. This generates filled bonding and empty antibonding orbitals, the energies of which are outside the mobility gap. Hydrogenation thus lowers the density of states in the mobility gap. Hydrogenated amorphous silicon (a-Si:H) is insulating in the dark, but is a good photoconductor because light absorption creates electrons and holes in mobile states that are outside the mobility gap.



Energy vs. DOS for an amorphous semiconductor. Disorder and dangling bonds result in localized mid-gap states.

The photoconductivity of **amorphous Se** is exploited in xerography. A conductive drum coated with a-Se, which is insulating, is charged with static electricity by corona discharge from a wire. When the drum is exposed to a pattern of light and dark (the image to be duplicated), the illuminated a-Se areas become conductive and the static charge is dissipated from those parts of the drum. Carbon-containing toner particles then adhere via static charge to the areas that were not exposed to light, and are transferred and

bonded to paper to make the copy. The speed of the process and the high resolution of pattern transfer depend on the very low conductivity of a-Se in the dark and its high conductivity under illumination.



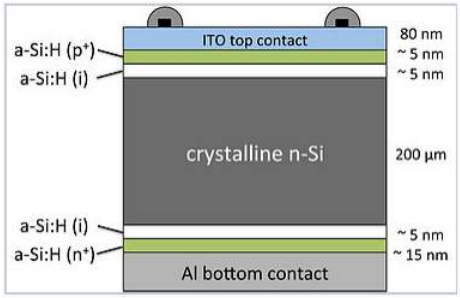
Charging of amorphous Se and pattern transfer in the xerographic cycle.

Amorphous hydrogenated Si is used in inexpensive thin film solar cells. The mobility gap is about 1.7 eV, which is larger than the bandgap crystalline of Si (1.1 eV). a-Si:H is a direct-gap material, and therefore thin films are good light absorbers. a-Si:H solar cells can be vapor-deposited in large-area sheets. p^+Si-a-Si:H-n^+Si cells have around 10% power conversion efficiency. However amorphous Si solar cells gradually lose efficiency as they are exposed to light. The mechanism of this efficiency loss, called the Staebler-Wronski effect,[9], involves photogenerated electron-hole pairs which have sufficient energy to cause chemical changes in the material. While the exact mechanism is still unclear, it has been proposed that the energy of electron-hole recombination breaks a weak Si-Si bond, and that one of the resulting dangling bonds abstracts a H atom, leaving a passivated Si-H center and a permanent dangling bond. The effect is minimized by hydrogenating a-Si and can be partially reversed by annealing.



A calculator that runs on solar and battery power

Thin layers of amorphous silicon are used in conjunction with crystalline silicon in heterojunction intrinsic thin-layer (HIT) solar cells.[10] Because the mobility gap of a-Si is wider than the bandgap of c-Si, there is a potential energy barrier at the amorphous-crystalline interface that reflects electrons and holes away from that interface. At the p^+ contact, only holes can tunnel through the barrier, whereas only electrons can tunnel through the barrier to the n^+ contact. The passivation of surface defects that are sites of electron-hole recombination prevents a major loss mechanism in solar cells, increasing both the photovoltage and the photocurrent relative to conventional c-Si p-n junction cells. Panasonic and Sanyo have announced the production of HIT cells with power conversion efficiencies as high as 23%.



Layered structure of a HIT solar cell. The layers are not drawn to scale. A thick crystalline n-silicon layer is the light absorber, and photogenerated holes, which are the minority carriers, are reflected away from the aluminum back contact by the thin intrinsic a-Si layer there.

11.8: Amorphous Semiconductors is shared under a CC BY-SA license and was authored, remixed, and/or curated by LibreTexts.

- **10.8: Amorphous Semiconductors** by Chemistry 310 is licensed CC BY-SA 4.0. Original source: https://en.wikibooks.org/wiki/Introduction_to_Inorganic_Chemistry.

11.9: Discussion Questions

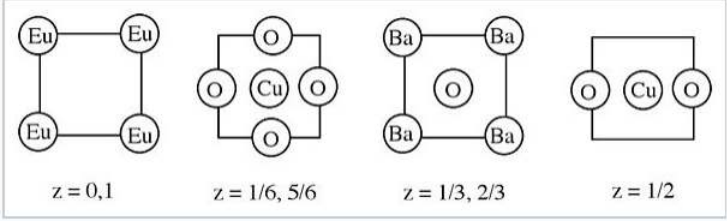
- How is magnetic ordering in the 3d transition metals (Fe, Co, Ni) and the absence of magnetism in the elements just below them (Ru, Ir, Pd) related to the metal-insulator transition?
- Why are good metals bad superconductors and vice-versa?
- Discuss why semiconducting oxides of early transition metals such as TiO_2 and Nb_2O_5 can be doped n-type but not p-type. Conversely, semiconducting late transition metal oxides such as NiO and Cu_2O can be doped p-type but not n-type.

11.9: Discussion Questions is shared under a CC BY-SA license and was authored, remixed, and/or curated by LibreTexts.

- **10.9: Discussion Questions** by Chemistry 310 is licensed CC BY-SA 4.0. Original source: https://en.wikibooks.org/wiki/Introduction_to_Inorganic_Chemistry.

11.10: Problems

1. The structure of a high temperature superconductor containing barium, europium, copper, and oxygen is shown below. What are the coordination environments of Cu in this compound? This structure is actually closely related to perovskite, ABO_3. Explain the relationship between this structure and the ideal perovskite structure.



2. VO_2 can exist in insulating or metallic form, depending on temperature and pressure. Which form would be stabilized by increasing the temperature? Explain your answer.

3. Explain briefly how and why the bandgaps for octet p-block semiconductors vary (1) with the average principal quantum number, and (2) with the electronegativity difference between anion and cation.

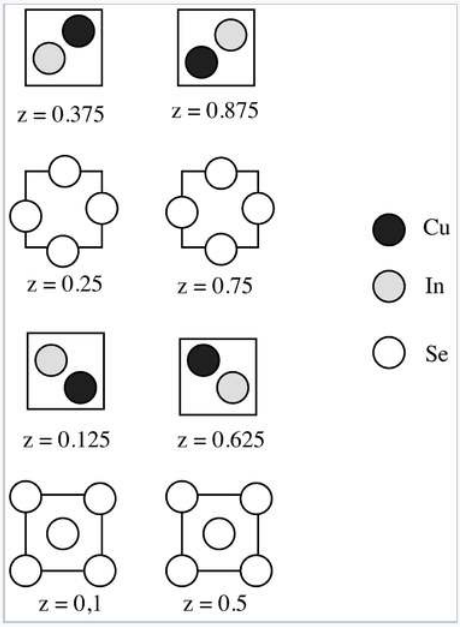
4. Indicate the type of conduction (n or p) in the following: (a) Se-doped GaAs, (b) $InAs_{1-x}$, where $x << 1$, (c) $Li_{0.05}Ni_{0.95}O$, (d) Li_xWO_3, where $x << 1$.

5. The structure of copper indium selenide, a semiconductor used in thin film solar cells, is shown below in sections.

(a) What is the stoichiometry of the compound?

(b) What kind of doping (n or p) will occur if a small amount of iodine is substituted for selenium?

(c) What kind of doping (n or p) will occur if a small fraction of the indium sites are occupied by copper atoms?

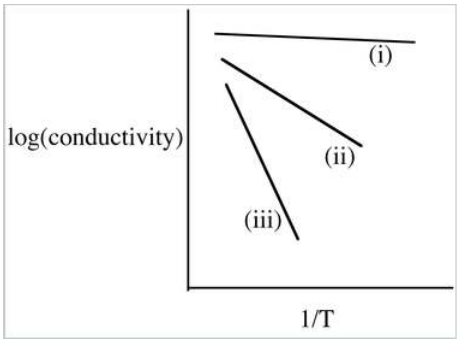


6. Using 1 eV = 1240 nm, predict the colors of anatase TiO_2 (Eg = 3.1 eV), SiC (2.0 eV), $ZnSnP_2$ (1.7 eV), $ZnGeP_2$ (1.9 eV), and InP (1.27 eV).

7. The conductivity of a certain intrinsic (undoped) semiconductor increases by a factor of two when the temperature is raised from 300 to 330 K. What is the bandgap (in eV)? R = 8.314 J/mol-K, 1 eV/atom = 96.52 kJ/mole.

8. Pure Ge is much more conductive than pure Si. Given their bandgaps (0.74 and 1.15 eV, respectively), estimate the ratio of their conductivities at room temperature.

9. The figure below illustrates the trends in conductivity vs. inverse temperature for Si, Ge, and As-doped Ge. Identify lines (i), (ii), and (iii) with the appropriate materials. Explain why the slope of line (i) is close to zero.



10. Sketch a silicon p-n junction, showing the depletion region, band bending, and the Fermi level in the absence of light or applied potential. In the dark, the p-n junction acts as a rectifier. (a) Which way do electrons and holes flow most easily in the dark? (b) Does the built in electric field increase or decrease under forward bias? (c) In the light, the junction acts as a photodiode. In this case, under short circuit conditions, do electrons flow in the same direction or in the opposite direction as in (a)? Explain.

11.10: Problems is shared under a CC BY-SA license and was authored, remixed, and/or curated by LibreTexts.

- **10.10: Problems** by Chemistry 310 is licensed CC BY-SA 4.0. Original source: https://en.wikibooks.org/wiki/Introduction_to_Inorganic_Chemistry.

11.11: References

1. Hubbard, J. (1963). "Electron Correlations in Narrow Energy Bands". *Proceedings of the Royal Society of London* **276** (1365): 238–257. doi:10.1098/rspa.1963.0204. Bibcode: 1963RSPSA.276..238H.
2. T. Mizokawa, Metal-insulator transitions: orbital control, Nature Physics 9, 612–613 (2013), doi: doi:10.1038/nphys2769
3. N. F. Mott, (1961) "The Transition to the Metallic State," Phil. Mag. 6, 287. DOI: 10.1080/14786436108243318.
4. P. P. Edwards and M. J. Sienko (1982) "The Transition to the Metallic State," Acc. Chem. Res. 15, 87-93. DOI: 10.1021/ar00075a004
5. Recent data have disproven this assertion; MacDonalds has finally responded to public opinion and is offering breakfast after 10:30 AM. But the laws of thermodynamics remain immutable and eternal
6. E. Yablonovitch, O. Miller, and S. Kurtz, "Strong Internal and External Luminescence as Solar Cells Approach the Shockley–Queisser Limit," IEEE Journal of Photovoltaics, vol. 2, no. 3, pp. 303-311, July 2012.
7. "Recent facts about photovoltaics in Germany". Fraunhofer ISE. 7 January 2015. Retrieved 17 February 2015.
8. Energy Information Administration, (November 2010). Levelized Cost of New Generation Resources in the Annual Energy Outlook 2011.
9. Staebler, D. L. and Wronski, C. R. Optically induced conductivity changes in discharge-produced hydrogenated amorphous silicon. J. Appl. Physics. 51(6), June 1980.
10. Mishima, T., Taguchi, M., Sakata, H., Maruyama, E., 2011. Development status of high efficiency HIT solar cells. Sol. Energy Mater. Sol. Cell. 95, 18–21. doi:10.1016/j.solmat.2010.04.030

11.11: References is shared under a CC BY-SA license and was authored, remixed, and/or curated by LibreTexts.

- **10.11: References** by Chemistry 310 is licensed CC BY-SA 4.0. Original source: https://en.wikibooks.org/wiki/Introduction_to_Inorganic_Chemistry.

12: Physical Techniques in Inorganic Chemistry

12: Physical Techniques in Inorganic Chemistry is shared under a not declared license and was authored, remixed, and/or curated by LibreTexts.

CHAPTER OVERVIEW

13: Coordination Chemistry IV - Electronic Spectra

13.1: Microstates and Terms

13.2: Term splitting in ligand fields, selection rules, Tanabe-Sugano diagrams. Metal to ligand, and ligand to metal transitions

13.3: Concept Review Questions Chapter 8

13.4: Homework Problems Chapter 8

This page titled 13: Coordination Chemistry IV - Electronic Spectra is shared under a not declared license and was authored, remixed, and/or curated by Kai Landskron.

13.1: Microstates and Terms

A closer look at electronic spectra

Let us take a closer look at optical absorption spectra, also called electronic spectra of coordination compounds. We have previously argued that ligand field theory can predict and explain the electronic spectra. However, only in relatively few cases ligand field theory (LFT) is sufficient to explain the spectra. For example the hexaaqua nickel (2+) complex ion is an octahedral d^8-complex ion. According to ligand field theory the metal d-orbitals in an octahedral field are the t_{2g} and the e_g–orbitals (Fig. 8.1.1). Six electrons are in the t_{2g} orbitals, and two electrons are in the e_g orbitals. Ligand field theory would predict that there is one electron transition possible, namely the promotion of an electron from a t_{2g} into an e_g orbital. This process would be triggered by the absorption of light whereby the wavelength of the light would depend on the Δ_o between the t_{2g} and the e_g orbitals. Overall, this should lead to a single absorption band in the absorption spectrum of the complex. We can check this prediction by experimentally recording the absorption spectrum of the complex (Fig. 8.1.1).

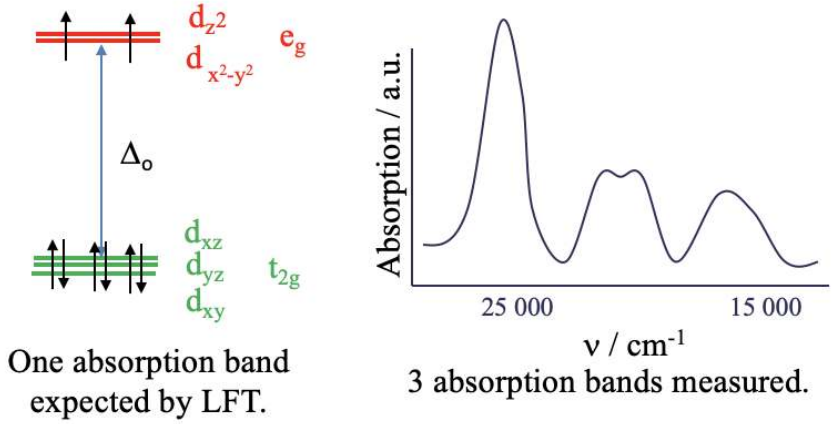


Figure 8.1.1 Electron transition according to LFT and actual absorption spectrum of the hexaaqua nickel (2+) complex ion. Attribution: E.R. Schofield.

What we find is that the absorption spectrum is far more complex than expected. Instead of just a single absorption band there are multiple ones. Obviously, ligand field theory is unable to explain this spectrum. The question is why? The answer is: LFT assumes that there are no electron-electron interactions. However, in reality there is repulsion between electron in d-orbitals and this has an effect on their energy.

Effect of Electron-Electron Interactions

Let us look closer at this. To simplify the problem let us consider a d^2 ion in an octahedral ligand field first (Fig. 8.1.2).

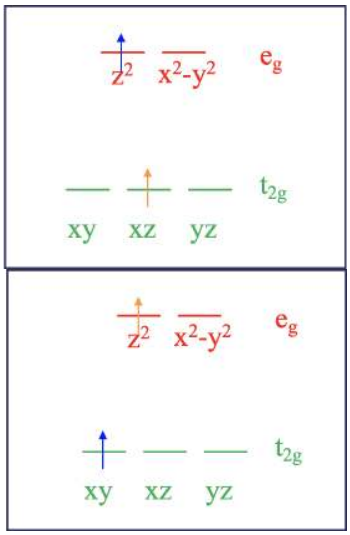


Figure 8.1.2 Two microstates with different energies for a d^2 ion in an octahedral ligand field

According to ligand field theory, the two electrons would be in the t_{2g} orbitals when in the ground state. For instance, they could be in the xy, and the xz orbitals. This is called a microstate. It is called a microstate of a state because there are other combinations of orbitals possible. For example, the ground state would also be realized if the two electrons were in the xz and the yz orbitals. This combination would be another microstate associated with the ground state electron configuration. Upon excitation using light the electron in the d_{xy} orbital could be promoted into an e_g orbital, which could be either the d_{z^2} or the $d_{x^2-y^2}$. Those two possibilities reflect to different microstates associated with the excited state (Fig. 8.1.2). Let us assume the electron goes into the d_{z^2} orbital. In this microstate one electron would be in the d_{xz} orbital and the other one in the d_{z^2} orbital. Now there us another possibility how to excite an electron. We could assume that not the d_{xy} electron is promoted into the d_{z^2} orbital, but the d_{xz} electron gets promoted. In this case, we would realize a microstate in which one electron in the d_{xy} orbital and the other one in the d_{z^2} orbital.



Figure 8.1.3 Orbitals associated with the two different microstates

Now let us compare the two cases. Ligand field theory would argue that both excited microstates have the same energy. However, in fact they do not. Why? That is because the electrons in the two excited microstates interact differently. This becomes plausible when considering the orbital shapes (Fig. 8.1.3). The d_{xz} orbital has electron density on the z-axis, while the d_{xy} orbital has not. Therefore, electrons in these orbitals would be expected to interact differently with an electron in a d_{z^2} orbital which has most of its electron density on the z-axis. As a result, the two excited microstates do not have the same energy. This means that in order to promote the electron into the two different microstates we need different amounts of energies. Thus, the complex would absorb light with more than just one wavelength. This is in contrast to what ligand field theory predicts. What will we need to do in order to correctly predict how many absorption bands we get? The answer is, we must find all possible microstates for the d^2 electron configuration and group those together which have the same energy. A group of microstates with the same energy is called a term. The number of electron transitions can then be predicted from the number of terms.

Russell Saunders Coupling of Electrons in Free Ions

Our task is now to find all the terms for the octahedral complex with d^2 electron configuration. To simplify matters let us first look at a free d^2 ion. A free ion is an ion which is not coordinated by any ligand.

m_l = magnetic quantum number of a single electron (m_l = -l.....l)

$$M_L = \Sigma\, m_l$$

M_L= total orbital angular momentum (of all electrons)

maximum M_L value = L

L = total orbital angular momentum quantum number

of microstates in the term due to angular momentum = 2L+1

This is because M_L can vary between –L and +L.

Figure 8.1.4. Relationships between angular momentum, total orbitals angular momentum, total angular orbital quantum number, and associated number of microstates of a term

The energy of the microstates depends on the quantum numbers m_l and m_s of the electrons (Fig. 8.1.4 and Fig. 8.1.5). This is because these quantum numbers of determine how the electrons interact. This is also called the Russell-Saunders coupling of electrons. Let us first see how the quantum number m_l of the electrons influences the term symbol. The term is determined by the microstate with the highest quantum number M_L, whereby M_L is the sum of the quantum numbers m_l of the individual electrons. The maximum M_L value is also called the total orbital angular momentum quantum number L. The L value also tells you how many microstates belong to a term due to these magnetic interactions. The number of microstates is 2L+1. This is because M_L can vary between –L and +L. So for instance if L=2, M_L can adopt the values -2, -1, 0, +1, and +2, and that translates to 2L+1=5 microstates.

The quantum number L alone does not define the term yet. In addition, we must also consider the interaction of the spins of the electrons (Fig. 8.1.5).

m_s = spin quantum number of a single electron

$M_S = \Sigma\, m_s$ (Total spin angular momentum)

maximum M_s value = S

S = total spin angular momentum quantum number

of microstates in the term due to spin = 2S+1

Figure 8.1.5 Relationships between the spin quantum number of the electron, the total spin angular quantum number, and the number of associated microstates.

The spin quantum number m_s of a single electron can be either +1/2 or -1/2. When the spins of the electrons interact, their spin quantum numbers add up, defining the total spin angular momentum M_s. The microstate with the maximum M_s value defines the total spin angular momentum quantum number S. The number of microstates due to the spin-spin interactions that belong to the term is 2S+1. This is also called the spin multiplicity (Fig. 8.1.6).

$$\#\text{ of overall microstates in the term} = (2L+1)\,2S+1$$

Figure 8.1.6 Equation for the overall number of microstates from L and S.

Overall the term has (2L+1)(2S+1) microstates. The total orbital angular quantum number L and the total orbital spin quantum number S define the term symbol (Fig. 8.1.7).

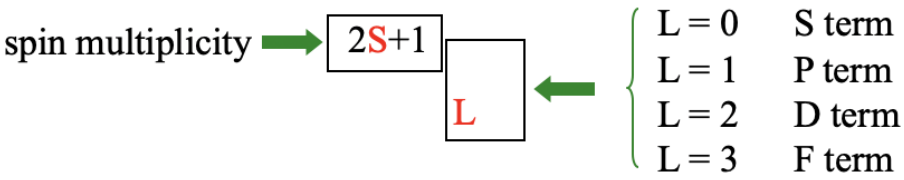


Figure 8.1.7 Term symbols. Attribution: E.R. Schofield.

When L=0 we have an S term, when L=1, we have a P term, when L=2, we call it a D term, and when L=3 we call it an F term. These symbols are chosen in analogy to the symbols s, p, d, and f for orbitals. The spin multiplicity 2S+1 is then written as a superscript in front of the letter defined by L. This gives the overall term symbol for a term. We call a term with a spin multiplicity of 1 a singlet term, when 2S+1=2, we call the term a doublet term. A term with a spin multiplicity of three is called a triplet term, one with a spin-multiplicity of 4 a quartet term, and so forth.

Microstates for a free d^2 ion

What are the possible microstates and the overall number of microstates for a free ion with d^2-electron configuration? We can express this in a so-called microstate table (Fig. 8.1.8).

M_s \ M_L	-4	-3	-2	-1	0	+1	+2	+3	+4
-1	Not possible (Pauli principle)	$-2^{-}\,-1^{-}$	$-2^{-}\,0^{-}$	$-2^{-}\,1^{-}$ $-1^{-}\,0^{-}$	$-2^{-}\,2^{-}$ $-1^{-}\,1^{-}$	$-1^{-}\,2^{-}$ $0^{-}\,1^{-}$	$0^{-}\,2^{-}$	$1^{-}2^{-}$	Not possible (Pauli principle)
0	$-2^{-}\,-2^{+}$	$-2^{-}\,-1^{+}$ $-2^{+}\,-1^{-}$	$-2^{-}\,0^{+}$ $-2^{+}\,0^{-}$ $-1^{-}\,-1^{+}$	$-2^{-}\,1^{+}$ $-2^{+}\,1^{-}$ $-1^{-}\,0^{+}$ $-1^{+}\,0^{-}$	$-2^{-}\,2^{+}$ $-2^{+}\,2^{-}$ $-1^{-}\,1^{+}$ $-1^{+}\,1^{-}$ $0^{-}\,0^{+}$	$-1^{-}\,2^{+}$ $-1^{+}\,2^{-}$ $0^{-}\,1^{+}$ $0^{+}\,1^{-}$	$0^{-}\,2^{+}$ $0^{+}\,2^{-}$ $1^{-}\,1^{+}$	$1^{-}2^{+}$ $1^{+}2^{-}$	$2^{-}\,2^{+}$
+1	Not possible (Pauli principle)	$-2^{+}\,-1^{+}$	$-2^{+}\,0^{+}$	$-2^{+}\,1^{+}$ $-1^{+}\,0^{+}$	$-2^{+}\,2^{+}$ $-1^{+}\,1^{+}$	$-1^{+}\,2^{+}$ $0^{+}\,1^{+}$	$0^{+}\,2^{+}$	$1^{+}2^{+}$	Not possible (Pauli principle)

Figure 8.1.8 d^2 electron configuration microstate table

You can see the microstate table for the d^2 electron configuration depicted above. Each column represents a possible value M_L. For the d^2 configuration, M_L can adopt values from -4 to +4, hence there there are 9 columns. Each row represents possible M_s value. For the d^2 electron configuration, M_s can vary between +1 and -1. +1 means both electrons have the spin +1/2, 0 means one electron has the spin +1/2 and the other one has the spin -1/2. The M_s value of -1/2 is adopted when both electrons have the spin -1/2. Now we can combine each M_s value with each M_L value which defines a particular field in the table. You can see that some fields are empty due to the Pauli principle. For example, the field for M_L=-4 and M_s=-1 is not filled because in this case both electrons would have the same quantum numbers, namely m_l=-2, and m_s =-1/2. We can further see that for some fields only one combination of electrons is possible, while for others there are multiple. For example, for the field with M_L=4 and M_s=0 there is only one combination of electrons possible. You can see the symbol "$2^{-}2^{+}$" in this field. This means that the first electron has an m_l value of 2 and and a spin of -1/2 and the second electron also has an m_l value of 2 and an m_s value of +1/2. The most populated field is the field for M_L=0 and M_s=0. There are overall five microstates with that combination of M_L and M_s values. If we count the overall number of microstates in the table then we arrive at the number 45. This is consistent with what we would expect according to the formula #microstates = (2L+1)(2S+1). In our example L=4 and S = 1, and thus the number of microstates is ((2x4)+1)((2x1)+1)=45. In general for a d^n electron configuration with *n* d-electrons the number of microstates is (10!)/((10-n)!n!).

One useful property of a microstate table is that we can derive the terms and term symbols for a particular electron configuration from it. For simplification sake, we indicate a possible microstate in the table just by an "x". Then we draw the largest possible rectangular box into the microstable that contains only fields with at least one possible electron combination (Fig. 8.1.9).

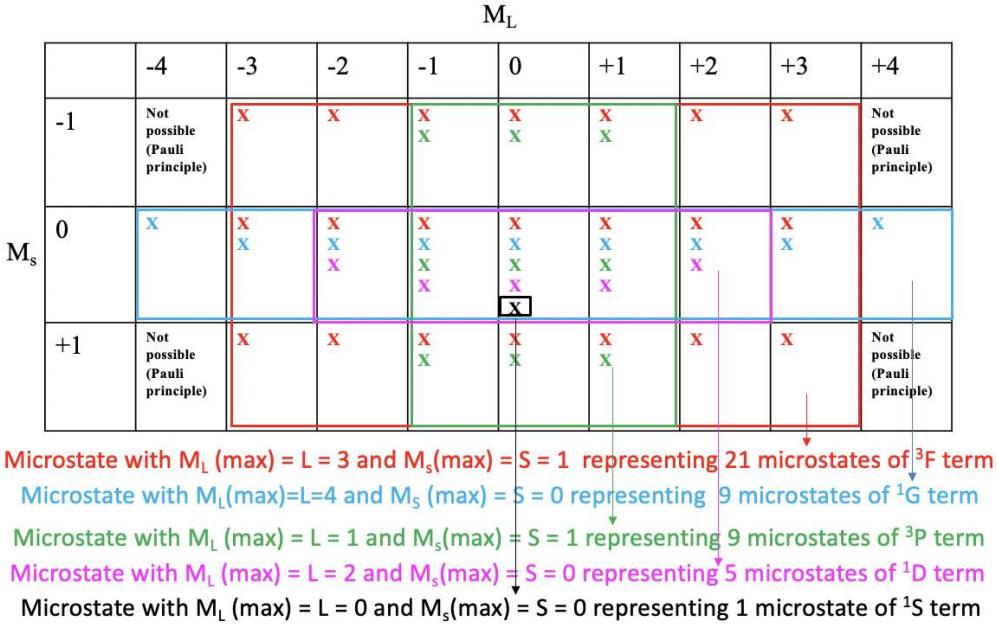


Figure 8.1.9 Deriving the terms and term symbols for the d^2 electron configuration from the microstate table

You can see that the largest possible box is the red box drawn (Fig. 8.1.9). This box contains the microstates that belong to the first term of the electron configuration d^2. The number of microstates is equal to the number of fields within the red box. That makes 7x3=21 microstates. What is the term symbol for this term? In order to answer this question we need to find the microstate in the red box that has the highest M_L and the highest M_s value. You can see that it is the one with M_L=3 and M_s = 2. Thus, L=3 and S=1. This defines the term as a ^{3}F term because 2S+1 = 3, and L=3 corresponds to the term symbol F. This term is a triplet term. Note that a triplet term also includes microstates with paired spins. Overall seven of the 21 microstates have M_s=0.

Next, we look what is the next-largest rectangular box we can draw, and which contains microstates we did not consider yet. We can see that the blue box contains nine fields equaling nine microstates. The microstate within this box that has the highest M_L and M_s values is the one with M_L=4 and M_s=0. This defines a ^{1}G term. This is a singlet term. Note that a singlet term ONLY has microstates with paired spins (M_s=0).

There is another rectangular box which also contains nine microstates. It is the green one. The microstate with the highest M_L and M_s values is the one with M_L=1 and M_s=1. Thus, L =1, and 2S+1=3 which defines a ^{3}P term. Note that despite this being a triplet term, the term also contains three microstates with paired spins.

The next-largest box is the purple one containing five fields and five microstates. What is the term with the highest M_L and M_s values? It is the one with M_L=2 and M_s=0. This means that L=2 and S=0 which defined a ^{1}D term. This is a singlet term. A singlet term contains only microstates with paired spins. There is one microstate left we did not consider thus far. It is one with M_L=0 and M_s = 0. These are the highest M_L and M_s values because there is no other microstate. Thus, this term contains only one microstate and the term symbol is ^{1}S. Now we have found all terms and term symbols.

The Energy of Terms

What is the relative energy of the terms? First we need to consider Hund's rule which states that the higher the spin multiplicity, the lower the energy of a term.

Rule 1: The higher spin multiplicity the lowest energy (Hund's rule).

We therefore first need to rank the terms with regards to the spin multiplicity. Secondly, we need to consider the value of the total orbital angular momentum quantum number L. The higher the value the lower the energy for the term. This means that the energy of terms decreases from S, to P, to D, to F.

Rule 2: When the spin-multiplicity is the same then the energy increases with increasing L value.

Note that this is contrary to orbital energies which increase from s, to p, to d, to f. Therefore, what would be the expected energy sequence for the terms associated with a d^2 free ion? It should be: $^3F<^3P<^1D<^1S$. However, the actual energy sequence is $^3F<^1D<^3P<^1G<^1S$. This means that, unexpectedly, the ^1D term is energetically lower than the ^3P term. We can understand from this is why Hund's rule is a called a rule and not a law because there are exceptions. In most but not all cases a triplet term has a lower energy than a singlet term.

Free-Ion Terms of Other d Electron Configurations

What are the term of the other d-electron configurations (Fig. 8.1.10)?

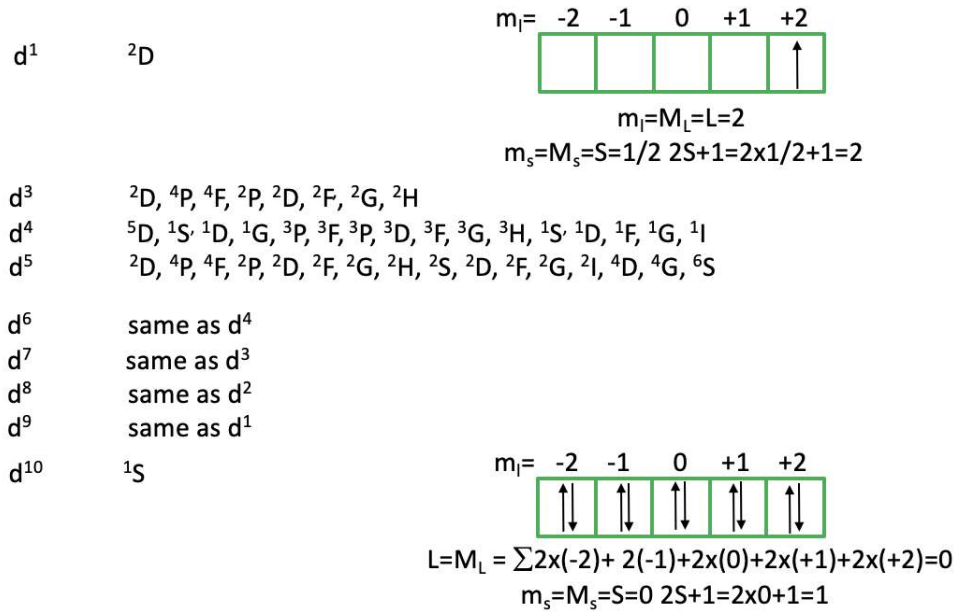


Figure 8.1.10 Terms for all d-electron configurations.

You can see above that there is only a single ^2D term for a d^1 free ion. How can we explain this term? Because there is no other electron, there are no electron-electron interactions, and thus every possible microstate has the same energy. This explains why there is only one term. Why is it ^2D? The term symbol is determined by the microstate with the highest M_L value and the highest M_S value. This is achieved when we fill the electron spin-up into the d-orbital with $m_l=2$ (Fig. 8.1.10). Because there is only one electron, $m_l=M_L=L=2$. This makes the term a D term. It is a doublet term because M_s is maximized when the electron is spin-up or $m_s=+1/2$. Thus, $m_s=M_s=S=1/2$. $2S+1=2\times1/2+1=2$, thus we have a doublet state. How many microstates are associated with this term? $(2L+1)(2S+1)=5\times2=10$. What does that mean? This means that we can fill the one electron that we have either spin-up or spin down in any of the five d-orbitals. All the 10 microstates are energetically equal.

When you go from d^2 to d^3 to d^4 to d^5 you can see that the number of the terms increases dramatically. This is because with increasing electron numbers the number of possible permutations increases, and thus the number of possible microstates. As a consequence, there are more terms. From d^6 to d^{10} the number of terms decreases again. The terms for d^6 are the same as the terms for d^4, the d^7-terms are identical to those for d^3, the d^8-terms are the same as the d^2 and the d^9-terms are the same as terms for the electron configuration d^1. Why is that? This is because unoccupied states in orbitals permute the same way as occupied ones do. For instance, in the d^3 electron configuration has three occupied states and seven unoccupied ones, while the d^7 electron configuration has seven occupied states and three unoccupied ones. The d^{10} electron configuration has also only one term with the term symbol ^1S (Fig. 8.1.10). Can we explain this? In the d^{10} electron configuration, there is no way to permute the electrons,

hence there is only one microstate possible. In this microstate L=0. Why is that? When we sum up the individual m_l-values of the ten electrons, then this sum is M_L = L = 2×(-2)+2(-1)+2×(0)+2×(+1)+2×(+2)=0. The spin multiplicity of the term is 1 because all electrons are paired (2S+1=(2×0)+1=1). Hence, we have a singlet ^{1}S term.

Spin-Orbit Coupling

We have still not considered all electron-electron interactions. In addition to the interaction between the angular magnetic momenta, and the magnetic interactions between the spins, there are also magnetic interactions between the angular momenta and the spins. This is called the spin-orbit coupling. It is expressed by an additional quantum number J. J can run from L+S to L-S.

$$J = L+S \ldots\ldots\ldots L-S$$

The quantum number J is added as a subscript behind letter describing the term. So a full term symbol is described as $^{2S+1}L_J$. Spin-orbit coupling may lead to additional terms depending on L and S (Fig. 8.1.11).

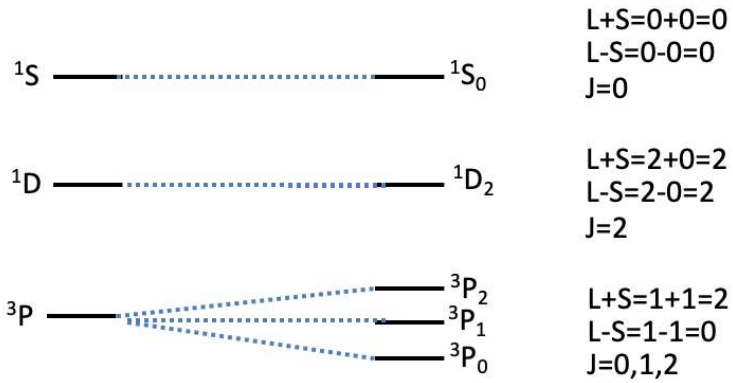


Figure 8.1.11. Spin-orbit coupling in ^{1}S, ^{1}D, and ^{3}P terms.

For instance, for a ^{3}P term, S=1, and L=1. Thus J can adopt values between L+S=1+1=2 and L-S=1-1=0. Thus, overall J can adopt the values, 0, 1, 2. This means a ^{3}P term splits into three terms due to the spin-orbit coupling. Their term symbols are $^3P_0$, $^3P_1$, and $^3P_2$. Their energy increases with increasing quantum number J. ^{1}S and ^{1}D terms on the other hand to do not split into additional terms. For a ^{1}S term L+S=0+0=0, and L-S=0-0=0. The full term symbol is $^1S_0$. For the ^{1}D term, L+S=2+0=2 and L-S=2-0=2, thus the full term symbol is $^1D_2$. Overall, the energy differences between terms due to J are very small, in the order of tens of wavenumbers, and orders of magnitudes smaller than energy differences due to RS-coupling, which are typically in the order of tens of thousands of wavenumbers. Thus, we usually ignore the effect of J when interpreting electronic spectra.

Dr. Kai Landskron (Lehigh University). If you like this textbook, please consider to make a donation to support the author's research at Lehigh University: Click Here to Donate.

This page titled 13.1: Microstates and Terms is shared under a not declared license and was authored, remixed, and/or curated by Kai Landskron.

- **8.1: Microstates and Terms** by Kai Landskron is licensed CC BY 4.0.

13.2: Term splitting in ligand fields, selection rules, Tanabe-Sugano diagrams. Metal to ligand, and ligand to metal transitions

Term Splitting of Terms in an Octahedral Field

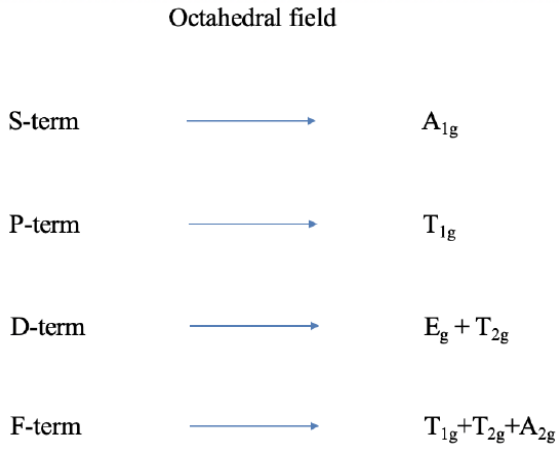


Figure **13.2.1**: Octahedral field term splitting

Thus far we have only considered free ion terms, that means terms without the presence of a ligand field. Let us next think about the influence of an octahedral field on a term. Terms are wavefunctions, just like orbitals, and therefore they behave like orbitals in a ligand field. D-orbitals split into t_{2g} and e_g orbitals in an octahedral ligand field. A D-term behaves similarly. It splits into T_{2g} and E_g terms. P-orbitals are triple-degenerate having T_{1g} symmetry in the point group O_h and do not split in energy. P-terms have the same symmetry and also do not split. We can call a P-term in an octahedral ligand field a T_{1g} term. Following analogous arguments, S terms become A_{1g} terms. F terms do split in energy like f-orbitals and become T_{1g}, T_{2g}, and A_{2g} terms. Overall, the presence of the octahedral field increases the number of terms from four to seven (Fig. **13.2.1**). It is easy to see that the ligand field leads to many states, and many potential electron transitions. Thus, we would expect quite complicated spectra. For other ligand fields, the terms also behave analogously to orbitals. For, instance in a tetrahedral field D-terms split into E and T_2 terms, and so forth.

Term Splitting for octahedral d^2 metal complexes

Now let us think about how the term energies of our free d^2-ion changes when placed in an octahedral ligand field, depending on the ligand field strength. We can express this by a correlation diagram (Fig. 8.2.2). In a correlation diagram, we plot the energies of the terms relative to the field strength.

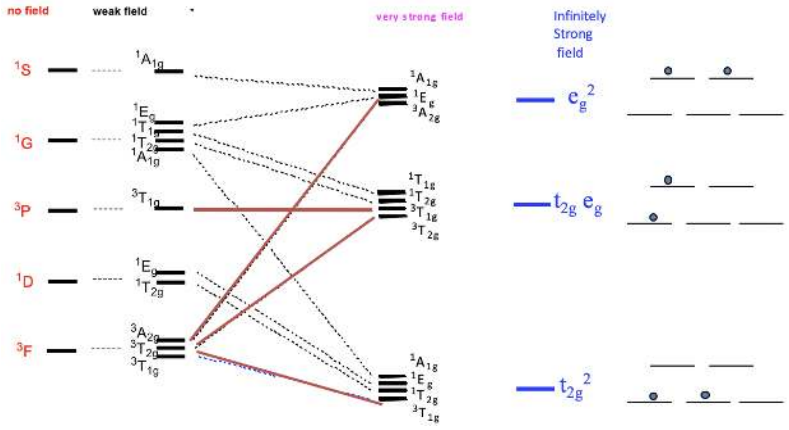


Figure 8.2.2 Correlation diagram

On the left side we plot the terms without any field according to their energies. In the case of a d^2 ion, the energies are $^3F<^1D<^3P<^1G<^1S$. Next, we plot the relative energies in a weak octahedral ligand field, and label the terms according to their

symmetry. We can see that the D, F, and G terms split in energy, while the S and P terms do not. Because of the weak field, energy differences are very small. Now let us increase the ligand field strength continuously, until we have reached a very strong ligand field. We see that some of the terms move up in energy, while other terms move down as the ligand field increases. For example, two of the three terms resulting from the F-terms increase in energy while one decreases. It is also possible that a term does not change its energy. For example, the $^3T_{1g}$ term from the ^3P term does not change its energy. In very strong ligand field there are three groups of terms that have similar energy. In the hypothetical case of an infinitely strong ligand field, the terms that belong to a particular group become identical in energy. In this case, there are only three states for the electrons possible. The field is considered so strong so that the energy associated with electron-electron interactions become negligible compared to the energy of the field. The electrons behave as though there were no electron-electron interactions. Therefore, we can call the lowest energy state the t_{2g}^2 state. It is equivalent to the state of the two electrons being in the t_{2g} orbitals. The second state is called the $t_{2g}e_g$ state. It is equivalent to the state of one electron being in the t_{2g} and one electron being in the e_g orbitals. The third state is called the e_g^2 state, which is equivalent to the state with both electrons in the e_g^2-orbitals.

Selection Rules

In most cases, the ligand field strength is in between the very weak and very strong case, and thus, we could expect very complicated spectra. Fortunately, nature does not make things quite as complicated, because not all possible electron transitions are quantum-mechanically allowed. The allowed transitions are defined by two rules: The spin selection rule and the Laporte rule.

The **spin selection rule** states that transitions with $\Delta S = 0$ are allowed.

The spin selection rule states that only transitions are allowed in which the total spin quantum number S does not change. When S does not change also the spin multiplicity does not change. Thus, electron transitions are only allowed for transitions that do not involve a change in spin multiplicity. For example, it would be allowed to excite an electron from a triplet term to another triplet term, but not from a triplet term to a doublet or singlet term.

The **Laporte rule** states that the transitions with the change of parity, g → u or u → g are allowed.

The Laporte rule state that transitions are only allowed when there is a change of parity. This means a transition from a gerade (g) to an ungerade (u)-term and vice versa is possible, but not a transition from a g-term to another g-term, or the transition from a u-term to another u-term. For example, the transition from a T_{2g} to a T_{1u} term would be allowed, but not the transition from a T_{2g} to a T_{1g} term.

Tanabe-Sugano diagram of a d^2 octahedral complex

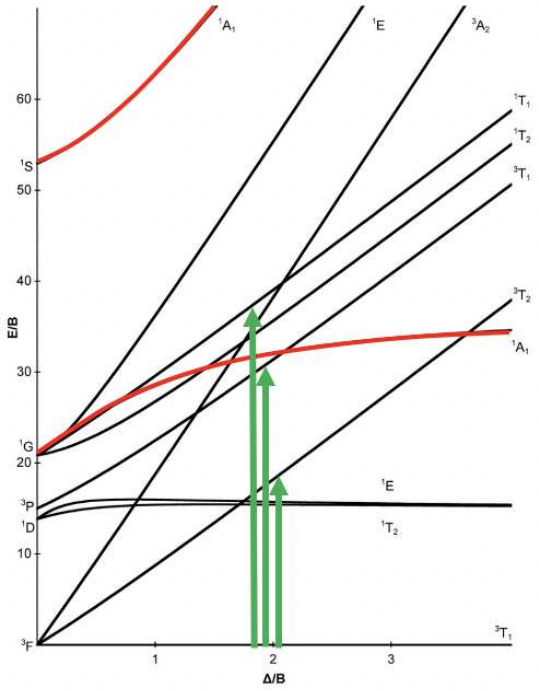


Figure 8.2.3 Tanabe-Sugano diagram of a d^2 octahedral complex (Attribution: Chem507f091 / Public domain https://commons.wikimedia.org/wiki/F...o_diagrams.png)

A particular correlation diagram is the Tanabe-Sugano diagram (Fig. 8.2.3). It is illustrated here for an octahedral d^2 complex. The difference to the previously discussed correlation diagram is that the energy of the ground state is plotted horizontally, and the energy of all other terms are plotted relative to that. In the case of the d^2 electron configuration, the $^3T_{1g}$ term is the ground term and is plotted as a horizontal line. We can see that the ligand field strength on the x-axis is given in units of B, and the energy of the terms is also given in units of B. B is a so-called Racah parameter, that is a quantum-mechanical energy unit for the electromagnetic interactions between the electrons. It is chosen because it provides “handy” numbers.

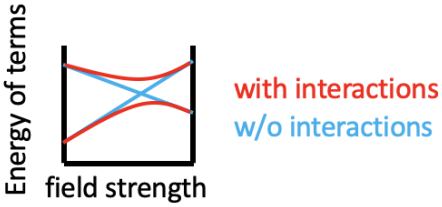


Figure 8.2.4 Origin of line-bending in Tanabe-Sugano diagrams.

You can see that some lines in the diagram are bent, and some are straight. Bending of lines occurs when two terms interact with each other because they are close in energy and have the same symmetry. This is again an analogy to orbitals. Like orbitals interact when they have the same symmetry type and similar energy, also terms interact when they have the same symmetry and the similar energy. Without taking their interactions into account, their energies can cross when the energy of term A declines and the energy of term B increases with increasing field strength (Fig. 8.2.4). The closer the terms come to the point where they cross, the stronger their interactions, because their energies become more and more similar. The interactions lead to the fact that the terms "bend away" from each other, leading to bent curves. This means that curves for two terms of the same symmetry type will bend away in a Tanabe-Sugano diagram and never cross. For example the terms for the two $^1A_{1g}$ terms bend away from each other and do not cross.

Next, let us think about which electron transitions would be allowed under the consideration of the spin selection and the Laporte rule. We notice that in the symmetry types the “g” for gerade has been omitted (Fig. 8.2.3). This is a common simplification made in the literature. We have to remind us that all the terms in the diagram are “g” terms. What does this mean for the allowance of

electron transitions? It means that no electron transition would be allowed, and that would imply that the complex could not absorb light. The Laporte selection rule however does not hold strictly. It only says that the probability of the electron-transition is reduced, however, not forbidden. This means that an absorption band that disobeys the Laporte rule will have lower intensity compared to one that follows the Laporte rule, but it can still be observed. The spin-selection rule, however, holds strictly, and transitions between terms of different spin multiplicity are strictly forbidden, meaning that they have near zero probability to occur. Overall, we can therefore excite an electron from the $^3T_1$ ground state to other triplet terms, namely the $^3T_2$ term, and the $^3A_2$ term (Fig. 8.2.3).

Tanabe-Sugano diagram of d^3 octahedral complexes

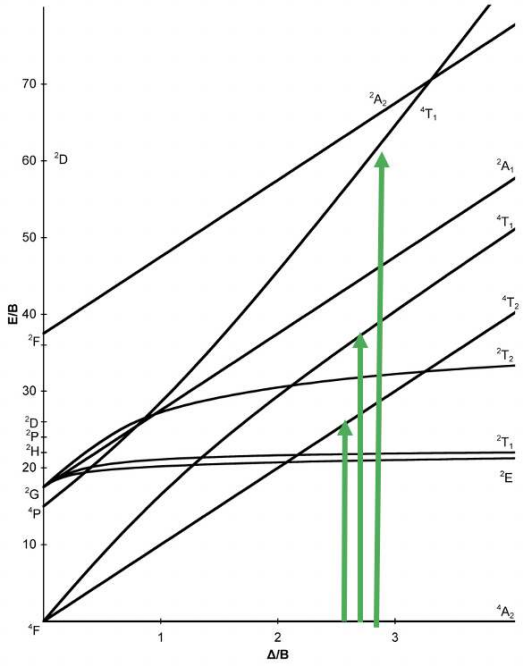


Figure 8.2.7 Tanabe-Sugano diagram of d^3 octahedral complexes (Attribution: Chem507f091 / Public domain https://commons.wikimedia.org/wiki/F...no_diagram.png)

Now, let us have a look at the Tanabe-Sugano diagram of a d^3 ion in an octahedral ligand field (Fig. 8.2.7). What is the ground term? We can see the term designation on the horizontal line reads "$^4A_2$", therefore this term is the ground term. How many electron transitions from the ground state should we expect? To answer this question we need to count the number of other quartet terms. There is the $^4T_2$, the $^4T_1$, and another $^4T_1$. Thus, there are overall three electron transitions possible. Can we understand why the ground state is a quartet term?

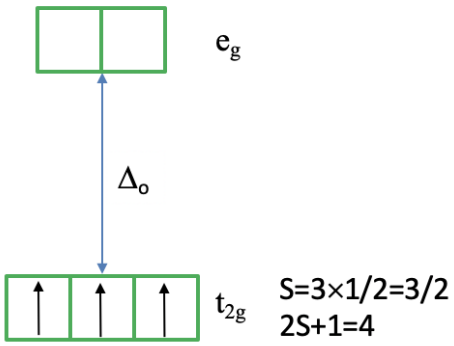


Figure 8.2.8 d-orbitals in an octahedral ligand field for the electron configuration d^3

It helps to consider how we would fill the electrons into the d-orbitals for the electron configuration d^3. All three electrons would be filled spin-up in the t_{2g} orbital following Hund's rule (Fig. 8.2.8). Because each electron has the spin +1/2 the total spin of all

three electrons is 3x1/2=3/2. Thus, the spin multiplicity is ((3x3/2)+1)=4. Note that the microstate we have drawn is actually only one of the (2L+1)(2S+1) microstates. S=3x1/2=3/2, but what is L? You can see one the left side of the diagram that the $^4A_2$ term originated from a ^4F term. This means L=3, and (2L+1)((2S+1)=7x4=28. This means that there are actually 27 other microstates that have the same energy as the microstate that we drew. Why did we draw this microstate in favor of the others? This is because this microstate is the state with the maximum M_L (=L) and M_s (=S) values determining the term symbol.

Tanabe-Sugano diagram of d^4 octahedral complexes

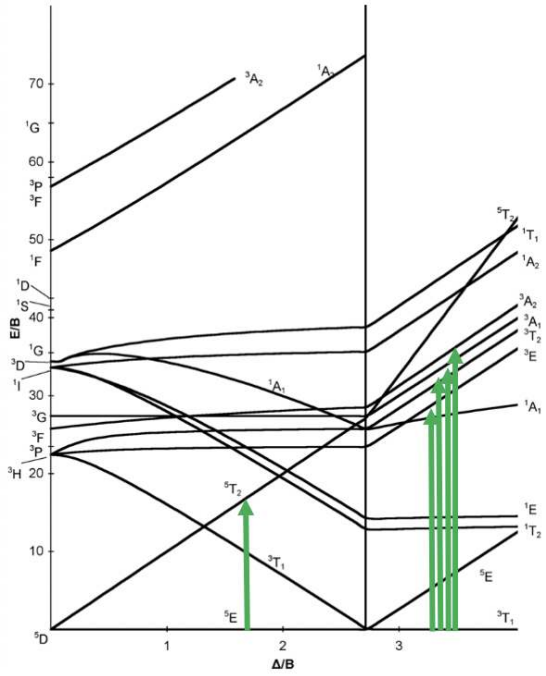


Figure 8.2.9 Tanabe-Sugano diagram of the d^4 octahedral complex (Attribution: Chem507f091 / Public domain https://commons.wikimedia.org/wiki/F...no_diagram.png)

Now let us look at the Tanabe-Sugano diagram of a d^4 octahedral complex. You can see that this diagram is separated into two parts separated by a vertical line. The line indicates the ligand field strength at which the complex changes from a high spin complex. At lower ligand field strengths, the ground term is a ^5E term. At higher field strength the ground term is a ^3T term.

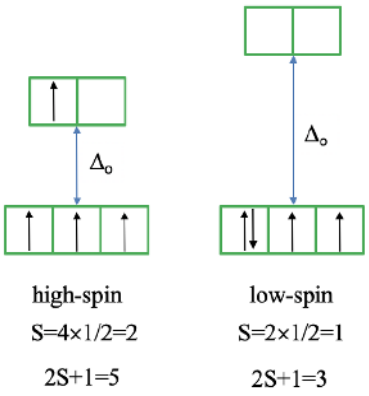


Figure 8.2.10 d-orbitals in the octahedral ligand field for the electron configuration d^4

We can rationalize this again by drawing the orbital box representation of the d-orbitals in the octahedral ligand field. In the high spin state, there are four unpaired electrons, thus S=4x1/2=2, and 2S+1=5. In the low spin state, there are two unpaired electrons, and thus S=2x1/2=1, and 2S+1=3. This explains the quintet and the triplet nature of the high and low spin ground terms. Note again, that the two microstates represented by the orbital box diagrams (Fig. 8.2.10) are not the only microstates that have the respective energy. They are only the "representative" microstates because the have the maximum M_L and M_S values.

How many electron transitions are possible from the ground term? For a high spin complex there is only one because the is only one other quintet term, namely the $^5T_2$ term. For the low spin complex, there are five transitions because there are five other triplet terms.

Tananbe-Sugano diagram of d^5 octahedral complexes

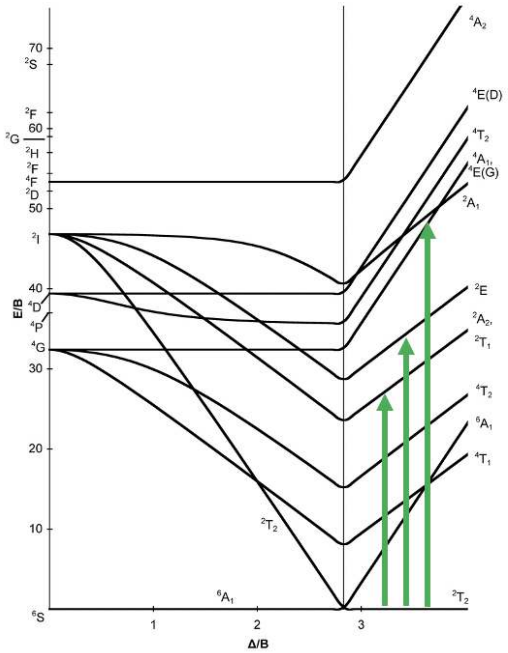


Figure 8.2.11 Tanabe-Sugano diagram of the d^5 octahedral complex (Attribution: Chem507f091 / Public domain https://commons.wikimedia.org/wiki/F...no_diagram.png)

Also the Tanabe-Sugano diagram of a d^5 octahedral complex is divided into two parts separated by a vertical line (Fig. 8.2.11). The left part reflects the high spin and the right part the low spin complex.

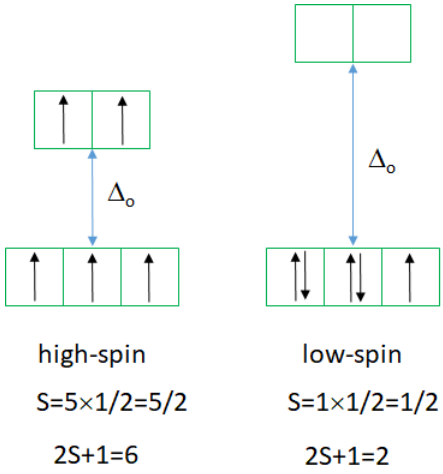


Figure 8.2.12 d-orbitals in the octahedral ligand field for the electron configuration d^5

The high spin ground state is a sextet term, and the low spin ground state is a doublet term. We can understand the sextet and doublet nature of the terms when considering that the associated electron box diagram have five and one unpaired electrons respectively. S=5x1/2=5/2 and 2S+1=6 for the high spin term, and S=1x1/2=1/2 and 2S+1=2 for the low spin term. What are the possible electron transitions from the ground state? For the high-spin complex there is no other sextet term, meaning that there is no electron transition possible. Hence, high-spin octahedral d^5-complexes are colorless. An example is the hexaaqua manganese (2+) complex. A solution of this complex is near colorless, only very slightly pinkish. The slight color is because also spin-forbidden

transitions can occur, albeit at a very low probability. For a d^5-low spin complex there are three additional doublet states, and thus there are three electron transitions possible.

Tanabe-Sugano diagram of d^6 octahedral complexes

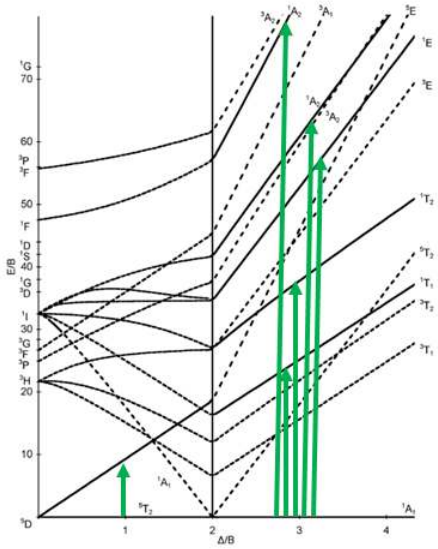


Figure 8.2.13 Tanabe-Sugano diagram of the d^6 octahedral complex (Chem507f091 / Public domain https://commons.wikimedia.org/wiki/F...no_diagram.png)

The next diagram is the one for the d^6 electron configuration (Fig. 8.2.13). Again, the diagram is separated into parts for high and low spin complexes. You can see dotted lines in the diagram. They indicate the terms that have a different spin multiplicity than the ground term. This way we can more easily see how many electron transitions are allowed.

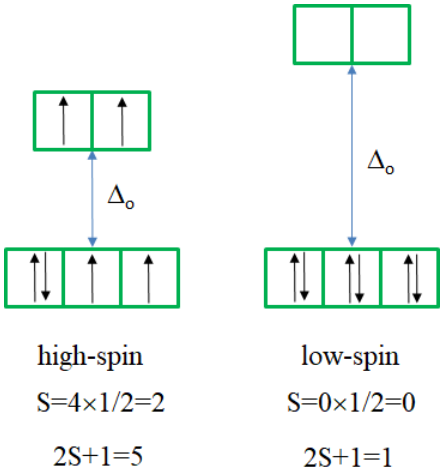


Figure 8.2.14 d-orbitals in the octahedral ligand field for the electron configuration d^6

The ground term for the high-spin complex is the quintet $^5T_2$ term. It is a quintet term because four electrons in the d-orbitals are unpaired, and two are paired. The value for S is thus 4x1/2=2, and the spin multiplicity is 2S+1=5. The ground term for the low spin complex is a $^1A_1$ term. It is a singlet term because all electrons are paired, and thus S=0, and 2S+1=1. How many electron transitions are there for the high-spin complex? There is only one because the ^5E term is the only other quintet term. There are five transitions possible for the low-spin case because there are five additional singlet terms.

Tanabe-Sugano diagram of d^7 octahedral complexes

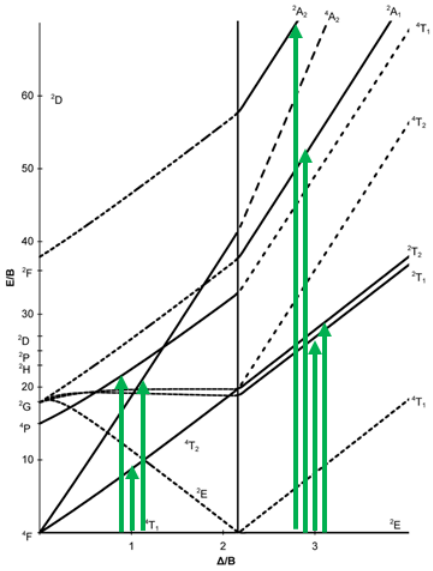


Figure 8.2.15 Tanabe-Sugano diagram of the d^7 octahedral complex (Attribution: Chem507f091 / Public domain https://commons.wikimedia.org/wiki/F...no_diagram.png)

Next, let us look at the Tanabe-Sugano diagram of a d^7 octahedral complex (Fig. 8.2.15). In this case, the high spin complex has a $^4T_1$ ground term, and the low spin complex has a ^2E ground term.

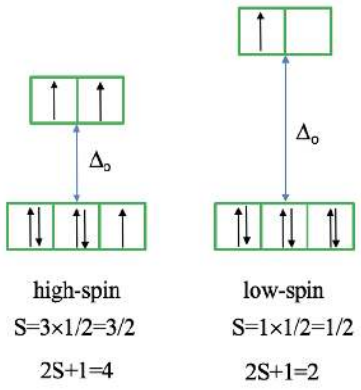


Figure 8.2.16 d-orbitals in the octahedral ligand field for the electron configuration d^7

The microstate that "represents" the high spin ground term has three unpaired electrons, hence the spin quantum number S=3/2 and the spin multiplicity is 2S+1=4. The microstate that represents the low spin ground term has one unpaired electron, an S value of ½, and a spin multiplicity of 2. There are three other quartet terms, and four other doublet terms, hence there are three electrons transitions for the high-spin complex, and four for the low spin complex.

Tanabe-Sugano diagram of d^8 octahedral complexes

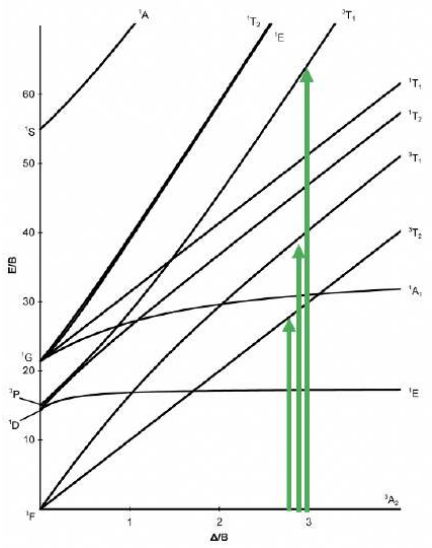


Figure 8.2.17 Tanabe-Sugano diagram of the d^8 octahedral complex (Attribution: Chem507f091 / Public domain https://commons.wikimedia.org/wiki/F...no_diagram.png)

Now let us look at an octahedral complex with d^8 electron configuration. For this electron configuration, there are no high and low spin complexes possible, therefore, the Tanabe-Sugano diagram is no longer divided into two parts (Fig. 8.2.17).

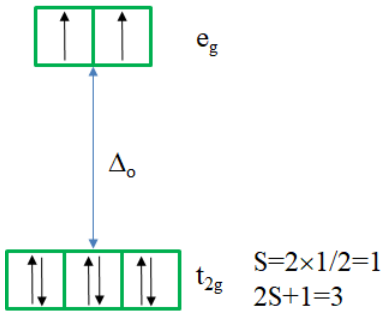


Figure 8.2.18 d-orbitals in the octahedral ligand field for the electron configuration d^8

There is a single ground term of the type $^3A_2$. It is a triplet state because the microstate representing the term has two unpaired electrons in the e_g orbitals (Fig. 8.2.18). Thus, S=2x1/2=1, and the spin multiplicity is 2S+1=2. How many electron transitions would you expect? There are three other triplet states, namely the $^3T_2$ and two $^3T_1$ terms. Therefore, there are three electron transitions possible.

We could also ask: Are there Tanabe-Sugano diagrams for d^1, d^9, and d^{10}? For, d^1 there are no electron-electron interactions, thus the simple orbital picture is sufficient. The ^2D term splits into T_{2g} and E_g terms, and there is only one electron transition possible. The d^9 electron configuration is the “hole-analog” of the d^1 electron configuration. It has also just one ^2D term which splits into a T_{2g} and an E_g term in the octahedral ligand field. Therefore, also in this case there is only one electron transition from the T_{2g} into the E_g term possible. In the case of d^{10} all microstates are filled with orbitals, and there is only the ^1S term which does not split in an octahedral ligand field. Therefore, there are no electron transitions in this case.

Finally, it should be mentioned that it is also possible to construct Tanabe-Sugano diagrams for other shapes such as the tetrahedral shape, but we will not discuss these further here.

Zn^{2+}		d^{10} ion	white
$[Cu(MeCN)_4]^+$	Cu(I)	d^{10} ion	colourless
$[Cu(phen)_2]^+$	Cu(I)	d^{10} ion	dark orange
TiF_4		d^0 ion	white
$TiCl_4$		d^0 ion	white
$TiBr_4$		d^0 ion	orange
TiI_4		d^0 ion	dark brown
$[MnO_4]^-$	Mn(VII)	d^0 ion	extremely purple
$[Cr_2O_7]^-$	Cr(VI)	d^0 ion	bright orange

Figure 8.2.19 Some examples of complexes with d^0 and d^{10} electron configurations, and their color. Attribution: E.R. Schofield.

We are still not done with our electronic spectra. Thus, far we have only considered transitions of d-electrons between d-orbitals, and their terms. They are called d-d transitions. However, there are also so-called charge transfer transitions possible, that are not d-d transitions. We can easily see that there must be other transitions but d-d transitions when we look at the color of d^{10} and d^0 ions. For those, the are no d-d transitions possible. Therefore, they all should be colorless. However, that is not always true. Some of these ions are indeed colorless, but some are not (Fig. 8.2.19). For example, Zn^{2+}, a d^{10} ion is colorless in complexes, but not Cu(I) which is also d^{10}. While tetrakis(acetonitrile)copper (+) is colorless, bis(phenanthrene) copper(+) is dark orange. Similar is true for d^0 ions. While TiF_4 and $TiCl_4$ are colorless, $TiBr_4$ is orange, and TiI_4 is brown. Some d^0 species are even extremely colorful, for example permanganate with Mn^{7+} which is extremely purple, and dichromate with Cr(VI) which is bright orange.

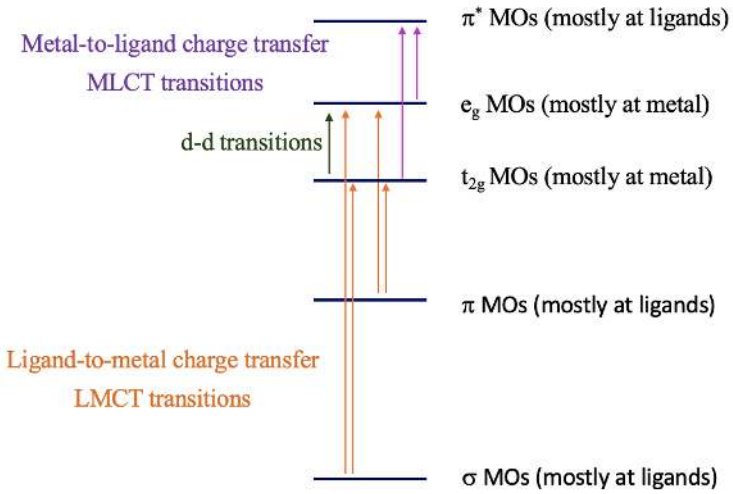


Figure 8.2.20 Charge-transfer transitions. Attribution: E.R. Schofield.

The explanation of these phenomena are charge-transfer transitions (Fig. 8.2.20). There are two types of charge-transfer transitions, the ligand-to-metal (LMCT) and the metal-to-ligand (MLCT) charge transfer transitions. For the ligand-to-metal transitions, electrons from bonding σ and π-orbitals get excited into metal d-orbitals in the ligand field, for example the t_{2g} and the e_g orbitals in an octahedral complex. If the energy difference between the σ/π-orbitals and the d-orbitals is small enough, then this electron-transition is associated with the absorption of visible light. The transition is called a ligand-to-metal transition because the ligand σ/π-orbitals are mostly located at the ligands, while the metal-d-orbitals in a ligand field are mostly located at the metal. Vice versa, the metal-to-ligand transition involves the transition of an electron from metal d-orbitals in a ligand field to ligand π*-orbitals. This essentially moves electron density from the metal to the ligand, hence the name ligand-to-metal-charge transfer transition. If the energy-difference between the ligand π* and the metal orbitals is small enough, then the absorption occurs in the visible range.

Charge-transfer transitions are usually both spin- and Laporte allowed, hence if they occur the color is often very intense. How can we distinguish between d-d and charge transfer transitions? Charge transfer transitions often change in energy as the solvent polarity is varied (solvatochromic) as there is a change in polarity of the complex associated with the charge transfer transition. This can be used to distinguish between d-d transitions and charge-transfer bands.

LMCT Transitions

Can we predict when the energy windows between the bonding molecular orbitals and the metal d-orbitals are small enough so that LMCT transitions in the visible can take place? Generally, it would be desirable if the energy of the metal orbitals was as low as possible and the energy of the bonding ligand orbitals are as high as possible. The energy of metal d-orbitals decreases with increasing positive charge at the metal because the effective nuclear charge on the metal increases. This means that very high metal oxidation states favor an LMCT transition. The d-orbitals should have few or no electrons, so that electrons can be promoted into the orbitals, and orbital energy decreases because electron-electron repulsion is minimized. Examples are Mn(VII), Cr(VI), and Ti(IV). The energy of MOs from bonding ligand orbitals increases when the ligand orbitals have high energy this is typically the case for π-donor ligand with negative charge (Fig. 8.2.21).

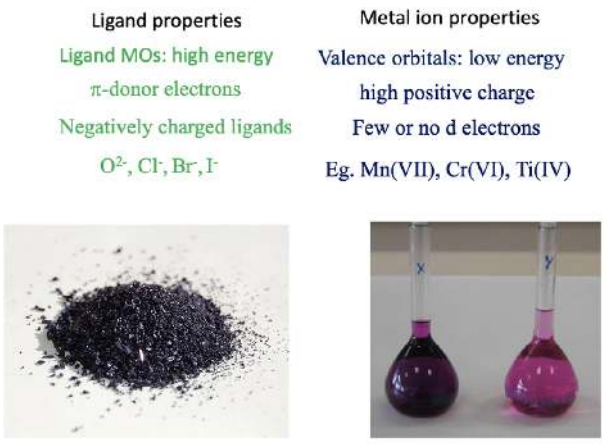


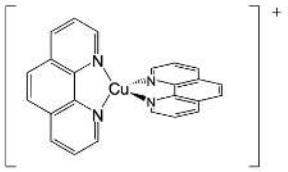
Figure 8.2.21 The properties of the metal ion and ligands suitable for LMCT transitions. MnO_4^- is deep purple due to LMCT transitions (Attribution: Benjah-bmm27 / Public domain https://commons.wikimedia.org/wiki/F...ate-sample.jpg) and (Attribution: Pradana Aumars / CC0 https://commons.wikimedia.org/wiki/F...entrations.jpg), respectively.

Examples of ligands are oxo- and halo ligands. This explains for example the LMCT transitions in permanganate. The Mn is in the very high oxidation state +7, and the ligands are are oxo-ligands wich are π-donors with a 2- negative charge. The transitions are both Laporte and spin-allowed leading to very high intensity of light absorption, and thus color (Fig. 8.2.21).

MLCT Transitions

What are favorable metal ion and ligand properties for a metal-to-ligand transition, then? In this case we would like to keep the energy of the metal orbitals as high as possible so that the energy difference between a metal d-orbital and a π*-orbital is minimized. This is accomplished when the positive charge at the metal ion is small, and there are many d-electrons that can repel each other, thereby increasing orbital energies, for examples Cu(I), Fig. 8.2.22.

Metal ion properties	Ligand properties
low metal ion charge	π-acceptor ligand with low-lying π* orbitals
many electrons	
Cu(I), d^{10} ion	1,10-phenanthroline, CN^-, CO, SCN^-



$[Cu(phen)_2]^+$, dark orange

Figure 8.2.22 bis(phenanthroline) copper(+). Attribution: E.R. Schofield.

The ligand should be a π-acceptor with low-lying π*-orbitals, for example phenanthroline, CN^-, SCN^-, and CO. For instance, the bis(phenanthroline) copper(+) is dark-orange and has a MLCT absorption band at 458 nm. Also, the MLCT transfer is both spin and Laporte-allowed.

It should be mentioned that some complexes allow for both metal-to-ligand and ligand to metal transitions. For example, in the $Cr(CO)_6$ complex the σ-orbitals are high enough and the π*-orbitals are low enough in energy to allow for light absorption in the visible range. Finally, also intraligand bands are possible when the ligand is a chromophore.

Dr. Kai Landskron (Lehigh University). If you like this textbook, please consider to make a donation to support the author's research at Lehigh University: Click Here to Donate.

This page titled 13.2: Term splitting in ligand fields, selection rules, Tanabe-Sugano diagrams. Metal to ligand, and ligand to metal transitions is shared under a not declared license and was authored, remixed, and/or curated by Kai Landskron.

- **8.2: Term splitting in ligand fields, selection rules, Tanabe-Sugano diagrams. Metal to ligand, and ligand to metal transitions** by Kai Landskron is licensed CC BY 4.0.

13.3: Concept Review Questions Chapter 8

Concept Review Questions

Section 1

1. Explain the difference between a microstate and a state.

2. Explain what is meant by a term? Why do we need terms to explain electronic spectra?

3. What is meant by “Russell-Saunders coupling”?

3. What is the definition of the total angular momentum quantum number L?

4. What is the definition of the quantum number M_l?

5. What is the definition of the quantum number m_l?

6. What is definition of the total spin quantum number S?

7. What is the definition of the quantum number M_s?

8. What is the definition of the quantum number m_s?

9. How many microstates are associated with a term defined by a quantum number L and S respectively?

10. Which formula can be used to calculate the number of microstates with a specific d electron configuration?

11. What is meant by the spin-orbit coupling?

12. Why is the spin-orbit coupling usually neglected for electronic spectra?

13. What is the dependency between the quantum number L and the energy of a term?

14. What is the dependency between the quantum number S and the energy of a term?

15. What is meant by a “free ion term”?

Section 2

1. How do D, P, and S terms split in an octahedral and tetrahedral ligand field, respectively?

2. What is a correlation diagram?

3. What is meant by t_{2g}^2, $t_{2g}e_g$, and e_g^2 terms in octahedral complexes? Explain their relationship to molecular orbitals.

4. What is the major difference between a Tanabe-Sugano diagram and a correlation diagram?

5. Why do terms with the same symmetry never cross in Tanabe-Sugano diagrams?

6. When are lines in Tanabe diagrams straight and when are they bent?

7. What is a metal-to-ligand charge transfer (MLCT) transition?

8. What is a ligand-to-metal charge (LMCT) transfer transition?

9. Under which conditions does a MLCT transition occur in the visible range? Name one example of a complex that does MLCT.

10. Under which conditions does a LMCT transiton occur in the visible range? Name one example of a complex that does LMCT?

Dr. Kai Landskron (Lehigh University). If you like this textbook, please consider to make a donation to support the author's research at Lehigh University: Click Here to Donate.

13.3: Concept Review Questions Chapter 8 is shared under a not declared license and was authored, remixed, and/or curated by LibreTexts.

- **Concept Review Questions Chapter 8** by Kai Landskron is licensed CC BY 4.0.

13.4: Homework Problems Chapter 8

Homework Problems

Section 1

Exercise 1

How many microstates exist for the electron configurations

a) p^3

b) f^2

c) d^3

Answer

a) p^3 - 6!/((6-3)!3!) = 20

b) f^2 -14!/((14-2)!2!)=91

c) d^3 -10!/((10-3)!3!)=120

Exercise 2

What is the term symbol for the one term associated with the following electron configurations?

a) p^6

b) p^1

c) f^{14}

d) s^1

Answer

a) p^6 - ^1S

b) p^1 - ^2P

c) f^{14} - ^1S

d) s^1 - ^2S

Exercise 3

What is the number of microstates for a

a) ^5D term

b) ^4G term

c) ^2F term

Answer

a) (2L+1)(2S+1) = 5 x 5 = 25

b) (2L+1)(2S+1) = 9 x 4 = 36

c) (2L+1)(2S+1) = 7 x 2 = 14

Exercise 4

In a triplet term there are

a) only microstates with unpaired electrons.

b) only microstates with paired electrons.

c) microstates with paired and unpaired electrons.

Answer

c) microstates with paired and unpaired electrons.

Exercise 5

In a singlet term there are

a) only microstates with unpaired electrons.

b) only microstates with paired electrons.

c) microstates with paired and unpaired electrons.

Answer

b) only microstates with paired electrons.

Dr. Kai Landskron (Lehigh University). If you like this textbook, please consider to make a donation to support the author's research at Lehigh University: Click Here to Donate.

13.4: Homework Problems Chapter 8 is shared under a not declared license and was authored, remixed, and/or curated by LibreTexts.

- **Homework Problems Chapter 8** by Kai Landskron is licensed CC BY 4.0.

CHAPTER OVERVIEW

14: Coordination Chemistry V - Reactions and Mechanisms

14.1: Substitution Reactions and their Mechanisms

14.2: Concept Review Questions Chapter 9

14.3: Homework Problems Chapter 9

Dr. Kai Landskron (Lehigh University). If you like this textbook, please consider to make a donation to support the author's research at Lehigh University: Click Here to Donate.

This page titled 14: Coordination Chemistry V - Reactions and Mechanisms is shared under a not declared license and was authored, remixed, and/or curated by Kai Landskron.

14.1: Substitution Reactions and their Mechanisms

Chemical Reactivity and Reactions of Complexes

In this chapter we will discuss the chemical reactivity and reactions of coordination compounds. First, let us briefly review what are the basic parameters that define if a reaction can be observed or not. The first parameter is the Gibbs free energy of reaction ΔG. The Gibbs free energy defines the thermodynamic driving force for the reaction. The more negative ΔG is, the greater the thermodynamic driving force. The Gibbs free energy of reaction is a measure for the difference in the stability of the reactants and products. The less stable the reactants, and the more stable the products, the more negative ΔG. The second parameter is the kinetics of a reaction. The kinetics is a measure of the speed at which a reaction occurs. The kinetics is independent from the thermodynamics. This means that even if there is a strong thermodynamic driving force for the reaction, the rate of the reaction may be extremely slow, and practically no reaction is observed. For example, graphite is thermodynamically more stable than diamond at ambient pressure and temperature, but the kinetics of the conversion at room temperature is so slow, so that practically no reaction is observed. The rate of the reaction is determined by the the activation energy that needs to be overcome to make the reaction happen. The lower the activation energy, the faster the reaction. In coordination chemistry the activation energy and the reaction rates are associated with the inertness and the lability of complexes. The more inert and the less labile a complex is the higher the activation barrier and the more slowly it reacts. The lability is the opposite of the inertness and is defined by the half-life time of a dative bond. The greater the half-life time, the more inert, and the less labile the complex.

Inert and Labile Complexes

The greater the half-life time of a dative bond, the more inert, and the less labile the complex. Where do we actually draw the borderline between a labile and an inert complex? A commonly accepted definition is that complexes with metal-ligand bond half life times of <30 s at standard conditions are considered labile complexes with a low activation energy. Those complexes undergo fast substitution reactions, and the chemical equilibrium is reached fast (Fig. 9.1.1).

Fast ligand exchange: *Labile* complex

$$M\text{-}L \rightleftharpoons M + L \quad (t_{1/2} < 30\ s;\ \text{low activation energy})$$

Labile complexes undergo fast substitution reaction:

$$[Fe(H_2O)_5(SCN)]^{2+} + F^- \rightarrow [Fe(H_2O)_5F]^{2+} + SCN^- \quad (t_{1/2} < 1s)$$

The chemical equilibrium will be reached very fast.

Figure 9.1.1 Properties of labile complexes

An example is the substitution of a thiocyanato ligand in a pentaaquathiocyanato iron (2+) complex by a fluoro ligand. This substitution reaction is fast because the half-life time of the metal-ligand bond is smaller than a second.

Slow ligand exchange: *Inert* complex

$$M\text{-}L \rightleftharpoons M + L \quad (t_{1/2} > 30\ s,\ \text{high activation energy})$$

Inert complexes undergo slow substitution reaction:

$$[Co(NH_3)_6]^{3+} + 6\ H_3O^+ \rightarrow [Co(H_2O)_6]^{3+} + 6\ NH_4^+ \quad (t_{1/2} > 1d)$$

The chemical equilibrium will be reached slowly.

Figure 9.1.2 Properties of inert complexes

If the half-life time is greater than 30s, then the complex is considered inert. For example, the hydrolysis of hexaammine cobalt (3+) is slow because the half-life time of the Co-N bond is larger than a day. The chemical equilibrium is reached only slowly (Fig. 9.1.2).

Can we predict which complexes are labile, and which ones are inert? Many factors determine this, but there are some trends we can keep in mind. For transition metals, octahedral d^3, low spin d^4-d^6, and square planar d^8 complexes tend to be inert. A second trend is that the lability decreases with the period within a group. For instance, we would expect that in group 10 the lability decreases from Ni to Pd to Pt. This is because covalency of the bonds tends to increase with increasing period due to the softer

nature of higher period metals. A third trend is that higher positive charges at the metal ion lead to a decrease in liability. Metal ions with higher oxidation numbers also tend to make more covalent bonds because the high positive charge at the metal is stabilized by covalent interactions (Fig. 9.1.3).

Trends for d-block metal ions:

Electron configuration: octahedral d^3, low spin d^4-d^6, square planar d^8 tend to be inert.

Higher period of metal ion → less labile

Higher positive charge of metal ion → less labile

Figure 9.1.3 Trends for d-block metal ions

We can also compare the d-block metals with the other blocks. S-block metal complexes tend to have the greatest lability, followed by the f-block, followed by the d-block. P-block metal complexes can widely vary in lability (Fig. 9.1.4).

Comparison of d- block metal ions with other blocks:

Lability s>f>d block ions; p: can vary a lot

Leaving group effect: good leaving group → labile

Figure 9.1.4 Trends for the blocks and leaving groups

Also the nature of the ligand influences the lability. Generally, when the ligand is a good leaving group, then the bond tends to be labile. A ligand is usually a good leaving group when it is stable in the uncoordinated form. For instance, a chloro ligand is a good leaving group because chloride anions are quite stable in their non-coordinated form. An alkyl ligand on the other hand would not be considered as a good leaving group because the an alkylide anion is not a very stable species in the free form.

Stability of Complexes

Now let us have a closer look at the stability of complexes. The more negative the Gibbs free energy of formation, the greater the equilibrium constant of formation K. The larger the equilibrium constant K of formation, the more stable the complex. This can be expressed by the van't Hoff equation $\Delta G = -RT\ln K$.

$$M + L \rightarrow M\text{-}L \quad \Delta G<0$$

$$K = \frac{[ML]}{[M]\,[L]}$$

Figure 9.1.5 Equilibrium constant for a reaction that forms a single metal-ligand bond. Reaction proceeds to the right if $\Delta G<0$.

For the formation of a single dative bond M-L the constant of formation is given by K=[ML]/[M][L] (Fig. 9.1.5). The greater K, the farther the equilibrium is on the side of the product. K is usually reported as logK because K can vary over 35 orders of magnitude.

Rationalizing the Different Stability of Complexes

How can we rationalize the different stabilities of coordination bonds, and coordination compounds? Here, the HSAB concept is very useful. Hard-hard and soft-soft interactions are typically strong and lead to high constants of formation and stable complexes. Hard-soft interactions lead to small constants of formation and less stable complexes.

hardest softest

	NH_3	F^-	Cl^-	Br^-
Ag^+	3.30	-0.17	3.08	4.30

soft

Figure 9.1.6 Formation constants log K for Ag^+ complexes

Let us understand this better by the example of the interaction of Ag^+ with different ligands (Fig. 9.1.6). You can see in the table the logK values for the different ligands. Br^- has the largest one, followed by NH_3 and Cl^-. F^- has the smallest one. Can we explain this with the HSAB concept? Ag^+ is a soft cation, thus it would be expected to make the strongest interactions with the softest ligand. Bromide is the softest of the four, and hence HSAB correctly predicts the stability. F^- is the hardest ligand and would be expected to make the weakest complex. This is in accordance with the small logK value for F^-. NH_3 and Cl^- have similar intermediate hardness, which is consistent with the similar, intermediate logK values.

Stabilities of Multi-ligand Complexes

Example ML_4

1. $M + L \rightarrow ML$ $\quad K_1 = [ML] / [M] [L]$
2. $ML + L \rightarrow ML_2$ $\quad K_2 = [ML_2] / [ML] [L]$
3. $ML_2 + L \rightarrow ML_3$ $\quad K_3 = [ML_3] / [ML_2] [L]$
4. $ML_3 + L \rightarrow ML_4$ $\quad K_4 = [ML_4] / [ML_3] [L]$

$$K_1 > K_2 > K_3 > K_4$$

Figure 9.1.7 Equilibria associated with a complex of the composition ML_4

How does the stability of a complex change as more ligands are added? Let us take a look at the constants of formation to answer the question. The addition of an additional ligand is associated with an additional chemical equilibrium which relates to an additional constant of formation. The number of equilibrium constants is equal to the number of ligands. For instance, when we have a complex ML_4 with four ligands, then for the addition of the first ligand we get a constant $K_1 = [ML] / [M] [L]$, for the second ligand we get a constant $K_2=[ML_2] / [ML] [L]$, for the third ligand there is a constant $K_3=[ML_3] / [ML_2] [L]$, and for the fourth ligand there is a constant $K_4=[ML_4] / [ML_3] [L]$. When we analyze the K-values, we notice that they decline from K_1 to K_4. For a general complex ML_n we find that the constants decline from K_1 to K_n. How can this be explained? The explanation is that the more ligands are getting added, the less many free ligands are available that could be further added. Thus, the probability that further ligands are added decreases, and this results in a smaller equilibrium constant. So it is a statistical effect that explains the phenomenon.

The stepwise and overall stability constants K are related as follows:

ML_4: $K = K_1.K_2.K_3.K_4$

ML_n: $K = K_1.K_2.....K_n$

Figure 9.1.8 Overall stability constants for a general complex ML_n

Then what is the overall stability constant K of the complex associated with the equation $M + 4\ L \rightarrow ML_4$ and more general $M + nL \rightarrow ML_n$? It is the product of the constants associated with each step. For the complex ML_4 it is $K=K_1K_2K_3K_4$. For the general complex ML_n it is $K=K_1K_2.....K_n$ (Fig. 9.1.8).

There are exceptions from the rule that the stability constants of complexes associated with the addition of one ligand decreases with the number of ligands. If there is an exception, then this is because the ligand addition causes a major change in the electronic structure of the complex. Here are a couple of examples.

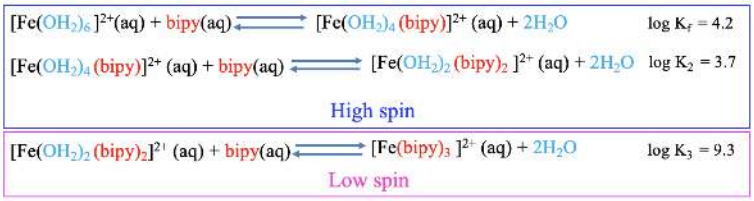


Figure 9.1.9 Example 1 for exceptions to the rule for stability constants

In the first example (Fig. 9.1.9) the aqua ligands of a hexaaqua iron (2+) complex are substituted by bipyridyl ligands. The bipyridyl ligand is a bidentate ligand, and so one bipydridyl ligand substitutes two aqua ligands. In the first substitution, the two aqua ligands get replaced by one bipyridyl ligand to form a tetraaqua(bipyridyl) iron (2+) complex. This step is associated with a $\log K_1$ value of 4.2.

In the second substitution step, two aqua ligands of the tetraaqua(bipyridyl) iron (2+) complex get replaced by another bipyridyl ligand to form a diaqua bis(bipyridyl) iron(2+) complex. As expected this step is associated with a smaller $\log K_2$ value of 3.7.

In the third step, the last two aqua ligands get substituted by another bipyridyl ligand forming a tris(bipyridyl) iron(2+) complex. What is the $\log K_3$ value? It is 9.3! This is much larger than $\log K_1$ and $\log K_2$, so this result is unexpected. A major change in electronic structure must have occurred. What is it? In this case it is a change from a high-spin to a low spin complex. The bipyridyl ligands are strong π-acceptors that increase Δ_o. Substitution of the first four aqua ligands increases Δ_O but the increase is not large enough yet so that it induces a switch from a high-spin to a low-spin complex. Only the third bipyridyl ligand does that. As a consequence, the formation constant $\log K_3$ is unusually large.

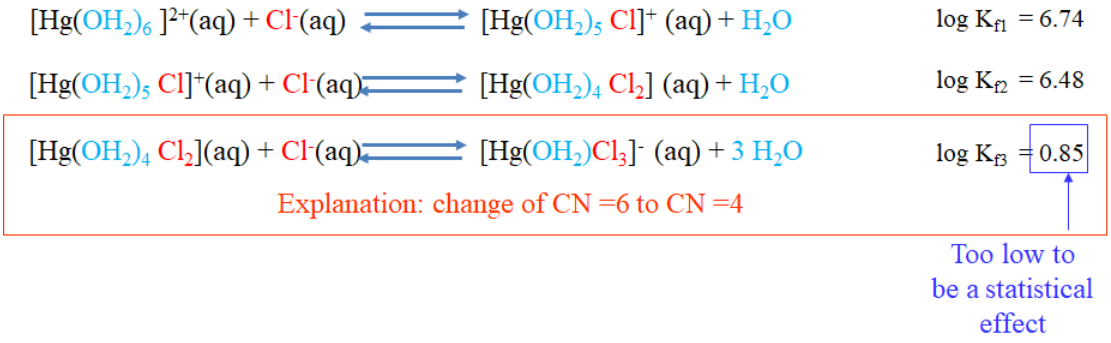


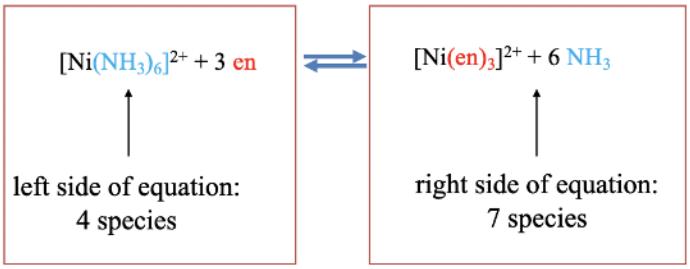
Figure 9.1.10 Example 2 for exceptions to the rule for stability constants

In the second example (Fig. 9.1.10) we subsequently substitute aqua ligands by chloroligands in a hexaaqua mercury(2+) complex. The first substitution leads to a pentaaquachloro mercury(+) complex. This reaction is associated with a $\log K_1$ value of 6.74. The second substitution leads to a tetraaquadichloro mercury(0) complex, and this reaction is associated with a smaller $\log K_2$ value of 6.48. The third substitution reaction leads to an aquatrichloro mercury(1-) complex. The $\log K_3$ value for this reaction is 0.85. We see that this value is smaller than $\log K_2$, and this is what we expected, but the difference between $\log K_3$ and $\log K_2$ is much larger than that between $\log K_1$ and $\log K_2$. The increased difference is too large to be just caused by a statistical effect, but must be induced by a change in electronic structure. In this case it is a change in coordination number. As the third chloro ligand is added, the complex does not lose only one but three aqua ligands. This reduces the coordination number from six to four.

Stability of Chelate Complexes

The Thermodynamic Chelate Effect

Chelating complexes tend to be more stable than complexes with monodentate ligands. This is called the “thermodynamic chelate effect”. The effect deserves an explanation. The explanation is the increase of entropy that occurs when two or more monodentate ligands are replaced by a chelating ligand. The entropy increases because the overall number of particles increases as the substitution takes place.



$\Delta S° = +88\ J\ K^{-1}\ mol^{-1}$

Figure 9.1.11 Example of the thermodynamic chelate effect

For example, the substitution of six ammine ligands in the hexaammine nickel (2+) complex by three ethylenediamine chelating ligands increases the number of molecules from four to seven, and hence the entropy increases, in this case by 88 J K^{-1} and mol^{-1} (Fig. 9.1.11)

The Kinetic Chelate Effect

In addition to the thermodynamic chelate effect, there is the kinetic chelate effect. Chelate complexes are frequently more inert than complexes with monodentate ligands. Chelate complexes are more inert for two reasons (Fig. 9.1.12).

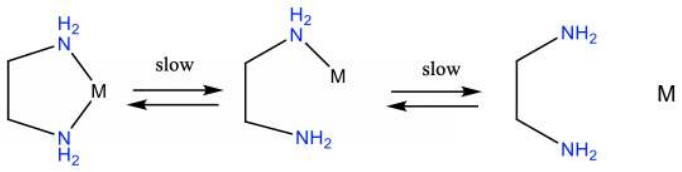
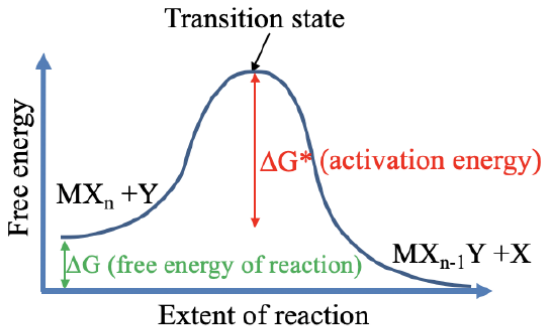


Figure 9.1.12 Illustration of the kinetic chelate effect

Firstly, the whole ligands needs to rotate and bend in order to cleave the first metal-ligand bond. This requires time and slows the kinetics of the bond cleavage. The second reason is that the detached donor atom cannot leave the proximity of the complex because the ligand is still attached via the other donor atom. This increases the probability of the re-formation of the metal-ligand bond which decreases the probability of both bonds being cleaved.

Mechanism of Ligand Substitution Reactions

Now let us talk about the mechanism of ligand substitution reactions. We know two basic mechanisms according to which a ligand substitution can occur. One is called the intimate mechanism, and the other one is called the stoichiometric mechanism.



Intimate mechanism

Figure 9.1.13 Intimate mechanism

The intimate mechanism goes through a single transition state as the reaction proceeds.

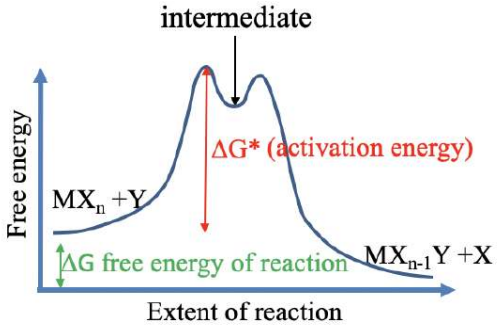


Figure 9.1.14 Stoichiometric mechanism

The stoichiometric mechanism goes through an intermediate. The intermediate is a shallow local minimum on the reaction coordinate. The transition state is the maximum on the reaction coordinate. For both mechanisms the principle of microscopic reversibility holds. This means that the reverse reaction follows the same free energy path as the forward reaction. For both mechanisms the free Gibbs energy of reaction is given by the difference between the free energy of the products and the free energy of the reactants. The reaction can only spontaneously occur if the free energy of the products is smaller than the free energy of the reactants. The activation energy is the free energy difference between the transition state and the reactants.

Classifications of Mechanisms

There are two forms of the stoichiometric mechanism: The dissociate mechanism D and the associative mechanism A. In the dissociative mechanism (Fig. 9.1.15), an old ligand X is lost first, and the intermediate has a lower coordination number. In the associative mechanism (Fig. 9.1.16), the new ligand Y is added first and the intermediate has a higher coordination number. The intermediates must be detectable, thus must be present in relatively high concentration to measurable with an analytical technique. This requires are relatively deep local thermodynamic minimum for the intermediate. In practice, many local minima are too shallow to allow for the clear detection of the intermediate. We call such a mechanism an Interchange mechanism. There are two forms of interchange mechanisms: I_a and I_d. I_a stands for associative interchange mechanism and I_D stands for dissociative interchange mechanism. Overall we can have a continuous range of mechanisms that range from A to I_a to intimate to I_d to D.

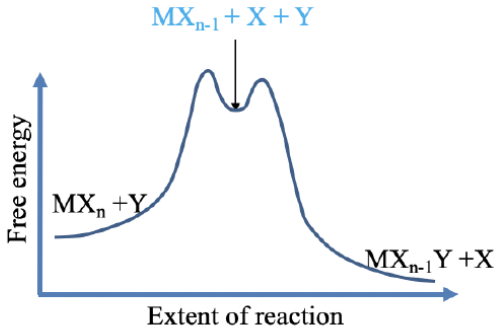


Figure 9.1.15 Dissociative mechanism

For a dissociative and the I_d mechanism the dissociation is the rate limiting step. This is because the activation energy is associated with the dissociative step. We need to go strongly uphill to achieve dissociation, and go into the local thermodynamic minimum. From, there we only need to go slightly uphill to add the new ligand.

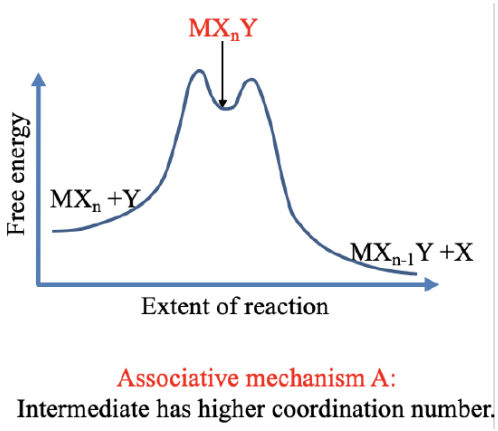


Figure 9.1.16 Associative mechanism

For the associative and the I_a mechanism (Fig. 9.1.16), the associative step is the rate limiting step because the activation energy is associated with the associative step. In this case we first need to go energetically strongly uphill to achieve association and reach the local thermodynamic minimum. We only need to go slightly uphill from the local thermodynamic minimum to lose the old ligand.

How to Distinguish Between D/I_d and A/A_d

We can use the relationships between the rate determining step and the mechanism to experimentally distinguish between associative A/I_a and dissociative D/I_d mechanisms. If the reaction rate strongly depends on the new ligand, then we likely have an associative or I_a mechanism. This is because the associative step is the rate determining step. If the reaction rate does not strongly depend on the new ligand, then the mechanism is likely dissociative D or I_d. This is because in the dissociate mechanism, the addition of the new ligand is not the rate-determining step.

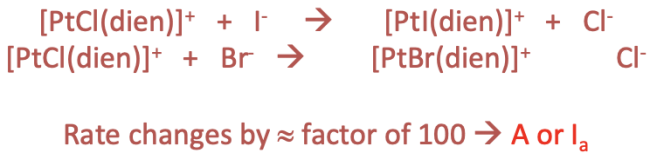


Figure 9.1.17 Distinguishing between D/I_d and A/A_d

For example, we can substitute a chloro ligand in a $[PtCl(dien)]^+$ complex by iodo and bromo ligands, respectively (Fig. 9.1.17). What we measure is that the reaction rates are by a factor of 100 different. This means that the reaction rates does depend on the new ligand and this indicates an associative or I_a mechanism.

Steric arguments can help to predict if a mechanism is associative or dissociative. Lower coordination numbers and little steric crowding tends to favor A and I_a mechanisms, while higher coordination numbers and greater steric crowding tend to favor the dissociative mechanism.

Dr. Kai Landskron (Lehigh University). If you like this textbook, please consider to make a donation to support the author's research at Lehigh University: Click Here to Donate.

This page titled 14.1: Substitution Reactions and their Mechanisms is shared under a not declared license and was authored, remixed, and/or curated by Kai Landskron.

- **9.1: Substitution Reactions and their Mechanisms** by Kai Landskron is licensed CC BY 4.0.

14.2: Concept Review Questions Chapter 9

Concept Review Questions

Section 1

1. When in general does a chemical reaction occur?

2. What is meant by an inert and a labile complex?

3. For which d electron configuration would you expect inert complexes?

4. How does the leaving group effect influence the inertness of a coordination compound?

5. With which concept can the stability of coordination compounds be estimated?

6. What is the linear free energy relationship? Explain its origins qualitatively.

7. Explain why the constant of formation for multi-ligand complexes decreases with the addition of additional ligands? Under which circumstances are there exceptions?

8. What is the “thermodynamic chelate effect”?

9. What is the “kinetic chelate effect”?

10. What is meant by an “intimate” and a “stoichiometric” mechanism respectively?

11. What is the difference between a transition state and an intermediate?

12. What is the difference between an associate mechanism A and an interchange mechanism I_a?

13. What is the difference between a dissociative mechanism D and an interchange mechanism I_d?

14. How can one experimentally distinguish between an associative and a dissociative mechanism?

15. Which factors favor associative mechanisms and dissociative mechanisms respectively?

Dr. Kai Landskron (Lehigh University). If you like this textbook, please consider to make a donation to support the author's research at Lehigh University: Click Here to Donate.

14.2: Concept Review Questions Chapter 9 is shared under a not declared license and was authored, remixed, and/or curated by LibreTexts.

- **Concept Review Questions Chapter 9** by Kai Landskron is licensed CC BY 4.0.

14.3: Homework Problems Chapter 9

Homework Problems

Section 1

Exercise 1

An associative mechanism is favored when

a) the oxidation state of the metal is high

b) the coordination number of the metal is low

c) the complex has bulky ligands

d) the metal –ligand bonds are labile.

Answer

b) the coordination number of the metal is low

Exercise 2

Which of the following metal-ligand bonds would you expect to have the highest thermodynamic stability?

a) Hg-S

b) Hg-O

c) Hg-N

d) Hg-F

Answer

a) Hg-S

Exercise 3

Chelate complexes are thermodynamically particularly stable because

a) The substitution of a simple ligand by a chelating ligand is enthalpically particularly favorable.

b) The substitution of a simple ligand by a chelating ligand is entropically particularly favorable.

c) Chelating ligands are more inert than simple ligands.

Answer

b) The substitution of a simple ligand by a chelating ligand is entropically particularly favorable.

Exercise 4

What is true about intimate mechanisms?

a) The intimate mechanism involves an intermediate that is detectable

b) The intimate mechanism involves an intermediate that is not detectable.

c) The intimate mechanism involves a transition state.

Answer

c) The intimate mechanism involves a transition state.

Exercise 5

What is true about complexes that undergo metal to ligand charge transfer?

a) The metal ion has no or few d electrons

b) The ligands are good pi-acceptors

c) The metal ions have a high charge.

Answer

b) The ligands are good pi-acceptors

14.3: Homework Problems Chapter 9 is shared under a not declared license and was authored, remixed, and/or curated by LibreTexts.

- **Homework Problems Chapter 9** by Kai Landskron is licensed CC BY 4.0.

CHAPTER OVERVIEW

15: Acid-Base Chemistry

Learning Objectives

- Understand the Brønsted and Lewis definitions of acids and bases.
- Identify conjugate acids and bases, and rules for strong & weak acids/bases, in both Brønsted and Lewis acid-base systems.
- Use Pauling's rules to predict the pK_as of oxoacids.
- Understand the periodic trends of acidic, basic, and amphoteric compounds
- Predict, describe, and rationalize acid/base chemistry in non-aqueous systems, including acidic and basic solvents, aprotic solvents, and molten salts.
- Apply the principles of acid-base chemistry to the design of molecules and Lewis acids with target functions.
- Understand the connection between acid-base chemistry and the stabilization of oxidation states.
- Predict favorable and stable compounds using hard-soft acid-base (HSAB) theory.
- Understand the applications of the ECW model.

Acid-base reactions form the basis of the most common kinds of equilibrium problems which you will encounter in almost any application of chemistry. There are three major classifications of acids and bases: (1) The Arrhenius definition states that an acid produces H^+ in solution and a base produces OH^- and the (2) Brønsted-Lowry and (3) Lewis definitions of acids and bases. Of particular importance in inorganic chemistry is the "hard and soft (Lewis) acids and bases" (HSAB) theory that is widely used for explaining stability of compounds, reaction mechanisms, and reaction pathways.

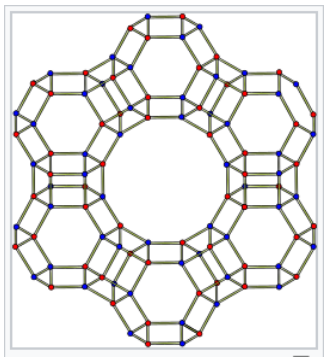
15.1: Prelude to Acid-Base Chemistry
15.2: Brønsted and Lewis Acids and Bases
15.3: Hard and Soft Acids and Bases
15.4: The Electrostatic-Covalent (ECW) Model for Acid-Base Reactions
15.5: Frustrated Lewis Pairs
15.6: Discussion Questions
15.7: Problems
15.8: References

15: Acid-Base Chemistry is shared under a CC BY-SA license and was authored, remixed, and/or curated by LibreTexts.

15.1: Prelude to Acid-Base Chemistry

Acids and bases are important for a number reasons in inorganic chemistry.

- Many industrially useful catalytic reactions involve inorganic acids and superacids, such as zeolites, anhydrous hydrogen fluoride, and sulfated zirconia. These acids are sufficiently strong in anhydrous media that they can protonate olefins and alcohols to produce carbocations. Carbocations are key intermediates in the transformations of hydrocarbons.
- Inorganic compounds are sometimes synthesized in strongly acidic or basic media. For example, ternary metal oxides can be synthesized and crystallized in molten NaOH or KOH, which are strongly basic. Organic fluorination reactions are often done in strongly acidic media, such as anhydrous HF. Understanding the familiar chemistry of acids and bases in water helps us understand how these non-aqueous media work.
- The acidic or basic environment of metal ions affects the stability of their oxidation states. We will learn more about this in Chapter 4.
- Transition metal complexes (coordination compounds and organometallic compounds) are essentially Lewis acid-base complexes. We can understand a great deal about their stability and reactivity by considering the acid-base character of metals and ligands. We will learn about this in Chapter 5.



Solid acid catalysts, such as zeolite Y, are used to isomerize hydrocarbons in the processing of crude oil into gasoline. Edith Flanigen(below with President Barack Obama) received the 2014 National Medal of Technology for her research on the synthesis of zeolite Y.



15.1: Prelude to Acid-Base Chemistry is shared under a CC BY-SA license and was authored, remixed, and/or curated by LibreTexts.

- **3.1: Prelude to Acid-Base Chemistry** by Chemistry 310 is licensed CC BY-SA 4.0. Original source: https://en.wikibooks.org/wiki/Introduction_to_Inorganic_Chemistry.

15.2: Brønsted and Lewis Acids and Bases

Three theories of acids and bases

There are three major classifications of substances known as acids or bases. The Arrhenius definition states that an acid produces H^+ in solution and a base produces OH^-. This theory was developed by Svante Arrhenius in 1883. Later, two more sophisticated and general theories were proposed. These are the Brønsted-Lowry and the Lewis definitions of acids and bases. The relationship between these theories is illustrated in the figure below.

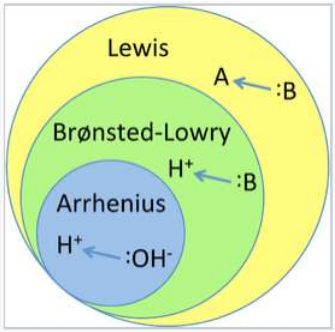


Illustration of the hierarchy of acid-base theories. Arrhenius acids and bases are a sub-class of Brønsted acids and bases, which are themselves a subclass of Lewis acids and bases.

The Arrhenius theory, which is the simplest and least general description of acids and bases, includes acids such as $HClO_4$ and bases such as NaOH or $Mg(OH)_2$. This theory successfully describes how acids and bases react with each other to make water and salts. However, it does not explain why some substances that do not contain hydroxide ions, for example F^- and NO_2^-, can make basic solutions in water. The Brønsted-Lowry definition of acids and bases addresses this problem. In this theory an **acid is a substance that can release a proton** (like in the Arrhenius theory) and a **base is a substance that can accept a proton**. A basic salt such as Na^+F^- generates OH^- ions in water by taking protons from water itself (to make HF):

$$\mathrm{F^-_{(aq)} + H_2O_{(l)} \rightleftharpoons HF_{(aq)} + OH^-} \tag{15.2.1}$$

When a Brønsted acid dissociates, it increases the concentration of hydrogen ions in the solution, $[H^+]$; conversely, Brønsted bases dissociate by taking a proton from the solvent (water) to generate $[OH^-]$.

Acid Dissociation: $\mathrm{HA_{(aq)} \rightleftharpoons A^-_{(aq)} + H^+_{(aq)}}$

$$K_a = \frac{[A^-][H^+]}{[HA]} \tag{15.2.2}$$

Base dissociation: $\mathrm{B_{(aq)} + H_2O_{(l)} \rightleftharpoons HB^+_{(aq)} + OH^-(aq)}$

$$K_b = \frac{[HB^+][OH^-]}{[B]} \tag{15.2.3}$$

Conjugate acids and bases

One important consequence of these equilibria is that every **acid** (HA) has a **conjugate base** (A-), and vice-versa. In the base dissociation equilibrium above the conjugate acid of base B is HB^+.

For a given acid or base, these equilibria are linked by the water dissociation equilibrium:

$$\mathrm{H_2O_{(l)} \rightleftharpoons H^+_{(aq)} + OH^-_{(aq)}} \tag{15.2.4}$$

$$K_w = [H^+][OH^-] \tag{15.2.5}$$

for which the equilibrium constant K_w is 1.00×10^{-14} at 25°C. It can be easily shown that the product of the acid and base dissociation constants K_a and K_b is K_w.

Strong and weak acids and bases

Acids and bases that dissociate completely are said to be strong:

$$HClO_{4\,(aq)} \longrightarrow H^+_{(aq)} + ClO_4{}^-_{(aq)} \tag{15.2.6}$$

$$HBr_{(aq)} \longrightarrow H^+_{(aq)} + Br^-_{(aq)} \tag{15.2.7}$$

$$CH_3O^-_{(aq)} + H_2O_{(l)} \longrightarrow CH_3OH_{(aq)} + OH^-_{(aq)} \tag{15.2.8}$$

$$NH_2{}^-_{(aq)} + H_2O_{(l)} \longrightarrow NH_{3\,(aq)} + OH^-_{(aq)} \tag{15.2.9}$$

Here the right-handed arrow (→) implies that the reaction goes to completion. That is, a 1.0 M solution of $HClO_4$ in water actually contains 1.0 M H^+(aq) and 1.0 M ClO_4^-(aq), and very little undissociated $HClO_4$.

Conversely, weak acids such as acetic acid (CH_3COOH) and weak bases such as ammonia (NH_3) dissociate only slightly in water - typically a few percent, depending on their concentration and the values of K_a and K_b - and exist mostly as the undissociated molecules.



Antacid tablets typically contain calcium salts of the bicarbonate ion (HCO_3^-), a weak base. Its conjugate acid, carbonic acid (H_2CO_3) is a weak acid. The acid-base equilibrium between carbonic acid and bicarbonate is important in maintaining blood pH.

Example

Household ammonia is a solution of NH_3 in water that ranges from about 5-10% by weight. Let's calculate the percent ionization and the pH of the solution.

Solution

For a solution that is 8% ammonia by weight, assuming that the density is about the same as that of liquid water, the analytical concentration of ammonia is (80 g/L) / (17 g/mol) = 4.7 M.

The other thing we need to know to solve this problem is the base dissociation constant, K_b.

$$NH_3 + H_2O \rightleftharpoons NH_4{}^+ + OH^- \quad K_b = 1.8 \times 10^{-5}$$

We can solve this problem rigorously by invoking both charge balance ($[H^+] + [NH_4^+] = [OH^-]$) and mass balance (4.7 M = $[NH_3] + [NH_4^+]$) and using $K_W = [H^+][OH^-]$. But because the algebra becomes complicated with that method - leading to a cubic equation that is hard to solve - we'll invoke two simplifying assumptions:

$[NH_4^+] \approx [OH^-] \gg [H^+]$ (which is a reasonable assumption for a basic solution)

and

$[NH_3] \gg [NH_4^+]$ (also reasonable if the percent ionization is small)

Now we can write:

$$[NH_4^+][OH^-] \approx [OH^-]^2 = (4.7M)(K_b) = 8.4 \times 10^{-5}$$

$$[OH^-] = 9.2 \times 10^{-3} M\ (\approx [NH_4^+]),\ [H^+] = \frac{K_w}{[OH^-]} = 1.1 \times 10^{-12} M,\ \ \mathbf{pH = 11.97}$$

The percent ionization is:

$$100\% \times 9.2 \times 10^{-3} M / 4.7 M = 0.19$$

This example illustrates that it is technically incorrect to label a bottle of aqueous ammonia as “ammonium hydroxide,” since only about 2/10 of one percent of the weak base exists in that form.

Conjugate acids and bases

A common misconception is that strong acids have weak conjugate bases, and that weak acids have strong conjugate bases. It is easy to see that this is incorrect by remembering that $K_aK_b = K_w$. Our definition of a strong acid or base is that K >> 1, i.e., that the substance dissociates completely. Our definition of a weak acid or base is $1 > K > K_w$. It follows that if $K_a >> 1$ (strong) then K_b cannot be > K_w (weak).

In fact, **strong acids** such as HCl dissociate to produce **spectator ions** such as Cl^- as conjugate bases, whereas **weak acids** produce **weak conjugate bases**. This is illustrated below for acetic acid and its conjugate base, the acetate anion. Acetic acid is a weak acid ($K_a = 1.8 \times 10^{-5}$) and acetate is a weak base ($K_b = \frac{K_w}{K_a} = 5.6 \times 10^{10}$)



The strength of a conjugate acid/base varies inversely with the strength or weakness of its parent acid or base. Any acid or base is technically a conjugate acid or conjugate base also; these terms are simply used to identify species in solution (i.e acetic acid is the conjugate acid of the acetate anion, a base, while acetate is the conjugate base of acetic acid, an acid).

Neutral oxyacids (H_2SO_4, H_3PO_4, HNO_3, $HClO_2$, etc.) can be classified as strong or weak following a simple rule first noted by Linus Pauling. If the number of oxygen atoms exceeds the number of hydrogen atoms by two or more, then the acid is strong; otherwise it is weak. For example $HClO_4$ and $HClO_3$, where the difference is 3 and 2, respectively, are both strong acids. HNO_2 and $HClO_2$ are both weak because the difference is 1 in both cases. For weak acids, the relative strength depends on this difference (i.e., $HClO_2$ is a stronger weak acid than HOCl) and on the electronegativity of the central atom (HOCl is stronger than HOI).

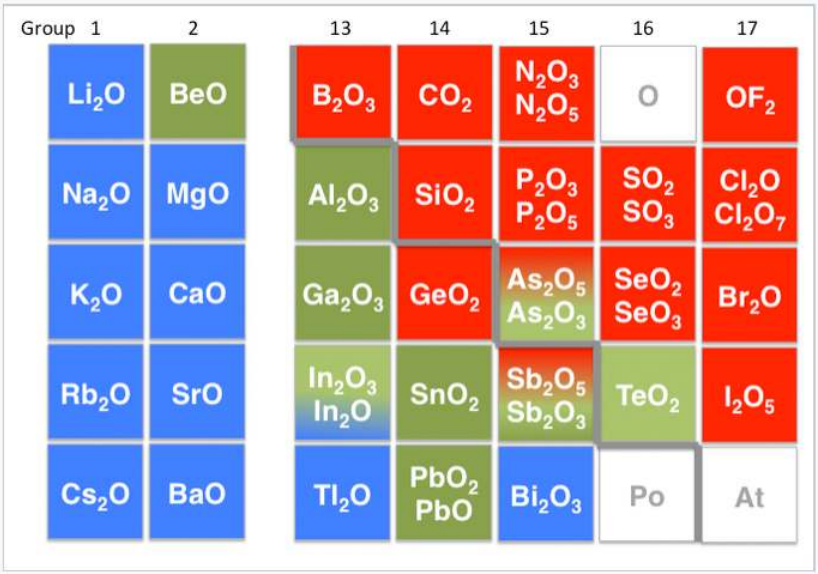
Acids that can donate more than one proton are called **polyprotic acids**. For example, sulfuric acid, H_2SO_4, is a strong acid that has a conjugate base that actually happens to be a weak acid itself. This means that every mole of H_2SO_4 in aqueous solution donates more than 1 mole of protons. Carbonic acid (H_2CO_3) and phosphoric acid (H_3PO_4) are weak polyprotic acids. Typically, the sequential pK_a's of polyprotic acid are separated by about 5 pH units, because it becomes progressively more difficult to remove protons as the ion becomes more negatively charged. For example, the three pK_a's of phosphoric acid are 2.15, 7.20, and 12.35.

Amphoteric compounds

Some substances can act either as an acid and as a base. An example is water. H_2O molecules may either donate a hydrogen ion or accept one. This property makes water an **amphoteric** solvent. In the situation where an acid dissociates in solution, water is acting as a base. Conversely, water acts as an acid when bases dissociate. The strongest acid we can make in H_2O is H^+ (aq), and the strongest base we can make in H_2O is OH^- (aq).

Other examples of amphoteric compounds are oxides and hydroxides of elements that lie on the border between the metallic and non-metallic elements in the periodic table. For example, aluminum hydroxide ($Al(OH)_3$) is insoluble at neutral pH, but can accept protons in acid to make $[Al(H_2O)_6]^{3+}$ or accept an OH^- ion in base to form $Al(OH)_4^-$ ions. Consequently, aluminum oxide is soluble in acid and in base, but not neutral water. Other examples of amphoteric oxides are BeO, ZnO, Ga_2O_3, Sb_2O_3, and PbO. Increasing

the oxidation state of a metal increases the acidity of its oxide by withdrawing electron density from the oxygen atoms. Thus, Sb_2O_5 is acidic, but Sb_2O_3 is amphoteric.



Periodic table showing basic (blue), amphoteric (green) and acidic (red) oxides. The metal-nonmetal boundary is indicated by the gray staircase line.

Solvent leveling

Solvent leveling is an effect that occurs when a strong acid is placed in a solvent such as (but not limited to) H_2O. Because strong acids donate their protons to the solvent, the strongest possible acid that can exist is the conjugate acid of the solvent. In aqueous solution, this is H_3O^+. This means that the strength of acids such as HCl and HBr cannot be differentiated in water as they both are dissociated 100% to H_3O^+. In the context of our discussion of conjugate bases above, we would say that both Cl^- and Br^- are spectator ions in water: neither one is a strong enough base to accept a proton from H_3O^+. In order to differentiate the acidities of strong acids such as $HClO_4$ and HCl, or the basicities of strong bases such as CH_3O^- and NH_2^-, we must typically work in non-aqueous solvents, as explained below.

Nonaqueous solutions

The Brønsted theory encompasses any type of solvent that can donate and accept H^+ ions, not just aqueous solutions. The strength of an acid or a base varies depending on the solvent. Non-aqueous acid-base chemistry follows similar rules to those developed for acids and bases in water. For example in liquid ammonia, the solvent autodissociates in the reaction:

$$2\,NH_{3\,(l)} \rightleftharpoons NH_4^+ + NH_2^- \tag{15.2.10}$$

This equilibrium is analogous to the autodissociation of water, but has a smaller equilibrium constant ($K \approx 10^{-30}$). It follows by analogy to water that NH_4^+ is the strongest acid and NH_2^- is the strongest base that can exist in liquid ammonia. Because ammonia is a basic solvent, it enhances the acidity and suppresses the basicity of substances dissolved in it. For example, the ammonium ion (NH_4^+) is a weak acid in water ($K_a = 6 \times 10^{-10}$), but it is a strong acid in ammonia. Similarly, acetic acid is weak in water but strong in ammonia. Solvent leveling in fact makes HCl, CH_3COOH, and NH_4Cl all strong acids in ammonia, where they have equivalent acid strength.

Strong acids that are leveled in water have different acid strengths in acidic solvents such as HF or anhydrous acetic acid. For example, acid dissociation of HX in acetic acid (CH_3COOH) involves protonating the solvent to make its conjugate acid ($CH_3COOH_2^+$) and the X^- anion. Because $CH_3COOH_2^+$ is a stronger acid that H_3O^+, the anion X^- (which is a spectator in water) can become a weak base in CH_3COOH:

$$HX + CH_3COOH \rightleftharpoons CH_3COOH_2^+ + X^- \tag{15.2.11}$$

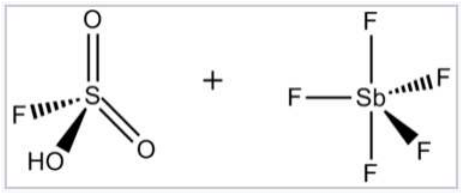
It follows that acidic solvents magnify the Brønsted basicities of substances that cannot accept protons in water. Conversely, basic solvents magnify the acidity of substances that cannot donate a proton to OH^-.

The acidity and basicity of non-aqueous solvents is difficult to quantify precisely, but one good relative measure is the Hammett acidity function, H_o. H_o is defined analogously to pH according to the Henderson-Hasselbach equation:

$$H_o = pK_a + \log(\frac{[base]}{[conjugate\ acid]}) \tag{15.2.12}$$

For non-aqueous solvents, or for acidic or basic compounds in dissolved in solvents that do not themselves dissociate, H_o is a rough measure of the pH of the solvent or compound in question. Anhydrous HF and H_2SO_4 have H_o values of approximately -10 and -12 respectively.

Superacids and superbases. The term *superacid* was originally coined by James Bryant Conant in 1927 to describe acids that were stronger than conventional mineral acids.[1] George A. Olah prepared the so-called magic acid, so-named for its ability to attack hydrocarbons, by mixing antimony pentafluoride (SbF_5) and fluorosulfonic acid (FSO_3H). The name was coined after a candle was placed in a sample of magic acid. The candle dissolved, showing the ability of the acid to protonate hydrocarbons, which under aqueous acidic conditions cannot be protonated.



Magic acid is made by mixing FSO_3H and SbF_5. Their reaction generates the $H_2SO_3F^+$ cation, which can protonate hydrocarbons.

At 140 °C , FSO_3H–SbF_5 converts methane into the tertiary-butyl carbocation, a reaction that begins with the protonation of methane:[2]

$$CH_4 + H^+ \longrightarrow CH_5^+ \tag{15.2.13}$$

$$CH_5^+ \longrightarrow CH_3^+ + H_2 \tag{15.2.14}$$

$$CH_3^+ + 3\,CH_4 \longrightarrow (CH_3)_3C^+ + 3\,H_2 \tag{15.2.15}$$

Fluoroantimonic acid, $HSbF_6$, can produce solutions with H_0 down to –28.[3] Fluoroantimonic acid is made by combining HF and SbF_5. In this system, HF releases its proton (H^+) concomitant with the binding of F^- by antimony pentafluoride, which (as described below) is a Lewis acid. The resulting anion (SbF_6-) is both a weak nucleophile and an extraordinarily weak base.

Superacids are useful in reactions such as the isomerization of alkanes. Industrially, anhydrous acid-exchanged zeolites, which are superacid catalysts, are used on a massive scale to isomerize hydrocarbons in the processing of crude oil to gasoline. Superbases such as lithium diethylamide ($LiNEt_2$), alkyllithium compounds (RLi), and Grignard reagents (RMgX) useful in a broad range of organic reactions. $LiNEt_2$ deprotonates C-H bonds to generate reactive carbanions. RLi and RMgX are powerful nucleophiles.

The use of superbases in nonaqueous media allows us to rank the acidities (and measure the pKa's) of different classes of molecules. This ranking is particularly important in understanding the reactions of organic molecules. Note that the order of acidities for hydrocarbons is alkynes >> alkenes, aromatics >> alkanes. This ordering has to do with the hybridization of the carbon atom that forms the carbanion. The negatively charged lone pair of the carbanion is stabilized in orbitals that have high s character (e.g., sp vs. sp^2 or sp^3). This is because s orbitals have finite probability density at the nucleus and "feel" the positive nuclear charge (thereby stabilizing the extra negative charge on carbon) more than p orbitals. Resonance effects also stabilize carbanions. Thus, cyclopentadiene is more acidic than even an alkyne because the negative charge is delocalized over the entire (aromatic) $C_5H_5^-$ ring when the C_5H_6 is deprotonated.

name	formula	structural formula	pKa
Methane	CH_4	Methane-2D-dimensions.svg	56
Propene	C_3H_6	Propylene skeletal.svg	44
Benzene	C_6H_6	Benzol.svg	43
Acetylene	C_2H_2	Acetylene-CRC-IR-dimensions-2D.png	25
Cyclopentadiene	C_5H_6	Cyclopentadiene.png	18

Table 1. Carbon acid acidities in pKa in DMSO [4].

Acid-base equilibria in molten salts

When a solid salt melts, it forms a solution of the cations and anions. For example, KOH melts at temperatures above 400 °C and dissociates into K^+ and OH^- ions which can act as a solvent for chemical reactions. Because of the autodissociation of the OH^- solvent, water is always present in a molten KOH flux, according to the acid-base equilibrium:

$$2\,OH^- \rightleftharpoons H_2O + O^{2-} \tag{15.2.16}$$

It follows that in this very basic solvent, water (the conjugate acid of the solvent) is the strongest acid that can exist. The conjugate base of the solvent, O^{2-}, is the strongest base. This autodissociation equilibrium allows for the acidity of a flux to be easily tuned through the addition or boiling off of water. A "wet" flux is more acidic, and can dissolve metal oxides that contain the basic O^{2-} anion. Conversely a "dry" flux is more basic and will cause oxides to precipitate. Molten hydroxide fluxes can thus be used in the synthesis of oxide crystals, such as the perovskite superconductor ($K_{1-X}Ba_XBiO_3$).[5]. Eutectic mixtures of NaOH and KOH are relatively low melting (≈ 200 °C) and can be used as solvents for crystallizing a variety of basic oxides.

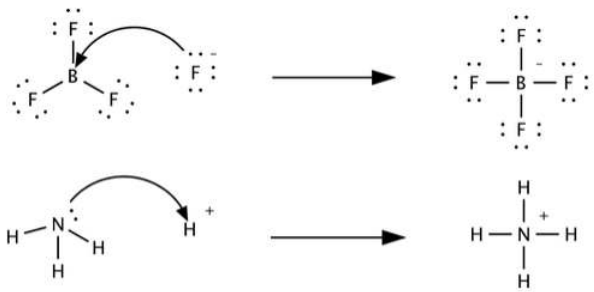
Lewis Acids and Bases

The Lewis classification of acids and bases is broader than the Brønsted-Lowry definition, and encompasses many more substances. Whereas the Brønsted-Lowry and the Arrhenius classifications are based on transfer of protons, Lewis acidity and basicity are based on the sharing of an electron pair. **Lewis acids** can accept an electron pair, while **Lewis bases** can donate an electron pair. This definition encompasses the Brønsted-Lowry definition, in that H^+ is an electron pair acceptor (when interacting with a base), and a base is an electron pair donor in its interaction with H^+. This is illustrated below for the protonation of ammonia.

Boron trifluoride, BF_3 acts as a Lewis acid when it combines with a basic ion or molecule that can donate an electron pair. Such a reaction is shown below.

\[\ce{BF3 + F^{-} <=> BF4^{-}}

Here, the acid is BF_3 and the base is F^-. This acid-base reaction allows boron (which is electron-deficient in BF_3) to complete its octet. Similarly, $AlCl_3$ is a Lewis acid that can react with Cl^- (a Lewis base) to make the Lewis "salt" $AlCl_4^-$. Note that in water Cl^- is a spectator ion (a weaker base than the solvent) in Brønsted acid-base reactions.



Additional examples of Lewis acid base reactions. In each, try to identify the acid, the base, and the salt, based on the concept that the base is the molecule or ion that donates an electron pair. In cases where you are not sure, it may help to draw the VSEPR structures of the molecules:

$$I_2 + I^- \rightleftharpoons I_3^-$$

$$AuCl_3 + Cl^- \rightleftharpoons [AuCl_4]^-$$

$$Fe^{3+} + 6\,H_2O \rightleftharpoons [Fe(H_2O)_6]^{3+}$$

$$TiF_4 + 2\,F^- \rightleftharpoons [TiF_6]^{2-}$$

$$SF_4 + SbF_5 \rightleftharpoons SSbF_9$$

In other Lewis acid base reactions both acid and base are molecules and the product is referred to as an adduct.

$$(CH_3)_3B + N(CH_3)_3 \longrightarrow (CH_3)_3B{-}N(CH_3)_3$$

$$I_2 + S(CH_3)_2 \longrightarrow I_2{-}S(CH_3)_2$$

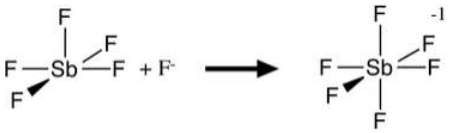
$$C_5N_5N + Cu(HFacac)_2 \longrightarrow C_5N_5N{-}Cu(HFacac)_2$$

Lewis acidity is the basis for coordination chemistry, a topic we will discuss in more detail in Chapter 5. This is because coordination chemistry involves **metal ions** that are Lewis acids, which bond to ligands that are Lewis bases.

Determining the strength of metal ion Lewis acids

There are three determining factors in the Lewis acid strength of a metal ion:
1. The higher positive charge on the metal, the more acidic it is. For example, Al^{3+} and Fe^{3+} are good Lewis acids and their salts make acidic solutions in water, but $K^+$and Na^+ are not.
2. The smaller the atomic radius of the metal ion, the more acidic it is. Going down the periodic table, the Lewis acidity of metal ions decreases (e.g., $Al^{3+} > Ga^{3+} > In^{3+}$) because the ionic radius increases.
3. For transition metal ions, more electronegative metals tend to make stronger Lewis acids. The electronegativity has maxima at W and Au in the 5d series, so metal ions near in that part of the periodic table are good Lewis acids.

Molecules with five coordinate geometries (e.g., PCl_5, AsF_5, SbF_5) are typically strong Lewis acids, because when accepting another pair of electrons from a base, they form an octahedral molecule or anion. Neither of the common five-coordinate geometries (trigonal bipyramidal or square pyramidal) is efficient in terms of packing. The Lewis acid-base reaction forms an additional bond with a relatively small energetic penalty of stretching the existing bonds:



Because F^- is a good Lewis base, and also a small anion, it can form stable octahedral anions with both main group elements and transition metals. For this reason, TiO_2 and SiO_2 dissolve in HF (but are unreactive with aqueous HCl and other strong acids):

$$TiO_2 + 4\,HF + 2\,F^- \rightleftharpoons TiF_6^{2-} + 2\,H_2O \tag{15.2.17}$$

$$SiO_2 + 4\,HF + 2\,F^- \rightleftharpoons SiF_6^{2-} + 2\,H_2O \tag{15.2.18}$$

Lewis bases stabilize high oxidation states.

An interesting example of using Lewis acid-base chemstry to drive reactions is the chemical synthesis of fluorine gas, which was devised by Karl O. Christe in 1986.[6] Christe at the time was organizing a symposium to commemorate the 100th anniversary of the isolation of elemental fluorine by Henri Moissan, which Moissan did in 1886 by electrolyzing a solution of anhydrous HF. 100 years later, there was still no direct (non-electrochemical) synthesis of F_2. Christe's reaction scheme followed two steps. The first was the known synthesis of K_2MnF_6 from $KMnO_4$:

$$4\,MnO_4^-{}_{(aq)} + 10\,H_2O_{(l)} + 24\,F^-{}_{(aq)} \longrightarrow 4\,MnF_6^{2-}{}_{(aq)} = 3\,O_{2\,(g)} + 20\,OH^-{}_{(aq)} \tag{15.2.19}$$

$$2\,K^{+}_{(aq)} + MnF_6{}^{2-}_{(aq)} \longrightarrow K_2MnF_{6\,(s)} \tag{15.2.20}$$

The second step involved reacting K_2MnF_6 with the powerful Lewis acid SbF_5, to make metastable MnF_4, which decomposes spontaneously to MnF_3 and fluorine gas:

$$K_2MnF_{6\,(s)} + 2\,SbF_{5\,(l)} \longrightarrow 2\,KSbF_{6\,(s)} + MnF_{4\,(s)} \tag{15.2.21}$$

$$MnF_{4\,(s)} \longrightarrow MnF_{3\,(s)} + \frac{1}{2}F_{2\,(g)} \tag{15.2.22}$$

This reaction teaches us something interesting and important about the connection between acid-base and redox chemistry. Acids tend to stabilize low oxidation states, and bases stabilize high oxidation states (We will see this again soon in Chapter 4, in the context of Pourbaix diagrams). Mn is stable in the +4 oxidation state in K_2MnF_6, where it is surrounded by six basic F^- anions. However, the highest stable neutral fluoride of Mn is MnF_3, and MnF_4 (transiently formed from K_2MnF_6) spontaneously decomposes to generate fluorine.

Oxide is a better base than fluoride. Interestingly, Mn can lose all its valence electrons to form Mn^{7+} in the permanganate ion, MnO_4^-. Here the 7+ oxidation state is stabilized electrostatically by coordination to four O^{2-} ions, and by the overall -1 charge on the MnO_4^- anion. Because of its 2- charge, O^{2-} is a stronger base and a better ion for stabilizing high oxidation states than F^-. This is a general trend among transition metals: the highest oxidation state is usually reached in the oxide, not in the fluoride, despite the fact that F is a more electronegative element than O. For example, Cr^{6+} is stable in the CrO_4^{2-} and $Cr_2O_7^{2-}$ anions, but not in any neutral fluoride or fluoroanion. The +8 oxidation state occurs in RuO_4 and OsO_4, but not in any fluoride of Ru or Os.

15.2: Brønsted and Lewis Acids and Bases is shared under a CC BY-SA license and was authored, remixed, and/or curated by LibreTexts.

- **3.2: Brønsted and Lewis Acids and Bases** by Chemistry 310 is licensed CC BY-SA 4.0. Original source: https://en.wikibooks.org/wiki/Introduction_to_Inorganic_Chemistry.

15.3: Hard and Soft Acids and Bases

Lewis acids and bases can be classified by designating them as hard or soft.

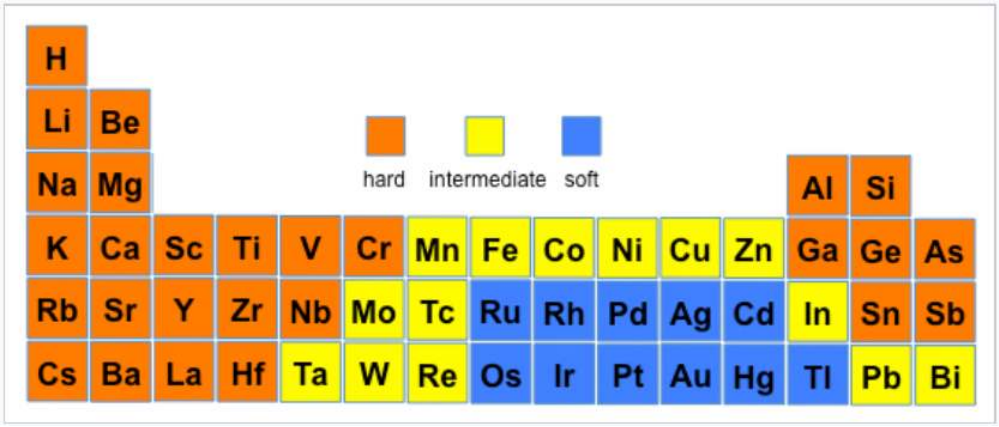
Hard Acids/Bases:

"Hard" acids and bases have a high charge (positive for acids, negative for bases) to ionic radius ratio along with higher oxidation states. Hard acids are not very polarizable and have high charge densities. Thus metal ions with high positive charges and smaller ionic sizes tend to be hard acids. Early transition metal ions in the 3d series tend to be hard Lewis acids. Hard bases are typically small anions and neutral molecules. Some examples of hard acids and bases include: H^+, O^{2-}, OH^-, F^-, Fe^{3+}, and Al^{3+}.

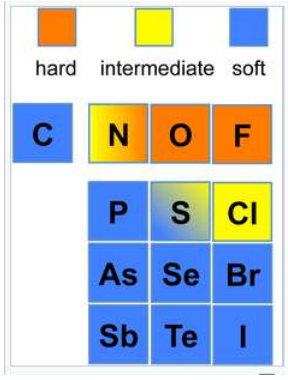
Soft Acids/Bases:

"Soft" acids or bases have a low charge to radius ratio, with low oxidation states. They are normally larger ions that are polarizable. For example, I^- and S^{2-} are soft bases and low charge density transition metals, such as Ag^+, are considered soft acids. Soft acids often include transition metals in the second and third row of the periodic table that have a +1 or +2 charge, as well as late transition metals (especially those in the 4d and 5d series) with filled or almost completely filled *d* orbitals.

Acids and bases are not strictly hard or soft, with many ions and compounds being classified as intermediate. For example, trimethylborane, Fe^{2+}, and Pb^{2+} cations are intermediate acids, and pyridine and aniline are examples of intermediate bases. An element can also change its hard/soft character depending on its oxidation state. The most extreme example is hydrogen, where H^+ is a hard acid and H^- is a soft base. Ni^{3+} (as in the layered compound NiOOH) is a hard acid, but Ni^0 (as in $Ni(CO)_4$) is a soft acid. The figures below show hard/soft trends for acids (left) and bases (right) in the periodic table. For bases, the major hard/soft discontinuity is between the 2nd row (N,O,F) and the rows below.



Hard-soft trends for acids



Hard-soft trends for bases

Like binds with Like

Hard acids interact more strongly with hard bases than they do with soft bases, and soft acids interact more strongly with soft bases than hard bases. Thus, the most stable complexes are those with hard-hard and soft-soft interactions. This tendency is illustrated in the table below, which shows the trend in formation constants for hard and soft acids. Hard acids bind halides in the order $F^- > Cl^- > Br^- > I^-$, whereas soft acids follow the opposite trend.

Log K_1	fluoride	chloride	bromide	iodide	acid classification
Fe^{3+}	6.0	1.4	0.5	-	Hard
Pb^{2+}	1.3	0.9	1.1	1.3	Intermediate
Ag^+	0.4	3.3	4.7	6.6	Soft
Hg^{2+}	1.0	6.7	8.9	12.9	Soft

The softest metal ion in the periodic table is $Au^+(aq)$. It forms stable complexes with soft bases such as phosphines and CN^-, but not with hard bases such as O^{2-} or F^-. The affinity of Au^+ for the soft base CN^- is high, and the resulting $[Au(CN)_2]^-$ complex is so stable that gold (which is normally very difficult to oxidize) can be oxidized by oxygen in the air:

$$4\,Au_{(s)} + 8\,CN^-{}_{(aq)} + O_{2\,(g)} + 2\,H_2O = 4\,[Au(CN)_2]^-{}_{(aq)} + 4\,OH^- \qquad (15.3.1)$$

This reaction is used in gold mining to separate small flakes of Au from large volumes of sand and other oxides. Ag is similarly dissolved by air oxidation in cyanide solutions. The precious metals are then isolated from the solution using chemical reducing agents or by electroplating. The use of cyanide ion on a large scale in mining, however, creates a potentially serious environmental hazard. In 2000, a spill at Baia Mare, Romania resulted in the worst environmental disaster in Europe since Chernobyl. Cyanide, which is highly toxic, is gradually oxidized by air to the less toxic cyanate (OCN^-) ion. On the laboratory scale, cyanide plating solutions are typically disposed of by using bleach to oxidize CN^- to OCN^-, and the metal is recovered as an insoluble chloride salt.



Netted solution pond next to cyanide heap leaching of gold ore near Elko, Nevada (1992).

The Au^{3+} ion, because of its higher positive charge, is a harder acid than Au^+ and can form complexes with harder bases such as H_2O and amines. In keeping with the "like binds like" principle, the compound AuI (soft-soft) is stable, but AuI_3 (hard-soft) is unknown. Conversely, AuF has never been isolated but AuF_3 (hard-hard) is stable.

15.3: Hard and Soft Acids and Bases is shared under a CC BY-SA license and was authored, remixed, and/or curated by LibreTexts.

- **3.3: Hard and Soft Acids and Bases** by Chemistry 310 is licensed CC BY-SA 4.0. Original source: https://en.wikibooks.org/wiki/Introduction_to_Inorganic_Chemistry.

15.4: The Electrostatic-Covalent (ECW) Model for Acid-Base Reactions

The classification of Lewis acids and bases as hard and soft is a useful qualitative approach to rationalize their behavior. The ECW Model is a more quantitative model that describes and predicts the strength of Lewis acid – Lewis base interactions. The strength of the acid-base interaction is measured as the enthalpy of adduct formation, $\triangle H$. Each acid is characterized by an E_A and a C_A. Each base is likewise characterized by its own E_B and C_B. The E and C parameters refer, respectively, to the electrostatic and covalent contributions to the strength of the bonds that the acid and base will form. These parameters have been empirically obtained by using enthalpies for adducts that *form only σ bonds between the acid and base as well as adducts that have no steric repulsion between the acid and base.*

$$-\Delta H = E_A E_B + C_A C_B + W$$

This equation reproduces and predicts the enthalpy change, $\triangle H$, of a reaction between many acids and a bases. $\triangle H$ is a measure of strength of the bond between the acid and the base, both in the gas phase and in weakly solvating media. The W term represents a constant energy for cleavage of a dimeric acid or base. For example, the enthalpy of cleavage of $[Rh(CO)_2Cl]_2$ by base B involves two steps. The first step is cleavage of the dimer, which is W:

$$\frac{1}{2}[Rh(CO)_2Cl]_2 \longrightarrow Rh(CO)_2Cl \;\; W = -43.5 kJ/mol \tag{15.4.1}$$

The second step is the binding of B to the $RhCl(CO)_2$ monomer. In another case, W is the enthalpy needed to cleave the internal hydrogen bonding of the H-bonding acid $(CF_3)_3COH$.

The calculation of the enthalpy of adduct formation for the reaction of pyridine, C_5H_5N and bis(hexafloroacetyacetonato)copper (II), $Cu(HFacac)_2$, shows how these parameters are used. In this case W =0 since neither the acid nor the base is a dimer. Selected parameters can be found at the Wikipedia page for the **ECW Model**

$$-\Delta H = E_A E_B + C_A C_B = (1.82)(1.78) + (2.86)(3.54) = 13.4 kcal/mol = -56.1 kJ/mol$$

$$\Delta H = -56.1 kJ/mol, \quad \Delta H_{measured} = -56.1 kJ/mol$$

However, the ΔH calculated for the reaction of Me_3B with Me_3N is less negative than that observed. This discrepancy is attributed to steric repulsion between the methyl groups on the B and N atoms. The difference between the calculated and observed values can then be taken as the amount of the steric effect, a value otherwise not attainable. Steric effects have also been identified with $(CH_3)_3SnCl$ and with $Cu(HFacac)_2$. When π bonding contributes to the measured enthalpy, the enthalpy calculated from the E and C parameters will be less than the measured enthalpy and the difference provides a measure of the extent of the π bonding contribution.

A graphical presentation of this model clearly shows that *there is no single ranking order of Lewis acid or Lewis base strengths,* a point often overlooked, and emphasizes that the magnitude of acid and base interactions requires two parameters (E & C) to account for the interactions. A **Cramer-Bopp plot**[7]using the three Lewis bases: acetonitrile, ammonia, and dimethyl sulfide illustrates that there is no unique ordering of Lewis base strengths. The Cramer-Bopp plot is a visual tool for comparing Lewis base strengths with the range of possible Lewis acid partners, and similar plots can be constructed to examine selected Lewis acids against the range of possible Lewis bases. These plots show that two properties are needed to completely define acid and base strength and that any attempt to define strength with one property or parameter is limited in its utility. For Drago's quantitative ECW model the two properties are electrostatic and covalent while for Pearson's qualitative HSAB theory the two properties are hardness and strength.

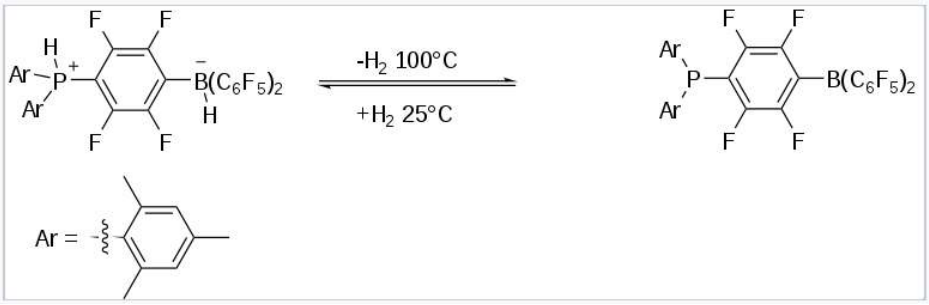
15.4: The Electrostatic-Covalent (ECW) Model for Acid-Base Reactions is shared under a CC BY-SA license and was authored, remixed, and/or curated by LibreTexts.

- **3.4: The Electrostatic-Covalent (ECW) Model for Acid-Base Reactions** by Chemistry 310 is licensed CC BY-SA 4.0. Original source: https://en.wikibooks.org/wiki/Introduction_to_Inorganic_Chemistry.

15.5: Frustrated Lewis Pairs

A **frustrated Lewis pair** (**FLP**) is a compound or mixture that contains a Lewis acid and a Lewis base which, because of steric hindrance, cannot combine to form a classical adduct.[8] Many kinds of FLPs have been devised, and their reactivity towards other molecules has been broadly developed.[9][10]

The hydrogen adduct of the original FLP, a phosphonium-borate salt, can be prepared by combining a phenylene bridged phosphinoborane and dihydrogen. The salt, which is colorless, is stable in the presence of air and moisture. It releases molecular H_2 when heated above 100 °C. This reactivity is remarkable considering the strength of the H-H bond, 432 kJ/mol.



Absorption and release of hydrogen from FLP

The discovery that some FLPs can split H_2[11] triggered the rapid growth of research into FLP's. Because of their "unquenched" reactivity, such systems are reactive toward substrates that can undergo heterolysis. For example, many FLP's split the hydrogen molecule. This reactivity suggested that FLP's can be useful for hydrogenation reactions. A sizable range of homogeneous and heterogeneous catalytic reactions have now been developed using FLP's.

Mixtures of sterically hindered Lewis acids and bases also can act as FLPs. One successful strategy is to mix sterically hindered triarylphosphines with triarylboranes. Small molecules such as CO_2 and ethylene can then form a bridge between the phosphine Lewis base and borane Lewis acid, e.g.,

$$\mathbf{P(\textit{t}\text{-}Bu)_3 + B(C_6F_5)_3 + CO_2 \longrightarrow (\textit{t}\text{-}Bu)_3P^+C(O)OB^-(C_6F_5)_3}$$

$$\mathbf{PCy_3 + B(C_6F_5)_3 + C_2H_4 \longrightarrow Cy_3P^+CH_2CH_2B^-(C_6F_5)_3}$$

Because FLPs behave at the same time as both nucleophiles and electrophiles, they can effect the ring-opening of cyclic ethers such as THF, 2,5-dihydrofuran, coumaran, and dioxane.[12]

15.5: Frustrated Lewis Pairs is shared under a CC BY-SA license and was authored, remixed, and/or curated by LibreTexts.

- **3.5: Frustrated Lewis Pairs** by Chemistry 310 is licensed CC BY-SA 4.0. Original source: https://en.wikibooks.org/wiki/Introduction_to_Inorganic_Chemistry.

15.6: Discussion Questions

- Discuss periodic trends in the Lewis acidity of metal ions.
- Explain what we mean by hard and soft acids and bases, using specific examples.
- Explain why hard and soft should not be equated with electrostatic and covalent.
- According to HSAB theory Cu and Zn are classified as intermediate acids while Cd is classified as soft. The base $(CH_2)_4O$ is considered hard while $(CH_2)_4S$ is soft. Using E and C numbers for $Cd[N(Si(CH_3)_3]_2$ and ZnTPP calculate the enthalpies for these two acids interacting with $(CH_2)_4O$ and $(CH_2)_4S$ and show that the HSAB model correctly predicts which base interacts more strongly with which acid. Do the same comparison using $Cu(HFacac)_2$ as the acid and show that HSAB fails to predict which base interacts more strongly. How are these results related to the Cramer-Bopp plot that show one property or one parameter cannot be used to rank Lewis acid or base strength?

15.6: Discussion Questions is shared under a CC BY-SA license and was authored, remixed, and/or curated by LibreTexts.

- **3.6: Discussion Questions** by Chemistry 310 is licensed CC BY-SA 4.0. Original source: https://en.wikibooks.org/wiki/Introduction_to_Inorganic_Chemistry.

15.7: Problems

1. Classify each of the substances below as an acid or base, and as strong or weak or as a spectator in the solvent listed. For each case, write out the dissociation reaction.

(a) H_3AsO_4 in water

(b) HCl in glacial acetic acid

(c) CH_3COOH in liquid ammonia

(d) H_2O in molten NaOH

(e) Cl^- in liquid ammonia

2. Write out the dissociation reactions for an acid HA and its conjugate base A^- in water. Use the equilibrium expressions for K_a and K_b to prove that $\boldsymbol{K_aK_b = K_w}$.

3. Calculate the percent ionization of 1 M acetic acid ($K_a = 1.8 \times 10^{-5}$) in water.

4. For each pair of compounds below, indicate which one is a stronger acid and explain your choice:

(a) $[Fe(H_2O)_6]^{3+}$ or $[Fe(H_2O)_6]^{2+}$

(b) H_3BO_3 or H_3PO_3

(c) $[Ga(H_2O)_6]^{3+}$ or $[Al(H_2O)_6]^{3+}$

(d) HIO_3 or HIO_4

(e) H_3PO_4 or H_2SeO_4

5. The Mg^{2+} and Cu^{2+} cations have similar ionic radii, but the acidities of aqueous nitrate solutions containing the two ions are different. Explain which ion is more acidic and why.

6. Cobalt reacts with excess fluorine to make CoF_3, but higher oxidation states of cobalt do not exist in binary fluorides. However, Co(IV) is stable in oxides such as CoO_2 and $BaCoO_3$. Explain why these oxides can stabilize a higher oxidation state of cobalt than fluorides.

7. (a) When solutions of the hydrosulfide (SH^-) salts of As^{3+}, Sb^{3+}, and Sn^{4+} are reacted with aqueous solutions of ammonium hydrosulfide ($NH_4^+SH^-$), the sulfide salts As_2S_3, Sb_2S_3, and SnS_2 precipitate. When excess aqueous Na_2S is added, however, these sulfides re-dissolve to form soluble anionic complexes. In contrast, solutions of Cu^{2+}, Pb^{2+}, Hg^{2+}, Bi^{3+} and Cd^{2+} precipitate as solid sulfides but do not re-dissolve in solutions that contain excess sulfide. We may consider the first group of ions to be amphoteric for soft acid-base reactions that involve SH^- instead of OH^-. The second group is more basic (less acidic) in the sense that it does not react with excess soft base. Use this information to locate the amphoteric diagonal in the periodic table for sulfides. Compare this with the diagonal that defines the amphoteric oxides, which dissolve in either acidic or basic solutions. Does your analysis agree with the description of S^{2-} as a softer base than O^{2-}?

(b) Au^+ is also precipitated by SH^- ions, and the sulfide Au_2S redissolves to form a soluble complex in excess SH^-. Does this fit the trend you discovered in part (a)? Does it make sense in terms of the electronegativity of Au? Explain.

8. Calculate the enthalpy for the adduct $(CH_3)_3B\text{-}N(CH_3)_3$ and compare it to the measured value of -73.6 kJ/mol. Parameters can be found at ECW Model.

9. Calculate the enthalpy for the adduct formation for the Lewis acid $(CH_3)_3SnCl$ with each of the following Lewis bases $(C_2H_5)_2O$, $(CH_2)_4O$, and CH_3CN. Their respective measured enthalpies are -9.2, -21.3 and -20.1 kJ/mol. Explain the any differences between the calculated and measured enthalpies. Parameters can be found at ECW Model.

10. Refer to the Cramer-Bopp plot found at ECW Model and indicate the order of Lewis base strength for

(a) An acid with Ra = -0.5

(b) An acid with Ra = 0.33

(c) An acid with Ra = -0.9

11. The Lewis acid $[Rh(CO)_2Cl]_2$ has a W value of -43.47 kJ/mol

(a) What does W refer to?

(b) The E, C, and W parameters found at ECW Model give the enthalpy for forming one mole adduct, that is, $\mathbf{B + \frac{1}{2}[RH(CO)_2Cl]_2 \longrightarrow B{-}RhCl(CO)_2}$

(1) What is the heat of dissociation of one mole of $[Rh(CO)_2Cl]_2$?

(2) What is the enthalpy of $\mathbf{2\,B + [Rh(CO)_2Cl]_2 \longrightarrow 2\,B{-}RhCl(CO)_2}$

(3) Calculate the enthalpy per mol of B- $RhCl(CO)_2$ for C_5H_5N, $(CH_3)_2CO$

15.7: Problems is shared under a CC BY-SA license and was authored, remixed, and/or curated by LibreTexts.

- **3.7: Problems** by Chemistry 310 is licensed CC BY-SA 4.0. Original source: https://en.wikibooks.org/wiki/Introduction_to_Inorganic_Chemistry.

15.8: References

1. Hall NF, Conant JB (1927). "A Study of Superacid Solutions". *Journal of the American Chemical Society* **49** (12): 3062–70. doi:10.1021/ja01411a010.
2. George A. Olah, Schlosberg RH (1968). "Chemistry in Super Acids. I. Hydrogen Exchange and Polycondensation of Methane and Alkanes in FSO_3H–SbF_5 ("Magic Acid") Solution. Protonation of Alkanes and the Intermediacy of CH_5^+ and Related Hydrocarbon Ions. The High Chemical Reactivity of "Paraffins" in Ionic Solution Reactions". *Journal of the American Chemical Society* **90** (10): 2726–7. doi:10.1021/ja01012a066.
3. Herlem, Michel (1977). "Are reactions in superacid media due to protons or to powerful oxidising species such as SO_3 or SbF_5?". *Pure & Applied Chemistry* **49**: 107–113. doi:10.1351/pac197749010107.
4. *Equilibrium acidities in dimethyl sulfoxide solution* Frederick G. Bordwell Acc. Chem. Res.; **1988**; 21(12) pp 456 - 463; DOI:10.1021/ar00156a004
5. R. J. Cava, et al. (1988). "Superconductivity near 30 K without copper: the $Ba_{0.6}K_{0.4}BiO_3$ perovskite". *Nature* **332**: 814–6. doi:10.1038/332814a0.
6. Christe, Karl O. (1986). "Chemical synthesis of elemental fluorine". Inorganic Chemistry 25 (21): 3721. doi:10.1021/ic00241a001.
7. Cramer RE, Bopp TT (1977). "Great E and C plot. Graphical display of the enthalpies of adduct formation for Lewis acids and bases". *Journal of Chemical Education* **54** (10): 612–613. doi:10.1021/ed054p612.
8. Stephan, D. W. (2008). "Frustrated Lewis pairs: a concept for new reactivity and catalysis". *Org. Biomol. Chem.* **6**: 1535–1539. doi:10.1039/b802575b.
9. Stephan, D. W.; Erker, G. (2010). "Frustrated Lewis Pairs: Metal-free Hydrogen Activation and More". *Angewandte Chemie International Edition* **49** (1): 46–76. doi:10.1002/anie.200903708. ISSN 1433-7851.
10. Stephan, D. W.; Erker, G. (2017). "Frustrated Lewis pair chemistry". *Philosophical Transactions of the Royal Society A: Mathematical, Physical and Engineering Sciences* (Royal Society) **375** (2101): 20170239. doi:10.1098/rsta.2017.0239. ISSN 1364-503X. PMID 28739971. Bibcode: 2017RSPTA.37570239S.
11. Welch, G. C.; San Juan, R. R.; Masuda, J. D.; Stephan, D. W. (2006). "Reversible, Metal-Free Hydrogen Activation". *Science* **314** (5802): 1124–1126. doi:10.1126/science.1134230. ISSN 0036-8075. PMID 17110572. Bibcode: 2006Sci...314.1124W.
12. Birkmann, B., et al. (2010). "Frustrated Lewis Pairs and Ring-Opening of THF, Dioxane, and Thioxane". *Organometallics* **29**: 5310–5319. doi:10.1021/om1003896.

15.8: References is shared under a CC BY-SA license and was authored, remixed, and/or curated by LibreTexts.

- **3.8: References** by Chemistry 310 is licensed CC BY-SA 4.0. Original source: https://en.wikibooks.org/wiki/Introduction_to_Inorganic_Chemistry.

CHAPTER OVERVIEW

16: Redox Stability and Redox Reactions

Learning Objectives

- Balance complex oxidation-reduction reactions by the ion-electron method.
- Understand periodic trends in the activity series and electrochemical series.
- Use the Nernst equation to determine half-cell and cell potentials.
- Derive the stability field of water and use this to rationalize aqueous redox chemistry.
- Construct and be proficient with Latimer diagrams, using them to determine unknown reduction potential values and to quickly identify stable and unstable species.
- Construct and be proficient with Frost diagrams, using them to identify stable and unstable species, as well as those that are strong oxidizers.
- Construct and be proficient with Pourbaix diagrams, using them to identify redox and non-redox reactions, reactions that are and are not pH-dependent, and ultimately to predict and rationalize stability, reactivity, corrosion, and passivation.

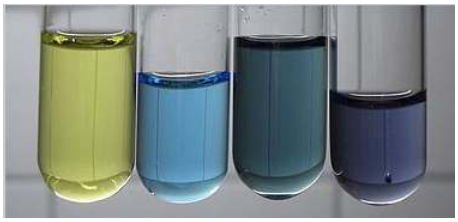
In redox reactions, one element or compound is reduced (gains electrons) and another is oxidized (loses electrons). In terms of everyday life, redox reactions occur all of the time around us. For example, the metabolism of sugars to CO_2, which stores energy in the form of ATP, is a redox reaction. Another example of redox is fire or combustion, such as in a car engine. In a car engine, hydrocarbons in the fuel are oxidized to carbon dioxide and water, while oxygen is reduced to water. Corrosion (i.e. the formation of rust on iron) is a redox reaction involving oxidation of a metal.

16.1: Prelude to Redox Stability and Redox Reactions
16.2: Balancing Redox Reactions
16.3: Electrochemical Potentials
16.4: Latimer and Frost Diagrams
16.5: Redox Reactions with Coupled Equilibria
16.6: Pourbaix Diagrams
16.7: Discussion Questions
16.8: Problems
16.9: References

16: Redox Stability and Redox Reactions is shared under a CC BY-SA license and was authored, remixed, and/or curated by LibreTexts.

16.1: Prelude to Redox Stability and Redox Reactions

In redox reactions, one element or compound is reduced (gains electrons) and another is oxidized (loses electrons). In terms of everyday life, redox reactions occur all of the time around us. For example, the metabolism of sugars to CO_2, which stores energy in the form of ATP, is a redox reaction. Another example of redox is fire or combustion, such as in a car engine. In a car engine, hydrocarbons in the fuel are oxidized to carbon dioxide and water, while oxygen is reduced to water. Corrosion (i.e. the formation of rust on iron) is a redox reaction involving oxidation of a metal.



Oxidation states of vanadium in acidic solution. From left to right the oxidation state goes from +5 to +2. These four oxidation states form the basis of the vanadium flow battery, a storage device for electricity generated from sunlight and wind.[1]

Oxidation-reduction reactions are important to understanding inorganic chemistry for several reasons:

- Transition metals can have multiple oxidation states
- Main group elements (N, halogens, O, S...) also have multiple oxidation states and important redox chemistry
- Many inorganic compounds catalyze redox reactions (which are especially useful in industrial and biological applications)
- Energy conversion and storage technologies (solar water splitting, batteries, electrolyzers, fuel cells) rely on inorganic redox reactions and catalysis
- Electrochemistry provides a way to measure equilibrium constants for dissolution/precipitation, complexation, and other reactions.
- Reaction mechanisms in organometallic chemistry (oxidative addition, reductive elimination) involve changes in the oxidation states of metals.

Not all oxidizers and reducers are created equal. The electrochemical series ranks substances according to their oxidizing and reducing power, i.e., their standard electrode potential. Strong oxidizing agents are typically compounds with elements in high oxidation states or with high electronegativity, which gain electrons in the redox reaction. Examples of strong oxidizers include hydrogen peroxide, permanganate, and osmium tetroxide. Reducing agents are typically electropositive elements such as hydrogen, lithium, sodium, iron, and aluminum, which lose electrons in redox reactions. Hydrides (compounds that contain hydrogen in the formal -1 oxidation state), such as sodium hydride, sodium borohydride and lithium aluminum hydride, are often used as reducing agents in organic and organometallic reactions.

16.1: Prelude to Redox Stability and Redox Reactions is shared under a CC BY-SA license and was authored, remixed, and/or curated by LibreTexts.

- **4.1: Prelude to Redox Stability and Redox Reactions** by Chemistry 310 is licensed CC BY-SA 4.0. Original source: https://en.wikibooks.org/wiki/Introduction_to_Inorganic_Chemistry.

16.2: Balancing Redox Reactions

In studying redox chemistry, it is important to begin by learning to balance electrochemical reactions. Simple redox reactions (for example, $H_2 + I_2 \rightarrow 2\ HI$) can be balanced by inspection, but for more complex reactions it is helpful to have a foolproof, systematic method. The **ion-electron method** allows one to balance redox reactions regardless of their complexity. We illustrate this method with two examples.

Example 1:
I^- is oxidized to **IO_3^-** by **MnO_4^-**, which is reduced to **Mn^{2+}**.

How can this reaction be balanced? In the ion-electron method we follow a series of four steps:

Step 1A: Write out the (unbalanced) reaction and identify the elements that are undergoing redox.

$\mathbf{Mn}O_4^- + \mathbf{I}^- \rightarrow \mathbf{I}O_3^- + \mathbf{Mn}^{2+}$ (The elements undergoing redox are **Mn** and **I**)

Step 1B: Separate the reaction into two **half reactions**, balancing the element undergoing redox in each.

$\mathbf{Mn}O_4^- \rightarrow \mathbf{Mn}^{2+}$
$\mathbf{I}^- \rightarrow \mathbf{I}O_3^-$

Step 2A: Balance the **oxygen** atoms by adding water to one side of each half reaction.

$Mn\mathbf{O_4}^- \rightarrow Mn^{2+} + 4H_2\mathbf{O}$
$3H_2\mathbf{O} + I^- \rightarrow I\mathbf{O_3}^-$

Step 2B: Balance the **hydrogen** atoms by adding H^+ ions.

$\mathbf{8H}^+ + MnO_4^- \rightarrow Mn^{2+} + \mathbf{4H_2}O$

The left side has a net charge of **+7** and the right side has a net charge of **+2**

$\mathbf{3H_2}O + I^- \rightarrow IO_3^- + \mathbf{6H}^+$

The left side has a net charge of **-1** and the right side has a net charge of **+5**

Step 2C: Balance the overall charge by adding **electrons**

$8H^+ + \mathbf{5e}^- + MnO_4^- \rightarrow Mn^{2+} + 4H_2O$

The left side has a charge of **+2** while the right side has a charge of **+2**. They are balanced.

$3H_2O + I^- \rightarrow IO_3^- + 6H^+ + \mathbf{6e}^-$

The left side has a charge of **-1** while the right side has a charge of **-1**. They are balanced.
Note: We did not need to explicitly determine the oxidation states of Mn or I to arrive at the correct number of electrons in each half reaction.

Step 3: Combine the half reactions so that there are equal numbers of electrons on the left and right sides

6 $(8H^+ + \mathbf{5e}^- + MnO_4^- \rightarrow Mn^{2+} + 4H_2O)$
5 $(3H_2O + I^- \rightarrow IO_3^- + 6H^+ + \mathbf{6e}^-)$

$48H^+ + \mathbf{30e}^- + 15H_2O + 6MnO_4^- + 5I^- \rightarrow 5IO_3^- + 6Mn^{2+} + 24H_2O + \mathbf{30e}^- + 30H^+$
Cancel the **H^+**, **electrons**, and **water**:
~~$48H^+$~~ + ~~$30e^-$~~ + ~~$15H_2O$~~ + $6MnO_4^- + 5I^- \rightarrow 5IO_3^- + 6Mn^{2+}$ + ~~$24H_2O$~~ + ~~$30e^-$~~ + ~~$30H^+$~~

The overall balanced reaction is therefore:
$\mathbf{18H^+ + 6MnO_4^- + 5I^- \rightarrow 5IO_3^- + 6Mn^{2+} + 9H_2O}$

Check your work by making sure that all **elements** and **charges** are balanced.

Step 4: If the reaction occurs under basic conditions, we add $\mathbf{OH^-}$ to each side to cancel $\mathbf{H^+}$
$\mathbf{18H^+}$ + $\mathbf{18OH^-}$ + $6MnO_4^-$ + $5I^-$ → $5IO_3^-$ + $6Mn^{2+}$ + $\mathbf{9H_2O}$ + $\mathbf{18OH^-}$

The $\mathbf{18H^+}$ + $\mathbf{18OH^-}$ will become $\mathbf{18H_2O}$ so the overall balanced reaction is:

$\mathbf{9H_2O + 6MnO_4^- + 5I^- \rightarrow 5IO_3^- + 6Mn^{2+} + 18OH^-}$

Again, it is a good idea to check and make sure that all of the elements are balanced, and that the charge is the same on both sides. If this is not the case, you need to find the error in one of the earlier steps.

Example 2:
Redox reaction of $\mathbf{S_2O_3^{2-}}$ and $\mathbf{H_2O_2}$
$\mathbf{S_2O_3^{2-}}$ + $\mathbf{H_2O_2}$ → $\mathbf{S_4O_6^{2-}}$ + $\mathbf{H_2O}$

Which elements are undergoing redox? **S** and **O**

Step 1: Write out half reactions, balancing the element undergoing redox

$\mathbf{2S_2O_3^{2-} \rightarrow S_4O_6^{2-}}$
$\mathbf{H_2O_2 \rightarrow 2H_2O}$

Step 2A: Balance oxygen (already balanced)

Step 2B: Balance hydrogen:

$\mathbf{2S_2O_3^{2-} \rightarrow S_4O_6^{2-}}$
$\mathbf{H_2O_2 + 2H^+ \rightarrow 2H_2O}$

Step 2C: Balance charge by adding electrons:

$\mathbf{2S_2O_3^{2-} \rightarrow S_4O_6^{2-} + 2e^-}$
$\mathbf{H_2O_2 + 2H^+ + 2e^- \rightarrow 2H_2O}$

Step 3: Combine the half reactions so that there are equal numbers of electrons on the left and right sides (already equal)
Overall balanced reaction:

$\mathbf{2S_2O_3^{2-} + H_2O_2 + 2H^+ \rightarrow S_4O_6^{2-} + 2H_2O}$

Note that again, we did not need to know the formal oxidation states of S or O in the reactants and products in order to balance the reaction. In this case, assigning the oxidation states would be rather complex, because $S_2O_3^{2-}$ and $S_4O_6^{2-}$ both contain sulfur in more than one oxidation state.

16.2: Balancing Redox Reactions is shared under a CC BY-SA license and was authored, remixed, and/or curated by LibreTexts.

- **4.2: Balancing Redox Reactions** by Chemistry 310 is licensed CC BY-SA 4.0. Original source: https://en.wikibooks.org/wiki/Introduction_to_Inorganic_Chemistry.

16.3: Electrochemical Potentials

In electrochemical cells, or in redox reactions that happen in solution, the thermodynamic driving force can be measured as the **cell potential**. Chemical reactions are spontaneous in the direction of -ΔG, which is also the direction in which the cell potential (defined as $E_{cathode}$ - E_{anode}) is positive. A cell operating in the **spontaneous** direction (for example, a battery that is discharging) is called a **galvanic cell**. A cell that is being driven in the **non-spontaneous** direction is called an **electrolytic cell**. For example, let us consider the reaction of hydrogen and oxygen to make water:

$$2\,H_{2\,(g)} + O_{2\,(g)} = 2\,H_2O_{(l)} \tag{16.3.1}$$

Thermodynamically, this reaction is spontaneous in the direction shown and has an overall standard free energy change (ΔG°) of -237 kJ per mole of water produced.

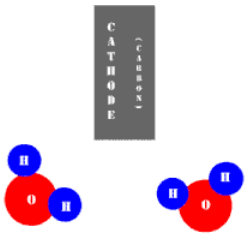
When this reaction occurs electrochemically in the spontaneous direction (e.g., in a hydrogen-air fuel cell), the two half cell reactions that occur are:

Anode: $H_{2\,(g)} \longrightarrow 2\,H^+_{(aq)} + 2\,e^-$

Cathode: $O_{2\,(g)} + 4\,H^+_{(aq)} + 4\,e^- \longrightarrow 2\,H_2O_{(l)}$

Here the anode is the negative electrode and the cathode is the positive electrode; under conditions of very low current density (where there are minimal resistive losses and kinetic overpotentials), the potential difference we would measure between the two electrodes would be 1.229 V.

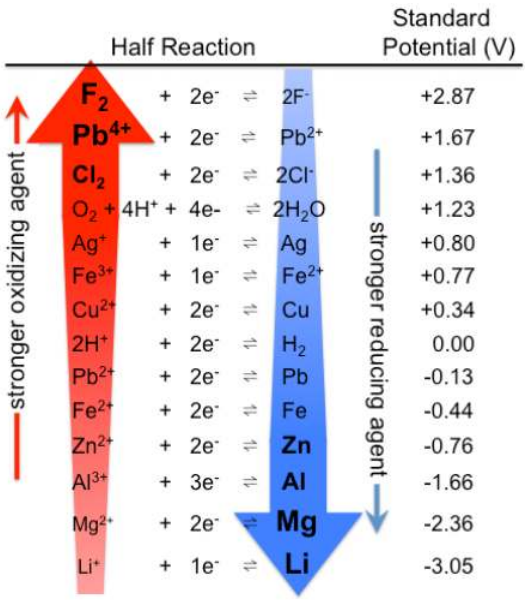
In an **electrolytic cell**, this reaction is run in reverse. That is, we put in electrical energy to split water into hydrogen and oxygen molecules. In this case, the half reactions (and their standard potentials) reverse. O_2(g) bubbles form at the anode and H_2(g) is formed at the cathode. Now the **anode** is the **positive** electrode and the **cathode** is **negative**. Electrons are extracted from the substance at the anode (water) and pumped into the solution at the cathode to make hydrogen. An animation of the cathode half reaction is shown below.



In both galvanic and electrolytic cells, **oxidation** occurs at the **anode** and **reduction** occurs at the **cathode**.

Half-cell potentials

As noted above, the equilibrium voltage of an electrochemical cell is proportional to the free energy change of the reaction. Because electrochemical reactions can be broken up into two half-reactions, it follows that the potentials of half reactions (like free energies) can be added and subtracted to give an overall value for the reaction. If we take the **standard hydrogen electrode** as our reference, i.e., if we assign it a value of zero volts, we can measure all the other half cells against it and thus obtain the voltage of each one. This allows us to rank redox couples according to their **standard reduction potentials** (or more simply their **standard potentials**), as shown in the table below.



Note that when we construct an electrochemical cell and calculate the voltage, we simply take the difference between the half cell potentials and do not worry about the number of electrons in the reaction. For example, for the displacement reaction in which silver ions are reduced by copper metal, the reaction is:

$$2\,Ag^{+}{}_{(aq)} + Cu_{(s)} = 2\,Ag_{(s)} + Cu^{2+}{}_{(aq)}$$

The two half-cell reactions are:

$$Ag^{+}_{(aq)} + e^{-} = Ag_{(s)} \quad +0.80V$$

$$Cu^{2+}_{(aq)} + 2e^{-} = Cu_{(s)} \quad +0.34V$$

and the standard potential $E^{o} = +0.80 - 0.34V = +0.46V$

The reason we don't need to multiply the Ag potential by 2 is that E^{o} is a measure of the free energy change **per electron**. Dividing the free energy change by the number of electrons (see below) makes E^{o} an **intensive property** (like pressure, temperature, etc.).

Relationship between E and ΔG. For systems that are in equilibrium, $\Delta G^{o} = -nFE^{o}_{cell}$, where n is number of moles of electrons per mole of products and F is the Faraday constant, ~96485 C/mol. Here the ^{o} symbol indicates that the substances involved in the reaction are in their standard states. For example, for the water electrolysis reaction, the standard states would be pure liquid water, H^{+} at 1M concentration (or more precisely, at unit activity), and O_2 and H_2(g) at 1 atmosphere pressure.

More generally (at any concentration or pressure), $\Delta G = -nFE$, where

$$E = E^{o} - \frac{RT}{nF} * lnQ \tag{16.3.2}$$

,

or at 298 K

$$E = E^{o} - \frac{0.0592}{n} * \log Q \tag{16.3.3}$$

where Q is the concentration ratio of products over reactants, raised to the powers of their coefficients in the reaction. This equation (in either form) is called the Nernst equation. The second term in the equation, when multiplied by -nF, is RT*lnQ. This is the free energy difference between ΔG and ΔG°. We can think of this as an entropic term that takes into account the positive entropy change of dilution, or the negative entropy change of concentrating a reactant or product, relative to its standard state.

Using the Nernst equation

Example 1:

For the half reaction $\mathbf{2H^+ + 2e^- = H_2}$, $E°_{1/2}$ = 0.000 V (by definition)

What is $E_{1/2}$ at pH 5 and P_{H_2} = 1 atm?
$\mathbf{pH = -\log[H^+] = 5}$, so $[H^+] = 10^{-5}$ M

$$E = E^o - \frac{0.0592}{2} * \log \frac{P_{H2}}{(H^+)^2} = E^o - \frac{0.0592}{2} * \log (10^5)^2 = E^o - \frac{0.0592}{2}(10) \qquad (16.3.4)$$
$$= 0.000 - 0.296 = -0.296V$$

Example 2:

What is the potential of a fuel cell (a galvanic H_2/O_2 cell) operating at pH 5?

Overall reaction: $\mathbf{2H_{2(g)} + O_{2(g)} = 2H_2O_{(l)}}$

In this reaction, H_2 is oxidized to H^+ and O_2 is reduced to H_2O. According to our convention, we write out and balance both half-cell reactions as reductions. For convenience, we do this in acid. (It is left as an exercise to the interested reader to try to work the problem in base)

Half cell reactions:

$\mathbf{2H_{2(g)} = 4H^+ + 4e^-}$

$\mathbf{O_{2(g)} + 4H^+_{(aq)} + 4e^- = 2H_2O_{(l)}}$



Toyota fuel cell hybrid bus. The bus runs on electrical energy obtained directly from the H_2/O_2 reaction. Individual fuel cells are connected in series to make a power train that charges a battery pack and drives an electric motor. Although the standard potential of the reaction is 1.23 V, because of kinetic overpotentials each fuel cell in the power train operates at a voltage of about 0.70 V. Despite this energy loss, the fuel cell system is still about twice as efficient as a combustion engine performing the same reaction.

To solve this problem we need to find the difference between the H_2/ H^+ and O_2/H_2O half cell potentials at pH 5.

$\mathbf{2H^+ + 2e^- \longrightarrow H_2}$ $E°_{1/2}$ = 0.000 V

Like all standard potentials, this is written as a reduction. We need to reverse it and change the sign of E^o since H_2 is being oxidized:

$\mathbf{H_2 \longrightarrow 2H^+ + 2e^-}$ $E°_{1/2}$ = -0.000 V

and add the standard potential of the substance being reduced at the cathode:

$O_2 + 4H^+ + 4e^- \longrightarrow 2H_2O$ $E°_{1/2}$ = +1.229 V

The difference between the two standard half cell potentials is +1.229 - 0.000 = +1.229 V

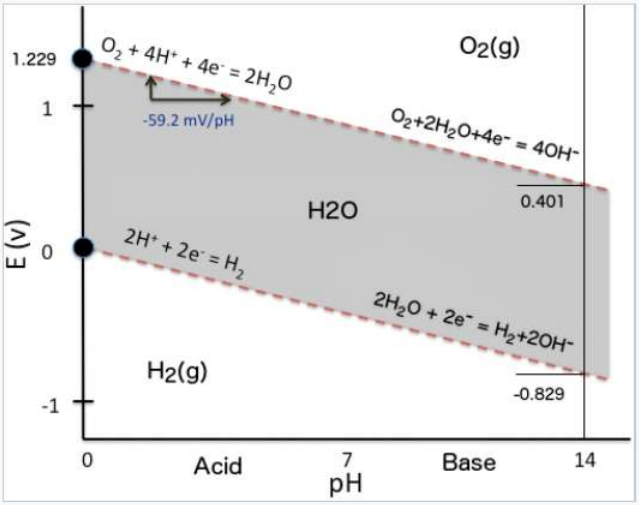
$E°_{cell}$ = +1.229 Volts

We now use the Nernst equation to account for the fact that H^+ is not in its standard state:

$$E_{cell} = E^o - \frac{0.0592}{4} * log\frac{[H^+]^4}{P_{O2}P_{H2}^2[H^+]^4} = E^o - \frac{0.0592}{4} * log(1) = E^o = +1.229V \quad (16.3.5)$$

Note that the value of E_{cell} **does not change** with pH since **both couples shift -59.2 mV/pH** according to the Nernst equation. This is the consequence of the fact that the number of electrons equals the number of protons in each of the half cell reactions. Another way to rationalize this result is to remember that the overall reaction ($2H_2 + O_2 = 2H_2O$) does not involve H^+ as a reactant or product, so ΔG and E should be independent of pH.

We can plot the shift in the H_2/H^+ and O_2/H_2O half-cell potentials with pH on a potential-pH diagram (also called a Pourbaix diagram) as shown below. The pH-dependent potentials of the H_2 and O_2 couples are shown as dotted lines. Notice that the potential difference between them is always 1.23 V. The dark circles represent the standard potentials.



Pourbaix diagram for water.

Pourbaix diagrams are essentially electrochemical **phase diagrams**, which plot regions of thermodynamic stability for redox-active substances. As in other kinds of phase diagrams, the lines represent conditions under which two phases coexist in equilibrium. The shaded area in the water Pourbaix diagram represents the conditions of potential and pH where liquid water is stable relative to hydrogen or oxygen. Outside the shaded region, water is thermodynamically unstable and is reduced to H_2(g) or oxidized to O_2(g). Although these processes are spontaneous in the thermodynamic sense (for example, water is unstable in the presence of Pb^{4+}, Cl_2, Fe, Zn, or Al), they are kinetically slow and require catalysis to proceed.

16.3: Electrochemical Potentials is shared under a CC BY-SA license and was authored, remixed, and/or curated by LibreTexts.

- **4.3: Electrochemical Potentials** by Chemistry 310 is licensed CC BY-SA 4.0. Original source: https://en.wikibooks.org/wiki/Introduction_to_Inorganic_Chemistry.

16.4: Latimer and Frost Diagrams

In addition to Pourbaix diagrams, there are two other kinds of redox stability diagrams known as Latimer and Frost diagrams. Each of these diagrams contains similar information, but one representation may be more useful in a given situation than the others.

Latimer and Frost diagrams help predict stability relative to higher and lower oxidation states, usually at one fixed pH. Pourbaix diagrams help understand pH-dependent equilibria, which are often coupled to solubility equilibria and corrosion (which will be talked about more later).



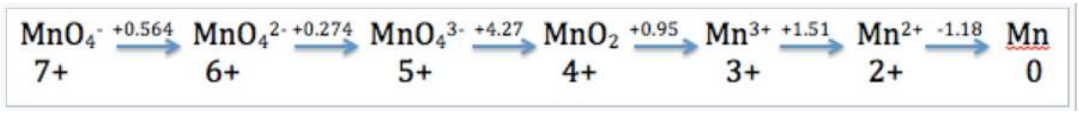
Manganese nodules on the sea floor contain Mn in oxidation states 2+, 3+, and 4+.

Latimer diagrams:

Latimer diagrams are the oldest and most compact way to represent electrochemical equilibria for substances that have multiple oxidation states. Electrochemical potential values are written for successive redox reactions (from highest to lowest oxidation state), typically under standard conditions in either strong acid ($[H^+]$ = 1 M, pH 0) or strong base ($[OH^-]$ = 1 M, pH 14). The oxidation states of successive substances in a Latimer diagram can differ by one or more electrons. Oxidation states for the element undergoing redox are typically determined by difference; we assign the oxygen atoms an oxidation state of -2 and the hydrogen atoms an oxidation state of +1.

Example:

Mn in Acid



The Latimer diagram for Mn illustrates its standard reduction potentials (in 1 M acid) in oxidation states from +7 to 0.

The Latimer diagram compresses into shorthand notation all the standard potentials for redox reactions of the element Mn. For example, the entry that connects Mn^{2+} and Mn gives the potential for the half-cell reaction:

$\mathbf{Mn^{2+}_{(aq)} + 2\,e^- \longrightarrow Mn_{(s)}}$ $E_{1/2}° = -1.18V$

and the entry connecting Mn^{4+} and Mn^{3+} represents the reaction:

$\mathbf{MnO_{2\,(s)} + 4\,H^+_{(aq)} + e^- \longrightarrow Mn^{3+}_{(aq)} + 2\,H_2O_{(l)}}$, :$E_{1/2}° = +0.95V$

We can also calculate values for **multi-electron reactions** by first adding $\Delta G°(=-nFE°)$ values and then dividing by the total number of electrons

For example, for the 5-electron reduction of MnO_4^- to Mn^{2+}, we write

$$E^o = \frac{1(0.564) + 1(0.274) + 1(4.27) + 1(0.95) + 1(1.51)}{5} = +1.51V \qquad (16.4.1)$$

and for the three-electron reduction of $MnO_4^-(aq)$ to $MnO_2(s)$,

$$E^o = \frac{1(0.564) + 1(0.274) + 1(4.27)}{3} = +1.70V \quad (16.4.2)$$

Remember to divide by the number of electrons involved in the oxidation number change (5 and 3 for the above equations).

Thermodynamically stable and unstable oxidation states

An unstable species on a Latimer diagram will have a lower standard potential to the left than to the right.

Example:

\(\ce{2MnO4^{3-} -> MnO2 + MnO4^{2-}}\) the MnO_4^{3-} species is unstable

$E^o = +4.27 - 0.274 = 3.997V$ (spontaneous disproportionation)

Which Mn species are unstable with respect to disproportionation?

MnO_4^{3-} 5+ → 6+,4+

Mn^{3+} 3+ → 4+,2+

So stable species are: MnO_4^-, MnO_4^{2-}, MnO_2, Mn^{2+}, and Mn^0.

But $\mathbf{MnO_4^{2-}}$ is also unstable - why?

$\mathbf{MnO_4^{2-} \longrightarrow MnO_2}$

$\mathbf{2\,MnO_4^{2-} \longrightarrow 2\,MnO_4^- + MnO_2}$ E° = 2.272 - 0.564 = +1.708 V

Moral: All possible disproportionation reactions must be considered in order to determine stability (this is often more convenient with a Frost diagram).

> **Note**
>
> Thermodynamically unstable ions can be quite stable kinetically. For example, most N-containing molecules (NO_2, NO, N_2H_4) are unstable relative to the elements (O_2, N_2, H_2), but they are still quite stable kinetically.

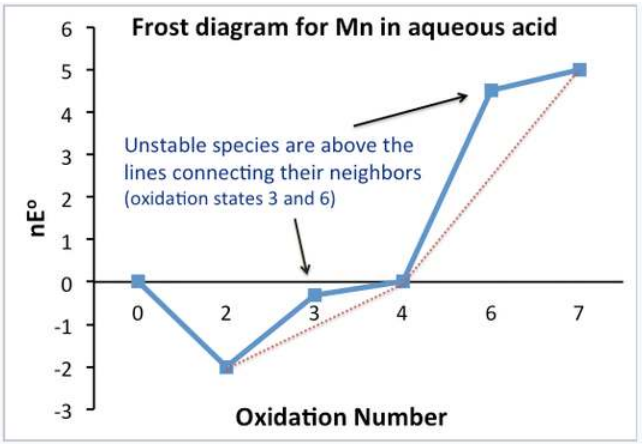
Frost diagrams:

In a Frost diagram, we plot ΔG°/F (= nE°) vs. oxidation number. The zero oxidation state is assigned a nE° value of zero.[2]

Stable and **unstable oxidation states** can be easily identified in the plot. Unstable compounds are higher on the plot than the line connecting their neighbors. Note that this is simply a graphical representation of what we did with the Latimer diagram to determine which oxidation states were stable and unstable.

The **standard potential** for any electrochemical reaction is given by the **slope** of the line connecting the two species on a Frost diagram. For example, the line connecting Mn^{3+} and MnO_2 on the Frost diagram has a slope of +0.95, the standard potential of

MnO_2 reduction to Mn^{3+}. This is the number that is written above the arrow in the Latimer diagram for Mn. Multielectron potentials can be calculated easily by connecting the dots in a Frost diagram.



A Frost diagram:

Contains the same information as in a Latimer diagram, but graphically shows stability and oxidizing power.

The lowest species on the diagram are the most stable (Mn^{2+}, MnO_2)

The highest species on diagram are the strongest oxidizers (MnO_4^-)

16.4: Latimer and Frost Diagrams is shared under a CC BY-SA license and was authored, remixed, and/or curated by LibreTexts.

- **4.4: Latimer and Frost Diagrams** by Chemistry 310 is licensed CC BY-SA 4.0. Original source: https://en.wikibooks.org/wiki/Introduction_to_Inorganic_Chemistry.

16.5: Redox Reactions with Coupled Equilibria

Redox Reactions with Coupled Equilibria

Coupled equilibria (solubility, complexation, acid-base, and other reactions) change the value of E°, effectively by changing the concentrations of free metal ions. We can use the Nernst equation to calculate the value of E° from the equilibrium constant for the coupled reaction. Alternatively, we can measure the half-cell potential with and without the coupled reaction to get the value of the equilibrium constant. This is one of the best ways to measure K_{sp}, K_a, and K_d values.

As an example, we consider the complexation of Fe^{2+} and Fe^{3+} by CN^- ions:

$$Fe^{2+}{}_{(aq)} + 6\,CN^-{}_{(aq)} \longrightarrow [Fe(CN)_6]^{4-} \tag{16.5.1}$$

$$Fe^{3+}{}_{(aq)} + 6\,CN^-{}_{(aq)} \longrightarrow [Fe(CN)_6]^{3-} \tag{16.5.2}$$

Which oxidation state of Fe is more strongly complexed by CN^-? We can answer this question by measuring the standard half-cell potential of the $[Fe(CN)_6]^{3-/4-}$ couple and comparing it to that of the $Fe^{3+/2+}$couple:

$Fe^{3+}{}_{(aq)} + e^- = Fe^{2+}{}_{(aq)}$ E° = +0.77 V (3)

$[Fe(CN)_6]^{3-} + 3^- = [Fe(CN)_6]^{4-}$ E° = +0.42 V (4)

Iron(III) is ***harder to reduce*** (i.e., **E° is less positive**) when it is complexed to CN^-

This implies that the equilibrium constant for complexation reaction (Equation 16.5.1) should be **smaller** than that for reaction (Equation 16.5.2). How much smaller?
We can calculate the ratio of equilibrium constants by adding and subtracting reactions:

$Fe^{3+} + 6\,CN^- \longrightarrow [Fe(CN)_6]^{3-}\ \ K = K_1$

$[Fe(CN)_6]^{4-} \longrightarrow Fe^{2+} + 6\,CN^-\ \ K = \frac{1}{K_2}$

$Fe^{3+} + Fe(CN)_6{}^{4-} \leftrightarrow Fe^{2+} + Fe(CN)_6{}^{3-}$

The equilibrium constant for this reaction is the product of the two reactions we added, i.e., $K = K_1/K_2$.

But we can make the same overall reaction by combining reactions (3) and (4)

$Fe^{3+}{}_{(aq)} + e^- = Fe^{2+}{}_{(aq)}\ \ E^o = +0.77V$

$[Fe(CN)_6]^{4-} = [Fe(CN)_6]^{3-} + e^-\ \ E^o = -0.42V$

$Fe^{3+} + Fe(CN)_6{}^{4-} \leftrightarrow Fe^{2+} + Fe(CN)_6{}^{3-}$

In this case, we can calculate E° = 0.77 - 0.42 = +0.35 V

It follows from $nFE° = -\Delta G° = RT\ln K$ that

$$E^o = \frac{RT}{nF} ln \frac{K_1}{K_2}$$

$$\frac{K_1}{K_2} = exp\frac{(nFE^o}{RT} = exp[(1\ equiv/mol)(96,500C/equiv)(0.35J/C)(8.314J/molK)(298)] = exp(13.63) = 8 \times 10^5$$

Thus we find that $Fe(CN)_6{}^{3-}$ is about a million times more stable as a complex than $Fe(CN)_6{}^{4-}$.

Solubility Equlibria

We can use a similar procedure to measure K_{sp} values electrochemically.
For example, the silver halides (AgCl, AgBr, AgI) are sparingly soluble. We can calculate the K_{sp} of AgCl by measuring the standard potential of the AgCl/Ag couple. This can be done very simply by measuring the potential of a silver wire, which is in contact with solid AgCl and 1 M Cl^-(aq), against a hydrogen reference electrode. That value is then compared to the standard potential of the Ag^+/Ag couple:

$$AgCl_{(s)} + e^- \longrightarrow Ag_{(s)} + Cl^-_{(aq)} \quad E^o + .207V$$

$$Ag^+_{(aq)} + e^- \longrightarrow Ag_{(s)} \quad E^o = +0.799V$$

Subtracting the second reaction from the first one we obtain:

$$AgCl_{(s)} = Ag^+_{(aq)} + Cl^-_{(aq)} \quad E^o = +0.207 - 0.799 = -0.592V$$

and again using nFE° = RTlnK, we obtain K = K_{sp} = **9.7 x 10^{-11} M^2**.



Because the solubility of the silver halides is so low, this would be a very difficult number to measure by other methods, e.g., by measuring the concentration of Ag+ spectroscopically, or by gravimetry. In practice almost all K_{sp} values involving electroactive substances are measured potentiometrically.

Acid-Base Equilibria

Many electrochemical reactions involve H^+ or OH^-. For these reactions, the half-cell potentials are **pH-dependent**.

Example: Recall that the disproportionation reaction $3\,MnO_4^{2-}{}_{(s)} \longrightarrow 2\,MnO_4^-{}_{(aq)} + MnO_{2\,(s)}$ is **spontaneous** at pH=0 ([H^+] = 1M), from the Latimer diagram or Frost plot.

However, when we properly balance this half reaction we see that it involves **protons as a reactant**:

$$3\,MnO_4^{2-}\,(aq) + 4\,H^+\,(aq) \rightleftharpoons 2\,MnO_4^-\,(aq) + MnO_2\,(s) + 2\,H_2O\,(l) \qquad (16.5.3)$$

By Le Chatelier's principle, it follows that **removing protons** (increasing the pH) should **stabilize** the reactant, MnO_4^{2-}. Thus we would expect the +6 oxidation state of Mn, which is unstable in acid, to be stabilized in basic media. We will examine these proton-coupled redox equilibria more thoroughly in the context of Pourbaix diagrams below.



Acid mine drainage occurs when sulfide rocks such as pyrite (FeS_2) are exposed to the air and oxidized. The reaction produces aqueous Fe^{3+} and H_2SO_4. When the acidic effluent of the mine meets a stream or lake at higher pH, solid $Fe(OH)_3$ precipitates, resulting in the characteristic orange muddy color downstream of the mine. The acidic effluent is toxic to plants and animals.

16.5: Redox Reactions with Coupled Equilibria is shared under a CC BY-SA license and was authored, remixed, and/or curated by LibreTexts.

- **4.5: Redox Reactions with Coupled Equilibria** by Chemistry 310 is licensed CC BY-SA 4.0. Original source: https://en.wikibooks.org/wiki/Introduction_to_Inorganic_Chemistry.

16.6: Pourbaix Diagrams

Pourbaix Diagrams plot electrochemical stability for different redox states of an element as a function of pH.[3] As noted above, these diagrams are essentially phase diagrams that map the conditions of potential and pH (most typically in aqueous solutions) where different redox species are stable. We saw a simple example of such a diagram in section 4.2 for H_2O. Typically, the water redox reactions are plotted as dotted lines on these more complicated diagrams for other elements.

The lines in Pourbaix diagrams represent redox and acid-base reactions, and are the parts of the diagram where two species can exist in equilibrium. For example, in the Pourbaix diagram for Fe below, the horizontal line between the Fe^{3+} and Fe^{2+} regions represents the reaction $\mathbf{Fe^{3+}_{(aq)} + e^- = Fe^{2+}_{(aq)}}$, which has a standard potential of +0.77 V. While we could use standard potentials for all these lines, in practice Pourbaix diagrams are usually plotted for lower ion concentrations (often 1 mM) that are more relevant to corrosion and electrochemical experiments.

Example: Iron Pourbaix diagram

Areas in the Pourbaix diagram mark regions where a single species (Fe^{2+}(aq), Fe_3O_4(s), etc.) is stable. More stable species tend to occupy larger areas.

Lines mark places where two species exist in equilibrium.

- **Pure redox** reactions are **horizontal** lines - these reactions are not pH-dependent
- **Pure acid-base** reactions are **vertical** lines - these do not depend on potential
- Reactions that are **both** acid-base and redox have a slope of -0.0592 V/pH x # H^+/# e^-)

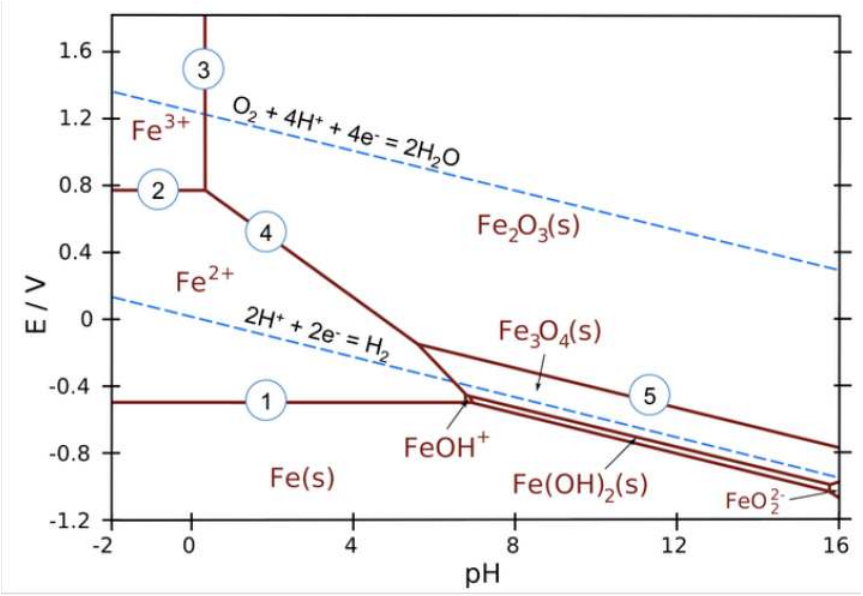


Figure **16.6.1**: Pourbaix diagram for iron at ionic concentrations of 1.0 mM. (CC BY-SA 3.0 Unported; Metallos via Wikipedia)

Examples of equilibria in the iron Pourbaix diagram (numbered on the plot):

1. $\mathbf{Fe^{2+} + 2e^- \longrightarrow Fe_{(s)}}$ (pure redox reaction - no pH dependence)
2. $\mathbf{Fe^{3+} + e^- \longrightarrow Fe^{2+}}$ (pure redox reaction - no pH dependence)
3. $\mathbf{2Fe^{3+} + 3H_2O \longrightarrow Fe_2O_{3\,(s)} + 6H^+}$ (pure acid-base, no redox)
4. $\mathbf{2Fe^{2+} + 3H_2O \longrightarrow Fe_2O_{3\,(s)} + 6H^+ + 2e^-}$ (slope = -59.2 x 6/2 = -178 mV/pH)
5. $\mathbf{2Fe_3O_{4\,(s)} + H_2O \longrightarrow 2H^+ + 2e^-}$ (slope = -59.2 x 2/2 = -59.2 mV/pH)

The water redox lines have special significance on a Pourbaix diagram for an element such as iron. Recall that liquid water is stable *only* in the region between the dotted lines. Below the H_2 line, water is unstable relative to hydrogen gas, and above the O_2 line, water is unstable with respect to oxygen. For active metals such as Fe, the region where the pure element is stable is typically below the H_2 line. This means that iron metal is unstable in contact with water, undergoing reactions:

$Fe_{(s)} + 2H^+ \longrightarrow Fe^{2+}{}_{(aq)} + H_2$ (in acid)

$fe_{(s)} + 2H_2O \longrightarrow Fe(OH)_{2\,(s)} + H_2$ (in base)

Iron (and most other metals) are also thermodynamically unstable in air-saturated water, where the potential of the solution is close to the O_2 line in the Pourbaix diagram. Here the spontaneous reactions are:

$4Fe_{(s)} + 3O_2 + 12H^+ \longrightarrow 4Fe^{3+} + 6H_2O$ (in acid)

\(\ce{4Fe_{(s)} + 3O2 -> 2Fe2O3_{(s)} (in base)

Corrosion and passivation. It certainly sounds bad for our friend Fe: unstable in water, no matter what the pH or potential. Given enough time, it will all turn into rust. But iron (and other active metals) can corrode, or can be stabilized against corrosion, depending on the conditions. Because our civilization is dependent on the use of active metals such as Fe, Al, Zn, Ti, Cr... for practically everything, it is important to understand this, and we can do so by referring to the Pourbaix diagram.

The **corrosion** of iron (and other active metals such as Al) is indeed rapid in parts of the Pourbaix diagram where the element is oxidized to a soluble, ionic product such as Fe^{3+}(aq) or Al^{3+}(aq). However, solids such as Fe_2O_3, and especially Al_2O_3, form a protective coating on the metal that greatly impedes the corrosion reaction. This phenomenon is called **passivation.**

Draw a vertical line through the iron Pourbaix diagram at the pH of tap water (about 6) and you will discover something interesting: at slightly acidic pH, iron is quite unstable with respect to corrosion by the reaction:

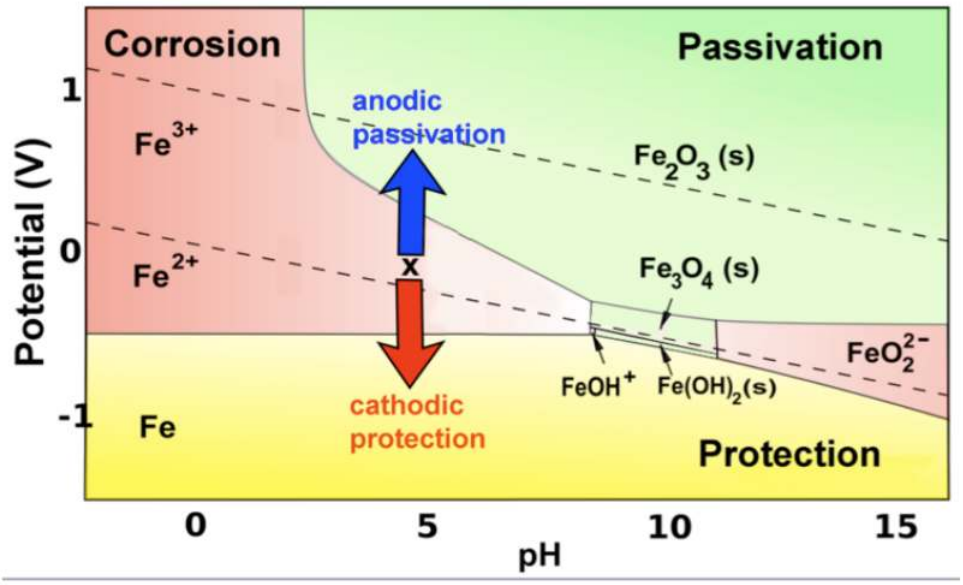
$$Fe_{(s)} + 2H^+ \longrightarrow Fe^{2+}{}_{(aq)} + H_2 \tag{16.6.1}$$

but *only in water that contains relatively little oxygen*, i.e., in solutions where the potential is near the H_2 line. Saturating the water with air or oxygen moves the system closer to the O_2 line, where the most stable species is Fe_2O_3 and the corrosion reaction is:

$$4Fe_{(s)} + 3O_2 \longrightarrow 2Fe_2O_{3\,(s)} \tag{16.6.2}$$

This oxidation reaction is orders of magnitude slower because the oxide that is formed *passivates* the surface. Therefore iron corrodes much more slowly in oxygenated solutions.

More generally, iron (and other active metals) are passivated whenever they oxidize to produce a solid product, and corrode whenever the product is ionic and soluble. This behavior can be summed up on the color-coded Pourbaix diagram below. The red and green regions represent conditions under which oxidation of iron produces soluble and insoluble products, respectively.



In the yellow part of the diagram, an active metal such as iron can be **protected** by a second mechanism, which is to bias it so that its potential is below the oxidation potential of the metal. This **cathodic protection** strategy is most frequently carried out by connecting a more active metal such as Mg or Zn to the iron or steel object (e.g., the hull of a ship, or an underground gas pipeline) that is being protected. The active metal (which must be higher than Fe in the activity series) is also in contact with the solution and slowly corrodes, so it must eventually be replaced. In some cases a battery or DC power supply - the anode of which oxidizes water to oxygen in the solution - is used instead to apply a negative bias.



The white patches visible on the ship's hull are zinc block sacrificial anodes.

Another common mode of corrosion of iron and carbon steel is **differential aeration.** In this case, part of the iron object - e.g., the base of a bridge, or the drill in an oil rig - is under water or in an anoxic environment such as mud or soil. The potential of the solution is close to the H_2 line in the Pourbaix diagram, where Fe can corrode to Fe^{2+} (aq). Another part of the iron object is in the air, or near the surface where water is well oxygenated. At that surface oxygen can be reduced to water, $O_2 + 4H^+ + 4e^- = 2\ H_2O$. The conductive iron object completes the circuit, carrying electrons from the anode (where Fe is oxidized) to the cathode (where O_2 is reduced). Corrosion by differential aeration can be rapid because soluble ions are produced, and the reaction has a driving force of over 1 V. Iron or carbon steel that is subjected to frequent weathering, such as the cast iron bridge and lamppost shown below, is corroded on the surface by differential aeration.



Rusty cast iron bridge and lamppost, North Ayrshire, Scotland

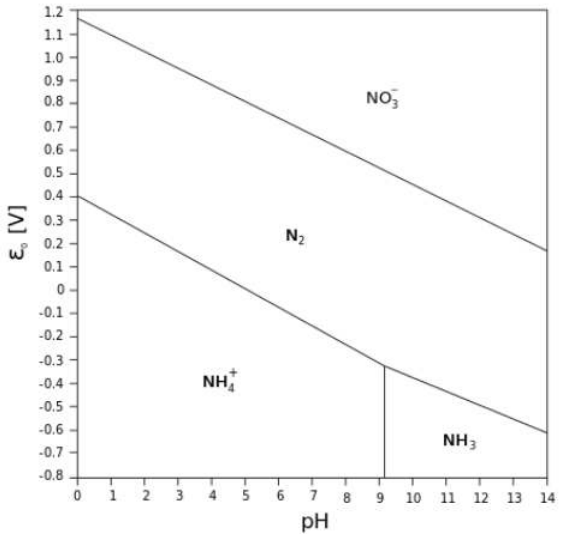
Differential aeration is involved in the formation of a rust ring around wet areas of cast iron, e.g., an iron frying pan left partially submerged in water for a day or more. (You may have seen this mechanism of corrosion in action when you did not get to the dirty dishes right away). Under the water, Fe is oxidized to soluble Fe^{2+}, and at the water line O_2 is reduced to H_2O. As Fe^{2+} ions diffuse towards the water surface, they encounter oxygen molecules and are oxidized to Fe^{3+}. However Fe^{3+} is insoluble at neutral pH and deposits as rust, typically just below the water line, forming the rust ring.

16.6: Pourbaix Diagrams is shared under a CC BY-SA license and was authored, remixed, and/or curated by LibreTexts.

- **4.6: Pourbaix Diagrams** by Chemistry 310 is licensed CC BY-SA 4.0. Original source: https://en.wikibooks.org/wiki/Introduction_to_Inorganic_Chemistry.

16.7: Discussion Questions

- Explain the simplified Pourbaix diagram for nitrogen, shown below. Discuss the reactions that are implied by the lines, and explain why they have the slopes they do.



- Use the information in the Pourbaix diagram to construct a Frost diagram for nitrogen at pH 7.

16.7: Discussion Questions is shared under a CC BY-SA license and was authored, remixed, and/or curated by LibreTexts.

- **4.7: Discussion Questions** by Chemistry 310 is licensed CC BY-SA 4.0. Original source: https://en.wikibooks.org/wiki/Introduction_to_Inorganic_Chemistry.

16.8: Problems

1. Balance the following redox reactions, adding H_2O and H^+ (or OH^-) as needed. Predict for each one whether the reaction would become more or less spontaneous at higher pH.

(a) $\mathbf{MnO_4^-{}_{(aq)} + N_2O_{(g)} = Mn^{2+}{}_{(aq)} + NO_3^-{}_{(aq)}}$ (in acid)

(b) $\mathbf{Cr_2O_7^{2-}{}_{(aq)} + S_2O_3^{2-}{}_{(aq)} = Cr_2O_3{}_{(s)} + SO_4^{2-}{}_{(aq)}}$ (in base)

(c) $\mathbf{H_2O_2{}_{(aq)} + HI_{(aq)} = I_3^-{}_{(aq)}}$ (in acid)

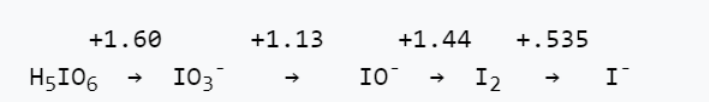
(d) $\mathbf{HOBr_{(aq)} = HBr_{(aq)} + HBrO_2{}_{(aq)}}$ (in acid)

(e) $\mathbf{C_{12}H_{22}O_{11}\ (sucrose, aq) + ClO_3^-{}_{(aq)} = HCO_3^-{}_{(aq)} + Cl^-{}_{(aq)}}$ (in base)

2. Silver metal is not easily oxidized, and does not react with oxygen-saturated water. However, when excess NaCN is added to a suspension of silver particles, some silver dissolves. If oxygen is removed (e.g., by bubbling nitrogen through the solution), the dissolution reaction stops. Write a balanced equation for the dissolution reaction (hint: it is a redox reaction).

3. The standard potentials for the Fe^{3+}/Fe^{2+} and Cl^-/Cl_2 couples are +0.77 and +1.36 V. Calculate the cell potential of a redox flow battery that has Fe^{3+}/Fe^{2+} and Cl^-/Cl_2 solutions on the two sides (both containing 1.0 M HCl as the electrolyte). The pressure of Cl_2 gas on the chlorine side is 0.2 atm, and the concentrations of Fe^{2+} and Fe^{3+} on the iron side are both 0.10 M.

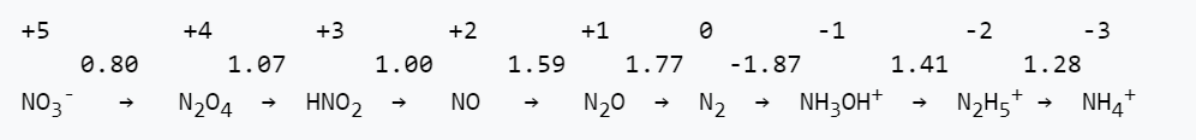
4. The Latimer potential diagram for iodine (in acidic solutions) is given below.



(a) What is the potential for the IO_3^-/I^- redox couple?

(b) Construct a Frost diagram and identify any species that are unstable with respect to disproportionation.

5. The Latimer diagram for nitrogen in acidic solutions is shown below:



(a) Write a balanced half reaction for reduction of NO to NH_4^+ in acid.

(b) What is the value of E^o for the half reaction in part (a)?

(c) Is this half reaction more thermodynamically favorable in acid or in base? Explain.

(d) All the nitrogen-containing molecules and ions listed above are kinetically stable, but only three are *thermodynamically* stable with respect to disproportionation in acid. Which ones are they?

6. Referring to the Pourbaix diagram for Mn below:

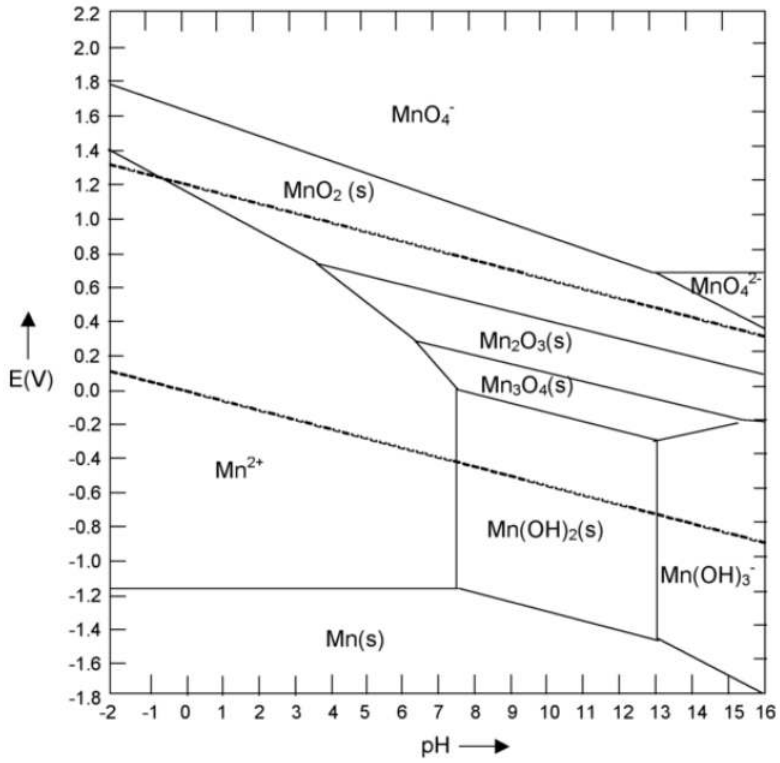
(a) Write out the balanced half reaction corresponding to the line separating Mn^{2+} and Mn_2O_3. Use your answer to calculate the slope of the line (give units).

(b) Is Mn metal stable in water at any pH? If so, in what range of pH?

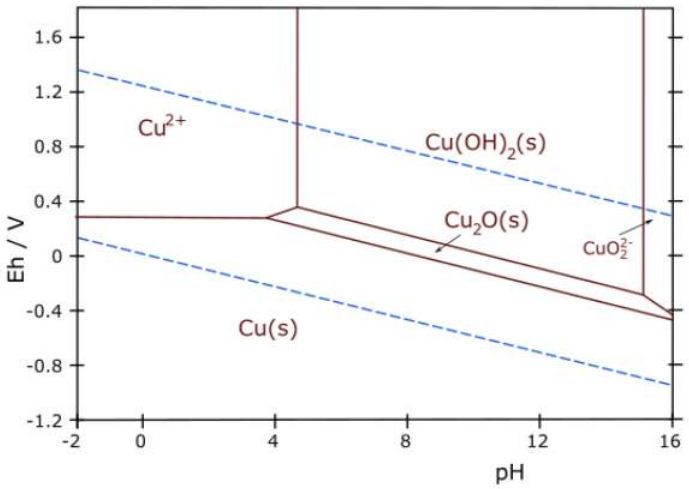
(c) What spontaneous reaction would you expect for an aqueous solution of MnO_4^- at pH 6?

(d) Describe an electrochemical procedure (specifying pH and potential) for making Mn_3O_4(s) from aqueous Mn^{2+}.

(e) Label the regions of the diagram that correspond to corrosion and passivation of Mn metal.



7. The Pourbaix diagram for copper is shown below.



(a) Write a balanced half-reaction that corresponds to the boundary between the $Cu_2O(s)$ and $Cu(OH)_2(s)$ regions of the diagram.

(b) What is the slope of the line (do not try to measure it from the graph!) that connects the $Cu^{2+}(aq)$ and $Cu_2O(s)$ regions? Explain your reasoning.

(c) Over what pH range (if any) is copper metal stable in contact with pure water?

(d) Thermodynamically, the reaction between coppper and oxygen is spontaneous at pH 7. Would you expect copper to corrode or to be passivated against corrosion in aerated water at neutral pH? Explain your reasoning.

(e) Some recent studies have suggested the use of Cu_2O as a water splitting photocatalyst. Would you expect Cu_2O to be stable in the presence of the oxygen formed in the reaction? Explain your reasoning.

16.8: Problems is shared under a CC BY-SA license and was authored, remixed, and/or curated by LibreTexts.

- **4.8: Problems** by Chemistry 310 is licensed CC BY-SA 4.0. Original source: https://en.wikibooks.org/wiki/Introduction_to_Inorganic_Chemistry.

16.9: References

1. Alotto, P.; Guarnieri, M.; Moro, F. (2014). "Redox Flow Batteries for the storage of renewable energy: a review". *Renewable & Sustainable Energy Reviews* **29**: 325–335. doi:10.1016/j.rser.2013.08.001.
2. Frost, Arthur (1951). "Oxidation Potential–Free Energy Diagrams". *Journal of the American Chemical Society* **73** (6): 2680–2682. doi:10.1021/ja01150a074.
3. Pourbaix, M., Atlas of electrochemical equilibria in aqueous solutions. 2d English ed. 1974, Houston, Tex.: National Association of Corrosion Engineers.

16.9: References is shared under a CC BY-SA license and was authored, remixed, and/or curated by LibreTexts.

- **4.9: References** by Chemistry 310 is licensed CC BY-SA 4.0. Original source: https://en.wikibooks.org/wiki/Introduction_to_Inorganic_Chemistry.

17: Transition-Metal Storage, Transport, and Biomineralization

Living organisms store and transport transition metals both to provide appropriate concentrations of them for use in metalloproteins or cofactors and to protect themselves against the toxic effects of metal excesses; metalloproteins and metal cofactors are found in plants, animals, and microorganisms. The normal concentration range for each metal in biological systems is narrow, with both deficiencies and excesses causing pathological changes. In multicellular organisms, composed of a variety of specialized cell types, the storage of transition metals and the synthesis of the transporter molecules are not carried out by all types of cells, but rather by specific cells that specialize in these tasks. The form of the metals is always ionic, but the oxidation state can vary, depending on biological needs. Transition metals for which biological storage and transport are significant are, in order of decreasing abundance in living organisms: iron, zinc, copper, molybdenum, cobalt, chromium, vanadium, and nickel. Although zinc is not strictly a transition metal, it shares many bioinorganic properties with transition metals and is considered with them in this chapter. Knowledge of iron storage and transport is more complete than for any other metal in the group.

I. General Principles

A. Biological Significance of Iron, Zinc, Copper, Molybdenum, Cobalt, Chromium, Vanadium, and Nickel

B. Chemical Properties Relative to Storage and Transport

1. Iron
2. Zinc, Copper, Vanadium, Chromium, Molybdenum, and Cobalt

II. Biological Systems of Metal Storage, Transport, and Mineralization

A. Storage

1. Iron
2. Zinc, Copper, Vanadium, Chromium, Molybdenum, Cobalt, Nickel, and Manganese

B. Transport

1. Iron
2. Zinc, Copper, Vanadium, Chromium, Molybdenum, and Cobalt

C. Iron Biomineralization

III. Summary

Transition metals (Fe, Cu, Mo, Cr, Co, Mn, V) play key roles in such biological processes as cell division (Fe, Co), respiration (Fe, Cu), nitrogen fixation (Fe, Mo, V), and photosynthesis (Mn, Fe). Zn participates in many hydrolytic reactions and in the control of gene activity by proteins with "zinc fingers." Among transition metals, Fe predominates in terrestial abundance; since Fe is involved in a vast number of biologically important reactions, its storage and transport have been studied extensively. Two types of Fe carriers are known: specific proteins and low-molecular-weight complexes. In higher animals, the transport protein transferrin binds two Fe atoms with high affinity; in microorganisms, iron is transported into cells complexed with catecholates or hydroxamates called siderophores; and in plants, small molecules such as citrate, and possibly plant siderophores, carry Fe. Iron complexes enter cells through complicated paths involving specific membrane sites (receptor proteins). A problem yet to be solved is the form of iron transported in the cell after release from transferrin or siderophores but before incorporation into Fe-proteins.

Iron is stored in the protein ferritin. The protein coat of ferritin is a hollow sphere of 24 polypeptide chains through which Fe^{2+} passes, is oxidized, and mineralizes inside in various forms of hydrated Fe_2O_3. Control of the formation and dissolution of the mineral core by the protein and control of protein synthesis by Fe are subjects of current study.

Biomineralization occurs in the ocean (e.g., Ca in shells, Si in coral reefs) and on land in both plants (e.g., Si in grasses) and animals (e.g., Ca in bone, Fe in ferritin, Fe in magnetic particles). Specific organic surfaces or matrices of protein and/or lipid allow living organisms to produce minerals of defined shape and composition, often in thermodynamically unstable states.

IV. References

1. (a) J. H. Martin and R. M. Gordon, *Deep Sea Research* **35** (1988), 177; (b) F. Egami, *J. Mol. Evol.* **4** (1974), 113.
2. J. F. Sullivan *et al.*, *J. Nutr.* **109** (1979), 1432.
3. M. D. McNeely *et al.*, *Clin. Chem.* **17** (1971), 1123
4. A. R. Byrne and L. Kosta, *Sci. Total Env.* **10** (1978), 17
5. A. S. Prasad, *Trace Elements and Iron in Human Metabolism*, Plenum Medical Book Company, 1978.
6. E. C. Theil, *Adv. Inorg. Biochem.* **5** (1983), 1.
7. E. C. Theil and P. Aisen, in D. van der Helm, J. Neilands, and G. Winkelmann, eds., *Iron Transport in Microbes, Plants, and Animals*, VCH, 1987, p. 421.
8. C. F. Mills, ed., *Zinc in Human Biology*, Springer-Verlag, 1989.
9. B. L. Vallee and D. S. Auld, *Biochemistry* **29** (1990), 5647.
10. J. Miller, A. D. McLachlan, and A. Klug, *EMBO J.* **4** (1985), 1609.
11. J. M. Berg, *J. Biol. Chem.* **265** (1990), 6513.
12. C. Sennett, L. E. G. Rosenberg, and I. S. Millman, *Annu. Rev. Biochem.* **50** (1981), 1053.
13. J. J. G. Moura *et al.*, in A. V. Xavier, ed., *Frontiers in Biochemistry*, VCH, 1986, p. 1.
14. C. T. Walsh and W. H. Orme-Johnson, *Biochemistry* **26** (1987), 4901.
15. H. Kim and R. J. Maier, *J. Biol. Chem.* **265** (1990), 18729.
16. Reference 5, p. 5.
17. V. L. Schramm and F. C. Wedler, eds., *Manganese in Metabolism and Enzyme Function*, Academic Press, 1986.
18. (a) D. W. Boyd and K. Kustin, *Adv. Inorg. Biochem.* **6** (1984), 312; (b) R. C. Bruening *et al.*, *J. Nat. Products* **49** (1986), 193.
19. T. G. Spiro, ed., *Molybdenum Biochemistry*, Wiley, 1985.
20. L. L. Fox, *Geochim. Cosmochim. Acta* **52** (1988), 771.
21. M. E. Farago, in A. V. Xavier, ed., *Frontiers in Bioinorganic Chemistry*, VCH, 1986, p. 106.
22. I. G. Macara, G. C. McCloud, and K. Kustin, *Biochem. J.* **181** (1979), 457.
23. R. C. Bruening *et al.*, *J. Am. Chem. Soc.* **107** (1985), 5298.
24. E. Bayer and H. H. Kneifel, *Z. Naturforsch.* **27B** (1972), 207.
25. E. Bayer and H. H. Kneifel, in A. V. Xavier, ed., *Frontiers in Bioinorganic Chemistry*, VCH, 1986, p. 98.
26. J. Felcman, J. J. R. Frausto da Silva, and M. M. Candida Vaz, *Inorg. Chim. Acta* **93** (1984), 101.
27. W. Mertz, *Nutr. Rev.* **3** (1975), 129.
28. E. C. Theil, *J. Biol. Chem.* **265** (1990), 4771; *Biofactors* **4** (1993), 87.
29. J. S. Rohrer *et al.*, *Biochemistry* **29** (1990), 259.
30. P. H. Connett and K. Wetterhahn, *Struct. Bonding* **54** (1983), 94.
31. E. C. Theil, *Ann. Rev. Biochem.* **56** (1987), 289; *Adv. Enzymol.* **63** (1990), 421.
32. G. C. Ford *et al.*, *Philos. Trans. Roy. Soc. Land. B*, **304** (1984),551.
33. G. D. Watt, R. B. Frankel, and G. C. Papaefthymiou, *Proc. Natl. Acad. Sci. USA* 82 (1985), 3640.
34. (a) J. S. Rohrer *et al.*, *J. Biol. Chem.* **262** (1987), 13385; (b) J. S. Rohrer *et al.*, *Inorg. Chem.* **28** (1989), 3393.
35. D. H. Hamer, *Ann. Rev. Biochem.* **55** (1986), 913.
36. A. H. Robbins, D. E. McRee, M. Williamson, S. A. Collett, N. H. Xuong, W. F. Furey, B. C. Want, and C. D. Stout, *J. Mol. Biol.* **221** (1991), 1269.
37. N. D. Chasteen, *Adv. Inorg. Biochem.* **5** (1983), 201.
38. P. Aisen and I. Listowsky, *Annu. Rev. Biochem.* **49** (1980), 357.
39. B. T. Anderson *et al.*, *Proc. Natl. Acad. Sci. USA* **84** (1987), 1768; E. N. Baker, B. F. Anderson, and H. M. Baker, *Int. J. Biol. Macromol.* **13** (1991), 122.
40. S. Bailey *et al.*, *Biochemistry* **27** (1988), 5804.
41. M. Ragland *et al.*, *J. BioI. Chem.* **263** (1990), 18339.
42. B. F. Matzanke, G. Muller, and K. N. Raymond, in T. M. Loehr, ed., *Iron Carriers and Iron Proteins*, VCH, 1989, pp. 1-121.
43. L. Stryer, *Biochemistry*, Freeman, 1981, pp. 110-116.
44. D. J. Ecker *et al.*, *J. Am. Chem. Soc.* **110** (1988), 2457.
45. Y. Sugiura and K. Nomoto, *Struct. Bonding* **58** (1984), 107.

46. S. Mann, *Struct. Bonding* **54** (1986), 125.
47. A. R. Bulls *et al.*, *J. Am. Chern. Soc.* **112** (1990), 2627.
48. J. Webb, in P. Westbroek and E. W. de Jong, eds., *Biomineralization and Biological Metal Accumulation*, Reidel, 1983, pp. 413-422.
49. K. Kustin *et al.*, *Struct. Bonding* **53** (1983), 139.
50. R. B. Frankel and R. P. Blakemore, *Philos. Trans. Roy. Soc. Lond. B* **304** (1984), 567.
51. S. J. Lippard, *Angew. Chemie* **22** (1988), 344.
52. K. E. Wieghardt, *Angew. Chemie* **28** (1989), 1153.
53. E. C. Theil, in R. B. Frankel, ed., *Iron Biomineralization*, Plenum Press, 1990.
54. S. Maun, J. P. Harrington, and R. J. P. Williams, *Nature* **234** (1986), 565.
55. W. H. Armstrong and S. J. Lippard, *J. Am. Chern. Soc.* **107** (1985), 3730.
56. L. Que, Jr. and R. C. Scarrow, in L. Que, ed., *Metal Clusters in Proteins*, ACS Symposium Series 372, American Chemical Society, Washington, DC, 1988, p. 152 and references therein.
57. S. M. Gorun aud S. J. Lippard, *J. Am. Chem. Soc.* **107** (1985), 4570.
58. S. M. Gorun *et al.*, *J. Am. Chern. Soc.* **109** (1987), 3337.
59. Q. Islam *et al.*, *J. Inorg. Biochem.* **36** (1989), 51.
60. C.-Y. Yang *et al.*, *J. Inorg. Biochem.* **28** (1986), 393.
61. A. N. Mansour *et aI.*, *J. Biol. Chern.* **260** (1985), 7975.
62. D. C. Hams and P. Aisen, in T. M. Loehr, ed., *Iron Carriers and Iron Proteins*, VCH, 1989, pp. 239-352.
63. P. M. Harrison and T. M. Lilley, in Reference 62, pp. 123-238.
64. G. S. Waldo *et al. Science* **259** (1993), 796.
65. J. Trikha, G. S. Waldo, F. A. Lewandowski, Y. Ha, E. C. Theil, P. C. Weber, and N. M. Allewell, *Protein* **18** (1994), issue #2, in press.

These references contain general reviews of the subjects indicated:

- Chromium: 27, 30
- Cobalt: 12
- Copper: 8
- Iron
  - Biochemistry; 7, 31, 37, 42
  - Biomineralization polynuclear models: 6, 42, 56, 57, 58
  - Siderophores: 42
  - Structure of storage and transport proteins: 32, 62, 63
- Manganese: 17
- Molybdenum: 19
- Nickel: 13, 14
- Vanadium: 18
- Zinc: 8, 9, 11, 35

Contributors and Attributions

- Elizabeth C. Theil (North Carolina State University, Department of Biochemistry)
- Kenneth N. Raymond (University of California at Berkeley, Department of Chemistry)

17: Transition-Metal Storage, Transport, and Biomineralization is shared under a not declared license and was authored, remixed, and/or curated by LibreTexts.

17.1: Biological Significance of Iron, Zinc, Copper, Molybdenum, Cobalt, Chromium, Vanadium, and Nickel

The transition metals and zinc are among the least abundant metal ions in the sea water from which contemporary organisms are thought to have evolved (Table 1.1).[1-5] For many of the metals, the concentration in human blood plasma greatly exceeds that in sea water. Such data indicate the importance of mechanisms for accumulation, storage, and transport of transition metals and zinc in living organisms.

Table 1.1: Concentrations of transition metals and zinc in sea water and human plasma.a*Data from References 1 - 5 and 12

Element	Sea Water (M) x 10^8	Human Plasma (M) x 10^8
Fe	0.005 - 2	2230
Zn	8.0	1720
Cu	1.0	1650
Mo	10.0	1000
Co	0.7	0.0025
Cr	0.4	5.5
V	4.0	17.7
Mn	0.7	10.9
Ni	0.5	4.4

The metals are generally found either bound directly to proteins or in cofactors such as porphyrins or cobalamins, or in clusters that are in turn bound by the protein; the ligands are usually O, N, S, or C. Proteins with which transition metals and zinc are most commonly associated catalyze the intramolecular or intermolecular rearrangement of electrons. Although the redox properties of the metals are important in many of the reactions, in others the metal appears to contribute to the structure of the active state, e.g., zinc in the Cu-Zn dismutases and some of the iron in the photosynthetic reaction center. Sometimes equivalent reactions are catalyzed by proteins with different metal centers; the metal binding sites and proteins have evolved separately for each type of metal center.

Iron is the most common transition metal in biology.[6,7] Its use has created a dependence that has survived the appearance of dioxygen in the atmosphere ca. 2.5 billion years ago, and the concomitant conversion of ferrous ion to ferric ion and insoluble rust (Figure 1.1 See color plate section, page C-1.). All plants, animals, and bacteria use iron, except for a lactobacillus that appears to maintain high concentrations of manganese instead of iron. The processes and reactions in which iron participates are crucial to the survival of terrestrial organisms, and include ribonucleotide reduction (DNA synthesis), energy production (respiration), energy conversion (photosynthesis), nitrogen reduction, oxygen transport (respiration, muscle contraction), and oxygenation (e.g., steroid synthesis, solubilization and detoxification of aromatic compounds). Among the transition metals used in living organisms, iron is the most abundant in the environment. Whether this fact alone explains the biological predominance of iron or whether specific features of iron chemistry contribute is not clear.

Many of the other transition metals participate in reactions equivalent to those involving iron, and can sometimes substitute for iron, albeit less effectively, in natural Fe-proteins. Additional biological reactions are unique to nonferrous transition metals.

Zinc is relatively abundant in biological materials.[8,9] The major location of zinc in the body is metallothionein, which also binds copper, chromium, mercury, and other metals. Among the other well-characterized zinc proteins are the Cu-Zn superoxide dismutases (other forms have Fe or Mn), carbonic anhydrase (an abundant protein in red blood cells responsible for maintaining the pH of the blood), alcohol dehydrogenase, and a variety of hydrolases involved in the metabolism of sugars, proteins, and nucleic acids. Zinc is a common element in nucleic-acid polymerases and transcription factors, where its role is considered to be structural rather than catalytic. Interestingly, zinc enhances the stereoselectivity of the polymerization of nucleotides under reaction

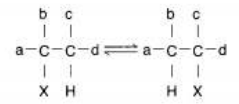
conditions designed to simulate the environment for prebiotic reactions. Recently a group of nucleic-acid binding proteins, with a repeated sequence containing the amino acids cysteine and histidine, were shown to bind as many as eleven zinc atoms necessary for protein function (transcribing DNA to RNA).[10] Zinc plays a structural role, forming the peptide into multiple domains or "zinc fingers" by means of coordination to cysteine and histidine (Figure 1.2A See color plate section, page C-l.). A survey of the sequences of many nucleic-acid binding proteins shows that many of them have the common motif required to form zinc fingers. Other zinc-finger proteins called steroid receptors bind both steroids such as progesterone and the progesterone gene DNA (Chapter 8). Much of the zinc in animals and plants has no known function, but it may be maintaining the structures of proteins that activate and deactivate genes.[11]

Copper and iron proteins participate in many of the same biological reactions:

1. reversible binding of dioxygen, e.g., hemocyanin (Cu), hemerythrin (Fe), and hemoglobin (Fe);
2. activation of dioxygen, e.g., dopamine hydroxylase (Cu) (important in the synthesis of the hormone epinephrine), tyrosinases (Cu), and catechol dioxygenases (Fe);
3. electron transfer, e.g., plastocyanins (Cu), ferredoxins, and c-type cytochromes (Fe);
4. dismutation of superoxide by Cu or Fe as the redox-active metal (superoxide dismutases).

The two metal ions also function in concert in proteins such as cytochrome oxidase, which catalyzes the transfer of four electrons to dioxygen to form water during respiration. Whether any types of biological reactions are unique to copper proteins is not clear. However, use of stored iron is reduced by copper deficiency, which suggests that iron metabolism may depend on copper proteins, such as the serum protein ceruloplasmin, which can function as a ferroxidase, and the cellular protein ascorbic acid oxidase, which also is a ferrireductase.

Cobalt is found in vitamin B_{12} , its only apparent biological site.[12] The vitamin is a cyano complex, but a methyl or methylene group replaces CN in native enzymes. Vitamin-B_{12} deficiency causes the severe disease of pernicious anemia in humans, which indicates the critical role of cobalt. The most common type of reaction in which cobalamin enzymes participate results in the reciprocal exchange of hydrogen atoms if they are on adjacent carbon atoms, yet not with hydrogen in solvent water:



(An important exception is the ribonucleotide reductase from some bacteria and lower plants, which converts ribonucleotides to the DNA precursors, deoxyribonucleotides, a reaction in which a sugar -OH is replaced by -H. Note that ribonucleotide reductases catalyzing the same reaction in higher organisms and viruses are proteins with an oxo-bridged dimeric iron center.) The cobalt in vitamin B_{12} is coordinated to five N atoms, four contributed by a tetrapyrrole (corrin); the sixth ligand is C, provided either by C5 of deoxyadenosine in enzymes such as methylmalonyl-CoA mutase (fatty acid metabolism) or by a methyl group in the enzyme that synthesizes the amino acid methionine in bacteria.

Nickel is a component of a hydrolase (urease), of hydrogenase, of CO dehydrogenase, and of S-methyl CoM reductase, which catalyzes the terminal step in methane production by methanogenic bacteria. All the Ni-proteins known to date are from plants or bacteria.[13,14] However, about 50 years elapsed between the crystallization of jack-bean urease in 1925 and the identification of the nickel component in the plant protein. Thus it is premature to exclude the possibility of Ni-proteins in animals. Despite the small number of characterized Ni-proteins, it is clear that many different environments exist, from apparently direct coordination to protein ligands (urease) to the tetrapyrrole F430 in methylreductase and the multiple metal sites of Ni and Fe-S in a hydrogenase from the bacterium *Desulfovibrio gigas*. Specific environments for nickel are also indicated for nucleic acids (or nucleic acid-binding proteins), since nickel activates the gene for hydrogenase.[15]

Manganese plays a critical role in oxygen evolution catalyzed by the proteins of the photosynthetic reaction center. The superoxide dismutase of bacteria and mitochondria, as well as pyruvate carboxylase in mammals, are also manganese proteins.[16,17] How the multiple manganese atoms of the photosynthetic reaction center participate in the removal of four electrons and protons from water is the subject of intense investigation by spectroscopists, synthetic inorganic chemists, and molecular biologists.[17]

Vanadium and chromium have several features in common, from a bioinorganic viewpoint.[18a] First, both metals are present in only small amounts in most organisms. Second, the biological roles of each remain largely unknown.[18] Finally, each has served as a

probe to characterize the sites of other metals, such as iron and zinc. Vanadium is required for normal health, and could act *in vivo* either as a metal cation or as a phosphate analogue, depending on the oxidation state, V(lV) or V(V), respectively. Vanadium in a sea squirt (tunicate), a primitive vertebrate (Figure 1.2B), is concentrated in blood cells, apparently as the major cellular transition metal, but whether it participates in the transport of dioxygen (as iron and copper do) is not known. In proteins, vanadium is a cofactor in an algal bromoperoxidase and in certain prokaryotic nitrogenases. Chromium imbalance affects sugar metabolism and has been associated with the glucose tolerance factor in animals. But little is known about the structure of the factor or of any other specific chromium complexes from plants, animals, or bacteria.

Molybdenum proteins catalyze the reduction of nitrogen and nitrate, as well as the oxidation of aldehydes, purines, and sulfite.[19] Few Mo-proteins are known compared to those involving other transition metals. Nitrogenases, which also contain iron, have been the focus of intense investigations by bioinorganic chemists and biologists; the iron is found in a cluster with molybdenum (the iron-molybdenum cofactor, or FeMoCo) and in an iron-sulfur center (Chapter 7). Interestingly, certain bacteria (*Azotobacter*) have alternative nitrogenases, which are produced when molybdenum is deficient and which contain vanadium and iron or only iron. All other known Mo-proteins are also Fe-proteins with iron centers, such as tetrapyrroles (heme and chlorins), Fe-sulfur clusters, and, apparently, non-heme/non-sulfur iron. Some Mo-proteins contain additional cofactors such as the Havins, e.g., in xanthine oxidase and aldehyde oxidase. The number of redox centers in some Mo-proteins exceeds the number of electrons transferred; reasons for this are unknown currently.

17.1: Biological Significance of Iron, Zinc, Copper, Molybdenum, Cobalt, Chromium, Vanadium, and Nickel is shared under a not declared license and was authored, remixed, and/or curated by LibreTexts.

17.2: Biological Systems of Metal Storage

Iron

Three properties of iron can account for its extensive use in terrestrial biological reactions:

a. facile redox reactions of iron ions;
b. an extensive repertoire of redox potentials available by ligand substitution or modification (Table 1.4);
c. abundance and availability (Table 1.1) under conditions apparently extant when terrestrial life began (see Section I.B.).

Ferrous ion appears to have been the environmentally stable form during prebiotic times. The combination of the reactivity of ferrous ion and the relatively large amounts of iron used by cells may have necessitated the storage of ferrous ion; recent results suggest that ferrous ion may be stabilized inside ferritin long enough to be used in some types of cells. As primitive organisms began to proliferate, the successful photosynthetic cells, which trapped solar energy by reducing CO_2 to make carbohydrates $(CH_2O)_n$ and produce O_2, exhausted from the environment the reductants from H_2 or H_2S or NH_3. The ability of primitive organisms to switch to the use of H_2O as a reductant, with the concomitant production of dioxygen, probably produced the worst case of environmental pollution in terrestrial history. As a result, the composition of the atmosphere, the course of biological evolution, and the oxidation state of environmental iron all changed profoundly. Paleogeologists and meteorologists estimate that there was a lag of about 200 - 300 million years between the first dioxygen production and the appearance of significant dioxygen concentrations in the atmosphere, because the dioxygen produced at first was consumed by the oxidation of ferrous ions in the oceans. The transition in the atmosphere, which occurred about 2.5 billion years ago, caused the bioavailability of iron to plummet and the need for iron storage to increase. Comparison of the solubility of Fe^{3+} at physiological conditions (about 10^{-18} M) to the iron content of cells (equivalent to 10^{-5} to 10^{-8} M) emphasizes the difficulty of acquiring sufficient iron.

Iron is stored mainly in the ferritins, a family* of proteins composed of a protein coat and an iron core of hydrous ferric oxide $[Fe_2O_3(H_2O)_n]$ with various amounts of phosphate.[6,7] As many as 4,500 iron atoms can be reversibly stored inside the protein coat in a complex that is soluble; iron concentrations equivalent to 0.25 M [about 10^{16}-fold more concentrated than Fe(III) ions] can be easily achieved *in vitro* (Figure 1.1). Ferritin is found in animals, plants, and even in bacteria; the role of the stored iron varies, and includes intracellular use for Fe-proteins or mineralization, long-term iron storage for other cells, and detoxification of excess iron. Iron regulates the synthesis of ferritin, with large amounts of ferritin associated with iron excess, small or undetectable amounts associated with iron deficiency. [Interestingly, the template (mRNA) for ferritin synthesis is itself stored in cells and is recruited by intracellular iron or a derivative for efficient translation into protein.[31] Iron does not appear to interact directly with ferritin mRNA nor with a ferritin mRNA-specific regulatory (binding) protein; however, the specific, mRNA regulatory (binding) protein has sequence homology to aconitase, and formation of an iron-sulfate cluster prevents RNA binding.] Because iron itself determines in part the amount of ferritin in an organism, the environmental concentration of iron needs to be considered before one can conclude that an organism or cell does not have ferritin.

Ferritin is thought to be the precursor of several forms of iron in living organisms, including hemosiderin, a form of storage iron found mainly in animals. The iron in hemosiderin is in a form very similar to that in ferritin, but the complex with protein is insoluble, and is usually located within an intracellular membrane (lysosomes). Magnetite (Fe_3O_4) is another form of biological iron derived, apparently, from the iron in ferritin. Magnetite plays a role in the behavior of magnetic bacteria, bees, and homing pigeons (see Section II.C).

The structure of ferritin is the most complete paradigm for bioinorganic chemistry because of three features: the protein coat, the iron-protein interface, and the iron core.[6,7]

---

* A family of proteins is a group of related but distinct proteins produced in a single organism and usually encoded by multiple, related genes.

Protein Coat

Twenty-four peptide chains (with about 175 amino acids each), folded into ellipsoids, pack to form the protein coat,* which is a hollow sphere about 100 Å in diameter; the organic surface is about 10 Å thick (Figure 1.9). Channels which occur in the protein coat at the trimer interfaces may be involved in the movement of iron in and out of the protein.[62,63,65] Since the protein coat is

stable with or without iron, the center of the hollow sphere may be filled with solvent, with $Fe_2O_3 \cdot H_2O$, or, more commonly, with both small aggregates of iron and solvent. Very similar amino-acid sequences are found in ferritin from animals and plants. Sorting out which amino acids are needed to form the shape of the protein coat and the ligands for iron core formation requires the continued dedication of bioinorganic chemists; identification of tyrosine as an Fe(III)-ligand adds a new perspective.[64]

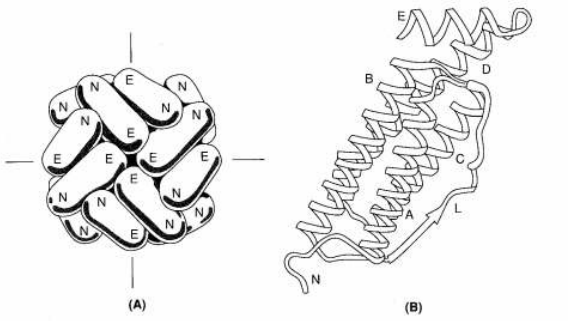


Figure 1.9 - (A) The protein coat of horse spleen apoferritin deduced from x-ray diffraction of crystals of the protein.[32] The outer surface of the protein coat shows the arrangement of the 24 ellipsoidal polypeptide subunits. N refers to the N-terminus of each polypeptide and E to the E-helix (see B). Note the channels that form at the four-fold axes where the E-helices interact, and at the threefold axes near the N-termini of the subunits. (B) A ribbon model of a subunit showing the packing of the four main alpha-helices (A, B, C, and D), the connecting L-loop and the E-helix.

* Some ferritin subunits, notably in ferritin from bacteria, bind heme in a ratio of less than one heme per two subunits. A possible role of such heme in the oxidation and reduction of iron in the core is being investigated.

Iron-Protein Interface

Formation of the iron core appears to be initiated at an Fe-protein interface where Fe(II)-O-Fe(Ill) dimers and small clusters of Fe(Ill) atoms have been detected attached to the protein and bridged to each other by oxo/hydroxo bridges. Evidence for multiple nucleation sites has been obtained from electron microscopy of individual ferritin molecules (multiple core crystallites were observed) and by measuring the stoichiometry of binding of metal ions, which compete with binding of monoatomic iron, e.g., VO(IV) and Tb(III) (about eight sites per molecule). EXAFS (*E*xtended *X*-ray *A*bsorption *F*ine *S*tructure) and Mössbauer spectroscopies suggest coordination of Fe to the protein by carboxyl groups from glutamic (Glu) and aspartic (Asp) acids. Although groups of Glu or Asp are conserved in all animal and plant ferritins, the ones that bind iron are not known. Tyrosine is an Fe(III)-ligand conserved in rapid mineralizing ferritins identified by Uv-vis and resonance Raman spectroscopy.[64]

Iron Core

Only a small fraction of the iron atoms in ferritin bind directly to the protein. The core contains the bulk of the iron in a polynuclear aggregate with properties similar to ferrihydrite, a mineral found in nature and formed experimentally by heating neutral aqueous solutions of $Fe(III)(NO_3)_3$. X-ray diffraction data from ferritin cores are best fit by a model with hexagonal close-packed layers of oxygen that are interrupted by irregularly incomplete layers of octahedrally coordinated Fe(III) atoms. The octahedral coordination is confirmed by Mössbauer spectroscopy and by EXAFS, which also shows that the average Fe(III) atom is surrounded by six oxygen atoms at a distance of 1.95 Å and six iron atoms at distances of 3.0 to 3.3 Å.

Until recently, all ferritin cores were thought to be microcrystalline and to be the same. However, x-ray absorption spectroscopy, Mössbauer spectroscopy, and high-resolution electron microscopy of ferritin from different sources have revealed variations in the degree of structural and magnetic ordering and/or the level of hydration. Structural differences in the iron core have been associated with variations in the anions present, e.g., phosphate[29] or sulfate, and with the electrochemical properties of iron. Anion concentrations in turn could reflect both the solvent composition and the properties of the protein coat. To understand iron storage, we need to define in more detail the relationship of the ferritin protein coat and the environment to the redox properties of iron in the ferritin core.

Experimental studies of ferritin formation show that Fe(II) and dioxygen are needed, at least in the early stages of core formation. Oxidation to Fe(III) and hydrolysis produce one electron and an average of 2.5 protons for iron atoms incorporated into the ferritin iron core. Thus, formation of a full iron core of 4,500 iron atoms would produce a total of 4,500 electrons and 11,250 protons. After

core formation by such a mechanism inside the protein coat, the pH would drop to 0.4 if all the protons were retained. It is known that protons are released and electrons are transferred to dioxygen. However, the relative rates of proton release, oxo-bridge formation, and electron transfer have not been studied in detail. Moreover, recent data indicate migration of iron atoms during the early stages of core formation and the possible persistence of Fe^{2+} for periods of time up to 24 hours. When large numbers of Fe(II) atoms are added, the protein coat appears to stabilize the encapsulated Fe(III).[34a,b] Formation of the iron core of ferritin has analogies to surface corrosion, in which electrochemical gradients are known to occur. Whether such gradients occur during ferritin formation and how different protein coats might influence proton release or alter the structure of the core are subjects only beginning to be examined.

Zinc, Copper, Vanadium, Chromium, Molybdenum, Cobalt, Nickel, and Manganese

Ions of nonferrous transition metals require a much less complex biological storage system, because the solubilities are much higher ($\geq 10^{-8}$ M) than those for Fe^{3+}. As a result, the storage of nonferrous transition metals is less obvious, and information is more limited. In addition, investigations are more difficult than for iron, because the amounts in biological systems are so small. Essentially nothing is known yet about the storage of vanadium, chromium, molybdenum, cobalt, nickel, and manganese, with the possible exception of accumulations of vanadium in the blood cells of tunicates.

Zinc and copper, which are used in the highest concentrations of any of the non-ferrous transition metals, are specifically bound by the protein metallothionein[35,36] (see Figure 1.10). Like the ferritins, the metallothioneins are a family of proteins, widespread in nature and regulated by the metals they bind. In contrast to ferritin, the amounts of metal stored in metallothioneins are smaller (up to twelve atoms per molecule), the amount of protein in cells is less, and the template (mRNA) is not stored. Because the cellular concentrations of the metallothioneins are relatively low and the amount of metal needed is relatively small, it has been difficult to study the biological fate of copper and zinc in living organisms, and to discover the natural role of metallothioneins. However, the regulation of metallothionein synthesis by metals, hormones, and growth factors attests to the biological importance of the proteins. The unusual metal environments of metallothioneins have attracted the attention of bioinorganic chemists.

Metallothioneins, especially in higher animals, are small proteins[35,36] rich in cysteine (20 per molecule) and devoid of the aromatic amino acids phenylalanine and tyrosine. The cysteine residues are distributed throughout the peptide chain. However, in the native form of the protein (Figure 1.10), the peptide chains fold to produce two clusters of -SH, which bind either three or four atoms of zinc, cadmium, cobalt, mercury, lead, or nickel. Copper binding is distinct from zinc, with 12 sites per molecule.

In summary, iron is stored in iron cores of a complicated protein. Ferritin, composed of a hollow protein coat, iron-protein interface, and an inorganic core, overcomes the problems of redox and hydrolysis by directing the formation of the quasi-stable mineral hydrous ferric oxide inside the protein coat. The outer surface of the protein is generally hydrophilic, making the complex highly soluble; equivalent concentrations of iron are ≤ 0.25 M. By contrast to iron, storage of zinc, copper, chromium, manganese, vanadium, and molybdenum is relatively simple, because solubility is high and abundance is lower. Little is known about the molecules that store these metals, with the possible exception of metallothionein, which binds small clusters of zinc or copper.

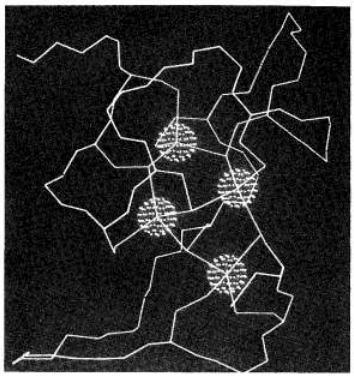


Figure 1.10 - The three-dimensional structure of the a domain from rat cd_7 metallothionein-2, determined by NMR in solution (Reference 36a), based on data in Reference 36b. The four metal atoms, bonded to the sulfur of cysteine side chains, are indicated as spherical collections of small dots. A recent description of the structure of the cd_5Zn_2 protein, determined from x-ray diffraction of crystals, agrees with the structure determined by NMR (Reference 36c).

17.2: Biological Systems of Metal Storage is shared under a not declared license and was authored, remixed, and/or curated by LibreTexts.

17.3: Chemical Properties Relative to Storage and Transport

Iron

Iron is the most abundant transition element in the Earth's crust and, in general, in all life forms. An outline of the distribution of iron in the Earth's crust[20,21] is shown in Table 1.2. As can be seen, approximately one-third of the Earth's mass is estimated to be iron. Of course, only the Earth's crust is relevant for life forms, but even there it is the most abundant transition element. Its concentration is relatively high in most crustal rocks (lowest in limestone, which is more or less pure calcium carbonate). In the oceans, which constitute 70 percent of the Earth's surface, the concentration of iron is low but increases with depth, since this iron exists as suspended particulate matter rather than as a soluble species. Iron is a limiting factor in plankton growth, and the rich fisheries associated with strong up-welling of ocean depths result at least in part from the biological growth allowed by these iron supplies. Properties that dominate the transport behavior of most transition metal ions are: (l) redox chemistry, (2) hydrolysis, and (3) the solubility of the metal ions in various complexes, particularly the hydroxides.

Table 1.2 - Iron: its terrestrial distribution.[a]

a) Data from References 1a and 20

One third of Earth's mass, most abundant element by weight

- Distribution in crustal rocks (weight %):
  - igneous 5.6
  - shale 4.7
  - sandstone 1.0
  - limestone 0.4
- Ocean (70% of Earth's surface):
  - 0.003 - 0.1 ppb, increasing with depth; limiting factor in plankton growth
- Rivers:
  - 0.07 - 7 ppm
- K_{sp} for $Fe(OH)_3$ is approximately 10^{-39}, hence at pH 7 $[Fe^{3+}]$ 10^{-18} M

As an example of the effects of solubility, consider the enormous variation in the concentration of iron in rivers, depending on whether the water is from a clear mountain stream running over rock or a muddy river carrying large amounts of sediment. However, the amount of dissolved iron in the form of free ferric ion or its hydrolysis products, whatever the source of water, is extremely low. As can be seen from the solubility of hydrated Fe(III) ($K_s \sim 10^{-18}$ M) (Table 1.2), the concentration of free ferric ion is extraordinarily low at neutral pH; so significant concentrations of soluble iron species can be attained only by strong complex formation.

One example of the versatility of iron as a function of its environment is how the ligand field can strongly alter the structural and ligand exchange properties of the metal ion (Figure 1.3). The ligand field can also alter the redox properties. For high-spin ferric ion, as found in the aquo complex or in many other complexes (including the class of microbial iron-transport agents called siderophores, to be discussed later), the coordination geometry is octahedral or pseudo-octahedral. In the relatively weak ligand field (high-spin ground state), the complex is highly labile. In a strong ligand field, such as an axially ligated porphyrin complex of ferric ion, or the simple example of the ferrocyanide anion, the low-spin complex is exchange-inert. Similarly, the high-spin octahedral ferrous complexes are exchange-labile, but the corresponding axially ligated porphyrin complexes, or the ferrocyanide complexes, are spin-paired (diamagnetic) and ligand exchange-inert. Large, bulky ligands or constrained ligands, such as those provided by metalloprotein and enzyme sites, can cause a tetrahedral environment, in which both ferrous ion and ferric ion form high-spin complexes.

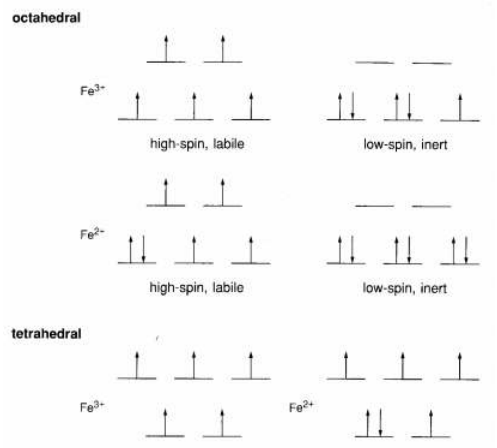


Figure 1.3 - Versatility of Fe coordination complexes.

The distribution of specific iron complexes in living organisms depends strongly on function. For example, although there are many different iron complexes in the average human, the relative amounts of each type differ more than 650-fold (Table 1.3). The total amount of iron in humans is quite large, averaging more than three and up to five grams for a healthy adult. Most of the iron is present as hemoglobin, the plasma oxygen-transport protein, where the function of the iron is to deliver oxygen for respiration. A much smaller amount of iron is present in myoglobin, a muscle oxygen-storage protein. For transport, the most important of these iron-containing proteins is transferrin, the plasma iron-transport protein that transfers iron from storage sites in the body to locations where cells synthesizing iron proteins reside; the major consumers of iron in vertebrates are the red blood cells. However, at any given time relatively little of the iron in the body is present in transferrin, in much the same way that at any given time in a large city only a small fraction of the population will be found in buses or taxis. Other examples of iron-containing proteins and their functions are included in Table 1.3 for comparison.

Table 1.3 - Average human Fe distribution

Protein	Function	Oxidation State of Fe	Amount of Fe (g)	Percent of Total
Hemoglobin	Plasma O_2 transport	2	2.6	65
Myoglobin	Muscle O_2 storage	2	0.13	6
Transferrin	Plasma Fe transport	3	0.007	0.2
Ferritin	Cell Fe storage	3	0.52	13
Hemosiderin	Cell Fe storage	3	0.48	12
Catalase	H_2O_2 metabolism	2	0.004	0.1
Cytochrome *c*	Electron transport	$\frac{2}{3}$ (17.3.1)	0.004	0.1
Other	Oxidases, other enzymes, etc.		0.14	3.6

An example of different iron-coordination environments, which alter the chemical properties of iron, is the difference in the redox potentials of hydrated Fe^{3+} and the electron-transport protein cytochrome *c* (Table 1.4). The coordination environment of iron in cytochrome *c* is illustrated in Figure 1.4. For example, the standard reduction potential for ferric ion in acid solution is 0.77 volts; so here ferric ion is quite a good oxidant. In contrast, cytochrome *c* has a redox potential of 0.25 volts. A wide range of redox potentials for iron is achieved in biology by subtle differences in protein structure, as listed in Table 1.4. Notice the large difference in the potential of cytochrome *c* and rubredoxin (Figure 1.5), 0.25 volts vs. -0.06 volts, respectively. In polynuclear ferredoxins, in

which each iron is tetrahedrally coordinated by sulfur, reduction potentials are near -0.4 volts. Thus, the entire range of redox potentials, as illustrated in Table 1.4, is more than one volt.

Table 1.4 - Fe redox potentials

Complex	Coord. no., type	Fe^{3+}/Fe^{2+} E^o (mV)
$Fe(OH_2)_6^{3+}$	6, aquo complex	770
Cytochrome a_3	6, heme	390
HIPIP	4, $Fe_4S_4(SR)_4^-$	350
Cytrochrome *c*	6, heme	250
Rubredoxin	4, $Fe(SR)_4$	-60
Ferredoxins	4, $Fe_4S_4(SR)_4^{2-}$	-400

Zinc, Copper, Vanadium, Chromium, Molybdenum, and Cobalt

The chemical properties of the other essential transition elements simplify their transport properties. For zinc there is only the +2 oxidation state, and the hydrolysis of this ion is not a limiting feature of its solubility or transport. Zinc is an essential element for both animals and plants.[8,9,20,21] In general, metal ion uptake into the roots of plants is an extremely complex phenomenon. A cross-sectional diagram of a root is shown in Figure 1.6. It is said that both diffusion and mass flow of the soil solution are of significance in the movement of metal ions to roots. Chelation and surface adsorption, which are pH dependent, also affect the availability of nutrient metal ions. Acid soil conditions in general retard uptake of essential divalent metal ions but increase the availability (sometimes with toxic results) of manganese, iron, and aluminum, all of which are normally of very limited availability because of hydrolysis of the trivalent ions.

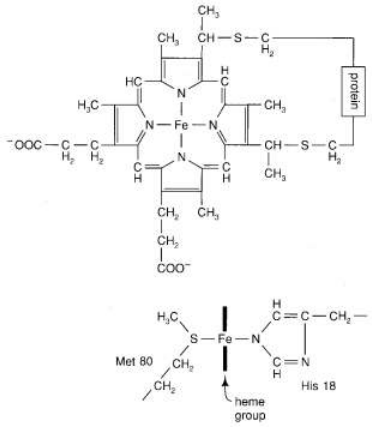


Figure 1.4 - Heme group and iron coordination in cytochrome c.

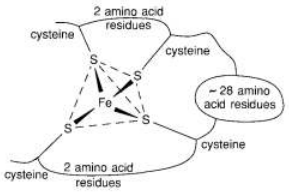


Figure 1.5 - $Fe^{3+/2+}$ coordination in rubredoxin.

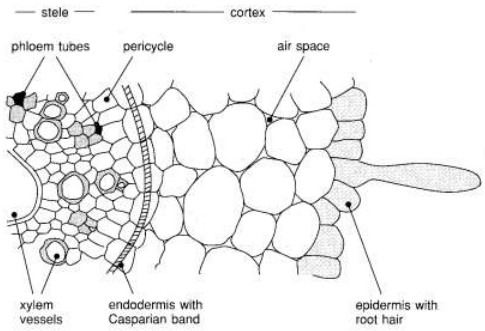


Figure 1.6 - Transverse section of a typical root.[20] The complex features of the root hair surface that regulate reductase and other activities in metal uptake are only beginning to be understood.

Vanadium is often taken up as vanadate, in a pathway parallel to phosphate.[18] However, its oxidation state within organisms seems to be highly variable. Unusually high concentrations of vanadium occur in certain ascidians (the specific transport behavior of which will be dealt with later). The workers who first characterized the vanadium-containing compound of the tunicate, *Ascidia nigra*, coined the name tunichrome.[22] The characterization of the compound as a dicatecholate has been reported.[23]

Quite a different chemical environment is found in the vanadium-containing material isolated from the mushroom *Amanita muscaria*. Bayer and Kneifel, who named and first described amavadine,[24] also suggested the structure shown in Figure 1.7.[25] Recently the preparation, proof of ligand structure, and (by implication) proof of the complex structure shown in Figure 1.7 have been established.[26] Although the exact role of the vanadium complex in the mushroom remains unclear, the fact that it is a vanadyl complex is now certain, although it may take a different oxidation state *in vivo*.

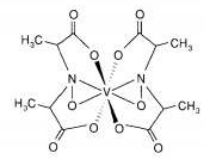


Figure 1.7 - A structure proposed for amavadine.[27]

The role of chromium in biology remains even more mysterious. In human beings the isolation of "glucose tolerance factor" and the discovery that it contains chromium goes back some time. This has been well reviewed by Mertz, who has played a major role in discovering what is known about this elusive and apparently quite labile compound.[27] It is well established that chromium is taken up as chromic ion, predominantly via foodstuffs, such as unrefined sugar, which presumably contain complexes of chromium, perhaps involving sugar hydroxyl groups. Although generally little chromium is taken up when it is administered as inorganic salts, such as chromic chloride, glucose tolerance in many adults and elderly people has been reported to be improved after supplementation with 150 - 250 mg of chromium per day in the form of chromic chloride. Similar results have been found in malnourished children in some studies in Third World countries. Studies using radioactively labeled chromium have shown that, although inorganic salts of chromium are relatively unavailable to mammals, brewer's yeast can convert the chromium into a usable form; so brewer's yeast is today the principal source in the isolation of glucose tolerance factor and has been used as a diet supplement.

Although chromium is essential in milligram amounts for human beings as the trivalent ion, as chromate it is quite toxic and a recognized carcinogen.[30] The uptake-reduction model for chromate carcinogenicity as suggested by Connett and Wetterhahn is shown in Figure 1.8. Chromate is mutagenic in bacterial and mammalian cell systems, and it has been hypothesized that the difference between chromium in the +6 and +3 oxidation states is explained by the "uptake-reduction" model. Chromium(III), like the ferric ion discussed above, is readily hydrolyzed at neutral pH and extremely insoluble. Unlike Fe^{3+}, it undergoes extremely slow ligand exchange. For both reasons, transport of chromium(III) into cells can be expected to be extremely slow unless it is present as specific complexes; for example, chromium(III) transport into bacterial cells has been reported to be rapid when iron is replaced by chromium in the siderophore iron-uptake mediators. However, chromate readily crosses cell membranes and enters cells, much as sulfate does. Because of its high oxidizing power, chromate can undergo reduction inside organelles to give chromium(m), which binds to small molecules, protein, and DNA, damaging these cellular components.

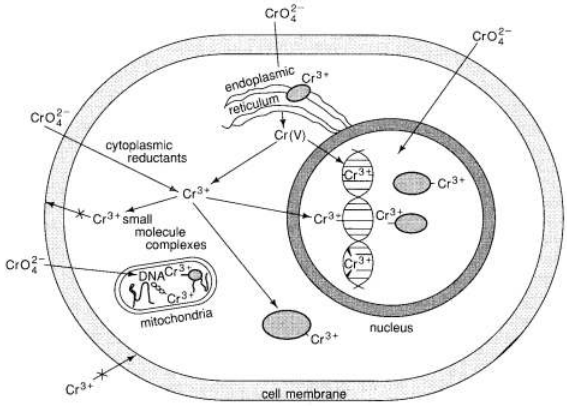


Figure 1.8 - The uptake-reduction model for chromate carcinogenicity. Possible sites for reduction of chromate include the cytoplasm, endoplasmic reticulum, mitochondria, and the nucleus.[27]

In marked contrast to its congener, molybdenum is very different from chromium in both its role in biology and its transport behavior, again because of fundamental differences in oxidation and coordination chemistry properties. In contrast to chromium, the higher oxidation states of molybdenum dominate its chemistry, and molybdate is a relatively poor oxidant. Molybdenum is an essential element in many enzymes, including xanthine oxidase, aldehyde reductase, and nitrate reductase.[19] The range of oxidation states and coordination geometries of molybdenum makes its bioinorganic chemistry particularly interesting and challenging.

The chemistry of iron storage and transport is dominated by high concentrations, redox chemistry (and production of toxic-acting oxygen species), hydrolysis (pK_a is about 3, far below physiological pH), and insolubility. High-affinity chelators or proteins are required for transport of iron and high-capacity sequestering protein for storage. By comparison to iron, storage and transport of the other metals are simple. Zinc, copper, vanadium, chromium, manganese, and molybdenum appear to be transported as simple salts or loosely bound protein complexes. In vanadium or molybdenum, the stable anion, vanadate or molybdate, appears to dominate transport. Little is known about biological storage of any metal except iron, which is stored in ferritin. However, zinc and copper are bound to metallothionein in a form that may participate in storage.

17.3: Chemical Properties Relative to Storage and Transport is shared under a not declared license and was authored, remixed, and/or curated by LibreTexts.

17.4: Iron Biomineralization

Many structures formed by living organisms are minerals. Examples include apatite [$Ca_2(OH)PO_4$] in bone and teeth, calcite or aragonite ($CaCO_3$) in the shells of marine organisms and in the otoconia (gravity device) of the mammalian ear, silica (SiO_2) in grasses and in the shells of small invertebrates such as radiolara, and iron oxides, such as magnetite (Fe_3O_4) in birds and bacteria (navigational devices) and ferrihydrite FeO(OH) in ferritin of mammals, plants, and bacteria. Biomineralization is the formation of such minerals by the influence of organic macromolecules, e.g., proteins, carbohydrates, and lipids, on the precipitation of amorphous phases, on the initiation of nucleation, on the growth of crystalline phases, and on the volume of the inorganic material.

Iron oxides, as one of the best-studied classes of biominerals containing transition metals, provide good examples for discussion. One of the most remarkable recent characterizations of such processes is the continual deposition of single-crystal ferric oxide in the teeth of chiton.[48] Teeth of chiton form on what is essentially a continually moving belt, in which new teeth are being grown and moved forward to replace mature teeth that have been abraded. However, the study of the mechanisms of biomineralization in general is relatively recent; a great deal of the information currently available, whether about iron in ferritin or about calcium in bone, is somewhat descriptive.

Three different forms of biological iron oxides appear to have distinct relationships to the proteins, lipids, or carbohydrates associated with their formation and with the degree of crystallinity.[49] Magnetite, on the one hand, often forms almost perfect crystals inside lipid vesicles of magneto-bacteria.[50] Ferrihydrite, on the other hand, exists as large single crystals, or collections of small crystals, inside the protein coat of ferritin; however, iron oxides in some ferritins that have large amounts of phosphate are very disordered. Finally, goethite [α-FeO(OH)] and lepidocrocite [γ-FeO(OH)] form as small single crystals in a complex matrix of carbohydrate and protein in the teeth of some shellfish (limpets and chitons); magnetite is also found in the lepidocrocite-containing teeth. The differences in the iron-oxide structures reflect differences in some or all of the following conditions during formation of the mineral: nature of co-precipitating ions, organic substrates or organic boundaries, surface defects, inhibitors, pH, and temperature. Magnetite can form in both lipid and protein/carbohydrate environments, and can sometimes be derived from amorphous or semicrystalline ferrihydrite-like material (ferritin). However, the precise relationship between the structure of the organic phase and that of the inorganic phase has yet to be discovered. When the goal of understanding how the shape and structure of biominerals is achieved, both intellectual satisfaction and practical commercial and medical information will be provided.

Synthetic iron complexes have provided models for two stages of ferritin iron storage and biomineralization:[51-59]

1. the early stages, when small numbers of clustered iron atoms are bound to the ferritin protein coat, and
2. the final stages, where the bulk iron is a mineral with relatively few contacts to the protein coat. In addition, models have begun to be examined for the microenvironment inside the protein coat.[54]

Among the models for the early or nucleation stage of iron-core formation are the binuclear Fe(III) complexes with $[Fe_2O(O_2CR_2)]^{2+}$ cores;[55,56] the three other Fe(III) ligands are N. The μ-oxo complexes, which are particularly accurate models for the binuclear iron centers in hemerythrin, purple acid phosphatases, and, possibly, ribonucleotide reductases, may also serve as models for ferritin, since an apparently transient Fe(II)-O-Fe(III) complex was detected during the reconstitution of ferritin from protein coats and Fe(II). The facile exchange of (O_2CR) for (O_2PR) in the binuclear complex is particularly significant as a model for ferritin, because the structure of ferritin cores varies with the phosphate content. An asymmetric trinuclear $(Fe_3O)^{7+}$ complex[57] and an $(FeO)_{11}$ complex (Figure 1.21) have been prepared; these appear to serve as models for later stages of core nucleation (or growth).[59]

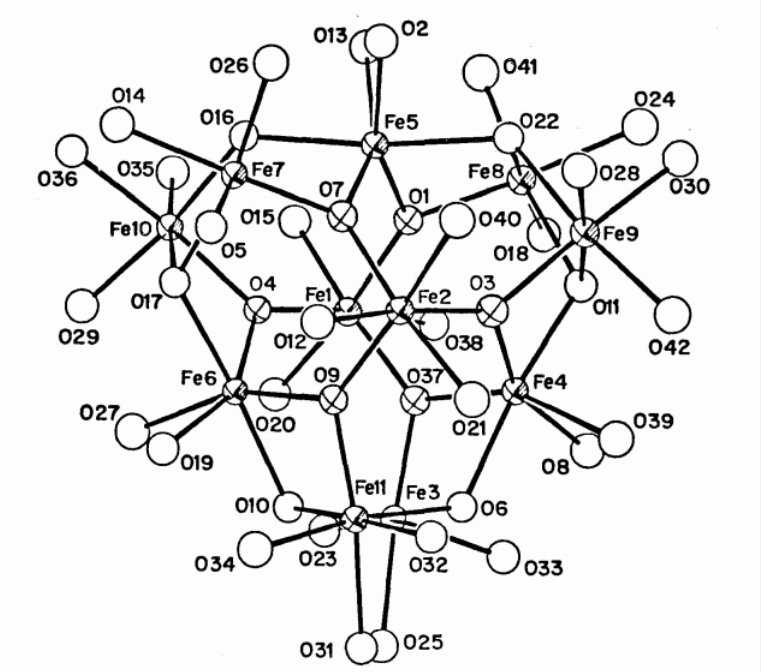


Figure 1.21 - The structure of a model for a possible intermediate in the formation of the ferritin iron core. The complex consists of 11 Fe(III) atoms with internal oxo-bridges and a coat of benzoate ligands; the Fe atoms define a twisted, pentacapped trigonal prism. See Reference 53.

Models for the full iron core of ferritin include ferrihydrite, which matches the ordered regions of ferritin cores that have little phosphate; however, the site vacancies in the lattice structure of ferrihydrite [FeO(OH)] appear to be more regular than in crystalline regions of ferritin cores. A polynuclear complex of iron and microbial dextran $(\alpha\text{-}1,4\text{-D-glucose})_n$ has spectroscopic (Mössbauer, EXAFS) properties very similar to those of mammalian ferritin, presumably because the organic ligands are similar to those of the protein (-OH, -COOH). In contrast, a polynuclear complex of iron and mammalian chondroitin sulfate $(\alpha\text{-}1,4\text{-}[\alpha\text{-}1,3\text{-D-glucuronic acid-N-acetyl-D-galactosamine-4-sulfate}]_n)$ contains two types of domains: one like mammalian ferritin [FeO(OH)] and one like hematite ($\alpha\text{-}Fe_2O_3$), which was apparently nucleated by the sulfate, emphasizing the importance of anions in the structure of iron cores.[60] Finally, a model for iron cores high in phosphate, such as those from bacteria, is Fe-ATP (4:1), in which the phosphate is distributed throughout the polynuclear iron complex, providing an average of 1 or 2 of the 6 oxygen ligands for iron.[61]

The microenvironment inside the protein coat of ferritin has recently been modeled by encapsulating ferrous ion inside phosphatidylcholine vesicles and studying the oxidation of iron as the pH is raised. The efficacy of such a model is indicated by the observation of relatively stable mixtures of Fe(II)/Fe(III) inside the vesicles, as have also been observed in ferritin reconstituted experimentally from protein coats and ferrous ion.[43,54]

Models for iron in ferritin must address both the features of traditional metalprotein interactions and the bulk properties of materials. Although such modeling may be more difficult than other types of bioinorganic modeling, the difficulties are balanced by the availability of vast amounts of information on Fe-protein interactions, corrosion, and mineralization. Furthermore, powerful tools such as x-ray absorption, Mössbauer and solid state NMR spectroscopy, scanning electron and proton microscopy, and transmission electron microscopy reduce the number of problems encountered in modeling the ferritin ion core.

Construction of models for biomineralization is clearly an extension of modeling for the bulk phase of iron in ferritin, since the major differences between the iron core of ferritin and that of other iron-biominerals are the size of the final structure, the generally higher degree of crystallinity, and, at this time, the more poorly defined organic phases. A model for magnetite formation has been provided by studying the coulometric reduction of half the Fe^{3+} atoms in the iron core of ferritin itself. Although the conditions for producing magnetite have .yet to be discovered, the unexpected observation of retention of the Fe^{2+} by the protein coat has provided lessons for understanding the iron core of ferritin. Phosphatidyl choline vesicles encapsulating Fe^{2+} appear to serve as models for both ferritin and magnetite; only further investigation will allow us to understand the unique features that convert Fe^{2+} to [FeO(OH)], on the one hand, and Fe_3O_4, on the other.

17.4: Iron Biomineralization is shared under a not declared license and was authored, remixed, and/or curated by LibreTexts.

17.5: Transport of Iron

The storage of iron in humans and other mammals has been dealt with in the previous section. Only a small fraction of the body's inventory of iron is in transit at any moment. The transport of iron from storage sites in cellular ferritin or hemosiderin occurs via the serum-transport protein transferrin. The transferrins are a class of proteins that are bilobal, with each lobe reversibly (and essentially independently) binding ferric ion.[37-39] This complexation of the metal cation occurs via prior complexation of a synergistic anion that *in vivo* is bicarbonate (or carbonate). Serum transferrin is a monomeric glycoprotein of molecular weight 80 kDa. The crystal structure of the related protein, lactoferrin,[39] has been reported, and recently the structure of a mammalian transferrin[40] has been deduced.

Ferritin is apparently a very ancient protein and is found in higher animals, plants, and even microbes; in plants and animals a common ferritin progenitor is indicated by sequence conservation.[41] In contrast, transferrin has been in existence only relatively recently, since it is only found ia the phylum Chordata. Although the two iron-binding sites of transferrin are sufficiently different to be distinguishable by kinetic and a few other studies, their coordination environments have been known for some time to be quite similar. This was first discovered by various spectroscopies, and most recently was confirmed by crystal-structure analysis, which shows that the environment involves two phenolate oxygens from tyrosine, two oxygens from the synergistic, bidentate bicarbonate anion, nitrogen from histidine, and (a surprise at the time of crystal-structure analysis) an oxygen from a carboxylate group of an aspartate.[39]

The transferrins are all glycoproteins, and human serum transferrin contains about 6 percent carbohydrate. These carbohydrate groups are linked to the protein, and apparently strongly affect the recognition and conformation of the native protein.

Although transferrins have a high molecular weight and bind only two iron atoms, transferrin is relatively efficient, because it is used in many cycles of iron transport in its interaction with the tissues to which it delivers iron. Transferrin releases iron *in vivo* by binding to the cell surface and forming a vesicle inside the cell (endosome) containing a piece of the membrane with transferrin and iron still complexed. The release of the iron from transferrin occurs in the relatively low pH of the endosome, and apoprotein is returned to the outside of the cell for delivery of another pair of iron atoms. This process in active reticulocytes (immature red blood cells active in iron uptake) can turn over roughly a million atoms of iron per cell per minute.[38] A schematic structure of the protein, deduced from crystal-structure analysis, is shown in Figure 1.11.

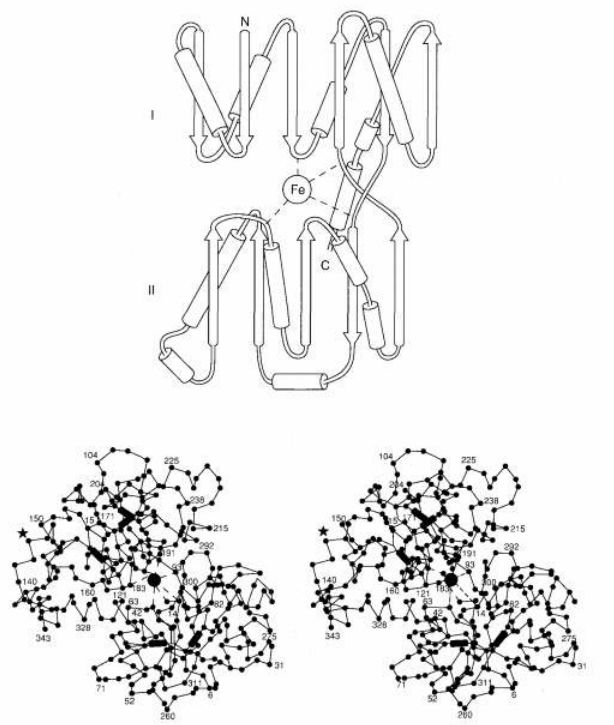


Figure 1.11: Three-dimensional structure of lactotransferrin. Top: schematic representation of the folding pattern of each lactoferrin lobe; Domain 1 is based on a beta-sheet of four parallel and two antiparallel domains; Domain II is formed from four parallel and one antiparallel strand. Bottom: stereo Ca diagram of the N lobe of lactoferrin; (●) *iron atom between domain 1 (residues 6 - 90+) and domain II (residues 91 - 251);* (⬛) *disulfide bridges;* (★) *carbohydrate attachment site. See Reference 39.*

Transferrin is an ellipsoidal protein with two subdomains or lobes, each of which binds iron. The two halves of each subunit are more or less identical, and are connected by a relatively small hinge. In human lactoferrin, the coordination site of the iron is the same as the closely related serotransferrin site. A major question that remains about the mechanism of iron binding and release is how the protein structure changes in the intracellular compartment of low pH to release the iron when it forms a specific complex with cell receptors (transferrin binding proteins) and whether the receptor protein is active or passive in the process. Recent studies suggest that the cell binding site for transferrin (a membrane, glycoprotein called the transferrin receptor) itself influences the stability of the iron-transferrin complex. The path of iron from the endosome to Feproteins has not been established; and the form of transported intracellular iron is not known.

Another major type of biological iron transport occurs at the biological opposite of the higher organisms. Although almost all microorganisms have iron as an essential element, bacteria, fungi, and other microorganisms (unlike humans and other higher organisms) cannot afford to make high-molecular-weight protein-complexing agents for this essential element when those complexing agents would be operating extracellularly and hence most of the time would be lost to the organism. As described earlier, the first life forms on the surface of the Earth grew in a reducing atmosphere, in which the iron was substantially more available because it was present as ferrous-containing compounds. In contrast to the profoundly insoluble ferric hydroxide, ferrous hydroxide is relatively soluble at near neutral pH. It has been proposed that this availability of iron in the ferrous state was one of the factors that led to its early incorporation in so many metabolic processes of the earliest chemistry of life.[6,38] In an oxidizing environment, microorganisms were forced to deal with the insolubility of ferric hydroxide and hence when facing iron deficiency secrete high-affinity iron-binding compounds called siderophores (from the Greek for iron carrier). More than 200 naturally occurring siderophores have been isolated and characterized to date.[42]

Most siderophore-mediated iron-uptake studies in microorganisms have been performed by using cells obtained under iron-deficient aerobic growth conditions. However, uptake studies in *E. coli* grown under anaerobic conditions have also established the presence of siderophore-specific mechanisms. In both cases, uptake of the siderophore-iron complex is both a receptor- and an energy-dependent process. In some studies the dependence of siderophore uptake rates on the concentration of the iron-siderophore complex has been found to conform to kinetics characteristic of protein catalysts, i.e., Michaelis-Menten kinetics. For example,

saturable processes with very low apparent dissociation constants of under one micromolar (1 μM) have been observed for ferric-enterobactin transport in *E. coli* (a bacterium), as shown in Figure 1.12.

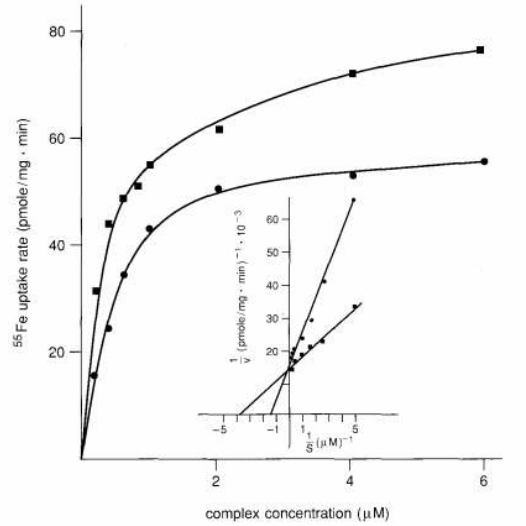


Figure 1.12 - Effect of MECAM analogues on iron uptake from E. coli. Iron transport by 2 μM ferric enterobactin is inhibited by ferric MECAM.

Similarly, in a very different microorganism, the yeast *Rhodoturala pilimanae*, Michaelis-Menten kinetics were seen again with a dissociation constant of approximately 6 μM for the ferric complex of rhodotoroulic acid; diagrams of some representative siderophores are shown in Figure 1.13. The siderophore used by the fungus *Neurospora crassa* was found to have a dissociation constant of about 5 μM and, again, saturable uptake kinetics.

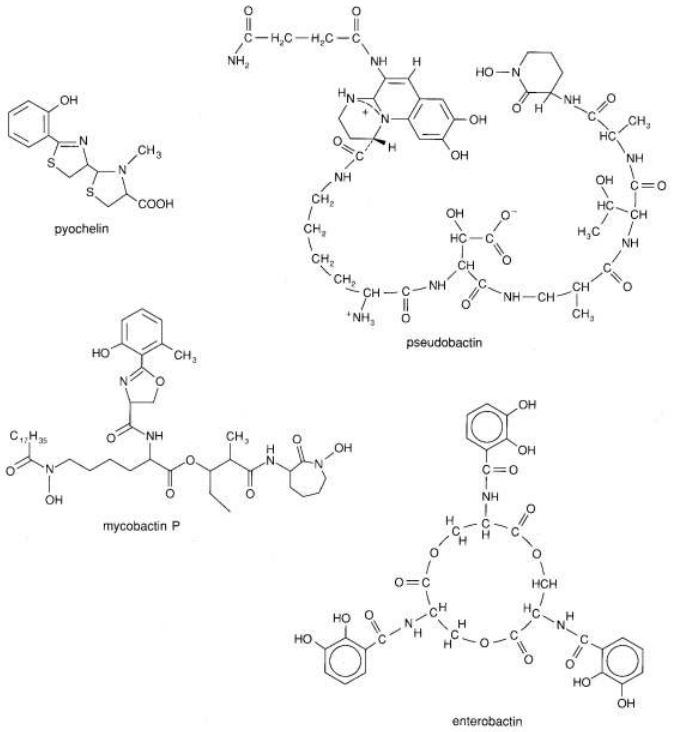


Figure 1.13 - Examples of bacterial siderophores. See Reference 42.

Although the behavior just described seems relatively simple, transport mechanisms in living cells probably have several more kinetically distinct steps than those assumed for the simple enzyme-substrate reactions underlying the Michaelis-Menten mechanism. For example, as ferric enterobactin is accumulated in *E. coli*, it has to pass through the outer membrane, the periplasm,

and the cytoplasm membrane, and is probably subjected to reduction of the metal in a low-pH compartment or to ligand destruction.

A sketch of a cell of E. coli and some aspects of its transport behavior are shown in Figure 1.14. Enterobactin-mediated iron uptake in *E. coli* is one of the best-characterized of the siderophore-mediated iron-uptake processes in microorganisms, and can be studied as a model. After this very potent iron-sequestering agent complexes iron, the ferric-enterobactin complex interacts with a specific receptor in the outer cell membrane (Figure 1.14), and the complex is taken into the cell by active transport. The ferric complexes of some synthetic analogs of enterobactin can act as growth agents in supplying iron to *E. coli*. Such a feature could be used to discover which parts of the molecule are involved in the sites of structural recognition of the ferric-enterobactin complex. Earlier results suggested that the metal-binding part of the molecule is recognized by the receptor, whereas the ligand platform (the triserine lactone ring; see Figure 1.13) is not specifically recognized.

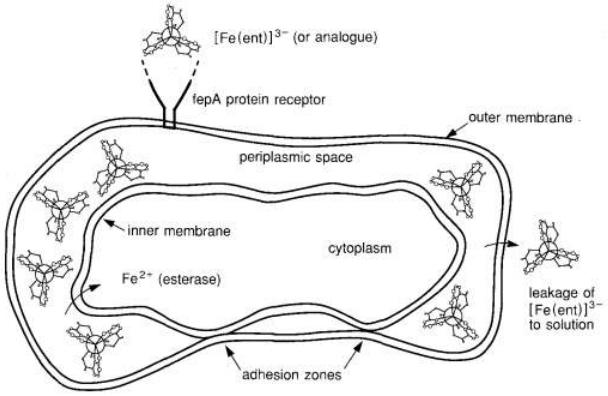


Figure 1.14 - Model for enterobactin-mediated Fe uptake in E. coli.

To find out which domains of enterobactin are required for iron uptake and recognition, rhodium complexes were prepared with various domains of enterobactin (Figure 1.15) as ligands to use as competitors for ferric enterobactin.[44] The goal was to find out if the amide groups (labeled Domain II in Figure 1.15), which linked the metal-binding catechol groups (Domain III, Figure 1.15) to the central ligand backbone (Domain I, Figure 1.15), are necessary for recognition by the receptor protein. In addition, synthetic ligands were prepared that differed from enterobactin by small changes at or near the catecholate ring. Finally, various labile trivalent metal cations, analogous to iron, were studied to see how varying the central metal ion would affect the ability of metal enterobactin complexes to inhibit competitively the uptake of ferric enterobactin by the organism. For example, if rhodium MECAM (Figure 1.16) is recognized by the receptor for ferric enterobactin on living microbial cells, a large excess of rhodium MECAM will block the uptake of radioactive iron added as ferric enterobactin. In fact, the rhodium complex completely inhibited ferric-enterobactin uptake, proving that Domain I is not required for recognition of ferric enterobactin.

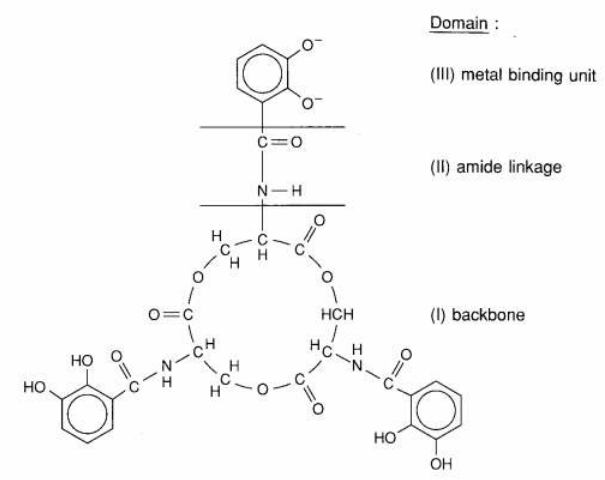


Figure 1.15 - Definition of recognition domains in enterobactin.

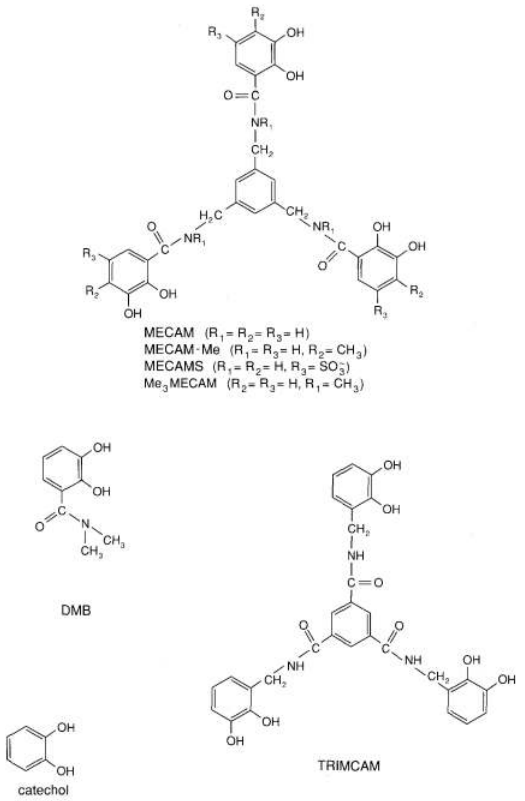


Figure 1.16 - MECAM and related enterobactin analogues.

However, if only Domain III is important in recognition, it would be expected that the simple tris(catecholato)-rhodium(III) complex would be an equally good inhibitor. In fact, even at concentrations in which the rhodium-catechol complex was in very large excess, no inhibition of iron uptake was observed, suggesting that Domain II is important in the recognition process.

The role of Domain II in the recognition process was probed by using a rhodium dimethyl amide of 2,3-dihydroxybenzene (DMB) as a catechol ligand, with one more carbonyl ligand than in the tris(catecholato)-rhodium(III) complex. Remarkably, this molecule shows substantially the same inhibition of enterobactin-mediated iron uptake in *E. coli* as does rhodium MECAM itself. Thus, in addition to the iron-catechol portion of the molecule, the carbonyl groups (Domain II) adjacent to the catechol-binding subunits of enterobactin and synthetic analogs are required for recognition by the ferric-enterobactin receptor. In contrast, when a methyl group was attached to the "top" of the rhodium MECAM complex, essentially no recognition occurred.

In summary, although the structure of the outer-membrane protein receptor of *E. coli* is not yet known, the composite of the results just described gives a sketch of what the ferric-enterobactin binding site must look like: a relatively rigid pocket for receiving the ferric-catecholate portion of the complex, and proton donor groups around this pocket positioned to hydrogen bond to the carbonyl oxygens of the ferric amide groups. The mechanisms of iron release from enterobactin, though followed phenomenologically, are still not known in detail.

17.5: Transport of Iron is shared under a not declared license and was authored, remixed, and/or curated by LibreTexts.

17.6: Transport of Zinc, Copper, Vanadium, Chromium, Molybdenum, and Cobalt

As described in an earlier section, transport problems posed by the six elements listed in the heading are somewhat simpler (with the exception of chromium) than those for iron. One very interesting recent development has been the characterization of sequestering agents produced by plants which complex a number of metal ions, not just ferric ions. A key compound, now well-characterized, is mugeneic acid (Figure 1.17).[45] The structural and chemical similarities of mugeneic acid to ethylenediaminetetraacetic acid (EDTA) have been noted. Like EDTA, mugeneic acid forms an extremely strong complex with ferric ion, but also forms quite strong complexes with copper, zinc, and other transition-metal ions. The structure of the cobalt complex (almost certainly essentially identical with that of the iron complex) is shown in Figure 1.18. Like the siderophores produced by microorganisms, the coordination environment accommodated by mugeneic acid is essentially octahedral. Although the coordination properties of this ligand are well laid out, and it has been shown that divalent metal cations, such as copper, competitively inhibit iron uptake by this ligand, the detailed process of metal-ion delivery by mugeneic acid and related compounds has not been elucidated.

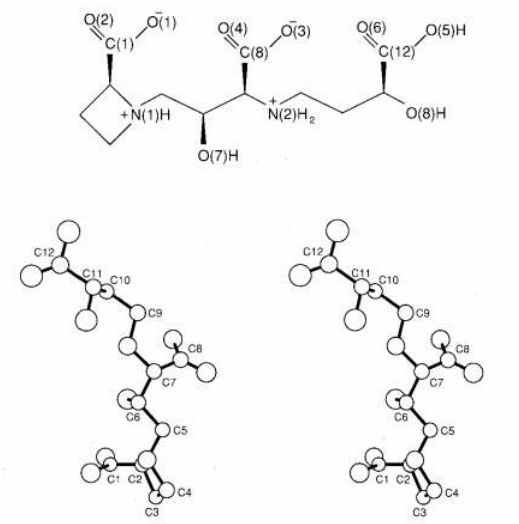


Figure 1.17 - Structure and a stereo view of mugeneic acid. See Reference 42.

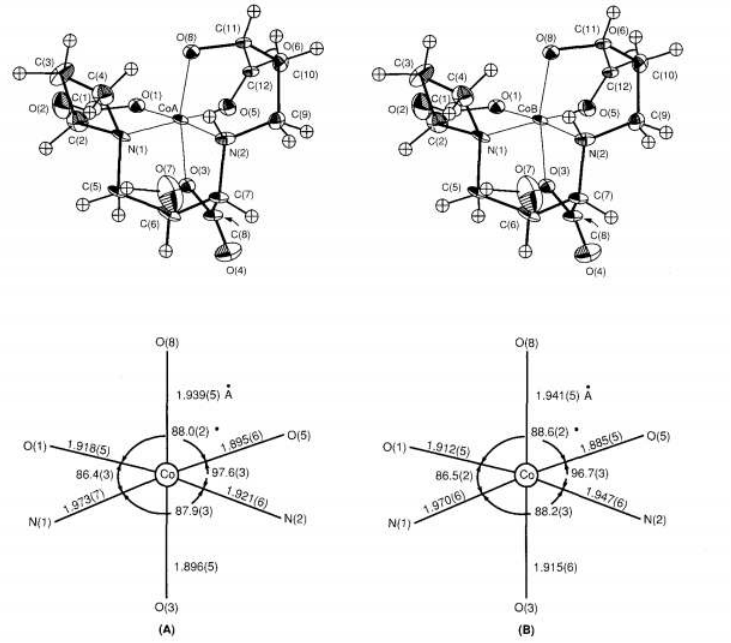


Figure 1.18 - Molecular structures of the complexes (molecules A and B) and coordination about the cobalt ion in molecules A and B of the mugeneic acid-Co(III) complex. Bond lengths in Å; angles in degrees. See Reference 42.

As noted in an earlier section, the biochemistry of vanadium potentially involves four oxidation states that are relatively stable in aqueous solution. These are V^{2+}, V^{3+}, VO^{2+} , and VO^{2+} (the oxidation states 2, 3, 4, and 5, respectively). Since even without added sequestering agents, V^{2+} slowly reduces water to hydrogen gas, it presumably has no biological significance. Examples of the remaining three oxidation states of vanadium have all been reported in various living systems. One of the most extensively investigated examples of transition-metal-ion accumulation in living organisms is the concentration of vanadium in sea squirts (tunicates), which is reported to be variable; many species have vanadium levels that are not exceptionally high. Others such as *Ascidia nigra* show exceptionally high vanadium concentrations.[46]

In addition to showing a remarkable concentration of a relatively exotic transition-metal ion, tunicates are a good laboratory model for uptake experiments, since they are relatively simple organisms. They possess a circulation system with a one-chambered heart, and a digestive system that is essentially a pump and an inlet and outlet valve connected by a digestive tract. The organism can absorb dissolved vanadium directly from sea water as it passes through the animal. The influx of vanadate into the blood cells of *A. nigra* has been studied by means of radioisotopes. The corresponding influx of phosphate, sulfate, and chromate (and the inhibition of vanadate uptake by these structurally similar oxoanions) has been measured. In the absence of inhibitors, the influx of vanadate is relatively rapid (a half-life on the order of a minute near 0 ºC) and the uptake process shows saturation behavior as the vanadate concentration is increased. The uptake process (in contrast to iron delivery in microorganisms, for example, and to many other uptake processes in microorganisms or higher animals) is *not* energy-dependent. Neither inhibitors of glycolysis nor decouplers of respiration-dependent energy processes show any significant effect on the rate of vanadate influx.

Phosphate, which is also readily taken up by the cells, is an inhibitor of vanadate influx. Neither sulfate nor chromate is taken up significantly, nor do they act as significant inhibitors for the vanadate uptake. Agents that inhibit transport of anions, in contrast, were found to inhibit uptake of vanadate into the organism. These results have led to the model proposed in Figure 1.19:

1. vanadate enters the cell through anionic channels; this process eliminates positively charged metal ion or metal-ion complexes present in sea water;
2. vanadate is reduced to vanadium(III); since the product is a cation, and so cannot be transported through the anionic channels by which vanadate entered the cell, the vanadium(III) is trapped inside the cell-the net result is an accumulation of vanadium. [It has been proposed that the tunichrome could act either as a reducing agent (as the complex) or (as the ligand) to stabilize the general vanadium(III); however, this seems inconsistent with its electrochemical properties (see below).]

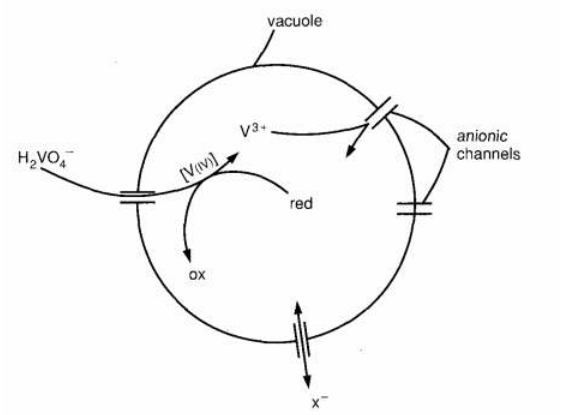


Figure 1.19 - Diagram of a vanadium accumulation mechanism. Vanadium enters the vacuole within the vanadocyte as mononegative $H_2VO_4^-$, although it may be possible for the dinegative anion, HVO_4^{2-}, to enter this channel as well (X^- stands for any negative ion such as Cl^- , $H_2PO_4^-$, etc., that may exchange across the membrane through the anionic channel). Reduction to V^{3+} takes place in two steps, via a V(IV) intermediate. The resulting cations may be trapped as tightly bound complexes, or as free ions that the anionic channel will not accept for transport. The nature of the reducing species is unknown.

Synthetic models of tunichrome b-1 (Figure 1.20) have been prepared. Tunichrome is a derivative of pyrogallol whose structure precludes the formation of an octahedral complex of vanadium as a simple 1:1 metal:ligand complex. The close analogue, described as 3,4,5-TRENPAMH$_9$, also cannot form a simple octahedral 1:1 complex. In contrast, the synthetic ligands TRENCAM and 2,3,4-TRENPAM can form pseudo-octahedral complexes. The structure of the vanadium TRENCAM complex shows that it is indeed a simple pseudo-octahedral tris-catechol complex.[47] The electrochemical behavior of these complexes is similar, with vanadium(IV/III) potentials of about -0.5 to -0.6 volts versus NHE. These results indicate that tunichrome b-1 complexes of

vanadium(IV/III) would show similar differences in their redox couples at high pH. At neutral pH, in the presence of excess pyrogallol groups, vanadium(IV) can be expected to form the intensely colored tris-catechol species. However, comparison of the EPR properties reported for vanadium-tunichrome preparations with model vanadium(lV)-complexes would indicate predominantly bis(catechol) vanadyl coordination. In any case, the vanadium(III) complexes must remain very highly reducing. It has been pointed out that the standard potential of pyrogallol is 0.79 V and decreases 60 mV per pH unit (up to about pH 9), so that at pH 7 the potential is about 0.4 V. The potentials of the vanadium couples for the tunichrome analogs are about -0.4 V. It has been concluded, therefore, that tunichrome or similar ligands cannot reduce the vanadium(IV) complex; so the highly reducing vanadium(III) complex of tunichrome must be generated in some other way.[47]

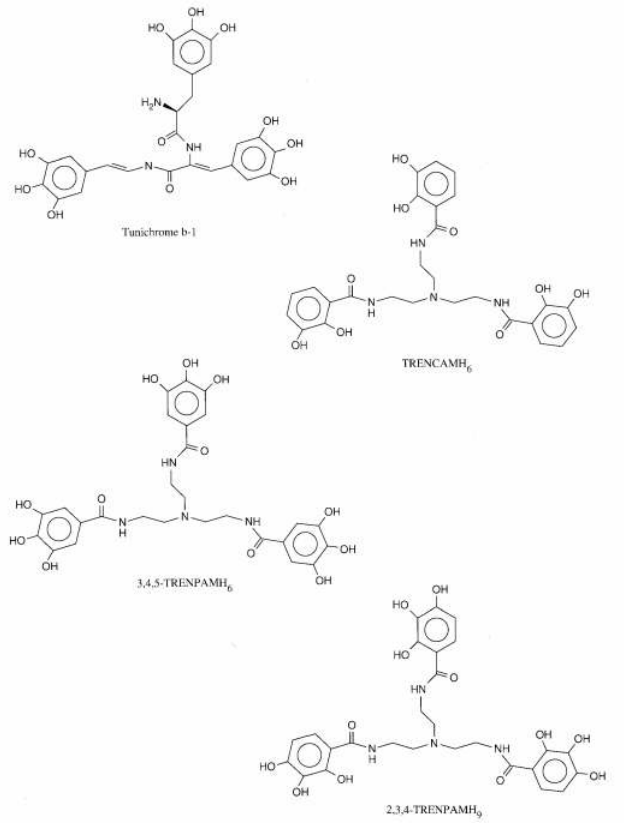


Figure 1.20 - Structures of tunichrome b-1 and synthetic analogues.[43]

Although a detailed presentation of examples of the known transport properties of essential transition-metal ions into various biological systems could be the subject of a large book, the examples that we have given show how the underlying inorganic chemistry of the elements is used in the biological transport systems that are specific for them. The regulation of metal-ion concentrations, including their specific concentration when necessary from relatively low concentrations of surrounding solution, is probably one of the first biochemical problems that was solved in the course of the evolution of life.

Iron is transported in forms in which it is tightly complexed to small chelators called siderophores (microorganisms) or to proteins called transferrins (animals) or to citrate or mugeneic acid (plants). The problem of how the iron is released in a controlled fashion is largely unresolved. The process of mineral formation, called biomineralization, is a subject of active investigation. Vanadium and molybdenum are transported as stable anions. Zinc and copper appear to be transported loosely associated with peptides or proteins (plants) and possibly mugeneic acid in plants. Much remains to be learned about the biological transport of nonferrous metal ions.

17.6: Transport of Zinc, Copper, Vanadium, Chromium, Molybdenum, and Cobalt is shared under a not declared license and was authored, remixed, and/or curated by LibreTexts.

Index

A

alkalides
- 10.8: Alkalides and Electrides

ambidentate isomerism
- 5.4: Isomerism

B

Berry pseudo rotation
- 5.3: Coordination Numbers and Structures

birefringence
- 9.3: Structures Related to NaCl and NiAs

C

constitutional isomers
- 5.4: Isomerism

coordination number
- 5.3: Coordination Numbers and Structures

D

Diode
- 11.7: Diodes, LEDs and Solar Cells
- 11.8: Amorphous Semiconductors
- 11.9: Discussion Questions
- 11.10: Problems
- 11.11: References

E

electrides
- 10.8: Alkalides and Electrides

enantiomers
- 5.4: Isomerism

F

fluorite (structure)
- 9.4: Tetrahedral Structures

H

Hund's rule
- 13.1: Microstates and Terms

hydrate isomerism
- 5.4: Isomerism

I

identity operation
- 2.1: Symmetry Elements and Operations

improper rotation
- 2.1: Symmetry Elements and Operations

inert complex
- 14.1: Substitution Reactions and their Mechanisms

ionization isomerism
- 5.4: Isomerism

isomerism
- 5.4: Isomerism

K

Kapustinskii equation
- 10.5: Kapustinskii Equation

L

labile complex
- 14.1: Substitution Reactions and their Mechanisms

Laporte Rule
- 13.2: Term splitting in ligand fields, selection rules, Tanabe-Sugano diagrams. Metal to ligand, and ligand to metal transitions

linkage isomerism
- 5.4: Isomerism

M

microstates
- 13.1: Microstates and Terms

O

overall symmetry
- 2.1: Symmetry Elements and Operations

P

Pourbaix diagrams
- 16.6: Pourbaix Diagrams

proper rotation
- 2.1: Symmetry Elements and Operations

pyrite structure
- 9.6: Bonding in TiS_2, MoS_2, and Pyrite Structures

S

Sabatier Principle
- 2.1: Symmetry Elements and Operations

Schoenflies symbol
- 2.1: Symmetry Elements and Operations

spectrochemical series
- 6.1: 7.1 Bonding in Coordination Compounds

stereoisomers
- 5.4: Isomerism

superconductor
- 11.3: Superconductors

symmetry elements
- 2.1: Symmetry Elements and Operations

symmetry operations
- 2.1: Symmetry Elements and Operations

T

term splitting
- 13.2: Term splitting in ligand fields, selection rules, Tanabe-Sugano diagrams. Metal to ligand, and ligand to metal transitions

terms
- 13.1: Microstates and Terms

V

valence bond theory
- 6.1: 7.1 Bonding in Coordination Compounds

Vasca’s complex
- 5.3: Coordination Numbers and Structures

Glossary

Sample Word 1 | Sample Definition 1

Detailed Licensing

Overview

Title: CHEM 4300: Inorganic Chemistry (Mink)

Webpages: 153

All licenses found:

- CC BY-SA 4.0: 67.3% (103 pages)
- Undeclared: 32.7% (50 pages)

By Page

- CHEM 4300: Inorganic Chemistry (Mink) - *Undeclared*
  - Front Matter - *Undeclared*
    - TitlePage - *Undeclared*
    - InfoPage - *Undeclared*
    - Table of Contents - *Undeclared*
    - Licensing - *Undeclared*
  - 1: Atomic Structure - *Undeclared*
    - 1.1: Historical Development of Atomic Theory - *Undeclared*
    - 1.2: The quantum-mechanical model of the atom - *Undeclared*
    - 1.3: Periodic Properties of Atoms - *Undeclared*
    - 1.4: Concept Review Questions Chapter 1 - *Undeclared*
    - 1.5: Homework Problems Chapter 1 - *Undeclared*
  - 2: Symmetry and Group Theory - *Undeclared*
    - 2.1: Symmetry Elements and Operations - *Undeclared*
    - 2.2: Point Groups - *Undeclared*
    - 2.3: Matrix Representations of Symmetry Operations and Character Tables - *Undeclared*
    - 2.4: Concept Review Questions Chapter 2 - *Undeclared*
    - 2.5: Homework Problems Chapter 2 - *Undeclared*
  - 3: Review of Chemical Bonding - *CC BY-SA 4.0*
    - 3.1: Prelude to Chemical Bonding - *CC BY-SA 4.0*
    - 3.2: Valence Bond Theory- Lewis Dot Structures, the Octet Rule, Formal Charge, Resonance, and the Isoelectronic Principle - *CC BY-SA 4.0*
    - 3.3: The Shapes of Molecules (VSEPR Theory) and Orbital Hybridization - *CC BY-SA 4.0*
    - 3.4: Bond Polarity and Bond Strength - *CC BY-SA 4.0*
    - 3.5: Discussion Questions - *CC BY-SA 4.0*
    - 3.6: Problems - *CC BY-SA 4.0*
    - 3.7: References - *CC BY-SA 4.0*
  - 4: Molecular Orbital Theory - *CC BY-SA 4.0*
    - 4.1: Prelude to Molecular Orbital Theory - *CC BY-SA 4.0*
    - 4.2: Constructing Molecular Orbitals from Atomic Orbitals - *CC BY-SA 4.0*
    - 4.3: Orbital Symmetry - *CC BY-SA 4.0*
    - 4.4: σ, π, and δ orbitals - *CC BY-SA 4.0*
    - 4.5: Diatomic Molecules - *CC BY-SA 4.0*
    - 4.6: Orbital Filling - *CC BY-SA 4.0*
    - 4.7: Periodic Trends in π Bonding - *CC BY-SA 4.0*
    - 4.8: Three-center Bonding - *CC BY-SA 4.0*
    - 4.9: Building up the MOs of More Complex Molecules- NH_3, P_4 - *CC BY-SA 4.0*
    - 4.10: Homology of σ and π orbitals in MO diagrams - *CC BY-SA 4.0*
    - 4.11: Chains and Rings of π-Conjugated Systems - *CC BY-SA 4.0*
    - 4.12: Discussion Questions - *CC BY-SA 4.0*
    - 4.13: Problems - *CC BY-SA 4.0*
    - 4.14: References - *CC BY-SA 4.0*
  - 5: Coordination Chemistry I - Structures and Isomers - *Undeclared*
    - 5.1: History - *Undeclared*
    - 5.2: Nomenclature - *Undeclared*
    - 5.3: Coordination Numbers and Structures - *Undeclared*
    - 5.4: Isomerism - *Undeclared*
    - 5.5: Concept Review Questions Chapter 5 - *Undeclared*
    - 5.6: Homework Problems Chapter 5 - *Undeclared*
  - 6: Coordination Chemistry III - Bonding - *Undeclared*
    - 6.1: 7.1 Bonding in Coordination Compounds - *Undeclared*
    - 6.2: Concept Review Questions Chapter 7 - *Undeclared*
    - 6.3: Homework Problems Chapter 7 - *Undeclared*
  - 7: Metals and Alloys- Structure, Bonding, Electronic and Magnetic Properties - *CC BY-SA 4.0*

- 7.1: Prelude to Metals and Alloys - *CC BY-SA 4.0*
- 7.2: Unit Cells and Crystal Structures - *CC BY-SA 4.0*
- 7.3: Bravais Lattices - *CC BY-SA 4.0*
- 7.4: Crystal Structures of Metals - *CC BY-SA 4.0*
- 7.5: Bonding in Metals - *CC BY-SA 4.0*
- 7.6: Conduction in Metals - *CC BY-SA 4.0*
- 7.7: Atomic Orbitals and Magnetism - *CC BY-SA 4.0*
- 7.8: Ferro-, Ferri- and Antiferromagnetism - *CC BY-SA 4.0*
- 7.9: Hard and Soft Magnets - *CC BY-SA 4.0*
- 7.10: Discussion Questions - *CC BY-SA 4.0*
- 7.11: Problems - *CC BY-SA 4.0*
- 7.12: References - *CC BY-SA 4.0*

- 8: Metals and Alloys - Mechanical Properties - *CC BY-SA 4.0*
  - 8.1: Defects in Metallic Crystals - *CC BY-SA 4.0*
  - 8.2: Work Hardening, Alloying, and Annealing - *CC BY-SA 4.0*
  - 8.3: Malleability of Metals and Alloys - *CC BY-SA 4.0*
  - 8.4: Iron and Steel - *CC BY-SA 4.0*
  - 8.5: Amorphous Alloys - *CC BY-SA 4.0*
  - 8.6: Discussion Questions - *CC BY-SA 4.0*
  - 8.7: Problems - *CC BY-SA 4.0*
  - 8.8: References - *CC BY-SA 4.0*
- 9: Ionic and Covalent Solids - Structures - *CC BY-SA 4.0*
  - 9.1: Prelude to Ionic and Covalent Solids - Structures - *CC BY-SA 4.0*
  - 9.2: Close-packing and Interstitial Sites - *CC BY-SA 4.0*
  - 9.3: Structures Related to NaCl and NiAs - *CC BY-SA 4.0*
  - 9.4: Tetrahedral Structures - *CC BY-SA 4.0*
  - 9.5: Layered Structures and Intercalation Reactions - *CC BY-SA 4.0*
  - 9.6: Bonding in TiS_2, MoS_2, and Pyrite Structures - *CC BY-SA 4.0*
  - 9.7: Spinel, Perovskite, and Rutile Structures - *CC BY-SA 4.0*
  - 9.8: Discussion Questions - *CC BY-SA 4.0*
  - 9.9: Problems - *CC BY-SA 4.0*
  - 9.10: References - *CC BY-SA 4.0*
- 10: Ionic and Covalent Solids - Energetics - *CC BY-SA 4.0*
  - 10.1: Ionic Radii and Radius Ratios - *CC BY-SA 4.0*
  - 10.2: Structure Maps - *CC BY-SA 4.0*
  - 10.3: Energetics of Crystalline Solids- The Ionic Model - *CC BY-SA 4.0*
  - 10.4: Born-Haber Cycles for NaCl and Silver Halides - *CC BY-SA 4.0*
  - 10.5: Kapustinskii Equation - *CC BY-SA 4.0*
  - 10.6: Discovery of Noble Gas Compounds - *CC BY-SA 4.0*
  - 10.7: Stabilization of High and Low Oxidation States - *CC BY-SA 4.0*
  - 10.8: Alkalides and Electrides - *CC BY-SA 4.0*
  - 10.9: Resonance Energy of Metals - *CC BY-SA 4.0*
  - 10.10: Prelude to Ionic and Covalent Solids - Energetics - *CC BY-SA 4.0*
  - 10.11: The Strange Case of the Alkali Oxides - *CC BY-SA 4.0*
  - 10.12: Lattice Energies and Solubility - *CC BY-SA 4.0*
  - 10.13: Discussion Questions - *CC BY-SA 4.0*
  - 10.14: Problems - *CC BY-SA 4.0*
  - 10.15: References - *CC BY-SA 4.0*
- 11: Electronic Properties of Materials - Superconductors and Semiconductors - *CC BY-SA 4.0*
  - 11.1: Prelude to Electronic Properties of Materials - Superconductors and Semiconductors - *CC BY-SA 4.0*
  - 11.2: Metal-Insulator Transitions - *CC BY-SA 4.0*
  - 11.3: Superconductors - *CC BY-SA 4.0*
  - 11.4: Periodic Trends- Metals, Semiconductors, and Insulators - *CC BY-SA 4.0*
  - 11.5: Semiconductors- Band Gaps, Colors, Conductivity and Doping - *CC BY-SA 4.0*
  - 11.6: Semiconductor p-n Junctions - *CC BY-SA 4.0*
  - 11.7: Diodes, LEDs and Solar Cells - *CC BY-SA 4.0*
  - 11.8: Amorphous Semiconductors - *CC BY-SA 4.0*
  - 11.9: Discussion Questions - *CC BY-SA 4.0*
  - 11.10: Problems - *CC BY-SA 4.0*
  - 11.11: References - *CC BY-SA 4.0*
- 12: Physical Techniques in Inorganic Chemistry - *Undeclared*
- 13: Coordination Chemistry IV - Electronic Spectra - *Undeclared*
  - 13.1: Microstates and Terms - *Undeclared*
  - 13.2: Term splitting in ligand fields, selection rules, Tanabe-Sugano diagrams. Metal to ligand, and ligand to metal transitions - *Undeclared*
  - 13.3: Concept Review Questions Chapter 8 - *Undeclared*
  - 13.4: Homework Problems Chapter 8 - *Undeclared*
- 14: Coordination Chemistry V - Reactions and Mechanisms - *Undeclared*
  - 14.1: Substitution Reactions and their Mechanisms - *Undeclared*

- 14.2: Concept Review Questions Chapter 9 - *Undeclared*
- 14.3: Homework Problems Chapter 9 - *Undeclared*

15: Acid-Base Chemistry - *CC BY-SA 4.0*

- 15.1: Prelude to Acid-Base Chemistry - *CC BY-SA 4.0*
- 15.2: Brønsted and Lewis Acids and Bases - *CC BY-SA 4.0*
- 15.3: Hard and Soft Acids and Bases - *CC BY-SA 4.0*
- 15.4: The Electrostatic-Covalent (ECW) Model for Acid-Base Reactions - *CC BY-SA 4.0*
- 15.5: Frustrated Lewis Pairs - *CC BY-SA 4.0*
- 15.6: Discussion Questions - *CC BY-SA 4.0*
- 15.7: Problems - *CC BY-SA 4.0*
- 15.8: References - *CC BY-SA 4.0*

16: Redox Stability and Redox Reactions - *CC BY-SA 4.0*

- 16.1: Prelude to Redox Stability and Redox Reactions - *CC BY-SA 4.0*
- 16.2: Balancing Redox Reactions - *CC BY-SA 4.0*
- 16.3: Electrochemical Potentials - *CC BY-SA 4.0*
- 16.4: Latimer and Frost Diagrams - *CC BY-SA 4.0*
- 16.5: Redox Reactions with Coupled Equilibria - *CC BY-SA 4.0*
- 16.6: Pourbaix Diagrams - *CC BY-SA 4.0*
- 16.7: Discussion Questions - *CC BY-SA 4.0*
- 16.8: Problems - *CC BY-SA 4.0*
- 16.9: References - *CC BY-SA 4.0*

17: Transition-Metal Storage, Transport, and Biomineralization - *Undeclared*

- 17.1: Biological Significance of Iron, Zinc, Copper, Molybdenum, Cobalt, Chromium, Vanadium, and Nickel - *Undeclared*
- 17.2: Biological Systems of Metal Storage - *Undeclared*
- 17.3: Chemical Properties Relative to Storage and Transport - *Undeclared*
- 17.4: Iron Biomineralization - *Undeclared*
- 17.5: Transport of Iron - *Undeclared*
- 17.6: Transport of Zinc, Copper, Vanadium, Chromium, Molybdenum, and Cobalt - *Undeclared*

Back Matter - *Undeclared*

- Index - *Undeclared*
- Glossary - *Undeclared*
- Detailed Licensing - *Undeclared*